PO Box 2345, Beijing 100023, China
Fax: +86-10-85381893
E-mail: wjg@wjgnet.com www.wjgnet.com

World J Gastroenterol 2004;10(12):1695-1696
World Journal of Gastroenterology
Copyright ©2004 by The WJG Press ISSN 1007-9327

• EDITORIAL •

Milling of wheat, maize and rice: Effects on fibre and lipid content and health

FI Tovey, M Hobsley

FI Tovey, Hon. Research Fellow, M Hobsley, Professor Emeritus, Dept. of Surgery, UCL, UK
Correspondence to: FI Tovey, 5 Crossborough Hill, Basingstoke RG21 4AG, UK. frank@tovey.fsnet.co.uk
Telephone: +44-01256-461521
Received: 2004-04-20 **Accepted:** 2004-05-06

Tovey FI, Hobsley M. Milling of wheat, maize and rice: Effects on fibre and lipid content and health. *World J Gastroenterol* 2004; 10(12): 1695-1696
http://www.wjgnet.com/1007-9327/10/1695.asp

During the last thirty years the main interest in the medical consequences of milling of staple carbohydrate foods, particularly wheat and maize, has been in its effect on the fibre content as a result of the milling. The late nineteenth and early twentieth centuries in the West saw great changes in milling processes, from stone milling using water or wind power, to increasingly sophisticated roller milling, with an increasing loss of fibre in the process. In the 1970s and onwards there was an enhanced interest in possible diseases which could be related to the loss of fibre in the diet. At one time the list included diverticulitis, appendicitis, varicose veins, deep vein thrombosis, carcinoma of the colon, Crohn' s disease, ulcerative colitis, irritable bowel syndrome, peptic ulcer, gall stones, hiatus hernia and gastro-oesophageal reflux, disorders of lipid metabolism and coronary heart disease! Over the course of time medical evidence has narrowed this list down to a much smaller number, of which the most important are diverticular disease and carcinoma of the colon.

The effect of fibre on peptic ulcer disease was attributed to its buffering effect on acid secretion. There seemed to be a relationship between the fibre content of staple diet and the geographical prevalence of duodenal ulceration. The prevalence was lower in populations using unrefined wheat, millets or maize with a high fibre content and higher in populations using refined wheat or maize flour or milled rice with low fibre contents[1-4]. There were, however, abnormalities which did not fit in with this pattern, such as the high prevalence of duodenal ulcer in the Highlands of Ethiopia, where the staple food was unrefined teff (Eragrastosis abyssinica) with a high fibre content[4]. A possible explanation of this abnormality may lie in the lipid content of teff (see next paragraph). However, in addition, acid secretion studies showed that, whilst fibre had an initial buffering effect on gastric acidity, the resulting antral stimulation led to a higher acid output[5].

A further effect of milling was on the lipid content of staple carbohydrate foods. Experiments on animal peptic ulcer models showed that the lipids present in the unrefined staple foods in areas with low prevalence of duodenal ulcer had a gastroprotective effect against ulceration and also promoted ulcer healing. These were not present in the refined staple foods of the areas with high duodenal ulcer prevalence[6-9].

Lipids are found in both the bran and the germ of staple carbohydrate foods. In wheat and rice more lipids are found in the bran, but in maize the bulk lies in the predominantly large germ. Lipases are also present principally in the germ.

Milling has different effects on the bran and germ. In the case of wheat the two come apart separately. They can be separated by sieving and are stable for a period of time without further treatment. In the case of maize and rice the bran and germ come away together and the resultant bruising releases the lipases which interact with the oil content leading, if left untreated, to early rancidity of the combined germ and bran. Thus wholemeal wheat flour has a stable shelf life for a variable period of time, but the only satisfactory way to eat whole maize is either on the cob or home-pounded and cooked on the same day. Rice can only be eaten in the unrefined state as brown or unmilled rice. Milled rice undergoes changes during storage. During the milling of rice some of the lipase present in the bran enters the endosperm and as the rice is stored it reacts with a small amount of oil present in the rice grain. Some say that this results in an improvement in taste. The resulting lipolysis results in the formation of free fatty acids followed by a process of peroxidation that produces ketoaldehydes. Experiments on animal peptic ulcer models have shown that the latter are ulcerogenic. Similar experiments have shown that freshly milled rice bran is protective, but that it rapidly becomes ulcerogenic[10,11]. Thus milled rice is not only deprived of gastroprotective lipids but also, on storage, becomes ulcerogenic, which is a possible factor in the high prevalence of duodenal ulceration in milled rice-eating countries.

With the discovery of *Helicobacter pylori* there has been much emphasis on its being the prime cause of duodenal ulceration. However, evidence is increasing to suggest that it may be a secondary infection affecting chronicity[12,13]. Moreover, it should be remembered that many other factors have been shown to be associated with duodenal ulceration. These include familial tendency, acute anxiety as in the Second World War, cigarette smoking and the introduction of roller milling. Of these factors, the latter two greatly increased at the beginning of the twentieth century, which is the time when the epidemic of duodenal ulceration began. A suggestive feature about smoking is that it results in an increase in the parietal cell mass and therefore in an increase in the maximal ability of the stomach to secrete acid[14], which itself is so strongly associated with duodenal ulceration[15]. Which of these factors are truly aetiological and which are confounding factors that happened to be increasing at the same time remain unknown. It is important to keep an open mind.

The results of experiments on animal peptic ulcer models, however, strongly support the possibility that the loss of certain protective lipids, resulting from the milling of staple carbohydrate foods, may be an important factor. More needs to be known about the nature and action of these lipids.

REFERENCES

1 **Tovey FI**. Peptic ulcer in India and Bangladesh. *Gut* 1979; **20**: 329-347
2 **Tovey FI**, Tunstall M. Duodenal ulcer in black populations in Africa south of the Sahara. *Gut* 1975; **16**: 564-576
3 **Tovey FI**. Duodenal ulcer in China. *J Gastroenterol Hepatol* 1992; **7**: 427-431
4 **Tovey FI**. Diet and duodenal ulcer. *J Gastroenterol Hepatol* 1994;

9: 177-185

5 **Tovey FI**. Aetiology of duodenal ulcer: an investigation into the buffering action and effect on pepsin of bran and unrefined carbohydrate foods. *Postgrad Med J* 1974; **50**: 683-688

6 **Jayaraj AP**, Tovey FI, Clark CG. Possible dietary factors in relation to the distribution of duodenal ulcer in India and Bangladesh. *Gut* 1980; **21**: 1068-1076

7 **Jayaraj AP**, Tovey FI, Lewin MR, Clark CG. Duodenal ulcer prevalence: Experimental evidence for the possible role of dietary lipids. *J Gastroenterol Hepatol* 2000; **15**: 610-616

8 **Jayaraj AP**, Tovey FI, Clark CG, Hobsley M. Dietary factors in relation to the distribution of duodenal ulcer in India as assessed by studies in rats. *J Gastroenterol Hepatol* 2001; **16**: 501-505

9 **Jayaraj AP**, Tovey FI, Hobsley M. Duodenal ulcer prevalence: Research into the nature of possible protective dietary lipids. *Phytother Res* 2003; **17**: 391-398

10 **Jayaraj AP**, Tovy FI, Clark CG, Rees KR, White JS, Lewin MR. The ulcerogenic and protective action of rice and rice fractions in experimental peptic ulceration. *Clin Sci* 1987; **72**: 463-466

11 **Jayaraj AP**, Rees KR, Tovey FI, White JS. A molecular basis for peptic ulceration due to diet. *Br J exp Path* 1986; **67**: 149-155

12 **Tovey FI**, Hobsley M. Is *Helicobacter pylori* the primary cause of duodenal ulceration? *J Gastroenterol Hepatol* 1999; **14**: 1053-1056

13 **Hobsley M**, Tovey FI. *Helicobacter pylori*: the primary cause of duodenal ulceration or a secondary infection? *World J Gastroenterol* 2001; **7**: 149-151

14 **Whitfield PF**, Hobsley M. Comparison of maximal gastric secretion in smokers and non-smokers with and without duodenal ulcer. *Gut* 1987; **28**: 557-560

15 **Hobsley M**, Whitfield PF. The likelihood of a disease in relation to the magnitude of a risk factor. The example of duodenal ulcer. *Theor Surg* 1987; **2**: 106-109

Edited by Xu XQ and Wang XL **Proofread by** Xu FM

PO Box 2345, Beijing 100023, China
Fax: +86-10-85381893
E-mail: wjg@wjgnet.com www.wjgnet.com

World J Gastroenterol 2004;10(12):1697-1698
World Journal of Gastroenterology
Copyright ©2004 by The WJG Press ISSN 1007-9327

• EDITORIAL •

Surgery for pancreatic necrosis: "Whom, when and what"

S Connor, JP Neoptolemos

S Connor, JP Neoptolemos, Department of Surgery, Royal Liverpool University Hospital, Daulby Street, Liverpool, L69 3GA, UK
Correspondence to: Professor JP Neoptolemos, Department of Surgery, Royal Liverpool University Hospital, 5th floor UCD, Daulby Street, Liverpool, L69 3GA, United Kingdom. j.p.neoptolemos@liv.ac.uk
Telephone: +44-151-7064177 **Fax:** +44-151-7065826
Received: 2004-01-14 **Accepted:** 2004-02-26

Connor S, Neoptolemos JP. Surgery for pancreatic necrosis: "Whom, when and what". *World J Gastroenterol* 2004; 10 (12): 1697-1698
http://www.wjgnet.com/1007-9327/10/1697.asp

Acute pancreatitis is a common condition in which 70% of patients will recover with simple medical management. For patients who develop extensive or infected pancreatic necrosis the outcome is significantly different with a high morbidity and mortality[1]. Surgery is the mainstay of treatment for these patients but several unresolved issues remain including *who requires surgery, when is the optimal time to intervene and what technique should be used.*

Infected necrosis is generally accepted as a strong indication for surgery[2]. This has developed not from randomised data but observational studies over time that seemed to show a reduction in the previously reported mortality[3-5]. A small number of recent reports[6-8] have attempted to cast doubt on whether all patients with infected pancreatic necrosis should undergo surgery. So should a randomised controlled trial be undertaken? On the available evidence most surgeons and gastroenterologists would lack the "equipoise" required to perform such a trial. The number of patients successfully responding to conservative treatment remains small compared to the overall population with infected pancreatic necrosis. Further identification of factors associated with spontaneous resolution of infected necrosis needs to be identified before conservative treatment can be recommended as an acceptable alternative.

With the main indication for surgery being infected necrosis, the absence of infection is not an absolute contraindication. Over 90% of patients with sterile necrosis can be successfully treated without surgical intervention[9,10], but a small subset with extensive necrosis warrants surgery. Indications in this setting include deteriorating organ failure despite maximal support[10,11] or persisting symptoms which preclude hospital discharge despite several weeks of optimum conservative treatment[9,12].

The timing of surgery is an important determinant of outcome with early surgery (within the first week) associated with a high mortality[13,14]. The development of infected necrosis is time dependant, increasing to a peak in weeks 2-4[15]. Some studies have suggested that antibiotics may reduce the incidence of infected necrosis[16-22] but other recent large randomized controlled trials now reject this notion[23,24]. Moreover whether prophylactic antibiotics can delay the onset of infected necrosis or the need for intervention is unknown. Another unknown factor is whether those patients who develop infected necrosis within the first 14 d of their illness should continue to be managed conservatively to allow the necrotic tissue to demarcate the reduction of complications associated with early debridement. Infected necrosis is almost universally associated with the progressive escalation of organ failure[17]. Increasing pre-operative organ dysfunction scores have been associated with an increase in mortality[25,26] and thus any delay in surgery following the diagnosis of infected necrosis is likely to be detrimental.

The aim of intervention in those with pancreatic necrosis is to remove the necrotic tissue and to provide adequate drainage for the remaining debris while preserving viable pancreatic tissue with minimal morbidity and mortality. It is generally accepted that debridement is preferable to resection[2] and the approaches to the pancreatic necrosis include trans-peritoneal, retro-peritoneal, minimally invasive and percutaneous techniques[4,12,14,25-32]. Post operative management includes laparostomy, packing, closed retroperitoneal lavage and repeat debridement[4,12,14,25-32]. There is no standardised optimal technique as there are no randomised trials that compared surgical techniques. In the largest reported series[17] the mortality was 39% but it has been reported as low as 6-8%[12,28], which was the same as that for the overall mortality associated with pancreatitis in the United Kingdom[33]. The reason for this wide inter-study variation is likely to be due to a number of factors. Firstly, there was an inter-study heterogeneity in both the reporting and the frequency of adverse patient prognostic factors. Secondly, intervention rates varied 10-fold[34,35], suggesting that the indications for intervention provided by guidelines are not uniformly interpreted. Thirdly, many studies were relatively small, retrospective or based over long time periods during which there was often a change in management.

The Regional Pancreas Centre at the Royal Liverpool University Hospital has adopted a minimally invasive approach in preference to an open approach because it was associated with a very high mortality despite expert surgery and intensive care[26,27]. Minimally, invasive retroperitoneal pancreatic necrosectomy has the dual advantages of removal of the solid necrotic material under direct vision through a wide bore tract[27,31,32] and the use of high volume post-operative lavage through the wide tract[27]. Moreover minimally invasive retroperitoneal pancreatic necrosectomy can be performed under local anaesthesia and reduces the need for post-operative intensive care, by avoiding an escalation in organ dysfunction which is usually seen after open surgery[26,31]. The disadvantages of minimally invasive retroperitoneal pancreatic necrosectomy include an increase in the number of procedures and possible increase in hospital stay[26,27]. Minimally invasive retroperitoneal pancreatic necrosectomy has not yet been shown to significantly reduce mortality although the trend is strong in this direction. Further experience with this technique and possible multi-centre randomised trials are needed.

Future studies on the outcome from intervention for pancreatic necrosis should incorporate standardised reporting of the precise profile of patients to allow for more valid comparisons between the different surgical techniques. In particular, there should be a clear description of the indications for intervention, the overall sample size from which the patients are selected, key prognostic indicators including age, organ dysfunction scores, extent of necrosis and the incidence of primary infection of the necrosis. It is notable that most studies failed to provide these critical factors and did not distinguish primary from secondary infection. Improving the reporting of studies will lead to the identification of the optimal patient at the optimal time undergoing the optimal procedure.

REFERENCES

1 **Neoptolemos JP**, Raraty M, Finch M, Sutton R. Acute pancreatitis: the substantial human and financial costs. *Gut* 1998; **42**: 886-891
2 **Uhl W**, Warshaw A, Imrie C, Bassi C, McKay CJ, Lankisch PG, Carter R, Di Magno E, Banks PA, Whitcomb DC, Dervenis C, Ulrich CD, Satake K, Ghaneh P, Hartwig W, Werner J, McEntee G, Neoptolemos JP, Buchler MW. International Association of Pancreatology. IAP Guidelines for the surgical management of acute pancreatitis. *Pancreatology* 2002; **2**: 565-573
3 **Altemeier WA**, Alexander JW. Pancreatic abscess. *Arch Surg* 1963; **87**: 80-85
4 **Bradley EL**. Management of infected pancreatic necrosis by open drainage. *Ann Surg* 1987; **204**: 542-549
5 **Sarr M**. Invited Commentary. *Dig Surg* 2003; **20**: 300
6 **Dubner H**, Steinberg W, Hill M, Bassi C, Chardavoyne R, Bank S. Infected pancreatic necrosis and peripancreatic fluid collections: Serendipitous response to antibiotic and medical therapy in three patients. *Pancreas* 1996; **12**: 298-302
7 **Salas CJ**, Gallego RFJ, Sanchez SJC, Diez GF. Medical treatment of infected pancreatic necrosis. *Gastroenterol Hepatol* 2001; **24**: 268-269
8 **Ramesh H**, Prakash K, Lekha V, Jacob G, Venugopal A. Are some cases of infected pancreatic necrosis treatable without intervention. *Dig Surg* 2003; **20**: 296
9 **Ashley SW**, Perez A, Pierce EA, Brooks DC, Moore FD Jr, Whang EE, Banks PA, Zinner MJ. Necrotising pancreatitis. *Ann Surg* 2001; **234**: 572-580
10 **Buchler MW**, Gloor B, Muller CA, Friess H, Seiler CA, Uhl W. Acute necrotising pancreatitis: treatment stratergy according to status of infection. *Ann Surg* 2000; **232**: 619-626
11 **Beger HG**, Isenmann R. Acute pancreatitis: Who needs an operation? *J Hepatobiliary Pancreat Surg* 2002; **9**: 436-442
12 **Fernadez-del Castillo C**, Rattner DW, Makary MA, Mostafavi A, McGrath D, Warshaw A. Debridement and closed packing for the treatment of necrotising pancreatitis. *Ann Surg* 2000; **228**: 676-684
13 **Mier J**, Leon EL, Castillo A, Robledo F, Blanco R. Early *versus* late necrosectomy in severe pancreatitis. *Am J Surg* 1997; **173**: 71-75
14 **Gotzinger P**, Wamser P, Exner R, Schwanzer E, Jakesz R, Fugger R, Sautner T. Surgical treatment of severe acute pancreatitis: timing of operation is crucial for survival. *Surg Infect* 2003; **4**: 205-211
15 **Beger HG**, Bittner R, Block S, Buchler M. Bacterial contamination of pancreatic necrosis. A prospective clinical study. *Gastroenterology* 1986; **91**: 433-438
16 **Pederzoli P**, Bassi C, Vesentini S, Campedelli A. A randomised multicentre clinical trial of antibiotic prophylaxis of septic complications in acute necrotising pancreatitis with imipenem. *Surg Gynecol Obstet* 1993; **176**: 480-483
17 **Gotzinger P**, Sautner T, Kriwanek S, Beckerhinn P, Barlan M, Armbruster C, Wamser P, Fugger R. Surgical treatment for severe acute pancreatitis: Extent and surgical control of necrosis determine outcome. *World J Surg* 2002; **26**: 474-478
18 **Pederzoli P**, Bassi C, Vesentini S, Girelli R, Cavallini G, Falconi M, Nifosi F, Riela A, Dagradi A. A randomised multi-centre clinical trial of antibiotic prophylaxis of septic complications in acute necrotising pancreatitis with imipenem. *Surg Gynecol Obstet* 1993; **176**: 480-483
19 **Sainio V**, Kemppainen E, Puolakkainen P, Taavitsainen M, Kivisaari L, Valtonen V, Haapiainen R, Schroder T, Kivilaakso E. Early antibiotic treatment in acute necrotising pancreatitis. *Lancet* 1995; **346**: 663-667
20 **Delcenserie R**, Yzet T, Ducroix JP. Prophylactic antibiotics in treatment of severe acute alcoholic pancreatitis. *Pancreas* 1996; **13**: 198-201
21 **Schwarz M**, Isenmann R, Meyer H, Beger HG. Antibiotic use in necrotizing pancreatitis. Results of a controlled study. *Dtsch Med Wochenschr* 1997; **122**: 356-361
22 **Nordback I**, Sand J, Saaristo R, Paajanen H. Early treatment with antibiotics reduces the need for surgery in acute necrotizing pancreatitis-a single-center randomized study. *J Gastrointest Surg* 2001; **5**: 113-118
23 **Isenmann R**, Runzi M, Kron M, Kahl S, Kraus D, Jung N, Maier L, Malfertheiner P, Goebell H, Beger HG. Prophylactic antibiotic treatment in patients with predicted severe acute pancreatitis: A placebo-controlled, double-blind trial. *Gastroenterology* 2004; **126**: 997-1004
24 **Spicak J**, Hejtmankova S, Cech P, Hoskovec D, Kostka R, Leffler J, Kasalicky M, Svoboda P, Bartova J. Antibiotic prophylaxis in severe acute pancreatitis: randomized multicenter prospective trial with meropenem. *Pancreatology* 2003; **3**: 220
25 **Beattie GC**, Mason J, Swan D, Madhavan KK, Siriwardena AK. Outcome of necrosectomy in acute pancreatitis. *Scand J Gastroenterol* 2002; **12**: 1450-1453
26 **Connor S**, Ghaneh P, Raraty M, Rosso E, Hartley MN, Garvey C, Hughes M, McWilliams R, Evans J, Rowlands P, Sutton R, Neoptolemos JP. Increasing age and APACHE II scores are the main determinants of outcome from pancreatic necrosectomy. *Br J Surg* 2003; **90**: 1542-1548
27 **Connor S**, Ghaneh P, Raraty M, Sutton R, Rosso E, Garvey CJ, Hughes ML, Evans JC, Rowlands P, Neoptolemos JP. Minimally invasive retroperitoneal pancreatic necrosectomy. *Dig Surg* 2003; **20**: 270-277
28 **Beger HG**, Buchler M, Bittner R, Block S, Nevalainen T, Roscher R. Necrosectomy and post-operative local lavage in necrotising pancreatitis. *Br J Surg* 1988; **75**: 207-212
29 **Lasko DS**, Habib FA, Sleeman D, Levi J, Shatz D, Livingstone A. Percutaneous lavage for infected pancreatic necrosis. *J Gastrointest Surg* 2003; **7**: 288-289
30 **Tzovaras G**, Parks RW, Diamond T, Rowlands BJ. Early and long term results of surgery for severe necrotising pancreatitis. *Dig Surg* 2004; **21**: 41-47
31 **Carter RC**, Mckay CJ, Imrie CW. Percutaneous necrosectomy and sinus tract endoscopy in the management of infected pancreatic necrosis: An initial experience. *Ann Surg* 2000; **232**: 175-180
32 **Gambiez LP**, Denimal FA, Porte HL, Saudemont A, Chambon JP, Quandalle PA. Retroperitoneal approach and endoscopic management of peripancreatic necrosis collections. *Arch Surg* 1998; **133**: 66-72
33 **Winslet M**, Hall C, London NJ, Neoptolemos JP. Relation serum amylase levels to aetiology and severity of acute pancreatitis. *Gut* 1992; **33**: 982-986
34 **Oleynikov D**, Cook C, Sellers B, Mone MC, Barton R. Decreased mortality from necrotising pancreatitis. *Am J Surg* 1998; **176**: 648-653
35 **Branum G**, Galloway J, Hirchowitz W, Fendley M, Hunter J. Pancreatic necrosis: results of necrosectomy, packing and ultimate closure over drains. *Ann Surg* 1998; **227**: 870-877

Edited by Xu XQ and Wang XL **Proofread by** Xu FM

PO Box 2345, Beijing 100023, China
Fax: +86-10-85381893
E-mail: wjg@wjgnet.com www.wjgnet.com

World J Gastroenterol 2004;10(12):1699-1708
World Journal of Gastroenterology
Copyright ©2004 by The WJG Press ISSN 1007-9327

• REVIEW •

Hyperhomocysteinemia, endoplasmic reticulum stress, and alcoholic liver injury

Cheng Ji, Neil Kaplowitz

Cheng Ji, Neil Kaplowitz, Gastroenterology/Liver Division, Keck School of Medicine, University of Southern California, Los Angeles, CA 90033, USA
Supported by the U.S. National Institute of Alcohol Abuse and Alcoholism, R01 AA014428 and by the Robert E. and May R. Wright Foundation, No. 263
Correspondence to: Cheng Ji, Ph.D., Faculty of Medicine, Gastroenterology/Liver Division, Keck School of Medicine, University of Southern California, HMR-101, 2011 Zonal Avenue, Los Angeles, CA 90033, USA. chengji@usc.edu
Telephone: +1-323-442-3452 **Fax:** +1-323-442-5425
Received: 2004-04-20 **Accepted:** 2004-05-06

Abstract

Deficiencies in vitamins or other factors (B6, B12, folic acid, betaine) and genetic disorders for the metabolism of the non-protein amino acid-homocysteine (Hcy) lead to hyperhomocysteinemia (HHcy). HHcy is an integral component of several disorders including cardiovascular disease, neurodegeneration, diabetes and alcoholic liver disease. HHcy unleashes mediators of inflammation such as NFκB, IL-1β, IL-6, and IL-8, increases production of intracellular superoxide anion causing oxidative stress and reducing intracellular level of nitric oxide (NO), and induces endoplasmic reticulum (ER) stress which can explain many processes of Hcy-promoted cell injury such as apoptosis, fat accumulation, and inflammation. Animal models have played an important role in determining the biological effects of HHcy. ER stress may also be involved in other liver diseases such as α_1-antitrypsin (α_1-AT) deficiency and hepatitis C and/or B virus infection. Future research should evaluate the possible potentiative effects of alcohol and hepatic virus infection on ER stress-induced liver injury, study potentially beneficial effects of lowering Hcy and preventing ER stress in alcoholic humans, and examine polymorphism of Hcy metabolizing enzymes as potential risk-factors for the development of HHcy and liver disease.

Ji C, Kaplowitz N. Hyperhomocysteinemia, endoplasmic reticulum stress, and alcoholic liver injury. *World J Gastroenterol* 2004; 10(12): 1699-1708

http://www.wjgnet.com/1007-9327/10/1699.asp

INTRODUCTION

Homocysteine (Hcy) is a toxic non-protein sulfur containing amino acids in humans. It is formed exclusively upon demethylation of the essential amino acid- methionine. Hcy is metabolized either through remethylation or transsulfuration pathways and is nutritionally regulated. Normal concentrations of total homocysteine in plasma are in the range of 5 to 16 μmol/L and the desired upper limit for Hcy concentration should be 10 μmol/L. An elevated plasma Hcy level is denoted hyperhomocysteinemia (HHcy). Three ranges of HHcy are defined: moderate (16 to 30 μmol/L), intermediate (31 to 100 μmol/L), and severe (>100 μmol/L). Individuals who consume a large amount of food rich in animal protein may ingest two to three grams of methionine, resulting in postprandial Hcy concentrations greater than 20 μmol/L. Clinical HHcy was first described more than 40 years ago in children with learning difficulties[1-3], and it has since been estimated that moderate HHcy occurs in 5-7% of the general population. Evidence now indicates that moderate HHcy is an important and independent risk factor for several disorders, including atherosclerosis, diabetes, fatty liver, immune activation, and neurodegenerations such as Alzheimer' s and Parkinson' s diseases[3-9].

Readers are referred to recent reviews on HHcy and functions of Hcy[10,11]. The main goal of this article is to provide information on major causes of HHcy, potential mechanisms of Hcy toxicity, with emphasis on endoplasmic reticulum (ER) stress mechanism, and animal models for the study of biological effects of HHcy. We would also summarize our ongoing work on ethanol-induced HHcy and liver injury in an intragastric ethanol fed murine model.

HCY METABOLISM AND HHCY

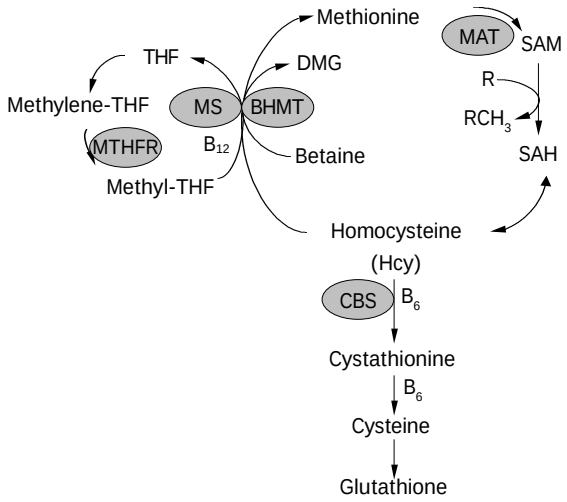

Figure 1 Homocysteine metabolism. Homocysteine has three main metabolic fates: to be remethylated to methionine, to enter the cysteine biosynthetic pathway, and to be released into the extracellular medium. CBS, cystathionine -synthase; MS, methionine synthase; THF, tetrahydrofolate; MTHFR, 5, 10-methylenetetrahydrofolate reductase; BHMT, betaine-homocysteine methyltransferase; DMG, dimethylglycine; MAT, methionine adenosyltransferase; SAM, S-adenosylmethionine; SAH, S-adenosylhomocysteine.

Hcy was formed from methionine after removal of the methyl group on S-adenosylmethionine (SAM) (Figure 1). Hcy metabolism involves reversible formation of S-adenosylhomocysteine (SAH), remethylation to methionine by betaine-homocysteine methyltransferase (BHMT) (liver and kidney restricted), which is vitamin-independent, and by the ubiquitous methionine synthase (MS), which is dependent on vitamin B12 and

methylenetetrahydrofolate (MTHF) production *via* 5, 10-methylenetetrahydrofolate reductase (MTHFR). Hcy can also be converted through transsulfuration to cystathionine for the formation of cysteine and glutathione (GSH). The transsulfuration is catalyzed by cystathionine-β-synthase (CBS) and is dependent on vitamin B6. In addition, Hcy can be converted to Hcy-tRNA. Although it was not incorporated into protein due to editing mechanisms, nitroso-Hcy-tRNA is stable and might play a role in Hcy-induced protein misfolding along with the formation of Hcy-protein-SH mixed disulfides and Hcy thiolactone covalent binding to lysine amino groups[11]. Hcy-t-RNA is edited through the action of methionyl-t-RNA synthetase (ATP consuming) by formation of a thioester thiolactone which could covalently bind to protein amino groups. Thus, homocysteinylation of proteins depends on the formation of thiolactone[12,13].

Tight regulation of Hcy metabolism depends on different affinities of MS, BHMT, and CBS for Hcy. MS and BHMT show low Km values for Hcy (<0.1 mmol/L), and CBS has high Km values for Hcy (>1 mmol/L). At low Hcy concentrations, methionine conservation was favored; and at high Hcy concentrations, immediate and long-term drainage of Hcy via the transsulfuration pathway was ensured[14]. SAM could play a key regulatory role by allosterically inhibiting MTHFR and BHMT and activating CBS[15-18]. Thus, SAM may be a regulatory switch in Hcy metabolism: low SAM favors remethylation and conservation of Hcy for methionine synthesis, whereas high levels favor transsulfuration. High Hcy levels can decrease the SAM/SAH ratio, since most methyltransferases bind to SAH with higher affinity than SAM, elevated SAH inhibits methylation. *In vitro*, under "physiological" conditions of concentrated 27 000 *g* postmitochondrial supernatant with 8 mmol/L GSH, 0.3 mmol/L serine, 2 mmol/L betaine, 60 μmol/L methionine, 50 μmol/L methyl THF, 60 μmol/L SAM and 10 μmol/L SAH, transsulfuration accounted for 46% of Hcy metabolism and the remainder was equally contributed to by MS and BHMT. The need to conserve methionine (*e.g.* low protein diet) resulted in decreased cystathionine production and increased Hcy remethylation. Conversely, in the presence of excess methionine, SAM activated the cystathionine pathway.

HHcy results from increased levels of intracellular Hcy that is readily released into the extracellular medium: plasma or body fluid. Kidney might be a major site for the removal and metabolism of Hcy primarily through the transsulfuration pathway[19]. Renal impairment often causes HHcy, reflecting a role of kidney in Hcy clearance from plasma. This fact might contribute to the high incidence of vascular complications in patients with chronic renal failure[20]. Genetic abnormalities, age, sex and various nutritional and hormonal determinants contribute to HHcy. However, genetic and nutritional disorders are the major factors. Genetic disorders involve polymorphism in the genes coding for MTHFR and CBS. The most common genetic defect associated with mild HHcy is a point mutation, namely, a C to T substitution at nucleotide 677 (C677→T) in the open reading frame of the gene for MTHFR. This point mutation could cause a substitution of valine for alanine in the functional enzyme[21], resulting in a thermolabile variant of the enzyme with decreased total activity. This is an autosomal recessive mutation, and the frequency of the C677→T polymorphism varied among racial and ethnic groups, with 13% of T/T homozygous and 50% C/T heterozygous among Caucasian and Asian populations, and very low incidence among African-Americans[21-27]. Premature atherosclerosis and thrombotic disease were observed in MTHFR deficiency[23-28]. The most common genetic cause associated with severe HHcy is homozygous CBS deficiency, which resulted in plasma Hcy concentrations of up to 400 μmol/L, compared to normal plasma levels of 10 μmol/L[28-30]. Homozygous CBS deficiency, T833→C and G919→A mutations, were inherited as an autosomal recessive disorder with pleiotropic clinical manifestations, including mental retardation, ectopia lentis, osteoporosis, skeletal abnormalities and hepatic steatosis[28-30]. Patients were usually at higher risk for premature atherosclerosis and thrombotic disease, which is the major cause of death[31-33]. CBS deficiency has a worldwide incidence of 1:344 000 live births, ranging from 1:58 000 to 1:1 000 000 in countries that perform newborn screening[31]. While homozygous CBS deficiency is rare, heterozygous CBS deficiency occurs in approximately 1% of the general population and is associated with premature atherosclerosis and thrombotic disease in phenotypically normal individuals[31-33].

Nutritional disorders that potentially lead to HHcy include deficiencies in vitamin B12, folate and vitamin B6, as the *de novo* synthesis of methionine methyl groups requires both vitamin B12 and folate cofactors whereas the synthesis of cystathionine requires pyridoxal 5-phosphate (vitamin B6). Although it has been shown that deficiencies of vitamin B12 and folate are related to increased plasma Hcy concentrations[32-35], the relationship of Hcy levels to vitamin B6 status is less clear[36,37]. In addition, excess dietary methionine in normal mice has been shown to induce HHcy[38]. Under normal conditions, several methylation reactions in the liver contribute to the bulk (90%) of SAM utilization and Hcy production via SAH. For example, phosphatidylethanolamine to phosphatidylcholine is mediated by phosphatidylethanolamine N-methyltransferase (PEMT). PEMT-/- mice had 50% decreased plasma Hcy despite being choline and betaine deficient[39]. PEMT null mice exhibited fatty liver and apoptosis but this was not prevented by betaine administration, impaired lipoprotein secretion rather than methyl donor deficiency appeared to be the dominant effect of choline deficiency[40]. The other major source of Hcy is the activity of hepatic guanidinoacetate (GAA) N-methyltransferase (NMT). GAA is produced in the kidney by L-arginine:glycine amidinotransferase. GAA is then converted to creatine in the liver by GAA-NMT, utilizing SAM and generating SAH. Creatine is exported to muscle and also represses the kidney enzyme which produces GAA. GAA supplementation could induce HHcy and creatine feeding lowers Hcy[41].

HCY TOXICITY

Possible cellular mechanisms by which elevated Hcy promotes liver disease are oxidative stress, endoplasmic reticulum (ER) stress and the activation of pro-inflammatory factors (Figure 2). Hcy enhances the production of several pro-inflammatory cytokines. Expression of monocyte chemoattractant protein 1 (MCP-1) was increased in cultured human vascular endothelial cells, smooth muscle cells and monocytes treated with Hcy[42-44]. Hcy has also been shown to increase expression of IL-8[42], a T-lymphocyte and neutrophil chemoattractant, in cultured endothelial cells. Hcy-induced expression of MCP-1 and IL-8 in monocytes and endothelial cells has been shown to occur through activation of NF-κB, a transcription factor involved in mediating downstream inflammatory processes[44,45]. Active NF-κB could stimulate production of cytokines, chemokines, interferons, leukocyte adhesion molecules, hemopoietic growth factors and major histocompatibility (MHC) class I molecules-all of which are thought to influence inflammation[45,46].

Hcy can generate a procoagulant state, which may be related to its proclivity to auto-oxidize, generating H_2O_2. Various *in vitro* studies using vascular tissues have implicated Hcy in causing abnormal vascular relaxation responses by enhancing the intracellular production of superoxide anion (O_2^-)[47-54]. O_2^- is believed to react with and decrease the availability of endothelial nitric oxide (NO) and yield peroxynitrite, thereby

limiting normal vasodilation responses[55,56]. Deceased GSH peroxidase transcription (reduction of peroxides protects NO) may play a role in this process[49,57], since overexpression of GSH peroxidase could restore the NO response[57]. O_2^- and peroxynitrite are also known to contribute to the oxidative modification of tissues, resulting in the formation of lipid peroxides and nitrosated end products such as 3-nitrotyrosine. The observations that Hcy decreased the expression of a wide range of antioxidant enzymes[57-59] and impaird endothelial NO bioavailability by inhibiting glutathione peroxidase activity raise the possibility that Hcy sensitizes cells to the cytotoxic effects of agents or conditions known to generate ROS. Decreased NO bioavailability has also been shown *in vitro* to increase the expression of MCP-1, which may enhance intravascular monocyte recruitment and lead to accelerated lesion formation[60].

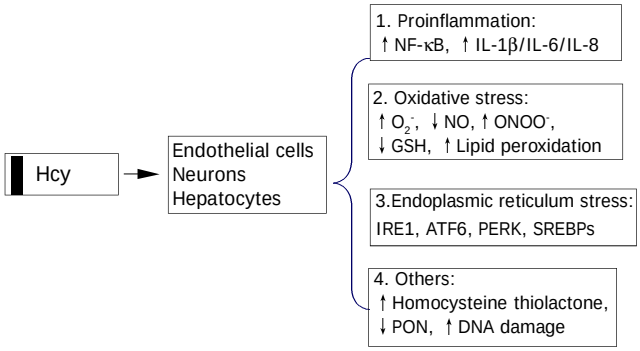

Figure 2 Cellular mechanisms by which homocysteine promotes cell injury. Homocysteine causes activation of necrosis factor-κB (NF-κB) and enhances production of cytokines (IL-1β, IL-6, and IL-8) resulting in inflammatory reactions, increases intracellular levels of superoxide anion causing oxidative stress, and induces endoplasmic reticulum (ER) stress by causing misfolding of proteins traversing the ER. Homocysteinyl-tRNA increases production of highly reactive derivative homocysteine thiolactone which damages enzymes and DNA. IRE1, type 1 ER transmembrane protein kinase; ATF6, the activating transcription factor 6; PERK, the PKR like ER kinase; SREBP, sterol regulatory element binding protein, PON, paraoxonase.

Intracellular Hcy can be converted by methionyl tRNA synthase into an Hcy-AMP complex, which is subsequently catabolised to Hcy thiolactone, thereby preventing the incorporation of Hcy into nascent polypeptide chains. Hcy thiolactone has unique reactive properties that can lead to the homocysteinylation of lysine residues and free amine groups on numerous cellular proteins, thereby resulting in decreased biological activity and premature degradation[61]. In addition, Hcy thiolactone secreted into the circulation may induce widespread modifications of plasma proteins that could potentially contribute to the development of liver and cardiovascular diseases. Recent studies have demonstrated that Hcy thiolactone decreases paraoxonase activity associated with HDL, thereby rendering HDL less protective against oxidative damage or against toxicity of Hcy thiolactone[62].

HCY-INDUCED ER STRESS

ER is a principal site for protein synthesis and folding, calcium storage and calcium signaling. It also serves as a site of biosynthesis for steroids, cholesterol and other lipids. The physiological roles of the ER include regulation of protein synthesis, folding and targeting and maintenance of cellular calcium homeostasis. The ER has a high concentration of numerous resident chaperone proteins such as glucose regulated protein-78 (GRP78) and GRP94, a high level of calcium and an oxidative environment to carry out these functions efficiently. Proteins that were translocated into the ER lumen underwent post-translational modifications and the folding required for optimal function. Properly folded proteins were allowed to reach their destiny via the secretory pathway, whereas unfolded and misfolded proteins were exported or dislocated from the ER and degraded by cytoplasmic proteasomes[63-68]. ER stress is a condition under which unfolded and misfolded proteins accumulate (Figure 3). ER stress triggers unfolded protein response (UPR), which is an intracellular signaling pathway and is mediated via three ER-resident sensors in mammalian cells: a type-I ER transmembrane protein kinase (IRE-1), the activating transcription factor 6 (ATF-6) and the PKR like ER kinase (PERK). Activation of these three pathways is mediated by GRP78, which is associated with each sensor in the absence of ER stress. As unfolded proteins accumulated in the ER, GRP78 dissociated from and thereby activating IRE-1, ATF-6 and PERK[68-70]. Activation of both IRE-1 and ATF-6 increases the expression of ER-resident chaperones. IRE-1 is a stress-activated transmembrane protein kinase having endoribonuclease activity. Following ER stress, IRE-1 dimerized and was autophosphorylated, thereby allowing IRE-1 to act as an endoribonuclease in the alternative splicing of XBP-1 mRNA. The removal of a 26 base pair intron resulted in a translation frameshift that permits XBP-1 to act as a transcriptional activator of genes containing upstream ER stress response elements (ERSE). Upon ER stress, ATF-6 was transported to the Golgi where the cytosolic transactivation domain of ATF-6 is cleaved from the membrane by specific proteases (S1P and S2P) that also recognize, cleave and activate sterol regulatory element-binding proteins (SREBPs) leading to increased lipids needed for ER membrane synthesis. Following release, the transactivation domain of ATF-6 localized to the nucleus where it interacts with ERSE, thereby activating transcription of numerous UPR-responsive genes, including GRP78, GADD153 (CHOP), XBP-1, ERp72, and Hcy-induced ER protein (Herp). ER stress could also lead to a rapid attenuation in protein synthesis, a cellular process mediated by the transmembrane protein kinase, PERK. Activation of PERK could cause phosphorylation of eukaryotic initiation factor-2α (eIF-2α), which blocks mRNA translation initiation to help relieve the unfolded protein burden on the ER. Recent studies have also demonstrated that PERK-dependent eIF-2α phosphorylation is required for transcriptional activation of a wide range of UPR-responsive genes[71,72]. The early UPR co-coordinately enhances cell survival by ensuring that the adverse effects of ER stress are dealt with in a timely and efficient manner. However, prolonged UPR following ER stress has severe consequences. It can lead to activation of the tumor necrosis factor receptor associated facter 2 (TRAF2), which activates caspases (e.g. caspase-12 in mice) and JNK resulting in programmed cell death. Overexpression of CHOP, a basic region leucine zipper transcription factor, could also promote cell death[71]. Overproduction of lipids by SREBP can lead to fat accumulation. In addition, ER stress is associated with release of ER Ca^{2+} stores which can trigger oxidative stress *via* effects on mitochondria and NF-κB activation leading to inflammatory reactions[73]. NF-κB activation could be blocked by calcium chelators and antioxidants[19]. Increased cytosol calcium also activates calpains which proteolytically cleave Bcl-X_L (inactivation) and caspase 12 (activation). ER stress could contribute to the pathogenesis of a number of human diseases, including diabetes, Alzheimer's disease, Parkinson's disease and cancer[72].

Hcy induced ER stress response has recently received much attention[6,74-79]. Hcy causes ER stress by disrupting disulphide bond formation and causing misfolding of proteins traversing

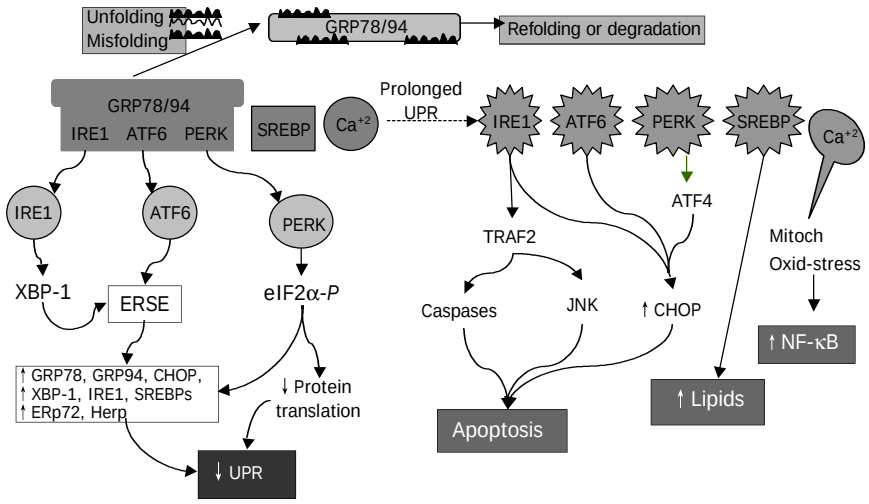

Figure 3 Consequences of endoplasmic reticulum (ER) stress response. In the early phase, unfolded proteins cause dissociation of chaperones such as Bip / GRP78 from ER resident kinases-IRE1 and PERK and transcription factor-ATF6. Activated PERK phosphorylates eIF2 resulting in translational attenuation. Activated IRE1 and ATF6 up-regulate genes encoding ER chaperone proteins such as GRP78 / 94 leading to increased protein-folding capacity. Overall, the unfolded protein response (UPR) goes down. In the late phase, IRE1 interacts with TRAF2 (tumor necrosis factor receptor associated factor 2) which activates caspases and JNK (cJUN NH2-terminal kinase) leads to apoptosis. ATF6 and PERK upregulate CHOP (C / EBP homologous protein) promoting cell death. SREBP upregulates lipid synthesis. Prolonged UPR leads to Ca^{2+} release from ER causing production of reactive oxygen intermediates which may lead to activation of NF-κB.

the ER. Elevated levels of intracellular Hcy could increase the expression of several ER stress response genes, including GRP78, GRP94, Herp and RTP[6,58,74,77,78,80-82]. Hcy could induce expression of GADD153[58,78,79] involved in ER stress-induced cell death[83]. Hcy-induced ER stress could cause dysregulation of lipid biosynthesis by activating the SREBPs[6,76-79], ER resident transcription factors are responsible for the induction of genes in the cholesterol/triglyceride biosynthesis and uptake pathways[6]. Hcy-induced cell death was mimicked by other ER stress agents and was dependent on IRE-1 signaling. Activation of IRE-1 by Hcy could lead to a rapid and sustained activation of JNK protein kinases[84,85], a result consistent with the finding that activation of JNK by ER stress involved binding of IRE-1 to TRAF2[86]. Because persistent activation of JNK correlated with cell death[87], these studies could provide further support for a mechanism involving Hcy-induced programmed cell death.

APPROACHES FOR STUDY OF HHCY

Cell and animal models with altered plasma Hcy are among the most useful approaches in determining the biological effects of HHcy. However, cell and transgenic animal models expressing Hcy metabolism-related genes/enzymes are not available. Nevertheless, diet- and, especially, genetic-induced animal models of HHcy have been developed. The gene knockout animals have significantly enhanced the status of Hcy as an independent risk factor for several disorders.

Homozygous and heterozygous CBS-deficient mice were generated in 1995[88]. Homozygous mutants completely lacking CBS were born at the expected frequency from mating of heterozygotes, but they suffered from severe growth retardation and a majority of them died within 5 wk after birth. Histological examination showed that the hepatocytes of homozygotes were enlarged, multinucleated, and filled with microvesicular lipid droplets. Plasma Hcy levels of the homozygotes (203.6±65.3 μmol/L) were 33 times higher than normal (6.1±0.8 μmol/L). The homozygous CBS deficient mice represented a model for severe HHcy. Heterozygous CBS deficient mice had 50% reduction in CBS mRNA and enzyme activity in the liver and had twice normal plasma Hcy levels (13.5± 3.2 μmol/L). The CBS knockouts significantly help elucidate the *in vivo* role of elevated levels of Hcy in the etiology of several HHcy-related disorders and in the cellular mechanisms by which Hcy promote cell injury. The CBS-deficient mice were predisposed to HHcy during dietary folate deficiency, and moderate HHcy was associated with marked impairment of endothelial function in mice[89]. Results from a subsequent study indicated that endothelial dysfunction occurred in HHcy mice even in the absence of folate deficiency[90]. Endothelial dysfunction in CBS (+/-) mice was associated with increased tissue levels of SAH, which suggests that altered SAM-dependent methylation may contribute to vascular dysfunction in HHcy[91]. Further studies with the CBS deficient mice revealed the importance of intracellular redox balance for nitric oxide bioactivity and endothelial function, and the importance of ER stress in abnormal hepatic accumulation of lipid[92,93]. Expression of several genes analyzed by DNA microarray was found to be reproducibly abnormal in the livers of heterozygous and homozygous CBS-deficient mice[94]. These genes encode ribosomal protein S3a and methylthioadenosine phosphorylase, suggesting cellular growth and proliferation perturbations may occur in homozygous CBS-deficient mice liver.

MTHFR-deficient mice have been recently developed to examine the effects of HHcy resulting from genetic deficiencies in the remethylation pathway[95]. MTHFR-deficient mice shared basic phenotypic similarities with CBS-deficient mice. However, they were unique in that they developed mild HHcy and atherosclerosis. Recent study has demonstrated the importance of choline metabolism in HHcy in this model[96]. Comparison study by administrating the alternate choline-derived methyl donor, betaine, to wild-type mice and MTHFR deficient mice revealed that plasma Hcy and liver choline metabolite levels were strongly dependent on the MTHFR genotype. Betaine supplementation decreased Hcy in all three genotypes, restored liver betaine and phosphocholine pools, and prevented severe steatosis in MTHFR-deficient mice. Since there was a significant negative correlation between plasma betaine and Hcy concentrations in humans with cardiovascular disease, the results emphasize the strong interrelationship between Hcy, folate, and choline metabolism. MTHFR-compromised mice with HHcy appeared to be much more sensitive to changes of choline/betaine intake than wild-type

animals. HHcy, in the range of that associated with folate deficiency or with homozygosity for the 677T MTHFR variant, may be associated with disturbed choline metabolism.

MS could directly catalyze the remethylation pathway and inactivation of this gene has been attempted recently[97]. Heterozygous MS knockout mice from an outbred background had slightly elevated plasma Hcy (6.1 mol/L) and methionine compared to wild-type mice (4.1 μmol/L) but seemed to be otherwise indistinguishable. Homozygous knockout embryos survived through implantation but died soon thereafter. Nutritional supplementation during pregnancy was unable to rescue embryos that were completely deficient in MS. This study indicated that MS activity was essential for early embryonic development of mice. Although the MS knockout mouse has not provided an immediately obvious animal model of human disease, heterozygotes with 50% reduction of MS activity may be useful. It is likely that MS heterozygote knockouts are more susceptible to dietary deficiencies than wild type mice and thus having merits as a model in which interactions between genetic status and nutritional status can be studied.

The animal models are valuable *in vivo* tools to further examine potential therapeutic approaches in lowering plasma Hcy while decreasing the prevalence of HHcy-induced disorders. However, the animal models neither have tissue or organ specificity nor exclude potential compensatory pathways of Hcy metabolism. Conditional disruption of Hcy metabolism-related genes and crossing between animal models that are deficient in different genes should be the future directions in the effort of creating animal models for study of HHcy.

ETHANOL-INDUCED HHCY AND LIVER INJURY

The pathogenesis of the pathologic features of alcoholic liver injury, namely steatosis, apoptosis, necrosis, inflammation and fibrosis, is an area of intense interest. Although much progress has been made over the past decade, we still do not have a complete understanding of this process[98]. We recently found that in a murine model of intragastric ethanol there was an upregulation of genes associated with endoplasmic reticulum (ER) stress response, including GRP78 and 94, CHOP and SREBP. The expression of these genes was associated with protein malfolding as well as apoptosis and lipid synthesis[78,79]. Since alcoholism and alcohol-related diseases constitute a severe health problem in the world and ER stress has been linked to Hcy in the pathogenesis of several disorders such as atherosclerosis, Alzheimer's disease, and liver steatosis, we would direct the readers' attention to ethanol-induced alterations in Hcy metabolism.

Alcoholic patients have been shown to have elevated plasma Hcy (average two-fold) which rangeed from 10-120 mol/L (normal 5-15 mol/L)[99-101]. Total folate, B_{12} and B_6 levels were normal. However, Hcy levels correlated with folate levels and blood alcohol levels. Well nourished alcoholics exhibited markedly lower levels of serum pyridoxal-phosphate (PLP) and mildly lower red cell folate[102]. Even "social" drinking (30 g/d×6 wk) caused 20% increased Hcy and decreased folate[99,103]. Heavy alcohol consumption is a risk factor for stroke and brain atrophy[103-105]. Rats fed ethanol exhibited a doubling of plasma Hcy despite normal levels of folate, PLP and B_{12}[106]. We have observed a 7 fold increase of plasma Hcy levels (22.3±2.8 μmol/L *vs* pair-fed control 3.0±0.9 μmol/L) in mice fed ethanol intragastrically for 4 wk[78].

With alcohol feeding of rats intragastrically for 9 wk liver specific MAT1A protein expression did not change, whereas MAT2A increased in conjunction with -40% decreased hepatic levels of methionine and SAM[107]. However, shorter exposure of rats and minipigs to ethanol was not associated with a decrease in methionine or SAM in most studies. Depending on route, ethanol dose and duration, variable changes in SAM and SAH have been described[107-110].

Ethanol feeding has been known to lower MS[111], leading to increased accumulation of 5-methyl THF and to increased BHMT leading to utilization-induced decreased betaine levels[111]. These effects depended on increased blood ethanol. Golden Syrian hamsters with high ADH fed a 360 mL/L ethanol diet did not develop increased blood ethanol levels or changes in Hcy metabolism unless ADH was inhibited[112]. Of note, the SAM levels were maintained by the utilization of betaine. However prolonged ethanol feeding eventually could lead to depletion of SAM. Chronic alcohol could increase choline uptake[113] and mitochondrial oxidation to betaine[114] suggesting compensation for increased demand for betaine. Feeding betaine (0.5%) raised SAM levels which was accentuated in alcohol fed animals (minimal to begin with) and prevented fatty liver[78,108,111]. Raised SAM was initially assumed to contribute to betaine's ameliorative effect on fatty liver. It may be equally important that the protective role of betaine was due to lowering Hcy directly through BHMT and indirectly by raised SAM leading to activation of CBS.

The mechanism of the ethanol induced decrease in MS is not well understood. Kenyon *et al*.[110] showed that the enzyme was inhibited by high concentrations of acetaldehyde, whereas we have found decreased mRNA. Increase in BHMT activity appeared to be a compensatory phenomenon to maintain methionine and was seen after 2 wk in ethanol fed rats and after 4 wk in ethanol fed mice.

In the chronic (12 mo) ethanol fed micropigs with adequate folate, MS activity decreased by 20% which was associated with slightly decreased serum methionine, 20% increased serum Hcy, and increased hepatic SAH but no change in SAM. These small changes due to ethanol were not associated with increased ALT or fatty liver but were associated with increased scattered apoptosis[115]. Interestingly addition of folate deficient diet to ethanol feeding of the castrated minipig accentuated plasma Hcy and liver injury[116] although ER stress was not considered in this study.

Betaine lowered Hcy and prevented ER stress and alcoholic liver injury in alcohol fed mice[78]. However, we need to be cognizant of other actions of betaine. Feeding rats betaine in drinking water (1.5 g/kg) blunted the TNF response to LPS and decreased concomitant liver injury[117]. Importantly, however, taurine was equally effective. Earlier work has suggested an indirect protective role of choline supplementation, suggesting choline oxidation to betaine could protect against Kupffer cell activation[118-120]. It has been suggested that betaine and taurine serve as organic osmolytes which are critical in regulating Kupffer cell function[121]. Hyperosmotic conditions induce Na^+ betaine transporter mRNA while hypoosmotic conditions do the opposite, this occurred in Kupffer cells but not hepatocytes. Betaine or taurine protects the liver against warm ischemia-reperfusion. Recently, betaine pretreatment was shown to protect the hepatocyte from bile acid induced apoptosis. The mechanism is not certain and high concentrations of betaine (mmol/L) were required[122,123]. We observed that increased gene expression of TNF and CD 14 was indicative of the alcohol-induced Kupffer cell activation[78]. However, betaine treatment did not significantly attenuate these changes, suggesting that betaine either acts downstream of alcohol-induced Kupffer cell activation or acts via an independent pathway.

The effect of SAM feeding is of interest since it was reported to decrease fatty liver and mitochondrial abnormalities[115]. SAM might be expected to inhibit re-methylation and promote transsulfuration of Hcy. It is unclear as to what the overall effect on Hcy would be. Severe SAM deficiency in MAT1A knockout did not alter Hcy but was associated with increased expression of BHMT and CBS[124]. SAM could transcriptionally

activate MAT1A and suppress MAT2A[125].

Overall chronic ethanol exposure seemed to cause a modest decrease in SAM and increase in SAH along with early-decreased MS and late-increased BHMT. All these changes were accompanied with increased Hcy which occurs despite adequate dietary folate, B_{12}, B_6 and choline. Thus there are possible contributions of decreased MS, unknown effects on CBS, and decreased SAM (decreased activation of CBS) leading to HHcy. The decrease in SAM levels was accompanied with increased SAH levels. Since both SAM and SAH activated CBS, it is doubtful that changes in levels of these metabolites exerted a significant regulatory role on transulfuration[11,16]. The increase in BHMT appeared insufficient to lower Hcy due to limitation on the availability of betaine and already-impaired cell function. Although high dietary choline might generate sufficient betaine in rodents, the choline oxidase pathway is normally low in primates. Thus, providing excess dietary betaine rather than choline would seem to be an approach more applicable to the human situation. Since betaine corrects hyperhomocysteinemia, fatty liver injury and ER stress, and homocysteine is known to cause all these changes, it is reasonable to state that an important mechanism by which betaine protects against alcoholic liver disease is the correction of hyperhomocysteinemia and proof of this hypothesis requires further work.

POSSIBLE ROLE OF ER STRESS IN OTHER LIVER DISEASES

ER stress may also be involved in liver injury caused by α_1-antitrypsin (α_1-AT) deficiency and hepatitis C virus (HCV) or hepatitis B virus (HBV) infection. α_1-antitrypsin (α_1-AT) deficiency was caused by a point mutation encoding a substitution of lysine for glutamate-342[126]. Aggregated mutant α_1-AT was retained in ER rather than secreted in the blood and body fluids where its function is to inhibit neutrophil proteases. Individuals with this deficiency had a markedly increased risk of developing emphysema by a loss of function mechanism by which reduced levels of α_1-AT in the lung inhibit connective tissue breakdown by neutrophil elastase, cathepsin G, and proteinase 3. Some individuals with α_1-AT deficiency developed liver injury and hepatocellular carcinoma by a gain of function mechanism, i.e., accumulation of aggregated mutant α_1-AT within the ER which is toxic to liver cells. However, the exact mechanism by which ER retention of this aggregated mutant protein leads to cellular injury is still unknown. Recent studies have demonstrated that ER retention of mutant α_1-AT induces a marked autophagic response in cell culture and transgenic mouse models of α_1-AT deficiency as well as in the liver of patients with α_1-AT deficiency[127]. The autophagic response is a general mechanism whereby cytosol and intracellular organelles, such as ER, are first sequestered from the rest of the cytoplasm within unique vacuoles and then degraded by fusion with lysosomes to clear the cells of senescent constituents. Under a fasting condition, a marked increase in fat accumulation was observed in α_1-AT-containing globules in the liver of α_1-AT deficient mice[128], suggesting a malfunction of ER caused by accumulation of mutant α_1-AT. Investigations of ER stress markers such as GRP78, CHOP, SREBP, XBP1, and ATF6 are needed to assess the direct involvement of ER stress in α_1-AT deficiency-induced liver injury.

Evidence of ER stress in HBV or HCV infection is emerging. HBV codes for three forms of surface protein. The minor and large forms are translated from transcripts specified by the preS1 promoter, while the middle and small forms are translated from transcripts specified by the downstream S promoter. Overexpression of the large surface protein of HBV could lead to a 10-fold activation of the S promoter but not of an unrelated promoter[129]. The large surface protein could also activate the cellular grp78 and grp94 promoters. Neither the middle nor the small surface protein, nor a secretable form of the large surface protein, could activate the S promoter, but agents that induced endoplasmic reticulum (ER) stress had an effect similar to that of the large surface protein, suggesting that HBV may evolve a feedback mechanism, such that ER stress induced by accumulation of the large surface protein increases the synthesis of the middle and small surface proteins, which in combination with the large surface protein can form mixed, secretable particles. HCV-induced ER stress was more evident. HCV replicates from a ribonucleoprotein (RNP) complex that is associated with ER membrane. The replication activities of the HCV subgenomic replicon have been shown to induce ER stress[130]. HCV replicons induce the UPR which is paralleled by the proteolytic cleavage of ATF6. The HCV non-structural protein 5A (NS5A) can bind to and inactivate the cellular double-stranded RNA-activated protein kinase, PKR. NS5A has recently been demonstrated to engage ER-nucleus signal transduction pathway[131]. Expression of NS5A in the ER could induce an ER stress leading to the activation of STAT-3 and NF-κB, which is sensitive to inhibitors of Ca^{2+} uptake. The NS5A-induced ER stress signaling has also been shown in the context of an HCV subgenomic replicon[131]. Another HCV component, the HCV envelope protein E2, is an ER-bound protein that contains a region of sequence homology with the PKR and its substrate, the eIF2α. E2 could modulate global translation by inhibition of the interferon-induced PKR through its PKR-eIF2α phosphorylation site homology domain (PePHD)[132]. E2 could also bind to and inhibit PERK[132]. At low expression levels, E2 induced ER stress, but at high expression levels, E2 inhibited PERK kinase activity *in vitro*. Mammalian cells that stably expressed E2 were refractory to the translation-inhibitory effects of ER stress inducers, and E2 relieved general translation inhibition induced by PERK. The PePHD of E2 was required for the rescue of translation that was inhibited by activated PERK. These findings may explain why the virus promotes persistent infection by overcoming the cellular ER stress response. In addition, HCV-induced ER stress resulted in a decline in protein glycosylation. Decreasing protein glycosylation could disrupt the proper protein folding of MHC class I molecules, preventing the assembly of MHC class I molecules. Cells expressing HCV subgenomic replicons had a lower MHC class I cell surface expression[133]. HCV-infected cells may thus be undetectable in the immune system by suppressing MHC class I antigen presentation to cytotoxic T lymphocytes. Therefore, the persistence and pathogenesis of HCV may depend upon the ER stress-mediated interference of MHC class I assembly and cell surface expression. Finally, HCV infection may suppress the degradation of misfolded proteins while stimulating the synthesis of its viral proteins in the ER. In the ER, IRE1-XBP1 pathway directs both protein refolding and degradation in response to ER stress. It was demonstrated that XBP1 expression was elevated in cells carrying HCV subgenomic replicons, but XBP1 transactivating activity was repressed[134]. This prevents the IRE1-XBP1 transcriptional induction of EDEM (ER degradation-enhancing -mannosidase-like protein), which is required for the degradation of misfolded proteins. Consequently, misfolded proteins are stable in cells expressing HCV replicons. Study with a cell line with a defective IRE1-XBP1 pathway showed elevated levels of HCV internal ribosome entry site-mediated translation[134]. This study indicated that the HCV suppression of misfolded protein degradation in the ER not only promoted HCV expression but also contributed to the persistence of the virus in infected hepatocytes.

HCV infection is common in alcoholic patients presenting with liver disease. Heavy alcohol intake would worsen the outcome of HCV infection[135-137], which has directed much attention to the interaction between alcohol and HCV infection.

Alcohol plays an important role in HCV infection resulting in increased viral replication, enhanced HCV quasispecies complexity, increased liver-cell death, suppression of immune responses, and iron overload[138]. However, the pathogenic mechanisms underlying the alcohol-HCV interactions are not fully understood. Based on the above evidence that both HCV and homocysteine could induce endoplasmic reticulum (ER) stress response[6,78,130] and that there was a link between alcohol-induced significant elevation of homocysteine level, ER stress, and the pathogenesis of liver injury[78], it is reasonable to hypothesize that a locus of the potentiative interaction between alcohol and HCV in accelerating the progression of liver disease is at the level of ER stress. In the case of both HBV and HCV infection, it is widely recognized that severely immunosuppressed patients may develop a paradoxically severe and rapidly progressive liver disease. This has been seen in the post-OLT setting and in patient with AIDS. Therefore, the loss of immune detection of viral-infected hepatocytes may lead to an unopposed massive overload of hepatocytes with viral proteins triggering ER stress. Future studies should examine the contribution of ER stress to these pathologic conditions.

CONCLUSION

HHcy is an integral component of several disorders including cardiovascular and cerebrovascular diseases, neurodegeneration, liver steatosis, diabetes, and cancer. HHcy can result from deficiencies of vitamin cofactors (B6, B12, folic acid) required for Hcy metabolism and/or from genetic disorders of its metabolism. Hcy unleashes inflammation mediators such as NFκB, IL-1β, IL-6, and IL-8. Hcy increases production of intracellular superoxide anion causing oxidative stress. Hcy-induced misfolding or malfunctioning of numerous intracellular proteins are increasingly important and attract much attention because the Hcy-induced ER stress mechanism can explain many processes of cell injury. Animal model creation and integral investigation of available animal models will certainly play important role in determining precisely the biological effects of HHcy. Our observations with the murine intragastric ethanol fed model have suggested a link between Hcy metabolism, ER stress, and the pathogenesis of alcohol induced liver injury. Figure 4 demonstrates our hypothesis in which ethanol feeding causes HHcy which then induces the ER stress response in parenchymal and nonparenchymal cells in the liver leading to fatty liver, apoptosis and possibly inflammation. The potential beneficial effects of lowering Hcy and preventing ER stress in alcoholic humans needs to be studied. In addition, since a minority of alcoholics develop liver disease and a wide range of Hcy levels are seen in alcoholics, it will be important to examine polymorphism of Hcy metabolizing enzymes as potential risk-factors for the development of HHcy and liver disease.

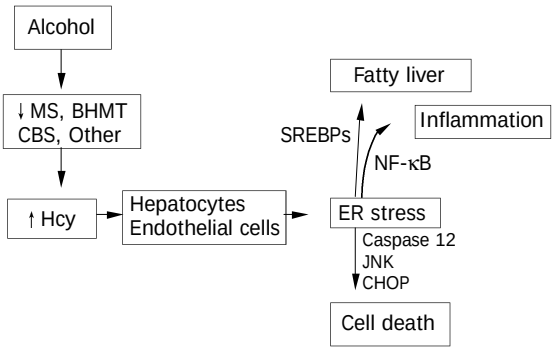

Figure 4 Hypothesis for the role of ethanol-induced HHcy in the pathogenesis of alcoholic liver disease.

REFERENCES

1 **Carson NAJ**, Neil DW. Metabolic abnormalities detected in a survey of mentally backward individuals in Northern Ireland. *Arch Dis Child* 1962; **37**: 505-513
2 **Gerritsen T**, Vaughn JG, Weisman HA. The identification of homocysteine in the urine. *Biochem Biophys Res Commun* 1962; **9**: 593-596
3 **Mudd SH**, Finkelstein JD, Irreverre F, Laster L. Homocystinuria: An Enzymatic Defect. *Science* 1964; **27**: 1443-1445
4 **Clarke R**, Daly L, Robinson K, Naughten E, Cahalane S, Fowler B, Graham I. Hyperhomocysteinemia: an independent risk factor for vascular disease. *N Engl J Med* 1991; **324**: 1149-1155
5 **Audelin MC**, Genest J Jr. Homocysteine and cardiovascular disease in diabetes mellitus. *Atherosclerosis* 2001; **159**: 497-511
6 **Werstuck GH**, Lentz SR, Dayal S, Hossain GS, Sood SK, Shi YY, Zhou J, Maeda N, Krisans SK, Malinow MR, Austin RC. Homocysteine-induced endoplasmic reticulum stress causes dysregulation of the cholesterol and triglyceride biosynthetic pathways. *J Clin Invest* 2001; **107**: 1263-1273
7 **Schroecksnadel K**, Frick B, Wirleitner B, Winkler C, Schennach H, Fuchs D. Moderate hyperhomocysteinemia and immune activation. *Curr Pharm Biotechnol* 2004; **5**: 107-118
8 **Herrmann W**, Knapp JP. Hyperhomocysteinemia: a new risk factor for degenerative diseases. *Clin Lab* 2002; **48**: 471-481
9 **Polidori MC**, Marvardi M, Cherubini A, Senin U, Mecocci P. Heart disease and vascular risk factors in the cognitively impaired elderly: implications for Alzheimer's dementia. *Aging* 2001; **13**: 231-239
10 **Lawrence de Koning AB**, Werstuck GH, Zhou J, Austin RC. Hyperhomocysteinemia and its role in the development of atherosclerosis. *Clin Biochem* 2003; **36**: 431-441
11 **Medina M**, Urdiales JL, Amores-Sanchez MI. Roles of homocysteine in cell metabolism: old and new functions. *Eur J Biochem* 2001; **268**: 3871-3882
12 **Jakubowski H**. Molecular basis of homocysteine toxicity in humans. *Cell Mol Life Sci* 2004; **61**: 470-487
13 **Jakubowski H**, Zhang L, Bardeguez A, Aviv A. Homocysteine thiolactone and protein homocysteinlylation in human endothelial cells: implications for atherosclerosis. *Circulation Research* 2000; **87**: 45-51
14 **Finkelstein JD**, Martin JJ, Harris BJ. Methionine metabolism in mammals. The methionine-sparing effect of cystine. *J Biol Chem* 1988; **263**: 11750-11754
15 **Finkelstein JD**. Pathways and regulation of homocysteine metabolism in mammals. *Semin Thromb Hemost* 2000; **26**: 219-225
16 **Finkelstein JD**. Homocysteine: a history in progress. *Nutr Rev* 2000; **58**: 193-204
17 **Finkelstein JD**, Martin JJ. Methionine metabolism in mammals. Distribution of homocysteine between competing pathways. *J Biol Chem* 1984; **259**: 9508-9513
18 **Mato JM**, Corrales FJ, Lu SC, Avila MA. S-Adenosylmethionine: a control switch that regulates liver function. *Faseb J* 2002; **16**: 15-26
19 **Bostom AG**, Lathrop L. Hyperhomocysteinemia in end-stage renal disease: prevalence, etiology, and potential relationship to arteriosclerotic outcomes. *Kidney Int* 1997; **52**: 10-20
20 **van Guldener C**, Stehouwer CD. Homocysteine metabolism in renal disease. *Clin Chem Lab Med* 2003; **41**: 1412-1417
21 **Mudd SH**, Lev HL, Skovby F. Disorders of transsulfuration. In Scriver CR, Beaudet AL, Sly WS, Valle D. (eds), *The Metabolic Basis of Inherited Disease. New York: McGraw-Hill* 1995: 1279–1327
22 **Rosenblatt DS**. Inherited disorders of folate transport and metabolism. In Scriver CR, Beaudet AL, Sly WS, Valle D. (eds), *The Metabolic Basis of Inherited Disease. New York: McGraw-Hill* 1995: 3111–3128
23 **Frosst P**, Blom HJ, Milos R, Goyette P, Sheppard CA, Matthews RG, Boers GJH, den Heiher M, Kluijtmans LAJ, van den Heuvel LP, Rozen RA. A candidate genetic risk factor for vascular disease: a common mutation in methylenetetrahydrofolate reductase. *Nature Genet* 1995; **10**: 111–113
24 **Ma J**, Stampfer MJ, Hennekens CH, Frosst P, Selhub J, Horsford J, Malinow MR, Willett WC, Rozen R. Methylenetetrahydrofolate reductase polymorphism, plasma folate, homocysteine, and risk of myocardial infarction in US physicians. *Circulation* 1996; **94**: 2410–2416

25 **Jacques PF**, Bostom AG, Williams RR, Ellison RC, Eckfeldt JH, Rosenberg IH, Selhub J, Rozen R. Relation between folate status, a common mutation in methylenetetrahydrofolate reductase, and plasma homocysteine concentrations. *Circulation* 1996; **93**: 7–9

26 **Jeng YL**, Wu MH, Huang HB, Lin WY, You SL, Chu TY, Chen CJ, Sun CA. The methylenetetrahydrofolate reductase 677C–> T polymorphism and lung cancer risk in a Chinese population. *Anticancer Res* 2003; **23**: 5149-5152

27 **Woo KS**, Qiao M, Chook P, Poon PY, Chan AK, Lau JT, Fung KP, Woo JL. Homocysteine, endothelial dysfunction, and coronary artery disease: emerging strategy for secondary prevention. *J Card Surg* 2002; **17**: 432-435

28 **Mudd SH**, Levy HL, Skovby F. Disorders of transsulfation. In: Scriver CR, Beadet AL, Sly WS, Vallee D, editors. *The Metabolic Basis for Inherited Disease. New York: McGraw-Hill* 1989: 693

29 **Kalra DK**. Homocysteine and cardiovascular disease. *Curr Atheroscler Rep* 2004; **6**: 101-106

30 **Wilcken DEL**, Dudman NPB. Homocystinuria and atherosclerosis. In: Lusis AJ, Rotter JI, Sparkes RS, editors. Molecular genetics of coronary artery disease; candidate genes and process in atherosclerosis. *Monograms in human genetics. New York: Karger* 1992: 311

31 **Mudd SH**, Levy HL, Kraus JP. Disorders of transsulfuration. In: Scriver CR, Beaudet AL, Sly WS, Eds. *The Metabolic and Molecular Bases of Inherited Disease. New York: McGraw-Hill* 2001: 2007-2056

32 **Ueland PM**, Refsum H. Plasma homocysteine, a risk factor for vascular disease: plasma levels in health, disease, and drug therapy. *J Lab Clin Med* 1989; **114**: 473–501

33 **Moat SJ**, Bao L, Fowler B, Bonham JR, Walter JH, Kraus JP. The molecular basis of cystathionine beta-synthase (CBS) deficiency in UK and US patients with homocystinuria. *Hum Mutat* 2004; **23**: 206

34 **Haynes WG**. Hyperhomocysteinemia, vascular function and atherosclerosis: effects of vitamins. *Cardiovasc Drugs Ther* 2002; **16**: 391-399

35 **Billion S**, Tribout B, Cadet E, Queinnec C, Rochette J, Wheatley P, Bataille P. Hyperhomocysteinaemia, folate and vitamin B12 in unsupplemented haemodialysis patients: effect of oral therapy with folic acid and vitamin B12. *Nephrol Dial Transplant* 2002; **17**: 455-461

36 **Lakshmi AV**, Maniprabha C, Krishna TP. Plasma homocysteine level in relation to folate and vitamin B6 status in apparently normal men. *Asia Pac J Clin Nutr* 2001; **10**: 194-196

37 **Cravo ML**, Camilo ME. Hyperhomocysteinemia in chronic alcoholism: relations to folic acid and vitamins B(6) and B(12) status. *Nutrition* 2000; **16**: 296-302

38 **Troen AM**, Lutgens E, Smith DE, Rosenberg IH, Selhub J. The atherogenic effect of excess methionine intake. *Proc Natl Acad Sci U S A* 2003; **100**: 15089-15094

39 **Noga AA**, Stead LM, Zhao Y, Brosnan ME, Brosnan JT, Vance DE. Plasma homocysteine is regulated by phospholipid methylation. *J Biol Chem* 2003; **278**: 5952-5955

40 **Shin OH**, Mar MH, Albright CD, Citarella MT, da Costa KA, Zeisel SH. Methyl-group donors cannot prevent apoptotic death of rat hepatocytes induced by choline-deficiency. *J Cell Biochem* 1997; **64**: 196-208

41 **Stead LM**, Au KP, Jacobs RL, Brosnan ME, Brosnan JT. Methylation demand and homocysteine metabolism: effects of dietary provision of creatine and guanidinoacetate. *Am J Physiol Endocrinol Metab* 2001; **281**: E1095-1100

42 **Poddar R**, Sivasubramanian N, Dibello PM, Robinson K, Jacobsen D. Homocysteine induces expression and secretion of monocyte chemoattractant protein-1 and interleukin-8 in human aortic endothelial cells: implications for vascular disease. *Circulation* 2001; **103**: 2717–2723

43 **Wang G**. Homocysteine stimulates the expression of monocyte chemoattractant protein-1 receptor (CCR2) in human monocytes: possible involvement of oxygen free radicals. *Biochem J* 2001; **357**: 233–240

44 **Wang G**, Siow YL. Homocysteine induces monocyte chemoattractant protein-1 expression by activating NF-kappa B in THP-1 macrophages. *Am J Physiol Heart Circ Physiol* 2001; **280**: H2840–2847

45 **Collins T**, Cybulsky MI. NF-kappaB: pivotal mediator or innocent bystander in atherogenesis? *J Clin Invest* 2001; **107**: 255–264

46 **Hofmann MA**, Lalla E, Lu Y, Gleason MR, Wolf BM, Tanji N, Ferran LJ Jr, Kohl B, Rao V, Kisiel W, Stern DM, Schmidt AM. Hyperhomocysteinemia enhances vascular inflammation and accelerates atherosclerosis in a murine model. *J Clin Invest* 2001; **107**: 675–683

47 **Loscalzo J**. The oxidant stress of hyperhomocyst(e)inemia. *J Clin Invest* 1996; **98**: 5–7

48 **Tawakol A**, Omland T, Gerhard M, Wu JT, Creager MA. Hyperhomocyst(e)inemia is associated with impaired endothelium-dependent vasodilation in humans. *Circulation* 1997; **95**: 1119–1121

49 **Weiss N**, Heydrick S, Zhang YY, Bierl C, Cap A, Loscalzo J. Cellular redox state and endothelial dysfunction in mildly hyperhomocysteinemic cystathionine beta-synthase-deficient mice. *Arterioscler Thromb Vasc Biol* 2002; **22**: 34–41

50 **Lang D**, Kredan MB, Moat SJ, Hussain SA, Powell CA, Bellamy MF, Powers HJ, Lewis MJ. Homocysteine-induced inhibition of endothelium-dependent relaxation in rabbit aorta: role for superoxide anions. *Arterioscler Thromb Vasc Biol* 2000; **20**: 422–427

51 **Chambers JC**, McGregor A, Jean-Marie J, Mbeid OA, Kooner JS. Demonstration of rapid onset vascular endothelial dysfunction after hyperhomocysteinemia: an effect reversible with vitamin C therapy. *Circulation* 1999; **99**: 1156–1160

52 **Stanger O**, Weger M. Interactions of homocysteine, nitric oxide, folate and radicals in the progressively damaged endothelium. *Clin Chem Lab Med* 2003; **41**: 1444-1454

53 **Franken DG**, Boers GHJ, Blom HJ, Trijibels FJM, Kloppenborg PW. Treatment of mild hyperhomocysteinemia in vascular disease patients. *Arterioscler Thromb* 1994; **14**: 465–470

54 **Mosharov E**, Cranford MR, Banerjee R. The quantitatively important relationship between homocysteine metabolism and glutathione synthesis by the transsulfuration pathway and its regulation by redox changes. *Biochemistry* 2000; **39**: 13005-13011

55 **Gryglewski RJ**, Palmer RM, Moncada S. Superoxide anion is involved in the breakdown of endothelium-derived vascular relaxing factor. *Nature* 1986; **320**: 454–456

56 **Heinecke JW**, Rosen H, Suzuki LA, Chait A. The role of sulfurcontaining amino acids in superoxide production and modification of low density lipoprotein by arterial smooth muscle cells. *J Biol Chem* 1987; **262**: 10098–10103

57 **Upchurch GR**, Welch GN, Fabian AJ, Freedman JE, Johnson JL, Keaney JF Jr, Loscalzo J. Homocyst(e)ine decreases bioavailable nitric oxide by a mechanism involving glutathione peroxidase. *J Biol Chem* 1997; **272**: 17012-17017

58 **Outinen PA**, Sood SK, Liaw PC, Sarge KD, Maeda N, Hirsh J, Ribau J, Podor TJ, Weitz JI, Austin RC. Characterization of the stress-inducing effects of homocysteine. *Biochem J* 1998; **332**: 213-221

59 **Dayal S**, Brown KL, Weydert CJ, Oberley LW, Arning E, Bottiglieri T, Faraci FM, Lentz SR. Deficiency of glutathione peroxidase-1 sensitizes hyperhomocysteinemic mice to endothelial dysfunction. *Arterioscler Thromb Vasc Biol* 2002; **22**: 1996-2002

60 **Yla-Herttuala S**, Palinski W, Rosenfeld ME, Parthasarathy S, Carew TE, Butler S, Witztum JL, Steinberg D. Evidence for the presence of oxidatively modified low density lipoprotein in atherosclerotic lesions of rabbit and man. *J Clin Invest* 1989; **84**: 1086-1095

61 **Jakubowski H**. Protein homocysteinylation: possible mechanism underlying pathological consequences of elevated homocysteine levels. *FASEB J* 1999; **13**: 2277-2283

62 **Ferretti G**, Bacchetti T, Marotti E, Curatola G. Effect of homocysteinylation on human high-density lipoproteins: a correlation with paraoxonase activity. *Metabolism* 2003; **52**: 146-151

63 **Kaufman RJ**. Stress signaling from the lumen of the endoplasmic reticulum: coordination of gene transcriptional and translational controls. *Genes Dev* 1999; **13**: 1211–1233

64 **Welihinda AA**, Tirasophon W, Kaufman RJ. The cellular response to protein misfolding in the endoplasmic reticulum. *Gene Expr* 1999; **7**: 293–300

65 **Kaufman RJ**, Scheuner D, Schroder M, Shen X, Lee K, Liu CY, Arnold SM. The unfolded protein response in nutrient sensing and differentiation. *Nat Rev Mol Cell Biol* 2002; **3**: 411–421

66 **Kaufman RJ**. Orchestrating the unfolded protein response in health and disease. *J Clin Invest* 2002; **110**: 1389–1398

67 **Ma Y**, Hendershot LM. The mammalian endoplasmic reticu-

lum as a sensor for cellular stress. *Cell Stress Chaperones* 2002; **7**: 222–229
68 **Shen J**, Chen X, Hendershot L, Prywes R. ER stress regulation of ATF6 localization by dissociation of BiP / GRP78 binding and unmasking of golgi localization signals. *Dev Cell* 2002; **3**: 99–111
69 **Liu CY**, Schroder M, Kaufman RJ. Ligand-independent dimerization activates the stress response kinases IRE1 and PERK in the lumen of the endoplasmic reticulum. *J Biol Chem* 2000; **275**: 24881–24885
70 **Liu CY**, Wong HN, Schauerte JA, Kaufman RJ. The protein kinase / endoribonuclease IRE1a that signals the unfolded protein response has a lumenal amino-terminal ligand-independent dimerization domain. *J Biol Chem* 2002; **277**: 18346–18356
71 **Rao RV**, Ellerby HM, Bredesen DE. Coupling endoplasmic reticulum stress to the cell death program. *Cell Death Differ* 2004; **11**: 372-380
72 **Kaufman RJ.** Regulation of mRNA translation by protein folding in the endoplasmic reticulum. *Trends Biochem Sci* 2004; **29**: 152-158
73 **Pahl HL**, Baeuerle PA. The ER-overload response: activation of NF-kappa B. *Trends Biochem Sci* 1997; **22**: 63-67
74 **Outinen PA**, Sood SK, Pfeifer SI, Pamidi S, Podor TJ, Li J, Weitz JI, Austin RC. Homocysteine-induced endoplasmic reticulum stress and growth arrest leads to specific changes in gene expression in human vascular endothelial cells. *Blood* 1999; **94**: 959-967
75 **Althausen S**, Paschen W. Homocysteine-induced changes in mRNA levels of genes coding for cytoplasmic- and endoplasmic reticulum-resident stress proteins in neuronal cell cultures. *Brain Res Mol Brain Res* 2000; **84**: 32-40
76 **Roybal CN**, Yang S, Sun CW, Hurtado D, Vander Jagt DL, Townes TM, Abcouwer SF. Homocysteine increases the expression of VEGF by a mechanism involving endoplasmic reticulum stress and transcription factor ATF4. *J Biol Chem* 2004; **279**: 14844-14852
77 **Zhang C**, Cai Y, Adachi MT, Oshiro S, Aso T, Kaufman RJ, Kitajima S. Homocysteine induces programmed cell death in human vascular endothelial cells through activation of the unfolded protein response. *J Biol Chem* 2001; **276**: 35867-35874
78 **Ji C**, Kaplowitz N. Betaine decreases hyperhomocysteinemia, endoplasmic reticulum stress, and liver injury in alcohol-fed mice. *Gastroenterology* 2003; **124**: 1488-1499
79 **Lluis JM**, Colell A, Garcia-Ruiz C, Kaplowitz N, Fernandez-Checa JC. Acetaldehyde impairs mitochondrial glutathione transport in HepG2 cells through endoplasmic reticulum stress. *Gastroenterology* 2003; **124**: 708-724
80 **Agarwala KL**, Kokame K, Kato H, Miyata T. Phosphorylation of RTP, an ER stress-responsive cytoplasmic protein. *Biochem Biophys Res Commun* 2000; **272**: 641-647
81 **Kokame K**, Agarwala KL, Kato H, Miyata T. Herp, a new ubiquitin-like membrane protein induced by endoplasmic reticulum stress. *J Biol Chem* 2000; **275**: 32846-32853
82 **Dimitrova KR**, DeGroot K, Myers AK, Kim YD. Estrogen and homocysteine. *Cardiovasc Res* 2002; **53**: 577-588
83 **Wang XZ**, Lawson B, Brewer JW, Zinszner H, Sanjay A, Mi LJ, Boorstein R, Kreibich G, Hendershot LM, Ron D. Signals from the stressed endoplasmic reticulum induce C / EBP-homologous protein(CHOP / GADD153). *Mol Cell Biol* 1996; **16**: 4273-4280
84 **Cai Y**, Zhang C, Nawa T, Aso T, Tanaka M, Oshiro S, Ichijo H, Kitajima S. Homocysteine-responsive ATF3 gene expression in human vascular endothelial cells: activation of c-Jun NH(2)-terminal kinase and promoter response element. *Blood* 2000; **96**: 2140-2148
85 **Zhang C**, Kawauchi J, Adachi MT, Hashimoto Y, Oshiro S, Aso T, Kitajima S. Activation of JNK and transcriptional repressor ATF3 / LRF1 through the IRE1 / TRAF2 pathway is implicated in human vascular endothelial cell death by homocysteine. *Biochem Biophys Res Commun* 2001; **289**: 718-724
86 **Urano F**, Wang X, Bertolotti A, Zhang Y, Chung P, Harding HP, Ron D. Coupling of stress in the ER to activation of JNK protein kinases by transmembrane protein kinase IRE1. *Science* 2000; **287**: 664-666
87 **Chen YR**, Meyer CF, Tan TH. Persistent activation of c-Jun N-terminal kinase 1 (JNK1) in gamma radiation-induced apoptosis. *J Biol Chem* 1996; **271**: 631-634
88 **Watanabe M**, Osada J, Aratani Y, Kluckman K, Reddick R, Malinow MR, Maeda N. Mice deficient in cystathionine beta-synthase: animal models for mild and severe homocyst(e)inemia. *Proc Natl Acad Sci U S A* 1995; **92**: 1585-1589
89 **Lentz SR**, Erger RA, Dayal S, Maeda N, Malinow MR, Heistad DD, Faraci FM. Folate dependence of hyperhomocysteinemia and vascular dysfunction in cystathionine beta-synthase-deficient mice. *Am J Physiol Heart Circ Physiol* 2000; **279**: H970-975
90 **Lentz SR**, Piegors DJ, Malinow RM, Heistad DD. Supplementation of atherogenic diet with B vitamins does not prevent atherosclerosis or vascular dysfunction in monkeys. *Circulation* 2001; **103**: 1006–1011
91 **Dayal S**, Bottiglieri T, Arning E, Maeda N, Malinow MR, Sigmund CD, Heistad DD, Faraci FM, Lentz SR. Endothelial dysfunction and elevation of S-adenosylhomocysteine in cystathionine beta-synthase-deficient mice. *Circ Res* 2001; **88**: 1203-1209
92 **Eberhardt RT,** Forgione MA, Cap A, Leopold JA, Rudd MA, Trolliet M, Heydrick S, Stark R, Klings ES, Moldovan NI, Yaghoubi M, Goldschmidt-Clermont PJ, Farber HW, Cohen R, Loscalzo J. Endothelial dysfunction in a murine model of mild hyperhomocyst(e)inemia. *J Clin Invest* 2000; **106**: 483–491
93 **Weiss N**, Heydrick S, Zhang YY, Bierl C, Cap A, Loscalzo J. Cellular redox state and endothelial dysfunction in mildly hyperhomocysteinemic cystathionine beta-synthase-deficient mice. *Arterioscler Thromb Vasc Biol* 2002; **22**: 34–41
94 **Robert K**, Chasse JF, Santiard-Baron D, Vayssettes C, Chabli A, Aupetit J, Maeda N, Kamoun P, London J, Janel N. Altered gene expression in liver from a murine model of hyperhomocysteinemia. *J Biol Chem* 2003; **278**: 31504-31511
95 **Chen Z**, Karaplis AC, Ackerman SL, Pogribny IP, Melnyk S, Lussier-Cacan S, Chen MF, Pai A, John SW, Smith RS, Bottiglieri T, Bagley P, Selhub J, Rudnicki MA, James SJ, Rozen R. Mice deficient in methylenetetrahydrofolate reductase exhibit hyperhomocysteinemia and decreased methylation capacity, with neuropathology and aortic lipid deposition. *Hum Mol Genet* 2001; **10**: 433-443
96 **Schwahn BC**, Chen Z, Laryea MD, Wendel U, Lussier-Cacan S, Genest J Jr, Mar MH, Zeisel SH, Castro C, Garrow T, Rozen R. Homocysteine-betaine interactions in a murine model of 5,10-methylenetetrahydrofolate reductase deficiency. *FASEB J* 2003; **17**: 512-514
97 **Swanson DA**, Liu ML, Baker PJ, Garrett L, Stitzel M, Wu J, Harris M, Banerjee R, Shane B, Brody LC. Targeted disruption of the methionine synthase gene in mice. *Mol Cell Biol* 2001; **21**: 1058-1065
98 **Tsukamoto H**, Lu SC. Current concepts in the pathogenesis of alcoholic liver injury. *FASEB J* 2001; **15**: 1335-1349
99 **Bleich S**, Bleich K, Kropp S, Bittermann HJ, Degner D, Sperling W, Ruther E, Kornhuber J. Moderate alcohol consumption in social drinkers raises plasma homocysteine levels: a contradiction to the 'French Paradox'? *Alcohol Alcohol* 2001; **36**: 189-192
100 **Stickel F**, Choi SW, Kim YI, Bagley PJ, Seitz HK, Russell RM, Selhub J, Mason JB. Effect of chronic alcohol consumption on total plasma homocysteine level in rats. *Alcohol Clin Exp Res* 2000; **24**: 259-264
101 **Carmel R**, James SJ. Alcohol abuse: an important cause of severe hyperhomocysteinemia. *Nutr Rev* 2002; **60**: 215-221
102 **Cravo ML**, Camilo ME. Hyperhomocysteinemia in chronic alcoholism: relations to folic acid and vitamins B(6) and B(12) status. *Nutrition* 2000; **16**: 296-302
103 **Bleich S**, Bandelow B, Javaheripour K, Muller A, Degner D, Wilhelm J, Havemann-Reinecke U, Sperling W, Ruther E, Kornhuber J. Hyperhomocysteinemia as a new risk factor for brain shrinkage in patients with alcoholism. *Neurosci Lett* 2003; **335**: 179-182
104 **Reynolds K**, Lewis B, Nolen JD, Kinney GL, Sathya B, He J. Alcohol consumption and risk of stroke: a meta-analysis. *JAMA* 2003; **289**: 579-588
105 **Bleich S**, Kornhuber J. Relationship between plasma homocysteine levels and brain atrophy in healthy elderly individuals. *Neurology* 2003; **60**: 1220
106 **Stickel F**, Choi SW, Kim YI, Bagley PJ, Seitz HK, Russell RM, Selhub J, Mason JB. Effect of chronic alcohol consumption on total plasma homocysteine level in rats. *Alcohol Clin Exp Res* 2000; **24**: 259-264

107 **Lu SC**, Huang ZZ, Yang H, Mato JM, Avila MA, Tsukamoto H. Changes in methionine adenosyltransferase and S-adenosylmethionine homeostasis in alcoholic rat liver. *Am J Physiol Gastrointest Liver Physiol* 2000; **279**: G178-185

108 **Barak AJ**, Beckenhauer HC, Junnila M, Tuma DJ. Dietary betaine promotes generation of hepatic S-adenosylmethionine and protects the liver from ethanol-induced fatty infiltration. *Alcohol Clin Exp Res* 1993; **17**: 552-555

109 **Trimble KC**, Molloy AM, Scott JM, Weir DG. The effect of ethanol on one-carbon metabolism: increased methionine catabolism and lipotrope methyl-group wastage. *Hepatology* 1993; **18**: 984-989

110 **Kenyon SH**, Nicolaou A, Gibbons WA. The effect of ethanol and its metabolites upon methionine synthase activity *in vitro*. *Alcohol* 1998; **15**: 305-309

111 **Barak AJ**, Beckenhauer HC, Tuma DJ. Betaine, ethanol, and the liver: a review. *Alcohol* 1996; **13**: 395-398

112 **Barak AJ**, Beckenhauer HC, Tuma DJ. Hepatic transmethylation and blood alcohol levels. *Alcohol Alcohol* 1991; **26**: 125-128

113 **Tuma DJ**, Keefer RC, Beckenhauer HC, Barak AJ. Effect of ethanol on uptake of choline by the isolated perfused rat liver. *Biochim Biophys Acta* 1970; **218**: 141-147

114 **Thompson JA**, Reitz RC. Studies of the acute and chronic effects of ethanol ingestion on choline oxidation. *Ann N Y Acad Sci* 1976; **273**: 194-204

115 **Halsted CH**, Villanueva J, Chandler CJ, Stabler SP, Allen RH, Muskhelishvili L, James SJ, Poirier L. Ethanol feeding of micropigs alters methionine metabolism and increases hepatocellular apoptosis and proliferation. *Hepatology* 1996; **23**: 497-505

116 **Halsted CH**, Villanueva JA, Devlin AM, Niemela O, Parkkila S, Garrow TA, Wallock LM, Shigenaga MK, Melnyk S, James SJ. Folate deficiency disturbs hepatic methionine metabolism and promotes liver injury in the ethanol-fed micropig. *Proc Natl Acad Sci U S A* 2002; **99**: 10072-10077

117 **Kim SK**, Kim YC. Attenuation of bacterial lipopolysaccharide-induced hepatotoxicity by betaine or taurine in rats. *Food Chem Toxicol* 2002; **40**: 545-549

118 **Rose ML**, Rivera CA, Bradford BU, Graves LM, Cattley RC, Schoonhoven R, Swenberg JA, Thurman RG. Kupffer cell oxidant production is central to the mechanism of peroxisome proliferators. *Carcinogenesis* 1999; **20**: 27-33

119 **Rivera CA**, Bradford BU, Seabra V, Thurman RG. Role of endotoxin in the hypermetabolic state after acute ethanol exposure. *Am J Physiol* 1998; **275**: G1252-1258

120 **Rivera CA**, Wheeler MD, Enomoto N, Thurman RG. A choline-rich diet improves survival in a rat model of endotoxin shock. *Am J Physiol* 1998; **275**: G862-867

121 **Zhang F**, Warskulat U, Wettstein M, Haussinger D. Identification of betaine as an osmolyte in rat liver macrophages (Kupffer cells). *Gastroenterology* 1996; **110**: 1543-1552

122 **Graf D**, Kurz AK, Reinehr R, FIscher R, Kircheis G, Haussinger D. Prevention of bile acid-induced apoptosis by betaine in rat liver. *Hepatology* 2002; **36**: 829-839

123 **Lieber CS**, Casini A, DeCarli LM, Kim CI, Lowe N, Sasaki R, Leo MA. S-adenosyl-L-methionine attenuates alcohol-induced liver injury in the baboon. *Hepatology* 1990; **11**: 165-172

124 **Lu SC**, Alvarez L, Huang ZZ, Chen L, An W, Corrales FJ, Avila MA, Kanel G, Mato JM. Methionine adenosyltransferase 1A knockout mice are predisposed to liver injury and exhibit increased expression of genes involved in proliferation. *Proc Natl Acad Sci U S A* 2001; **98**: 5560-5565

125 **Garcia-Trevijano** ER, Latasa MU, Carretero MV, Berasain C, Mato JM, Avila MA. S-adenosylmethionine regulates MAT1A and MAT2A gene expression in cultured rat hepatocytes: a new role for S-adenosylmethionine in the maintenance of the differentiated status of the liver. *Faseb J* 2000; **14**: 2511-2518

126 **Teckman JH**, Qu D, Perlmutter DH. Molecular pathogenesis of liver disease in alpha1-antitrypsin deficiency. *Hepatology* 1996; **24**: 1504-1516

127 **Perlmutter DH**. Liver injury in alpha1-antitrypsin deficiency: an aggregated protein induces mitochondrial injury. *J Clin Invest* 2002; **110**: 1579-1583

128 **Teckman JH**, An JK, Loethen S, Perlmutter DH. Fasting in alpha1-antitrypsin deficient liver: constitutive activation of autophagy. *Am J Physiol Gastrointest Liver Physiol* 2002; **283**: G1156-1165

129 **Xu Z**, Jensen G, Yen TS. Activation of hepatitis B virus S promoter by the viral large surface protein via induction of stress in the endoplasmic reticulum. *J Virol* 1997; **71**: 7387-7392

130 **Tardif KD**, Mori K, Siddiqui A. Hepatitis C virus subgenomic replicons induce endoplasmic reticulum stress activating an intracellular signaling pathway. *J Virol* 2002; **76**: 7453-7459

131 **Waris G**, Tardif KD, Siddiqui A. Endoplasmic reticulum (ER) stress: hepatitis C virus induces an ER-nucleus signal transduction pathway and activates NF-kappaB and STAT-3. *Biochem Pharmacol* 2002; **64**: 1425-1430

132 **Pavio N**, Romano PR, Graczyk TM, Feinstone SM, Taylor DR. Protein synthesis and endoplasmic reticulum stress can be modulated by the hepatitis **C** virus envelope protein E2 through the eukaryotic initiation factor 2alpha kinase PERK. *J Virol* 2003; **77**: 3578-3585

133 **Tardif KD**, Siddiqui A. Cell surface expression of major histocompatibility complex class I molecules is reduced in hepatitis C virus subgenomic replicon-expressing cells. *J Virol* 2003; **77**: 11644-11650

134 **Tardif KD**, Mori K, Kaufman RJ, Siddiqui A. Hepatitis C virus suppresses the IRE1-XBP1 pathway of the unfolded protein response. *J Biol Chem* 2004; **279**: 17158-17164

135 **Lieber CS**. Hepatitis C and alcohol. *J Clin Gastroenterol* 2003; **36**: 100-102

136 **Szabo G**. Pathogenic interactions between alcohol and hepatitis C. *Curr Gastroenterol Rep* 2003; **5**: 86-92

137 **Peters MG**, Terrault NA. Alcohol use and hepatitis C. *Hepatology* 2002; **36**: S220-225

138 **Bhattacharya R**, Shuhart MC. Hepatitis C and Alcohol. *J Clin Gastroenterol* 2003; **36**: 242-252

Edited by Wang XL and Xu XQ **Proofread by** Xu FM

PO Box 2345, Beijing 100023, China
Fax: +86-10-85381893
E-mail: wjg@wjgnet.com www.wjgnet.com

World J Gastroenterol 2004;10(12):1709-1715
World Journal of Gastroenterology
Copyright ©2004 by The WJG Press ISSN 1007-9327

• REVIEW •

Review of cytokine profiles in patients with hepatitis

Qiao-Ling Sun, Wei Ran

Qiao-Ling Sun, The Department of Biotechnological Pharmaceutics, Taishan Medical University, Tai' an 271000, Shangdong Province, China
Wei Ran, Basic Medical Research Institute, Taishan Medical University, Tai' an 271000, Shangdong Province, China
Correspondence to: Qiao-Ling Sun, The Department of Biotechnological Pharmaceutics, Taishan Medical University, Tai' an 271000, Shangdong Province, China. sunsunpublic@sina.com
Telephone: +86-538-6222435
Received: 2003-09-18 **Accepted:** 2003-10-12

Abstract

The development of T helper 1 versus T helper 2 cells is a major branch point in the immune response and is an important determinant of the body's response to an infectious pathogen, leading to protection of the host or dissemination of the disease. Resent studies have shown that there exist macrophage activation states in parallel to the T helper cell type 1/2 paradigm, and the T helper 1 development process is governed to a great degree by cytokine IL-12 provided mainly by antigen presenting cells such as macrophages and dendritic cells. A model in patients with hepatitis is proposed that links the pathogen, macrophage activation and T helper cell polarization.

Sun QL, Ran W. Review of cytokine profiles in patients with hepatitis. *World J Gastroenterol* 2004; 10(12): 1709-1715
http://www.wjgnet.com/1007-9327/10/1709.asp

INTRODUCTION

The immune response that occurs during infectious disease is characterized by plasticity in both its nature and its magnitude. This feature provides an important advantage that permits the immune system to tailor its defense strategy to particular groups of infectious pathogens. Interactions between CD4+T helper (Th) lymphocytes and antigen-presenting-macrophage cells in liver shape and amplify the subsequent immune response. The Th precursors differentiate into 2 subsets of effector Th cells with different functions[1,2]. Th1 cells produce IFN-γ, IL-2 and Th2 cells produce IL-4, IL-10 and IL-13. The ensuing Th1- and Th2-type immune responses include both potent humoral and cell-mediated components. Th1-derived IFN-γ suppresses Th2 response and Th2-derived IL-10 inhibits the development of Th1 populations[3]. In addition, the effector cells and antibody isotypes involved are quite distinct[4]. Th1 cells are responsible for activation of macrophages to a microbicidal state, induction of IgG2 a Abs that mediate phagocytosis, and support of CD8+ antiviral effector T cells. By contrast, Th2 cells stimulate the growth and differentiation of mast cells and eosinophils, as well as the production of Ab isotypes, including IgE and IgG4, which can mediate the activation of these cells. IL-12, a cytokine elaborated mainly by macrophages/monocytes, induces the maturation of Th1 cells. An imbalance of Th1 and Th2 appears to be important in the pathogenesis of chronic viral and nonviral infections in humans, such as infection with human immunodeficiency virus, leprosy, leishmaniasis[5-7],and viral hepatitis[8].

Recent studies have shown macrophage activation states in parallel to the Th cell type 1/2 paradigm. IFN-γ has long been known as the classical macrophage activating factor inducing cytokine secretion by macrophages to support Th1-driven immune responses. IL-4 which was historically regarded as macrophage deactivators is now thought to induce alternative immunological activation of macrophages[9], in that it enhances of the capacity of macrophages for endocytosis and antigen presentation by the induction of mannose receptor expression[10]. In normal immunological process, classical and alternative macrophage activation maintains the balance of macrophage.

IMBALANCE OF Th1/Th2

Th1 and Th2 type cytokines in patients with hepatitis

Chronic hepatitis is characterized by incomplete clearance of virus and damage hepatocytes. Since hepatitis B virus (HBV) is known to have no cytopathic effect on the infected hepatocytes, cell-mediated immunity is thought to play an important role in the pathogenesis of hepatocellular damage and HBV clearance[11]. Although immune evading mechanisms used by HBV are largely unknown, defects in T cell response have been suspected as a major factor involved in the pathogenesis of chronic hepatitis[11-15]. Different from acute self-limited hepatitis in which protective immunity develops after elimination of HBV, immune response fails to remove HBV-infected hepatocytes in chronic hepatitis B. Th1 type pattern of secreted immunity can be considered as an appropriate response of the immune system to inhibit viral replication and HBV eradication. Mechanisms by which IFN-γ favors the elimination of HBV may include enhancement of cytotoxic T lymphocyte (CTL) activation, direct anti-viral activity, increased expression of major histcompatibility complex class I molecules on infected cells, and activation of macrophages[16-18]. It has been shown in a transgenic mouse model that adoptive transfer of CTLs producing IFN-γ could inhibit HBV replication without cytolysis[19].

Studies have shown[18] that predominant Th1 (IFN-γ) cytokine profile of hepatitis B core Ag (HbcAg)-specific and hepatitis B surface Ag (HbsAg)-reactive T cells is associated with acute self-limited hepatitis B. In most patients with acute hepatitis, CTL responses to epitopes of HBsAg, while there are no such responses in patients with chronic hepatitis[20]. Thus, Th1 might be insufficient for complete removal of HBV in chronic hepatitis and positively correlated with hepatic inflammatory activity.

Meanwhile, Barnaba *et al.* cloned CD4+ HBV envelope antigen (HbeAg)-reactive T cells and showed signs of cytotoxicity only when they produced IFN-γ[21]. This is in agreement with findings that production of IFN-γ[22] by peripheral blood mononuclear cells (PBMCs) upon HBsAg stimulation was associated with higher level of hepatocyte damage. The dissociation between the mechanisms responsible for the immune-mediated hepatocytolysis, and for vural clearance in HBV infection was proposed[23]. It has been demonstrated that the interaction between Ag-specific CTL and target hepatocytes results in spotty necrosis which is limited to a very few hepatocytes[24]. Instead, the antiviral effect is mediated by IFN-γ, IL-2, and TNF-α released by HBV-specific CTLs or by antigen nonspecific macrophages, and these

cytokines profoundly suppress HBV gene expression in infected hepatocytes by noncytolytic mechanisms[25] through eliminating HBV nucleocapsid particles and destabiling the viral RNA[26]. Thus, after recognition of HBV antigens on the surface of infected hepatocytes, CTLs perform two distinct functions; they kill a small fraction of infected hepatocytes and secrete IFN-γ and TNF-α, which exert antiviral effects without destruction of hepatocytes. Effective clearance of duck HBV and woodchuck hepatitis virus has also been shown to occur without massive hepatocellular necrosis[27].

In addition, a cytokine balance favoring Th2 type cytokine production such as IL-4 and IL-10 has been associated with progressive virus infections. Co-activation of Th3 cells with Th2 cells can negatively regulate immune responses and may be associated with the immune tolerant state of chronic HBV infection[28]. The shift from Th1 to Th2 or Th0 profiles was observed in acquired immune deficiency syndrome[29]. Result also indicates the existence of a Th2 type response to HBsAg in chronic hepatitis B patients with more sever liver damage[30]. Th2 cells may be associated with the persistence of HBV infection[31]. Probably the virus can mutate effectively and evade T-cell immune defense mechanisms. Persistent infection upsets the balance between immunostimulatory and inhibitory cytokines which can prolong inflammation and lead to necrosis, fibrosis, and chronic liver disease[32].

In chronic hepatitis C virus (HCV) infection, Fan *et al*. observed that the elevated levels of Th2 cytokines were greater than Th1 cytokines measured by ELISA[33]. This result is in agreement with Kobayashi *et al.* who showed a significant increase in number of IL-4-producing Th2 cells and a significant decrease in number of IFN-γ-producing Th1 cells (PBMC stimulated by anti-CD3 antibody)[34]. They[34] suggested that, theoretically, stimulation with anti-CD3 antibody results in the expansion of T lymphocytes, whereas stimulation with HCV core protein results in the expansion of T lymphocytes responsive to HCV core antigen. The stimulation of PBMC with anti-CD3 antibody could reflect the patient' s real situation better than that with HCV core protein. In addition, they measured the IFN-γ after the depletion of CD8+ T cells –one of the major sources of IFN-γ production. This could explain that the increased production of IFN-γ (Th1) shown in others studies were due to IFN-γ secretion by CD8+T lymphocytes.

However, Iwata *et al.* found that in patients with chronic hepatitis C there was the increasing production of IFN-γ (Th1) by PBMC after stimulation with HCV core protein[35]. Bergamini *et al.* obtained the similar result that the percentage of Th1 cells was significantly increased in CD4+, CD8+, ' naive' -CD45RA+ and ' memory' -CD45RO+ T-cell subsets (PBMC by mitogen-stimulation) from patients versus controls[36], and Sobue1 *et al*.[37] also found that a shift to Th1 cytokine profile correlated with the progress of liver damage, which could be related to the higher proportion of CD4+T cells. Although in chronic hepatitis C infection, the levels of mononuclear cells derived from peripheral blood reflected the level of mononuclear cells derived from liver, the profile of Th1/Th2 in liver tissue and in peripheral blood was different[37]. In liver tissue, a predominance of Th1-type cytokines was seen in CD4+T cells[38], while a predominance of Th1 type cytokines was observed in CD8+ cells in peripheral blood. Thus, the elevated cytokine production may also have been caused by a higher proportion of CD4+T cells in the liver tissue of patients with chronic HCV infection compared with that in healthy controls, and intrahepatic CD4+T cells may be more important than CD8+T cells in the pathogenesis of liver damage in chronic hepatitis C infection. In addition, the percentage of CD4+T cells in liver correlated with the histological activity of hepatitis[38,39]. These results may indicate a preferential compartmentalization of Th1 cytokine-producing CD4+T cells in the liver[40], suggesting that some liver-derived CD4+T cells had a direct cytotoxic effect[41,21]. Meanwhile cytokines produced may inhibit viral replication, such as IFN-γ and TNF-α[26].

The probable mechanism of Th1 predominance in HCV infection is that in order to eliminate HCV and inhibit viral replication, the compartmentalized CD4+T cells may shift to a Th1 profile and induce nonspecific immune responses to activate nonspecific immune cells and effector molecules, resulting in liver cell damage. Nevertheless, further studies are needed to investigate the significance of CD4+T cells in liver tissue.

But the different result was observed regarding Th1 or Th2 predominance in patients with chronic hepatitis C, which was probably due to the administration of PBMC and the measurement for Th1 cytokines from CD4+T, or both CD4+ and CD8+ T cells. It is also possible that the HCV-related antigen influences T helper cells to produce a different cytokine profile from that in healthy subjects. For example, in transgenic mice with HBeAg, the T cell response against peptide 120-31 of HBeAg was predominantly Th1, whereas the response against peptide 129-40 was predominantly Th2-like[42]. Moreover, escaping variants of HCV epitope attenuate or fail to stimulate T-cell proliferation, which is accompanied by a shift in cytokine secretion patterns from one characteristic of a Th1 antiviral responses to a Th2 form[43]. Recent evidence suggests that the polymorphic nature of the MHC binding sites and differences in the T-cell repertoire among persons lead to highly variable binding affinity for the immunodominant HBV peptides, which in turn determines the outcome after acute HBV infection[44,45].

The role of IL-12 in hepatitis disease

IL-12, a heterodimer composed of 2 subunits of p40 and p35 and secreted mainly by antigen-presenting cells (APC) such as activated macrophages and dendritic cells (DCs), is a crucial mediator between innate and adaptive immune responses. The transcriptional factor T-bet, which can induce transcription of an IFN-γ reporter gene and is specifically expressed in Th1 cells generated in the presence of IL-12[46], suppresses the expression of genes encoding IL-4, IL-5 and induces the synthesis of IFN-γ. These studies suggest that Th1 development process is governed by cytokine IL-12 to a great degree.

IL-12 is a key cytokine not only promoting Th1–synergizing with IL-2, IL-12 induces rapid and efficient production of IFN-γ[47] by stimulation of the TCR–CD3 complex and activation of the CD28 receptor, but also maintaining Th1 responses[48] (Figure 1),- in that Th-cell differentiation is determined most probably early after infection by the balance between IL-12 and IL-10 ,IL-4, which favour Th1- and Th2-cell development, respectively. In addition, IL-12 correlates with virus clearance. In HBV-infected patients, a significant increase in IL-12 production was observed only in patients who cleared the virus. The peak of serum IL-12 associated with Th1 cytokines (IFN-γ) occurred after the ALT flare and preceded or coincided with the time of HBe seroconversion[8]. Thus, the findings in patients with chronic HBV infection support a proposed combination strategy for therapy with IL-12 plus vaccination[49,50]. After the ALT flare, the occurrence of IL-12 peak would be the reason that hepatocellular necrosis induced by CTL leads to the recruitment of macrophages and noncommitted T helper cells in the liver. Then the native particles of HBcAg are released from damaged hepatocytes and provide potent antigenic stimulation for these cells. In patients who are able to respond with an increase in IL-12 production, this will promote Th1 cell development and stimulate the production of IFN-γ and TNF-α, which will exert their noncytolytic antiviral effects.

IL-12 may be instrumental in the defense mechanism against HBV infection, and the elevation of its level can be indicative of hepatitis recovery[51]. The enhancing effect of IL-12 on IFN-γ production of PBMC in patients with chronic hepatitis B virus

infection is increased during IFN-α treatment. Therefore, IFN-α and IL-12 may enhance the efficacy for the treatment of chronic HBV infection[52], and HCV-related cellular immune defect in patients with hepatitis C can be restored in most patients by IL-12[53]. However, Quiroga *et al*[54] found that HCV-infected patients with greater necro-inflammatory activity of liver showed greater IL-12 production by PBMC than those with minimal or mild activity and normal donors. Massive induction of the proinflammatory cytokines IL-12 and IFN-γ in liver specimens is apparently not counterbalanced by the anti-inflammatory cytokine IL-10, which may play an important role in promoting inflammatory reactions leading to massive liver damage in murine models of fulminant hepatitis B[55].

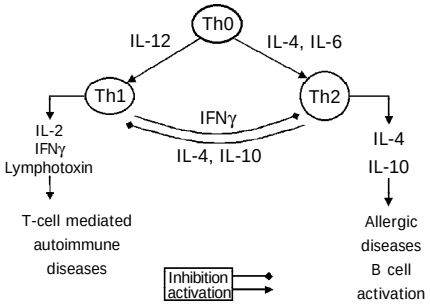

Figure 1 Development of Th1/Th2 From Marc and Weeber.

BLANCE OF MACROPHAGE IN PATIENTS WITH HEPATITIS

Macrophage and macrophage activation

Macrophages can be segregated into two broad groups: resident tissue macrophages and inflammatory macrophages. Tissue macrophages are heterogeneous, and those isolated from different anatomical sites differ in function presumably because of adaptive responses to the local micro-environment[56]. Inflammatory macrophages are derived largely from circulating monocytes, which infiltrate damaged tissue, but some arise by local cell division[57]. There is now increasing evidence for the heterogeneity of macrophages that have infiltrated inflamed or otherwise damaged tissue, depending on the type and severity of injury, the stage of its evolution and the localization of the macrophages within the tissue[58].

One major function of macrophages is to provide a defense line against microbial invasion and to recognize and kill tumor cells. Macrophages can accomplish this in a direct manner, involving the release of products such as oxygen radicals and tumor necrosis factor that are harmful to microorganisms or cancer cells. On the other hand, they play an indirect role in these anti-microbial or anti-tumor activities by secretion of cytokines or by antigen processing and presentation, thereby regulating the immune system[59].

The macrophage presents HBV-derived proteins which activates CD4+T cells. The effects of stimulation on macrophages include increased cytokine production (TNF-α, IFN-γ, IL-1), expression of inducible nitric oxide synthase, nitric oxide secretion, and up-regulation of adhesion molecules. All these processes can lead, directly or indirectly, to increased cytotoxicity of the macrophages. We also found the higher expression level of granulate and activation –linked surface antigen CD69 by CD14 macrophage from peripheral blood in patients with chronic hepatitis than in controls[60].This activity was associated with high level transcription of IL-1, IL-6 and TNF-α (unpublished data). Probably, plasma HBV antigens activate macrophages from peripheral blood. Subsequently, such cytokines are produced. In addition, the increasing number of macrophage functions and heterogeneity *in vitro* and *in vivo* has led to the definition of macrophage activation states in parallel to the Th 1/2 paradigm. IFN-γ has long been known as the classical macrophage activating factor inducing cytokine secretion by macrophages supporting Th1-driven immune responses. IL-4 which was historically regarded as macrophage deactivators is now thought to induce alternative immunological activation of macrophages[9], in that it enhances of the capacity of macrophages for endocytosis and antigen presentation by the induction of mannose receptor expression[10]. In normal immunological process, classical and alternative macrophage activation maintains the balance of macrophage.

Balanced macrophage activation hypothesis

Figure 2 shows a macrophage activation cycle wherein multiple steps occur during various forms of activation and recycling of macrophage function so as to achieve balanced macrophage activation (Steps 1-5)[61]. When hepatitis virus invades the body, tissue-resident macrophages undergo local activation and engulf the virus or antigen and enhanced recruitment of monocytes and precursors from bone-marrow pools results in the accumulation of tissue macrophages that have enhanced turnover and an altered phenotype[62].After the antigen presentation, Th cells are activated through MHC class II. Th1 (stand for active Th) cell produces IL-2 and IFN-γ and Th2 (stand for inhibitor T) cell secrets IL-4 and IL-10, which is involved in B cell activation as well as providing signals for balanced macrophage activation. Production of IL-4 is known to activate the alternative macrophage activation pathway[10] (step 5). Although IL-4 induces mannose receptor expression and enhance the capacity of macrophages for endocytosis and antigen presentation[62], alternative pathway activated macrophages *in vitro* actively inhibit mitogen-induced proliferation of peripheral blood lymphocytes[63] and CD4+T cells[64-66] These findings convincingly confirm that alternative activation generates immunosuppressive macrophage populations. In fact, co-induction of IL-10 with IL-4 secreted by Th2 cells, mainly contributes to the inhibition effect. The net result of excess IL-10 production shuts off the Th1 activation pathway[61]. Therefore, the balance of macrophage and these cytokines are closely related to viral infectious diseases such as AIDS and viral hepatitis.

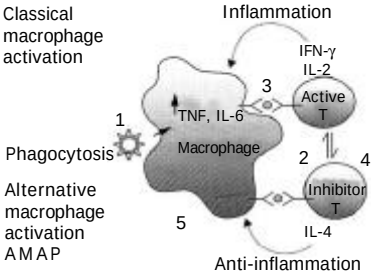

Figure 2 Blanced macrophage activation cycles From Michael[61].

Macrophages may contribute either directly or indirectly to the hepatonecrosis with fulminant virus infection[67] through classical macrophage pathway. Macrophages in the liver called Kupffer cells activate Th1(IFN-γ), IFN-γ will activate Kupffer cells[68,69]. This results in Kupffer overactivation, which in turn promotes cytokines production (TNF-α, IFN-γ), expression of inducible NOS (iNOS), nitric oxide (NO) secretion. All these processes can lead, directly or indirectly, to increased cytotoxicity of the macrophages-this is the classical macrophage activation pathway.

IL-12 is a cytokine secreted by APCs such as activated macrophages and DCs[70]. It has an important role against intracellular pathogens by promoting Th1 cell development, cell mediated cytotoxicity and IFN–γ production[71,72]. For

example, a significant increase in IL-12 production was observed only in patients with chronic hepatitis C who cleared the virus[73]. On the one hand, IFN-γ, activating macrophage and TNF-α secreted by macrophage, exert their noncytolytic antiviral effects. On the other hand, macrophage kills small fraction of infected hepatocytes. As mentioned above, the increase of serum IL-12 and Th1 cytokines always followed the ALT flare[73], confirming the function of IL-12 in promoting Th1 cell development, and binary function of macrophage. This also explains that HCV-infected patients with greater necro-inflammatory activity of liver showed greater IL-12 production by PBMC than those with minimal or mild activity in normal donors, and why Th1 predominance in HCV infection was correlated with the direct cytotoxic effect[41,21] and the inhibition of viral replication.

The greater production of IL-12 associated with greater necro-inflammatory activity of liver in HCV-infected patients[54] and response of IFN-γ to HCV core protein with chronic liver disease suggest a cellular immune response to the onset of the necroinflammatory process of hepatitis[35]. In murine model of fulminant hepatitis B, massive liver damage was associated with the massive induction of IL-12 and IFN-γ in liver specimens. Probably, the proinflammatory cytokines are apparently not counterbalanced by the anti-inflammatory cytokine IL-10. Thus IL-12 may play an important role in promoting inflammatory reactions[55]. These cases suggest that the macrophages are in the hyperactive situation, probably due to the imbalance of Th1/Th2 and failing to establish the alternative macrophage activation, which results in the imbalance of macrophage. Thus massive hepatocytes are killed by macrophages or overactivited CTLs.

The steps 2 and 3 in Figure 2 are continually stimulated when foreign virus can not be cleared by successful immune response for Lack of optimal T-cell reactivity that would reestablish balanced macrophage activation. The immunologic overstimulation would predictably lead to pathologic sequelae such as cirrhosis and hepatoma in chronic hepatitis B and C infections[74]

After long periods of time during which steps 2 and 3 are overemphasized, there would be a predicted shortage of cells to accomplish steps 5 and 1.There would also be an initial overdrive of Th1 cell population. Patients with HIV also have been observed to have a dramatic Th1 to Th2 shift as described in step 4 and patients with chronic hepatitis B appeared to be Th2 predominant[30]. The balanced macrophage activation theory predicts that this shift is compensatory in nature with the T cells attempting to regulate balanced macrophage activation through production of IL-4 which induces step5. Th2 predominance would be suffered by patients with chronic viral disease, which would cause secondary immunopathogenic changes, such as HCV-related liver cirrhosis(HCC)[75], while patients with histology of inflammation showed a significantly higher CD4+Th1 response to the HCV core antigen as compared to patients with histology of fibrosis/cirrhosis[76]. These findings suggest that Th1/Th2 imbalance in HCV-related cirrhosis would decrease the antitumor immunity and its improvement might present the protective effect from HCC[75]. At the same time, there exists the exhaustion of cells in steps 5 and 1.This would decrease the rate of phagecytosis.

Alternative macrophage pathway (step 4) has the following features: (1) the production of angiogenic factors, (2) inhibition of T cell responses, (3) associated downregulation of inflammatory-mediator production characteristic of classical activated macrophages, and (4) with the alternative macrophage activation chemokine-1 (AMAC-1)[77], also known as macrophage inflammatory protein-4 (MIP-4). But few studies were performed in aspect of macrophage, and little is known about the mechanism of the balanced macrophage theory in chronic virus liver infection.

CONCLUSION

Recent data have made a major shift in the role of macrophages in HIV[78] and inflammatory kidney disease. They can no longer be regarded solely as causing injury but rather as cells that can also promote resolution[79,80]. This means that strategies to prevent macrophage influx may be beneficial to patients with hepatitis. Future experiments will need to define methods for determining the functional attributes of macrophages in clinical liver biopsies, and effective ways to manipulate the function of inflammatory macrophages *in vivo*.

Given the diverse range of functions macrophages can assume, it becomes possible to modulate disease by altering macrophage activity. The classic view would be that the overall inflammatory environment is a balance between pro- and anti-inflammatory cytokines, determining infiltrating and resident cell function. An increase of pro-inflammatory cytokines from macrophages such as TNF-α or IL-1β thus worsens inflammation, whereas antagonists of these molecules such as IL-1 receptor antagonist (IL-1ra), IL-1 type II decoy receptor (IL-1RII) and soluble TNF receptor result in reduced injury[81]. A number of cytokines are described as anti-inflammatory, including the Th2 cytokines IL-4, IL-10 and IL-13, IL-6 and TGF-β. rIL-10 treatment of patients with advanced fibrosis who had failed antiviral therapy appeared to decrease disease activity[82]. TGF-β2 significantly suppressed IFN-γ production at the single-cell level, indicating that the enhanced down-regulation of Th1 by TGF-β2 in patients with HCVrelated liver cirrhosis might be effective against hepatoma[83]. But not all anti-inflammatory cytokines are equal in their ability to modulate macrophage function *in vivo*. In contrast to the results with the Th2 cytokines, IL-4 and IL-10, infusions of TGF-β do not modulate inflammatory macrophage function in glomerulonephritis. For example, Infusion of TGF-β3 in rats with NTN (nephrotoxic nephritis RANTES) before the onset of disease did not alter the degree of proteinuria, although the number of infiltrating macrophages was reduced[84]. The study about TGF-β treatment of animal models and patients with hepatitis is still unknown.

Advanced clinical studies of WF10 (completely blocked antigen activation of T cells responsiveness -in step 2) are currently underway in the USA for treatment of patients with HIV disease. The patients who received two cycles of WF10 showed chronic immunological changes by downregulating inflammatory macrophages and reestablished alternative macrophage activation, which was consistent with induction of balanced macrophage activation[85]. Similarly, it is possible to modify inflammatory virus liver disease using a range of cytokines (Th1/Th2 types) with well-defined effects on macrophage activation. For example, defects in T cell response have been suspected as a major factor involved in the pathogenesis of chronic hepatitis B[11-15], and favoring Th2 type cytokine may lead to chronic infections with HBV. Recent study has shown that activation of Th1 immunity accompanied by enhancement of CTL activity during therapy is a common immune mechanism for the successful treatment of hepatitis B and C[86]. Using HBV core gene transduced DCs as APCs, HBcAg specific CTLs and Th1 type immune responses could be generated in the mice, which would be a new way to deal with the viral hepatitis[87].Thus, treatment with IL-12 to drive T cell reactivity[88], and usage of IL-4 receptor antagonist are probably the practicable way to clear virus and remove HBV-infected hepatocytes. Although IL-12 as monotherapy in patients with HCV did not alter the production of regulatory cytokines produced by Th1/2 cells[89] and had low efficacy[90,91], IL-12 combining with IFN-α may enhance the efficacy for the treatment of chronic hepatitis B virus infection[92]and may be a predisposition for elimination of HBeAg and successful treatment of hepatitis B[93].

REFERENCES

1 **Mosmann TR**, Cherwinski H, Bond MW, Giedlin MA, Coffman RL. Two types of murine helper T cell clones. I. Definition according to profiles of lymphokine activities and secreted proteins. *J Immunol* 1986; **136**: 2348–2357

2 **Romagnani S**, Parronchi P, D'Elios MM, Romagnani P, Annunziato F, Piccinni MP, Manetti R, Sampognaro S, Mavilia C, De Carli M, Maggi E, Del Prete GF. An update on human Th1 and Th2 cells. *Int Arch Allergy Immunol* 1997; **113**: 153-156

3 **Racke MK**, Bonomo A, Scott DE, Cannella B, Levine A, Raine CS, Shevach EM, Rocken M. Cytokine-induced immune deviation as therapy for inflammatory autoimmune disease. *J Exp Med* 1994; **180**: 1961-1966

4 **Abbas AK**, Murphy KM, Sher A. Functional diversity of helper T lymphocytes. *Nature* 1996; **383**: 787–793

5 **Clerici M**, Shearer GM. The Th1-Th2 hypothesis of HIV infection: new insights. *Immunol Today* 1994; **15**: 575–581

6 **Yamamura M**, Uyemura K, Deans RJ, Weinberg K, Rea TH, Bloom BR, Modlin RL. Defining protective responses to pathogens: cytokine profiles in leprosy lesions. *Science* 1991; **254**: 277–279

7 **Sher A**, Coffman RL. Regulation of immunity to parasites by T cells and T cell-derived cytokines. *Annu Rev Immunol* 1992; **10**: 385–409

8 **Rossol S**, Marinos G, Carucci P, Singer MV, Williams R, Naoumov NV. Interleukin-12 induction of Th1 cytokines is important for viral clearance in chronic hepatitis B. *J Clin Invest* 1997; **99**: 3025-3033

9 **Birk RW**, Gratchev A, Hakiy N, Politz O, Schledzewski K, Guillot P, Orfanos CE, Goerdt S. Alternative activation of antigen-presenting cells: concepts and clinical relevance. *Hautarzt* 2001; **52**: 193-200

10 **Montaner LJ**, da Silva RP, Sun J, Sutterwala S, Hollinshead M, Vaux D, Gordon S. Type 1 and type 2 cytokine regulation of macrophages endocytosis: differential activation by IL-4/IL-13 as opposed to IFN-γ or IL-10. *J Immunol* 1999; **162**: 4606-4613

11 **Chisari FV**, Ferrari C. Hepatitis B virus immunopathogenesis. *Springer Semin Immunopathol* 1995; **13**: 29–60

12 **Ishikawa T**, Kakumu S, Yoshika K, Wakita T, Takayanagi M, Olido E. Immune response of peripheral blood mononuclear cells to antigenic determinants within hepatitis B core antigen in HB virus-infected man. *Liver* 1992; **12**: 100–105

13 **Marinos G**, Torre F, Chokshi S, Hussain M, Clarke BE, Rowlands DJ, Eddleston AL, Naoumov NV, Williams R. Induction of T-helper cell response to hepatitis B core antigen in chronic hepatitis B: a major factor in activation of the host immune response to the hepatitis B virus. *Hepatology* 1995; **22** (4 Pt 1): 1040-1049

14 **Ferrari C**, Penna A, Bertoletti A, Valli A, Antoni AD, Giuberti T, Cavalli A, Petit MA, Fiaccadori F. Cellular immune response to hepatitis B virus-encoded antigens in acute and chronic hepatitis B virus infection. *J Immuol* 1990; **145**: 3442-3449

15 **Lohr HF,** Weber W, Schlaak J, Goergen B, Meyer zum Buschenfelde KH, Gerken G. Proliferative response of CD4+T cells and hepatitis B virus clearance in chronic hepatitis with or without hepatitis B eminus hepatitis B virus mutants. *Hepatology* 1995; **22**: 61-68

16 **Toyonaga T**, Hino O, Sugai S, Wakasugi S, Abe K, Shichiri M, Yamamura K. Chronic active hepatitis in transgenic mice expression interferon–gamma in the liver. *Proc Natl Acad Sci U S A* 1994; **91**: 614-618

17 **Peters M**. Actions of cytokines on the immune response and viral interactions: an overview. *Hepatology* 1996; **23**: 909-916

18 **Ando K**, Moriyama T, Guidotti LG, Wirth S, Schreiber RD, Schlicht HJ, Huang SN, Chisari FV. Mechanisms of class I restricted immunopathology. A transgenic mouse model of fulminant hepatitis. *J Exp Med* 1993; **178**: 1541-1554

19 **Guidotti LG**, Ando K, Hobbs MV, Ishikawa T, Runkel L, Schreiber RD, Chisari FV. Cytotoxic T lymphocytes inhibit hepatitis B virus gene expression by a noncytolytic mechanism in transgenic mice. *Proc Natl Acad Sci U S A* 1994; **91**: 3764-3768

20 **Nayersina R**, Fowler P, Guilhot S, Missale G, Cerny A, Schlicht HJ, Vitiello A, Chesnut R, Person JL, Redeker AG. HLA A2 restricted cytotoxic T lymphocyte responses to multiple hepatitis B surface antigen epitopes during hepatitis B infection. *J Immunol* 1993; **150**: 4659-4671

21 **Barnaba V**, Franco A, Paroli M, Benvenuto R, De Petrillo G, Burgio VL, Santilio I, Balsano C, Bonavita MS, Cappelli G. Selective expansion of cytotoxic T lymphocytes with a CD4+CD56+surface phenotype and a T helper type 1 profile of cytokine secretion in the liver of patients chronically infected with Hepatitis B virus. *J Immunol* 1994; **152**: 3074-3087

22 **Clerici M**, Hakim FT, Venzon DJ, Blatt S, Hendrix CW, Wynn TA, Shearer GM. Changes in interleukin-2 and interleukin-4 production in asymptomatic, human immunodeficiency virus-seropositive individuals. *J Clin Invest* 1993; **91**: 759-765

23 **Chisari FV**. Hepatitis B virus transgenic mice: insights into the virus and the disease. *Hepatology* 1995; **22**(4 Pt 1): 1316-1325

24 **Ando K**, Guidotti LG, Wirth S, Ishikawa T, Missale G, Moriyama T, Schreiber RD, Schlicht HJ, Huang SN, Chisari FV. Class I-restricted cytotoxic T lymphocytes are directly cytopathic for their target cells *in vivo*. *J Immunol* 1994; **152**: 3245-3253

25 **Gilles PN**, Fey G, Chisari FV. Tumor necrosis factor alpha negatively regulates hepatitis B virus gene expression in transgenic mice. *J Virol* 1992; **66**: 3955-3960

26 **Guidotti LG**, Ishikawa T, Hobbs MV, Matzke B, Schreiber R, Chisari FV. Intracellular inactivation of the hepatitis B virus by cytotoxic T lymphocytes. *Immunity* 1996; **4**: 25-36

27 **Jilbert AR**, Wu TT, England JM, Hall PM, Carp NZ, O'Connell AP, Mason WS. Rapid resolution of duck hepatitis B virus infections occurs after massive hepatocellular involvement. *J Virol* 1992; **66**: 1377-1388

28 **Jiang R**, Lu Q, Hou J. Polarized populations of T helper cells in patients with chronic hepatitis B virus infection. *Zhonghua Yixue Zazhi* 2000; **80**: 741-744

29 **Maggi E**, Mazzetti M, Ravina A, Annunziato F, de Carli M, Piccinni MP, Manetti R, Carbonari M, Pesce AM, del Prete G. Ability of HIV to promote a TH1 to TH0 shift and to replicate preferentially in TH2 and TH0 cells. *Science* 1994; **265**: 244-248

30 **Lee M,** Lee SK, Son M, Cho SW, Park S, Kim HI. Expression of Th1 and Th2 type cytokines responding to HbsAg and HBxAg in chronic hepatitis B patients. *J Korean Med Sci* 1999; **14**: 175-181

31 **Jiang R**, Feng X, Guo Y, Lu Q, Hou J, Luo K, Fu N. T helper cells in patients with chronic hepatitis B virus infection. *Chin Med J* 2002; **115**: 422-424

32 **Jacobson Brown PM**, Neuman MG. Immunopathogenesis of hepatitis C viral infection: Th1/Th2 responses and the role of cytokines. *Clin Biochem* 2001; **34**: 167-171

33 **Fan XG**, Liu WE, Li CZ, Wang ZC, Luo LX, Tan DM, Hu GL, Zhang Z. Circulating Th1 and Th2 cytokines in patients with hepatitis C virus infection. *Mediators Inflamm* 1998; **7**: 295-297

34 **Kobayashi K**, Ishii M, Igarashi T, Satoh T, Miyazaki Y, Yajima Y, Ukai K, Suzuki H, Kanno A, Ueno Y, Miura T, Toyota T. Profiles of cytokines produced by CD4-positive T-lymphocytes stimulated by anti-CD3 antibody in patients with chronic hepatitis C. *J Gastroenterol* 1998; **33**: 500-507

35 **Iwata K**, Wakita T, Okumura A, Yoshioka K, Takayanagi M, Wands JR, Kakumu S. Interferon gamma production by peripheral blood lymphocytes to hepatitis C virus core protein in chronic hepatitis C infection. *Hepatology* 1995; **22**(4 Pt 1): 1057-1064

36 **Bergamini A**, Bolacchi F, Cerasari G, Carvelli C, Faggioli E, Cepparulo M, Demin F, Uccella I, Bongiovanni B, Niutta P, Capozzi M, Lupi M, Piscitelli E, Rocchi G, Angelico M. Lack of evidence for the Th2 predominance in patients with chronic hepatitis C. *Clin Exp Immunol* 2001; **123**: 451-458

37 **Sobue S**, Nomura T, Ishikawa T, Ito S, Saso K, Ohara H, Joh T, Itoh M, Kakumu S. Th1/Th2 cytokine profiles and their relationship to clinical features in patients with chronic hepatitis C virus infection. *J Gastroenterol* 2001; **36**: 544–551

38 **Tran A**, Yang G, Doglio A, Ticchioni M, Laffont C, Durant J, Bernard JL, Gugenheim J, Saint-Paul MC, Bernard A, Rampal P, Benzaken S. Phenotyping of intrahepatic and peripheral blood lymphocytes in patients with chronic hepatitis C. *Dig Dis Sci* 1997; **42**: 2495-2500

39 **Khakoo SI**, Soni PN, Savage K, Brown D, Dhillon AP, Poulter LW, Dusheiko GM. Lymphocyte and macrophage phenotypes

in chronic hepatitis C infection Correlation with disease activity. *Am J Pathol* 1997; **150**: 963–970

40 **Picker LJ**, Singh MK, Zdraveski Z, Treer JR, Waldrop SL, Bergstresser PR, Maino VC. Direct demonstration of cytokine synthesis heterogeneity among human memory/effector T cells by flow cytometry. *Blood* 1995; **86**: 1408–1419

41 **Minutello MA**, Pileri P, Unutmaz D, Censini S, Kuo G, Houghton M, Brunetto MR, Bonino F, Abrignani S. Compartmentalization of T lymphocytes to the site of disease: intrahepatic CD4+T cells specific for the protein NS4 of hepatitis C virus in patients with chronic hepatitis C. *J Exp Med* 1993; **178**: 17–25

42 **Milich DR**, Schodel F, Peterson DL, Jones JE, Hughes JL. Characterization of self-reactive T cells that evade tolerance in hepatitis Be antigen transgenic mice. *Eur J Immunol* 1995; **25**: 1663-1672

43 **Wang JH**, Layden TJ, Eckels DD. Modulation of the peripheral T-Cell response by CD4 mutants of hepatitis C virus: transition from a Th1 to a Th2 response. *Hum Immunol* 2003; **64**: 662-673

44 **Ferrari C**, Bertoletti A, Penna A, Cavalli A, Valli A, Missale G, Pilli M, Fowler P, Giuberti T, Chisari FV. Identification of immunodominant T cell epitopes of the hepatitis B virus nucleocapsid antigen. *J Clin Invest* 1991; **88**: 214-222

45 **Thursz MR**, Kwiatkowski D, Allsopp CE, Greenwood BM, Thomas HC, Hill AV. Association between an MHC class II allele and clearance of hepatitis B virus in the Gambia. *N Engl J Med* 1995; **332**: 1065-1069

46 **Szabo SJ**, Kim ST, Costa GL, Zhang X, Fathman CG, Glimcher LH. A novel transcription factor, T-bet, directs Th1 lineage commitment. *Cell* 2000; **100**: 655–669

47 **Chan SH**, Kobayashi M, Santoli D, Perussia B, Trinchieri G. Mechanisms of IFN-γ induction by natural killer) cell stimulatory factor (NKSF/IL-12): role of transcription and mRNA stability in the synergistic interaction between NKSF and IL-2. *J Immunol* 1992; **148**: 92–98

48 **Trinchieri G**. Interleukin-12 and the regulation of innate resistance and adaptive immunity. *Nat Rev Immunol* 2003; **3**: 133-146

49 **Milich DR**, Wolf SF, Hughes JL, Jones JE. Interleukin 12 suppresses autoantibody production by reversing helper T-cell phenotype in hepatitis B e antigen transgenic mice. *Proc Natl Acad Sci U S A* 1995; **92**: 6847-6851

50 **Gherardi MM**, Ramirez JC, Esteban M. Towards a new generation of vaccines: the cytokine IL-12 as an adjuvant to enhance cellular immune responses to pathogens during prime-booster vaccination regimens. *Histol Histopathol* 2001; **16**: 655-667

51 **Liu Q,** Feng GX, Lin YL, Peng YZ, Mo BQ. Detection of interleukin-6 and -12 in hepatitis B patients and its clinical significance. *Diyi Junyi Daxue Xuebao* 2001; **21**: 858-859

52 **Wang S,** Lin Y, Ma W, Zhang B, Qi S, Lan F. Effect of IL-12 on IFN-gamma and IL-10 produced by peripheral blood mononuclear cells in patients with chronic hepatitis B virus infection during IFN-alpha treatment. *Zhonghua Ganzangbing Zazhi* 2002; **10**: 116-119

53 **Schlaak JF**, Pitz T, Lohr HF, Meyer zum Buschenfelde KH, Gerken G. Interleukin 12 enhances deficient HCV-antigen-induced Th1-type immune response of peripheral blood mononuclear cells. *J Med Virol* 1998; **56**: 112-117

54 **Quiroga JA**, Martin J, Navas S, Carreno V. Induction of interleukin-12 production in chronic hepatitis C virus infection correlates with the hepatocelluar damage. *J Infect Dis* 1998; **178**: 247-251

55 **Leifeld L**, Cheng S, Ramakers J, Dumoulin FL, Trautwein C, Sauerbruch T, Spengler U. Imbalanced intrahepatic expression of interleukin 12, interferon gamma, and interleukin-10 in fulminant hepatitis B. *Hepatology* 2002; **36**(4 Pt 1): 1001-1008

56 **Henson PM**, Riches DW. Modulation of macrophage maturation by cytokines and lipid mediators: a potential role in resolution of pulmonary inflammation. *Ann N Y Acad Sci* 1994; **725**: 298-308

57 **Yang N**, Wu LL, Nikolic-Paterson DJ, Ng YY, Yang WC, Mu W, Gilbert RE, Cooper ME, Atkins RC, Lan HY. Local macrophage and myofibroblast proliferation in progressive renal injury in the rat remnant kidney. *Kidney Int* 1998; **54**: 143-151

58 **Segerer S**, MacK M, Regele H, Kerjaschki D, Schlondorff D. Expression of the C-C chemokine receptor 5 in human kidney diseases. *Kidney Int* 1999; **56**: 52-64

59 **Klimp AH**, de Vries EG, Scherphof GL, Daemen T. A potential role of macrophage activation in the treatment of cancer. *Crit Rev Oncol Hematol* 2002; **44**: 143–161

60 **Wel R**, Chen B, Gan TF, Zhou XM, Zhang YQ, Ren DL. Application of flow cytometry to analyzing the activation states of peripheral blood mononuclear cells CD14 macrophage. *Chin J Lab Med* 2003; **26**: 1-4

61 **Mcgrath MS**, Kodelja V. Balanced macrophage activation hypothesis: a biological model for development of drugs targeted at macrophage functional states. *Pathobiology* 1999; **67**: 277-281

62 **Gordon S**. Alternative activation of macrophages. *Nat Rev Immunol* 2003; **3**: 23-35

63 **Wand J**, Crawford K, Yuan M, Wang H, Gorry PR, Gabuzda D. Regulation of CC chemokine receptor 5 and CD4 expression and human immunodeficiency virus type 1 replication in human macrophages and microglia by T helper type 2 cytokines. *J Infect Dis* 2002; **185:** 885-897

64 **Kodellia V**, Muller C, Schebesch C, Orfanos CE, Tenorio S, Goerdt S. Differences in angiogenic potential of classically *vs* alternatively activated macrophages. *Immunobiology* 1997; **197**: 478-493

65 **Saha B**, Das G, Vohra H, Ganguly NK, Mishra GC. Macrophage-T cell interaction in experimental mycobacterial infection. Selective regulation of co-stimulatory molecules on mycobacterium-infected macrophages and its implication in the suppression of cell-mediated immune response. *Eur J Immunol* 1994; **24**: 2618-2624

66 **Kirschmann DA**, He X, Murasko DMl. Inhibition of macrophage-induced, antigen-specific T-cell proliferation by poly I : C role of suppressor macrophages. *Immunology* 1994; **82**: 238-243

67 **Liu M**, Chan CW, Mcgilvray I, Ning Q, Levy GA. Fulminant viral hepatitis: molecular and cellular basis, and clinical implications. *Expert Rev Mol Med* 2001; **28**: 1-9

68 **Shiratori Y**, Takikawa H, Kawase T, Sugimoto T. Superoxide anion generating capacity and lysosomal enzyme activities of Kupffer cells in galactosamine induced hepatitis. *Gastroenterol Jpn* 1986; **21**: 135–144

69 **Andus T**, Bauer J, Gerok W. Effects of cytokines on the liver. *Hepatology* 1991; **13**: 364-375

70 **D' Andrea A**, Rengaraju M, Valiante NM, Chehimi J, Kubin M, Aste M, Chan SH, Kobayashi M, Young D, Nickbarg E. Production of natural killer cell stimulatory factor (interleukin 12) by peripheral-blood mononuclear cells. *J Exp Med* 1992; **176**: 1387–1398

71 **Park AY**, Hondowicz BD, Scott P. IL-12 is required to maintain a Th1 response during Leishmania major infection. *J Immunol* 2000; **165**: 896–902

72 **Yap G**, Pesin M, Sher A. Cutting edge: IL-12 is required for the maintenance of IFN-gamma production in T cells mediating chronic resistance to the intracellular pathogen, Toxoplasma gondii. *J Immunol* 2000; **165**: 628–631

73 **Rossol S**, Marinos G, Carucci P, Singer MV, Williams R, Naoumov NV. Interleukin-12 induction of Th1 cytokines is important for viral clearance in chronic hepatitis B. *J Clin Invest* 1997; **99**: 3025-3033

74 **Chen YP**, Feng XR, Dai L, Ding HB, Zhang L. Screening and evaluation of non-invasive diagnosis markers for compensated liver cirrhosis in patients with chronic hepatitis B. *Zhonghua Ganzangbing Zazhi* 2003; **11**: 225-227

75 **Sakaguchi E**, Kayano K, Segawa M, Aoyagi M, Sakaida I, Okita K. Th1/Th2 imbalance in HCV-related liver cirrhosis. *Nippon Rinsho* 2001; **59**: 1259-1263

76 **Sreenarasimhaiah J**, Jaramillo A, Crippin J, Lisker-Melman M, Chapman WC, Mohanakumar T. Lack of optimal T-cell reactivity against the hepatitis C virus is associated with the development of fibrosis/cirrhosis during chronic hepatitis. *Hum Immunol* 2003; **64**: 224-230

77 **Kitching AR**, Tipping PG, Mutch DA, Huang XR, Holdsworth SR. Interleukin-4 deficiency enhances Th1 responses and crescentic glomerulonephritis in mice. *Kidney Int* 1998; **53**: 112-118

78 **Raffanti SP,** Schaffner W, Federspiel CF, Blackwell RB, Ching OA, Kuhne FW. Randomized, double-blind placebo-controlled

trial of the immune modulator WF10 in patients with advanced AIDS. *Infection* 1998; **26**: 202-207
79 **Rovin BH.** Chemokine blockade as a therapy for renal disease. *Curr Opin Nephrol Hypertens* 2000; **9**: 225-232
80 **Erwig LP**, Stewart K, Rees AJ. Macrophages from inflamed but not normal glomeruli are unresponsive to anti-inflammatory cytokines. *Am J Pathol* 2000; **156**: 295-301
81 **Kluth DC**, Rees AJ. New approaches to modify glomerular inflammation. *J Nephrol* 1999; **12**: 66-75
82 **Nelson DR**, Tu Z, Soldevila-Pico C, Abdelmalek M, Zhu H, Xu YL, Cabrera R, Liu C, Davis GL. Long-term interleukin 10 therapy in chronic hepatitis C patients has a proviral and anti-inflammatory effect. *Hepatology* 2003; **38**: 859-868
83 **Sakaguchi E**, Kayano K, Segawa M, Okamoto M, Sakaida I, Okita K. Th1 down-regulation at the single-lymphocyte level in HCV-related liver cirrhosis and the effect of TGF-beta on Th1 response: possible implications for the development of hepatoma. *Hepatol Res* 2002; **24**: 282
84 **Wilson HM**, Minto AW, Brown PA, Erwig LP, Rees AJ. Transforming growth factor-beta isoforms and glomerular injury in nephrotoxic nephritis. *Kidney Int* 2000; **57**: 2434-2444
85 **McGrath MS**, Benike C, Kuchne FW, Engleman E. Effect of WF10 (TCDO) on antigen presentation. *Transplant Proc* 1998; **30**: 4200-4204
86 **Tsai SL**, Sheen IS, Chien RN, Chu CM, Huang HC, Chuang YL, Lee TH, Liao SK, Lin CL, Kuo GC, Liaw YF. Activation of Th1 immunity is a common immune mechanism for the successful treatment of hepatitis B and C: tetramer assay and therapeutic implications. *J Biomed Sci* 2003; **10**: 120-135
87 **Ding CL**, Yao K, Zhang TT, Zhou F, Xu L, Xu JY. Generation of cytotoxic T cell against HBcAg using retrovirally transduced dendritic cells. *World J Gastroenterol* 2003; **9**: 1512-1515
88 **Teuber G**, Rossol S, Lee JH, Dietrich CF, Zeuzem S. TH1/TH2 serum cytokine profiles and soluble TNF-receptor response in patients with chronic hepatitis C during recombinant human interleukin-12 (rHuIL-12) treatment. Z *Gastroenterol* 2002; **40**: 487-495
89 **Barth H,** Klein R, Berg PA, Wiedenmann B, Hopf U, Berg T. Analysis of the effect of IL-12 therapy on immunoregulatory T-cell subsets in patients with chronic hepatitis C infection. *Hepatogastroenterology* 2003; **50**: 201-206
90 **Pockros PJ**, Patel K, O'Brien C, Tong M, Smith C, Rustgi V, Carithers RL, McHutchison JG, Olek E, Debruin MF. A multicenter study of recombinant human interleukin 12 for the treatment of chronic hepatitis C virus infection in patients nonresponsive to previous therapy. *Hepatology* 2003; **37**: 1368-1374
91 **Zeuzem S**, Carreno V. Interleukin-12 in the treatment of chronic hepatitis B and C. *Antiviral Res* 2001; **52**: 181-188
92 **Wang S**, Lin Y, Ma W, Zhang B, Qi S, Lan F. Effect of IL-12 on IFN-gamma and IL-10 produced by peripheral blood mononuclear cells in patients with chronic hepatitis B virus infection during IFN-alpha treatment. *Zhonghua Ganzangbing Zazhi* 2002; **10**: 116-119
93 **Barth H**, Klein R, Berg PA, Wiedenmann B, Hopf U, Berg T. Induction of T helper cell type 1 response and elimination of HBeAg during treatment with IL-12 in a patient with therapy-refractory chronic hepatitis B. *Hepatogastroenterology* 2001; **48**: 553-555

Edited by Liu HX and Xu FM

PO Box 2345, Beijing 100023, China
Fax: +86-10-85381893
E-mail: wjg@wjgnet.com www.wjgnet.com

World J Gastroenterol 2004;10(12):1716-1721
World Journal of Gastroenterology
Copyright ©2004 by The WJG Press ISSN 1007-9327

• ESOPHAGEAL CANCER •

Differential gene expression between squamous cell carcinoma of esophageus and its normal epithelium; altered pattern of mal, akr1c2, and rab11a expression

Sakineh Kazemi-Noureini, Sergio Colonna-Romano, Abed-Ali Ziaee, Mohammad-Ali Malboobi, Mansour Yazdanbod, Parviz Setayeshgar, Bruno Maresca

Sakineh Kazemi-Noureini, Abed-Ali Ziaee, Institute of Biochemistry and Biophysics, University of Tehran, Tehran, Iran; PO Box: 13145-1384
Sergio Colonna-Romano, International Institute of Genetics and Biophysics, National Research Council, Via Marconi 12, 80125 Naples, Italy
Mohammad-Ali Malboobi, National Research Center for Genetic Engineering and Biotechnology (NRCGEB), Tehran, Iran
Mansour Yazdanbod, Shariati Hospital, Department of Surgery, Medical University of Tehran, Tehran, Iran
Parviz Setayeshgar, Pathology department, Madaen Hospital, Tehran, Iran
Bruno Maresca, International Institute of Genetics and Biophysics, National Research Council, Via Marconi 12, 80125 Naples, Italy; and University of Salerno, School of Pharmacy, Dept. Pharmaceutical Sciences, Fisciano, Salerno, Italy
Correspondence to: Associate Professor Abed-Ali Ziaee (Ph.D.), Institute of Biochemistry and Biophysics,University of Tehran, PO Box: 13145-1384, Tehran, Iran. aa_ziaee@yahoo.uk.co
Telephone: +98-21-6956975 **Fax:** +98-21-6404680
Received: 2003-08-23 **Accepted:** 2003-12-01

Abstract

AIM: To identify the altered gene expression patterns in squamous cell carcinoma of esophagus (ESCC) in relation to adjacent normal esophageal epithelium.

METHODS: Total RNA was extracted using SV total RNA isolation kit from snap frozen tissues of ESCC samples and normal esophageal epithelium far from the tumor. Radio-labeled cDNA were synthesized from equal quantities of total RNAs of tumor and normal tissues using combinations of 24 arbitrary 13-mer primers and three different anchoring oligo-dT primers and separated on sequencing gels. cDNA with considerable different amounts of signals in tumor and normal tissue were reamplified and cloned. Using southern blot, the clones of each band were controlled for false positive results caused by probable heterogeneity of cDNA population with the same size. Clones that confirmed differential expression by slot blot selected for sequencing and northern analysis. Corresponding full-length gene sequences was predicted using human genome project data, related transcripts were translated and used for various protein/motif searches to speculate their probable functions.

RESULTS: The 97 genes showed different levels of cDNA in tumor and normal tissues of esophagus. The expression of mal gene was remarkably down regulated in all 10 surveyed tumor tissues. Akr1c2, a member of the aldo-keto reductase 1C family, which is involved in metabolism of sex hormones and xenobiotics, was up-regulated in 8 out of 10 inspected ESCC samples. Rab11a, RPL7, and RPL28 showed moderate levels of differential expression. Many other cDNAs remained to further studies.

CONCLUSION: The mal gene which is switched-off in all ESCC samples can be considered as a tumor suppressor gene that more studies in its regulation may lead to valuable explanations in ESCC development. Akr1c2 which is up-regulated in ESCC probably plays an important role in tumor development of esophagus and may be proposed as a potential molecular target in ESCC treatments. Differential display technique in spite of many disadvantages is still a valuable technique in gene function exploration studies to find new candidates for improved ones like gene chips.

Kazemi-Noureini S, Colonna-Romano S, Ziaee AA, Malboobi MA, Yazdanbod M, Setayeshgar P, Maresca B. Differential gene expression between squamous cell carcinoma of esophageus and its normal epithelium; altered pattern of mal, akr1c2, and rab11a expression. *World J Gastroenterol* 2004; 10(12): 1716-1721
http://www.wjgnet.com/1007-9327/10/1716.asp

INTRODUCTION

Esophageal squamous cell carcinoma (ESCC) is a predominant kind of cancer in the developing world as well as the north and northeast of Iran, which show age-standardized incidence rate of about 150 per 100 000 person-years for both sexes[1]. The exposure of esophageal cells to both exogenous agents such as food, alcohol, smoke and endogenous causes such as genetic and inflammation of esophagus tissue as well as the race and cultural habits have been accounted for high incidence in certain geographical regions[2]. Many genes including several oncogenes and tumor suppressor genes are deregulated in esophageal cancrcinoma[3, 4]. Some new publications reported gene expression profiles of normal and ESCC tissues recently[5-8].

Two-dimensional gel electrophoresis has been already studied in Institute of Biochemistry and Biophysics, University of Tehran, Tehran, Iran to compare the protein populations of normal esophagus and ESCC tissues[9]. A predominant transition of C to T at CpG dinucleotides has been reported for p53 gene as well as over expression of cox-2 gene and accumulation of nitrotyrosine was detected in ESCC tumors of Iranian patients[10] confirming the concept of chronic inflammatory stress and sensitivity of esophageal cells to exogenous risk factors are involved in ESCC development in Iranian patients.

In order to find new molecular markers suitable for diagnosis and to identify probable potent molecular targets for drug design we started to screen genes with different levels of expression in normal and ESCC tissues of patients that were operated in 2 000 in Madean Hospital. Using differential display methodology on fresh normal and cancer tissues in this propose we scanned expression of almost 6 000 genes. Using this

technique we tried to screen out all real mRNA population of transcribed genes in tumor and normal tissues in order to include the probable unknown genes too. Among them 97 cDNAs were found with lower or higher expression levels in comparing normal and tumor tissues. 47 cDNAs with remarkable different levels of expression between normal and tumor states were cloned. Six genes that confirmed to have different expression in normal and ESCC tumor tissues are reported here.

MATERIALS AND METHODS

Tissue collection and sample preparation

Tumor tissues of ESCC patients and normal adjacent parts were surgically removed and snap frozen in liquid nitrogen and stored at -80 ℃ until use. By histopathological examinations tumors were classified into three major groups of well, moderately, and poorly differentiated squamous cell carcinoma according to WHO classification by a pathologist. A brief pathological and clinical data of the patients were shown in Table 1[12]. Histological normal adjacent epithelium from the same patient was used as the normal pair. A pair of tumor and normal tissues both from the same patient (RP; as reference patient) was chosen randomly for differential display. According to the clinical date this patient is a 47-year-old woman carried moderately differentiated tumor with reactive lymph nodes, which is an indicative of non-metastatic tumor. For a survey of gene expression in other ECSS patients, northern blotting was conducted for RP and nine other ESCC patients at different stages of tumor development. Patients were middle- to old-age all living in north of Iran.

Table 1 Sex, age and histopathological status of the inspected ESCC patients

No	Sex	Age	Differentiation degree of ESCC tumor	Metastatic lymphnodes
1	F	47	Moderately differentiated	None
2	M	53	Well differentiated	3 out of 8
3	F	47	Well differentiated	2 out of 10
4	F	50	Moderately differentiated	1 out of 1
5	M	69	Moderately differentiated	3 out of 9
6	F	60	Moderately differentiated	1 out of 6
7	M	66	Moderately differentiated	All five
8	M	76	Moderately differentiated	None
9	F	55	Poorly differentiated	No evidence
10	F	70	Well differentiated	All three

RNA purification

Using SV Total RNA extraction Kit (Promega), total RNA was purified from ESCC tumor and normal tissue pairs of the same patient in parallel. After DNase-I treatment, DNA-free RNA was recovered in a solution of 0.01 mol/L dithiotriotol (DTT), 10 U/L RNasin (Promega) in diethyl pyrocarbonate-treated water. The quality of RNAs and quantifications were done by spectrophotometry of Absorbency at 260 nm and gel electrophoresis.

Differential display reverse transcriptase-PCR

After 5 min of incubation of 0.2 g of RNA samples at 65 ℃, reverse transcriptions were done in 20 L reactions RT buffer containing 50 mmol/L Tris-HCl (pH 8.3), 125 mmol/L KCl, 5 mmol/L $MgCl_2$, 0.01 mol/L DDT, 0.2 mol/L of a anchored oligo-dT11M (where M is A, C or G), 20 mol/L dNTPs and 200 U SuperScript™ RNase-H$^-$ Reverse Transcriptase (Gibco BRL), for 60 min at 37 ℃. For amplification 2.0 μL of each reverse transcribed RNA was added into a 20 l reaction containing 1.25 mmol/L $MgCl_2$, 2.0 μmol/L dNTPs, 0.2 μmol/L of the respective oligo-dT 11 mol/L, 0.2 mol/L of one 13-mer arbitrary primer, 1 μL [^{35}S]dATP [4.44×10^4 GBq/mmoL (1 200 Ci/mmoL), Amersham] and 1.0 U of Ampli-Taq (Perkin Elmer). PCR cycles/parameters were: a denaturation step at 94 ℃ for 5 min followed by 3 cycles at 94 ℃ for 30 s, 42 ℃ for 2 min, 72 ℃ for 30 s, and 37 cycles at 94 ℃ for 30 s, 45 ℃ for 2 min, 72 ℃ 30 s and a final extension at 72 ℃ for 5 min.

Identification and cloning of differentially expressed cDNA bands

The amplified products of DDRT-PCR were fractionated on standard 60 g/L poly-acrylamide/urea gel, and then transferred to 3 mm filter paper (Amersham) without methanol/acetic acid fixing, dried and exposed to X-ray film overnight. The putative differentially displayed bands that showed the same pattern of expression in repeated DDRT gels were eluted and re-amplified by the same primers used in related first amplification sets. Molecular mass and quality of re-amplified cDNA fragments were checked by gel electrophoresis before cloning into the cloning vector pCR2.1 (Invitrogen Co, CA). Escherichia coli TOP10 harboring recombinant plasmids of pCR2.1 were selected on agar plates containing ampicillin and X-gal. Since probable heterogeneity in cDNA populations of the same size existing in each band can leads to false positive results, for each cloned band six single well grown colonies were subjected to Southern blot. Radio-labeled probe was prepared from the inserted fragment of one of these six colonies.

Slot and northern blots analysis

For slot blots preparation, 2.0 g of RNA samples were vacuum-dried and resuspended in 50 L of DEPC-dd H_2O. Fifty microliters of formaldehyde/20SSC solution (1:1 vol/vol) was added and incubated for15 min at 60 ℃ before loading on nylon filters (Hybond, Amersham, UK). For northern blots, 30 g of N and T total RNAs were run on denaturing 1.2 g/L agarose gel and blotted onto Hybond membrane dried at 37 ℃ and fixed using UV cross-linking. As probes, gel purified cDNA fragments of interest were radio-labeled using High Prim™ DNA labeling system (Boheringer) and 4 of [-^{32}P]-dCTP [1.11×10^5 GBq/mmoL (3 000 Ci/mmoL), Amersham]. Blots were hybridized with respective probes in hybridization solution containing 0.5 mol/L phosphate buffer pH 7.2, 10 mmol/L EDTA and 50 g/L SDS at 60 ℃ overnight. Filters were washed twice at 55 ℃ in 0.1 hybridization solution for 15 min and scanned with a phosphor imager SF (Molecular Dynamics) following 4 h exposure at room temperature. Differentially expressed cDNA clones were sequenced using Sequenase kit Version 2.0 (USB) and fractionated on standard sequencing gels[13].

Analysis of the sequences

Data entry, sequence management, sequence alignment and protein sequence analysis were performed by Lasergene software package[12]. Sequence similarity search and several structural features were predicted by the use of online databases and related software including BLAST N, X and P (www.ncbi.nlm.nih.gov/BLAST/)[13,14], Pfam (www.sanger.ac.uk/Software/Pfam/search.shtml)[15], PRINTS (www.bioinf.man.ac.uk/dbbrowser/PRINTS/)[16,17], Blocks (condor.urbb.jussieu.fr/logiciels/Protein_Blocks/Structural_Words/motif_PB_m.html)[18], SMART (www.bork.embl-heidelberg.de/NAIL/RSmart)[19,20], PROSITE (www.expasy.org/prosite/)[21] and PSORT (psort.nibb.ac.jp/form.html)[22].

RESULTS

Isolation of differentially expressed genes

The expression pattern of about 6 000 genes was scanned using combinations of 24 arbitrary 13-mer primers and three different anchoring oligo-dT primers in differential display reverse transcription-PCR reactions. We identified 97 genes with

different levels of cDNA in tumor and normal tissues of esophagus. 47 bands with considerable differential level of cDNA signals in tumor and normal tissues (Figure 1 panel A; Table 2) were reamplified and cloned. The clones that confirmed differential expression by slot blot (Figure 1 panel B) were selected for sequencing and northern analysis on other tumor samples. To annotate the isolated cDNA fragments, corresponding full-length gene sequences was predicted by the use of human genome project data (Table 2). The generated transcripts were translated and used for various protein motif searches.

Down regulation of mal gene

A 360-bp cDNA fragment, ESC1 clone, was found down regulated in ESCC tumor cells (Figure 1). ESC1 sequence was localized to 2cen-q13 locus of chromosome 2 that encompass mal gene, a T-cell differentiation antigen. The amino acid sequence encoded by ESC1 aligned with the last 34 amino acids at the C-terminal of human MAL protein family members (Table 2). The available data shows that mal gene encodes four transcript variants as a result of alternative splicing. The detected band with estimated mRNA size of almost 1.1 kb by northern blot, strongly suggests that Mal-a variant is the only form expressed in normal esophagus. The expression of this gene was found to be down regulated in all 10 surveyed patients carrying tumors at different stages of ESCC (Figure 2).

Induced expression of a member of ras oncogene family

Another under-represented gene was found as a 273-bp cDNA fragment named ESC2 (Figure 1). The expression level of the related gene to ESC2, with approximate length of 1.0 kb mRNA,

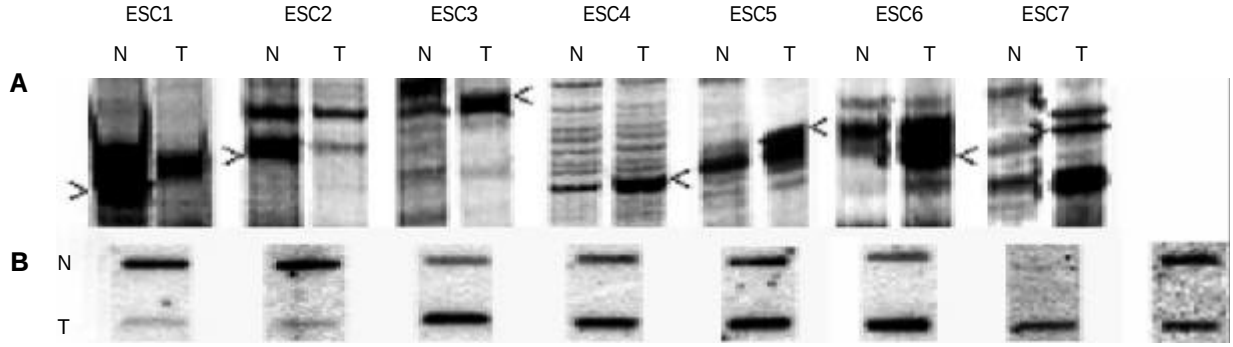

Figure 1 Parts of DDRT gels including cDNA fragments that show transcriptional alteration in comparing normal esophageal and ESCC tissues (have been pointed with arrows (panel A)), and the results of slot blots containing two microgram RNAs of normal (N) and tumor (T) tissues of esophagus in hybridization with radio-labeled related cDNAs (panel B). All of the slots have been prepared simultaneously and from the same RNA stocks of T and N. One piece of the slots has been hybridized with radio-labeled GADPH probe as shown in the right most side in panel B.

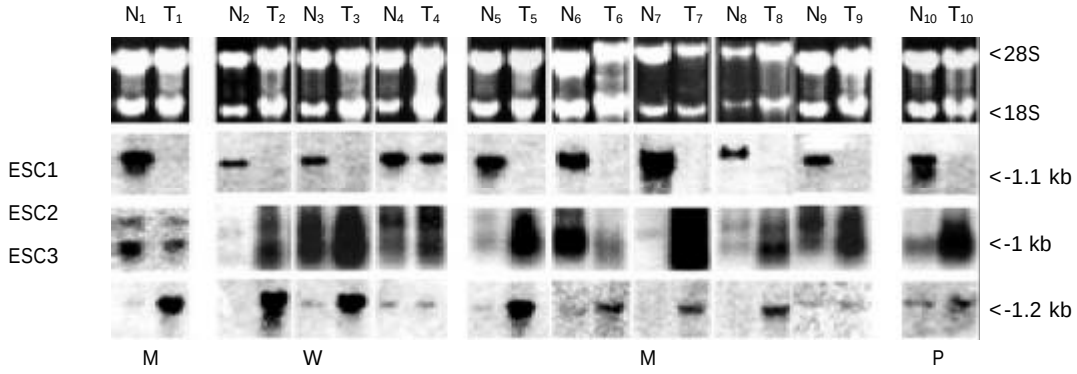

Figure 2 Northern results of patient 1 (RP) and other patients in hybridization with radio-labeled probes of ESC1, ESC2 and ESC3. Each northern membrane contains about 30 micrograms RNA of normal (N) and tumor (T) tissues of esophagus. The differentiation status of each tumor has been shown as W: Well differentiated tumor; M: Moderately differentiated tumor; P: poorly differentiated tumor. The estimated sizes of each bands has been shown on the right side and the ethidium bromide stained gel on top shows the relative amounts of RNAs loaded in each lane.

Table 2 The cDNAs, primers have been used in RT reactions and their related genes with different expression level in normal esophageal and ESCC tissues

cDNA name	cDNA's length (bp)	3' end primer (5'→3')	5' end primer (5'→3')	GeneBank accession number
ESC1	360	AAG CTT TTT TTT TTT G	AAG CTT TAC GTA C	BC000458
ESC2	273	AAG CTT TTT TTT TTT A	AAG CTT CTC AGA C	BC013348
ESC3	300	AAG CTT TTT TTT TTT C	AAG CTT CTC AGA C	BC007024
ESC4	325	AAG CTT TTT TTT TTT C	AAG CTT AAC GAGG	BC006095
ESC5	442	AAG CTT TTT TTT TTT G	AAG CTT GAT TCG C	BC000072
ESC6	271	AAG CTT TTT TTT TTT C	AAG CTT GCG ATG T	AF_061732
ESC7	273	AAG CTT TTT TTT TTT C	AAG CTT TGG TCA G	NM001759

in RP and patient no. 6 was consistent with that observation. However it showed increased level of expression in five tumors (no. 2, 5, 7, 9, 10) out of eight other patients (Figure 2). The sequence of ESC2 was identical to a sequence localized at chromosome 15q21 of human genome corresponding to the 3' region of human rab11a gene. The expression of this gene was down regulated in RP and patient no.6 while over-expressed in 5 other surveyed patients and unchanged in three others. No clear correlation was detected between the rab11a expression and pathological parameters and/or patients prognosis.

Up-regulation of an aldo-keto reductase encoding gene

A 300 bp of cDNA fragment, ESC3 clone, was clearly up regulated in ESCC tumor (Figure 1). ESC3 sequence identified a locus on chromosome 10 p15 encoding AKR1C1, 2 and 3 three members of aldo-keto reductase protein family 1C. The nucleotide sequence of ESC3 is identical to 3' end of AKR1C2. The corresponding protein sequence encompasses all six conserved blocks of the family. This gene is highly expressed in 8 out of 10 tumors of different stages of ESCC (Figure 2). Low abundance of its transcripts was detected in the other two patients. Again, no clear correlation was found between the expression level and histopathological classification of tumor samples (Figure 2) (Table 2).

Other differentially expressed genes

The expression of two cDNA fragments ESC4 and 5 with the length of 325 bp and 442 bp, respectively, were found to be induced in tumor tissues (Figure 1). They are localized on locus 5q32, the location of ribosomal protein L7 (RpL7), which is a member of RPL30 gene family, and on chromosome 19q13.4 that juxtaexpose the location of ribosomal protein 28 (RpL28) encoding gene respectively. Both of these ribosomal proteins are the components of 60S subunit of ribosome. Northern blots showed increase expression of RpL7 (ESC4) in three tumor samples of ESCC (pair no.1; 4 and 5 if RNA shown in the first panel is normalized), while there is no substatial alterations for its expression in other pairs (Figure 3). The over-expression of RpL28 (ESC5) was confirmed on at least 4 out of 6 ESCC tumor samples by northern (Figure 3, pair samples No: 1, 3, 5 and 8). ESC6 clone carries a 271 bp cDNA fragment that contains a sequence identical to100-amino acid hypothetical protein, which is moderately over expressed in tumor tissues of RP. A longer transcript of this sequence is also seen in related counting constructed from ESTs in TIGR and GeneBank (Table 2). This contig for ESC6 locates on 19p13.2 as shown by BLAST searches in Map Viewer. This aligned with a fetus brain protein called My029. The motif searches in BLOCKS, Pfam, CD, TIGR fam failed to identify any conserved motif, while there are two bipartite nuclear targeting sequence (RRqpslrglksrrkprc), three protein kinase C phosphorylation sites as showed by PSORT seraches. Northern analysis shows a moderate over expression of this gene in at least 4 out of 6 samples of well and moderately differentiated ESCC tumors (Figure 3).

The sequence of a 273 bp cDNA fragment, ESC7, localized in 12p13 that code for cyclin D2. Northern analysis on normal and tumor RNA of RP indicates the over expression of this gene in ESCC (Figure 1). No further work was done on this clone.

DISCUSSION

The expression level of two genes encoding MAL, and AKR1C2 have been enormously altered, so that they may be mentioned as switched off and on genes respectively, while the other genes as ribosomal proteins L7 and L28 and a hypothetical protein showed moderate differences of expression between normal and tumor tissues. Except for mal gene[23], differential expression of the other genes in ESCC is reported for the first time in this study.

ESC1 and 2 are the related clones for genes encode for two membrane proteins MAL and Rab11a respectively. A clear suppression of mal gene is seen in all ten ESCC samples (Figure 2). Mal gene has been already shown to express in four alternatively spliced forms of transcripts during intermediate and late stages of T-cell differentiation[24], also in differentiating epithelial cells[25]. The possible roles for MAL¨ Cglycosphingolipid complexes in cell signaling, differentiation and apical sorting have been suggested[25]. Here, we report down-regulation of this gene in all surveyed Iranian ESCC patients with different stages of tumor development, which is in good agreement by similar observations from China[23] and Japan[26]. As mal gene is up-regulated during the late stages of T-cell[24] and urothelial cells[25] differentiation, the switching-off of this gene in ESCC may suggest its involvement in a determining event in developing esophageal cancer. Although further studies are needed to clarify the role of MAL in normal esophageal cells and regulation of its expression, in a recent study the ectopic expression of MAL in carcinoma TE3 cells led to repressed formation of tumor induced by TE3 cells in nude mice, inhibition of cell motility and production of apoptosis by Fas pathway[26]. These observations suggest MAL protein as a potential candidate for ESCC diagnosis/ treatment and we expect it to be a tumor suppressor protein as it has been reported just recently[26].

Rab11a, a non-oncogene member of small GTPase Ras oncogene family, involves in secretory pathways, vesicle trafficking and apical recycling system in epithelial cells[27]. The most important role of Rab11a might be to facilitate cell migration

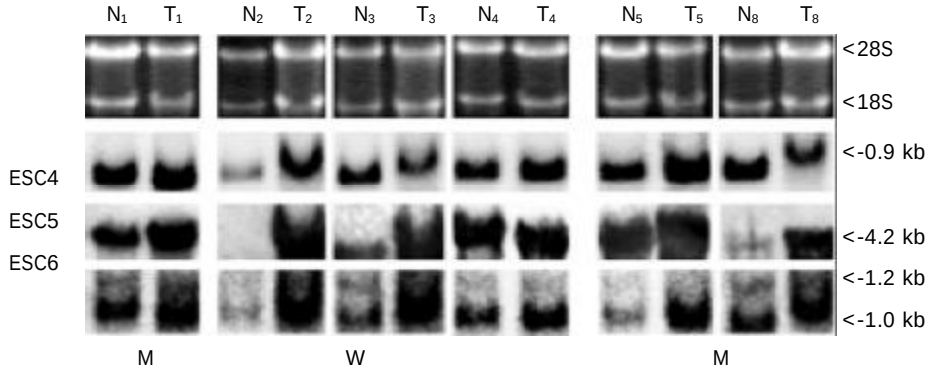

Figure 3 Northern results of patient 1 (RP) and other patients in hybridization with radio-labeled probes of ESC4, ESC5 and ESC6. Each northern membrane contains about 20 µg RNA of normal (N) and tumor (T) tissues of esophagus. The differentiation status of each tumor has been shown as W: Well differentiated tumor; M: Moderately differentiated tumor. The estimated sizes of each bands has been shown on the right side and the ethidium bromide stained gel on top shows the relative amounts of RNAs loaded in each lane.

by internalizing integrins at the rear of cell and transporting them forward at the leading edge to form new contacts with the extra cellular matrix[28]. To our knowledge, this is the first report of alterations of Rab11a expression in ESCC cancer. Similarly, massive synthesis of mRNA and protein of Rab11 was observed in cell line of esophagus adenocarcinoma and in low-grade dysplastic cells during esophageal adenocarcinoma development[29]. Roles rab11a can play in ESCC is to be studied.

One of the most important results of this study was demonstration of the up regulation of gene encoding AKR1C2 that catalyzes the interconversion of aldehydes and ketones to their corresponding alcohol compounds in sex hormones and similar substrates. Such reactions lead to the production of reactive oxygen species (ROS) and consequent DNA damage as carcinogenesis progresses[30]. Akr1c2 is also over expressed in lung carcinoma cell line[31], in non-small cell lung cancer[32], and in ovarian carcinoma cells[33]. The pertinent enzyme activity, dehydration dehydrogenase type 2 (DDH2), (EC 1.1.1.213) plays a critical role in metabolism of steroid hormone[34], drugs[35] and polycyclic aromatic hydrocarbons (PAH)[36]. As the esophagus tissue is not directly involved in steroid hormone metabolism the most probable substrate for this enzyme can be polycyclic aromatic hydrocarbons (PAH), some drugs and so on[35]. During metabolic pathway of these xenobiotic compounds, the resulting o-quinones lead to stable depurination of DNA adducts[36] that in turn can establish futile redox cycles and amplify ROS. These by-products are potent causative agents for establishing G to T transversion commonly found in ras and p53 genes[37,38] as shown to occur in ESCC tumors too[10]. Indeed oxidative stress has been considered as a major pathogenic factor in esophageal carcinoma[39].

Furthermore oxidative stress leads to 4-hydroxy-2-nonenal (HNE) formation during lipid peroxidation, which diffuses through the cell membranes and with a longer half-life, it is even more destructive than ROS[40]. On the other hand HNE specifically induces the expression of AKR1C1 isoform[40]. Since AKR1C2 and AKR1C1 differ for only seven amino acids, it is indistinguishable if AKR1C1 is also being over-expressed in ESCC. As these two enzymes differ just slightly in their untranslated 3' end regions, at least some portions of the signal in northern can belong to akr1c1 transcripts so that both enzymes may be up-regulated in ESCC.

A clear up-regulation of akr1c2 in 8 out of 10 tumor samples of Iranian ESCC patients with different degrees of tumor development was shown in Figure 2. This enzyme is suggested to be involved in esophageal carcinogenesis at least indirectly, and this speculation is in a good agreement with the hypothesis of PAH exposure association with carcinogenesis of this tissue[41]. However AKR1C2 is of special interest in cancer biology and drug design for prostate cancer[42] and may be considered also as a potent molecular target in ESCC treatments.

The expression of RpL7 is higher in tumor tissues of all three samples of ESCC, wherein the amount of normal and tumor RNA can be normalized, considering the signals showed in Figure 2 for ESC4. The up-regulation of RpL7 has been reported recently in prostate cancer too[43]. Several ribosomal proteins are suggested to be involved in cell proliferation, apoptosis, DNA repair, regulation of development and malignancies as their second function[44], however the possible role of this protein in cancer cells remains to be clear. ESC5 cDNA fragment, that identified as RpL28 shows a higher expression in tumor tissues of ESCC. RpL28 seems to have a regulatory role as it is strongly ubiquitinated during S phase in Saccharomyces cerevisiae, while the levels of RpL28 ubiquitination is reduced in G1. As the human ortholog of RpL28 is also ubiquitinated, this modification is highly conserved in evolution, and a probable regulatory role for multiubiquitin of RpL28 has been speculated not necessarily as a target for degradation[45].

We have seen also the over expression of cyclin D2 using Northern blot on RNA samples of RP, but no more experiments have done on other patients because of low amounts of available RNA. Although the over expression of Cyclin D2 in different kinds of squamous carcinoma cell lines has been shown to modulate proliferation after induced quiescence and enhance *in vivo* aggressive growth behavior[46], however the RP sample has no metstasis in pathology report of tumor.

It is obviously anticipated that many genes are involved in carcinogenesis of esophagus, although differential expression of these genes could be the consequence rather than a cause. Many complicated events like cell to cell/matrix interactions, cell communications and transportations, normal regulation of protein synthesis, translation and cell cycle regulation as well as metabolic enzymes are affected by cancer development of esophagus.

ACKNOWLEDGEMNETS

We would like to thank Alfredo Franco Romano for his technical assists. This work has been done in collaboration between Molecular Biology Lab, Institute of Biochemistry and Biophysics, University of Tehran and Cell Stress Lab, International Institute of Biophysics and Genetics, Naples as a part of Ph.D. thesis of Sakineh Kazemi-Noureini.

REFERENCES

1 **Saidi F**, Sepehr A, Fahimi S, Farahvash MJ, Salehian P, Esmailzadeh A, Keshoofy M, Pirmoazen N, Yazdanbod M, Roshan MK. Oesophageal cancer among the Turkomans of northeast Iran. *Br J Cancer* 2000; **83**: 1249-1254

2 **Munoz N**. Epidemiological aspects of oesophageal cancer. *Endoscopy* 1993; **23**: 609-612

3 **Lam AK**. Molecular biology of oesophageal squamous cell carcinoma. *Crit Rev Oncol Hematol* 2000; **33**: 71-90

4 **Mandard AM**, Hainaut P, Hollstein M. Genetic steps in the development of squamous cell carcinoma of the esophagus. *Mutat Res* 2000; **462**: 335-342

5 **Graber MW**, Schweinfest CW, Reed CE, Papas TS, Baron PL. Isolation of differentially expressed genes in carcinoma of the esophagus. *Ann Surg Oncol* 1996; **3**: 192-197

6 **Xu Z**, Wang MR, Xu X, Cai Y, Han YL, Wu KM, Wang J, Chen BS, Wang XQ, Wu M. Novel human esophagus-specific gene C1orf10: cDNA cloning, gene structure, and frequent loss of expression in oesophageal cancer. *Genomics* 2000; **69**: 322-330

7 **Hu YC**, Lam KY, Law S, Wong J, Srivastava G. Identification of differentially expressed genes in esophageal squamous cell carcinoma (ESCC) by cDNA expression array: overexpression of Fra-1, Neogenin, Id-1 and CDC25B genes in ESCC. *Clin Cancer Res* 2001; **7:** 2213-2221

8 **Zhou J**, Zhao LQ, Xiong MM, Wang XQ, Yang GR, Qiu ZL, Wu M, Liu ZH. Gene expression profiles at different stages of human esophageal squamous cell carcinoma. *World J Gastroenterol* 2003; **9**: 9-15

9 **Rastegar-Jazii F**, Ziaee AA, Yazdanbod M. Application of two-dimensional electrophoresis and HIH 3T3 cell transfection assay in the study of tumor-associated proteins and genomic DNA tumorigenicity in malignant human oesophageal specimens. *J Sciences IRI* 1998; **9**: 216-225

10 **Sepehr A**, Taniere P, Martel-Planche G, Ziaee AA, Rastegar-Jazi F, Yazdanbod M, Etemad-Moghadam G, Kamangar F, Saidi F, Hainaut P. Distinct pattern of TP53 mutations in squamous cell carcinoma of the esophagus in Iran. *Oncogene* 2001; **20**: 7368-7374

11 **Watanabe H**, Jass JR, Sobin LH. Histological typing of oesophageal and gastric tumors. In: International Histological Classification of Tumors, Ed. 2. *Berlin: Springer-Verlag* 1990

12 **Burland TG**. DNASTAR's Lasergene sequence analysis software. *Methods Mol Biol* 2000; **132**: 71-91

13 **Gish W**, States DJ. Identification of protein coding regions by database similarity search. *Nat Genet* 1993; **3**: 266-272

14 **Pertsemlidis A**, Fondon JW 3rd. Having a BLAST with bioinformatics (and avoiding BLASTphemy). *Genome Biol* 2001; **2**: REVIEWS 2002
15 **Bateman A**, Birney E, Durbin R, Eddy SR, Howe KL, Sonnhammer ELL. The Pfam protein families database. *Nucleic Acid Res* 2000; **28**: 263-266
16 **Attwood TK**, Croning MD, Flower DR, Lewis AP, Mabey JE, Scordis P, Selley NL, Wright W. PRINTS-S: the database formerly known as PRINTS. *Nucleic Acid Res* 2000; **28**: 225-227
17 **Attwood TK**, Blythe MJ, Flower DR, Gaulton A, Mabey JE, Maudling N, McGregor L, Mitchell AL, Moulton G, Paine K, Scordis P. PRINTS and PRINTS-S shed light on protein ancestry. *Nucleic Acids Res* 2002; **30**: 239-241
18 **Pietrokovski S.** Searching databases of conserved seqeuence regions by aligning protein multiple-alignments. *Nucleic Acids Res* 1996; **24**: 3836-3845
19 **Schultz J**, Copley RR, Doerks T, Ponting CP, Bork P. A web-based tool for the study of genetically mobile domains. *Nucleic Acid Res* 2000; **28**: 231-234
20 **Letunic I**, Goodstadt L, Dickens NJ, Doerks T, Schultz J, Mott R, Ciccarelli F, Copley RR, Ponting CP, Bork P. Recent improvements to the SMART domain-based sequence annotation resource. *Nucleic Acids Res* 2002; **30**: 242-244
21 **Falquet L**, Pagni M, Bucher P, Hulo N, Sigrist CJ, Hofmann K, Bairoch A. The PROSITE database, its status in 2002. *Nucleic Acids Res* 2002; **30:** 235-238
22 **Nakai K**, Horton P. PSORT: a program for detecting sorting signals in proteins and predicting their subcellular localization. *Trends Biochem Sci* 1999; **24**: 34-36
23 **Wang Z**, Wang M, Xu X, Xu Z, Han Y, Cai Y, Sun Y, Wu M. Studies of MAL gene in human oesophageal cancer by RNA in situ hybridization. *Zhonghua Yixue Yichuanxue Zazhi* 2000; **17**: 329-331
24 **Alonso MA**, Weissman SM. cDNA cloning and sequence of MAL, a hydrophobic protein associated with human T-cell differentiation. *Proc Natl Acad Sci U S A* 1987; **84**: 1997-2001
25 **Liebert M,** Hubbel A, Chung M, Wedemeyer G, Lomax MI, Hegeman A, Yuan TY, Brozovich M, Wheelock MJ, Grossman HB. Expression of mal is associated with urothelial differentiation *in vitro*: identification by differential display reverse-transcriptase polymerase chain reaction. *Differentiation* 1997; **61**: 177-185
26 **Mimori K**, Shiraishi T, Mashino K, Sonoda H, Yamashita K, Yoshinaga K, Masuda T, Utsunomiya T, Alonso MA, Inoue H, Mori M. MAL gene expression in esophageal cancer suppresses motility, invasion and tumorigenicity and enhances apoptosis through the Fas pathway. *Oncogene* 2003; **22**: 3463-3471
27 **Somsel Rodman J**, Wandinger-Ness A. Rab GTPases coordinate endocytosis. *J Cell Sci* 2000; **113**(Pt 2): 183-192
28 **Kamei T**, Matozaki T, Takai Y. Mechanisms of cell adhesion and migration. *Gan To Kagaku Ryoho* 1999; **26**: 1359-1366
29 **Goldenring JR**, Ray GS, Lee JR. Rab11 in displasia of Barrett's epithelia. *Yale J Biol Med* 1999; **72**: 113-120
30 **Burczynski ME**, Lin HK, Penning TM. Isoform-specific induction of a human aldo-keto reductase by polycyclic aromatic hydrocarbons (PAHs), electrophiles, and oxidative stress: implications for the alternative pathway of PAH activation catalyzed by human dihydrodiol dehydrogenase. *Cancer Res* 1999; **59**: 607-614
31 **Palackal NT,** Lee SH, Harvey RG, Blair IA, Penning TM. Activation of polycyclic aromatic hydrocarbon trans-dihydrodiol proximate carcinogens by human aldo-keto reductase (AKR1C) enzymes and their functional overexpression in human lung carcinoma (A549) cells. *J Biol Chem* 2002; **277:** 24799-24808
32 **Hsu NY**, Ho HC, Chow KC, Lin TY, Shih CS, Wang LS, Tsai CM. Overexpression of dihydrodiol dehydrogenase as a prognostic marker of non-small cell lung cancer. *Cancer Res* 2001; **61**: 2727-2731
33 **Deng HB**, Parekh HK, Chow KC, Simpkins H. Increased expression of dihydrodiol dehydrogenase induces resistance to cisplatin in human ovarian carcinoma cells. *J Biol Chem* 2002; **277:** 15035-15043
34 **Penning TM**, Burczynski ME, Jez JM, Hung CF, Lin HK, Ma H, Moore M, Palackal N, Ratnam K. Human 3alpha-hydroxysteroid dehydrogenase isoforms (AKR1C1-AKR1C4) of the aldo-keto reductase superfamily: functional plasticity and tissue distribution reveals roles in the inactivation and formation of male and female sex hormones. *Biochem J* 2000; **351**(Pt 1): 67-77
35 **Breyer-Pfaff U**, Nill K. High-affinity stereoselective reduction of the enantiomers of ketotifen and ketonic nortriptyline metabolites by aldo-keto reductases from human liver. *Biochem Pharmacol* 1999; **59**: 249-260
36 **Shou M**, Harvey RG, Penning TM. Reactivity of benzo[a]pyrene-7,8-dione with DNA. Evidence for the formation of deoxyguanosine adducts. *Carcinogenesis* 1993; **14**: 475-482
37 **Esterbauer H**, Schaur RJ, Zollner H. forming propano-dGuo adducts which can lead to a pre-mutagenic lesion. *Free Radic Biol Med* 1991; **11**: 81-128
38 **Penning MT**, Burczynski ME, Hung CF, McCoull KD, Palackal NT, Tsuruda LS. Dihydrodiol dehydrogenase and polycyclic aromatic hydrocarbon activation: generation of reactive and redox active o-quinones. *Chem Res Toxicol* 1999; **12**: 1-18
39 **Lee JS,** Oh TY, Abn BO, Cho H, Kim WB, Kim YB, Surh YJ, Kim HJ, Hahm KB. Involvement of oxidative stress in experimentally induced reflex esophagitis and Barrett's esophagus: clue for the chemoprevention of esophageal carcinoma by antioxidants. *Mutat Res* 2001; **480-481**: 189-200
40 **Burczynski ME**, Sridhar GR, Palackal NT, Penning TM. The reactive oxygen species- and Michael acceptor-inducible human aldo-keto reductase AKR1C1 reduces the α,β-unsaturated aldehyde 4-hydroxy-2-nonenal to 1,4-dihyroxy-2-nonene. *J Biol Chem* 2001; **276:** 2890-2897
41 **Nadon L**, Siemiatycki J, Dewar R, Krewski D, Gerin M. Cancer risk due to occupation exposure to polycyclic aromatic hydrocarbons. *Am J Ind Med* 1995; **28**: 303-324
42 **Lin HK**, Jez JM, Overby AM, Burcynski ME, Peehl DM, Penning TM. Type 3 3-hydroxysteroid dehydrogenase (3-HSD) accumulate 5-DHTand activates the androgen receptor in human prostate cancer PC3 cell. *Proc Am Assoc Cancer Res* 2000; **41**: 1510
43 **Wang Q**, Holmes DI, Powell SM, Lu QL, Waxman J. Analysis of stromal-epithelial interactions in prostate cancer identifies PTPCAAX2 as a potential oncogene. *Cancer Lett* 2002; **175**: 63-69
44 **Cehn FW**, Ioannou YA. Ribosomal proteins in cell proliferation and apoptosis. *Int Rev Immunol* 1999; **18**: 429-448
45 **Spence J**, Gali RR, Dittmar G, Sherman F, Karin M, Finley D. Cell cycle-regulated modification of the ribosome by a variant multiubiquitin chain. *Cell* 2000; **102**: 67-76
46 **Liu SC**, Bassi DE, Zhang SY, Holoran D, Conti CJ, Klein-Szanto AJ. Overexpression of cyclin D2 is associated with increased *in vivo* invasiveness of human squamous carcinoma cells. *Mol Carcinog* 2002; **34**: 131-139

Edited by Wang XL and Xu CT **Proofread by** Xu FM

PO Box 2345, Beijing 100023, China
Fax: +86-10-85381893
E-mail: wjg@wjgnet.com www.wjgnet.com

World J Gastroenterol 2004;10(12):1722-1725
World Journal of Gastroenterology
Copyright ©2004 by The WJG Press ISSN 1007-9327

• GASTRIC CANCER •

Reversal of multidrug resistance in drug-resistant human gastric cancer cell line SGC7901/VCR by antiprogestin drug mifepristone

Da-Qiang Li, Zhi-Biao Wang, Jin Bai, Jie Zhao, Yuan Wang, Kai Hu, Yong-Hong Du

Da-Qiang Li, Zhi-Biao Wang, Jin Bai, Jie Zhao, Yuan Wang, Kai Hu, Yong-Hong Du, State Key Laboratory of Ultrasound Engineering in Medicine, Chongqing Medical University, Chongqing 400016, China
Supported by the National Key Research Project Fundation of China, No. 96-905-02-01, and the National Natural Science Fundation of China, No. 39630340
Correspondence to: Dr. Da-Qiang Li, State Key Laboratory of Ultrasound Engineering in Medicine, Chongqing Medical University, PO Box 153, Chongqing 400016, China. lidaqiang1974@ sohu.com
Telephone: +86-23-68485022 **Fax:** +86-23-68485023
Received: 2003-07-04 **Accepted:** 2003-08-16

Abstract

AIM: To explore the reversal effect of mifepristone on multidrug resistance (MDR) in drug-resistant human gastric cancer cell line SGC7901/VCR and its mechanisms.

METHODS: Expression of multidrug resistance-associated protein(MRP) was detected using reverse transcription-polymerase chain reaction(RT-PCR). Flow cytometry was used to assay the expression of P-glycoprotein(P-gp), Bcl-2, Bax, and the mean fluorescent intensity of intracellular rhodamine 123 in the cells. Meanwhile, the protein levels of Bcl-2 and Bax were also detected by Western blotting analysis. The sensitivity of cells to the anticancer agent, vincrimycin(VCR), and the intracellular [^{3}H]VCR accumulation were determined by tetrazolium blue (MTT) assay and a liquid scintillation counter, respectively.

RESULTS: Expression of MRP and P-gp in SGC7901/VCR cells was 6.04-and 8.37-fold higher as compared with its parental SGC7901 cells, respectively. After treatment with 1, 5, 10, and 20 μmol/L mifepristone, SGC7901/VCR cells showed a 1.34-, 2.29-, 3.11-, and 3.71-fold increase in the accumulation of intracellular VCR, a known substrate of MRP, and a 1.03-, 2.04-, 3.08-, and 3.68-fold increase in the retention of rhodamine 123, an indicator of P-gp function, respectively. MTT assay revealed that the resistance of SGC7901/VCR cells to VCR was 11.96-fold higher than that of its parental cells. The chemosensitivity of SGC7901/VCR cells to VCR was enhanced by 1.02-, 7.19-, 12.84-, and 21.17-fold after treatment with mifepristone at above-mentioned dose. After 96 h of incubation with mifepristone 10 μmol/L, a concentration close to plasma concentrations achievable in human, the expression of Bcl-2 protein was decreased to (9.21±0.65)% from (25.32±1.44)%, whereas the expression of Bax protein was increased to (19.69±1.13)% from (1.24±0.78)% ($P<0.01$). Additionally, the effects of mifepristone on the expression of Bcl-2 and Bax proteins in SGC7901/VCR cells were further demonstrated by Western blotting analysis.

CONCLUSION: Mifepristone has potent reversal effect on MDR in SGC7901/VCR via inhibiting the function of MRP and P-gp, modulating the expression of Bcl-2 and Bax proteins, and enhancing the sensitivity to anticancer agent VCR.

Li DQ, Wang ZB, Bai J, Zhao J, Wang Y, Hu K, Du YH. Reversal of multidrug resistance in drug-resistant human gastric cancer cell line SGC7901/VCR by antiprogestin drug mifepristone. *World J Gastroenterol* 2004; 10(12): 1722-1725
http://www.wjgnet.com/1007-9327/10/1722.asp

INTRODUCTION

Gastric cancer is still the second most common cancer and the second most cause of cancer-related mortality[1-2]. Surgery is effective for the majority of cases but chemotherapy plays an important role in the management of the patients with advanced gastric cancer[3-4]. However, intrinsic or acquired resistance of gastric cancer cells to a broad spectrum of structurally and functionally unrelated anticancer agents, termed multidrug resistance(MDR), is a major obstacle to effective chemotherapy[5-7]. Thus, there is an urgent need to identify effective reversal agents against the tumor.

The accumulating evidence[8-12] showed that the mechanisms responsible for the MDR of gastric cancer involve, at least in part, overexpression of two ATP-dependent drug transporter proteins, P-glycoprotein(P-gp) and multidrug resistance-associated protein(MRP), as well as maladjustment of apoptosis-related genes Bcl-2 and Bax. Recent studies[13-15] proved that mifepristone, as a potent antiprogestin agent, effectively reversed P-gp-and MRP-mediated MDR in mouse S7CD-5 thymoma cells and human GLC4/sb30 lung cancer cells, and induced apoptosis in human LNCaP prostate cancer cells by regulating the expression of Bcl-2 and Bax. However, the effects of mifepristone on MDR in human gastric cancer cells remain unknown. The present study was therefore undertaken to explore the reversal effect of mifepristone on the MDR in drug-resistant human gastric cancer cell line SGC7901/VCR and its mechanisms.

MATERIALS AND METHODS

Cell culture and treatment

Human gastric cancer cell line SGC7901, and its drug-resistant counterpart SGC7901/VCR selected by stepwise exposure of parental SGC7901 cells to increasing concentrations of vincristine (VCR), were purchased from Wuhan University Type Culture Collection (Wuhan, China). Both cell lines were maintained in RPMI1640 medium (Gibco BRL, Grand Island, NY) supplemented with 100 mL/L heat-inactivated fetal bovine serum(Hyclone, Logan, UT), 10^5 U/L penicillin and 100 mg/L streptomycin in a incubator containing 50 mL/L CO_2 at 37 ℃. When cells were grown to approximately 50% confluence, the medium was then replaced with serum- free RPMI1640. After 24 h, fresh media containing 1, 5, 10, and 20 μmol/L mifepristone (Sigma Chemical Co., St Louis, MO) was added, respectively. Control cells were treated with the same volume of vehicle (ethanol). Unless otherwise indicated, the cells were harvested after 96 h of incubation.

RT-PCR for MRP

Total RNA was extracted form the cultured cells using Trizol reagent (Gibco BRL) according to the manufacturer's instructions. Two milligrams of total RNA was used for reverse transcription in a total volume of 20 μL with the SuperScript

preamplification system (Gibco BRL). Aliquots of 2 μL cDNA were then amplified using a PCR kit (Promega,USA) following conditions recommended by the manufacturer. The sense and antisense primers for MRP, designed according to the sequences published previously[16], were 5' -AGGAGAGAT-CATCATCGATGG-3' and5' -GCCTCCTGCACATTCATGG-3' , respectively. The sense and anti-sense primers for β-actin were 5' -ATCTG-GCACCACACCTTCTACAATGAGCTGC-G-3' and 5' -CGTCATACTCCTGCTTGCTGATCCACATCTGC-3' , respectively. The cycling conditions were 95 ℃ for 1 min, followed by 30 cycles of 94 ℃ for 60 s, 58 ℃ for 45 s, and 72 ℃ for 1 min and a final extension of 72 ℃ for 8 min. PCR products were separated on a 20 g/L agarose gel and visualized by ethidium bromide staining. The density of each band was measured on a densitometer, and the relative level of MRP mRNA expression in cells was calculated according to the ratio of MRP gene to β-actin.

Detection of P-gp, Bcl-2, Bax by flow cytometry

The harvested cells were fixed with 40 g/L paraformaldehyde for 10 min, followed by treatment with 2 g/L Triton X-100 for 10 min. After incubation with normal rabbit serum for 10 min to block non-specific binding, the cells were incubated for 1 h at 4 ℃ with mouse anti-human monoclonal antibodies against P-gp, Bcl-2, Bax(Santa Cruz Biotechnology, Inc., USA) respectively, followed by treatment with FITC-conjugated goat anti-mouse IgG for 30 min at 4 ℃. The percentage of positive cells were determined using the FACS Calibur flow cytometry (Becton & Dickinson) with an excitation wavelength of 488 nm.

Western blotting analysis of Bcl-2 and Bax

Western blotting analysis was made to detect Bcl-2 and Bax protein levels according to the published method with some modifications[17]. Briefly, proteins were extracted from the harvested cells using a lysis buffer containing 50 mmol/L HEPES, pH7.2, 100 mmol/L NaCl, 200 mL/L glycerol, 0.1 mmol/L EDTA, pH8.0, 2 g/L Triton X-100, 2 mmol/L phenylmethylsulfonyl fluoride (PMSF) and 1 mmol/L dithiothreitol(DTT), and then quantitated using the Bio-Rad Detergent Compatible Protein Assay kit(Bio-Rad, Hercules, CA). Equal amounts of protein (10-20 μg) were resolved on a 100 g/L minigel by SDS-polyacrylamide gel electrophoresis. Proteins were transferred to a PVDF membrane(Millipore, Bedford, MA) using the Multiphor Novoblot electrophoresis transfer system, followed by immunoblotting using a monoclonal mouse anti- human antibody against Bcl-2 and Bax (Santa Cruz Biotechnology, Inc., USA), respectively. A horseradish peroxidase-conjugated secondary antibody (goat anti-mouse HRP, Amersham, Arlington Heights, IL) was used at a dilution of 1:3 000. The membranes were subsequently developed using Enhanced Chemiluminescence (ECL, Amersham) and exposed to film.

Intracellular [^{3}H]VCR accumulation

Cells were incubated with 20 nmol/L [^{3}H]VCR(specific activity 5.8 Ci/mmol, Amersham Pharmacia Biotech Co.) at 37 ℃ for 90 min in the absence or presence of various concentrations of mifepristone. Cells were then washed three times with ice-cold PBS and lyzed in distilled water by ultrasonication. Radioactivity of [^{3}H]VCR in the cell extract was then determined with a liquid scintillation counter (Beckman LS1801, USA) and normalized to cellular protein content.

Rhodamine 123 retention assay

Retention of rhodamine 123(Sigma) was determined by flow cytometry as a functional index of P-gp activity. Cells (2×10^5) were treated with various concentrations of mifepristone for 24 h prior to the addition of 10 g/L rhodamine 123. After incubation at 37 ℃ for 1 h, cells were harvested and centrifuged at 300 g for 10 min. Cell pellets were resuspended with 500 μL of PBS and immediately used for flow cytometric analysis of rhodamine 123 retention.

Drug-sensitivity assay

The sensitivity of cells to VCR was determined using the MTT assay as described previously[18]. The drug concentration producing 50% inhibition of growth (IC_{50}) was determined graphically for VCR using the relative survival curves. The reversal effects of mifepristone were determined as the IC_{50} value in the absence of mifepristone to that in the presence of mifepristone. Assays were performed in quadruplicate for at least three times.

Statistical analysis

Data were expressed as mean±SD. Statistical analysis of the data was performed using the Student's *t* test and the Chi-square test. $P<0.05$ was considered statistically significant.

RESULTS

Expression of MRP mRNA and P-gp protein

To examine the relationship between the levels of MRP and P-gp expression in SGC7901 /VCR and SGC7901 cells and the changes in drug resistance, RT-PCR and flow cytometry were used to detect the expression of MRP mRNA and P-gp protein. As indicated in Figure.1, a 6.04-fold overexpression of MRP mRNA was found in SGC7901/VCR cells as compared with the parental line. The relative level of MRP mRNA expression in drug-resistant cells and drug-sensitive cells was 1.45±0.23 and 0.24±0.17, respectively. Similarly, the expression of P-gp was significantly increased in the SGC7901/VCR cells in comparison with the parental cells (57.64±8.56% *vs* 6.89±1.25%, 8.37-fold, $P<0.005$).

Intracellular [^{3}H]VCR accumulation and rhodamine 123 retention

Intracellular accumulation of [^{3}H]VCR, a known substrate of MRP, was measured in the presence or the absence of various concentrations of mifepristone in both cell lines. After treatment with 1, 5, 10, and 20 μmol/L mifepristone for 90 min, the

Table 1 Effects of of mifepristone on intracellular VCR accumulation and rhodamine 123 retention in drug-resistant human gastric cancer cell line SGC7901 / VCR and its parental counterpart SGC7901

Mifepristone (μmol / L)	Intracellular [^{3}H]VCR accumulation (pmol / mg protein)		Fluorescent intensity of intracellular rhodamine 123	
	SGC7901	SGC7901 / VCR	SGC7901	SGC7901 / VCR
0 (control)	3.36±0.54	0.98±0.20	82.36±4.23	22.32±3.14
1	3.41±0.49	1.31±0.29[a]	83.21±5.50	28.89±4.25[a]
5	3.54±0.68	2.24±0.62[b]	85.12±4.89	45.63±6.34[b]
10	3.65±0.87	3.05±0.75[b]	86.01±6.12	68.69±7.40[b]
20	3.84±0.79	3.64±0.84[b]	88.20±6.45	82.10±9.21[b]

[a]$P<0.05$, [b]$P<0.01$ *vs* control group.

accumulation of intracellular VCR in SGC7901/VCR cells was enhanced by 1.34-, 2.29-, 3.11-, and 3.71-fold as compared with medium control, respectively (Table 1). It had been documented that the efflux of rhodamine 123 correlated with well P-gp expression. By this rational, we used rhodamine 123 to evaluate the function of P-gp. As shown in Table 1, after treatment with various concentrations of mifepristone for 24 h, the retention of rhodamine 123 in SGC7901/ VCR cells was increased by 1.03-, 2.04-, 3.08-, and 3.68-fold as compared with the medium control. In contrast, no significant increase in the intracellular rhodamine 123 retention and VCR accumulation was observed in mifepristone-treated SGC7901 cells.

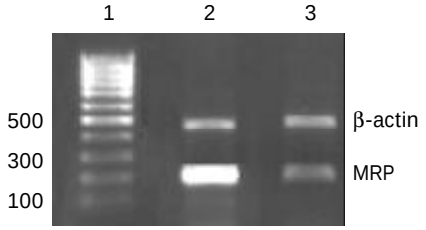

Figure 1 RT-PCR analysis of MRP mRNA expression in human gastric cancer cell line SGC7901 and its drug-resistant counterpart SGC7901/VCR. Lane 1-3: marker(bp), SGC7901/VCR, SGC7901, respectively.

Expression of Bcl-2 and Bax

Flow cytometric assay revealed that the expression of Bcl-2 protein was significantly increased, whereas the expression of Bax was decreased in SGC-7901/VCR cells as compared with drug-sensitive SGC7901 cells (Table 2). Mifepristone when used at 10 μmol/L, a concentration close to plasma concentrations achievable in human, markedly up- regulated the expression of Bax and simultaneously down-regulated the expression of Bcl-2 in SGC7901/ VCR cells (Table 3). Additionally, the results were further demonstrated by Western blotting analysis (Figure 2). Western blotting revealed that mifepristone dose-dependently modulated the expression of Bcl-2 and Bax proteins, which was especially remarkable at the 20 μmol/L concentration.

Table 2 Flow cytometric analysis of Bcl-2 and Bax expression in human gastric cancer cell line SGC7901 and its drug-resistant counterpart SGC7901/VCR

Cell line	Bcl-2(%)	Bax(%)
SGC7901	17.23±0.86	5.85±0.56
SGC7901/VCR	25.32±1.44[a]	1.24±0.78[a]

[a] $P<0.05$ *vs* SGC7901 cell line.

Table 3 Effect of mifepristone on Bcl-2 and Bax expression in SGC7901/VCR cells

Mifepristone (μmol/L)	Bcl-2(%)	Bax(%)
0 (control)	25.32±1.44	1.24±0.78
10	9.21±0.65[a]	19.69±1.13[a]

[a] $P<0.05$ *vs* control group.

Drug sensitivity assay

The sensitivity of SGC7901/VCR cells and its parental cells to VCR is shown in Table 4. Our results showed that the resistance of the SGC7901/VCR cells to VCR was 11.96-fold higher than that of its parental counterparts in terms of IC_{50} value. After incubation with 1, 5, 10, and 20 μmol/L mifepristone for 96 h, the sensitivity of SGC7901/VCR cells to VCR was enhanced by 1.02, 7.19, 12.84, and 21.17 times, respectively. In contrast, mifepristone did not obviously alter the sensitivity to VCR in parental SGC-7901 cells.

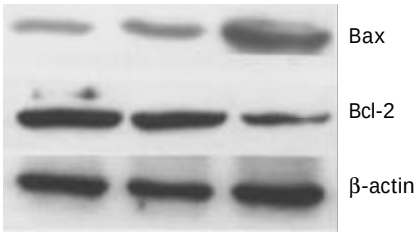

Figure 2 Western blotting analysis of Bcl-2 and Bax proteins in cellular extracts of SGC7901/ VCR cells cultured for 96 h in the absence or the presence of miferpstone. Lane1-3: control, 1 μmol/L and 10 μmol/L mifepristone, respectively.

Table 4 Effects of mifepristone on the sensitivity of SGC7901 cells and its drug-resistant counterpart SGC7901/VCR to VCR

Mifepristone (μmol/L)	SGC7901		SGC7901/VCR	
	IC_{50}	Reversal fold	IC_{50}	Reversal fold
0 (control)	4.23±1.02		46.36±5.14	
1	4.19±1.00	1.01	45.23±4.21	1.02
5	4.05±0.94	1.04	6.45±1.23[b]	7.19
10	3.81±0.89	1.11	3.61±0.87[b]	12.84
20	3.49±0.74	1.21	2.19±0.54[a]	21.17

Data represent IC_{50} values of VCR (nmol/L) expressed as mean±SD of 3 independent experiments. [a]$P<0.005$, [b]$P<0.01$, *vs* control group.

DISCUSSION

Mifepristone is a potent antiprogestin agent that has been widely used as the first-line drug for the termination of early pregnancy[19,20]. Interestingly, recent studies[21-25] have proved that mifepristone exerts markedly anticancer effects and reversal effects on MDR in some cancer cells with no serious side-effects. Thus, there is an increasing interest in exploring the reversal effect of mifepristone on MDR in human gastric cancer cells. In the present study, we reported for the first time that mifepristone effectively reversed MDR in SGC7901/VCR via multiple mechanisms.

Previous studies[26-28] have proved that MDR in gastric cancer cells is closely related to overexpression of two ATP-dependent transporter proteins, P-gp encoded by MDR1 gene and MRP identified by Cole *et al*.[16] from adriamycin-selected MDR lung cancer cell line H69/ ADR. Both proteins belong to the ATP-binding cassette(ABC) protein superfamily, and efflux anticancer agents out of cells and therefore decrease their intracellular accumulation. Thus, we firstly determined the relationship between the levels of P-gp and MRP expression in SGC7901/ VCR and its parental cells and the changes of drug resistance. Results showed that the expression of P-gp and MRP in SGC7901/VCR cells was 8.37- and 6.04-fold higher as compared with its parental counterparts. The data indicate that the overexpression P-gp and MRP confers, at least in part, the MDR phenotype of VCR-selected SGC7901/VCR cells.

To determine the effects of mifepristone on the function of P-gp and MRP, we further investigated the accumulation of intracellular VCR, a substrate of MRP, and the retention of rhodamine 123, an indicator of P-gp function, in both cell lines. Results revealed that mifepristone dose-dependently enhanced the intracellular VCR accumulation and rhodamine 123 retention in SGC7901/VCR cells. In contrast, mifepristone had no significant effects on the drug-sensitive SGC7901 cells. The results were further proved by the drug sensitivity assay. We found that, after incubation with 1, 5, 10, and 20 μmol/L mifepristone for 96 h, the sensitivity of SGC7901/ VCR cells to VCR was enhanced by 1.02, 7.19, 12.84, and 21.17 times, whereas

no significant changes in the sensitivity to VCR were observed in mifepristone-treated SGC901 cells. The findings are in agreement with those of previous studies on other cancer cell lines *in vitro*[13,14]. Taken together, it seems reasonable to conclude that mifepristone can inhibit the function of P-gp and MRP and therefore enchance the sensitivity of cells to anticancer agent VCR.

Although overexpression of the P-gp and MRP plays an important role in the MDR of gastric cancer, this does not explain all of the MDR[29]. Recent studies have shown that overexpression of anti-apoptotic proteins, such as Bcl-2, Bcl-X_L and Mcl-1, induces cancer cells resistance to chemotherapeutic agents in cancer cells that act by apoptosis, whereas high levels of pro-apoptotic proteins, Bcl-Xs and Bax, contribute to sensitize MCF-7 breast cancer cells to etoposide (VP16), taxol and epirubicin. These data were also proved by the work of Zhao *et al*.[10], who reported that the Bax gene-transfected SGC7901/VCR cells were more sensitive to adriamycin and VCR than mock vector transfected cells. In a word, Bcl-2/ Bax pathway may be an alternative mechanism of drug resistance in gastric cancer. In this study, we proved that mifepristone when used at 10 μmol/L, a concentration close to plasma concentrations achievable in human, significantly up-regulated the expression of Bcl-2 and simultaneously down-regulated the expression of Bax in SGC7901/VCR cells. In addition, the modulating effects of mifepristone on the expression of Bcl-2 and Bax proteins in SGC7901/ VCR cells were further demonstrated by Western blotting analysis. These results may partly explain the reversal effects of mifepristone on SGC7901/VCR.

In conclusion, mifepristone exerts potent reversal effect on MDR in SGC7901/VCR via inhibiting MRP- and P-gp-mediated drug transporter, modulating the expression of apoptosis-related genes Bcl-2 and Bax, and enhancing the sensitivity of cells to anticancer agents such as VCR. These results indicate that mifepristone may be a promising chemosensitizer likely allowing to reverse the MDR of human gastric cancer cells although further studies are clearly needed to prove the possibility.

REFERENCES

1 **Albert C.** Clinical aspects of gastric cancer. In: Rustgi AK, eds. Gastrointestinal cancer: biology, diagnosis and therapy. *Philadelphia: Lippincott Raven* 1995: 197-216

2 **Lu JB,** Sun XB, Dai DX, Zhu SK, Chang QL, Liu SZ, Duan WJ. Epidemiology of gastroenterologic cancer in Henan Province, China. *World J Gastroenterol* 2003; **9**: 2400-2403

3 **Sasako M.** Principles of surgical treatment for curable gastric cancer. *J Clin Oncol* 2003; **21**: 274s-275s

4 **Roth AD.** Chemotherapy in gastric cancer: a never ending saga. *Ann Oncol* 2003; **14**: 175-177

5 **Choi JH,** Lim HY, Joo HJ, Kim HS, Yi JW, Kim HC, Cho YK, Kim MW, Lee KB. Expression of multidrug resistance-associated protein1, P-glycoprotein, and thymidylate synthase in gastric cancer patients treated with 5-fluorouracil and doxorubicin-based adjuvant chemotherapy after curative resection. *Br J Cancer* 2002; **86**: 1578-1585

6 **Ludwig A,** Dietel M, Lage H. Identification of differentially expressed genes in classical and atypical multidrug-resistant gastric carcinoma cells. *Anticancer Res* 2002; **22**: 3213- 3221

7 **Kowalski P,** Stein U, Scheffer GL, Lage H. Modulation of the atypical multidrug-resistant phenotype by a hammerhead ribozyme directed against the ABC transporter BCRP / MXR / ABCG2. *Cancer Gene Ther* 2002; **9**: 579-586

8 **Endo K,** Maehara Y, Kusumoto T, Ichiyoshi Y, Kuwano M, Sugimachi K. Expression of multidrug-resistance-associated protein (MRP) and chemosensitivity in human gastric cancer. *Int J Cancer* 1996; **68**: 372-377

9 **Fan K,** Fan D, Cheng LF, Li C. Expression of multidrug resistance-related markers in gastric cancer. *Anticancer Res* 2000; **20**: 4809-4814

10 **Zhao Y,** Xiao B, Chen B, Qiao T, Fan D. Upregulation of drug sensitivity of multidrug- resistant SGC7901/ VCR human gastric cancer cells by bax gene transduction. *Chin J Med* 2000; **113**: 977-980

11 **Ramesh S,** Shanthi P, Krishnan KB, Shanthi AV, Taralakshmi VV, Subulakshmi S. Multidrug resistance 1 gene expression in Indian patients with gastric carcinoma. *Indian J Gastroenterol* 2003; **22**: 19-21

12 **Pohl A,** Lage H, Muller P, Pomorski T, Herrmann A. Transport of phosphatidylserine via MDR1 (multidrug resistance 1) P-glycoprotein in a human gastric carcinoma cell line. *Biochem J* 2002; **365**: 259-268

13 **Payen L,** Delugin L, Courtois A, Trinquart Y, Guillouzo A, Fardel O. Reversal of MRP -mediated multidrug resistance in human lung cancer cells by the antiprogestatin drug RU486. *Biochem Biophys Res Commun* 1999; **258**: 513-518

14 **Gruol DJ,** Zee MC, Trotter J, Bourgeois S. Reversal of multidurg resistance by RU486. *Cancer Res* 1994; **54**: 3088-3091

15 **El Etreby MF,** Liang Y, Lewis RW. Induction of apoptosis by mifepristone and tamoxifen in human LNCaP prostate cancer cells in culture. *Prostate* 2000; **43**: 31-42

16 **Cole SP,** Bhardwaj G, Gerlach H, Mackie JE, Grant CE, Almquist KC, Stewart AJ, Kurz EU, Duncan AM, Deeley RG. Overexpression of a transporter gene in multidrug- resistant human lung cancer cell line. *Science* 1992; **258**: 1650-1654

17 **Kamradt MC,** Mohideen N, Vaughan ATM. RU486 increases radiosensitivity and restores apoptosis through modulation of HPV E6 / E7 in dexamethasone-treated cervical carcinoma cells. *Gynecol Oncol* 2000; **77**: 177-182

18 **Hotta T,** Tanimura H, Iwahashi M, Tani M, Tsunoda T, Noguchi K, Mizobata S, Arii K, Terasawa H, Nakamori M, Yamaue H. P-glycoprotein-expressing tumor cells are resistant to anticancer drugs in human gastrointestinal cancer. *Surg Today* 1999; **29**: 591- 596

19 **Mahajan DK,** London SN. Mifepristone(RU486): a review. *Fertil Steril* 1997; **68**: 967-976

20 **Basu R,** Gundlach T, Tasker M. Mifepristone and misoprostol for medical termination of pregnancy: the effectiveness of a flexible regimen. *J Fam Plann Reprod Health Care* 2003; **29**: 139-141

21 **Rocereto TF,** Saul HM, Aikins JA Jr, Paulson J. Phase II study of mifepristone(RU486) in refractory ovarian cancer. *Gynecol Oncol* 2000; **77**: 429-432

22 **Hyder SM,** Chiappetta C, Stancel GM. Pharmacological and endogenous progestins induce vascular endothelial growth factor expression in human breast cancer cells. *Int J Cancer* 2001; **92**: 469-473

23 **Peters MG,** Vanzulli S, Elizalde PV, Charreau EH, Goin MM. Effects of antiprogestins RU486 and ZK98299 on the expression of cell cycle proteins of a medroxyprogesterone acetate (MPA)-induced murine mammary tumor. *Oncol Rep* 2001; **8**: 445-449

24 **Yokoyama Y,** Shinohara A, Takahashi Y, Wan X, Takahashi S, Niwa K, Tamaya T. Synergistic effects of danazol and mifepristone on the cytotoxicity of UCN-01 in hormone-responsive breast cancer cells. *Anticancer Res* 2000; **20**: 3131-3135

25 **Liang Y,** Hou M, Kallab AM, Barrett JT, El Etreby F, Schoenlein PV. Induction of antiproliferation and apoptosis in estrogen receptor negative MDA-231 human breast cancer cells by mifepristone and 4-hydroxytamoxifen combination therapy: a role for TGFbeta1. *Int J Oncol* 2003; **23**: 369-380

26 **Stein U,** Lage H, Jordan A, Walther W, Bates SE, Litman T, Hohenberger P, Dietel M. Impact of BCRP / MXR, MRP1 and MDR1 / P-Glycoprotein on thermoresistant variants of atypical and classical multidrug resistant cancer cells. *Int J Cancer* 2002; **97**: 751-760

27 **Lin HL,** Liu TY, Wu CW, Chi CW. Berberine modulates expression of mdr1 gene product and the responses of digestive track cancer cells to Paclitaxel. *Br J Cancer* 1999; **81**: 416- 422

28 **Alexander D**, Yamamoto T, Kato S, Kasai S. Histopathological assessment of multidrug resistance in gastric cancer:expression of P-glycoprotein, multidrug resistance-associated protein, and lung-resistance protein. *Surg Today* 1999; **29**: 401-406

29 **Kim R,** Ohi Y, Inoue H, Aogi K, Toge T. Introduction of gadd153 gene into gastric cancer cells can modulate sensitivity to anticancer agents in association with apoptosis. *Anticancer Res* 1999; **19**: 1779-1783

Edited by Ma JY and Xu FM

PO Box 2345, Beijing 100023, China
Fax: +86-10-85381893
E-mail: wjg@wjgnet.com www.wjgnet.com

World J Gastroenterol 2004;10(12):1726-1729
World Journal of Gastroenterology
Copyright ©2004 by The WJG Press ISSN 1007-9327

• GASTRIC CANCER •

Effects of mifepristone on invasive and metastatic potential of human gastric adenocarcinoma cell line MKN-45 *in vitro* and *in vivo*

Da-Qiang Li, Zhi-Biao Wang, Jin Bai, Jie Zhao, Yuan Wang, Kai Hu, Yong-Hong Du

Da-Qiang Li, Zhi-Biao Wang, Jin Bai, Jie Zhao, Yuan Wang, Kai Hu, Yong-Hong Du, State Key Laboratory of Ultrasound Engineering in Medicine, Chongqing Medical University, Chongqing 400016, China
Supported by the National Key Research Project Foundation of China, No.96-905- 02-01, and the National Natural Science Foundation of China, No. 39630340
Correspondence to: Dr. Zhi-Biao Wang, State Key Laboratory of Ultrasound Engineering in Medicine, Chongqing Medical University (PO Box 153), Chongqing 400016, China. wangzhibiao@netease.com
Telephone: +86-23-68485022 **Fax:** +86-23-68485023
Received: 2003-08-23 **Accepted:** 2003-12-06

Abstract

AIM: To investigate the effects of mifepristone on the invasive and metastatic potential of human gastric adenocarcinoma cell line MKN-45 and its mechanisms.

METHODS: After incubation with various concentrations of mifepristone (5, 10, 20 μmol/L), the adhesion to artificial basement membrane, Matrigel, and the migration of MKN-45 cells were assayed using MTT assay and Transwell cell culture chambers, respectively. Enzyme- linked immunoabsorbent assay (ELISA) and flow cytometry were used to determine the expression of vascular endothelial growth factor (VEGF) and integrin β3 in the cells. After subcutaneous transplantation of MKN-45 cells in nude mice, mifepristone (50 mg/kg·d) was administrated subcutaneously for 8 wk to assess its effects on tumor metastasis. Immunohistochemical analysis was used to detect the expression of VEGF and microvascular density (MVD) in xenografted tumors.

RESULTS: Mifepristone dose-dependently inhibited the heterotypic adhesion to Matrigel of MKN-45 cells. The inhibition was accompanied by a significant down-regulation of integrin β3 expression in the cells. After incubation with 5, 10, 20 μmol/L mifepristone, the number of migrated MKN-45 cells was 72±8, 50±6, 41±5 in experiment group, and 94±16 in control group (P<0.01). Meanwhile, secreted VEGF protein of MKN-45 cells in mifepristone-treated group (14.2±2.9, 8.9±3.1, 5.4±2.1 ng/g per liter) was significantly lower than that in control group (22.7±4.3 ng/g per liter, P<0.01). *In vivo*, mifepristone decreased the number of metastatic foci in lungs of nude mice and down-regulated the expression of VEGF and MVD in the xenograted tumors.

CONCLUSION: Mifepristone can effectively inhibit the invasive and metastatic potential of human gastric adenocarcinoma cell line MKN-45 *in vitro* and *in vivo* through inhibition of heterotypic adhesion to basement membrane, cell migration and angiogenesis.

Li DQ, Wang ZB, Bai J, Zhao J, Wang Y, Hu K, Du YH. Effects of mifepristone on invasive and metastatic potential of human gastric adenocarcinoma cell line MKN-45 *in vitro* and *in vivo*.*World J Gastroenterol* 2004; 10(12): 1726-1729
http://www.wjgnet.com/1007-9327/10/1726.asp

INTRODUCTION

Mifepristone is a progesterone receptor (PR) antagonist that has been widely used as the first- line drug for the termination of early pregnancy[1]. Recently, considerable studies[2,3] have proved that mifepristone exerts markedly anti-tumor effects on PR-positive tumor cells, such as breast cancer and ovarian cancer, without obvious side-effects and drug resistance. Its similar effect on PR-positive human gastric adenocarcinoma cell line MKN-45 was also demonstrated in our laboratory.

More interestingly, accumulating evidences show that embryo implantation and tumor metastasis share striking similarities in biological behaviors, such as cell adhesion[4], immune escape[5], angiogenesis[6], invasion[7] and tumor metastasis-related gene expression[8]. By this rational, there is an increasing interest in addressing the role of mifepristone, an agent against embryo implantation, in anti-tumor invasion and metastasis. Therefore, the present study was undertaken to further investigate the effects of mifepristone on the invasive and metastatic potential of MKN-45 cells *in vitro* and *in vivo* and its possible mechanisms.

MATERIALS AND METHODS

Cell culture and treatment

Human gastric adenocarcinoma cell line MKN-45 was obtained from Wuhan University Type Culture Collection (Wuhan, China), and maintained in phenol red-free RPMI1640 (Gibco BRL, Grand Island, NY) supplemented with 100 mL/L[1] fetal bovine serum (Hyclone, Logan, UT), 10^5 U/L penicillin and 100 mg/L streptomycin at 37 ℃ in a humidified atmosphere containing 50 mL/L CO_2 in air. When cells were grown to approximately 50% confluence, the medium was then replaced with serum-free RPMI1640. After 24 h, fresh media containing 5, 10, 20 μmol/L mifepristone (Sigma Chemical Co., St Louis, MO) were added, respectively. Control cells were treated with the same volumes of vehicle (ethanol). Unless otherwise stated, the cells were harvested after 96 h of incubation.

Adhesion assay

Each well in 96-well tissue culture plates was coated with 2 μg of Matrigel (Collaborative Research Inc., Bedford, MA) and allowed to dry in a laminar flow cabinet overnight at room temperature. After washed three times with PBS to remove excess and unbound Matrigel, the wells were blocked with 20 μL of a 20 mg/L bovine serum albumin (BSA, Sigma) solution in RPMI1640 medium for 1 h at 37 ℃. Aliquots of 8×10^4 cells, in 100 μL of serum-free RPMI1640 medium containing various concentrations of mifepristone, were added to each well and the cells were allowed to adhere for 1 h at 37 ℃. When the incubation was completed, the wells were washed three times with PBS to remove unbound cells. Then, the remaining cells were continuously incubated with MTT solutions (40 μg/well) for 4 h at 37 ℃, followed by treatment with 200 μL of dimethyl sulfoxide (DMSO) for 10 min. Finally, A_{570nm} of each well was measured using an ELISA plate reader(Bio-Rad, USA). Results were expressed as the adhesive rate(%) that was calculated according to the

following formula: (A_{570nm} of the adhered cells/A_{570nm} of total cells)×100%.

Detection of integrin β3 by flow cytometry

The harvested cells were fixed with 40 mg/L paraformaldehyde for 10 min, followed by treatment with 2 mg/L Triton X-100 for 10 min. After treatment with normal rabbit serum for 10 min to block non-specific binding, the cells were incubated for 1 h at 4 ℃ with mouse anti- human monoclonal antibody against β3(Santa Cruz, USA), followed by treatment with FITC-conjugated goat anti-mouse IgG (Vector, Burlingame, CA) for 30 min at 4 ℃. The percentage of positive cells was determined using the FACS Calibur flow cytometry (Becton & Dickinson) with an excitation wavelength of 488 nm.

Migration assay

Migration of MKN-45 cells was assayed in Transwell cell culture chambers with 6.5-mm- diameter polycarbonate membrane filters containing 8-μm-pore size (Becton Dickinson Labware, Bedford, MA). Fibroblast-conditioned medium, obtained from confluent NIH 3T3 cell cultures in serum-free RPMI 1640, was used as the chemoattractant and added to the lower wells of the chambers. Aliquots of 2×10^4 cells in 300 μL fresh medium containing various concentrations of mifepristone were seeded into the upper wells of the cell inserts. After 24 h of incubation at 37 ℃, the non-migrating cells were removed from the upper surface of the membrane with a cotton swab. The cells on the lower surface of the membrane were fixed with ice-cold methanol and then stained with haematoxylin and eosin. The number of migrated cells was counted under a light microscope. Five random microscopic fields (×400) were counted per well and the mean was determined.

Measurement of VEGF by ELISA

The media were collected after 48 h for VEGF ELISA determinations as described below. The cells were taken through three freeze-thaw cycles, centrifuged and supernatant was collected for determination of protein concentration as described previously. VEGF levels in the cell culture media were measured using a Quantikine kit from R & D Diagnostics (Minneapolis, MN) using the procedure provided by the supplier. Human recombinant VEGF included in the kit was used to construct a standard curve and obtain absolute values of VEGF protein content. The values were then normalized to the total protein concentration in each dish.

Xenografts of MKN-45 cells in nude mice

Two×10^7 MKN-45 cells were subcutaneously xenografted in the right flank of 8-wk-old male BALB/c-*nu*/*nu* mice (Shanghai Experimental Animal Center, Chinese Academy of Sciences, China). When tumors reached a mean volume of 100 mm^3, mice were randomly divided into two groups (8 mice in per group) and treated as the following. Mice in experiment group were administrated subcutaneously with mifepristone at the dose of 50 mg/kg· d, whereas mice in control were subcutaneouely injected with saline every day. After 8 wk of treatment, lungs were harvested, and the weights of lungs were determined. The number of metastatic foci in lungs fixed with Bouin' s solution for 24 h was counted under a stereomicroscope. Meanwhile, the tumors were resected, fixed with 40 g/L formaldehyde in PBS, embedded in paraffin and sliced into 4-μm-thick sections for immunohistochemical analysis.

Immunohistochemical staining for VEGF and MVD

The expression of VEGF and MVD in harvested tumors was determined immunohisto- chemically using an avidin-biotin-peroxidase complex (ABC) kit (Vector Laboratories, USA). Unless otherwise stated, all steps were performed at room temperature. Briefly, after removal of wax, tissue sections were treated with 30 mL/L hydrogen peroxidase for 30 min to block endogenous peroxidase activity, and microwaved in 10 mmol/L citrate buffer for 10 min to retrieve antigens. After blocked with normal goat serum, rabbit anti-human polyclonal antibody against VEGF and factor VIII-related antigen (Santa Cruz Biotechnology, USA) at a 100-fold dilution were separately applied to sections and incubated overnight at 4 ℃. This was followed by treatment with biotin-labeled goat anti-rabbit IgG for 60 min. The ABC complex was added and allowed to stand for 30 min. Sites of immunoreaction were visualized with 3, 3' -diaminobenzidine (DAB), followed by counterstaining with Mayer' s haematoxylin, if necessary. Between each step, the sections were washed three times with 100 mmol/L Tris-HCl buffer containing 0.1 mg/L Triton X-100. For a positive control, breast cancer tissue was used and the primary antibody was replaced by normal rabbit serum as a negative control.

Statistical analysis

Data were expressed as mean±SD. Statistical analysis was performed using the Student' s *t* test and chi-square test. $P<0.05$ was considered statistically significant.

RESULTS

Adhesion assay and expression of integrin β3

MTT assay revealed that mifepristone dose-dependently inhibited the cell adhesion to artificial basement membrane, Matrigel. The adhesive rate of MKN-45 cells was 78.2±5.0%, 65.4±4.7%, 49.8±4.2% in mifepristone-treated group, and 85.6±6.3% in control group ($P<0.05$). To further explore whether the change of cell adhesion molecule expression in MKN-45 cells contributed to the inhibition, flow cytometry was used to detect the expression of integrin β3 in the cells. Results showed that the expression of integrin β3 in MKN-45 cells treated with 5, 10, 20 μmol/L mifepristone was significantly lower than that in control group (25.4±3.6%, 19.6±2.9%, 15.8±2.2% *vs* 31.8±4.1%, $P<0.05$).

Migration assay

The effect of mifepristone on the migration of MKN-45 cells was evaluated in the Transwell cell culture chambers. As shown in Figure 1, there was a significant decrease in the number of migrated MKN-45 cells in mifepristone-treated group (72±8, 50±6, 41±5) as compared with that in control group (94±16, $P<0.01$).

Expression of VEGF protein

After treatment with 5, 10, 20 μmol/L mifepristone for 48 h, secreted VEGF protein in the cell culture media measured by ELISA assay, was 14.2±2.9, 8.9±3.1 and 5.4±2.1 ng/g per liter, respectively. There was a significant difference in VEGF expression as compared with that in the control cells (22.7±4.3 ng/g per liter, $P<0.01$).

Xenografts of MKN-45 cells in nude mice

During necropsy, lung metastasis of gastric cancer was found in 6 mice of the control group, and in 4 mice of mifepristone group (Figure 2). As far as the number of metastatic foci in lungs was concerned, there was a significant difference in mifepristone-treated group as compared with control group (8±2 *vs* 18±7, $P<0.05$). In addition, the weights of xenografted tumors in nude mice treated with mifepristone (201±36 mg) were significantly lower than those in control group (298±54 mg, $P<0.05$). To evaluate the effects of mifepristone on MVD and VEGF expression in xenografted tumors, immnunohistochemical

staining was performed using ABC method. Results revealed that VEGF was highly expressed in xenografted gastric cancer in nude mice (Figure 3A). After treatment with mifepristone for 8 wk, the expression of VEGF was markedly down-regualted in the tumors (Figure 3B). In addition, MVD of xenografted tumors was (11.2±2.5)/400×visual field in mifepristone-treated group, and (29.8±7.6)/400×in the control group (P<0.01).

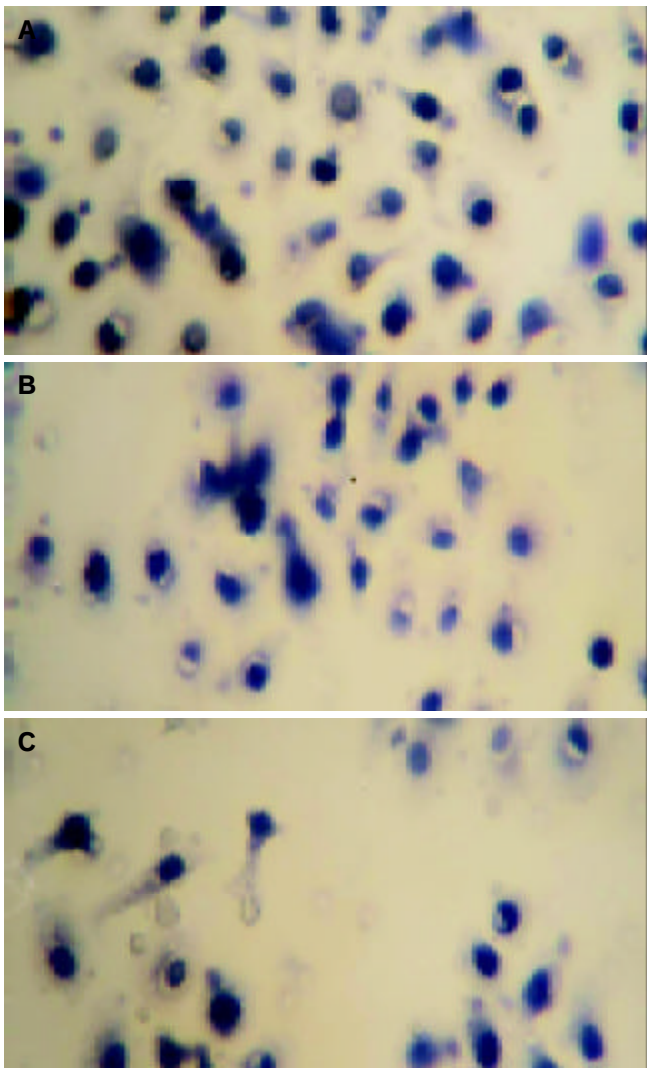

Figure 1 Effect of mifepristone on migration of MKN-45 cells incubated in Transwell cell culture chambers for 24 h in the absence (A) or presence of 10 μmol/L (B) and 20 μmol/L (C) mifepristone (H.E, ×200).

Figure 2 Metastatic foci in lungs of nude mice (arrow). After 24 h of fixation with Bouin's solution, lung tissues exhibited yellow, whereas the tumors exhibited white.

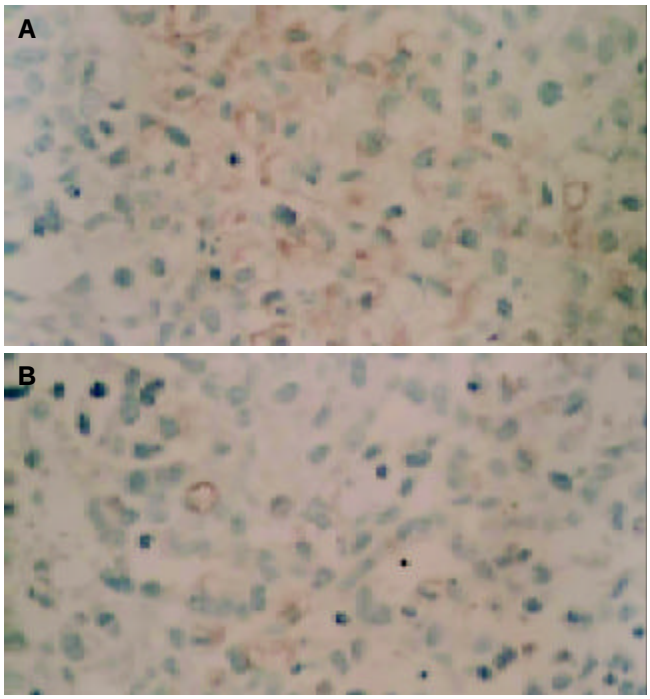

Figure 3 Immunohistochemical detection of VEGF expression in xenografted gastric cancer tissues of nude mice treated for 8 wk without (A) or with (B) 50 mg/kg·d mifepristone (ABC, ×100).

DISCUSSION

Although considerable evidence[9,10], both clinical and experimental, has demonstrated that mifepristone exerts markedly anti-proliferative effects on PR-positive malignant tumor cells, the role of mifepristone in anti-tumor invasion and metastasis, especially on gastric cancer, is poorly understood. In the presnet study, we demonstrated that mifepristone effectively inhibited the invasive and metastatic potential of human gastric adenocarcinoma cell line MKN-45 *in vitro* and *in vivo* through multiple mechanisms.

For tumor cells, increase of heterotypic adhesion to basement membrane and decrease of homotypic adhesion to the same cells have been defined as the critical event of tumor invasion that signals the initiation of metastatic cascade[11,12]. In the present study, heterotypic adhesion of MKN-45 cells to artificial basement membrane, Matrigel, was examined with MTT dye assay to stain the adhered cells. Results showed that mifepristone dose-dependently decreased the adhesive rate of MKN-45 cells. Moreover, the findings were further proved by the down- regulation of integrin β3 expression in the cells treated with mifepristone.

Integrin β3, one member of integrins superfamily, plays a fundamental role in tumor cell heterotypic adhesion to extracellular matrix and basement membrane, which has been found to be mediated through a specific arginine-glycine-aspartic acid (RGD) amino acid sequence[13]. Brakebusch *et al.*[14] reported that high expression of integrin β3 directly correlated with tumorigenicity and tumor progression. To further explore whether the change of integrin β3 expression in MKN- 45 cells contributed to the inhibitory effect of mifepristone on cell adhesion, flow cytometry was perfomed. We found that mifepristone down-regulated the expression of integrin β3 in MKN-45 cells in a dose-dependent manner. The results were also demonstrated by the work of Li *et al.*[15], who reported that mifepristone significantly down-regulated the expression of integrin β3 in decidua and chorionic villi of early pregnancy, and the effect might be related with the anti-pregnancy mechanism of mifepristone. Taken together, the inhibitory

effect of mifepristone on heterotypic adhesion of MKN-45 cells may be associated with the down-regulation of integrin β3. Moreover, integrin β3 has been found to function not only as a cell adhesion molecule, but also as a signaling molecule for regulation of angiogenesis[16]. Therefore, down- regulation of integrin β3 expression in MKN-45 cells may be partially responsible for the inhibition of angiogenesis in the cells by mifepristone.

Continuous growth, invasion and metastasis of malignant tumors including human gastric cancer are dependent on angiogenesis factors regulated by peptide growth factors, of which VEGF is one of the most selective and potent[17]. Hyder *et al*.[18] reported that progestins could induce the expression of VEGF mRNA and protein in human breast cancer cell line T47D, and this effect was blocked by the antiprogestin agent mifepristone. The finding suggests that mifepristone may be useful to inhibit proliferation and metastasis in some tumors by blocking VEGF production. Thus, there is a great interest in exploring the effect of mifepristone on the expression of VEGF in MKN-45 cells. After exposure of MKN-45 cells to various concentrations of mifepristone for 48 h, a dose-dependent decrease in the media levels of VEGF was observed. Furthermore, the results were further supported by animal experiments. Immunohistochemical analysis showed that mifepristone significantly down-regulated the expression of VEGF and MVD in xenografted gastric cancer in nude mice. Summarily, it seems reasonable to conclude that the inhibitory effect of mifepristone on the invasive and metastatic potential of MKN-45 cells is medicated partially via blocking VEGF production.

On the other hand, tumor cell migration was necessary at the initiation of metastatic cascade, when the tumor cells left the primary site and gained access to the circulation and also at the end of invasion, when they were entering the secondary site[19]. Theoretically, the decrease of tumor cell migration would contribute to the inhibition of tumor invasion and metastasis. In the study, the effect of mifepristone on the migaration of MKN-45 cells was estimated in Transwell cell culture chambers. Results showed that a significant decrease in the number of migrated MKN-45 cells was observed in mifepristone-treated group as compared with control group.

In summary, mifepristone effectively inhibited the invasive and metastatic potential of human MKN-45 gastric adenocarcinoma cells through inhibition of the heterotypic adhesion to basement membrane, cell migration and angiogenesis. These findings, linked to its anti- proliferative effects, indicate that mifepristone may be a beneficial agent for additional and complementary use in the management of gastric cancer.

REFERENCES

1 **Mahajan DK**, London SN. Mifepristone(RU486): a review. *Fertil Steril* 1997; **68**: 967- 976

2 **Rocereto TF**, Saul HM, Aikins JA Jr, Paulson J. Phase II study of mifepristone (RU486) in refractory ovarian cancer. *Gynecol Oncol* 2000; **77**: 429-432

3 **Thomas M**, Monet JD. Combined effects of RU486 and tamoxifen on the growth and cell cycle phases of the MCF-7 cell line. *J Clin Endocrinol Metab* 1992; **75**: 865-870

4 **Lash GE**, Fitzpatrick TE, Graham CH. Effect of hypoxia on cellular adhesion to vitronectin and fibronectin. *Biochem Biophys Res Commun* 2001; **287**: 622-629

5 **Arck PC**, Hertwig K, Hagen E, Hildebrandt M, Klapp BF. Pregnancy as a model of controlled invasion might be attributed to the ratio of CD3/CD8 to CD56. *Am J Reprod Immunol* 2000; **44**: 1-8

6 **Murray MJ**, Lessey BA. Embryo implantation and tumor metastasis: common pathways of invasion and angiogenesis. *Semin Reprod Endocrinol* 1999; **17**: 275-290

7 **Fitzpatrick TE**, Lash GE, Yanaihara A, Charnock-Jones DS, Macdonald-Goodfellow SK, Graham CH. Inhibition of breast carcinoma and trophoblast cell invasiveness by vascular endothelial growth factor. *Exp Cell Res* 2003; **283**: 247-255

8 **Janneau JL**, Maldonado-Estrada J, Tachdjian G, Miran I, Motte N, Saulnier P, Sabourin JC, Cote JF, Simon B, Frydman R, Chaouat G, Bellet D. Transcriptional expression of genes involved in cell invasion and migration by normal and tumoral trophoblast cells. *J Clin Endocrinol Metab* 2002; **87**: 5336-5339

9 **Yokoyama Y,** Shinohara A, Takahashi Y, Wan X, Takahashi S, Niwa K, Tamaya T. Synergistic effects of danazol and mifepristone on the cytotoxicity of UCN-01 in hormone-responsive breast cancer cells. *Anticancer Res* 2000; **20**: 3131-3135

10 **El Etreby MF**, Liang Y, Lewis RW. Induction of apoptosis by mifepristone and tamoxifen in human LNCaP prostate cancer cells in culture. *Prostate* 2000; **43**: 31-42

11 **Stetler-Stevenson WG**, Kleiner DE. Molecular biology of cancer: invasion and metastases. In: Devita VT, Hellman S, Rosenberg SA, eds. Cancer principles and practice of oncology. 6th ed. *Philadelphia: Lippincott Williams Willkins* 2001: 123-136

12 **Hanahan D**, Weinberg RA. The hallmarks of cancer. *Cell* 2000; **100**: 57-70

13 **Liotta LA**, Kohn EC. Invasion and metastases. In: Frin H, eds. Cancer medicine. 5th ed. *Baltimore: Williams Wilkins* 2001: 121-131

14 **Brakebusch C,** Bouvard D, Stanchi F, Sakai T, Fassler R. Integrins in invasive growth. *J Clin Invest* 2002; **109:** 999-1006

15 **Li RZ,** Wang ZH, Wu RF, Lu SY, Shi B. Expression of integrin b3 and extracellular matrix: fibronectin and laminin in deciduas and chorionic chill of medical abortion for early pregnancy. *J Reprod Med* 1999; **8**: 214-216

16 **Kohn EC**, Liotta LA. Metastasis and angiogenesis: molecular dissection and noval applications. In: Mendelsohn J, Howley PM, Israel MA, Liota LA. eds. The molecular basis of cancer. 2nd ed. *Philadephia: W.B Saunders Company* 2001: 163-172

17 **Folkman J**. Tumor angiogenesis. In:Abeloff MD, Arimitage JO, Lichter AS, Niederbuber JE, eds. Clinical oncology. 2nd ed. *Orlando: Harcourt Publishers Limited* 2001: 132-151

18 **Hyder SM**, Chiappetta C, Stancel GM. Pharmacological and endogenous progestins induce vascular endothelial growth factor expression in human breast cancer cells. *Int J Cancer* 2001; **92**: 469-473

19 **Fidler IJ**. Cancer biology: invasion and metastasis. In: Abeloff MD, Arimitage JO, Lichter AS, Niederbuber JE, eds. Clinical oncology. 2nd ed. *Orlando: Harcourt Publishers Limited* 2001: 29-53

Edited by Xu FM and Wang XL

PO Box 2345, Beijing 100023, China
Fax: +86-10-85381893
E-mail: wjg@wjgnet.com www.wjgnet.com

World J Gastroenterol 2004;10(12):1730-1734
World Journal of Gastroenterology
Copyright ©2004 by The WJG Press ISSN 1007-9327

• LIVER CANCER •

Microvessel density of malignant and benign hepatic lesions and MRI evaluation

Jian-Ping Lu, Jian Wang, Tao Wang, Yi Wang, Wei-Qing Wu, Li Gao

Jian-Ping Lu, Jian Wang, Department of Radiology, Changhai Hospital, Second Military Medical University, Shanghai 200433, China
Tao Wang, Yi Wang, Wei-Qing Wu, Eastern Hepatobiliary Surgery Institute, Second Military Medical University, Shanghai 200433, China
Li Gao, Department of Pathology, Changhai Hospital, Second Military Medical University, Shanghai 200433, China
Supported by the National Natural Science Foundation of China, No. 39970728
Correspondence to: Dr. Jian-Ping Lu, Department of Radiology, Changhai Hospital, Second Military Medical University, Shanghai 200433, China
Telephone: +86-21-25072133
Received: 2003-08-23 **Accepted:** 2003-10-12

Abstract

AIM: To study the difference of microvessel density (MVD) between malignant and benign hepatic lesions and study the relationship between MVD and dynamic enhanced magnetic resonance imaging (MRI) for evaluation of microvessels within malignant and benign hepatic lesions.

METHODS: A total of 265 specimens of hepatocellular carcinoma (HCC), 122 cirrhosis tissues and 22 hepatic benign lesions were enrolled for MVD by immunohistochemistry on tissue microarray, of which 49 underwent MRI examination before surgery, then contrast-to-noise ratios (CNR) and enhancement index (EI) in all the phases were calculated. Pearson correlation was performed for correlation analysis between CNR, EI and MVD.

RESULTS: MVD of HCC was 22.7±15.8 (mean±SD), which was obviously higher than that of cirrhosis tissue (8.3±7.6, $P<0.01$), but was not statistically different from that of benign lesions (31.3±22.7, $P>0.05$). Among HCC, MVD of gradesI-II was 29.9±18.6, which was much higher than those of grade III (22.2±18.2, $P<0.01$) and gradeIV (22.9±19.0, $P<0.01$). MVD of HCC ($P=0.018$) and of benign lesions ($P=0.014$) were both correlative with CNR in arterial phase.

CONCLUSION: Neoangiogenesis is an important feature for malignant tumor, and MVD may act as a biological marker in differentiating malignant from benign hepatic lesions. Dynamic enhanced MRI, especially image in arterial phase, may act as an MVD evaluation criterion for malignant and benign hepatic lesions.

Lu JP, Wang J, Wang T, Wang Y, Wu WQ, Gao L. Microvessel density of malignant and benign hepatic lesions and MRI evaluation. *World J Gastroenterol* 2004; 10(12): 1730-1734
http://www.wjgnet.com/1007-9327/10/1730.asp

INTRODUCTION

It is well known that hepatocellular carcinoma (HCC) is a type of hypervascular lesion[1], but there were seldom reports on difference of microvessel density (MVD) between HCC and benign hepatic lesions. The tissue microarray, which has been developed recently as a high-throughput technique for rapid scanning hundreds or thousands of samples at the same time, can be applied in analyzing expression of some DNA, RNA or protein[2]. In this research, differences of MVD of a large number of hepatic malignant and benign lesions were studied with tissue microarray, which further demonstrated some biological features of HCC.

Recent advances in magnetic resonance imaging (MRI) have led to the establishment of fast scan techniques, which, combined with bolus injection of contrast material, allows the acquisition of dynamic enhanced MRI for higher confident detection of HCC[3-5]. There have been reports on correlation among digital subtraction angiography (DSA), ultrasound angiography (USAG), computed tomography during arterial portography (CTAP) and immunohistochemical findings[6], but the relationship between MVD and dynamic MRI has been seldom reported. In this research, correlation between MVD and dynamic enhanced MRI of hepatic malignant and benign lesions was studied in order to establish a theoretical foundation for microvessels evaluation within these lesions with MRI images, which will give more references to clinical diagnosis or HCC therapy.

MATERIALS AND METHODS

Tissue specimens

Tissue specimens were obtained at surgery from Eastern Hepatobiliary Surgery Institute, including 265 of HCC, 122 of cirrhosis tissue adjacent to carcinoma, 5 of hepatocellular adenoma and 17 of focal nodular hyperplasia (FNH). The 265 specimens of HCC included 45 of small HCC (tumor diameter$\leqslant$3 cm). All the case of HCC were graded by Edmondson-Steiner's pathological criteria into 3 groups: grades I-II (37 cases), grade III (218 cases) and grade IV (10 cases). All the specimens were fixed in 10% formalin and embedded in paraffin. All the pathologic diagnoses were confirmed by two the pathologists.

Constructing tissue microarray

For tissue microarray construction, a hematoxylin and eosin (H&E)-stained section was made from each block to define representative regions. With a tissue-microarray-constructor (Beecher Instruments, Silver Spring, MD), a hole (diameter=6 mm) was punched into a recipient paraffin block, and then a cylindrical core sample (diameter=6 mm), which had been punched from the donor tissue block, was deposited into the hole. This process was repeated till all the samples were deposited into the recipient block. After finishing the recipient block, multiple sections were cut from the block with a microtome.

Immunohistochemical staining and evaluation criteria

Avidin-biotin-peroxidase complex (ABC) method was used for immunohistochemical staining with monoclonal antibody CD-34 (Antibody Dignostic Inc., U.S.A.). After staining, the tubular, sinusoidal, cystiform or vacuolar structures shaped by endothelial cells or immature endothelial cells, which were stained yellow

or brown by CD34, were considered as positive microvessels. In high power microscopic views, all the positive microvessels were counted for MVD.

MRI technique

Forty-eight patients with 49 of the lesions underwent MRI examination before surgery, including 33 HCC (only one belonged to grade IV, and the others belonged to grade III and all diameters were≤3 cm) and 16 benign lesions. MRI was performed with a 1.5 T system (Symphony, Siemens) and a phased array coil was used. All the patients underwent axial T1 weighted (fast low angle shot, FLASH, TR=123 ms, TE=4.8 ms), T2 weighted (half-fourier acquisition single-shot turbo spin echo, HASTE, TR=1 200 ms, TE=57 ms) and multiphase dynamic gadolinium-DTPA enhanced (the same sequence as T1 weighted) imaging. The section thickness was 8 mm, with an intersection gap of 0.5-2 mm. The contrast material dose was 0.2 mmol/kg·b.w. and was administered as a rapid bolus. Arterial phase images were obtained in 15-20 s after the start of bolus administration. Portal venous and equilibrium phase images were obtained in the 45 s and 90 s, respectively.

Image analyses

In all the images, signal intensities of lesions (SI_l), liver parenchyma (SI_p) and background noise (SI_n) were evaluated, respectively. Signal-to-noise ratios (SNR) of lesions and parenchyma were both calculated as $SNR=SI_{l/p}/SI_n$. Contrast-to-noise ratios (CNR) in all the phases were calculated as $CNR=SNR_l-SNR_p$. Enhancement indexes (EI) of lesions in all the phases were calculated as $EI= (SNR_{contrasted}-SNR_{uncontrased})/ SNR_{uncontrased}$.

Statistical analyses

All data were analyzed by SPSS 9.0. Analysis of variance was used to determine significant differences of MVD among HCC, cirrhosis and benign lesion, of MVD of HCC among different pathological grades and tumor diameters, and of CNR between HCC and benign lesion among nonenhanced, arterial, portal venous and equilibrium phases. Pearson correlation was performed for correlation analysis among CNRs, EIs and MVD in arterial, portal venous and equilibrium phases of HCC or benign lesion, respectively.

RESULTS

Outcome of tissue microarray constructing, immunohistochemical staining and MRI

Overview of a piece of tissue microarray is shown in Figure 1. Microvessel density stained by immunohistochemistry and dynamic MR images of HCC, hepatocellular adenoma and FNH are shown in Figures 2, 3 and 4, respectively.

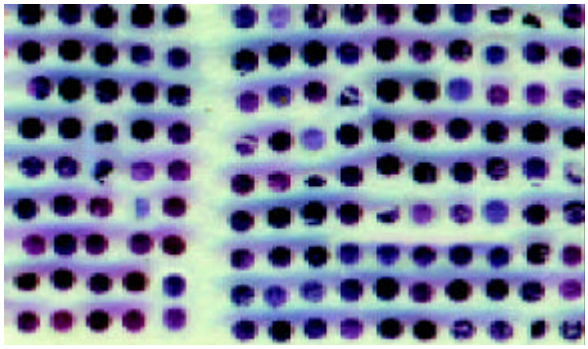

Figure 1 Overview of a piece of tissue microarray including 234 samples (HE staining).

Table 1 MVD of malignant and benign liver lesions

	Number	MVD (mean±SD)
HCC	265	22.7±15.8[b]
Cirrhosis	122	8.3±7.6
Benign lesion	22	31.3±22.7

[b]$P<0.01$ *vs* cirrhosis.

MVD of hepatic benign and malignant lesions

MVD of HCC was significantly higher than that of cirrhosis, but there was no significant difference between those of HCC and of benign lesions (Table 1).

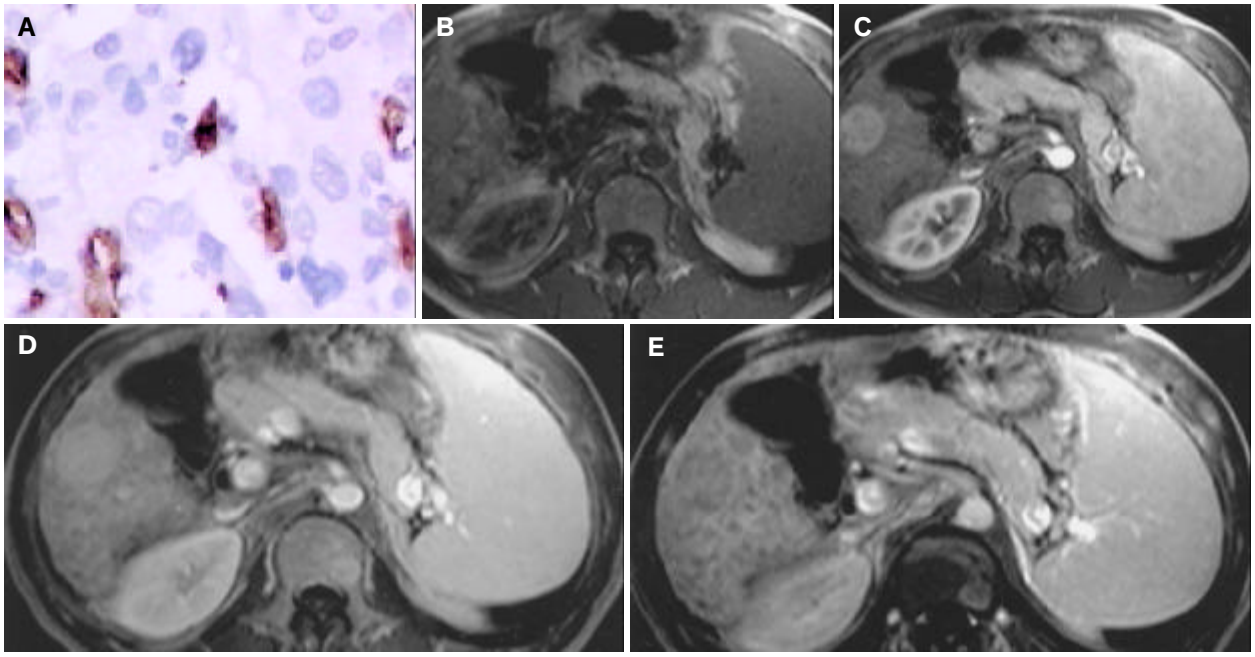

Figure 2 HCC in right lobar of liver. A: Microvessel density, stained by CD34 (Original magnification: ×200); B: MR image, T1 weighted, nonenhanced, CNR=-1.50; C: MR image, arterial phase, CNR=11.00; D: MR image, portal venous phase, CNR=10.50; E: MR image, equilibrium phase, CNR=-6.00.

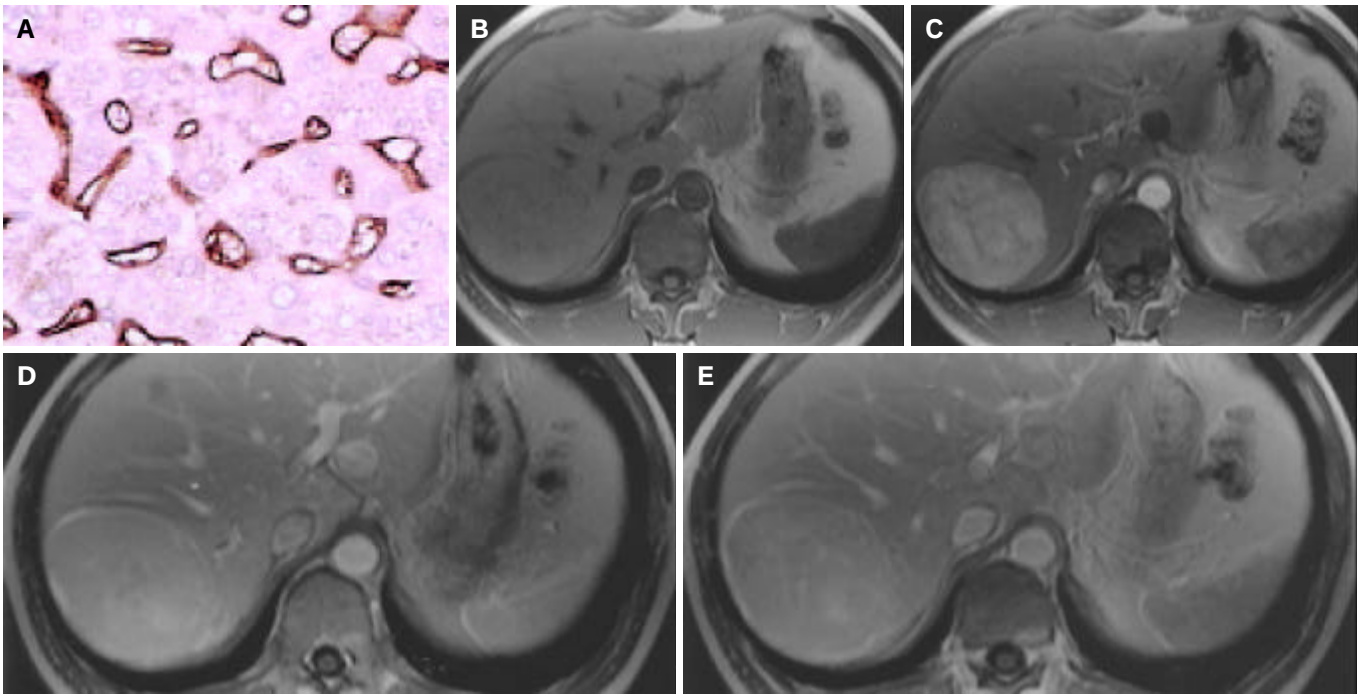

Figure 3 Hepatocellular adenoma in right lobar of liver. A: Microvessel density, stained by CD34 (Original magnification: ×200); B: MR image, T1 weighted, nonenhanced, CNR=-0.10; C: MR image, arterial phase, CNR=16.93; D: MR image, portal venous phase, CNR=9.42; E: MR image, equilibrium phase, CNR=6.42.

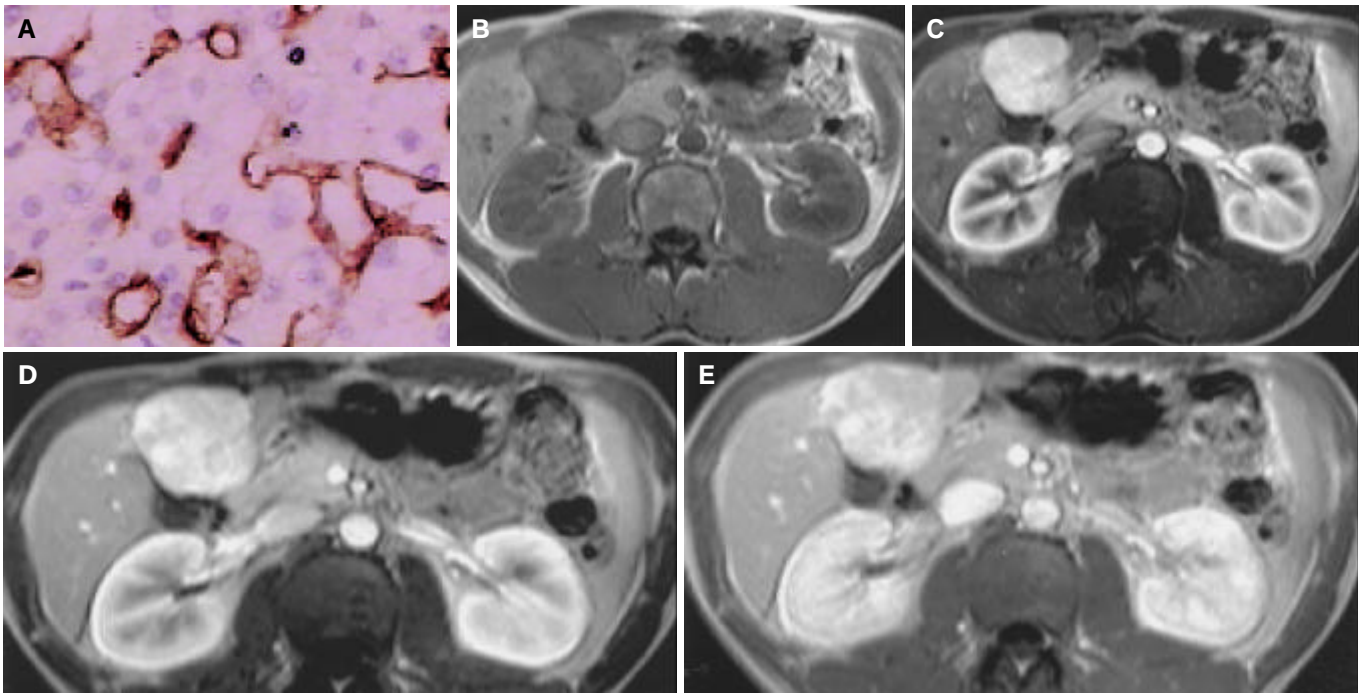

Figure 4 FNH in left inner lobar of liver. A: Microvessel density, stained by CD34 (Original magnification: ×200); B: MR image, T1 weighted, nonenhanced, CNR=-3.48; C: MR image, arterial phase, CNR=15.43; D: MR image, portal venous phase, CNR=5.81; E: MR image, equilibrium phase, CNR=2.97.

MVD of HCC among different pathological grades and tumor sizes

MVD of grades I-II was 29.9±18.6 (mean±SD), which was much higher than those of grade III (22.2±18.2, $P<0.01$) and grade IV (22.9±19.0, $P<0.01$). There was no significant difference in MVD between small HCC (26.1±115.3) and those HCC whose diameters were more than 3 cm (22.1±15.8).

CNR of HCC and benign lesion in all the phases

CNRs of HCC and benign lesion in T1 weighted nonenhanced, arterial, portal venous and equilibrium phases are shown in Table 2. There was significant difference among all the phases ($F=9.761$, $P<0.001$), but no significant difference among nonenhanced, portal venous and equilibrium phases ($P=0.279$) or between HCC and benign lesion ($F=0.380$, $P=0.539$).

Correlation between MVD and CNRs

Forty-eight patients with 49 of the lesions underwent MRI examination before surgery, including 33 HCC (only one belonged to grade IV, and the others belonged to grade III and all the diameters were≤3 cm) and 16 benign lesions. Pearson

Correlation coefficients among MVD and CNRs of HCC in arterial, portal venous and equilibrium phases were 0.409 (P=0.018), 0.264 (P=0.138) and 0.212 (P=0.236), respectively, while Pearson Correlation coefficients between MVD and CNRs of benign lesions in arterial, portal venous and equilibrium phases were 0.599 (P=0.014), 0.581 (P=0.018) and 0.540 (P=0.031), respectively.

Table 2 CNR of HCC and benign lesion (mean±SD)

	Nonenhanced	Arterial phase	Portal venous phase	Equilibrium phases
HCC				
(n=33)	-2.86±2.94	3.88±5.63	-1.43±8.39	-1.08±2.80
Benign lesion				
(n=16)	-2.91±2.79	2.12±9.08	-2.05±8.56	-0.92±6.59

Correlation between MVD and EIs

Pearson Correlation coefficients between MVD and EIs of the 33 specimens of HCC in arterial, portal venous and equilibrium phases were 0.155 (P=0.389), 0.072 (P=0.692) and -0.122 (P=0.497), respectively, while Pearson Correlation coefficients between MVD and EIs of the 16 specimens of benign lesions in arterial, portal venous and equilibrium phases were 0.077 (P=0.776), 0.180 (P=0.506) and -0.062 (P=0.821), respectively.

DISCUSSION

Utilization of tissue microarray technique in detecting nucleic acid and protein has recently made great progress in basic research of tumor. A large number of samples in one section of tissue microarray can be stained under the same pre-treatment condition, the same antibody titer and the same detection systems. And reproducibility of the staining reaction, as well as the speed and reliability of the interpretation, is improved, since all the samples are on the same slide[7,8]. Then, quickly and efficiently scanning a great number of specimens with tissue microarray can reduce mistakes not only from sample selecting and statistical analysis but also from tumor heterogeneity. In MVD counting, utilization of tissue microarray can standardize sample areas and overcome manual deviation. In this research, tissue microarray technique, combined with immunohistochemistry, was used to study difference of MVD between malignant and benign hepatic lesions in order to further demonstrate some biological features of these lesions.

CD34, which is expressed in blood stem cells and neovessel endothelial cells, is the most distinctive marker for demonstrating vessel endothelial cells[9,10], especially for demonstrating sinusoid-like vessels in tumor tissues[11,12]. Angiogenesis is very common within normal and pathologic tissues and is regulated by many factors, such as hypoxia-inducible factor 1alpha (HIF-1α), vascular endothelial growth factor (VEGF), human macrophage metalloelastase (HME), basic fibroblast growth factor (bFGF) and so on[13-16]. Vessels, as an important part of tumorous interstitial tissue, interact with tumor cells to construct microenvironment of tumor. Researches showed that angiogenesis plays an important role in tumor invasion[17], MVD is a novel prognostic marker in patients after resection of small HCC[11,18-20], and high expression of CD34-positive sinusoidal endothelial cells is a risk factor for HCC in patients with chronic liver diseases[21]. Sun *et al*.[18] reported that MVD level was not related to tumor size, capsule status, Edmondson-Steiner's grade, alpha-fetoprotein (AFP) level, associated cirrhosis, gamma-glutamyltransferase and serum HBsAg status. Yamamoto *et al*.[22] demonstrated that sinusoidal capillarization occurring in well-differentiated HCC is related to dedifferentiation of parenchymal tumor cells, but not to tumor size. But some reports showed that tumor size, poor differentiation and portal invasion are significantly related to MVD[11,23]. In this research, MVD of HCC was significantly higher than that of cirrhosis, but there was no significant difference between those of HCC and of benign lesion, which probably means that microvessels play an important role not only in occurrence and development of HCC, but also in some other benign lesions, thus may be helpful to identify malignant lesions or precancerous lesions (for example, high-grade dysplastic nodule) from regenerative nodules or low-grade dysplastic nodules[24,25]. MVD in grades I-II was higher than those in grade III and grade IV, suggesting that angiogenesis is more active during the beginning of hepatocarcinogenesis.

DSA and CTAP have been used for assessing angiogenesis of HCC[6], but these examinations are all invasive and expensive with dangerousnesses of ionized radiation and allergy induced by iodic contrast material. Shimizu *et al*.[26] used xenon-enhanced CT to quantitatively measure tissue blood flow in HCC, but xenon is a kind of scarce gas. Compared with DSA, CTAP and xenon-enhanced CT, MRI is uninvasive, safe, rapid, and cheap. Gadolinium has a strong hydrogen-proton spin-lattice relaxation effect, which will increase the signal intensity of adjacent tissue on T1 weighted images. The MRI contrast agent, gadolinium-DTPA, does not penetrate cell membrane and only diffuses into vascular space and interstitial space, which may reveal that the signal intensity of tissue on enhanced T1 weighted image is correlated with the vascularity. There have been reports on correlation of dynamic contrast enhancement MRI with MVD in prostate cancer and in breast cancer[27,28]. With development of fast scan technique, rapid MRI is available to image the whole liver during the arterial phase[29]. In this research, CNR in arterial phase, regardless of malignant or benign lesions, was correlative with MVD. Since MVD of HCC is much higher than that of cirrhosis, arterial phase images of MRI could be a useful method to distinguish HCC from regenerative nodules. Some reports have confirmed this view[30,31]. In this research, CNR of HCC in portal venous or equilibrium phase was not correlated with MVD. This phenomenon probably demonstrates that CNR is regulated by many factors besides MVD. Reports have shown that with small HCC increasing in size and becoming increasingly dedifferentiated, the number of portal tracts apparently decreases and intratumoral arteriole develops[22,23]. Because of portal tracts' decreasing and intratumoral arteriols' developing, there was no unified blood supply in HCC nodules, which would not demonstrate unified relationship between MVD and CNR in portal venous or equilibrium phase. There was no change of blood supply in benign nodules, so unified relationship between MVD and CNR in portal venous or equilibrium phase was demonstrated. CNR in arterial phase is mostly regulated by MVD, while in portal venous or equilibrium phase, blood supply plays a more important role. This hypothesis should be tested by advanced research.

In conclusion, angiogenesis is secondary to occurrence and development of benign and malignant tumors. Since dynamic MRI could evaluate microvessel of lesions, it is a very useful method to demonstrate HCC.

REFERENCES

1 **El-Assal ON**, Yamanoi A, Soda Y, Yamaguchi M, Igarashi M, Ymamoto A, Nabika T, Nagasue N. Clinical significance of microvessel density and vascular endothelial growth factor expression in hepatocellular carcinoma and surrounding liver: possible involvement of vascular endothelial growth factor in the angiogenesis of cirrhotic liver. *Hepatology* 1998; **27**: 1554-1562

2 **Kallioniemi OP**, Wagner U, Kononen J, Sauter G. Tissue microarray technology for high-throughput molecular profiling of cancer. *Hum Mol Genet* 2001; **10**: 657-662

3 **Tomemori T**,Yamakado K, Nakatsuka A, Sakuma H, Matsumura K, Takeda K. Fast 3D dynamic MR imaging of the liver with MR SmartPrep: comparison with helical CT in de-

tecting hypervascular hepatocellular carcinoma. *Clin Imaging* 2001; **25**: 355-361

4 **Shinozaki K**, Honda H, Yoshimitsu K, Taguchi K, Kuroiwa T, Irie H, Aibe H, Nishie A, Nakayama T, Shimada M, Masuda K. Optimal multi-phase three-dimensional fast imaging with steady-state free precession dynamic MRI and its clinical application to the diagnosis of hepatocellular carcinoma. *Radiat Med* 2002; **20**: 111-119

5 **Noguchi Y**, Murakami T, Kim T, Hori M, Osuga K, Kawata S, Okada A, Sugiura T, Tomoda K, Narumi Y, Nakamura H. Detection of hypervascular hepatocellular carcinoma by dynamic magnetic resonance imaging with double-echo chemical shift in-phase and opposed-phase gradient echo technique: comparison with dynamic helical computed tomography imaging with double arterial phase. *J Comput Assist Tomogr* 2002; **26**: 981-987

6 **Toyoda H**, Fukuda Y, Hayakawa T, Kumada T, Nakano S. Changes in blood supply in small hepatocellular carcinoma: correlation of angiographic images and immunohistochemical findings. *J Hepatol* 1997; **27**: 654-660

7 **Bubendorf L**, Kononen J, Koivisto P, Schraml P, Moch H, Gasser TC, Willi N, Mihatsch MJ, Sauter G, Kallioniemi OP. Survey of gene amplifications during prostate cancer progression by high-throughout fluorescence *in situ* hybridization on tissue microarrays. *Cancer Res* 1999; **59**: 803-806

8 **Richter J**, Wagner U, Kononen J, Fijan A, Bruderer J, Schmid U, Ackermann D, Maurer R, Alund G, Knönagel H, Rist M, Wilber K, Anabitarte M, Hering F, Hardmeier T, Schönenberger A, Flury R, Jager P, Fehr JL, Schraml P, Moch H, Mihatsch MJ, Gasser T, Källioniemi OP, Sauter G. High-throughput tissue microarray analysis of cyclin E gene amplification and overexpression in urinary bladder cancer. *Am J Pathol* 2000; **157**: 787-794

9 **Kimura H**, Nakajima T, Kagawa K, Deguchi T, Kakusui M, Katagishi T, Okanoue T, Kashima K, Ashihara T. Angiogenesis in hepatocellular carcinoma as evaluated by CD34 immunohistochemistry. *Liver* 1998; **18**: 14-19

10 **Frachon S**, Gouysse G, Dumortier J, Couvelard A, Nejjari M, Mion F, Berger F, Paliard P, Boillot O, Scoazec JY. Endothelial cell marker expression in dysplastic lesions of the liver: an immunohistochemical study. *J Hepatol* 2001; **34**: 850-857

11 **Tanigawa N**, Lu C, Mitsui T, Miura S. Quantitation of sinusoid-like vessels in hepatocellular carcinoma: its clinical and prognostic significance. *Hepatology* 1997; **26**: 1216-1223

12 **Gottschalk-Sabag S**, Ron N, Glick T. Use of CD34 and factor VIII to diagnose hepatocellular carcinoma on fine needle aspirates. *Acta Cytol* 1998; **42**: 691-696

13 **Ravi R**, Mookerjee B, Bhujwalla ZM, Sutter CH, Artemov D, Zeng Q, Dillehay LE, Madan A, Semenza GL, Bedi A. Regulation of tumor angiogenesis by p53-induced degradation of hypoxia-inducible factor 1alpha. *Genes Dev* 2000; **14**: 34-44

14 **Gorrin-Rivas MJ**, Arii S, Mori A, Takeda Y, Mizumoto M, Furutani M, Imamura M. Implications of human macrophage metalloelastase and vascular endothelial growth factor gene expression in angiogenesis of hepatocellular carcinoma. *Ann Surg* 2000; **231**: 67-73

15 **Yoshiji H**, Kuriyama S, Yoshii J, Ikenaka Y, Noguchi R, Hicklin DJ, Huber J, Nakatani T, Tsujinoue H, Yanase K, Imazu H, Fukui H. Synergistic effect of basic fibroblast growth factor and vascular endothelial growth factor in murine hepatocellular carcinoma. *Hepatology* 2002; **35**: 834-842

16 **Park YN**, Kim YB, Yang KM, Park C. Increased expression of vascular endothelial growth factor and angiogenesis in the early stage of multistep hepatocarcinogenesis. *Arch Pathol Lab Med* 2000; **124**: 1061-1065

17 **Ker CG**, Chen HY, Juan CC, Lo HW, Shen YY, Chen JS, Lee KT, Sheen PC. Role of angiogenesis in hepatitis and hepatocellular carcinoma. *Hepatogastroenterology* 1999; **46**: 646-650

18 **Sun HC**, Tang ZY, Li XM, Zhou YN, Sun BR, Ma ZC. Microvessel density of hepatocellular carcinoma: its relationship with prognosis. *J Cancer Res Clin Oncol* 1999; **125**: 419-426

19 **Salizzoni M**, Romagnoli R, Lupo F, David E, Mirabella S, Cerutti E, Ottobrelli A. Microscopic vascular invasion detected by anti-CD34 immunohistochemistry as a predictor of recurrence of hepatocellular carcinoma after liver transplantation. *Transplantation* 2003; **76**: 844-848

20 **Poon RT**, Ng IO, Lau C, Yu WC, Yang ZF, Fan ST, Wong J. Tumor microvessel density as a predictor of recurrence after resection of hepatocellular carcinoma: a prospective study. *J Clin Oncol* 2002; **20**: 1775-1785

21 **Ohmori S**, Shiraki K, Sugimoto K, Sakai T, Fujikawa K, Wagayama H, Takase K, Nakano T. High expression of CD34-positive sinusoidal endothelial cells is a risk factor for hepatocellular carcinoma in patients with HCV-associated chronic liver diseases. *Hum Pathol* 2001; **32**: 1363-1370

22 **Yamamoto T**, Hirohashi K, Kaneda K, Ikebe T, Mikami S, Uenishi T, Kanazawa A, Takemura S, Shuto T, Tanaka H, Kubo S, Sakurai M, Kinoshita H. Relationship of the microvascular type to the tumor size, arterialization and dedifferentiation of human hepatocellular carcinoma. *Jap J Cancer Res* 2001; **92**: 1207-1213

23 **Nakashima Y**, Nakashima O, Hsia CC, Kojiro M, Tabor E. Vascularization of small hepatocellular carcinomas: correlation with differentiation. *Liver* 1999; **19**: 12-18

24 **Roncalli M**, Roz E, Coggi G, Di Rocco MG, Bossi P, Minola E, Gambacorta M, Borzio M. The vascular profile of regenerative and dysplastic nodules of the cirrhotic liver: implications for diagnosis and classification. *Hepatology* 1999; **30**: 1174-1178

25 **de Boer WB**, Segal A, Frost FA, Sterrett GF. Can CD34 discriminate between benign and malignant hepatocytic lesions in fine-needle aspirates and thin core biopsies? *Cancer* 2000; **90**: 273-278

26 **Shimizu J**, Oka H, Dono K, Sakon M, Takamura M, Murakami T, Hayashi S, Nagano H, Nakamori S, Umeshita K, Sase S, Gotoh M, Wakasa K, Nakamura H, Monden M. Noninvasive quantitative measurement of tissue blood flow in hepatocellular carcinoma using xenon-enhanced computed tomography. *Dig Dis Sci* 2003; **48**: 1510-1516

27 **Schlemmer HP**, Merkle J, Grobholz R, Jaeger T, Michel MS, Werner A, Rabe J, van Kaick G. Can pre-operative contrast-enhanced dynamic MR imaging for prostate cancer predict microvessel density in prostatectomy specimens? *Eur Radiol* 2004; **14**: 309-317

28 **Su MY**, Cheung YC, Fruehauf JP, Yu H, Nalcioglu O, Mechetner E, Kyshtoobayeva A, Chen SC, Hsueh S, McLaren CE, Wan YL. Correlation of dynamic contrast enhancement MRI parameters with microvessel density and VEGF for assessment of angiogenesis in breast cancer. *J Magn Reson Imaging* 2003; **18**: 467-477

29 **Van Beers BE**, Materne R, Lacrosse M, Jamart J, Smith AM, Horsmans Y, Gigot JF, Gilon R, Pringot J. MR imaging of hypervascular liver tumors: timing optimization during the arterial phase. *J Magn Reson Imaging* 1999; **9**: 562-567

30 **Yoshimitsu K**, Honda H, Jimi M, Kuroiwa T, Irie H, Aibe H, Shinozaki K, Asayama Y, Shimada M, Masuda K. Correlation of three-dimensional gradient echo dynamic MR imaging with CT during hepatic arteriography in patients with hypervascular hepatocellular carcinomas: preliminary clinical experience. *J Magn Reson Imaging* 2001; **13**: 258-262

31 **Noguchi Y**, Murakami T, Kim T, Hori M, Osuga K, Kawata S, Kumano S, Okada A, Sugiura T, Nakamura H. Detection of hepatocellular carcinoma: comparison of dynamic MR imaging with dynamic double arterial phase helical CT. *Am J Roentgenol* 2003; **180**: 455-460

Edited by Hu DK and Chen WW **Proofread by** Xu FM

PO Box 2345, Beijing 100023, China
Fax: +86-10-85381893
E-mail: wjg@wjgnet.com www.wjgnet.com

World J Gastroenterol 2004;10(12):1735-1739
World Journal of Gastroenterology
Copyright ©2004 by The WJG Press ISSN 1007-9327

• VIRAL HEPATITIS •

Cloning and identification of *NS5ATP2* gene and its spliced variant transactivated by hepatitis C virus non-structural protein 5A

Qian Yang, Jun Cheng, Yan Liu, Yuan Hong, Jian-Jun Wang, Shu-Lin Zhang

Qian Yang, Shu-Lin Zhang, Department of Infectious Disease, First Hospital of Xi' an Jiaotong University, Xi' an 710061, Shaanxi Province, China
Jun Cheng, Yan Liu, Yuan Hong, Jian-Jun Wang, Gene Therapy Research Center, Institute of Infectious Diseases, 302 Hospital of PLA, 100 Xisihuanzhong Road, Beijing 100039, China
Supported by the National Natural Science Foundation of China, No. C03011402, No. C30070690 and the 9th Five-year Plan Period Research and Development Foundation of PLA, No. 98D063 and the Start-up for Students Studying Overseas of PLA, No. 98H038 and the 10th Five-year period Youth Research and Technology Foundation of PLA, No. 01Q138 and the 10th Five-year period Research and Technology Foundation of PLA, No. 01MB135
Correspondence to: Dr. Jun Cheng, Gene Therapy Research Center, Institute of Infectious Diseases, 302 Hospital of PLA, 100 Xisihuanzhong Road, Beijing 100039, China. cj@genetherapy.com.cn
Telephone: +86-10-66933391 **Fax:** +86-10-63801283
Received: 2003-11-21 **Accepted:** 2003-12-29

Abstract

AIM: To clone, identify and study new *NS5ATP2* gene and its spliced variant transactivated by hepatitis C virus non-structural protein 5A.

METHODS: On the basis of subtractive cDNA library of genes transactivated by NS5A protein of hepatitis C virus, the coding sequence of new gene and its spliced variant were obtained by bioinformatics method. Polymerase chain reaction (PCR) was conducted to amplify *NS5ATP2* gene.

RESULTS: The coding sequence of a new gene and its spliced variant were cloned and identified successfully.

CONCLUSION: A new gene has been recognized as the new target transactivated by HCV NS5A protein. These results brought some new clues for studying the biological functions of new genes and pathogenesis of the viral proteins.

Yang Q, Cheng J, Liu Y, Hong Y, Wang JJ, Zhang SL. Cloning and identification of *NS5ATP2* gene and its spliced variant transactivated by hepatitis C virus non-structural protein 5A. *World J Gastroenterol* 2004; 10(12): 1735-1739
http://www.wjgnet.com/1007-9327/10/1735.asp

INTRODUCTION

Hepatitis C virus (HCV) is the major causative agent of non-A, non-B hepatitis worldwide, which often leads to cirrhosis and an increased risk of hepatocellular carcinoma. The single-stranded RNA genome of HCV is a 9.6 kb-long positive-sense molecule, belonging to the *Flaviviridae* family. The viral genome encodes a single polyprotein precursor of approximately 3 010 amino acids, which is cleaved by both host and viral proteases to generate putative structural proteins (core, E1, and E2/p7) and the nonstructural proteins (NS2, NS3, NS4A, NS4B, NS5A, and NS5B)[1-3]. The nonstructural protein 5A (NS5A) is a phosphoprotein consisting of 447 amino acid residues. NS5A exists in two forms of polypeptide p56 and p58, which are phosphorylated mainly at serine residues both *in vitro* and *in vivo*[4,5].

It was previously shown that NS5A could function as a transcriptional trans-activator. Although these reports implicate a functional role of NS5A in transcription, the exact nature of its role or the mechanism (s) involved in regulating the cellular transcription has not been investigated. NS5A is localized to the endocytoplasmic reticulum (ER), whereas transcriptional trans-activation traditionally requires the protein to be in the nucleus. The NS5A protein must participate in signal transduction pathways that are initiated in the cytoplasm where it resides[6,7]. However, some studies show NS5A protein possesses a nuclear localization-like signal sequence and is present in the nuclear periplasmic membrane fraction related to transcription or translation[8]. The present study shows NS5A protein has transactivating effect on SV40 early promoter.

MATERIALS AND METHODS

Plasmid construction

The HCV-NS5A sequences were generated by PCR amplification of HCV plasmid (HCV strain 1b). The plasmid contains coding sequences for all of the nonstructural proteins. The PCR conditions were as follows: 94 ℃ for 40 s. 10 ng of PCR product was cloned with pEGM-T vector (Promega). The primary structure of insert was confirmed by direct sequencing. To create pcDNA3.1 (-)-NS5A, the fragments of encoding NS5A were released from the pEGM-T-NS5A by digestion with *Eco*R I and *Kpn* I, and ligated to pcDNA3.1 (-)[9].

Cell culture and transfection

The hepatoblastoma cell line HepG2 was propagated in DMEM supplemented with 10% FBS, 200 μmol/L L-glutamine, penicillin, and streptomycin. The HepG2 cells were plated at a density of 1×10^6 /well in 35-mm dishes. About 60-70% confluent HepG2 cells were cotransfected with plasmids pcDNA3. 1(-)-NS5A and pCAT3-promoter, transfected with pcDNA3.1 (-)-NS5A, pcDNA3.1 (-) with FuGENE 6(Roche).

Confirmation of protein expression of HCV-NS5A

Expression plasmid pcDNA3.1 (-)-NS5A was transfected using FuGENE 6 into HepG2 cells. The proteins expressed in these cells were analyzed on an immunoblot using the NS5A-specific antibody. The proteins were resolved by electrophoresis on a sodium dodecyl sulfate 125 g/L polyacrylamide gel. The lysate of cells transfected with expression vector pcDNA3. 1(-) served as negative control[10].

CAT assay

Cells were then harvested after 48 h for CAT assay. Lysates of transfected cells were analyzed for CAT density using a commercial enzyme-linked immunosorbent assay (Roche Molecular Biochemicals). The absorbance of the samples was measured at 405 nm[11].

RNA extraction and SSH

mRNAs from HepG2 cells transfected with plasmids pcDNA3.1

(-)-NS5A and pcDNA3.1(-) were extracted by using QuickPrep micro mRNA Purification Kit (Amersham Pharmacia). The amount of mRNA from two samples was 3-4 μg.

SSH was performed with the cDNA Substraction Kit (Clontech) according to the manufacturer' s protocol. cDNA was synthesized from 2 μg of poly A+RNA from two samples being compared. The cDNA from pcDNA3.1 (-)-NS5A acted as the tester, the cDNA from pcDNA3.1 (-) as the driver. The tester and driver cDNAs were digested with *Rsa* I, which yielded blunt ends. Two different PCR adaptors that could join only 5' ends DNA were ligated to different aliquots of tester DNA. These ligated DNAs were denatured, mixed with an excess of driver DNA (that had no adaptors), and allowed to anneal. The two DNA pools were then mixed together, and more denatured driver DNAs were added to further bind tester that was also present in the driver. Remaining complementary single strands of tester DNA were allowed to anneal, and the adaptor sequences were copied into their 3' ends. PCR was then performed to obtain exponential amplification of tester DNAs with different adaptors at each end. PCR amplifications products were directly purified by using Wizard PCR Preps DNA Purification System (Promega), and subcloned into pEGM-T easy vectors (Promega) to set up the subtractive library[12,13].

New gene cloned

On the basis of subtractive cDNA library of genes transactivated by NS5A protein of hepatitis C virus, the coding sequence of a new gene, named NS5ATP2, was obtained by bioinformatics methods. The standard PCR cloning technique was used to amplify NS5ATP2 gene. Cytoplasmic RNA was isolated from HepG2 cells. RNA was used for RT-PCR as described previously, primers were: sense 5' -GGA TTC ATG GCT TCG GTC TCC TCT GC-3' , antisense 5' -GGT ACC TCA GGA GTG TGG CTC ACT GG -3' (HepG2 cDNA). The PCR condition was as follows: at 94 ℃ for 60 s, at 60 ℃ for 60 s, at 72 ℃ for 60 s, for 30 cycles. The PCR product was cloned with pGEM-T vector (Promega). The primary structure of insert was confirmed by direct sequencing.

RESULTS

NS5A protein expressed in HepG2 cells

NS5A protein expressed in cells was analyzed by Western blot. The lysates of cells transfected with plasmid pcDNA3.1 (-)-NS5A were specifically detected by NS5A specific antibody (Figure 1).

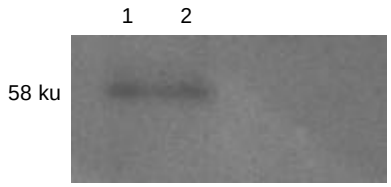

Figure 1 Western blotting of NS5A protein expression in HepG2 cells. Lane 1: Expression plasmid pcDNA3.1 (-)-NS5A; Lane 2: Plasmid pcDNA3.1 (-)-vector.

Transactivating effect of NS5A on SV40 early promoter

To determine whether NS5A protein has transactivating effect, we constructed plasmid pcDNA3.1 (-)-NS5A, and HCV NS5A protein expressed in Hep G2 cells was detected by reverse transcription PCR (RT-PCR) and Western blotting. HepG2 cells were transiently cotransfected with pcDNA3.1 (-)-NS5A/pCAT3-promoter, pcDNA3.1(-)/pCAT3-promoter. Chloramphenicol acetyltransferase (CAT) activity in cells that were cotransfected with pcDNA3.1 (-)-NS5A/pCAT3-promoter is shown in Figure 2.

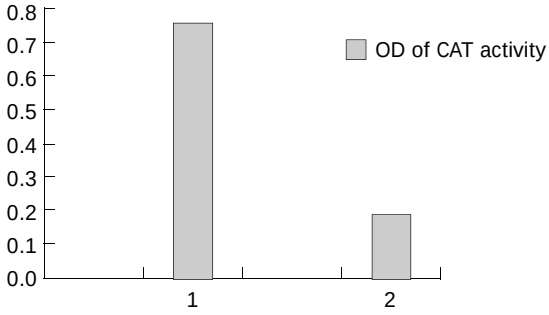

Figure 2 Transactivation on SV40 promoter by NS5A. 1: Plasmid pcDNA3.1 (-)-NS5A was cotransfected with pCAT3-promoter in HepG2 cells. 2: Plasmid pcDNA3.1 (-) was cotransfected with pCAT3-promoter in HepG2 cells.

Construction of subtractive cDNA library

Our studies showed NS5A protein had transactivation effect on SV40 promoter. In order to investigate influence of NS5A protein on cells gene expression, Suppression subtraction hybridization (SSH) was introduced to establish substractive cDNA library of HepG2 transfected with plasmid pcDNA3.1 (-)-NS5A. We performed the PCR experiment to analyse the ligation efficiency. The result showed that at least 25% of the cDNA had adaptors at both ends. The efficiency of subtraction was estimated by PCR experiment. The test was done by comparison of the abundance of G3PDH before and after subtraction. G3PDH primers were provided by the kit (Figure 3).

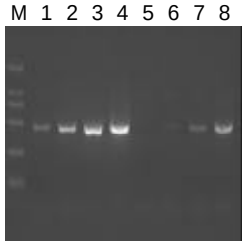

Figure 3 Reduction of G3PDH amount by PCR-selective subtraction. PCR was performed on unsubtracted (Lanes 1-4) and subtracted (Lanes 5-8) secondary PCR products with the G3PDH 5' and 3' primers. Lanes 1, 5: 18 cycles; Lanes 2,6: 23 cycles; Lanes 3,7: 28 cycles.

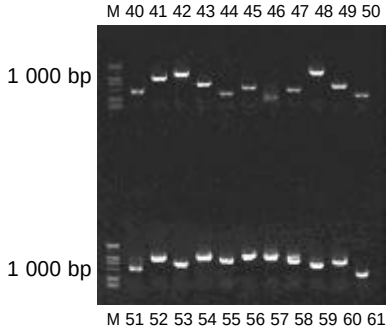

Figure 4 Map of colony PCR on 9 g/L agarose/EtBr gel.

After tester cDNA was hybridized with driver cDNA twice and underwent nested PCR twice, they were then subcloned into pGEM-T easy vectors to set up the subtractive library. Amplification of the library was carried out with *E. coli* strain JM109. The amplified library contained 121 positive clones.

Colony PCR showed that 115 clones contained 200-1 000 bp inserts (Figure 4). The nucleotide sequences of 90 clones from this cDNA library was analyzed, the full length sequences were obtained with Vector NTI 6 and BLAST database homology search (http://www. ncbi. nlm. nih. gov/). Altogether 44 kinds of coding sequences were obtained, consisting of 29 known and 15 unknown ones. Some genes code for proteins involved in cell cycle regulation, cell apoptosis, signal transduction pathway and tumour (Table 1).

Table 1 Sequence analysis of 46 clones isolated from subtractive cDNA library

Known genes	Number of clones	Homology (%)
Ribosomal protein	15	99
Eukaryotic translation initiation factor	4	99
HCV NS5A protein	4	98
Sentrin	4	99
Pro-oncosis receptor inducing membrane injury (Porimin)	3	100
Importin	3	98
Serine/threonine kinase	3	100
Cadherin-associated protein	2	100
Mitogen-activated protein kinase phosphatase	2	99
Adenylyl cyclase-associated protein	2	100
Serum response element	2	100
Rho GTPase activating protein	2	100
Fibronectin	3	99
Laminin	3	99
Lysophospholipase A2	2	100
Lysophospholipase B	2	100
Dual specificity phosphatase 6	1	99
Putative homeodomain transcription factor	2	92
Transcription factor B2 NF-E2-like basic leucine zipper	2	100
Transcriptional activator	2	98
Transcriptional elongation factor (TFIIS)	2	100
MHC-I binding protein	1	100
C response protein binding protein (CRPBP)	1	99
Integrin	2	99
Iron-regulated transporter (IREG)	1	99
Tumor associated protein L6	2	100
WW domain-containing protein 1 (WWP1)	1	100
Nascent polypeptide-associate complex α(NACA)	1	99
Thioredoxin reductase	1	99

Confirmation of new gene expression by RT-PCR

We found the spliced variant of NS5A-TP2 (Figures 5, 6). After EST database homology search (http://www. ncbi. nlm. nih. gov/), the locations of NS5A-TP2 and its spliced variant were detected on chromosome 6q22. 1-23. 3. The exons and introns of two new genes were compared (Figure 7). The direct sequencing showed we acquired the ORF of NS5A-TP2 (Figure 8).

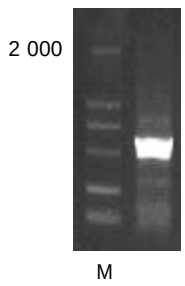

Figure 5 NS5A-TP2 fragment amplified by RT-PCR. M: Marker.

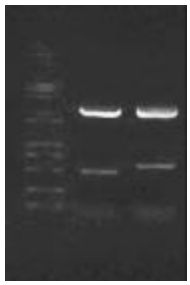

Figure 6 pEGM-T-NS5A-TP2 cut by EcoR I/Kpn I. M: Marker; Lane 1: A 512-bp fragment; Lane 2: A 615-bp fragment.

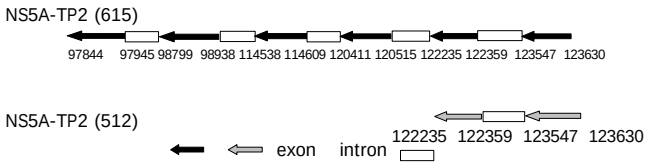

Figure 7 Comparison of exons and introns of NS5A-TP2 (615) and (512) gene.

615 **ATG** GCT TCG GTC TCC TCT GCG ACC TTC TCG
512 **ATG** GCT TCG GTC TCC TCT GCG ACC TTC TCG

615 GGC CAC GGG GCT CGG TCC CTA CTG CAG TTC
512 GGC CAC GGG GCT CGG TCC CTA CTG CAG TTC

615 CTG CGG CTG GTA GGG CAG CTC AAG AGA GTC
512 CTG CGG CTG GTA GGG CAG CTC AAG AGA GTC

615 CCA CGA ACT GGC TGG GTA TAC AGA AAT GTC
512 CCA CGA ACT GGC TGG GTA TAC AGA AAT GTC

615 CAG AGG CCG GAG AGC GTT TCA GAT CAC ATG
512 CAG AGG CCG GAG AGC GTT TCA GAT CAC ATG

615 TAC CGG ATG GCA GTT ATG GCT ATG GTG ATC
513 TAC CGG ATG GCA GTT ATG GCT ATG GTG ATC

615 AAA GAT GAC CGT CTT AAC AAA GAC CGA TGT
512 AAA GAT GAC CGT CTT AAC AAA GAC C-- ---

615 GTA CGC CTA GCC CTG GTT CAT GAT ATG GCA
512 --- --- --- --- --- --- --- --- --- ---

615 GAA TGC ATC GTT GGG GAC ATA GCA CCA GCA
512 --- --- --- --- --- --- --- --- --- ---

615 GAT AAC ATC CCC AAA GAA GAA AAA CAT AGG
512 --- --- --- --- --- --- --- --- --- ---

615 CGA GAA GAG GAA GCT ATG AAG CAG ATA ACC
512 --- --- --- G GAA GCT A**TG A**AG CAG ATA ACC

615 CAG CTC CTA CCA GAG GAC CTC AGA AAG GAG
512 CAG CTC CTA CCA GAG GAC CTC AGA AAG GAG

615 CTC TAT GAA CTT TGG GAA GAG TAC GAG ACC
512 CTC TAT GAA CTT TGG GAA GAG TAC GAG ACC

615 CAA TCT AGT GCA GAA GCC AAA TTT GTG AAG
512 CAA TCT AGT GCA GAA GCC AAA TTT GTG AAG

615 CAG CTA GAC CAA TGT GAA ATG ATT CTT CAA
512 CAG CTA GAC CAA TGT GAA ATG ATT CTT CAA

615 GCA TCT GAA TAT GAA GAC CTT GAA CAC AAA
512 GCA TCT GAA TAT GAA GAC CTT GAA CAC AAA

615 CCT GGG AGA CTG CAA GAC TTC TAT GAT TCC
512 CCT GGG AGA CTG CAA GAC TTC TAT GAT TCC
615 ACA GCA GGA AAA TTC AAT CAC CCT GAG ATA
512 ACA GCA GGA AAA TTC AAT CAC CCT GAG ATA

615 GTC CAG CTT GTT TCT GAA CTT GAG GCA GAA
512 GTC CAG CTT GTT TCT GAA CTT GAG GCA GAA

615 AGA AGC ACT AAC ATA GCT GCA GCT GCC AGT
512 AGA AGC ACT AAC ATA GCT GCA GCT GCC AGT

615 GAG CCA CAC TCC **TGA**
512 GAG CCA CAC TCC TGA

Figure 8 ORF comparison of NS5A-TP2 (615) and (512).

DISCUSSION

Hepatitis C virus often causes persistent infection with a significant risk of end-stage cirrhosis and hepatocellular carcinoma. HCV may benefit by regulation of celluar genes leading to the disruption of normal cell growth. Viral genes can override cellular control mechanisms, which in untransformed cells regulate cell cycle progression in response to various antiproliferative signals. In HCV persistently infected cells, the continued presence of viral gene products is likely to be detrimental for host cells. Many studies demonstrated NS5A protein of HCV transcriptionally modulates cellular genes and promotes murine fibroblast cell growth into a tumorigenic phenotype. It may be possible that the NS5A protein plays a role in hepatocarcinogenesis, since many other viral proteins that play a role in carcinogenesis often function as transcriptional activators[14-17]. However, the precise mechanism is still unknown.

In the present study, we investigated the possible mechanism by which NS5A protein transactivated gene expression and its role in hepatocarcinogenesis. NS5A protein in Hep G2 cells was detected by RT-PCR and Western blotting. HepG2 cells were transiently cotransfected with pcDNA3.1 (-)-NS5A/ pCAT3-promoter. CAT activity was evidently higher in the cotransfected cells than in control. It is suggested that NS5A protein has transactivating effect on SV40 early promoter. We predicted that NS5A protein transcriptionally regulated gene expression through regulating promoter activity, either directly or through signal transduction pathways.

On the basis of this study, we constructed subtractive cDNA library by SSH. After sequencing analysis, we obtained coding sequences of 46 genes, which consisted of 26 kinds of known and 15 kinds of unknown ones. Some genes code for proteins involved in cell cycle regulation, cell apoptosis, and tumor angiogenesis. Sentrin is a 101-amino acid ubiquitin-like protein that interacts with the death domains of Fas and TNFR1, with PML, a tumor suppressor implicated in the pathogenesis of promyelocytic leukemia, with Rad51 and Rad52, proteins that are involved in repairing double-stranded DNA breaks, and with RanGAP1, a GTPase-activating protein that is critically involved in nuclear protein transport[18-20]. Overexpression of sentrin in mammalian cells protects them against anti-Fas or tumor necrosis factor-induced cell death[21]. Porimin is a highly glycosylated protein that can be classified as a member of the cell membrane-associated mucin family[22]. Porimin is a membrane mucin that mediates cell death. Although mucins mainly affect cell adhesion and ligand binding, several membrane mucins have also been documented to trigger cell death or inhibit cell proliferation, such as CD43 (leukosialin, sialophorin), CD162 (PSGL-1), and CD164 (MGC-24v)[23]. Likewise, serine/threonine kinase, cadherin-associated protein, adenylyl cyclase-associated protein, mitogen-activated protein kinase phosphatase involving in cell cycle regulation, and cell growth may be correlated with hepatocarcinogenesis of NS5A protein[24-28].

Alternative pre-mRNA splicing is a fundamental mechanism for differential gene expression that has been reported to regulate the tissue distribution, the intracellular localization, and the activity of different protein kinases. In the process of our study on new genes, we accidentally acquired the spliced variant of NS5A-TP2 and confirmed the ORF of NS5A-TP2 (516) and its location on chromosome. Both of NS5A-TP2 (615) and its spliced variant- NS5A-TP2 (516) locate on 6q22.1-23.3, but they have different exons and introns[29-31].

The result of this study shows that the NS5A protein is a potent transcriptional activator and transactivates some genes involved in cell cycle regulation, cell apoptosis, and tumor angiogenesis. The study on new genes NS5A-TP2 (516), and NS5A-TP2 (615) brings some new clues to the biological functions of novel genes and pathogenesis of the viral proteins.

REFERENCES

1 **Pawlotsky JM**. Hepatitis C virus (HCV) NS5A protein: role in HCV replication and resistance to interferon-alpha. *J Viral Hepat* 1999; **6**(Suppl 1): 47-48

2 **Kumar U**, Tuthill T, Thomas HC, Monjardino J. Sequence, expression and reconstitution of an HCV genome from a British isolate derived from a single blood donation. *J Viral Hepat* 2000; **7**: 459-465

3 **Sandres K**, Dubois M, Pasquier C, Payen JL, Alric L, Duffaut M, Vinel JP, Pascal JP, Puel J, Izopet J. Genetic heterogeneity of hypervariable region 1 of the hepatitis C virus (HCV) genome and sensitivity of HCV to alpha interferon therapy. *J Virol* 2000; **74**: 661-668

4 **Neddermann P**, Clementi A, De Francesco R. Hyperphosphorylation of the hepatitis C virus NS5A protein requires an active NS3 protease, NS4A, NS4B, and NS5A encoded on the same polyprotein. *J Virol* 1999; **73**: 9984-9991

5 **Reed KE**, Rice CM. Identification of the major phosphorylation site of the hepatitis C virus H strain NS5A protein as serine 2321. *J Biol Chem* 1999; **274**: 28011-28018

6 **Ghosh AK**, Steele R, Meyer K, Ray R, Ray RB. Hepatitis C virus NS5A protein modulates cell cycle regulatory genes and promotes cell growth. *J Gen Virol* 1999; **80**(Pt 5): 1179-1183

7 **Ghosh AK**, Majumder M, Steele R, Yaciuk P, Chrivia J, Ray R, Ray RB. Hepatitis C virus NS5A protein modulates transcription through a novel cellular transcription factor SRCAP. *J Biol Chem* 2000; **275**: 7184-7188

8 **Song J**, Nagano-Fujii M, Wang F, Florese R, Fujita T, Ishido S, Hotta H. Nuclear localization and intramolecular cleavage of N-terminally deleted NS5A protein of hepatitis C virus. *Virus Res* 2000; **69**: 109-117

9 **Liu Y**, Cheng J, Lu YY. Cloning of genes transactivated by hepatitis B virus X protein. *Zhonghua Ganzangbing Zazhi* 2003; **11**: 5-7

10 **Wang L**, Li K, Cheng J, Chen TY, Hong Y, Liu Y, Wang G, Zhong YW. Screening of gene encoding of hepatic protein interacting with Hcbp6 via yeast two hybridization. *Shijie Huanren Xiaohua Zazhi* 2003; **11**: 385-388

11 **Liu Y**, Dong J, Cheng J, Lu YY. The study of transactivating effect of HBV X protein on SV40 early promoter. *Jiefangjun Yixue Zazhi* 2001; **26**: 404-406

12 **Shridhar V**, Sen A, Chien J, Staub J, Avula R, Kovats S, Lee J, Lillie J, Smith DI. Identification of underexpressed genes in early- and late-stage primary ovarian tumors by suppression subtraction hybridization. *Cancer Res* 2002; **62**: 262-270

13 **Diatchenko L**, Lau YF, Campbell AP, Chenchik A, Moqadam F, Huang B, Lukyanov S, Lukyanov K, Gurskaya N, Sverdlov ED, Siebert PD. Suppression subtractive hybridization: a method for generating differentially regulated or tissue-specific cDNA probes and libraries. *Proc Natl Acad Sci U S A* 1996; **93**: 6025-6030

14 **Majumder M**, Ghosh AK, Steele R, Ray R, Ray RB. Hepatitis C virus NS5A physically associates with p53 and regulates p21/ waf1 gene expression in a p53-dependent manner. *J Virol* 2001; **75**: 1401-1407

15 **De Mitri MS**, Morsica G, Cassini R, Bagaglio S, Zoli M, Alberti A, Bernardi M. Prevalence of wild-type in NS5A-PKR protein kinase binding domain in HCV-related hepatocellular carcinoma. *J Hepatol* 2002; **36**: 116-122

16 **Park KJ**, Choi SH, Choi DH, Park JM, Yie SW, Lee SY, Hwang SB. 1Hepatitis C virus NS5A protein modulates c-Jun N-terminal kinase through interaction with tumor necrosis factor receptor-associated factor 2. *J Biol Chem* 2003; **278**: 30711-30718

17 **Reyes GR**. The nonstructural NS5A protein of hepatitis C virus: an expanding, multifunctional role in enhancing hepatitis C virus pathogenesis. *J Biomed Sci* 2002; **9**: 187-197

18 **Ryu SW**, Chae SK, Kim E. Interaction of Daxx, a Fas binding protein, with sentrin and Ubc9. *Biochem Biophys Res Commun* 2000; **279**: 6-10

19 **Okura T**, Gong L, Kamitani T, Wada T, Okura I, Wei CF, Chang

HM, Yeh ET. Protection against Fas / APO-1- and tumor necrosis factor-mediated cell death by a novel protein, sentrin. *J Immunol* 1996; **157**: 4277-42781

20 **Kretz-Remy C**, Tanguay RM. SUMO / sentrin: protein modifiers regulating important cellular functions. *Biochem Cell Biol* 1999; **77**: 299-309

21 **Kamitani T**, Kito K, Nguyen HP, Fukuda-Kamitani T, Yeh ET. Characterization of a second member of the sentrin family of ubiquitin-like proteins. *J Biol Chem* 1998; **273**: 11349-11353

22 **Ma F**, Zhang C, Prasad KV, Freeman GJ, Schlossman SF. Molecular cloning of Porimin, a novel cell surface receptor mediating oncotic cell death. *Proc Natl Acad Sci U S A* 2001; **98**: 9778-9783

23 **Zhang C**, Xu Y, Gu J, Schlossman SF. A cell surface receptor defined by a mAb mediates a unique type of cell death similar to oncosis. *Proc Natl Acad Sci U S A* 1998; **95**: 6290-6295

24 **Tamari M**, Daigo Y, Nakamura Y. Isolation and characterization of a novel serine threonine kinase gene on chromosome 3p22-21.3. *J Hum Genet* 1999; **44**: 116-120

25 **Ohteki T**, Parsons M, Zakarian A, Jones RG, Nguyen LT, Woodgett JR, Ohashi PS. Negative regulation of T cell proliferation and interleukin 2 production by the serine threonine kinase GSK-3. *J Exp Med* 2000; **192**: 99-104

26 **Ratcliffe MJ**, Rubin LL, Staddon JM. Dephosphorylation of the cadherin-associated p100 / p120 proteins in response to activation of protein kinase C in epithelial cells. *J Biol Chem* 1997; **272**: 31894-31901

27 **Nagafuchi A**, Takeichi M, Tsukita S. The 102 kd cadherin-associated protein: similarity to vinculin and posttranscriptional regulation of expression. *Cell* 1991; **65**: 849-857

28 **Zelicof A**, Gatica J, Gerst JE. Molecular cloning and characterization of a rat homolog of CAP, the adenylyl cyclase-associated protein from Saccharomyces cerevisiae. *J Biol Chem* 1993; **268**: 13448-13453

29 **Shima F**, Yamawaki-Kataoka Y, Yanagihara C, Tamada M, Okada T, Kariya K, Kataoka T. Effect of association with adenylyl cyclase-associated protein on the interaction of yeast adenylyl cyclase with Ras protein. *Mol Cell Biol* 1997; **17**: 1057-1064

30 **Chen P**, Li J, Barnes J, Kokkonen GC, Lee JC, Liu Y. Restraint of proinflammatory cytokine biosynthesis by mitogen-activated protein kinase phosphatase-1 in lipopolysaccharide-stimulated macrophages. *J Immunol* 2002; **169**: 6408-6416

31 **Cheng J**, Li K, Lu YY, Wang L, Liu Y. Bioinformatics analysis of human hepatitis C virus core protein-binding protein 6 gene and protein. *Shijie Huanren Xiaohua Zazhi* 2003; **11**: 378-384

Edited by Zhu LH and Chen WW **Proofread by** Xu FM

PO Box 2345, Beijing 100023, China
Fax: +86-10-85381893
E-mail: wjg@wjgnet.com www.wjgnet.com

World J Gastroenterol 2004;10(12):1740-1745
World Journal of Gastroenterology
Copyright ©2004 by The WJG Press ISSN 1007-9327

• VIRAL HEPATITIS •

Gene expression profiles in an hepatitis B virus transfected hepatoblastoma cell line and differentially regulated gene expression by interferon-a

Xun Wang, Zheng-Hong Yuan, Ling-Jie Zheng, Feng Yu, Wei Xiong, Jiang-Xia Liu, Gen-Xi Hu, Yao Li

Xun Wang, Zheng-Hong Yuan, Ling-Jie Zheng, Wei Xiong, Jiang-Xia Liu, Department of Molecular Virology, Shanghai Medical College, Fudan University, Shanghai 200032, China
Feng Yu, Gen-Xi Hu, Institute of Biochemistry and Cell Biology, CAS, Shanghai 200031, China
Yao Li, State Key Laboratory of Genetics, Fudan University School of Life Science, Shanghai 200433, China
Supported by the Chinese State Basic Science Foundation, No. 1999054105 and Med-X Foundation of Fudan University
Correspondence to: Zheng-Hong Yuan, Department of Molecular Virology, Shanghai Medical College, Fudan University Fudan, 138 Yi Xue Yuan Road, Shanghai 200032, China. zhyuan@shmu.edu.cn
Telephone: +86-21-64161928 **Fax:** +86-21-64227201
Received: 2003-10-15 **Accepted:** 2003-12-22

Abstract

AIM: To study interactions between hepatitis B virus (HBV) and interferon-α in liver- derived cells.

METHODS: mRNAs were separately isolated from an HBV-transfected cell line ($HepG_2$2.2.15) and its parental cell line ($HepG_2$) pre- and post-interferon-α (IFN-α) treatment at 6, 24 and 48 h, followed by hybridization with a cDNA microarray filter dotted with 14 000 human genes. After hybridization and scanning of the arrays, the data were analyzed using ArrayGauge software. The microarray data were further verified by Northern blot analysis.

RESULTS: Compared to $HepG_2$ cells, 14 genes with known functions were down-regulated 3 to 12- magnitudes, while 7 genes were up-regulated 3-13 magnitudes in $HepG_2$2.2.15 cells prior to IFN-α treatment. After interferon-α treatment, the expression of four genes (vascular endothelial growth factor, tyrosine phosphate 1E, serine protein with IGF-binding motif and one gene of clathrin light chain) in $HepG_2$2.2.15 were up-regulated, while one gene encoding a GTP-binding protein, two genes of interferon-induced kinases and two proto-oncogenes were further down- regulated. Interestingly, under IFN-α treatment, a number of differentially regulated genes were new ESTs or genes with unknown functions.

CONCLUSION: The up-regulated genes in $HepG_2$2.2.15 cell line suggested that under IFN-α treatment, these repressed cellular genes in HBV infected hepatocytes could be partially restored, while the down- regulated genes were most likely the cellular genes which could not be restored under interferon treatment. These down-regulated genes identified by microarray analysis could serve as new targets for anti-HBV drug development or for novel therapies.

Wang X, Yuan ZH, Zheng LJ, Yu F, Xiong W, Liu JX, Hu GX, Li Y. Gene expression profiles in an hepatitis B virus transfected hepatoblastoma cell line and differentially regulated gene expression by interferon-α. *World J Gastroenterol* 2004; 10 (12): 1740-1745
http://www.wjgnet.com/1007-9327/10/1740.asp

INTRODUCTION

Viral hepatitis B continues to be a significant global problem. It is estimated that there are approximately 350 million chronic hepatitis B virus (HBV) carriers world-wide. Furthermore, chronic hepatitis B patients are at high risk of developing liver cirrhosis and hepatocellular carcinoma with high mortality rates.

In the past two decades, interferon-α (IFN-α) has proven effective in the treatment of chronic hepatitis B patients. However, sustained responses were observed in only one-third of chronic hepatitis B patients[1-3]. In the normal physiological state, interferon-α is expressed at a low level and is induced to high levels by viral or bacterial infections and the exposure to double-stranded RNA[4]. In contrast to other types of viral infections, IFN-α was either non-detectable or present in extremely low levels in HBV chronically infected patients[5,6]. Additionally, decreased synthesis of 2'-5' A synthetase, belonging to a family of enzymes induced by IFNs, has been reported in chronic hepatitis B patients[7,8]. To date, mechanisms underlying defective production of IFN or defective responses to IFN in chronic hepatitis B patients have not been fully elucidated.

Development of microarray technology has provided a powerful tool for study of the complicated biological process in cells which results in altered global gene expression. cDNA microarray has been used to analyze virus-host cell interactions in Human Immunodeficiency Virus (HIV), Human Cytomegalovirus (HCMV), Herpes Simplex Virus (HSV) and Influenza Virus infected cell cultures[9-13]. By comparing virus infected cell cultures with non-infected cell cultures, a number of differentially expressed genes were identified. For HBV, although several studies have been undertaken to clarify the effects of HBV infection on hepatocytes[14-16], the global effects of all HBV proteins or HBV replication on host cells, especially the interaction between HBV and interferon remain unclear. Therefore, in this study, cDNA microarray filters dotted with 14 000 human genes were used to analyze transcriptional changes between an HBV DNA-transfected cell line ($HepG_2$2.2.15)[17,18] and its parental cell line ($HepG_2$) pre- and post- IFN treatment. Based on analysis of altered mRNA expression, several IFN-differentially regulated genes including new ESTs or genes with unknown functions were further investigated for their potential antiviral activity.

MATERIALS AND METHODS

Cell culture

The HBV DNA transfected hepatoblastoma cell line $HepG_2$2.2.15, that has been confirmed to produce infectious virus[18,19], and its parental cell line $HepG_2$ were maintained in Dulbecco's modified Eagle's medium supplemented with 10 mL/L fetal calf serum and antibiotics. The cells were incubated at 37 ℃ in 50 mL/LCO_2. Cell viability was estimated by the trypan blue dye exclusion method.

Preparation of cell samples for cDNA microarray

The cells were separately seeded into T-75 flasks at 40%

confluence (4×104 cells/cm^2) one day prior to the experiment. After overnight culture, two flasks of cells for each cell line were harvested before treatment with IFN-α for RNA preparation and were regarded as 0 h cells for IFN-α treatment. The other cells were exposed to 5×10^3 IU/mL of IFN-α (Calbiochem, San Diego, CA, USA) and harvested 6, 24 and 48 h after IFN-α treatment. The culture media were removed and stored at -70 ℃. For each flask of cells, 5 mL of TRIzol Reagent (Gibco BRL) was added directly into the flask.

RNA extraction

Total RNA was extracted using standard TRIzol RNA isolation protocol (Gibco BRL). The isolated total RNA was divided into two aliquots, one for RNA slot analysis and the other for mRNA preparation.

Generation of microarray

Generation of microarrays and microarray analysis were carried out by the Institute of Biochemistry and Cell Biology, CAS as described previously[20]. Human cDNA clones were derived from liver, hepatocarcinoma cell lines and hypothalamus-pituitary-adrenal libraries[21] or purchased from Research Genetics (Huntsville, AL, USA). A cDNA array was assembled with 14 000 cDNA clones representing the same number of independent cDNA clusters, of which 7 565 clusters were homologous to that in the UniGene Database. All cDNA fragments were amplified and verified by gel electrophoresis and sequencing. The average length of the cDNA fragments was ~1 kb. PCR products were precipitated in isopropanol, redissolved in 10 μL of denaturing buffer (1.5 mol/L NaCl, 0.5 mol/L NaOH) and spotted onto 8×12 cm Hybond-N nylon membranes (Amersham Pharmacia, Buckinghamshire, UK) using an arrayer (BioRobotics, Cambridge, UK). Each spot carried ~100 nL in volume and was 0.4 mm in diameter; each cDNA fragment was spotted as two different spots (double-offset). Lambda phage and pUC18 vector DNA were spotted as negative controls.

Eight housekeeping genes encoding ribosomal protein S9 (RPS9), β-actin (ACTB), glyceraldehydes-3-phosphate dehydrogenase, hypoxanthine phosphoribosyltransferase 1, M_r 23 000 highly basic protein (RPL13A), ubiquitin C, phospholipase A2, and ubiquitin thiolesterase (UCHL1) were each evenly distributed in 12 spots on each 8×12 cm array as an intramembrane control. Hybridization data were considered invalid if the intensity of the darkest spot exceeded 1.5 times that of the weakest spot among the 12 spots representing the same gene.

mRNA isolation and probe preparation

The poly (A)$^+$ mRNA was isolated from the total RNA using a poly (dT) resin (Qiagen, Hilden, Germany). Approximately 1 - 2 μg of mRNA were labeled in a reverse transcription reaction in the presence of 200 μCi [α^{33}P] deoxyadenosine 5' -triphosphate (DuPont NEN, Boston, MA, USA) using Moloney murine leukemia virus reverse transcriptase as recommended by the manufacturer (Promega Corp., Madison, WI, USA).

Hybridization and Image Procession

Prehybridization was carried out in 20 mL of prehybridization solution (6×SSC, 5 g/L SDS, 5×Denhardt's and 100 μg/mL denatured salmon sperm DNA) at 68 ℃ for 3 h. Overnight hybridization with the ^{33}P-labeled cDNA in 6 mL of hybridization solution (6×SSC, 5 g/L SDS, and 100 μg/mL denatured salmon sperm DNA) was followed by stringent washing (0.1×SSC, 5 g/L SDS, at 65 ℃ for 1 h). Membranes were exposed to Phosphor Screen overnight and scanned with an FLA-3 000A Plate/ Fluorescent Image Analyzer (Fuji Photo Film, Tokyo, Japan). Radioactive intensity of each spot was linearly digitalized to 65 536 gray-grade in a pixel size of 50 μm in the Image Reader and recorded using the Array Gauge software (Fuji Photo Film, Tokyo, Japan). After subtraction of background (3±3) chosen from an area where no cDNA was spotted, genes with intensities >10 were considered as positive signals to ensure that they were distinguished from background with statistical significance >99.9%. Normalization among arrays was based on the sum of background-subtracted signals from all genes on the membrane[22].

RNA slot analysis

Total cellular RNA, 10 μg/sample was mixed with 7 μL formaldehyde, 20 μL formamide and 2 μL 20×SSC (1×SSC=0.15 mol/L NaCl plus 0.015 mol/L sodium citrate). After being denatured at 65 ℃ for 15 min and immediately cooled in an ice bath, the RNA sample was applied to the nylon membrane (Boehringer Mannheim, Germany) with Minifold I (Schleicher & Schuell). After fixation at 120 ℃ for 30 min, the membrane was pre-hybridized in 20 mL of prehybridization solution (6×SSC, 5 g/L SDS, 5×Denhardt's and 100 μg/mL denatured salmon sperm DNA) at 42 ℃ for 6 h, and followed by hybridization with 20 mL hybridization solution (6×SSC, 5 g/L SDS, 5×Denhardt's and 100 μg/mL denatured salmon sperm DNA) including [α-^{32}P]dCTP labeled cDNA probes (Random labeling kit, Boehringer Mannheim, Germany) at 42 ℃ for 16 h. The cDNA probes represented the unique sequence of IFN related P27, KIAA0919, beta3gal-T5 and FLJ12673. After stringent membrane washing process (0.1×SSC, 5 g/L SDS at 68 ℃ for 30 min, thrice), autoradiographs were exposed to X-ray film (Fijifilm, Japan) overnight at -70 ℃. Quantitative analysis was undertaken by scanning the intensity of the membranes. In order to normalize the total RNA quantity in each blot, an [α^{32}-P]dCTP labeled β-actin probe was hybridized to the membrane again after the first probe was removed. The change of regulated gene expression between different cell samples could be detected by comparing the intensity ratio of specific gene and β-actin.

RESULTS

Validation of microarray results

Similar to previous study, results from the reproducible analysis confirmed that the replicated experiments were in concordance with an R^2 (square of Pearson correlation coefficiency, measuring similarity in gene expression pattern) of 0.97-0.98 on scatterplot[20].

To confirm the altered expression level, 4 genes (interferon related genes P27, KIAA0919, β-3-gal-T5 gene and FLJ12673 human cDNA clone) were selected and tested by RNA slot

Table 1 Comparison of microarray and RNA slot analyses on 4 selected genes

Accession ID	X67325		AB023136		AA622328		NM_018300	
	Ratio of arrays	Ratio of slot	Ratio of arrays	Ratio of slot	Ratio of arrays	Ratio of slot	Ratio of arrays	Ratio of slot
6 h/0 h	3.6	Undetectable	3.4	1.3	2.0	0.5	1.1	2.9
24 h/0 h	5.9	>31	7.2	3.5	3.9	1.6	4.9	3.4
48 h/0 h	6.1	>33	8.4	6.2	3.8	5.7	1.0	1.3
Description	IFN-inducible P27		Sec15B(vesicle traffic protein)		beta3gal-T5 gene		cDNA FLJ12673	

analysis (Figure 1). The ratios of the signal intensity of specific genes and β-actin and their comparison with microarray result are listed in Table 1. It is observed that the results of RNA slot analysis are aligned with those from the microarray analyses (Figure 1 and Table 1).

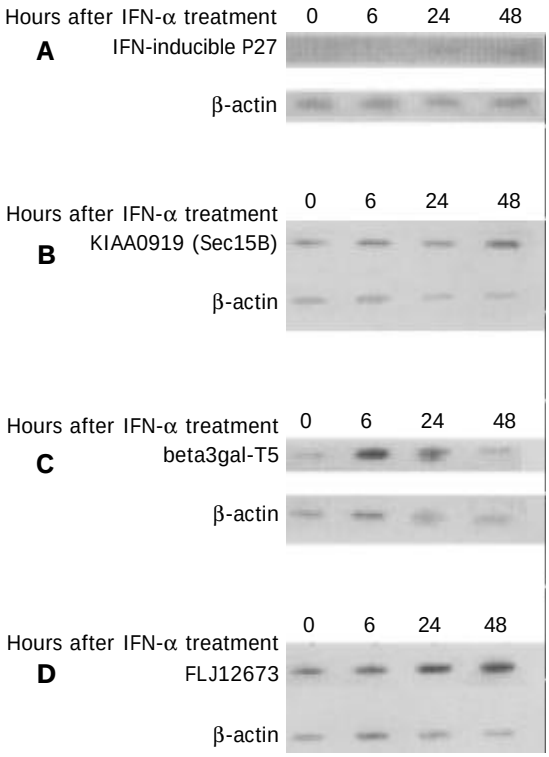

Figure 1 RNA slot analyses of IFN-inducible P27, KIAA0919 (Sec15B), beta3gal-T5 and FLJ12673 genes in $HepG_2$2.2.15 before and after IFN treatment Four genes (interferon related genes P27, KIAA0919, β-3-gal-T5 gene and FLJ12673 human cDNA clone) were selected and tested by RNA slot analysis to confirm the altered expression level indicated by the results of the microarrays.10 μg/sample total cellular RNA was blotted to the nylon membrane. The membrane was then hybridized with [α-^{32}P]dCTP labeled cDNA probes. Autoradiographs were exposed to X-ray film overnight at -70 ℃. The β-actin gene was used as the control to normalize the total RNA quantity.

Differentially expressed genes in $HepG_2$2.2.15 cell line and $HepG_2$ cell line prior to IFN-α treatment

To study the basic differentiated expressed genes between $HepG_2$2.2.15 cell line and its parental cell line $HepG_2$, systematic comparison of gene expression profiles from both cell lines before treatment with IFN-α was done at 0 h. Totally 89 genes were either up- or down-regulated three-fold (Table 2). In these 89 genes, 22 genes have defined functional activities (Table 3) while 67 genes were new ESTs with unknown functions. Fifteen of the 22 known genes were down-regulated by three- to twelve-fold, while 7 genes were up-regulated by three- to thirteen-fold. 4 genes could be catalogued in four classes, such as cell cycle (Y13467), ligands and receptors (AF022375), phosphatase (U12128), and transcription factors (D87258).

Differentially regulated genes in $HepG_2$2.2.15 cell line and $HepG_2$ after IFN-α treatment

Six hours after treatment with interferon-α, significant changes in mRNA expression were observed in both $HepG_2$ and $HepG_2$2.2.15 cells, with 83 and 34 genes up- or down-regulated by at least three-fold (Table 2). A moderate increase in changes of cellular gene expression was detected at 24 h, at which time, 103 and 48 genes were up- or down-regulated respectively by at least three-fold (Table 2). Approximately half of these genes could be classified in functional categories, including interferon responsive proteins, signal transducing genes such as kinase, phosphatase and ligand as well as receptors (Table 4). It is interesting to note that the number of differentially expressed cellular genes in $HepG_2$ and $HepG_2$2.2.15 cell lines could be decreased by interferon-α treatment from 89 to 40, 33 and 36 genes at 6, 24, 48 h post treatment (Table 2). The differentially regulated gene expressed profile in $HepG_2$2.2.15 and $HepG_2$ cell lines after IFN-α treatment are available at http://www.mvlab-fudan.cn/microarray databases.

Kinetics of IFN-treated gene expression profile in 23 genes from $HepG_2$ and $HepG_2$2.2.15 cell lines

Twenty three selected genes, belonging catalogues of interferon induced proteins kinase/phosphatase, ligands and receptors, phosphatase, protein degradation, viral and clathrin receptors, protooncogenes and transcription factors respectively, were further compared between $HepG_2$2.2.15 and its parental cell line $HepG_2$ to study the effect of interferon-α treatment on HBV and cellular gene expressions (Table 5). From this table, it is noted that most of these selected genes with known functions have two- three-fold expression regulated in both $HepG_2$ cell line and $HepG_2$2.2.15 cell post interferon treatment. However, five genes (U02680, U07358, U52969, U50529 and U70321), were up-regulated only in HepG2 cell line, while down-regulated in $HepG_2$2.2.15 cells.

DISCUSSION

DNA microarray is an important and powerful tool for surveying changes in cellular gene expression on a large scale. Several groups have used this approach to analyze virus-host cell interactions in HBV infection. Rho *et al*. constructed a $HepG_2$ cell line stably expressing HBx (HepG2-HBx), and performed cDNA microarray analysis on 588 cellular cDNAs to study the effect of HBx on the transcriptional regulation in the human liver cell[15]. To gain more information on how HBV proteins regulate host cellular gene expression, Otsuka *et al*. examined the differences in the gene expression profiles of $HepG_2$2.2.15 and $HepG_2$ cells, using an in-house cDNA microarray dotted with 2 304 cellular genes[16]. To identify hepatocellular genes whose transcriptional regulation is tightly linked with IFN-γ- and IFN-α/β-mediated inhibition of HBV replication, Chisari *et al*. used DNA microarrays and a high-throughput cDNA differential display method (total gene expression analysis (TOGA) to examine the gene expression profiles of HBV transgenic mouse livers before and after the intrahepatic induction of IFN-α/β and IFN-γ[23]. To further understand molecular mechanisms underlying HBV pathogenesis and identify novel cellular genes as new targets for anti-HBV drug development or for novel

Table 2 Gene expression profiling in the microarray analysis

Ratio	Gene differences in $HepG_2$2.2.15			Gene differences in $HepG_2$			Gene differences in $HepG_2$2.2.15/$HepG_2$			
	6 h/0 h	24 h/0 h	48 h/0 h	6 h/0 h	24 h/0 h	48 h/0 h	0 h	6 h	24 h	48 h
3	34	48	45	83	103	48	89	40	33	36
5	10	18	12	37	37	23	27	12	8	11

Table 3 Differently expressed known genes in $HepG_2$2.2.15 and $HepG_2$ cell lines before IFN-α treatment

Accession ID	$HepG_2$	$HepG_2$2.2.15	Ratio	Description	Unigene
Cell cycle					
Y13467	101.95	29.54	-3.45	RB18A	Hs.15589
Ligands and receptors					
AF022375	16.17	5.19	-3.12	vascular endothelial growth factor	Hs.73793
Phosphatase					
U12128	152.03	27.26	-5.58	tyrosine phosphatase 1E (PTP1E)	Hs.211595
Transcription factors					
D87258	156.76	37.78	-4.15	serin protease with IGF-binding motif	Hs.75111
Miscellaneous					
X69962	242.93	73.77	-3.29	FMR-1	Hs.89764
X56597	1.64	21.98	13.40	humFib mRNA for fibrillarin	Hs.99853
U76713	403.90	123.59	-3.27	apobec-1 binding protein 1	Hs.81361
U50410	189.94	27.03	-7.03	heparan sulphate proteoglycan (OCI5)	Hs.119651
U23070	5.35	16.82	3.14	putative transmembrane protein (nma)	Hs.78776
S68805	4.12	12.74	3.09	L-arginine:glycine amidinotransferase	Hs.75335
M22430	13.63	50.17	3.68	RASF-A PLA2	Hs.76422
M16961	221.65	61.50	-3.60	alpha-2-HS-glycoprotein alpha and beta chain	Hs.75430
M13928	21.15	163.32	7.72	delta-aminolevulinate dehydratase	Hs.1227
L40157	14.58	92.98	6.38	endosome-associated protein (EEA1)	Hs.2864
L24123	1 309.05	430.92	-3.04	NRF1 protein (NRF1)	Hs.83469
D00096	7.61	31.28	4.11	Prealbumin	Hs.194366
AJ006835	150.29	49.21	-3.05	U17 small nucleolar RNA host gene	Hs.196769
AF073308	237.11	78.45	-3.02	nonsyndromic hearing impairment protein (DFNA5)	Hs.13530
AF050127	823.97	71.21	-11.57	hypoxia inducible factor (aHIF)	Hs.197540
AC002045	237.87	67.71	-3.51	Chromosome 16 BAC clone CIT987SK-A-589H1	Hs.253182
AB027013	15.62	2.31	-6.76	Nucleosome Assembly Protein 1-like 2	Hs.66180
AB023136	544.25	44.18	-12.32	KIAA0919	Hs.44175

Table 4 Functional catalogues of 3 fold regulated genes in $HepG_2$ and $HepG_2$2.2.15 cell lines post IFN-α treatment

Catalogue	3-fold regulated gene number in $HepG_2$2.2.15			3-fold regulated gene number in $HepG_2$		
	6 h/0 h	24 h/0 h	48 h/0 h	6 h/0 h	24 h/0 h	48 h/0 h
Cell cycle	-	1	1	-	-	-
Coagulation	-	1	1	-	1	-
Cytokine/receptors	1	2	2	1	1	-
Extracellular matrix and cell adhesion	-	-	1	-	1	-
GTP binding proteins and signal transduction	2	-	1	-	1	1
Interferon	8	6	3	6	5	5
Kinase and phosphatase	-	-	1	-	2	-
Ligands and receptors	-	1	2	-	-	-
Mitochondrial	-	1	1	-	2	-
Phosphatase and phosphodiesterase	2	2	2	1	2	1
Protooncogenes	-	1	-	1	-	-
Transcription factors	-	-	-	1	1	1
Viral and clathrin receptors	-	1	1	-	1	-
Miscellaneous	7	8	8	14	18	13
New ESTs	14	24	21	59	68	27
Total	34	48	45	83	103	48

therapies, we used cDNA microarray filters dotted with 14 000 human genes to analyze transcriptional changes between an HBV DNA-transfected cell line ($HepG_2$2.2.15) and its parental cell line ($HepG_2$) pre- and post-IFN treatment. The $HepG_2$2.2.15 cell line, that has four copies of HBV genome integrated in the cellular chromosome and can persistently secrete HBV virions, was used for HBV infected liver-derived cells[17,18]. The parental hepatoblastoma cell line, $HepG_2$, from which $HepG_2$2.2.15 cell line was generated, was used as the uninfected cell control. In this study, the differentially expressed cellular genes detected between these two cell lines could be due to the integration of HBV DNA, the replication of HBV or the expression of HBV proteins. In chronic HBV infections, the virus usually persists in hepatocytes similar to the status of HBV in $HepG_2$2.2.15 cell line; the differentially expressed cellular genes in $HepG_2$2.2.15 cell line could reveal similar changes in the hepatocytes of HBV chronically infected patients.

Prior to interferon-α treatment, compared to $HepG_2$ cells, 15 known genes were more than three-fold down-regulated, while 7 genes were more than 3-fold up-regulated (Table 3) in $HepG_2$2.2.15 cells. To concentrate on the down-regulated genes, 4 genes belonging to the categories of cell cycle, ligands and receptors,

Table 5 Kinetics of IFN-treated gene expression profiles in 23 selected genes from $HepG_2$ and $HepG_2$2.2.15 cells

Accession ID	$HepG_2$2.2.15 cell lines			$HepG_2$ cell lines			Description
	6 h/0 h	24 h/0 h	48 h/0 h	6 h/0 h	24 h/0 h	48 h/0 h	
Interferon							
X57352	3.8	3.1	2.5	6.5	8.1	6.4	1-8U gene from interferon-inducible gene family
X57351	3.4	2.2	2.2	4.3	4.4	4.4	1-8U gene from interferon-inducible gene family
M87503	2.3	1.7	1.7	3.2	2.4	2.6	IFN-responsive transcription factor subunit
M33882	2.4	1.6	1.5	2.5	2.1	1.6	p78 protein
M11810	9.1	5.7	4.4	8.4	7.7	3.9	(2'-5') oligo A synthetase E gene
L07633	2.0	1.3	1.5	2.0	2.7	1.3	(clone 1950.2) interferon-gamma IEF SSP 5111
J04164	6.7	5.0	2.9	6.4	7.0	6.5	Interferon-inducible protein 9-27
D28137	3.0	3.3	2.8	2.7	2.6	1.8	BST-2
AJ225089	3.9	1.3	1.1	1.9	2.1	1.2	2'-5' oligoadenylate synthetase 59 kDa isoform
Kinase/Phosphate							
U07358	-1.3	-1.3	-2.5	1.1	2.4	1.4	Protein kinase (zpk)
U02680	-1.1	1.4	-2.5	1.5	7.1	1.6	Protein tyrosine kinase
AF032437	-1.1	-2.5	-1.7	-1.3	-3.3	-2.0	Mitogen activated protein kinase activated protein kinase
Ligands and receptors							
D86096	2.3	4.6	3.5	1.9	1.8	2.3	Prostaglandin E receptor EP3 subtype
AF022375	1.8	1.8	3.2	-1.2	-1.1	1.1	Vascular endothelial growth factor
Phosphatase							
U12128	3.0	4.8	4.7	-1.2	-1.1	-1.2	Protein tyrosine phosphatase 1E (PTP1E)
Protein degradation							
Z14977	2.2	1.2	1.4	2.7	1.3	1.6	Major histocompatibility complex encoded proteasome subunit LMP2
AF061736	2.6	1.5	1.4	2.3	2.3	2.0	Ubiquitin-conjugating enzyme RIG-B
Protooncogenes							
U52969	1.1	-2.0	-1.3	2.2	1.6	2.1	PEP19 (PCP4)
U50529	-2.5	-5.0	-2.5	1.7	1.5	2.2	BRCA2 region, mRNA sequence CG016
Transcription factors							
D87258	1.6	2.3	2.5	1.0	-1.1	-1.5	Serin protease with IGF-binding motif
Viral and clathrin receptors							
X81636	1.1	5.5	5.2	-1.1	6.4	-1.7	Clathrin light chain a
U70321	-1.3	-2.0	1.1	2.0	1.2	1.6	Herpesvirus entry mediator
AF079221	1.0	1.2	2.9	1.7	2.2	1.9	BCL2/adenovirus E1B 19kDa-interacting protein 3 a

phosphatase and transcription factors were down-regulated more than three-fold in $HepG_2$ 2.2.15 cells (Table 3). In a microarray study on HCMV-host cell interactions compared to non-infected human fibroblasts, down-regulated genes belonging to these categories were also reported in HCMV infected cells[10]. Though identical down-regulated genes from these categories were not found in the HCMV infected and HBV transfected cells, changes in the expression of cellular genes in these categories could reflect the common adverse effects of virus infections on host cells. In future studies, when more microarray analyses on virus-host interactions will be performed, it may be possible to identify significant changes of cellular gene expression due to HBV-hepatocyte interactions.

The effects of IFN-α on the global gene expression of $HepG_2$ and $HepG_2$2.2.15 cells revealed interesting differences (data available at http://www.mvlab-fudan.cn/microarray databases). In $HepG_2$ cells, compared with the expression of cellular genes at 0 h, no known gene was three-fold down-regulated 48 hr after IFN-α treatment. In contrast, 21 genes were up-regulated three-fold or more, and among these, five were IFN-induced genes, one belonging to the GTP-binding protein and signal transduction category, and one belonging to the phosphatase and phosphodiesterase category associated with the IFN-induced cascade. In $HepG_2$ 2.2.15 cells, after being treated with IFN-α for 48 h, eight genes remained down-regulated three-fold or more. In comparison to the known functional genes, one gene was predicted as encoding the regulatory G protein beta subunit, one was predicted as encoding an antigen of B cell differentiation, one encoding the thymosin beta 4Y isoform, one encoding a LDL-receptor related protein, which was also reported as encoding a human IFN-γ receptor, and one was an exon encoding a protein of the phosphatase and phosphodiesterase category, and the other 3 genes belonged to coagulation, mitochondrial and miscellaneous categories, respectively. These genes remained down-regulated and thus seemed refractory to the treatment of IFN-α. Since 2 of these genes are associated with thymosin and IFN-γ, microarray studies of $HepG_2$2.2.15 cells treated with IFN-γ and/or cytokines may be able to elucidate whether these defects in cellular functions could be reversed. In $HepG_2$2.2.15 cells, a number of IFN induced genes were up-regulated post IFN-α treatment; among these, genes p27 and 2' -5' A synthetase E were the top two up-regulated genes, being 6.1 and 9.1 respectively. Compared to the increases in these two genes up-regulated in $HepG_2$ (being 7.1 and 8.4 respectively), IFN-α was as effective in inducing these two genes in HBV infected cells as that in the uninfected hepatocytes.

To analyze whether there were HBV specific down-regulated cellular genes, which could be restored by IFN-α treatment, 23 matched genes from $HepG_2$ and $HepG_2$2.2.15 cell lines were compared post IFN-α treatment. As shown in Table 5, the three genes which were found down-regulated in $HepG_2$2.2.15 prior to IFN-α treatment (Table 3), namely described as encoding vascular endothelial growth factor, tyrosine phosphatase 1E,

serine protease with IGF-binding motif were all up-regulated by IFN-α treatment. In addition, a gene described as coding for clathrin light chain, which belongs to the viral and clathrin receptor category was also up-regulated 5.2 times. However, even after IFN-α treatment, the down-regulated protein kinase zpk and protein tyrosine kinase genes could not be restored (Table 5), which suggested a possible defective link in the IFN-α induced cascade. Measures for restoring the functions of the kinases could help to improve the therapeutic efficacy of IFN-α. The clinical implications of non-restorable down-regulated protooncogenes in $HepG_2$ 2.2.15 cell lines merit further study.

Analysis of gene expression profiles in HBV-hepatocyte interaction by microarray is an interesting field. The information gathered in this study, though preliminary in scope, provides an important basis for further study. The differentially expressed genes detected in this study should be further evaluated by cell transfection or by *in vivo* studies and should provide new insight into the molecular mechanisms of HBV infection. In addition, there were approximately 200 unknown genes or ESTs being up- or down-regulated in $HepG_2$2.2.15 cells. Preliminary transiently co-transfected functional assay has already shown that some of cellular genes significantly regulated by HBV infection and IFN are associated with the inhibition of HBV gene replication and expression (data not shown). It is predicted that other IFN-inducible proteins could be discovered and new mechanisms of this cytokine may be revealed.

ACKNOWLEDGMENTS

This work was supported by the Chinese State Basic Science Foundation (No.1999054105) and Med-X Foundation of Fudan University. Xun Wang and Wei Xiong are Ph.D. students supported by the Chinese Ministry of Education.

REFERENCES

1 **Hoofnagle JH**. Alpha-interferon therapy of chronic hepatitis B: Current status and recommendations. *J Hepatol* 1990; **11** (Suppl 1): S100-107

2 **Korenman JB**, Baker B, Waggoner J, Everhart JE, Di Bisceglie AM, Hoofnagle JH. Long-term remission of chronic hepatitis B after alpha-interferon therapy. *Ann Intern Med* 1991; **114**: 629-634

3 **Caselmann WH**, Eisenburg J, Hofschneider PH, Koshy R. Beta- and gamma-interferon in chronic active hepatitis B. A pilot trial of short-term combination therapy. *Gastroenterology* 1989; **96**(2 Pt 1): 449-455

4 **Samuel CE**. Antiviral actions of interferons. *Clin Microbiol Rev* 2001; **14**: 778-809

5 **Wen YM**, Qian LS, Lou HZ, Gao JQ, Wu XH, Yang PZ. Studies on production of interferon I by peripheral blood mononuclear cells in chronic hepatitis B patients. *Chin Med J* 1980; **60**: 239-241

6 **Wen YM**, Luo HZ, Qian LS, Duan SC, Zhu QR, Wu XH. Serial study on production of interferon by leucocytes in viral hepatitis B. *Chin J Microb Immunol* 1981; **1:** 342-345

7 **Wen YM**, Yu CZ, Huang YX, Wu XH, Zheng HD, Liu XY. Studies on 2'-5' oligo-isoadenylate synthetase and virus replication in hepatitis B. *Chin J Inf Dis* 1985; **3**: 106-109

8 **Fujisawa K**, Yamazaki K, Kawase H, Kitahara T, Kimura K, Ogura K, Kameda H. Interferon therapy for chronic viral hepatitis and the use of peripheral lymphocytic 2'-5'-oligoadenylate synthetase In: Zuckerman AJ, eds. Viral hepatitis and liver disease. *New York: Alan R Liss Inc* 1988: 834-839

9 **Geiss GK**, Bumgarner RE, An MC, Agy MB, van't Wout AB, Hammersmark E, Carter VS, Upchurch D, Mullins JI, Katze MG. Large-scale monitoring of host cell gene expression during HIV-1 infection using cDNA microarrays. *Virology* 2000; **266**: 8-16

10 **Zhu H**, Cong JP, Mamtora G, Gingeras T, Shenk T. Cellular gene expression altered by human cytomegalovirus: global monitoring with oligonucleotide arrays. *Proc Natl Acad Sci U S A* 1998; **95**: 14470-14475

11 **Browne EP**, Wing B, Coleman D, Shenk T. Altered cellular mRNA levels in human cytomegalovirus-infected fibroblasts: viral block to the accumulation of antiviral mRNAs. *J Virol* 2001; **75**: 12319-12330

12 **Stingley SW**, Ramirez JJ, Aguilar SA, Simmen K, Sandri-Goldin RM, Ghazal P, Wagner EK. Global analysis of herpes simplex virus type 1 transcription using an oligonucleotide-based DNA microarray. *J Virol* 2000; **74**: 9916-9927

13 **Geiss GK**, An MC, Bumgarner RE, Hammersmark E, Cunningham D, Katze MG. Global impact of influenza virus on cellular pathways is mediated by both replication-dependent and –independent events. *J Virol* 2001; **75**: 4321-4331

14 **Lara-Pezzi E**, Majano PL, Gomez-Gonzalo M, Garcia-Monzon C, Moreno-Otero R, Levrero M, Lopez-Cabrera M. The hepatitis B virus X protein up-regulates tumor necrosis factor α gene expression in hepatocytes. *Hepatology* 1998; **28**: 1013-1021

15 **Han J**, Yoo HY, Choi BH, Rho HM. Selective transcriptional regulations in the human liver cell by hepatitis B viral X protein. *Biochem Biophys Res Commun* 2000; **272**: 525-530

16 **Otsuka M**, Aizaki H, Kato N, Suzuki T, Miyamura T, Omata M, Seki N. Differential cellular gene expression induced by hepatitis B and C viruses. *Biochem Biophys Res Commun* 2003; **300**: 443-447

17 **Knowles BB**, Howe CC, Aden DP. Human cell lines secrete the major plasma proteins and hepatitis B surface antigen. *Science* 1980; **209**: 497-499

18 **Sells MA**, Chen ML, Acs G. Production of hepatitis B virus particles in Hep G_2 cells transfected with cloned hepatitis B virus DNA. *Proc Natl Acad Sci U S A* 1987; **84**: 1005-1009

19 **Gerber MA**, Sells MA, Chen ML, Thung SN, Tabibzadeh SS, Hood A, Acs G. Morphologic immunohistochemical and ultrastructural studies of the production of hepatitis B virus *in vitro*. *Lab Invest* 1988; **59**: 173-180

20 **Xu L**, Hui L, Wang S, Gong J, Jin Y, Wang Y, Ji Y, Wu X, Han Z, Hu G. Expression profiling suggested a regulateory role of liver-enriched transcription factors in human hepatocellular carcinoma. *Cancer Res* 2001; **61**: 3176-3181

21 **Hu RM**, Han ZG, Song HD, Peng YD, Huang QH, Ren SX, Gu YJ, Huang CH, Li YB, Jiang CL, Fu G, Zhang QH, Gu BW, Dai M, Mao YF, Gao GF, Rong R, Ye M, Zhou J, Xu SH, Gu J, Shi JX, Jin WR, Zhang CK, Wu TM, Huang GY, Chen Z, Chen MD, Chen JL. Gene expression profiling in the human hypothalamus-pituitary-adrenal axis and full-length cDNA cloning. *Proc Natl Acad Sci U S A* 2000; **97**: 9543-9548

22 **Rhee CH**, Hess K, Jabbur J, Ruiz M, Yang Y, Chen S, Chenchik A, Fuller GN, Zhang W. cDNA expression array reveals heterogeneous gene expression profiles in three glioblastoma cell lines. *Oncogene* 1999; **18**: 2711-2717

23 **Wieland SF**, Vega RG, Muller R, Evans CF, Hilbush B, Guidotti LG, Sutcliffe JG, Schultz PG, Chisari FV. Searching for interferon-induced genes that inhibit hepatitis B virus replication in transgenic mouse hepatocytes. *J Virol* 2003; **77**: 1227-1236

Edited by Xu FM and Wang XL

PO Box 2345, Beijing 100023, China
Fax: +86-10-85381893
E-mail: wjg@wjgnet.com www.wjgnet.com

World J Gastroenterol 2004;10(12):1746-1749
World Journal of Gastroenterology
Copyright ©2004 by The WJG Press ISSN 1007-9327

• VIRAL HEPATITIS •

Transactivating effect of hepatitis C virus core protein: A suppression subtractive hybridization study

Min Liu, Yan Liu, Jun Cheng, Shu-Lin Zhang, Lin Wang, Qing Shao, Jian Zhang, Qian Yang

Min Liu, Shu-Lin Zhang, Qian Yang, Department of Infectious Diseases, The First Hospital of Xi' an Jiaotong University, Xi' an 710061, Shaanxi Province, China
Yan Liu, Jun Cheng, Lin Wang, Qing Shao, Jian Zhang, Gene Therapy Research Center, Institute of Infectious Diseases, 302 Hospital of PLA, Beijing 100039, China
Supported by the National Natural Science Foundation of China, No.39970674
Correspondence to: Dr. Jun Cheng, Gene Therapy Research Center, Institute of Infectious Diseases, 302 Hospital of PLA, 100 Xisihuanzhong Road, Beijing 100039, China. cj@genetherapy.com.cn
Telephone: +86-10-66933392 **Fax**: +86-10-63801283
Received: 2003-11-21 **Accepted:** 2003-12-29

Abstract

AIM: To investigate the transactivating effect of hepatitis C virus (HCV) core protein and to screen genes transactivated by HCV core protein.

METHODS: pcDNA3.1(-)-core containing full-length HCV core gene was constructed by insertion of HCV core gene into *Eco*RI/*Bam*HI site. HepG2 cells were cotransfected with pcDNA3.1(-)-core and pSV-lacZ. After 48 h, cells were collected and detected for the expression of β-gal by an enzyme-linked immunosorbent assay (ELISA) kit. HepG2 cells were transiently transfected with pcDNA3.1(-)-core using Lipofectamine reagent. Cells were collected and total mRNA was isolated. A subtracted cDNA library was generated and constructed into a pGEM-Teasy vector. The library was amplified with *E. coli* strain JM109. The cDNAs were sequenced and analyzed in GenBank with BLAST search after polymerase chain reaction (PCR).

RESULTS: The core mRNA and protein could be detected in HepG2 cell lysate which was transfected by the pcDNA3.1(-)-core. The activity of β-galactosidase in HepG2 cells transfected by the pcDNA3.1(-)-core was 5.4 times higher than that of HepG2 cells transfected by control plasmid. The subtractive library of genes transactivated by HCV core protein was constructed successfully. The amplified library contained 233 positive clones. Colony PCR showed that 213 clones contained 100-1 000 bp inserts. Sequence analysis was performed in 63 clones. Six of the sequences were unknown genes. The full length sequences were obtained with bioinformatics method, accepted by GenBank. It was suggested that six novel cDNA sequences might be target genes transactivated by HCV core protein.

CONCLUSION: The core protein of HCV has transactivating effects on SV40 early promoter/enhancer. A total of 63 clones from cDNA library were randomly chosen and sequenced. Using the BLAST program at the National Center for Biotechnology Information, six of the sequences were unknown genes. The other 57 sequences were highly similar to known genes.

Liu M, Liu Y, Cheng J, Zhang SL, Wang L, Shao Q, Zhang J, Yang Q. Transactivating effect of hepatitis C virus core protein: A suppression subtractive hybridization study. *World J Gastroenterol* 2004; 10(12): 1746-1749
http://www.wjgnet.com/1007-9327/10/1746.asp

INTRODUCTION

Hepatitis C virus (HCV) is a major causative agent of chronic liver diseases including chronic hepatitis, liver cirrhosis, and hepatocellular carcinoma worldwide[1-4]. The majority of individuals infected with HCV cannot resolve their infection and suffer from persistent chronic hepatitis. The molecular mechanism of HCV persistence and pathogenesis is not well understood. HCV contains a single-stranded positive-sense RNA genome which encodes a precursor polypeptide of approximately 3 000 amino acids. After translation, a capsid protein (core), envelope glycoproteins (E1 and E2), and nonstructural proteins (NS2, NS3a, NS3b, NS4A, NS4B, NS5A, and NS5B) are processed from the polyprotein by cellular and viral proteases[5-10].

HCV core gene contains the most conserved sequences in the coding region of most HCV genotypes, which implies an important biological function. Since suitable viral culture systems are not generally available[10-13], analysis of HCV genome organization and viral-product function is important to understand the viral life cycle and the pathogenesis of HCV infection. In order to understand the pathogenesis of HCV infection, we investigated the transactivating effect of HCV core protein.

MATERIALS AND METHODS

Construction and identification of expression vectors

pcDNA3.1(-)-core containing full-length HCV core gene was constructed by insertion of HCV core gene into *EcoRI*/*BamHI* site, which could directly express core protein. pcDNA3.1(-) was obtained from Invitrogen. The gene was identified by PCR and digested by *Eco*R I, *Bam*H I, and Hind III (Takara). PCR primers were: up primer, 5' -GAA TTC AAT GAG CAC GAA TCC TAA-3' ;down primer, 5' -GGA TCC AGG CTG AAG CGG GCA CA-3' (Shanghai BioAsia Biotechnology Co., Ltd).

Cotransfection with reporter vectors pSV-lacZ

HepG2 cells were transfected by various concentrations of pSV-lacZ (0.1-1.8 μg) (Promega). Expression of β-gal was detected by using β-gal assay kit (Promega). The best concentration of pSV-lacZ was selected, HepG2 cells with pcDNA3.1(-)-core and pSV-lacZ were cotransfected. At the same time, HepG2 cells were cotransfected with empty pcDNA3.1(-) and pSV-lacZ as control. After 48 h, cells were collected and the expression of β-gal was detected.

Expression of pcDNA3.1(-)-core in HepG2 cells

HepG2 cells were transiently transfected with pcDNA3.1(-)-core using Lipofectamine. At the same time, empty vectors were also transfected into cells as control. HepG2 cells were

plated at a density of 1×10^6 on a 35 mm plate in RPMI1640 containing 100 U/mL of penicillin, 100 μg/mL of streptomycin, and 100 mL/L heat-inactivated FBS. After 24 h of growth to 40-50% confluentce, the cells were transfected with plasmids by using Lipofectamine according to the manufacturer' s protocol (Gibco Co.).

mRNA and cDNA isolation

Total cellular RNA was isolated using TRIzol (Invitrogen) according to the manufacturer' s instructions. cDNAs were reversely-transcribed from total RNA. The result was identified by PCR. Cells were collected and mRNA was isolated by using a micro mRNA purification kit (Amersham Biosciences).

Generation of a subtracted cDNA library

Genome comparisons were performed by suppression subtraction hybridization according to the manufacturer' s instructions of PCR-selectTM cDNA subtraction kit (Clontech). In brief, 2 μg aliquots each of poly(A)+ mRNA from the tester and the pooled driver were subjected to cDNA synthesis. Tester and driver cDNAs were digested with *RsaI*. The tester cDNA was subdivided into two portions, and each was ligated with a different cDNA adapter. In the first hybridization reaction, an excess of driver was added to each sample of tester. The samples were heat denatured and allowed to be annealed. Because of the second-order kinetics of hybridization, the concentration of high- and low-abundance sequences was equalized among the single-stranded tester molecules. At the same time single-stranded tester molecules were significantly enriched for differentially expressed sequences. During the second hybridization, the two primary hybridization samples were mixed without denaturation. Only the remaining equalized and subtracted single-stranded tester cDNAs could reassociate, forming double-stranded tester molecules with different ends. After the ends were filled with DNA polymerase, the entire population of molecules was subjected to nested PCR with two adapter-specific primer pairs.

Cloning subtracted library into pGEM-Teasy vector

Products of these amplified A overhangs containing a subtracted cDNA library (3 μL) were ligated into a pGEM-Teasy plasmid (Promega). Subsequently, the plasmid was introduced into Escherichia coli strain JM109. Bacteria were transferred into 800 μL of SOC medium and allowed to be incubated for 45 min at 37 ℃ and centrifuged at 225 rpm. Then they were plated onto agar plates containing ampicillin (50 μg/mL), 5-bromo-4-chloro-3-indolyl-β-D-galactoside (X-Gal; 20 μg/cm^2), and isopropyl-β-D-thiogalactoside (IPTG; 12.1 μg/cm^2) and incubated overnight at 37 ℃. White colonies were picked and identified by PCR. Primers were T7/SP6 primer of pGEM-Teasy plasmid. After the positive colonies (Shanghai BioAsia Biotechnology Co., Ltd) were sequenced, nucleic acid homology searches were performed using the BLAST (basic local alignment search tool) server at the National Center for Biotechnology Information.

RESULTS

Identification of expression vector

Figure 1 shows pcDNA3.1(-)-core of the PCR assay for plasmid and digestion of restriction enzyme analysis. Restriction enzyme analysis of pcDNA3.1(-)-core plasmid with *Eco*RI/*Bam*H I yielded two bands: 4 900 bp empty pcDNA3.1 (-) and 573 bp HCV core. Cleavage with *Hind* III produced only one 5 500 bp band (4 900 bp+573 bp). The products of plasmid were amplified by PCR. Analysis of the PCR reaction products by agarose gel electrophoresis showed a clear band with the expected size (573 bp). Sequence of the PCR product was correct.

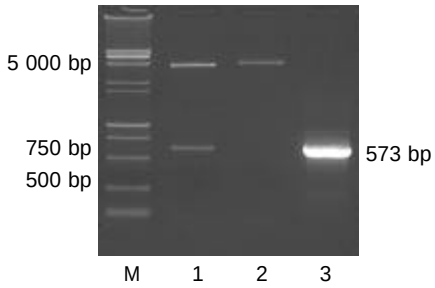

Figure 1 Products of pcDNA3.1(-)-core PCR and restriction enzyme cleavage were electrophoresed in 1% agarose gel. Lane 1: *Eco*RI / *Bam*HI cleaved; lane 2: *Hind*III cleaved; lane 3: products of plasmid PCR; M: DNA marker, (15 000 bp+ 2 000 bp).

Identification of HCV core transient expression

The total mRNA was reversely-transcribed by three different Oligo dT, identification of cDNA by PCR yielded a common 573 bp band (Figure 2). Table 1 shows co-transfected pcDNA3.1 (-)-core and pSV-lacZ into HepG2 cells, transient expression of HCV core was positive. On the contrary, empty pcDNA3.1 (-) co-tranfected HepG2 cells were negative.

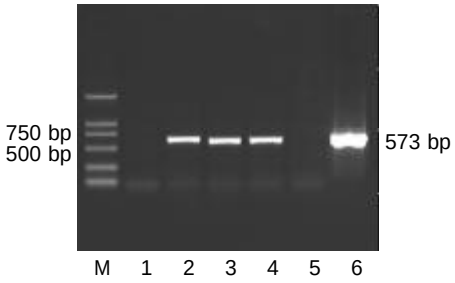

Figure 2 RT-PCR products were electrophoresed in 1% agarose gel. Lane 1: negative control; lanes 2-4: total RNA was isolated from pcDNA3.1(-)-core and RT-PCR was performed by three different Oligo dT; lane 5: blank control; lane 6: positive control; M: DNA marker (2 000 bp).

Table 1 Transient expression of pcDNA3.1(-)-core in HepG2 cells

Group	Coat Ag	*P*	P / N (n=0.05)	Results (+ / -)
pcDNA3.1(-)-core	pcDNA3.1(-)-core lysate	0.219	4.38	+
Blank plasmid	pcDNA3.1(-) lysate	0.034	0.68	-
Positive control	HCV core Ag	1.299	24.60	+
Negative control	PBS	0.012	0.24	-

Result of pcDNA3.1(-)-core and pSV-lacZ cotransfection

Selection of 0.3 μg pSV-lacZ served as the best concentration by analysis. After cotransfection of pcDNA3.1(-)-core and pSV-lacZ, the *A* value of expression of β-gal was 0.219. In contrast, the *A* value of expression of β-gal by cotransfected empty pcDNA3.1(-) and pSV-lacZ was 0.034. Expression of β-gal was 5.4-fold higher in cotransfected pcDNA3.1(-)-core and pSV-lacZ than in cotransfected empty pcDNA3.1(-) and pSV-lacZ (Figure 3). The significant increase of expression of β-gal was attributed to the transactivating effect of HCV core on early promoter of SV40, leading to the increased expression of downstream gene lacZ.

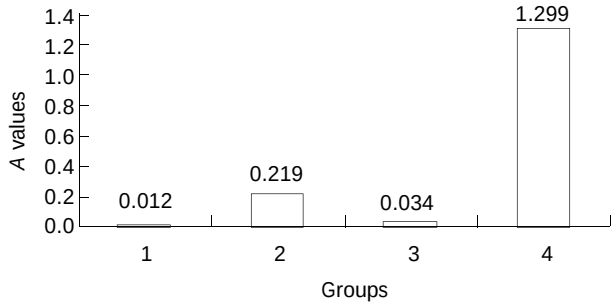

Figure 3 Comparison of *A* values among transfection groups. 1. Negative control (PBS); 2. pcDNA3.1(-)-core; 3. Blank plasmid; 4. Positive control.

Analysis of subtraction library

Using suppression subtractive hybridization technique (SSH), we obtained a total of 233 positive clones. These clones were prescreened by using PCR amplification to make sure that only clones with different inserts were subjected to sequencing (Figure 4). Two hundred and thirteen clones contained 100-1 000 bp inserts. A total of 63 clones from cDNA library were randomly chosen and sequenced. Using the BLAST program at the National Center for Biotechnology Information, six of the sequences were unknown genes. The full length sequences accepted by GenBank were obtained with bioinformatics method. The other 57 sequences had a high similarity to known genes. Twenty-one of the sequences were 100% identical in nucleotide sequence to previously described sequences. Summary of the data is presented in Table 2.

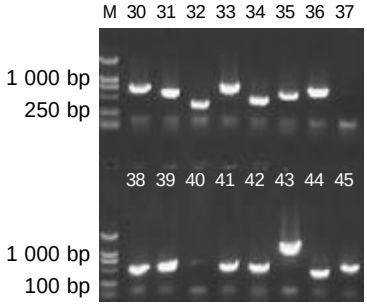

Figure 4 Agarose gel electrophoresis of PCR products of some clones (30-45). M: DNA marker (2 000 bp).

Table 2 Comparison between positive clones and similar sequences in GenBank

High similarity to known genes	Number of similar clones
Ribosomal protein	21
Eukaryotic translation elongation factor	6
Eukaryotic translation initiation factor	5
Heat shock factor binding protein (HSBP)	5
Apolipoprotein	5
NADH dehydrogenase	3
Heterogeneous nuclear ribonucleoprotein	3
D-like (HNRPDL), transcript variant	
Alpha-2-macroglobulin (A2M)	2
Bile acid-binding protein (BABP)	2
Cathepsin C (CTSC)	1
Fibronectin (FN precursor)	1
Magnesium-dependent protein phosphatase	1
Thioredoxin-related transmembrane protein	1
WEE1 gene for protein kinase	1

DISCUSSION

The diverse functional activities of HCV putative core protein have already been noted by a number of investigators. These include nucleocytoplasmic localization[14], regulation of cellular and unrelated viral promoters in *in vitro* studies[15-18], inhibition of apoptosis under certain conditions[19], physical association with apolipoprotein II[20] and cytoplasmic tail of the lymphotoxin β-receptor[21,22], promotion of normal cells to a transformed phenotype[23], and transactivation of suppression of cell growth[12,24].

We cotransfected HepG2 cells with pcDNA3.1(-)-core and pSV-lacZ and demonstrated that the HCV core was successfully expressed in transfected HepG2 cells. Expression of β-gal was 5.4-fold higher in cotransfected pcDNA3.1(-)-core and pSV-lacZ than in cotransfected empty pcDNA3.1(-) and pSV-lacZ. HCV core had significant transactivating effects on the early promoter of SV40, through increasing the expression of downstream gene lacZ. This result indicates that the HCV core protein expressed in HepG2 cells retains its biological activity in terms of transcriptional activation, which was inconsistent with the previous report[23].

The nucleocapsid core protein of HCV has been shown to trans-act on several viral or cellular promoters[15,16,25,26]. To get insight into the trans-action mechanism of HCV core protein, an SSH was used for identification of relatively transactivated target genes of HCV core protein. HCV core protein relatively transactivated gene subtractive library was set up successfully. Sequence analysis was performed in 63 clones. Five of the sequences matched strongly (>97% nucleotide identity) with the apolipoprotein (Apo) sequence. Two of those sequences matched strongly (>97% nucleotide identity) with the bile acid-binding protein (BABP).

Several lines of evidence suggest that HCV core protein may modulate cellular transduction signals and alter lipid metabolism. A characteristic of HCV infection is the presence of liver steatosis. It is plausible that this steatosis could arise, at least in part, from direct effects of HCV proteins on lipid metabolism. The levels of apoAI and high density lipoprotein are independent predictive factors response to treatment[27]. Apo, a protein that bind to lipids and renders them water soluble in the form of lipoproteins, could be a good candidate for an interaction with the core protein. HCV has been described as a lipid-containing virus and in plasma of patients shows a heterogeneous density distribution partially due to its binding to low density lipoprotein, very low density lipoprotein, IgG, and to a minor degree of IgM and high density lipoprotein[28]. Barba *et al*.[20] by double immunofluorescence and confocal analysis of the core and apo revealed colocalization of apoAII and the HCV core protein in the globular structures. Sabile *et al*.[29] investigated the binding of HCV core protein to cellular proteins expressed in HepG2 cells by combining 2 yeast hybrid, confocal and surface plasmon resonance assays. The results showed the direct binding of the viral protein to apolipoprotein AII (apoAII) and mapped the interaction domain to the C-terminal of HCV core protein. Taking advantage of the well-established increase in apoAII expression caused by fibers in HepG2 cells, they identified that apoAII was one of the cellular targets for HCV core protein and the intervention of fenofibric acid in cellular lipid metabolism directly affected the expression pattern of HCV core protein.

It has been discovered that bile acids are the natural ligand for a nuclear receptor termed farnesoid X receptor (FXR; NR1H4)[30-32]. Therefore, bile acids may be important regulators of gene expression in the liver and intestines. To date, the genes that have been shown to be responsive to regulation by FXR encoded proteins are involved in the biosynthesis and transport of bile acids[33]. Bile acids have been shown to modulate a variety of other cellular functions, such as secretion of lipoproteins

from hepatocytes[34,35] and translocation of bile acid transporters to the hepatocyte canalicular membrane[36]. Our results indicate that HCV core protein interacts with bile acid-binding proteins. Maybe it is a way that HCV core protein affects cellular lipid metabolism.

Our results revealed a number of novel and known genes that responded to HCV core. The 6 unknown nucleotide sequences of SSH fragments are deposited in GenBank under accession numbers of AY038359, AY038361, AY039041, AY039042, AY039043, and AY039044.

REFERENCES

1 **Choo QL**, Kuo G, Weiner AJ, Overby LR, Bradley DW, Houghton M. Isolation of a cDNA clone derived from a blood-borne non-A, non-B viral hepatitis genome. *Science* 1989; **244**: 359-362

2 **Di Bisceglie AM**. Hepatitis C and hepatocellular carcinoma. *Hepatology* 1997; **26**(3 Suppl 1): 34S-38S

3 **Hasan F**, Jeffers LJ, De Medina M, Reddy KR, Parker T, Schiff ER, Houghton M, Choo QL, Kuo G. Hepatitis C-associated hepatocellular carcinoma. *Hepatology* 1990; **12**(3 Pt 1): 589-591

4 **Ito T**, Mukaigawa J, Zuo J, Hirabayashi Y, Mitamura K, Yasui K. Cultivation of hepatitis C virus in primary hepatocyte culture from patients with chronic hepatitis C results in release of high titre infectious virus. *J Gen Virol* 1996; **77**(Pt 5): 1043-1054

5 **Clarke B**. Molecular virology of hepatitis C virus. *J Gen Virol* 1997; **78**(Pt 10): 2397-2410

6 **Bukh J**, Purcell RH, Miller RH. Sequence analysis of the 5' noncoding region of hepatitis C virus. *Proc Natl Acad Sci U S A* 1992; **89**: 4942-4946

7 **Grakoui A**, McCourt DW, Wychowski C, Feinstone SM, Rice CM. Characterization of the hepatitis C virus-encoded serine proteinase: determination of proteinase-dependent polyprotein cleavage sites. *J Virol* 1993; **67**: 2832-2843

8 **Takamizawa A**, Mori C, Fuke I, Manabe S, Murakami S, Fujita J, Onishi E, Andoh T, Yoshida I, Okayama H. Structure and organization of the hepatitis C virus genome isolated from human carriers. *J Virol* 1991; **65**: 1105-1113

9 **Grakoui A**, Wychowski C, Lin C, Feinstone SM, Rice CM. Expression and identification of hepatitis C virus polyprotein cleavage products. *J Virol* 1993; **67**: 1385-1395

10 **Hijikata M**, Kato N, Ootsuyama Y, Nakagawa M, Shimotohno K. Gene mapping of the putative structural region of the hepatitis C virus genome by *in vitro* processing analysis. *Proc Natl Acad Sci U S A* 1991; **88**: 5547-5551

11 **Kato N**, Nakazawa T, Mizutani T, Shimotohno K. Susceptibility of human T-lymphotropic virus type I infected cell line MT-2 to hepatitis C virus infection. *Biochem Biophys Res Commun* 1995; **206**: 863-869

12 **Lanford RE**, Sureau C, Jacob JR, White R, Fuerst TR. Demonstration of *in vitro* infection of chimpanzee hepatocytes with hepatitis C virus using strand-specific RT/PCR. *Virology* 1994; **202**: 606-614

13 **Shimizu YK**, Purcell RH, Yoshikura H. Correlation between the infectivity of hepatitis C virus *in vivo* and its infectivity *in vitro*. *Proc Natl Acad Sci U S A* 1993; **90**: 6037-6041

14 **Yasui K**, Wakita T, Tsukiyama-Kohara K, Funahashi SI, Ichikawa M, Kajita T, Moradpour D, Wands JR, Kohara M. The native form and maturation process of hepatitis C virus core protein. *J Virol* 1998; **72**: 6048-6055

15 **Ray RB**, Lagging LM, Meyer K, Steele R, Ray R. Transcriptional regulation of cellular and viral promoters by the hepatitis C virus core protein. *Virus Res* 1995; **37**: 209-220

16 **Ray RB**, Steele R, Meyer K, Ray R. Transcriptional repression of p53 promoter by hepatitis C virus core protein. *J Biol Chem* 1997; **272**: 10983-10986

17 **Ray RB**, Steele R, Meyer K, Ray R. Hepatitis C virus core protein represses p21WAF1/Cip1/Sid1 promoter activity. *Gene* 1998; **208**: 331-336

18 **Shih CM**, Lo SJ, Miyamura T, Chen SY, Lee YH. Suppression of hepatitis B virus expression and replication by hepatitis C virus core protein in HuH-7 cells. *J Virol* 1993; **67**: 5823-5832

19 **Ray RB**, Meyer K, Ray R. Suppression of apoptotic cell death by hepatitis C virus core protein. *Virology* 1996; **226**: 176-182

20 **Barba G**, Harper F, Harada T, Kohara M, Goulinet S, Matsuura Y, Eder G, Schaff Z, Chapman MJ, Miyamura T, Brechot C. Hepatitis C virus core protein shows a cytoplasmic localization and associates to cellular lipid storage droplets. *Proc Natl Acad Sci U S A* 1997; **94**: 1200-1205

21 **Chen CM**, You LR, Hwang LH, Lee YH. Direct interaction of hepatitis C virus core protein with the cellular lymphotoxin-beta receptor modulates the signal pathway of the lymphotoxin-beta receptor. *J Virol* 1997; **71**: 9417-9426

22 **Matsumoto M**, Hsieh TY, Zhu N, VanArsdale T, Hwang SB, Jeng KS, Gorbalenya AE, Lo SY, Ou JH, Ware CF, Lai MM. Hepatitis C virus core protein interacts with the cytoplasmic tail of lymphotoxin-beta receptor. *J Virol* 1997; **71**: 1301-1309

23 **Chang J**, Yang SH, Cho YG, Hwang SB, Hahn YS, Sung YC. Hepatitis C virus core from two different genotypes has an oncogenic potential but is not sufficient for transforming primary rat embryo fibroblasts in cooperation with the H-ras oncogene. *J Virol* 1998; **72**: 3060-3065

24 **Ray RB**, Lagging LM, Meyer K, Ray R. Hepatitis C virus core protein cooperates with ras and transforms primary rat embryo fibroblasts to tumorigenic phenotype. *J Virol* 1996; **70**: 4438-4443

25 **Kim DW**, Suzuki R, Harada T, Saito I, Miyamura T. Trans-suppression of gene expression by hepatitis C viral core protein. *Jpn J Med Sci Biol* 1994; **47**: 211-220

26 **Shih CM**, Lo SJ, Miyamura T, Chen SY, Lee YH. Suppression of hepatitis B virus expression and replication by hepatitis C virus core protein in HuH-7 cells. *J Virol* 1993; **67**: 5823-5832

27 **Soardo G**, Pirisi M, Fonda M, Fabris C, Falleti E, Toniutto P, Vitulli D, Cattin L, Gonano F, Bartoli E. Changes in blood lipid composition and response to interferon treatment in chronic hepatitis C. *J Interferon Cytokine Res* 1995; **15**: 705-712

28 **Thomssen R**, Bonk S, Thiele A. Density heterogeneities of hepatitis C virus in human sera due to the binding of beta-lipoproteins and immunoglobulins. *Med Microbiol Immunol* 1993; **182**: 329-334

29 **Sabile A**, Perlemuter G, Bono F, Kohara K, Demaugre F, Kohara M, Matsuura Y, Miyamura T, Brechot C, Barba G. Hepatitis C virus core protein binds to apolipoprotein AII and its secretion is modulated by fibrates. *Hepatology* 1999; **30**: 1064-1076

30 **Makishima M**, Okamoto AY, Repa JJ, Tu H, Learned RM, Luk A, Hull MV, Lustig KD, Mangelsdorf DJ, Shan B. Identification of a nuclear receptor for bile acids. *Science* 1999; **284**: 1362-1365

31 **Parks DJ**, Blanchard SG, Bledsoe RK, Chandra G, Consler TG, Kliewer SA, Stimmel JB, Willson TM, Zavacki AM, Moore DD, Lehmann JM. Bile acids: natural ligands for an orphan nuclear receptor. *Science* 1999; **284**: 1365-1368

32 **Wang H**, Chen J, Hollister K, Sowers LC, Forman BM. Endogenous bile acids are ligands for the nuclear receptor FXR/BAR. *Mol Cell* 1999; **3**: 543-553

33 **Russell DW**. Nuclear orphan receptors control cholesterol catabolism. *Cell* 1999; **97**: 539-542

34 **Lin Y**, Havinga R, Schippers IJ, Verkade HJ, Vonk RJ, Kuipers F. Characterization of the inhibitory effects of bile acids on very-low-density lipoprotein secretion by rat hepatocytes in primary culture. *Biochem J* 1996; **316**(Pt 2): 531-538

35 **Lin Y**, Havinga R, Verkade HJ, Moshage H, Slooff MJ, Vonk RJ, Kuipers F. Bile acids suppress the secretion of very-low-density lipoprotein by human hepatocytes in primary culture. *Hepatology* 1996; **23**: 218-228

36 **Misra S**, Ujhazy P, Gatmaitan Z, Varticovski L, Arias IM. The role of phosphoinositide 3-kinase in taurocholate-induced trafficking of ATP-dependent canalicular transporters in rat liver. *J Biol Chem* 1998; **273**: 26638-26644

Edited by Zhu LH and Wang XL **Proofread by** Xu FM

PO Box 2345, Beijing 100023, China
Fax: +86-10-85381893
E-mail: wjg@wjgnet.com www.wjgnet.com

World J Gastroenterol 2004;10(12):1750-1754
World Journal of Gastroenterology
Copyright ©2004 by The WJG Press ISSN 1007-9327

Effects of *Helicobacter pylori* infection on gastric emptying rate in patients with non-ulcer dyspepsia

Grigoris I Leontiadis, George I Minopoulos, Efstratios Maltezos, Stamatia Kotsiou, Konstantinos I Manolas, Konstantinos Simopoulos, Dimitrios Hatseras

Grigoris I Leontiadis, Efstratios Maltezos, 2nd Department of Internal Medicine, Democritus University of Thrace, Alexandroupolis, Greece
George I Minopoulos, Department of Endoscopic Surgery, Democritus University of Thrace, Alexandroupolis, Greece
Stamatia Kotsiou, 1st Department of Internal Medicine, Democritus University of Thrace, Alexandroupolis, Greece
Konstantinos I Manolas, 1st Department Surgery, Democritus University of Thrace, Alexandroupolis, Greece
Konstantinos Simopoulos, 2nd Department of Surgery, Democritus University of Thrace, Alexandroupolis, Greece
Dimitrios Hatseras, Department of Cardiology, Democritus University of Thrace, Alexandroupolis, Greece
Correspondence to: Dr. Grigoris I Leontiadis, 4 Karailia Street, Thessaloniki 546 44, Greece. grleo@yahoo.com
Telephone: +30-2310-323535 **Fax:** +30-2310-323535
Received: 2003-12-11 **Accepted:** 2004-01-30

Abstract

AIM: The pathogenesis of delayed gastric emptying in patients with non-ulcer dyspepsia (NUD) remains unclear. We aimed to examine whether gastric emptying rate in NUD patients was associated with *Helicobacter pylori* (*H pylori)* infection and whether it was affected by eradication of the infection.

METHODS: Gastric emptying rate of a mixed solid-liquid meal was assessed by the paracetamol absorption method in NUD patients and asymptomatic controls (n=17). *H pylori* status was assessed by serology and biopsy urease test. *H pylori*-positive NUD patients (n=23) received 10-day triple eradication therapy. *H pylori* status was re-assessed by biopsy urease test four weeks later, and if eradication was confirmed, gastric emptying rate was re-evaluated.

RESULTS: Thirty-three NUD patients and 17 controls were evaluated. NUD patients had significantly delayed gastric emptying compared with controls. The mean maximum plasma paracetamol concentration divided by body mass (Cmax/BM) was 0.173 and 0.224 mg/L·kg respectively (P=0.02), the mean area under plasma paracetamol concentration-time curve divided by body mass (AUC/BM) was 18.42 and 24.39 mg·min/L·kg respectively (P=0.01). Gastric emptying rate did not differ significantly between *H pylori*-positive and *H pylori*-negative NUD patients. The mean Cmax/BM was 0.172 and 0.177 mg/L·kg respectively (P=0.58), the mean AUC/BM was 18.43 and 18.38 mg·min/L·kg respectively (P=0.91). Among 14 NUD patients who were initially *H pylori*-positive, confirmed eradication of the infection did not significantly alter gastric emptying rate. The mean Cmax/BM was 0.171 and 0.160 mg/L·kg before and after *Hp* eradication, respectively (P=0.64), the mean AUC/BM was 17.41 and 18.02 mg·min/L·kg before and after eradication, respectively (P=0.93).

CONCLUSION: Although gastric emptying is delayed in NUD patients compared with controls, gastric emptying rate is not associated with *H pylori* status nor it is affected by eradication of the infection.

Leontiadis GI, Minopoulos GI, Maltezos E, Kotsiou S, Manolas KI, Simopoulos K, Hatseras D. Effects of *Helicobacter pylori* infection on gastric emptying rate in patients with non-ulcer dyspepsia. *World J Gastroenterol* 2004; 10(12): 1750-1754
http://www.wjgnet.com/1007-9327/10/1750.asp

INTRODUCTION

Dyspepsia is defined as pain or discomfort centered in the upper abdomen, according to the Rome II criteria[1]. Discomfort refers to a subjective, unpleasant feeling that the patient does not interpret as pain and which can include any of the following: upper abdominal fullness, early satiety, bloating, or nausea. Functional or non-ulcer dyspepsia (NUD) is defined as persistent or recurrent dyspepsia for at least 12 wk, which need not to be consecutive, within the preceding 12 mo of persistent or recurrent dyspepsia, with no evidence of organic disease that is likely to explain the symptoms, and no evidence that symptoms are exclusively relieved by defecation or associated with the onset of a change in stool frequency or stool form (*i.e.*, not irritable bowel syndrome)[1].

NUD is a common healthcare problem: The estimated annual prevalence in Western countries is 15%[2]. Despite a great deal of scientific attention, little is known about the pathogenesis of NUD. *Helicobacter pylori* (*H pylori)* infection and delayed gastric emptying have both been documented to have higher prevalence in patients with NUD compared with asymptomatic controls[3, 4]. However, it is unknown if *H pylori* infection and/or delayed gastric emptying are involved in the pathogenesis of NUD. Furthermore, it is still unclear whether there is a causal association between these two factors in patients with NUD.

Therefore, we designed this study to investigate whether gastric emptying rate in patients with NUD was associated with the presence of *H pylori* infection, and whether the eradication of the infection affected the gastric emptying rate in these patients. We also sought to confirm in our population the well-known finding of delayed gastric emptying in patients with NUD compared with asymptomatic controls.

MATERIALS AND METHODS

Subjects

Consecutive patients with dyspeptic symptoms who attended the self-referred out-patient clinic of the 2nd Department of Internal Medicine, General Regional Hospital of Alexandroupolis were candidates for inclusion in the study. Inclusion criteria were: (1) age between 18 and 65 years; (2) presence of dyspeptic symptoms, defined as upper abdominal pain, upper abdominal discomfort, upper abdominal fullness, early satiety, or nausea/vomiting, continuously or intermittently for at least three mo; (3) no relevant findings revealed by physical examination other

than epigastric tenderness; (4) normal gastroscopy except mild erythema of gastric or duodenal mucosa; (5) normal abdominal ultrasound scan; (6) normal full blood count, liver function tests, fasting glucose, urea, creatinine, electrolytes, amylase and thyroid function tests. Exclusion criteria were: (1) presence of any organic or psychiatric disease that could affect the evaluation, treatment or compliance of the patient; (2) heartburn as the predominant symptom; (3) predominant symptoms being compatible with the diagnosis of irritable bowel syndrome or functional constipation as defined by Rome I criteria[5]; (4) pregnancy or breast feeding; (5) chronic alcoholism or drug abuse; (6) past medical history of peptic ulcer disease, oesophagitis, pancreatitis, abdominal trauma, or abdominal surgery other than uncomplicated appendectomy; (7) intake of antibiotics 4 wk prior to inclusion; (8) regular intake of non steroidal anti-inflammatory drugs, including aspirin, or other medications that could cause dyspepsia during the 3 mo prior to inclusion.

The asymptomatic controls were recruited from the employees of General Regional Hospital of Alexandroupolis. Eligibility criteria were: (1) age between 18 and 65 years; (2) absence of dyspeptic symptoms; (3) absence of any organic or psychiatric disease that could affect the evaluation, treatment or compliance of the participant; (4) intake of antibiotics 4 wk prior to inclusion.

Proton pump inhibitors and H_2-receptor antagonists were withheld from all participants for 7 d before gastroscopy or gastric emptying testing. Paracetamol and all medications with any known potential effect on gastrointestinal motility were withheld for, respectively, two and three days before gastric emptying testing.

Study prolocol

Study procedures were timed as follows: NUD patients underwent gastroscopy and two biopsy specimens were collected, one from the antrum and one from the corpus, for urease testing for *H pylori* (*CLOtest®, Delta West Ltd, Australia*). The presence of *H pylori* IgG antibodies in serum was assessed by ELISA (*H pylori GVE 57311 IgG, PLK, Italy*). On the following day, gastric emptying rate was assessed by the paracetamol absorption method as described below. *H pylori* -positive NUD patients received 10 d of *H pylori* eradication therapy consisting of omeprazole 20 mg twice daily, amoxicillin 1 000 mg twice daily and clarithromycin 500 mg twice daily. Four weeks later, *H pylori* status was re-assessed by biopsy urease test. If eradication of *H pylori* infection was confirmed, gastric emptying rate was re-evaluated. Asymptomatic controls were tested for *H pylori* infection by serology (*H pylori* IgG ELISA) and had gastric emptying rate assessed by the paracetamol absorption method.

The study protocol conformed to the World Medical Association Helsinki Declaration in 1964 as amended in 1996 and was approved by the regional Ethics Committee. Informed consent was obtained from all study subjects. This work was not financially supported by any outside agency or pharmaceutical company.

Assessment of gastric emptying rate

Gastric emptying rate was assessed by the paracetamol absorption method, which was conceived by Heading *et al*[6,7] and recently re-evaluated[8, 9]. The test meal was administered following overnight fasting and consisted of: (1) three cream crackers (total mass is 35 g); (2) a 200-mL carton of *Fortimel®* (*Nutritcia Clinical, Holland;* liquid nutritional supplement; 410 mOsm/L; 4.184×10^3 kJ/L; containing 19.4 g of protein, 4.2 g of fat and 20.8 g of carbohydrates per carton); (3) 1 g of paracetamol as two tablets 500 mg *Depon®, Bristol-Myers Squibb*; (4) 100 mL of tap water. Peripheral venous blood samples were obtained *via* a heparinised cannula immediately after the ingestion of paracetamol (time 0) and at 30 min intervals over a 3-h period (7 samples in total). During the 3-h test period, the subjects were free to sit, stand or walk; they were not allowed to eat, drink or smoke.

Paracetamol plasma concentration was determined with the *TDxFLx® System* (*Abbott, IL, USA*) by using fluorescence polarization immunoassay technology. The following parameters were calculated: time to detect paracetamol in plasma (lag phase), maximum plasma paracetamol concentration divided by body mass (C_{max} /BM); time to reach maximum plasma paracetamol concentration (T_{max}), area under the plasma paracetamol concentration – time curve divided by body weight (AUC/BM).

Primary outcomes were the absolute difference in gastric emptying rate as assessed by Cmax/BW and AUC/BW in *H pylori*-positive and *H pylori*-negative NUD patients, and in *H pylori*- positive NUD patients before and after eradication.

Secondary outcomes were the absolute difference in gastric emptying rate as assessed by Cmax/BM and AUC/BM in NUD patients compared to asymptomatic controls. We also assessed gastric emptying lag phase and T_{max} in all study groups.

Sample size calculation

Sample size was calculated *a priori* with the Altman nomogram[10]. A pilot study of five *H pylori*-positive NUD patients provided an estimate of mean C_{max} /BM (19.0 mg· min/L· kg) and standard deviation (5.0 mg· min/L· kg). We calculated that at least 10 subjects were required in each study group (*H pylori*-negative NUD patients, *H pylori*-positive NUD patients, post-eradication NUD patients, asymptomatic controls) in order to detect a clinically important relative difference (*a priori* set as $\geqslant$25%) between two study groups or within person comparison before and after *H pylori* eradication ($1-\beta=0.8$, $\alpha=0.05$, two tailed significance).

Statistic analysis

Statistical analysis was carried out according to a pre-established analysis plan. Proportions were compared by χ^2 test with Fisher's exact test when appropriate. Regarding continuous outcomes, study groups were compared by the Mann-Whitney *U* test, while differences before and after *H pylori* eradication were assessed by Wilcoxon matched pairs signed rank test. Two sided significance tests were used throughout. The software used was Statistical Package for the Social Sciences 10.0.1 for Windows (release 1999, SPSS Inc., Chicago, IL). Confidence intervals were calculated with Confidence Interval Analysis software 2.0.0 (release 2000, T. Bryant, Univ. of Southampton).

RESULTS

Thirty-three patients with NUD and 17 asymptomatic volunteers were included in the study during two recruitment periods (January to March 1997 and March to April 1998). All participants were Caucasian. Twenty-three of the NUD patients (70%) had both a positive serum anti-*H pylori* IgG and biopsy urease test and were considered *H pylori*- positive. The remaining 10 NUD patients had both tests negative and were considered *H pylori*- negative. The baseline characteristics of the study groups are displayed in Table 1. The only significant difference found was a difference in age between control group and NUD group (P=0.02). Nevertheless multiple regression (ANOVA) revealed that age had no effect on any of the study outcomes. There was, therefore, no need for adjustment for age.

All study subjects underwent evaluation of gastric emptying. There was no significant difference in gastric emptying rate between *H pylori*-positive and *H pylori*-negative NUD patients as assessed by the primary study parameters C_{max}/BM and

AUC/BM (Table 2). NUD patients had significantly delayed gastric emptying compared with asymptomatic controls as assessed by C_{max} /BM and AUC/BM (Table 3). Gastric emptying lag phase and T_{max} did not differ significantly in any comparison (data not shown).

All 23 *H pylori*-positive NUD patients received eradication therapy. Of those, 18 completed the 10-d course and 4 wk later underwent repeat gastroscopy and biopsy urease test, eradication was confirmed in 14 patients (per protocol eradication rate 77.8%). Of the remaining five patients who received eradication therapy, 4 did not consent to repeat gastroscopy and 1 discontinued the course on the third day due to severe diarrhea (*C. difficile* toxin negative). No other side effects of the eradication regimen were reported on direct questioning.

All 14 NUD patients with confirmed *H pylori* eradication underwent repeat assessment of gastric emptying. No significant difference was found in the gastric emptying parameters C_{max} /BM and AUC/BM compared with the values prior to eradication (intra-individual comparisons) as shown in Table 4. Neither gastric emptying lag phase nor T_{max} differed significantly compared with the values prior to eradication (data not shown).

DISCUSSION

This study confirmed that gastric emptying is significantly delayed in patients with NUD compared to asymptomatic controls (Table 3). This has been well established for years[3, 11]. In fact, our results showed that the 95% confidence interval (CI) for the absolute difference between the medians of gastric emptying parameters, C_{max} /BW and AUC/BW, was compatible with a relative difference encompassing the predefined limit of clinical importance (*i.e.* 25%). Consequently, our results need to be interpreted as evidence of a statistically significant difference in gastric emptying rate between patients with NUD and asymptomatic controls, which however is unclear if it is clinically relevant. The above comparison was not the primary outcome of our; Nonethelss the fact that these results are in agreement with the current medical literature corroborates the methodological validity of our study and the credibility of the main outcomes.

The pathophysiology of delayed gastric emptying in patients with NUD, as well as its clinical implications, remains unknown. *H pylori* gastritis - which was also more prevalent in patients with NUD[3] - has been suggested as a causal factor for the gastric motility disorders found in these patients. There is no solid evidence supporting this hypothesis although there is some biological plausibility since a mucosal inflammatory reaction could affect the function of enteric nerves and smooth muscle[12].

In our attempt to investigate the potential role of *H pylori* in the above mentioned motility disorders, we found that the gastric emptying rate in patients with NUD did not differ significantly between *H pylori*-positive and *H pylori*-negative patients (Table 2). Furthermore, eradication of *H pylori* infection in patients with NUD did not induce any significant modification

Table 1 Baseline characteristics of patients with non-ulcer dyspepsia (NUD)

Charateristics	Controls (*n*=17)	All NUD pts (*n*=33)	Hp positive NUD pts (*n*=23)	Hp negative NUD pts (*n*=10)
Sex (Male:Female)	9:8	20:13	13:10	7:3
Age (yr) (mean±SD)	27.7±6.7	37.3±14.5	39.3±14.2	35.2±18.4
Body mass (kg) (mean±SD)	66.6±13.8	74.3±10.0	75.6±9.8	71.2±10.1
Hp(+) (%)	9 (52.9)	23 (69.7)	23 (100)	0 (0)
Smokers (%)	8 (47.1)	10 (30.3)	7 (30.4)	3 (30)

Table 2 Gastric emptying: *H pylori*-positive NUD patients *vs H pylori*-negative NUD patients

parameters (mean±SD, M)	*Hp* positiveNUD pts (*n*=23)	*Hp* negative NUD pts (*n*=10)	Mann-Whitney *U* test	95% CI for difference between medians (*Hp* pos. –*Hp* neg.)
Cmax/BM(mg/L·kg)	0.172±0.070 (0.153)	0.177±0.050 (0.176)	*P*=0.58	-0.050 to 0.037
AUC/BM(mg·min/L·kg)	18.43±6.93 (18.53)	18.38±5.94 (19.42)	*P*=0.91	-5.36 to 4.62

C_{max} /BM: maximum plasma paracetamol concentration divided by body mass; AUC/BW: area under the plasma paracetamol concentration-time curve divided by body mass. M: median.

Table 3 Gastric emptying: NUD patients *vs* asymptomatic controls

Parameters (mean±SD, M)	NUD pts (*n*=33)	Controls (*n*=17)	Mann-Whitney *U* test	95% CI for difference between medians (NUD pts–Controls)
Cmax/BM (mg/L·kg)	0.173±0.064 (0.163)	0.224±0.076 (0.221)	*P*=0.02	-0.012 to-0.095
AUC/BM (mg·min/L·kg)	18.42±6.56 (18.53)	24.34±8.06 (25.53)	*P*=0.01	-2.11 to-10.93

C_{max} /BM: maximum plasma paracetamol concentration divided by body mass; AUC/BM: area under the plasma paracetamol concentration – time curve divided by body mass. M: median.

Table 4 Gastric emptying: *H pylori*-positive NUD patients before and after eradication (intra-individual comparisons)

Parameters (mean±SD, M)	Initially *Hp* positive NUD pts (*n*=14)		Wilcoxon matched pairs test	95%CI for the median difference (after – before)
	Before eradication	After eradication		
Cmax/BM (mg/L·kg)	0.171±0.074 (0.167)	0.160±0.064 (0.146)	*P*=0.64	-0.047 to 0.278
AUC/BM (mg·min/L·kg)	17.41±5.25 (18.95)	18.02±7.25 (16.88)	*P*=0.93	-3.04 to 4.38

C_{max} /BM: maximum plasma paracetamol concentration divided by body mass. AUC/BM: area under the plasma paracetamol concentration–time curve divided by body mass. M: median.

of the gastric emptying rate (Table 4). However, for both comparisons, the 95% CI for the absolute difference between the medians of gastric emptying parameters was marginally compatible with the pre-defined level of a clinically important relative difference of 25%. This should be interpreted, therefore, as insufficient evidence to confirm or exclude a clinically important difference in gastric emptying rate between *H pylori*-positive and *H pylori*-negative patients with NUD. The same conclusion applies to the changes of gastric emptying rate following eradication of *H pylori* infection in patients with NUD.

Our results are in agreement with most previous publications, which did not detect any influence of *H pylori* status on gastric emptying rate in patients with NUD[13-23]. However, it is possible that some of these studies were not adequately powered to detect the targeted difference. Some investigators were able to demonstrate significant differences, but their conclusions differed. For example, Fock *et al*.[24] found that gastric emptying was slower in *H pylori*-positive NUD patients compared to *H pylori*-negative NUD patients, while Tucci *et al*.[25] found the opposite. No meta-analysis has yet addressed this issue.

Regarding the effect of the eradication of *H pylori* infection on gastric emptying rate in NUD patients, our results are in line with three other trials, which were unable to detect any changes in gastric emptying rate after a follow up period of one[26], six[27] and 12 mo[28]. Nonetheless, other investigators found that eradication of the infection significantly increased gastric emptying rate after a follow-up of 1 mo[29] or "normalised" previously abnormal (*i.e*. rapid or delayed) gastric emptying after a 2-mo follow up[30]. There was considerable methodological heterogeneity among these trials, which complicates any attempts to draw a conclusive answer.

Further larger trials would be helpful. These would be facilitated by using safe and non-invasive methods of gastric emptying assessment, such as the parecetamol absorption method, ultrasonography[31], or ^{13}C octanoic acid breath test. Utilization of urea breath testing for confirmation of *H pylori* eradication[32], which was not available to us at the time of the research, might improve the compliance of participants and could allow investigators to lengthen the post-eradication follow-up time without a significant dropout rate. Future studies should also explore whether specific *H pylori* characteristics, such as CagA phenotype[19], or differences in host response are implicated in the pathogenesis of gastric emptying disorders in patients with NUD.

In conclusion, gastric emptying is delayed in patients with NUD but is unrelated to *H pylori* status. Eradication of *H pylori* infection in *H pylori*-positive patients with NUD does not significantly alter the gastric emptying rate. Although our results are not definitive, they will contribute to a better understanding of the pathogenesis of NUD - especially when quantitatively synthesised with analogous data in future meta-analyses.

ACKNOWLEDGMENTS

The authors thank Professor Nikolaos Gotsis for his help in the design of the study, Professor Colin Howden for helpful discussions, Associate Professor Areti Hitoglou-Makedou for performing the *H pylori* serology and expert technical advice and Ms. Vasiliki Katsilaki for her excellent technical assistance.

REFERENCES

1 **Talley NJ**, Stanghellini V, Heading RC, Koch KL, Malagelada JR, Tytgat GNJ. Functional gastroduodenal disorders. *Gut* 1999; **45**(Suppl 2): 37-42
2 **Talley NJ**, Silverstein MD, Agreus L, Nyren O, Sonnenberg A, Holtmann G. AGA Technical Review: Evaluation of dyspepsia. *Gastroenterology* 1998; **114**: 582-595
3 **Jaakkimainen RL**, Boyle E, Tudiver F. Is *Helicobacter pylori* associated with non-ulcer dyspepsia and will eradication improve symptoms? A meta-analysis. *BMJ* 1999; **319**: 1040-1044
4 **Quartero AO,** de Wit NJ, Lodder AC, Numans ME, Smout AJ, Hoes AW. Disturbed solid-phase gastric emptying in functional dyspepsia: a meta-analysis. *Dig Dis Sci* 1998; **43**: 2028-2033
5 **Thompson WG**, Creed F, Drossman DA, Heaton KW, Mazzacca G. Functional bowel disease and functional abdominal pain. *Gastroenterol Int* 1992; **5**: 75-91
6 **Heading RC**, Nimmo J, Prescott LF, Tothill P. The dependence of paracetamol absorption on the rate of gastric emptying. *Br J Pharmacol* 1973; **47**: 415-421
7 **Clements JA**, Heading RC, Nimmo WS, Prescott LF. Kinetics of acetaminophen absorption and gastric emptying in man. *Clin Pharmacol Ther* 1978; **24**: 420-431
8 **Medhus AW**, Sandstad O, Bredesesn J, Husebye E. Delay of gastric emptying by duodenal intubation: sensitive measurement of gastric emptying by the paracetamol absorption test. *Aliment Pharmacol Ther* 1999; **13**: 609-620
9 **Medhus AW**, Lofthus CM, Bredesesn J, Husebye E. The validity of a novel paracetamol absorption test for gastric emptying. *Gastroenterology* 2000; **118**(Suppl 2): A142
10 **Altman D**. Practical statistics for medical research. London: *Chapman & Hall* 1991: 455-459
11 **Malagelada JR**. Functional dyspepsia. Insights on mechanisms and management strategies. *Gastroenterol Clin North Am* 1996; **25**: 103-112
12 **Olbe L**, Malfertheiner P. Gastric pathophysiology – emphasis on acid secretion and gastrointestinal motility. *Curr Opin Gastroenterol* 1996; **12**(Suppl 1): 16-20
13 **Caballero-Plasencia AM**, Muros-Navarro MC, Martin-Ruiz JL, Valenzuela-Barranco M, de los Reyes-Garcia MC, Casado-Caballero FJ, Rodriguez-Tellez M, Lopez-Manas JG. Dyspeptic symptoms and gastric emptying of solids in patients with functional dyspepsia. Role of *Helicobacter pylori* infection. *Scand J Gastroenterol* 1995; **30**: 745-751
14 **Chang CS**, Chen GH, Kao CH, Wang SJ, Peng SN, Huang CK. The effect of *H pylori* infection on gastric emptying of digestible and indigestible solids in patients with nonulcer dyspepsia. *Am J Gastroenterol* 1996; **91**: 474-479
15 **Perri F**, Clemente R, Festa V, Annese V, Quitadamo M, Rutgeerts P, Andriulli A. Patterns of symptoms in functional dyspepsia: role of *H pylori* infection and delayed gastric emptying. *Am J Gastroenterol* 1998; **93**: 2082-2088
16 **Wegener M**, Borsch G, Schaffstein J, Schulz-Flake C, Mai U, Leverkus F. Are dyspeptic symptoms in patients with *Campylobacter pylori*-associated type B gastritis linked to delayed gastric emptying? *Am J Gastroenterol* 1988; **83**: 737-740
17 **Dumitrascu DL**, Pascu O, Drãghini A, Andreica A, Nagy Z. *Helicobacter pylori* infection does not influence the gastric emptying of a semisolid meal. *Rom J Gastroenterol* 1996; **5**: 167-174
18 **Marzio L,** Falcucci M, Ciccaglione AF, Malatesta MG, Lapenna D, Ballone E, Antonelli C, Grossi L. Relationship between gastric and gallblader emptying and refilling in normal subjects and patients with *H pylori*-positive and -negative idiopathic dyspepsia and correlation with symptoms. *Dig Dis Sci* 1996; **41**: 26-31
19 **Parente F**, Imbesi V, Maconi G, Cucino C, Sangaletti O, Vago L, Bianchi Porro G. Influence of bacterial CagA status on gastritis, gastric function indices, and pattern of symptoms in *H pylori*-positive dyspeptic patients. *Am J Gastroenterol* 1998; **93**: 1073-1079
20 **Minocha A**, Mokshagundam S, Gallo SH, Rahal PS. Alterations in upper gastrointestinal motility in *Helicobacter pylori*-positive nonulcer dyspepsia. *Am J Gastroenterol* 1994; **89**: 1797-1800
21 **Koskenpato J**, Kairemo K, Korppi-Tommola T, Farkkila M. Role of gastric emptying in functional dyspepsia: a scintigraphic study of 94 subjects. *Dig Dis Sci* 1998; **43**: 1154-1158
22 **Rhee PI**, Kim YH, Son HJ, Kim JJ, Koh KC, Paik SW, Rhee JC, Choi KW. Lack of association of *Helicobacter pylori* infection with gastric hypersensitivity or delayed gastric emptying in functional dyspepsia. *Am J Gastroenterol* 1999; **94**: 3165-3169

23 **Scott AM**, Kellow JE, Shuter B, Cowan H, Corbett AM, Riley JW, Lunzer MR, Eckstein RP, Hoschl R, Lam SK, Jones MP. Intragastric distribution and gastric emptying of solids and liquids in functional dyspepsia. Lack of influence of symptom subgroups and *H pylori*-associated gastritis. *Dig Dis Sci* 1993; **38:** 2247-2254

24 **Fock KM**, Khoo TK, Chia KS, Sim CS. *Helicobacter pylori* infection and gastric emptying of indigestible solids in patients with dysmotility-like dyspepsia. *Scand J Gastroenterol* 1997; **32**: 676-680

25 **Tucci A,** Corinaldesi R, Stanghellini V, Tosetti C, Di Febo G, Paparo GF, Varoli O, Paganelli GM, Labate AM, Masci C, Zoccoli G, Monetti N, Barbara L. *Helicobacter pylori* infection and gastric function in patients with chronic idiopathic dyspepsia. *Gastroenterology* 1992; **103**: 768-774

26 **Goh KL**, Paramsothy M, Azian M, Parasakthi N, Peh SC, Bux S, Lo YL, Ong KK. Does *H pylori* infection affect gastric emptying in patients with functional dyspepsia? *J Gastroenterol Hepatol* 1997; **12**: 790-794

27 **Parente F**, Imbesi V, Maconi G, Cucino C, Manzionna G, Vago L, Bianchi Porro G. Effects of *Helicobacter pylori* eradication on gastric function indices in functional dyspepsia. *Scand J Gastroenterol* 1998; **33**: 461-467

28 **Koskenpato J**, Korppi-Tommola T, Kairemo K, Farkkila M. Long-term follow-up study of gastric emptying and *Helicobacter pylori* eradication among patients with functional dyspepsia. *Dig Dis Sci* 2000; **45**: 1763-1768

29 **Murakami K**, Fujioka T, Shiota K, Ito A, Fujiyama K, Kodama R, Kawasaki Y, Kubota T, Nasu M. Influence of *Helicobacter pylori* infection and the effects of its eradication on gastric emptying in non-ulcerative dyspepsia. *Eur J Gastroenterol Hepatol* 1995; **7**(Suppl 1): 93-97

30 **Miyaji H**, Azuma T, Ito S, Abe Y, Ono H, Suto H, Ito Y, Yamazaki Y, Kohli Y, Kuriyama M. The effect of *Helicobacter pylori* eradication therapy on gastric antral myoelectrical activity and gastric emptying in patients with non-ulcer dyspepsia. *Aliment Pharmacol Ther* 1999; **13**: 1473-1480

31 **Gilja OH**, Hausken T, Degaard S, Berstad A. Gastric emptying measured by ultrasonography. *World J Gastroenterol* 1999; **5**: 93-94

32 **Howden CW**, Hunt RH. Guidelines for the management of *Helicobacter pylori* infection. *Am J Gastroenterol* 1998; **93**: 2330-2338

Edited by Xu CT and Wang XL **Proofread by** Pan BR and Xu FM

PO Box 2345, Beijing 100023, China
Fax: +86-10-85381893
E-mail: wjg@wjgnet.com www.wjgnet.com

World J Gastroenterol 2004;10(12):1755-1758
World Journal of Gastroenterology
Copyright ©2004 by The WJG Press ISSN 1007-9327

Effects of lactose as an inducer on expression of *Helicobacter pylori* rUreB and rHpaA, and *Escherichia coli* rLTKA63 and rLTB

Jie Yan, Shou-Feng Zhao, Ya-Fei Mao, Yi-Hui Luo

Jie Yan, Shou-Feng Zhao, Ya-Fei Mao, Yi-Hui Luo, Department of Medical Microbiology and Parasitology, College of Medical Science, Zhejiang University, Hangzhou 310031, Zhejiang Province, China
Supported by the Excellent Young Teacher Fund of Ministry of Education of China and the General Science and Technology Research Plan of Zhejiang Province, No. 001110438
Correspondence to: Jie Yan, Department of Medical Microbiology and Parasitology, College of Medical Science, Zhejiang University, 353 Yan An Road, Hangzhou 310031, Zhejiang Province, China. yanchen@mail.hz.zj.cn
Telephone: +86-571-87217385 **Fax:** +86-571-87217044
Received: 2003-10-15 **Accepted:** 2003-12-16

Abstract

AIM: To demonstrate the effect of lactose as an inducer on expression of the recombinant proteins encoded by *Helicobacter pylori* ureB and hpaA, and *Escherichia coli* LTB and LTKA63 genes and to determine the optimal expression parameters.

METHODS: By using SDS-PAGE and BIO-RAD gel image analysis system, the outputs of the target recombinant proteins expressed by *pET32a-ureB-E.coliBL21, pET32a-hpaA-E.coliBL21, pET32a-LTKA63-E.coliBL21 and pET32a-LTB-E.coliBL21* were measured when using lactose as inducer at different dosages, original bacterial concentrations, various inducing temperatures and times. The results of the target protein expression induced by lactose were compared to those by isopropyl-β-D-thiogalactoside (IPTG). The proteins were expressed in *E.coli*.

RESULTS: Lactose showed higher efficiency of inducing the expression of rHpaA, rUreB, rLTB and rLTKA63 than IPTG. The expression outputs of the target recombinant proteins induced at 37 ℃ were remarkably higher than those at 28 ℃. Other optimal expression parameters for the original bacterial concentrations, dosages of lactose and inducing time were 0.8, 50 g/L and 4 h for rHpaA; 0.8, 100 g/L and 4 h for rLTKA63; 1.2, 100 g/L and 5 h for both rUreB and rLTB, respectively.

CONCLUSION: Lactose, a sugar with non-toxicity and low cost, is able to induce the recombinant genes to express the target proteins with higher efficiency than IPTG. The results in this study establish a beneficial foundation for industrial production of *H pylori* genetic engineering vaccine.

Yan J, Zhao SF, Mao YF, Luo YH. Effects of lactose as an inducer on expression of *Helicobacter pylori* rUreB and rHpaA, and *Escherichia coli* rLTKA63 and rLTB. *World J Gastroenterol* 2004; 10(12): 1755-1758
http://www.wjgnet.com/1007-9327/10/1755.asp

INTRODUCTION

In China, chronic gastritis and peptic ulcer are two most common gastric diseases[1], and gastric cancer is one of the malignant tumors with high mortalities and morbidities.

Helicobacter pylori (*H pylori*), a microaerophilic, spiral and Gram-negative bacterium, is recognized as a human-specific gastric pathogen that colonizes the stomachs of at least half of the world's populations. Most infected individuals are asymptomatic. However, in some subjects, *H pylori* infection causes acute, chronic gastritis and peptic ulceration[2-4], and acts as a high risk factor on development of gastric adenocarcinoma[5-10], and mucosa-associated lymphoid tissue (MALT) lymphoma[10-13].

It is generally considered inoculation of *H pylori* vaccine is a most efficient measure for prevention and control of *H pylori* infection[14]. However, high nutrition requirements, poor growth for a long time, easy contamination during the cultivation and difficulty of bacterial strain conservation make whole cell vaccine of *H pylori* impracticable. Genetic engineering vaccine seems to be a possible pathway for developing *H pylori* vaccine.

Isopropyl-β-D-thiogalactoside (IPTG), a highly stable and effective inducer on T7lac promoter for target recombinant protein expression, is widely used in laboratories. However, IPTG is a reagent with potential toxicity and high cost[15], which limited it as a practical inducer for industrial production of genetic engineering vaccines. It was reported that lactose, a common disaccharide, is also able to induce T7lac promoter after it is transformed into allolactose[16]. The low-cost and non-toxicity make lactose a practical potential for engineering products. In comparison with IPTG, the parameters of lactose inducing different recombinant protein expression vary greatly and its optimal working conditions are established usually by a large number of laboratory tests[17]. In our previous studies, urease subunit B (UreB) and *H pylori* adhesin (HpaA) were demonstrated as fine candidates in *H pylori* engineering vaccine[18,19]. For improving immunogenicity of the vaccine, heat-labile enterotoxin subunit A mutant at the 63rd position (LTKA63) and subunit B (LTB) of *Escherichia coli* were selected as adjuvants[20]. In this study, 4 constructed prokaryotic expression systems of ureB, hpaA, LTKA63 and LTB were used as the target genes to determine the inducing effects with different lactose dosages, temperatures and times, and original bacterial concentrations on expression of the recombinant proteins.

MATERIALS AND METHODS

Materials

Four prokaryotic expression systems of *pET32a-ureB-E.coliBL21, pET32a-hpaA-E.coli BL21, pET32a-LTKA63-E.coliBL21 and pET32a-LTB-E.coliBL21* were constructed and offered by our laboratory. Tryptone, yeast extract for LB medium were purchased from OXOID (Basingstoke, Hampshire, England). IPTG and lactose used for inducement, and SDS, glycine and DTT were offered by BBST (Shanghai, China). Acrylamide, N, N' -methylen-bis-acrylamid and TEMED were obtained from Serva (Heidelberg, Germany).

Methods

Determination of optimal inducing concentrations of lactose

and temperatures A colony of each the four engineering bacteria in LB agar plates was inoculated into 5 mL of LB liquid medium and then incubated on rotator with 200 r/min at 37 ℃ for 12 h. The values at A_{600} measured by spectrophotometry were used to indicate the bacterial concentrations. Lactose at the final concentrations of 5, 10, 50 and 100 g/L were added into the cultures of the 4 strains with the A_{600} values of 1.2, respectively, and then incubated on 200 r/min shaking at 28 ℃ or 37 ℃ for 4 h. The bacteria in the medium were collected by centrifugation. By using SDS-PAGE, the expression and outputs of the target recombinant proteins (rUreB, rHpaA, rLTKA63 and rLTB) were examined and estimated, respectively. BIO-RAD gel image analysis system was applied to measure the outputs of target protein fragments by their area percentages in the total bacterial proteins. 0.5 mmol/L IPTG was simultaneously used as an inducer control, which inducing effects for the four recombinant proteins had been confirmed in our previous studies[18-20].

Determination of optimal original bacterium concerntrations for inducement Four engineering bacterial strains were inoculated with proportion of 1:100 (V/V) into LB liquid medium and then incubated on 200 r/min shaking at 37 ℃. According to the results obtained above, lactose at the final concentrations of 100, 50, 100 and 100 g/L for inducement of rUreB, rHpaA, rLTKA63 and rLTB expression was added into the cultures with the A_{600} values of 0.2, 0.4, 0.8, 1.2, 1.6, 2.0 and 2.4, respectively. The lactose added cultures were continuously incubated on 200 r/min shaking at 37 ℃ for 4 h. The outputs of rUreB, rHpaA, rLTKA63 and rLTB were examined by SDS-PAGE and BIO-RAD gel image analysis system.

Effects of the target protein expression by using different inducing time According to the results obtained above, the optimal original bacterial concerntration for inducement was 1.2 (A_{600}). The four different bacterial cultures (A_{600}=1.2), which expressing rUreB, rHpaA, rLTKA63 or rLTB, were added with lactose at the final concentrations of 100, 50, 100, 100 g/L, respectively. The cultures were continuously incubated on 200 r/min shaker at 37 ℃ for 1, 2, 3, 4, 5, 6 and 7 h, respectively. The outputs of rUreB, rHpaA, rLTKA63 and rLTB were examined by SDS-PAGE and BIO-RAD gel image analysis system.

SDS-PAGE A vertical discontinious plate polyacrylamide gel eletrophoresis was applied[21]. The isolation gels with 8%, 10%, 12% and 15% concentrations (W/V) were used to detect the expressed rUreB, rLTKA63, rHpaA and rLTB, respectively, based on their different molecular weights. The start voltage was 8 V/cm and then changed to 15 V/cm while the samples went into isolation gels. The gels after electrophoresis were stained by Coomassie brilliant blue and then decolorized with methanol-acetic acid solution.

RESULTS

Optimal inducing concentrations and temperatures of lactose

Lactose with multiple appropriate concentrations could effectively induce expression of 4 target recombinant proteins (Figure 1). Beginning with the original bacterial concentrations of 1.2 A_{600} values, the outputs of rUreB, rHpaA, rLTKA63 and rLTB at the inducing temperature of 37 ℃ were 27.3-53.9%, 7.4-30.9%, 0.8-79.8% and 12.7-119.1% increased as compared with those of 28 ℃, respectively (Table 1). When the concentrations of lactose were 100, 50, 100 and 100 g/L inducing at 37 ℃ for 4 h, outputs of the 4 recombinant proteins reached the highest (Table 1). In comparison with the inducing expression effects of 0.5 mmol/L IPTG, the highest outputs of rUreB, rHpaA, rLTKA63 and rLTB induced by lactose were 203.2%, 98.4%, 114.0% and 245.1% increased, respectively (Table 1).

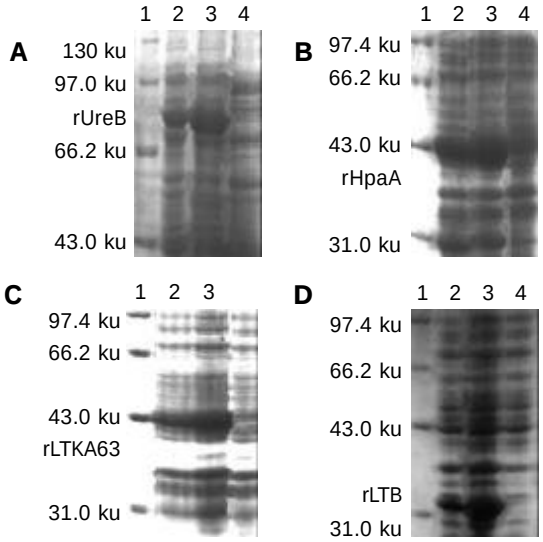

Figure 1 Effects of lactose on inducing expression of target recombinant proteins compared to IPTG. A: rUreB; Lane 1: Marker; Lane 2: Induced with 0.5 mmol/L IPTG; Lane 3: Induced with 100 g/L lactose; Lane 4: Non-induced. B: rHpaA; Lane 1: Marker; Lane 2: Induced with 0.5 mmol/L IPTG; Lane 3: Induced with 50 g/L lactose; Lane 4: Non-induced. C: rLTKA63 expression; Lane 1: Marker; Lane 2: Induced with 0.5 mmol/L IPTG; Lane 3: Induced with 100 g/L lactose. Lane 4: Non-induced; D: rLTB; Lane 1: Marker; Lane 2: Induced with 0.5 mmol/L IPTG; Lane 3: Induced with 100 g/L lactose; Lane 4: Non-induced.

Effects of the target protein expression of original bacteria with different A_{600} values under inducement by lactose

By using the inducing concentrations of lactose with 100, 50, 100 and 100 g/L inducing at 37 ℃ for 4 h, the expression outputs of the 4 recombinant proteins with the different original bacterial concentrations (0.2-2.4 A_{600} values) are showed in Figure 2. The results indicated that a better expression effect for any of the 4 recombinant proteins was present when the original bacterial concentration used was higher (A_{600}=0.8-1.2).

Table 1 Expression outputs of rUreB, rHpaA, rLTKA63 and rLTB proteins induced by different concentrations of lactose and temperatures

Concentrations of lactose(g/L) and IPTG(mmol/L)	Expression outputs (% of total bacterial proteins)							
	rUreB		rHpaA		rLTKA63		rLTB	
	(37 ℃)	(28 ℃)	(37 ℃)	(28 ℃)	(37 ℃)	(28 ℃)	(37 ℃)	(28 ℃)
Lactose (50)	40.59	26.38	50.35	44.72	23.36	22.41	39.55	21.91
(10)	50.52	39.70	57.61	44.86	35.84	27.09	42.66	26.17
(5)	30.51	22.17	60.80	46.42	35.64	22.09	26.99	23.94
(1)	27.33	18.92	54.00	50.29	21.91	21.73	23.33	10.65
(0.5)	20.78	13.63	42.29	36.05	22.01	12.24	14.72	10.31
IPTG (0.5)	16.66	14.72	30.65	22.61	16.75	14.48	12.36	10.06

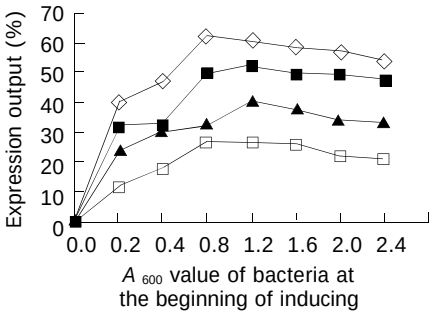

Figure 2 Expression of target recombinant proteins of original bacteria with different A_{600} values under inducement by lactose. ◇: rHpaA; ■: rUreB; ▲: rLTB; □: rLTKA63.

Effects of the target protein expression using different inducing time

When the original bacterial concentrations as A_{600} values of 1.2 and the lactose concentrations of 100, 50, 100 and 100 g/L, the outputs of rUreB, rHpaA, rLTKA63 and rLTB were shown in Figure 3. The results indicated that a higher output for any of the 4 recombinant proteins was present when the inducing time was 4-5 h.

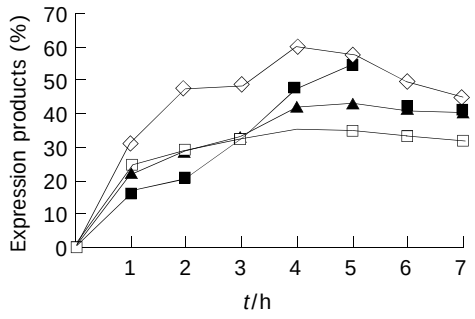

Figure 3 Expression outputs of the target proteins by using different inducing time. ◇: rHpaA; ■: rUreB; ▲: rLTB; □: rLTKA63.

DISCUSSION

H pylori causes a local superficial infection in human stomach and duodenum[22]. So orally inoculating of *H pylori* vaccine has a good protective effect[23]. So far, no commercial *H pylori* engineering vaccine has been available. An engineering vaccine has many advantages but its immunoprotective effect is usually poor because of the unitarity for antigen components. Using adjuvant is an efficient measure to improve immune effect of engineering vaccines[24]. UreB and HpaA were demonstrated to be excellent antigen candidates as their stable and high expression, strong antigenicity, universal distribution in different *H pylori* isolates and exposure on the surface of the bacterium[25,26]. *E. coli* LTKA63 and LTB were recently found and were generally considered as the most efficient adjuvants for mucosal immunization so far[27,28]. So we planed to use the rUreB and rHpaA as antigens and LTB or LTKA63 as adjuvants to develop an oral-taken double-valence genetic engineering vaccine of *H pylori*.

Almost of all the recombinant proteins show a very low expression or non-expression without inducement. IPTG is a routinely laboratory used inducer with high efficiency on recombinant protein expression in *E. coli* but it must be removed by complicated methods from the induced products because of its toxicity. When at the efficient inducing dosages, the cost of IPTG is approximate hundredfold of lactose. Therefore, lactose as an inducer has industrially remarkable advantages. Lactose, differs from IPTG, is unable to enter the bacterial body. It must be helped by a special enzyme called as primase to be transported into host bacterium. The lactose in bacterial cell must be transferred into allolactose by β- galactosidase and the latter is able to start T7 Lac promotor. In the process inducing expression of recombinant protein, lactose is much more complex than IPTG. So lactose, if used it as an efficient inducer, must be clarified its inducing parameters such as dosage, temperature, time and original bacterial concentration.

It was proved by our study that lactose at the multiple tested concentrations could efficiently induce the expression of rUreB, rHpaA, rLTKA63 and rLTB. The effects of lactose on inducing expression of the 4 recombinant proteins were much stronger than that by IPTG, which demonstrated by 98.4-245.1% increased outputs (Table 1). Furthermore, it was reported that lactose is a carbon source for bacteria to promote growth and increase number of bacteria in culture, which results in the increase of output of the target recombinant protein.

The results of this study indicated that at 37 ℃ for 4 h inducement the lactose concentration to obtain the highest expression outputs of rUreB, rHpaA, rLTKA63 and rLTB were 100, 50, 100 and 100 g/L, respectively. It was found in the study that inducing temperatures can obviously affect the expression of the recombinant proteins. For example, with the original bacterial concentration of 1.2 A_{600} value for 4 h inducement, using 37 ℃ as the inducing temperature could increase the expression outputs of rUreB, rHpaA, rLTKA63 and rLTB with 27.3-53.9%, 7.4-30.9%, 0.8-79.8% and 12.7-119.1% of those induced by 28 ℃. The original bacterial concentrations when lactose addition was found to affect the outputs of the recombinant proteins. There were preferable expression effects of the recombinant proteins to add lactose when the original bacterial concentrations with the A_{600} values of 0.8-1.2. With the original bacterial concentration of 1.2 A_{600} values and at temperature 37 ℃, the outputs of the recombinant proteins for 4-5 h inducement by the optimal concentrations of lactose were relatively higher.

Summarily, using lactose as an inducer on the expression of *pET32a-ureB-E.coliBL21, pET32a-hpaA-E.coli BL21, pET32a-LTKA63-E.coliBL21 and pET32a-LTB-E.coliBL21*, the optimal temperature was 37 ℃. The rest optimal parameters for the original bacterial concentrations, dosages of lactose and inducing time were 0.8, 50 g/L and 4 h for rHpaA; 0.8, 100 g/L and 4 h for rLTKA63; 1.2, 100 g/L and 5 h for both rUreB and rLTB, respectively. The results from this study established a beneficial foundation for industrial production of *H pylori* genetic engineering vaccines.

REFERENCES

1 **Niu WX**, Qin XY, Liu H, Wang CP. Clinicopathological analysis of patients with gastric. *World J Gastroenterol* 2001; **7**: 281-284
2 **Peng ZS**, Liang ZC, Liu MC, Ouyang NT. Studies on gastric epithelial cell proliferation and apoptosis in *Hp* associated gastric ulcer. *Shijie Huaren Xiaohua Zazhi* 1999; **7**: 218-219
3 **Kate V**, Ananthakrishnan N, Badrinath S. Effect of *Helicobacter pylori* eradication on the ulcer recurrence rate after simple closure of perforated duodenal ulcer: retrospective and prospective randomized controlled studies. *Br J Surg* 2001; **88**: 1054-1058
4 **Yao YL**, Zhang WD. Relation between *Helicobacter pylori* and gastric cancer. *Shijie Huaren Xiaohua Zazhi* 2001; **9**: 1045-1049
5 **Lu SY**, Pan XZ, Peng XW, Shi ZL. Effect of *Hp* infection on gastric epithelial cell kinetics in stomach diseases. *Shijie Huaren Xiaohua Zazhi* 1999; **7**: 760-762
6 **Liu HF**, Liu WW, Fang DC. Study of the relationship between apoptosis and proliferation in gastric carcinoma and its precancerous lesion. *Shijie Huaren Xiaohua Zazhi* 1999; **7**: 649-651
7 **Zhu ZH**, Xia ZS, He SG. The effects of ATRA and 5-Fu on telomerase activity and cell growth of gastric cancer cells *in vitro*. *Shijie Huaren Xiaohua Zazhi* 2000; **8**: 669-673
8 **Cai L**, Yu SZ. A molecular epidemiologic study on gastric

cancer in Changle, Fujian Province. *Shijie Huaren Xiaohua Zazhi* 1999; **7**: 652-655

9 **Suganuma M**, Kurusu M, Okabe S, Sueoka N, Yoshida M, Wakatsuki Y, Fujiki H. *Helicobacter pylori* membrane protein 1: a new carcinogenic factor of *Helicobacter pylori*. *Cancer Res* 2001; **61**: 6356-6359

10 **Uemura N**, Okamoto S, Yamamoto S, Matsumura N, Yamaguchi S, Yamakido M, Taniyama K, Sasaki N, Schlemper RJ. *Helicobacter pylori* infection and the development of gastric cancer. *N Engl J Med* 2001; **345**: 8298-8332

11 **Hiyama T**, Haruma K, Kitadai Y, Miyamoto M, Tanaka S, Yoshihara M, Sumii K, Shimamoto F, Kajiyama G. B-cell monoclonality in *Helicobacter pylori*-associated chronic atrophic gastritis. *Virchows Arch* 2001; **483**: 232-237

12 **Nakamura S**, Matsumoto T, Suekane H, Takeshita M, Hizawa K, Kawasaki M, Yao T, Tsuneyoshi M, Iida M, Fujishima M. Predictive value of endoscopic ultrasonography for regression of gastric low grade and high grade MALT lymphomas after eradication of *Helicobacter pylori*. *Gut* 2001; **48**: 454-460

13 **Morgner A**, Miehlke S, Fischbach W, Schmitt W, Muller-Hermelink H, Greiner A, Thiede C, Schetelig J, Neubauer A, Stolte M, Ehninger G, Bayerdorffer E. Complete remission of primary high-grade B-cell gastric lymphoma after cure of *Helicobacter pylori* infection. *J Clin Oncol* 2001; **19**: 2041-2048

14 **Houben MH,** van de Beek D, Hensen EF, Craen AJ, Rauws EA, Tytgat GN. A systematic review of *Helicobacter pylori* eradication therapy- the impact of antimicrobial resistance on eradication rates. *Aliment Pharmacol Ther* 1999; **13**: 1047-1055

15 **Donovan RS**, Robinson CW, Glick BR. Review: optimizing inducer and culture conditions for expression of foreign proteins under the control of the lac promoter. *J Ind Microbiol* 1996; **16**: 145-154

16 **Yildirim N,** Mackey MC. Feedback regulation in the lactose operon: a mathematical modeling study and comparison with experimental data. *Biophys J* 2003; **84**: 2841-2851

17 **Menzella HG**, Ceccarelli EA, Gramajo HC. Novel *Escherichia coli* strain allows efficient recombinant protein production using lactose as inducer. *Biotechnol Bioeng* 2003; **82**: 809-817

18 **Mao YF,** Yan J, LI LW. Cloning, expression and identification of hpaA gene from a clinical isolate of *Helicobacter pylori*. *Zhejiang Daxue Xuebao* 2003; **32**: 9-12

19 **Chen Z**, Yan J, Mao YF. Construction of prokaryotic expression system of ureB gene from a clinical isolate of *Helicobacter pylori* and identification of immunogenicity of the fusion protein. *Zhejiang Daxue Xuebao* 2003; **32**: 4-8

20 **Xia XP**, Yan J, Zhao SF. Cloning, expression and identification of *Escherichia coli* LTB gene and *Vibrio cholerae* CTB gene. *Zhejiang Daxue Xuebao* 2003; **32**: 17-20

21 **Sambrook J,** Fritsch EF, Maniatis T**.** Molecular Cloning. *Cold Spring Harbor Laboratory Press* 1989: pp 18.47-18.61

22 **Recavarren Ascencios R**, Recavarren Arce S. Chronic atrophic gastritis: pathogenic mechanisms due to cellular hypersensitivity. *Rev Gastroenterol Peru* 2002; **22**: 199-205

23 **Crabtree JE**. Eradication of chronic *Helicobacter pylori* infaction by therapeutic vaccination. *Gut* 1998; **43**: 7-8

24 **Yuki Y**, Kiyono H. New generation of mucosal adjuvants for the induction of protective immunity. *Rev Med Virol* 2003; **13**: 293-310

25 **Corthesy-Theulaz I**, Porta N, Glauser M, Saraga E, Vaney AC, Haas R, Kraehenbuhl JP, Blum AL, Michetti P. Oral immunization with *Helicobacter pylori* urease B subunit as a treatment against *Helicobactor pylori* infection in mice. *Gastroenterology* 1995; **109**: 115-121

26 **Opazo P,** Muller I, Rollan A, Valenzuela P, Yudelevich A, Garcia-de la Guarda R, Urra S, Venegas A. Serological response to *Helicobacter pylori* recombiant antigens in Chilean infected patients with duodenal ulcer, non-ulcer dyspepsia and gastric cancer. *Apmis* 1999; **107**: 1069-1078

27 **Verweij WR,** de Haan L, Holtrop M, Agsteribbe E, Brands R, van Scharrenburg GJ, Wilschut J. Mucosal immunoadjuvant activity of recombinant *Escherichia coli* heat-labile enterotoxin and its B subunit: induction of systemic IgG and secretory IgA responses in mice by intranasal immunization with influenza virus surface antigen. *Vaccine* 1998; **16**: 2069-2076

28 **Baudner BC,** Giuliani MM, Verhoef JC, Rappuoli R, Junginger HE, Giudice GD. The concomitant use of the LTK63 mucosal adjuvant and of chitosan-based delivery system enhances the immunogenicity and efficacy of intranasally administered vaccines. *Vaccine* 2003; **21**: 3837-3844

Edited by Zhang JZ **Proofread by** Chen WW and Xu FM

PO Box 2345, Beijing 100023, China
Fax: +86-10-85381893
E-mail: wjg@wjgnet.com www.wjgnet.com

World J Gastroenterol 2004;10(12):1759-1762
World Journal of Gastroenterology
Copyright ©2004 by The WJG Press ISSN 1007-9327

Coordinate increase of telomerase activity and c-Myc expression in *Helicobacter pylori*-associated gastric diseases

Guo-Xin Zhang, Yan-Hong Gu, Zhi-Quan Zhao, Shun-Fu Xu, Hong-Ji Zhang, Hong-Di Wang, Bo Hao

Guo-Xin Zhang, Yan-Hong Gu, Zhi-Quan Zhao, Shun-Fu Xu, Hong-Ji Zhang, Hong-Di Wang, Bo Hao, Department of Gastroenterology, the First Affiliated Hospital of Nanjing Medical University, Nanjing 210029, Jiangsu Province, China
Supported by the Ministry of Health of China, No. 8-1-323
Correspondence to: Dr. Guo-Xin Zhang, Department of Gastroenterology, the First Affiliated Hospital of Nanjing Medical University, 300 Guangzhou Road, Nanjing 210029, Jiangsu Province, China. guoxinz2002@yahoo.com
Telephone: +86-25-3718836-6973 **Fax:** +86-25-3724440
Received: 2003-08-06 **Accepted:** 2003-10-07

Abstract

AIM: To detect the telomerase activity and c-Myc expression in gastric diseases and to examine the relation between these values and *Helicobacter pylori* (*H pylori*) as a risk factor for gastric cancer.

METHODS: One hundred and seventy-one gastric samples were studied to detect telomerase activity using a telomerase polymerase chain reaction enzyme linked immunosorbent assay (PCR-ELISA), and c-Myc expression using immunohistochemistry.

RESULTS: The telomerase activity and c-Myc expression were higher in cancers (87.69% and 61.54%) than in noncancerous tissues. They were higher in chronic atrophic gastritis with severe intestinal metaplasia (52.38% and 47.62%) than in chronic atrophic gastritis with mild intestinal metaplasia (13.33% and 16.67%). In chronic atrophic gastritis with severe intestinal metaplasia, the telomerase activity and c-Myc expression were higher in cases with *H pylori* infection (67.86% and 67.86%) than in those without infection (21.43% and 7.14%). c-Myc expression was higher in gastric cancer with *H pylori* infection (77.27%) than in that without infection (28.57%). The telomerase activity and c-Myc expression were coordinately up-regulated in *H pylori* infected gastric cancer and chronic atrophic gastritis with severe intestinal metaplasia.

CONCLUSION: *H pylori* infection may influence both telomerase activity and c-Myc expression in gastric diseases, especially in chronic atrophic gastritis.

Zhang GX, Gu YH, Zhao ZQ, Xu SF, Zhang HJ, Wang HD, Hao B. Coordinate increase of telomerase activity and c-Myc expression in *Helicobacter pylori*-associated gastric diseases. *World J Gastroenterol* 2004; 10(12): 1759-1762
http://www.wjgnet.com/1007-9327/10/1759.asp

INTRODUCTION

Gastric cancer is one of the most common malignant tumors in the world. Gastric carcinogenesis is a multi-step process progressing from chronic gastritis to glandular atrophy, metaplasia, and dysplasia[1-3]. Genetic analyses of gastric cancers suggest alterations are involved in the structures and functions of several oncogenes and tumor suppressor genes as well as genetic instability[3,4]. However, in addition to these genetic changes, cell immortality is important for the sustained growth properties of gastric cancer cells[4,5]. The ribonucleoprotein enzyme telomerase that synthesizes the G-rich strand of telomeric DNA in germline tissues and in immortal tumor cells plays a critical role in the maintenance of telomeres[6]. By using a highly sensitive PCR-based TRAP assay, telomerase activity has been observed in a wide range of human cancers, including cancers of breast, bladder, stomach, colon, prostate, and liver, so telomerase may be regarded as a molecular marker for cancer diagnosis and therapeutic strategies[7-13]. Telomerase activity is also positive in gastric preneoplastic lesions[14]. Therefore it is thought that reactivation of telomerase may occur at an early stage of carcinogenesis[14].

Myc network proteins are known to be oncoproteins, which are involved in the control of cell porliferation, differentiation and apoptosis[15,16]. The c-Myc oncogene is implicated in the transformation and progression of mutated cells[17-19]. Deregulation of Myc genes is usually caused by chromosomal translocation involving the c-myc gene as well as by gene amplification. Overexpression of Myc is frequently observed in a wide variety of tumor types, and affects both the development and progression of hyperproliferations[20,21].

It is well known that *Helicobacter pylori* (*H pylori*), the main cause of chronic gastritis, is a class I gastric carcinogen[22]. It contributes to the induction of chronic gastritis to cancer through precursor lesions, such as atrophy, metaplasia and dysplasia[23]. Precancerous phenotypic expression is generally associated with acquired genomic instability and activation of telomerase activity[24]. *H pylori* inoculation into Mongolian gerbils has been reported to induce chronic gastritis and intestinal metaplasia. Chronic infection with *H pylori* induces activations of telomerase in gastric mucosa exhibiting intestinal metaplasia[25]. In patients with intestinal-type gastric cancer, telomerase activity was higher in intestinal metaplasia with *H pylori* infection than in that without infection[25,26]. These data indicate that *H pylori* infection may contribute to the precancerous stage through induction of telomerase activity, and that telomerase activation in intestinal metaplasia with *H pylori* infection may be correlated with oncogenesis, though the mechanism remains to be defined. To our knowledge, little is known about whether *H pylori* infection induces both genetic alterations and cell immortality in gastric mucosa. Recent evidence suggested that Myc protein was implicated in the regulation of hTERT[27-29]. Therefore we measured telomerase activity and c-Myc expression in *H pylori* infected gastric cancer, chronic atrophic gastritis and chronic superficial gastritis. The results indicate that *H pylori* infection may induce telomerase activity and c-Myc protein expression in the process of carcinogenesis.

MATERIALS AND METHODS

Tissue samples

Samples were obtained from upper gastrointestinal endoscopy or surgical operation during the period of September 2000 to May 2001. It included 20 of chronic superficial gastritis(CSG),

30 of chronic atrophic gastritis(CAG) with mild intestinal metaplasia(IM), 42 of chronic atrophic gastritis with severe intestinal metaplasia, 14 of dysplasia(Dys) and 65 of gastric cancer(GC). Haematoxylin and eosin stains were used for the histopathological diagnosis. Degree of inflammatory reaction and glandular atrophy, intestinal metaplasia, and cellular dysplasia were evaluated according to the criteria of the updated Sydney system. The diagnosis of each sample was based on agreement between two pathologists.

H pylori infection

H pylori infection was detected by rapid urease test and bacteria culture. Infection was defined as positive when *H pylori* was detected and/or urease test was positive.

Immunohistochemistry

For each case, 4-μm thick serial sections were cut from paraffin wax blocks, mounted on acid-cleaned glass slides, and heated at 55 ℃ for 60 min. Slides were dewaxed and rehydrated, then endogenous peroxidase activity was inhibited by incubation with 30 mL/L H_2O_2 in methanol for 20 min at room temperature. To reduce non-specific background staining, slides were incubated with 50 mL/L goat serum for 15 min at room temperature. To enhance immunostaining, sections were treated with an antigen retrieval solution (10 mmol/L citric acid monohydrate, pH 6.0, adjusted with 2 mol/L NaOH) and heated three times in a microwave oven at high power for five min. Finally, slides were incubated with appropriate primary antiserum in a moist chamber overnight at 4 ℃. The monoclonal primary antibody, anti-c-Myc, was purchased from Maxim Biotech, Inc. (USA). S-P kit was purchased from Fujian Maixin Ltd (China). Samples were detected according to manufacturer's instructions. The degree of immunopositivity was evaluated semi-quantitatively. A total of 300 cells were counted in random fields from representative areas of the lesions, and the immunoreactive cells were roughly assessed and expressed as percentages. The scoring system for the antibody tested was: 0-5%(negative), 5-25%(low positivity), 25-50%(moderate positivity), >50%(high positivity).

Telomerase assay

Telomerase activity was measured by a modified version of the standard TRAP method, using PCR-ELISA detection kit (Roche Molecular Biochemicals), according to its manufacturer's instructions. Five 10-μm thick cryostat sections of were transferred into a sterile reaction tube containing 200 μL ice-cold lysis reagent. The lysates were homogenized and incubated on ice for 30 min. After centrifuged at 16 000 *g* for twenty minutes at 4 ℃, 175 μL of the supernatant was collected and transferred to a fresh tube. Three micro-litter of tissue extract was incubated with 25 μL of reaction mixture including a biotin labeled P1-TS primer and P2 primer, telomerase substrate, and Taq polymerase for 20 min at 25 ℃. After further incubation at 94 ℃ for 5 min for telomerase inactivation, the resulting mixture was subjected to PCR for 30 cycles at 94 ℃ for 30 s, at 50 ℃ for 30 s, and at 72 ℃ for 90 s, the reaction was held at 72 ℃ for 10 min.

PCR products were denatured and hybridized with a digoxigenin labeled, telomeric repeat specific detection probe. The resulting product was immobilized through the biotin labeled TS primer to a streptavidin coated microtitre plate and detected with antidigoxigenin antibody conjugated with peroxidase. Absorbance values were measured using a microtitre (ELISA) reader at 450 nm with a reference wavelength of approximately 690 nm within 30 min after addition of the stop reagent. Heat-treatment of the cell extract for 10 min at 65 ℃ prior to the TRAP reaction was used to inactivate telomerase protein for producing negative controls. Positive controls were the 293 cells that expressed the telomerase activity. Samples were regarded as telomerase-positive if the difference in absorbance (△A) was higher than 0.2 (A 450 nm–A 690 nm units).

Statistical analyses

The correlations between qualitative data were studied with the χ^2 and Fisher tests. A probability P value <0.05 was considered statistically significant.

RESULTS

H pylori infection

One hundred and twelve of 171 cases were *H pylori* positive. The *H pylori* infection rate was 65%(13/20) in CSG, 63.89%(46/72) in CAG, 64.29%(9/14) in Dys, and 67.69%(44/65) in GC. It had no significant difference among these groups.

Telomerase activity

Telomerase activity was measured by a telomerase polymerase chain reaction (PCR) enzyme linked immunosorbent assay, which does not require radioactive PCR amplification and yields a semiquantitative measurement. Telomerase activity was detected in 57(87.69%) of 65 gastric carcinomas examined, 46(63.89%) of 72 CAG and 9(64.29%)of 14 Dys. No telomerase activity was detected in all the 20 CSG. The mean telomerase activity was higher in gastric cancer than in CAG, CSG and Dys (P<0.01 or P<0.05). Based on intestinal metaplasia, CAG was classified into two groups, severe IM and mild IM. The telomerase activity was higher in CAG with severe IM than that in mild IM (P<0.01).

Twenty-nine gastric cancers with complete clinical data were classified by histologic parameters such as gender, tumor location, tumor size and microscopic morphology. The telomerase activity among these groups had no significant difference (data not shown).

H pylori infection and telomerase activity in patients with gastric cancer and CAG are shown in Table 1. The mean telomerase activity was higher in CAG with severe intestinal metaplasia and *H pylori* infection than in that without infection (P<0.05), but there was no significant difference between those with and without *H pylori* infection in gastric cancer and CAG with mild intestinal metaplasia.

Table 1 Telomerase activity and c-Myc expression in *H pylori* infected gastric diseases

Diagnosis	Samples number	*H pylori* infection	Telomerase activity + (%)	*P*	c-Myc expression + (%)	*P*
GC	65	+(44)	38 (86.36)	>0.05	34 (77.27)	<0.05[a]
		-(21)	19 (90.48)		6 (28.57)	
CAG with MM	30	+(18)	3 (16.67)	>0.05	4 (22.22)	>0.05
		-(12)	1 (8.33)		1 (8.33)	
CAG with SM	42	+(28)	19 (67.86)	<0.01[b]	19 (67.86)	<0.01[d]
		-(14)	3 (21.43)		1 (7.14)	

χ^2 test and Fisher's exact test. [a]P<0.05 *vs* c-Myc expression from samples without *H pylori* infection. [b]P<0.01 *vs* telomerase activity from samples without *H pylori* infection. [d]P<0.01 *vs* c-Myc expression from samples without *H pylori* infection. MM, mild intestinal metaplasia SM, severe intestinal metaplasia.

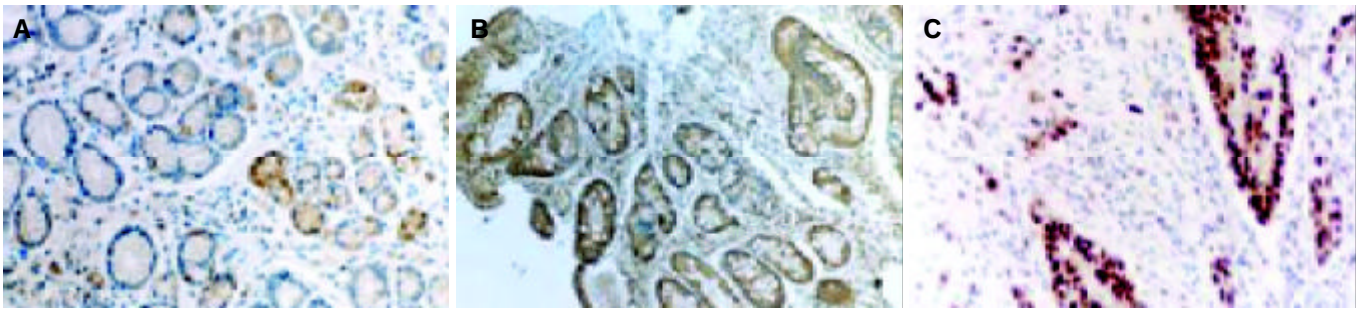

Figure 1 c-Myc protein expression in chronic superficial gastritis, chronic atrophic gastritis and gastric adenocarcinoma. A: c-Myc protein expression in chronic superficial gastritis. B: c-Myc protein expression in chronic atrophic gastritis. C: c-Myc protein expression in gastric adenocarcinoma.

c-Myc expression

c-Myc was expressed in 40 of 65(61.5%) gastric cancers, 20 of 42(47.62%) CAG with severe IM, 5 of 30(16.67%) CAG with mild IM, 8 of 14(57.14%) Dys and 1 of 20(5%) CSG. The expression of c-Myc was highest in gastric cancer, and c-Myc expression in CAG with severe IM was significantly higher than that in CAG with mild IM. The c-Myc immunoreactivity was localized in both cytoplasm and nucleus (Figure 1).

H pylori infection and c-Myc expression in patients with gastric cancer and CAG are shown in Table 1. The expression of c-Myc was higher in *H pylori* infected gastric cancer and CAG with severe IM than in those without infection ($P<0.01$), but there was no significant difference between those with and without *H pylori* infection in CAG with mild IM.

Coordinate up-regulation of telomerase activity and c-Myc expression in H pylori infected gastric cancer and CAG with severe intestinal metaplasia

The telomerase activity and c-Myc expression were coordinately increased in *H pylori* infected gastric cancer and CAG with severe IM (Figure 2). The rate of co-expression was 89.47%(34/38) and 100%(19/19), respectively.

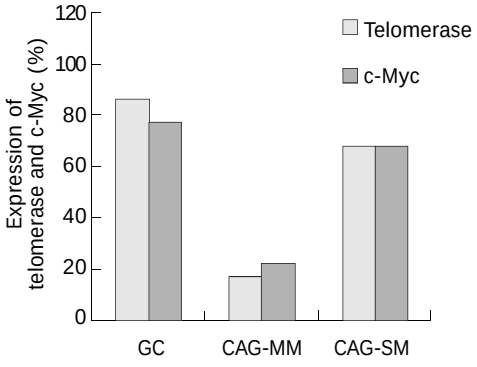

Figure 2 Coordinate increase of telomerase activity and c-Myc expression in *H pylori* infected gastric cancer and CAG with severe intestinal metaplasia. The rate of co-expression was 89.47%(34/38) and 100%(19/19), respectively. (CAG-MM: chronic atrophic gastritis with mild metaplasia; CAG-SM: chronic atrophic gastritis with severe metaplasia.).

DISCUSSION

In the present study, we demonstrated that most gastric tumors displayed telomerase activity, regardless of histological types. Telomerase activity was highest in cancer tissue, followed by chronic atrophic gastritis with complete intestinal metaplasia, dysplasia, chronic atrophic gastritis with mild intestinal metaplasia and chronic superficial gastritis. Telomerase activity was higher in CAG with severe metaplasia and *H pylori* infection than in that without *H pylori* infection ($P<0.01$). Our results indicate that telomerase activity is one of the most common and fundamental events of gastric cancers. What is more important is that telomerase was activated in precursor lesions, such as chronic atrophic gastritis with intestinal metaplasia and dysplasia. It suggested that there were a certain number of immortal cells existing in these lesions. In addition, *H pylori* infection might induce telomerase activity in chronic atrophic gastritis with intestinal metaplasia.

Recently, it was reported that *H pylori* infection played a role in activation of telomerase. Chronic infection with *H pylori* induced the activation of telomerase in gastric mucosa exhibiting intestinal metaplasia[25]. In patients with intestinal-type gastric cancer, telomerase activity was higher in intestinal metaplasia with *H pylori* infection than in that without infection[26]. We found that telomerase was activated in *H pylori* infected precursor lesions, such as chronic atrophic gastritis and dysplasia, and telomerase activity rose higher during the progression of the lesions. These data indicate that *H pylori* infection may contribute to gastric tumorigenesis through induction of telomerase activity, and that telomerase activation in *H pylori* infected chronic atrophic gastritis with intestinal metaplasia and dysplasia may be correlated with oncogenesis. It remains to be defined how *H pylori* infection activates telomerase. *H pylori* infection might influence the negative regulator of telomerase activity during early stages of stomach carcinogenesis[26]. In addition, inflammatory gastric mucosa caused by *H pylori* infection could produce free radicals and cytokines that may induce telomerase activity[30].

Frequent genetic alterations, such as c-myc proto-oncogene have been found in gastric pre-malignant lesions[31,32]. Amplified c-Myc, which controls cell growth and cellular differentiation[33,34], has been reported in small percent of gastric carcinomas[35,36]. Expression of c-Myc was proved to be more frequent in poorly differentiated gastric cancer cells, and more frequent in gastric adenocarcinoma than in adenoma and has also been proposed as an aid to differentiate between the two conditions[37,38]. In the present study, c-Myc was expressed in 61.54%(40/65) of gastric cancers, 47.62%(20/42) of chronic atrophic gastritis with severe IM, 16.67%(5/30) of CAG with mild IM, and 5%(1/20) of chronic superficial gastritis patients. The expression of c-Myc was highest in gastric cancers, and c-Myc expression in CAG with severe intestinal metaplasia was significantly higher than that in CAG with mild intestinal metaplasia. The expression of c-Myc was higher in *H pylori* infected gastric cancer and CAG with severe intestinal metaplasia than in that without infection ($P<0.01$). We found that c-Myc expression in both gastric cancer and chronic atrophic gastritis with severe intestinal metaplasia is correlated with *H pylori* status. Previously, a study by Nardone *et al* showed that *H pylori* infection affected the expression of c-Myc in chronic gastritis, but the positive rate was very low (15%). The expression of c-Myc was very high in *H pylori* infected CAG in our study because we classified chronic gastritis as CSG

and CAG, the latter was further classified as CAG with mild intestinal metaplasia and with severe intestinal metaplasia.

Recent evidence suggested that the Myc protein could bind to the promotor of human telomerase reverse transcriptase (hTERT), the catalytic subunit of telomerase[27-29] . It has been shown that hTERT is the determinant of telomerase activity control. A study by Hiyama *et al*. demonstrated a close association between a high level of telomerase activity and amplification of the myc locus in neuroblastomas. Thus, up-regulation of Myc due to gene alterations leading to subsequent activation of hTERT expression, may be one cause for telomerase activation in tumors. Interestingly, we found that telomerase activity and c-Myc were co-expressed in *H pylori* infected chronic atrophic gastritis. The correlation was not significant in patients without *H pylori* infection or in patients with *H pylori* infection but without gastric atrophy. Therefore, it is suggested that the presence of both gastric atrophy and chronic *H pylori* infection is essential for cell immortality and genomic instability.

REFERENCES

1 **Correa P**. *Helicobacter pylori* and gastric carcinogenesis. *Am J Surg Pathol* 1995; **19**(Suppl 1): S37-43
2 **Correa P,** Chen VW. Gastric cancer. *Cancer Surv* 1994; **19-20**: 55-76
3 **Rugge M**, Cassaro M, Leandro G, Baffa R, Avellini C, Bufo P, Stracca V, Battaglia G, Fabiano A, Guerini A, Di Mario F. *Helicobacter pylori* in promotion of gastric carcinogenesis. *Dig Dis Dci* 1996; **41**: 950-955
4 **Wright PA**, Williams GT. Molecular biology and gastric carcinoma. *Gut* 1993; **34**: 145-147
5 **Harley CB**, Kim NW, Prowse KR, Weinrech SL, Hirsch KS, West MD, Bacchetti S, Hirte HW, Counter CM, Greider CW, Wright WE, Shay JW. Telomerase, cell immortality, and cancer. *Cold Spring Harb Symp Quant Biol* 1994; **59**: 307-315
6 **Avilion AA**, Piatyszek MA, Gupta J, Shay JW, Bacchetti S, Greider CW. Human telomerase RNA and telomerase activity in immortal cell lines and tumor tissues. *Cancer Res* 1996; **56**: 645-650
7 **Kim NW**, Piatszek MA, Prowse KR, Harley CB, West MD, Ho PL, Coviello GM, Wright WE, Weinrich SL, Shay JW. Specific association of human telomerase activity with immortal cells and cancer. *Science* 1994; **226**: 2011-2015
8 **Hiyama E**, Gollahon L, Kataoka T, Kuroi K, Yokohama T, Gazdar AF, Hiyama K, Piatyszek MA, Shay JW. Telomerase activity in human breast tumors. *J Natl Cancer Inst* 1996; **88**: 116-122
9 **Hiyama E**, Yokoyama T, Tatsumoto N, Hiyama K, Jmamura Y, Murakami Y, Kodama T, Piatyszek MA, Shay JW, Matsuura Y. Telomerase activity in gastric cancer. *Cancer Res* 1995; **55**: 3258-3262
10 **Shay JW**, Bacchetti S. A survey of telomerase activity in human cancer. *Eur J Cancer* 1997; **33**: 787-791
11 **Lin Y**, Miyamoto H, Fujinami K, Uemura H, Hosaka M, Iwasaki Y, Kubota Y. Telomerase activity in human bladder cancer. *Clin Cancer Res* 1996; **2**: 929-932
12 **Sommerfeld HJ**, Meeker AK, Piatyszek MA, Bova GS, Shay JW, Coffey DS. Telomerase activity: a prevalent marker of malignant human prostate tissue. *Cancer Res* 1996; **56**: 218-222
13 **Kojima H**, Yokosuka O, Imazeki F, Saisho H, Omata M. Telomerase activity and telomere length in hepatocellular carcinoma and chronic liver disease. *Gastroenterology* 1997; **112**: 493-500
14 **Tahara H**, Kuniyasu H, Yokozaki H, Yasui W, Shay JW, Ide T, Tahara E. Telomerase activity in preneoplastic and neoplastic gastric and colorectal lesions. *Clin Cancer Res* 1995; **1**: 1245-1251
15 **Henriksson M,** Lüscher B. Proteins of the Myc network: essential regulators of cell growth and differentiation. *Adv Cancer Res* 1996; **68**: 109-182
16 **Hurlin PJ**, Foley KP, Ayer DE, Eisenman RN, Hanahan D, Arbeit JM. Regulation of c-Myc and Mad during epidermal differentiation and HPV-associated tumorigenesis. *Oncogene* 1995; **11**: 2487-2501
17 **Xu D**, Popov N, Hou M, Wang Q, Bjorkholm M, Gruber A, Menkel AR, Henriksson M. Switch from Myc/Max to Mad1/Max binding and decrease in histone acetylation at the telomerase reverse transcriptase promoter during differentiation of HL60 cells. *Proc Natl Acad Sci U S A* 2001; **98**: 3826-3831
18 **Kuschak TI**, Taylor C, McMillan Ward E, Israels S, Henderson DW, Mushinski JF, Wright JA, Mai S. The ribonucleotide reductase R2 gene is a non-transcribed target of c-Myc-induced genomic instability. *Gene* 1999; **238**: 351-365
19 **Vaux DL**, Cory S, Adamas JM. Bcl-2 gene promotes haemopoietic cell survival and cooperates with c-Myc to immortalize pre-B cells. *Nature* 1988; **335**: 440-442
20 **Bissonnette RP**, Echeverri F, Mahboubi A, Green DR. Apoptotic cell death induced by c-Myc is inhibited by bcl-2. *Nature* 1992; **359**: 552-554
21 **Fanidi A**, Harrington EA, Evan GI. Cooperative interaction between c-Myc and bcl-2 proto-oncogenes. *Nature 1*992; **359**: 554-556
22 **Correa P**, Miller MJ. *Helicobacter pylori* and gastric atrophy-cancer paradoxes. *J Natl Cancer Inst* 1995; **87**: 1731-1732
23 **Kuipers EJ**, Uyterlinde AM, Pena AS, Roosendaal R, Pals G, Nelis GF, Festen HP, Meuwissen SG. Long-term sequelae of *Helicobacter pylori* gastritis. *Lancet* 1995; **345**: 1525-1528
24 **Craanen ME**, Dekker W, Blok P, Ferwerda J, Tytgat GN. Intestinal metaplasia and *Helicobacter pylori*: an endoscopic bioptic study of the gastric antrum. *Gut* 1992; **33**: 16-20
25 **Kameshima H**, Yagihashi A, Yajima T, Watanabe N, Ikeda Y. *Helicobacter pylori* infection induces telomerase activity in premalignant lesions. *Am J Gastroenterol* 1999; **94**: 547-548
26 **Kameshima H**, Yagihashi A, Yajima T, Kobayashi D, Denno R, Hirata K, Watanabe N. *Helicobacter pylori* infection: augmentation of telomerase activity in cancer and noncancerous tissues. *World J Surg* 2000; **24**: 1243-1249
27 **Horikawa I**, Cable PL, Mazur SJ, Appella E, Afshari CA, Barrett JC. Downstream E-box-mediated regulation of the human telomerase reverse transcriptase (hTERT) gene transcription: evidence for an endogenous mechanism of transcriptional repression. *Mol Biol Cell* 2002; **13**: 2585-2597
28 **Cong YS**, Wen J, Bacchetti S. The human telomerase catalytic subunit hTERT: organization of the gene and characterization of the promoter. *Hum Mol Genet* 1999; **8**: 137-142
29 **Gunes** C, Lichtsteiner S, Vasserot AP, Englert C. Expression of the hTERT gene is regulated at the level of transcriptional initiation and repressed by Mad1. *Cancer Res* 2000; **60**: 2116-2121
30 **Tahara E**. Molecular mechanism of human stomach carcinogenesis implicated in *Helicobacter pylori* infection. *Exp Toxicol Pathol* 1998; **50**: 375-378
31 **Fest T**, Mougey V, Dalstein V, Hagerty M, Milette D, Silva S, Mai S. C-Myc overexpression in Ba/F3 cells simultaneously elicits genomic instability and apoptosis. *Oncogene* 2002; **21**: 2981-2990
32 **Wang J**, Chi D, Kalin G, Sosinski C, Miller LE, Burja I, Thomas E. *Helicobacter pylori* infection and oncogene rxpressions in hastric varcinoma and its precursor lesions. *Dig Dis Sci* 2002; **47**: 107-113
33 **Peng H**, Diss T, Isaacson PG, Pan L. C-myc gene abnormalities in mucosa-associated lymphoid tissue (MALT) lymphomas. *J Pathol* 1997; **181**: 381-386
34 **O'Leary JJ**, Landers RJ, Crowley M, Healy I, Kealy WF, Hogan J, Doyle CT. Alterations in exon 1 of c-myc and expression of p62 c-myc in cervical squamous cell carcinoma. *J Clin Pathol* 1997; **50**: 896-903
35 **Hajdu J**, Kozma L, Kiss I, Szentkereszty Z, Szakall S, Ember I. Is the presence of distant metastasis associated with c-myc amplification in gastric cancer? *Acta Chir Hung* 1997; **36**: 119-121
36 **Amadori D**, Maltoni M, Volpi A, Nanni O, Scarpi E, Renault B, Pellgata NS, Gaudio M, Magni E, Ranzani GN. Gene amplification and proliferative kinetics in relation to prognosis of patients with gastric carcinoma. *Cancer* 1997; **79**: 226-232
37 **Han S**, Kim HY, Park K, Cho HJ, Lee MS, Kim HJ, Kim YD. c-myc expression is related with cell proliferation and associated with poor clinical outcome in human gastric cancer. *J Korean Med Sci* 1999; **14**: 526-530
38 **Lee LA**, Dolde C, Barrett J, Wu CS, Dang CV. A link between c-Myc-mediated transcriptional repression and neoplastic transformation. *J Clin Invest* 1996; **97**: 1687-1695

Edited by Zhu LH and Wang XL **Proofread by** Xu FM

PO Box 2345, Beijing 100023, China
Fax: +86-10-85381893
E-mail: wjg@wjgnet.com www.wjgnet.com

World J Gastroenterol 2004;10(12):1763-1768
World Journal of Gastroenterology
Copyright ©2004 by The WJG Press ISSN 1007-9327

• BASIC RESEARCH •

Differential Cl^- and HCO_3^- mediated anion secretion by different colonic cell types in response to tetromethylpyrazine

Jin-Xia Zhu, Ning Yang, Qiong He, Lai-Ling Tsang, Wen-Chao Zhao, Yiu-Wa Chung, Hsiao-Chang Chan

Jin-Xia Zhu, Lai-Ling Tsang, Yiu-Wa Chung, Hsiao-Chang Chan, Epithelial Cell Biology Research Center, Department of Physiology, Faculty of Medicine, The Chinese University of Hong Kong, Shatin, Hong Kong
Jin-Xia Zhu, Ning Yang, Qiong He, Wen-Chao Zhao, Department of Physiology, Medical School, Zhengzhou University, Zhengzhou, 450052, Henan Province, China
Supported by the Innovation and Technology Commission of Hong Kong SAR, and Strategic program of The Chinese University of Hong Kong
Correspondence to: Professor Hsiao-Chang Chan, Epithelial Cell Biology Research Center, Department of Physiology, Faculty of Medicine, The Chinese University of Hong Kong, Shatin, NT, Hong Kong, China. hsiaocchan@cuhk.edu.hk
Telephone: +852-26096839 **Fax:** +852-26035022
Received: 2003-10-20 **Accepted:** 2004-01-31

Abstract

AIM: Colonic epithelium is known to secrete both Cl^- and HCO_3^-, but the secretory mechanisms of different colonic cell types are not fully understood. The present study aimed to investigate the differential activation of Cl^- and HCO_3^- secretion by tetramethylpyrazine (TMP) in human crypt-like cell line, T84, and villus-like cell line, Caco-2, in comparison to the TMP-induced secretory response in freshly isolated rat colonic mucosa.

METHODS: Colonic epithelial anion secretion was studied by using the short circuit current (I_{SC}) technique. RT-PCR was used to examine the expression of Na^+-HCO_3^--cotranspoter in different epithelial cell types.

RESULTS: TMP produced a concentration-dependent I_{SC} which was increase in both T84 and Caco-2 cells. When extracellular Cl^- was removed, TMP-induced I_{SC} was abolished by 76.6% in T84 cells, but not in Caco-2 cells. However, after both Cl^- and HCO_3^- were removed, TMP-induced I_{SC} in Caco-2 cells was reduced to 10%. Bumetanide, an inhibitor of Na^+-K^+-Cl^--cotranspoter, inhibited the TMP-induced I_{SC} by 96.7% in T84 cells, but only 47.9% in Caco-2 cells. In the presence of bumetanide and 4, 4'-diisothiocyanostilbene-2, 2'-disulfonic acid, an inhibitor of Na^+-HCO_3^- cotransporter, inhibited the TMP-induced current in Caco-2 cells by 93.3%. In freshly isolated rat colonic mucosa, TMP stimulated distinct I_{SC} responses similar to that observed in T84 and Caco-2 cells depending on the concentration used. RT-PCR revealed that the expression of Na^+-HCO_3^- cotransporter in Caco-2 cells was 4-fold more greater than that in T84 cells.

CONCLUSION: TMP exerts concentration-dependent differential effects on different colonic cell types with stimulation of predominant Cl^- secretion by crypt cells at a lower concentration, but predominant HCO_3^- secretion by villus cells at a higher concentration, suggesting different roles of these cells in colonic Cl^- and HCO_3^- secretion.

Zhu JX, Yang N, He Q, Tsang LL, Zhao WC, Chung YW, Chan HC. Differential Cl^- and HCO_3^- mediated anion secretion by different colonic cell types in response to tetromethylpyrazine. *World J Gastroenterol* 2004; 10(12): 1763-1768
http://www.wjgnet.com/1007-9327/10/1763.asp

INTRODUCTION

Colonic epithelium, which lines the surface of both crypts and villi, plays an important role in the maintenance of water and electrolyte balance. While it is well established that colonic fluid secretion is driven by electrogenic colonic Cl^- secretion[1], HCO_3^- secretion has also been shown to be important in the human colon. In many diarrhea disorders, a high concentration of HCO_3^- was frequently found in stool water and patients with severe diarrhea often suffered from metabolic acidosis due to sustained HCO_3^- losses in the stool[2]. However, the contribution of crypts and villus epithelia to colonic Cl^- and HCO_3^- secretion is not known. Although it has been generally believed that colonic villus (or surface) epithelium is mainly involved in NaCl and water absorption while crypt epithelium is involved in secretion[1,3]. There is now clear evidence that electrolyte secretion is located in both[1,4]. The cystic fibrosis transmembrane conductance regulator (CFTR), a cAMP-dependent Cl^- channel known to mediate both Cl^-[5] and HCO_3^- secretion[6,7], has been shown to be present in both crypt and villus epithelial cells although higher expression level of CFTR was found in crypts than in villi[8,9]. Human colonic cell lines have been derived to provide useful models in studying electrolyte transport properties of colonic crypts and villus epithelial cells. T84 cell line is a well-characterized colonic epithelial model that maintains a secretory phenotype similar to crypt base cells, and has been widely used to examine the regulation of intestinal Cl^- secretion since CFTR and Na^+-K^+-Cl^- cotransporter (NKCC) are highly expressed in this cell line[1,10,11]. The properties of human colonic Caco-2 cells are mostly close to those of mature absorptive villus/surface cells but they possess a certain CFTR characteristic of secretory cells[1,12,13]. However, few studies have been conducted to compare the secretory properties of these cell lines.

Tetramethylpyrazine (TMP, also named ligustrazine), a compound purified from *Ligustium Wollichii Francha*, is a widely used active ingredient in Chinese herbal medicine for the treatment of cardiovascular diseases due to its vasodilatory actions and antiplatelet activity[14-16]. TMP has been proposed to act as an inhibitor of phosphodiesterase (PDE) and thereby it increases intracellular cAMP[15]. We have recently demonstrated a stimulatory effect of a TMP-containing herbal formula on the anion secretion in human colonic[17] and pancreatic duct cell lines[18], indicating the involvement of cAMP and activation of CFTR. The present study aimed to compare the stimulatory effects of TMP on colonic anion secretion in different colonic cell types, T84 and Caco-2, as well as freshly isolated rat colonic mucosa, in an attempt to assess the different contribution of these two cell types to colonic anion secretion.

MATERIALS AND METHODS

Chemicals and solutions

Tetramethylpyrazine was purchased from Beijing Fourth

Pharmacy (Beijing, China). Diphenylamine-2, 2' -dicarboxylic acid (DPC) was obtained from Riedel-de Haen Chemicals (Hannover, Germany). Amilorode hydrochloride was obtained from Sigma Chemical Company (St. Louis, MO). Calbiochem (San Diego, CA) was the source for 4, 4' -diisothiocyanostilbene-2, 2' -disulfonic acid (DIDS), bumetanide, tetrodotoxin (TTX), indomethacin and glybenclamide. Dulbecco' s modified Eagle' s medium (DMEM)/F12, Hanks' balanced salt solution (HBSS) and fetal bovine serum were from Gibco Laboratory (New York, NY). Krebs-Henseleit solution (K-HS) had the following compositions (mmol/L): NaCl, 117; KCl, 4.5; $CaCl_2$, 2.5; $MgCl_2$, 1.2; $NaHCO_3$, 24.8; KH_2PO_4, 1.2; glucose, 11.1. The solution was gassed with 950 mL/L O_2 and 50 mL/L CO_2, and kept the pH at 7.4. In some experiments gluconate was used to replace anions Cl^- or Cl^-/HCO_3^- for making a Cl^- free or Cl^-/HCO_3^- free K-HS. For Cl^-/HCO_3^--free K-HS, HEPES and Tris were used and the solution was gassed with absolute O_2.

Cell culture

Human colonic T84 and Caco-2 cells were purchased from American Type Culture Collection (Rockville, MD). The cells were routinely maintained in DMEM/F12 for T84 or in DMEM for Caco-2 with 100 mL/L fetal bovine serum, 100 kU/L penicillin and 100 mg/L streptomycin. The cells were fed 3 times a week, and (2-3)×10^5 cells were plated on to the floating permeable support, which was made of a Millipore filter with a silicone rubber ring attached on top of it for confining the cells (0.45 cm^2). Cultures were incubated at 37 ℃ in 950 mL/L O_2 - 50 mL/L CO_2 for 4-5 d before experiments.

Colonic mucosa preparation

Adult male Sprague-Dawley rats (Laboratory Animal Services Center, the Chinese University of Hong Kong) ranging in age from 8 to 12 wk had free access to standard rodent laboratory food and water until the day of the experiments. The animals were killed by exposure to absolute CO_2. Segments of distal colon about 8 cm proximal to the anus were quickly removed, cut along the mesenteric border into flat sheets and flushed with ice-cold K-HS bubbled with 950 mL/L O_2-50 mL/L CO_2. The tissues were pinned flat with the mucosal side down in a Sylgard-lined petri dish containing ice-cold oxygenated solution. The serosa, submucosa, and muscular layer were stripped away with fine forceps to obtain a mucosa preparation which was pretreated with indomethacin (10 μmol/L), a synthesis inhibitor of prostaglandins (PG), and 1 μmol/L of tetrodotoxin (TTX), a blocker of neuron sodium channel, 30 min before treatment with TMP. Three or four of these stripped mucosal preparations were obtained from each animal.

Short-circuit current measurements

The measurement of I_{SC} was described previously[19]. Between the two halves of the Ussing chamber, in which the total cross-sectional area was 0.45 cm^2, monolayers of cell lines grown on permeable supports were clamped and flat sheets of rat stripped colonic mucosa were mounted, which were bathed in both sides with K-HS and maintained at 37 ℃ by a water jacket enclosing the reservoir. K-HS was bubbled with 950 mL/L O_2 -50 mL/L CO_2 to maintain the pH of the solution at 7.4. Drugs could be added directly to apical or basolateral side of the epithelium. Transepithelial potential difference for every monolayer or colonic mucosa was measured by the Ag/AgCl reference electrodes (World Precision Instrument, USA) connected to a preamplifier that was in turn connected to a voltage-clamp amplifier DVC-1000 (World Precision Instrument, USA). In most of the experiments, the change in I_{SC} was defined as the maximal rise in I_{SC} following agonist stimulation and it was normalized to current change per unit area of the epithelial monolayer (μA/cm^2). The total charge transported for 15 min (the area under the curve of the agonist-induced I_{SC} response) was also used to describe the agonist-induced response (μC/cm^2). Experiments were normally repeated in different batches of culture to ensure that the data were reproducible.

Reverse transcription PCR (RT-PCR) analysis

Total RNA (15 μg) was extracted from T84, Caco-2 cells and rat colonic mucosa. Human pancreatic duct epithelial cells, CAPAN-1, were used as a positive control. Expression of NBC was analyzed by competitive RT-PCR. The specific oligo nucleotide primers for NBC were CCT CAG CTC TTC ACG GAA CT for sense and AGC ATG ACA GCC TGC TGT AG for antisense corresponding to nucleotides 333-949 with expected cDNA of 616 bp[20]. Internal marker, GAPDH was used for semi-quantitative analysis of NBC expression in Caco-2 and T84 cells. The specific oligo nucleotide primers for GAPDH were TCC CAT CAC CAT CTT CCA G for sense and TCC ACC ACT GAC ACG TTG for antisense corresponding to nucleotides 249-764 bp with expected cDNA of 515 bp[20].

Statitical analysis

Results were expressed as mean±SE. The number of experiments represented independent measurements on separate monolayers. Comparisons between groups of data were made by either the Student' s *t*-test (2-group comparison) or one-way ANOVA with Newman-Keuls *post-hoc* test (3-group comparison). A P value less than 0.05 was considered statistically significant. EC_{50} values were determined by nonlinear regression using GraphPad Prism software.

RESULTS

TMP- induced I_{SC} responses in T84 and Caco-2 cells

TMP stimulation increased I_{SC} in both T_{84} and Caco-2 cells when the drug was added to either the apical or basolateral membrane. However, greater responses were achieved when TMP was added to apical membrane of T84 and basolateral membrane of Caco-2. The TMP-induced responses were concentration-dependent with an apparent EC_{50} at 0.5 and 5.1 mmol/L for T84 and Caco-2 cells respectively (Figure 1A). The TMP-induced changes in I_{SC} were calculated as the total charge transported for 15 min (the area under the curve of the TMP-induced I_{SC} response for the given time period) since the current kinetics was different in the two cell types. TMP produced a fast and sustained increase of I_{SC} in T84 cells with averaged total charge of 6100±451 μC/cm^2 (n=8, Figure 1B) transported over 15 min in response to TMP at a concentration close to corresponding EC_{50} (1 mmol/L). However, TMP produced a I_{SC} response in Caco-2 cells with a fast transient peak followed by a lower but sustained plateau with averaged total charge of 2 293±214.7 μC/cm^2 (n=7) in response to TMP at corresponding EC_{50} (5 mmol/L, Figure 1C). Similar TMP-induced I_{SC} characteristics were observed in the same cell type at all concentrations of TMP used.

Involvement of Cl^- and HCO_3^- in TMP-induced I_{SC} responses in colonic cell lines

Removal of Cl^- from the bathing solution inhibited TMP-induced I_{SC} increase by 76%, from 6 100±451 μC/cm^2 to 1 375±103 μC/cm^2 in T84 cells (n=7, P<0.001, Figure 2). In Caco-2 cells the TMP-induced current in Cl^--free solution was not reduced, but rather increased to 3 700±388 μC/cm^2 (n=6, P<0.001, Figure 3). However, the TMP-induced I_{SC} in Caco-2 was reduced by 90%, to 228.9±27.6 μC/cm^2 (n=6, P<0.001) when both extracellular Cl^- and HCO_3^- were removed (Figure 3). Apical addition of Cl^- channel blockers, DPC (2 mmol/L) or

glibenclamide (1 mmol/L), could completely abolish the TMP-induced response in T84 (Figure 2A,B) and Caco-2 cells (Figure 3A,B). Basolateral addition of Na^+-K^+-$2Cl^-$ cotransporter (NKCC) inhibitor, bumetanide (100 μmol/L), inhibited TMP-induced I_{SC} in T84 cells by 96.7%, from 6 100±451 μC/cm^2 (n=8) to 200±71 μC/cm^2 (n=5, P<0.001, Figure 4A), but only 47.9% in Caco-2 cells, from 2 720±144 μC/cm^2 (n=6) to 1 304±200 μC/cm^2 (n=5, P<0.001, Figure 4B). However, when an inhibitor of NBC, DIDS (200 μmol/L), was combined with bumetanide, it reduced TMP-induced current in Caco-2 cells to 181±41 μC/cm^2 by 93.3% (n=5, P<0.001, Figure 4B). Pretreatment with epithelial Na^+ channel (ENaC) blocker, amiloride (10 μmol/L) (n=5, P>0.05) or removal of Na^+ from apical solution (n=4, P>0.05) did not significantly affect the TMP-induced I_{SC} (data not shown), indicating that TMP-produced responses were mediated by Cl^-/HCO_3^- secretion, but not Na^+ absorption.

TMP-induced I_{SC} response in colonic mucosa

In freshly isolated rat colonic mucosa, TMP induced different I_{SC} responses depending on the concentration used. One mmol/L of TMP evoked a sustained I_{SC} increase (Figure 5A) similar to that observed in T84 cells, with averaged total charge of 5 133±465 μC/cm^2 (Figure 5C, n=11). However, at the concentration greater than 5 mmol/L, TMP induced a I_{SC} response similar to that observed in Caco-2 cells, a transient peak followed by a more sustained phase (Figure 5B), with averaged total charge of 18 945±2 023 μC/cm^2 (Figure 5C, n=11). Removal of extracellular Cl^- inhibited 65.5% of the I_{SC} induced by 1 mmol/L TMP (Figure 5C, n=10, P<0.001). However, the I_{SC} induced by 5 mmol/L of TMP was not significantly reduced by Cl^- removal (n=6, P>0.05) but was reduced by 71.6% in Cl^- and HCO_3^- -free solution (Figure 5, n=5), indicating a greater extent of the involvement of HCO_3^- in the response to 5 mmol/L TMP as compared to the response

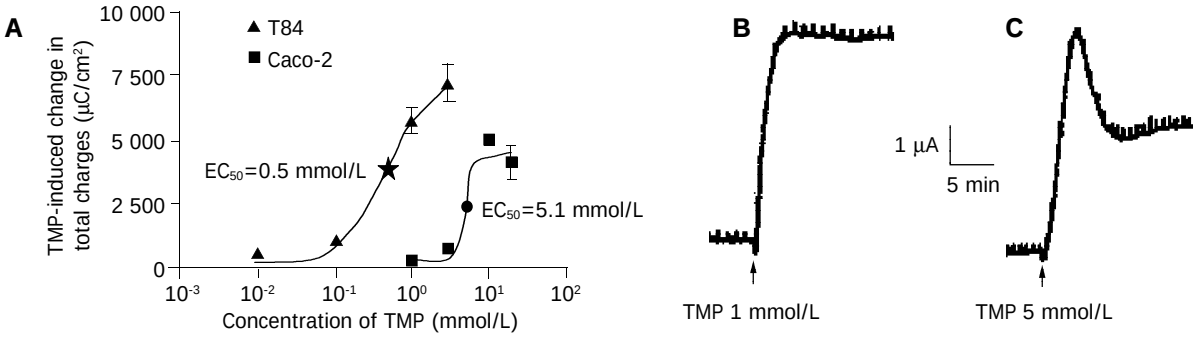

Figure 1 TMP-induced I_{SC} response in T84 and Caco-2 cell lines. The concentration-response curve for TMP-induced response in T84 and Caco-2 cells, and each datum was obtained from at least 4 individual experiments. A: Values are mean±SE of maximal I_{SC} increase; B: Representative I_{SC} recordings in response to apical addition of TMP (1 mmol/L) in T84 cells; C: Basolateral application of TMP (5 mmol/L) in Caco-2 cells.

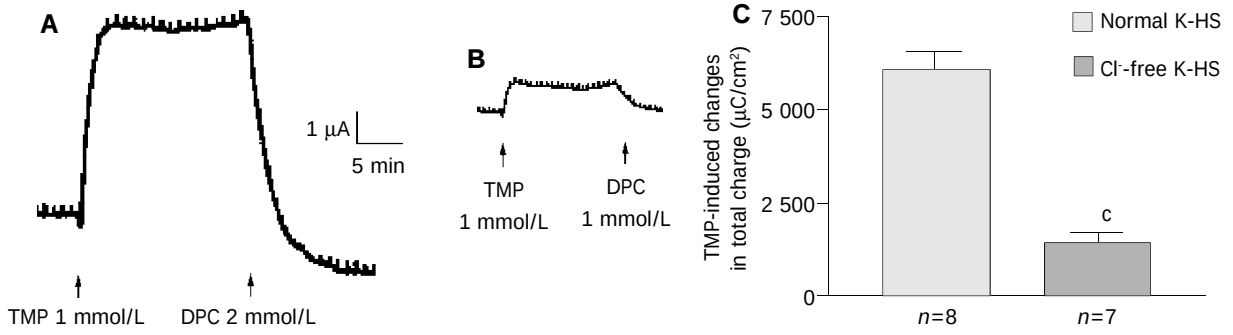

Figure 2 Cl^- dependence of TMP-induced I_{SC} increase in T84 cells. Representative I_{SC} recording with arrows indicating TMP (1mmol/L) added apically, which was blocked by apical adding DPC. Values are mean±SE; ^cP<0.001. A: Normal; B: Cl^-free; C: K-HS, comparison of TMP-induced total charge transferred in normal and Cl^--free K-HS.

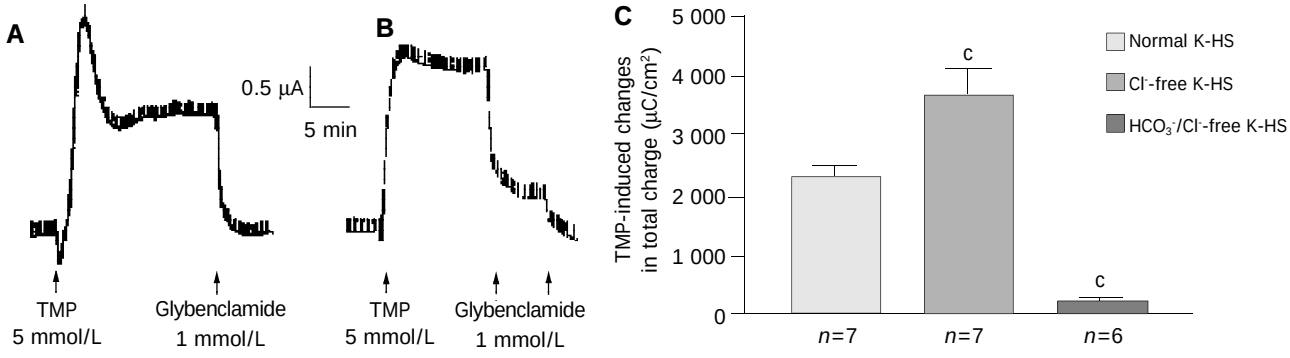

Figure 3 HCO_3^- dependence of TMP-induced I_{SC} increase in Caco-2 cells. Representative I_{SC} recording with arrows indicating TMP (5 mmol/L) added basolaterally, which was abolished by apical application of glybenclamide. Values are mean±SE; ^aP<0.05, ^bP<0.01 and ^cP<0.001. A: Normal; B: Cl-free; C: K-HS, comparison of TMP-induced total charges transferred in normal and Cl^--free K-HS.

to 1 mmol/L TMP. Basolateral addition of bumetanide (100 μmol/L) blocked 80.9% responses induced by 1 mmol/L TMP, from 5 133±465 μC/cm^2 to 978±357 μC/cm^2 (n=9, P<0.001, Figure 5D), but only blocked 43.2% of the responses induced by 5 mmol/L of TMP, from 18 945±2 023μC/cm^2 to 1 0762±2 513 μC/cm^2 (n=7, P<0.05). Basolateral addition of DIDS (100 μmol/L) had no significant effect on the response induced by 1 mmol/L of TMP (n=7, P>0.05), but inhibited 66.5% of the responses induced by 5 mmol/L of TMP, from 17 143±2 408 μC/cm^2 to 8 248±2 328 μC/cm^2 (n=7, P<0.001), indicating possible involvement of NBC in the 5 mmol/L TMP-induced response.

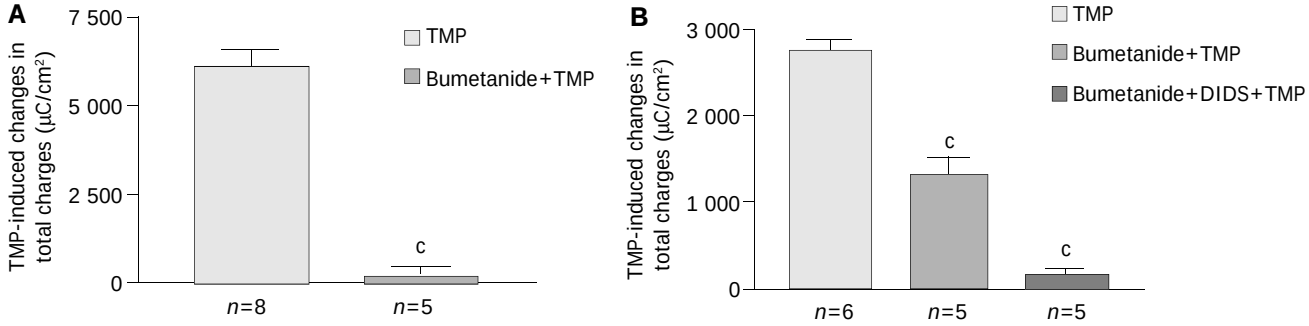

Figure 4 Effect of inhibitors of basolateral anion transporters on TMP-induced I_{SC} responses. Values are mean±SE; ^cP<0.001. A: Comparison of TMP (1 mmol/L)-induced I_{SC} responses in T84 cells in the absence and presence of basolateral addition of bumetanide (100 μmol/L); B: Comparison of TMP (5 mmol/L) -induced I_{SC} responses in Caco-2 cells in the absence and presence of basolateral addition of inhibitors indicated.

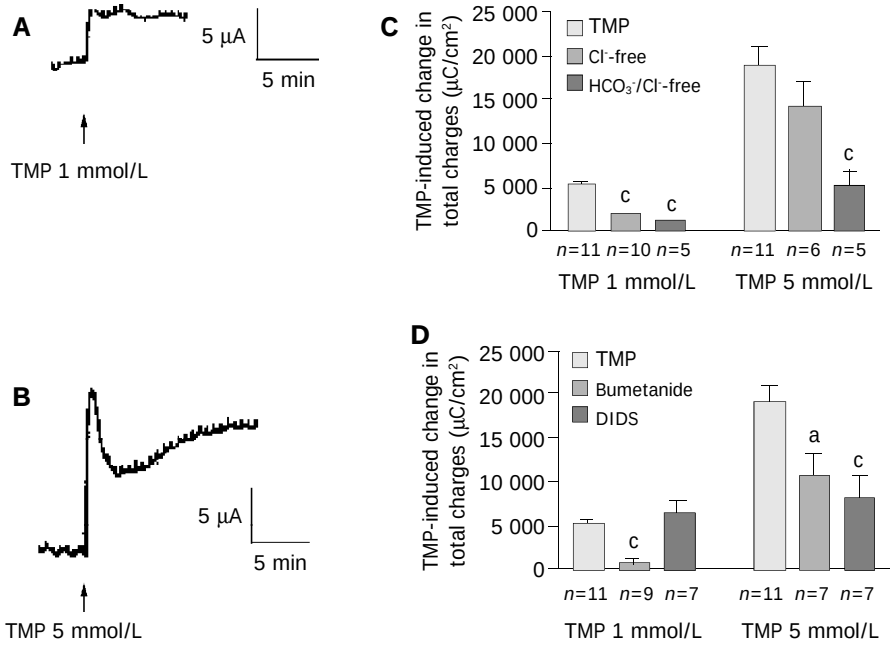

Figure 5 TMP-induced anion secretions in rat colonic mucosa. Representative I_{SC} recording values are mean±SE; ^aP<0.05, ^bP<0.01, ^cP<0.001. A: 1 mmol/L; B: 5 mmol/L of TMP added basolaterally in normal K-HS; C: Comparison of TMP (1 and 5 mmol/L)-induced I_{SC} obtained in normal and Cl^--free as well as both of Cl^- and HCO_3^- -free solutions; D: Comparison of TMP (1 and 5 mmol/L)-induced I_{SC} obtained in basolateral pretreatment of colonic mucosa with bumetanide (100 μmol/L) and DIDS (100 μmol/L).

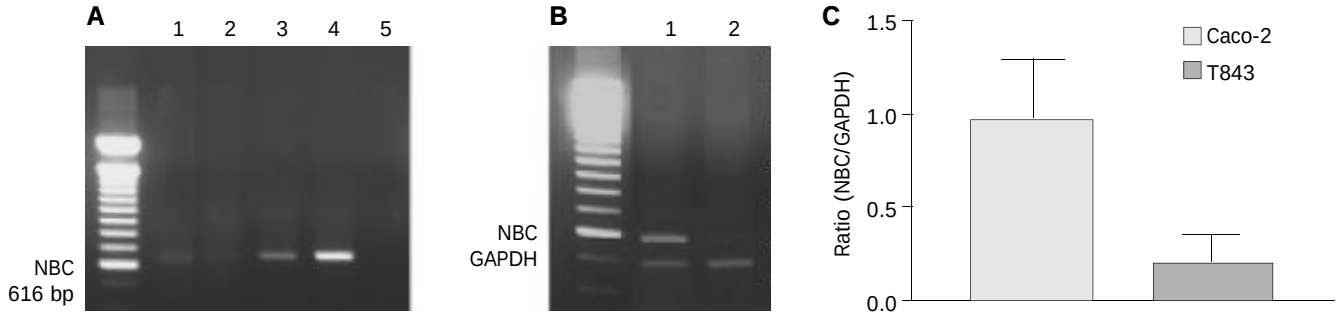

Figure 6 RT-PCR analysis of mRNA expression of Na^+- HCO_3^- cotransporter (NBC) in colonic cells. A: RT-PCR results with products as expected of NBC found in rat colon (1), T84 (2) and Caco-2 (3) with positive control (4) using pancreatic duct cells (CAPAN-1) and negative control (5) where cDNA was omitted. B: Semi-quantitative analysis of NBC expression in Caco-2 (1) ; C: T84 (2) cells with NBC to GAPDH (internal marker) ratio shown.

RT-PCR analysis of NBC expression in T84, Caco-2 cells and colonic mucosa

NBC was expressed in all cells and tissues examined by RT-PCR (Figure 6A). However, semi-quantitative analysis showed that the nucleotide expression level in Caco-2 cells was 4.8-fold over that of T84 (Figure 6B). The NBC nucleotide fragment was confirmed by nucleotide sequencing (Figure 6C).

DISCUSSION

The present study has demonstrated for the first time the effects of TMP on the colonic anion secretion and revealed that the different doses of TMP could induce differential Cl^- and HCO_3^- mediated anion secretion by different colonic cell types. The differential effects of TMP on T84 and Caco-2 cells were not only reflected by the differences in the concentration-dependent I_{SC} responses and the I_{SC} kinetics, but also in the extents to which Cl^- and HCO_3^- were involved in mediating the TMP responses. This was supported by the observation that the TMP-induced response in T84 was sensitive to extracellular Cl^- replacement or an inhibitor of basolateral NKCC, bumetanide, while the response in Caco-2 cells was relatively insensitive to these treatments, at least to a much less extent. Instead, the response in Caco-2 cells was sensitive to the removal of extracellular HCO_3^- and an inhibitor of basolateral NBC, which has been shown to mediate HCO_3^- entry into the cells in a number of tissues including the pancreas[21,22], intestine[23], kidney[24] and endometrium[25]. Although DIDS is also known to inhibit Cl^-/HCO_3^- exchanger (AE), the involvement of AE in this case was unlikely since it was not electrogenic. The high expression of NBC in Caco-2 cells but not T84 cells was also consistent with the DIDS sensitivity profiles in the two cell types, suggesting the involvement of NBC in mediating basolateral HCO_3^- transport in Caco-2 cells. The observed predominant Cl^- secretion elicited by TMP in T84 cells was consistent with the Cl^-- secreting characteristics of this colonic crypt-like cell model. Although secretory properties were less well characterized in Caco-2 cells, a previous study[26] has demonstrated I_{SC} increases in response to cAMP-evoking agents including PDE inhibitor, 3-isobutyl-1-methylxanthine (IBMX), in Caco-2 cells with biphasic current kinetics and DIDS sensitivity similar to that of the TMP-induced I_{SC} response observed in the present study. Interestingly, in the same study alkalization of the apical solution could be induced which was also inhibited by basolateral addition of DIDS. Similar HCO_3^--dependent and DIDS-sensitive I_{SC} was also observed in the intestine[27-29]. Together with the presently demonstrated NBC expression in Caco-2 cells, these results strongly indicate a role of villus-like Caco-2 cells in HCO_3^--potentiated secretion. Thus, it appears that colonic Cl^- and HCO_3^- potentiated secretion may be differentially mediated by different colonic cell types.

The observed difference between T84 and Caco-2 cells in their I_{SC} responses to different concentrations of TMP suggested that colonic Cl^- and HCO_3^- mediated secretions might be differentially elicited by the same agent depending on the concentrations used, probably due to differential expression of receptors, cotranspoters, exchangers and ion channels[10-13] leading to differential responses to TMP. This notion is supported by the observation that TMP at different concentrations could elicit different I_{SC} responses from freshly isolated rat colon mucosa with distinct current characteristics. Interestingly, the colonic mucosal I_{SC} response elicited by 1 mmol/L of TMP had characteristics similar to the TMP-induced response in T84 cells (e.g. sensitive to Cl^- removal and bumetanide but insensitive to DIDS), indicating predominant Cl^- secretion, whereas the colonic mucosal I_{SC} response elicited by TMP at concentrations greater than 5 mmol/L resembled the response observed in Caco-2 cells (e.g., more sensitive to DIDS than to Cl^- removal and bumetanide), indicating predominant HCO_3^--potentiated secretion at this concentration range. The fact that distinct TMP-induced I_{SC} responses with characteristics similar to those observed in human colonic T84 and Caco-2 cells could be observed in intact rat colonic mucosa suggests that the secretory activities of T84 and Caco-2 cells may reflect the secretory properties of the colon, which may be similar in rats and humans. The present findings suggest that by having different sensitivities to stimulation in distinct colonic cell types, the colon in rats or humans, may be able to secrete either Cl^--rich fluid or HCO_3^--rich fluid. In other words, colonic Cl^- and HCO_3^--mediated secretions may be differentially regulated by the same physiological regulator depending on its local concentration. Possible candidates of physiological regulators may include prostaglandins, VIP and secretin, all of which are known to be present in the colon and able to increase intracellular cAMP[30-32]. In fact, secretin has been shown to stimulate Cl^- secretion in the colon[33] and HCO_3^- secretion in Caco-2 cells[26]. It should be noted that TMP has been shown to be a cAMP-evoking agent having an action similar to PDE inhibitor in antiplatelet activity[15]. The further study is required to identify the signaling pathway in mediating TMP effects on colonic cells.

The present finding of predominant HCO_3^--mediated secretion by villus-like Caco-2 cells is of physiological interest. Although a constant pH microclimate at the luminal surface has been considered to have a decisive influence on the reabsorption of Cl^- and absorption of weak electrolytes such as short-chain fatty acids[34], the mechanisms involved in the maintenance and regulation of the pH microclimate are poorly understood. A recent study has demonstrated that HCO_3^- is the most important factor in maintaining a constant pH microclimate at the luminal surface[35]. However, the origin of HCO_3^- responsible for this was not demonstrated although a continuous secretion of HCO_3^- at the luminal surface of the colonic epithelium has been observed[36]. The present study suggested that the villus/surface-like epithelial cells were capable of secreting HCO_3^- upon stimulation, and thus, they are likely to contribute to the maintenance and regulation of the pH microclimate observed at the luminal surface of the colon. Being situated at the luminal surface, villus epithelial cells have the advantage over crypt cells in that they can sense the small variations in the pH microclimate at the luminal surface and secrete HCO_3^- directly adjusting the luminal microclimate. This suggests that the secretory role of villus/surface epithelium is distinct from that of crypts which are mainly responsible for Cl^- secretion on which colonic fluid secretion depends. The differential expression of NBC, the major basolateral transport mechanism for HCO_3^- entry[23], in the two human colonic cells lines also supports this contention.

The mechanism(s) by which Cl^- and HCO_3^- exit through the apical membrane remains to be elucidated. The fact that both Cl^- and HCO_3^- secretions could be completely blocked by DPC and glibenclamide, both of which are known to inhibit CFTR, suggest that a common mechanism may be involved. CFTR appears to be a possible candidate since its involvement in Cl^- and HCO_3^- secretion has been demonstrated[5-7]. The investigation of detail mechanism involved in mediating the TMP-stimulated anion secretions is currently undertaken in our laboratory.

It should be noted that while TMP has been used clinically to treat cardiovascular disorders[14], no study has been reported, at the time of writing, on its effect on colonic secretion. The present results suggest that potential application of TMP as an alternative treatment of GI disorders may be further explored, considering its natural origin and differential effects on colonic Cl^- and HCO_3^- secretion.

REFERENCES

1 **Kunzelmann K**, Mall M. Electrolyte transport in the mammalian colon: mechanisms and implications for disease. *Physiol Rev* 2002; **82**: 245-289

2 **Fordtran JS**. Speculations on the pathogenesis of diarrhea. *Fed Proc* 1967; **26**: 1405-1414

3 **Welsh MJ**, Smith PL, Fromm M, Frizzell RA. Crypts are the site of intestinal fluid and electrolyte secretion. *Science* 1982; **218**: 1219-1221

4 **Stewart CP**, Turnberg LA. A microelectrode study of responses to secretagogues by epithelial cells on villus and crypt of rat small intestine. *Am J Physiol* 1989; **257**(3 Pt 1): G334-343

5 **O'Grady SM**, Jiang X, Maniak PJ, Birmachu W, Scribner LR, Bulbulian B, Gullikson GW. Cyclic AMP-dependent Cl secretion is regulated by multiple phosphodiesterase subtypes in human colonic epithelial cells. *J Membr Biol* 2002; **185**: 137-144

6 **Clarke LL**, Harline MC. Dual role of CFTR in cAMP-stimulated HCO_3^- secretion across murine duodenum. *Am J Physiol* 1998; **274** (4 Pt 1): G718-726

7 **Seidler U**, Blumenstein I, Kretz A, Viellard-Baron D, Rossmann H, Colledge WH, Evans M, Ratcliff R, Gregor M. A functional CFTR protein is required for mouse intestinal cAMP-, cGMP- and Ca(2+)-dependent HCO_3^--secretion. *J Physiol* 1997; **505**(Pt 2): 411-423

8 **Sood R**, Bear C, Auerbach W, Reyes E, Jensen T, Kartner N, Riordan JR, Buchwald M. Regulation of CFTR expression and function during differentiation of intestinal epithelial cells. *EMBO J* 1992; **11**: 2487-2494

9 **Strong TV**, Boehm K, Collins FS. Localization of cystic fibrosis transmembrane conductance regulator mRNA in the human gastrointestinal tract by *in situ* hybridization. *J Clin Invest* 1994; **93**: 347-354

10 **Merlin D**, Jiang L, Strohmeier GR, Nusrat A, Alper SL, Lencer WI, Madara JL. Distinct Ca^{2+}- and cAMP-dependent anion conductances in the apical membrane of polarized T84 cells. *Am J Physiol* 1998; **275**(2 Pt 1): C484-495

11 **Barrett KE**. Positive and negative regulation of chloride secretion in T84 cells. *Am J Physiol* 1993; **265**(4 Pt 1): C859-868

12 **Grasset E**, Bernabeu J, Pinto M. Epithelial properties of human colonic carcinoma cell line Caco-2: effect of secretagogues. *Am J Physiol* 1985; **248**(5 Pt 1): C410-418

13 **Osypiw JC**, Gleeson D, Lobley RW, Pemberton PW, McMahon RF. Acid-base transport systems in a polarized human intestinal cell monolayer: Caco-2. *Exp Physiol* 1994; **79**: 723-739

14 **Liao F**. Herbs of activating blood circulation to remove blood stasis. *Clin Hemorheol Microcirc* 2000; **23**: 127-131

15 **Liu SY**, Sylvester DM. Antiplatelet activity of tetramethylpyrazine. *Thromb Res* 1994; **75**: 51-62

16 **Kwan CY**. Plant-derived drugs acting on cellular Ca^{2+} mobilization in vascular smooth muscle: tetramethylpyrazine and tetrandrine. *Stem Cells* 1994; **12**: 64-67

17 Z**hu JX**, Chan YM, Tsang LL, Chan LN, Zhou Q, Zhou CX, Chan HC. Cellular signaling mechanisms underlying pharmacological action of Bak Foong Pills on gastrointestinal secretion. *Jpn J Physiol* 2002; **52**: 129-134

18 **Zhu JX**, Lo PS, Zhao WC, Tang N, Zhou Q, Rowlands DK, Gou YL, Chung YW, Chan HC. Bak Foong Pills stimulate anion secretion across normal and cystic fibrosis pancreatic duct epithelia. *Cell Biol Int* 2002; **26**: 1011-1018

19 **Ussing HH**, Zerahn K. Active transport of sodium as the source of electric current in the short-circuited isolated frog skin. *J Am Soc Nephrol* 1999; **10**: 2056-2065

20 **Usui T**, Hara M, Satoh H, Moriyama N, Kagaya H, Amano S, Oshika T, Ishii Y, Ibaraki N, Hara C, Kunimi M, Noiri E, Tsukamoto K, Inatomi J, Kawakami H, Endou H, Igarashi T, Goto A, Fujita T, Araie M, Seki G. Molecular basis of ocular abnormalities associated with proximal renal tubular acidosis. *J Clin Invest* 2001; **108**: 107-115

21 **Marino CR**, Jeanes V, Boron WF, Schmitt BM. Expression and distribution of the Na^+-HCO_3^- cotransporter in human pancreas. *Am J Physiol* 1999; **277**(2 Pt 1): G487-494

22 **Satoh H**, Moriyama N, Hara C, Yamada H, Horita S, Kunimi M, Tsukamoto K, Iso-O N, Inatomi J, Kawakami H, Kudo A, Endou H, Igarashi T, Goto A, Fujita T, Seki G. Localization of Na^+-HCO_3^- cotransporter (NBC-1) variants in rat and human pancreas. *Am J Physiol Cell Physiol* 2003; **284**: C729-737

23 **Bachmann O**, Rossmann H, Berger UV, Colledge WH, Ratcliff R, Evans MJ, Gregor M, Seidler U. cAMP-mediated regulation of murine intestinal/pancreatic Na^+- HCO_3^- cotransporter subtype pNBC1. *Am J Physiol Gastrointest Liver Physiol* 2003; **284**: G37-45

24 **Romero MF**, Hediger MA, Boulpaep EL, Boron WF. Expression cloning and characterization of a renal electrogenic Na^+-/HCO_3^- cotransporter. *Nature* 1997; **387**: 409-413

25 **Wang XF**, Yu MK, Leung KM, Yip CY, Ko WH, Liu CQ, Chan HC. Involvement of Na^+ HCO_3^- cotransporter in mediating cyclic adenosine 3', 5'-monophosphate-dependent HCO_3^- secretion by mouse endometrial epithelium. *Biol Reprod* 2002; **66**: 1846-1852

26 **Fukuda M**, Ohara A, Bamba T, Saek Y. Activation of transepithelial ion transport by secretin in human intestinal Caco-2 cells. *Jpn J Physiol* 2000; **50**: 215-225

27 **Taylor J**, Hamilton KL, Butt AG. HCO_3^- potentiates the cAMP-dependent secretory response of the human distal colon through a DIDS-sensitive pathway. *Pflugers Arch* 2001; **442**: 256-262

28 **Schultheiss G**, Horger S, Diener M. The bumetanide-resistant part of forskolin-induced anion secretion in rat colon. *Acta Physiol Scand* 1998; **164**: 219-228

29 **Joo NS**, London RM, Kim HD, Forte LR, Clarke LL. Regulation of intestinal Cl- and HCO3-secretion by uroguanylin. *Am J Physiol* 1998; **274**(4 Pt 1): G633-644

30 **Simon B**, Kather H, Kommerell B. Colonic mucosal adenylate cyclase by prostaglandins. *Adv Prostaglandin Thromboxane Res* 1980; **8**: 1617-1620

31 **Dupont C**, Laburthe M, Broyart JP, Bataille D, Rosselin G. Cyclic AMP production in isolated colonic epithelial crypts: a highly sensitive model for the evaluation of vasoactive intestinal peptide action in human intestine. *Eur J Clin Invest* 1980; **10**: 67-76

32 **Chow BK**. Molecular cloning and functional characterization of a human secretin receptor. *Biochem Biophys Res Commun* 1995; **212**: 204-211

33 **Eto B**, Boisset M, Griesmar B, Desjeux JF. Effect of sorbin on electrolyte transport in rat and human intestine. *Am J Physiol* 1999; **276**(1 Pt 1): G107-114

34 **Rechkemmer G**, Wahl M, Kuschinsky W, von Engelhardt W. pH-microclimate at the luminal surface of the intestinal mucosa of guinea pig and rat. *Pflugers Arch* 1986; **407**: 33-40

35 **Genz AK**, v Engelhardt W, Busche R. Maintenance and regulation of the pH microclimate at the luminal surface of the distal colon of guinea-pig. *J Physiol* 1999; **517**(Pt 2): 507-519

36 **Feldman GM**, Berman SF, Stephenson RL. Bicarbonate secretion in rat distal colon *in vitro*: a measurement technique. *Am J Physiol* 1988; **254**(3 Pt 1): C383-390

Edited by Wang XL and Xu CT **Proofread by** Pan BR and Xu FM

PO Box 2345, Beijing 100023, China
Fax: +86-10-85381893
E-mail: wjg@wjgnet.com www.wjgnet.com

World J Gastroenterol 2004;10(12):1769-1774
World Journal of Gastroenterology
Copyright ©2004 by The WJG Press ISSN 1007-9327

• BASIC RESEARCH •

Time- and pH-dependent colon-specific drug delivery for orally administered diclofenac sodium and 5-aminosalicylic acid

Gang Cheng, Feng An, Mei-Juan Zou, Jin Sun, Xiu-Hua Hao, Yun-Xia He

Gang Cheng, Feng An, Mei-Juan Zou, Jin Sun, Yun-Xia He, Department of Biopharmaceutics, School of Pharmacy, Shenyang Pharmaceutical University, Shenyang 110016, Liaoning Province, China
Xiu-Hua Hao, School of Pharmacy, Jilin University, Changchun 130021, Jilin Province, China
Supported by the Foundation of Ministry of Education of China for distinguished Teachers, No. 903 and the Natural Science Foundation of Liaoning Province, No. 9910500504
Correspondence to: Gang Cheng, Department of Biopharmaceutics, School of Pharmacy, Shenyang Pharmaceutical University, PO Box 32, 103 Wenhua Road, Shenyang 110016, Liaoning Province, China. chenggang63@hotmail.com
Telephone: +86-24-23843711-3536 **Fax:** +86-24-23953047
Received: 2004-01-09 **Accepted:** 2004-02-21

Abstract

AIM: To investigate Time- and pH-dependent colon-specific drug delivery systems (CDDS) for orally administered diclofenac sodium (DS) and 5-aminosalicylic acid (5-ASA), respectively.

METHODS: DS tablets and 5-ASA pellets were coated by ethylcellulose (EC) and methacrylic acid copolymers (Eudragit® L100 and S100), respectively. The *in vitro* release behavior of the DS coated tablets and 5-ASA coated pellets were examined, and then *in vivo* absorption kinetics of DS coated tablets in dogs were further studied.

RESULTS: Release profile of time-dependent DS coated tablets was not influenced by pH of the dissolution medium, but the lag time of DS release was primarily controlled by the thickness of the coating layer. The thicker the coating layer, the longer the lag time of DS release is. On the contrary, in view of the pH-dependent 5-ASA coated pellets, 5-ASA release was significantly governed by pH. Moreover, the 5-ASA release features from the coated pellets depended upon both the combination ratio of the Eudragit® L100 and S100 pH-sensitive copolymers in the coating formulation and the thickness of the coating layer. The absorption kinetic studies of the DS coated tablets in dogs demonstrated that *in vivo* lag time of absorption was in a good agreement with *in vitro* lag time of release.

CONCLUSION: Two types of CDDS, prepared herein by means of the regular coating technique, are able to achieve site-specific drug delivery targeting at colon following oral administration, and provide a promising strategy to control drug release targeting the desired lower gastrointestinal region.

Cheng G, An F, Zou MJ, Sun J, Hao XH, He YX. Time- and pH-dependent colon-specific drug delivery for orally administered diclofenac sodium and 5-aminosalicylic acid. *World J Gastroenterol* 2004; 10(12): 1769-1774
http://www.wjgnet.com/1007-9327/10/1769.asp

INTRODUCTION

Currently, a novel oral colon-specific drug delivery system (CDDS) has been developing as one of the site-specific drug delivery systems. This delivery system, by means of combination of one or more controlled release mechanisms, hardly releases drug in the upper part of the gastrointestinal (GI) tract, but rapidly releases drug in the colon following oral administration. The necessity and advantage of CDDS have been well recognized and reviewed recently[1-3]. In view of CDDS specifically delivering drug to the colon, a lot of benefits would be acquired in terms of improving safety and reducing toxicity when treating local or systemic chronic diseases. First, as for treating localized colonic diseases, i.e. ulcerative colitis, Crohn' s disease and constipation *etc.*, the optimal drug delivery system, such as CDDS, should selectively deliver drug to the colon, but not to the upper GI tract[1]. For this reason, the drug concentration was significantly lessened in the upper GI tract, while increased considerably in the colon, resulting in alleviated GI side effects. Second, the colon is referred to as the optimal absorption site for protein and polypeptide after oral administration, because of the existence of relatively low proteolytic enzyme activities and quite long transit time in the colon[2, 3]. To our knowledge, CDDS could provide reliable protection against GI enzymatic degradation by releasing the polypeptide and protein nearly unchanged and fully efficacious in the preferred colon, thereafter resulting in remarkably increased bioavailability for protein and polypeptide. Finally, CDDS would be advantageous when a delay in absorption is desirable from a therapeutical point of view, as for the treatment of diseases that have peak symptoms in the early morning and that exhibit circadian rhythms, such as nocturnal asthma, angina and rheumatoid arthritis[1,4,5].

There were currently a few strategies to achieve colonic specificity, such as bacterially triggered and pressure-controlled CDDS[6]. The aim of this study was to explore the feasibility of the time- and pH-dependent CDDS, diclofenac sodium (DS) and 5-aminosalicylic acid (5-ASA) being selected as model drugs, respectively. Besides, we were intended to exploit the typical pharmaceutical coating technology to attain the time- and pH-dependent colon-specific drug delivery. Time-dependent colon-specific DS coated tablets consisted of a tablet core and a coating layer composed of a water-insoluble ethylcellulose (EC) and a water-soluble channeling agent. pH-dependent colon-specific 5-ASA coated pellets consisted of a pellet core and a coating layer of the pH-sensitive methacrylic acid copolymers (Eudragit® L100 and S100).

DS was frequently used for treating rheumatoid arthritis[2], which had apparent circadian rhythms and peak symptoms in the early morning. When orally administering DS conventional formulation, it was difficult to achieve the desired clinical effect, because it elicited patients' incompliance of administration in the early morning to coordinate the rhythm of rheumatoid arthritis, due to rapid absorption of the conventional formulation. However, colon-specific DS delivery was not only effective, but also more convenient for administration than the conventional formulation. On the other hand, 5-ASA was usually used to effectively treat ulcerative colitis and Crohn' s disease in clinical practice[7]. It was unstable in the stomach, and readily absorbed in the small intestine, eliciting the undesirable adverse effect. Thereby, 5-ASA was prepared as

the CDDS in this study, which protected 5-ASA from the upper GI conditions[1] and allowed for 5-ASA rapid release in the designated colonic region.

MATERIALS AND METHODS

Preparation of time-dependent colon-specific DS coated tablets and in vitro/in vivo tests

Preparation of DS core tablets Core tablets consisted of 40% (w/w) diclofenac sodium (Yanzhou Pharm., China), 40% (w/w) sodium carboxymethyl starch sodium, 8% (w/w) sodium chloride, 2% (w/w) other excipients. Drug and excipients were blended and sieved (mesh 80); the mixtures were granulated with adhesives and dried 1 h at 55 ℃. Core tablets with average weight of 100 mg were prepared using a single punch tablet machine (Type-TDP, 1st Pharm Machine Manu. Co., Shanghai, China). The diameter of core tablets was 6 mm.

Tablet coating The core tablets were coated in a conventional rotating pan. For the coating process, the rotation speed was adjusted to 36 r/min with the coating pan set at an angle of 45°, nozzle port size 0.8 mm; inlet air temperature was 35 ℃; tablet bed temperature was 25 ℃; the coating solution was sprayed onto the tablets at a flow rate of 0.8 mL/min. The coating solution was 30 g/L EC (Colorcon Co., China) in ethanol solution which contained diethyl phthalate (20% of EC, w/w) as plasticizer, and PEG 400 (15% of EC, w/w, Pharm. Med. Supply Ltd. Co., China) as channeling agent.

Dissolution test Dissolution studies were carried out with paddle method at a rotation speed of 100 r/min and 900 mL distilled water as medium at 37 ℃ (n=6). Samples were collected at predetermined time points, analyzed for DS contents using a UV-spectrophotometer (UV-9100, Ruili Co., China) at 276±1 nm and calculated cumulative release amounts of DS over the sampling times.

Absorption kinetics of time-dependent colon-specific DS coated tablets

Experimental protocol Six male dogs (weight 20±2.5 kg) were randomly assigned to one of two crossover experiments with a 7-d washout period. Dogs were fasted overnight for 12 h before administration and free access to water was allowed. Each dog was orally administered either reference formulation (four enteric coated tablets, Liaodong Pharm. Ltd. Co., batch: 010910, tablet containing 25 mg of DS) or test formulation (four EC coated tablets, each tablet containing 25 mg of DS with 7.5% coating level), respectively. Blood samples were collected at predetermined times for each protocol, respectively: (1) 1, 2, 2.5, 3, 3.5, 4, 4.5, 5, 6, 7, 8, 10, and 24 h for the reference; (2) 1, 3, 4, 5, 5.5, 6, 6.5, 7, 7.5, 8, 9, 10, 12, and 24 h for the test. Plasma was immediately obtained by centrifuging the blood samples at 3 000 r/min for 10 min. The plasma samples were maintained in a freezer at -20 ℃ until analysis.

Chromatographic conditions The quantitative determination was performed on a high-performance liquid chromatograph equipped with a PU-1580 pump (Jasco, Japan) and 970/975 UV detector (Jasco, Japan). The column was a Hypersil ODS C-18 (250 mm×4.6 mm, 5 μm). The mobile phase consisted of methanol: water: triethylamine: glacial acetic acid (68:22:0.044:0.044, v/v)[8]. The eluate was monitored at 274 nm, with a sensitivity of 0.001 AUFS. A flow rate was 1.0 mL/min, and the column temperature was maintained at 35 ℃.

Sample preparation A 0.5 mL plasma sample was mixed with 20 μL of 4.8 mmol/L inuprofen (internal standard) and 0.6 mL of 1.0 mol/L phosphate buffer in a glass centrifuge tube. The solution was mixed on a vortex mixer for 2 min, and then added 3 mL of a solution of hexane and isopropyl alcohol (4:1, v/v). The mixture was mixed on a vortex mixer for 2 min again and centrifuged at 3 000 r/min for 5 min. The organic layer was transferred into a clean tube and evaporated to dryness under nitrogen at 35 ℃. The residue was dissolved in 100 μL of mobile phase and 20 μL of the solution were injected into the HPLC system.

Data analysis C_{max} represents the maximum drug concentration, t_{max} the time to reach peak concentration, and t_{lag} the lag time of drug. These values were obtained as directly measured values. The elimination rate constant (K_e) was calculated from the slope of the logarithm plasma concentration to time at the end four points. The areas under the plasma concentration-time curve ($AUC_{0\text{-}tn}$) were calculated by the trapezoidal method. The relative bioavailability (F %) was calculated by the equation: $F(\%)=(AUC_{\text{Test formulation}}\cdot \text{Dose}_{\text{Reference formulation}})/(AUC_{\text{Reference formulation}}\cdot \text{Dose}_{\text{Test formulation}})$. The percentages of absorption *in vivo* were calculated by the Wagner-Nelson method.

Preparation of pH-dependent colon-specific 5-ASA coated pellets

Preparation of 5-ASA pellets Pellets (1.0-1.2 mm in diameter) consisted of 5-aminosalicylic acid (5-ASA, Genlou Chem. Ltd. Co., China), microcrystalline cellulose (MCC, Avicel PH101, Asahi Chem. Ind. Ltd. Co., Japan) and lactose. Drug and excipients were blended and sieved (mesh 80); the mixtures were prepared as wet mass with adhesives. Pellets were prepared by extruder and spheronizer (Institute of Machinery for Chemical Industry East China University of Science and Technology, Shanghai, China). The speed of the extrusion was 30 r/min. The speed of the spheronization was 1 200 r/min and the time of the spheronization was 5 min[9,10].

Pellet coating The pellets were coated in a fluidized-bed coating apparatus (Shenyang Pharm. Univer., China). For the coating process, nozzle port size was 0.8 mm; inlet air temperature 45 ℃; atomizing pressure 1.2 kg/cm^2; coating solution was sprayed onto the pellets at a flow rate of 0.8 mL/min. The coating solution was aqueous dispersions of various proportions of Eudragit® L100 and Eudragit® S100 (Röhm Pharma GmbH, Germany). The plasticizer TEC was added directly to the polymer dispersions[11].

Dissolution test Dissolution studies were carried out with a basket method at a 100 r/min rotation speed and 37 ℃, 900 mL dissolution medium according to ChP 2000. The dissolution tests were performed in HCl pH 1.2, phosphate buffer solution pH 6.0, 6.8, 7.2 or 7.5, respectively. Samples were collected at predetermined time points, analyzed for 5-ASA content using a UV-spectrophotometer (UV-9100, Ruili Co., China) at 302 nm and 330 nm for 5-ASA assay in 0.1 mol/L HCl and the phosphate buffer solutions, respectively.

In order to simulate the pH changes along the GI tract, three dissolution media with pH 1.2, pH 6.0, and pH 7.2, were sequentially used, referred to as the sequential pH change method (Table 1). pH 6.0, and pH 7.2 media were 0.05 mol/L phosphate buffer solution. When performing release experiments, the pH 1.2 medium was first used for 2 h, then removed, and the fresh pH 6.0 dissolution medium was added. After 1 h, the medium was removed again, and fresh pH 7.2 dissolution medium added. The UV readings were taken at 302 nm and 330 nm for 5-ASA measurement in 0.1 mol/L HCl and the buffer media, respectively[12,13]. And then the 5-ASA cumulative release percentage was calculated over the sampling times.

Table 1 Dissolution conditions of 5-ASA coated pellets

pH	λ_{max} (nm)	Time (h)	Simulated GI region
1.2	302	2	Stomach
6.0	330	1	Duodenum
7.2	330	5	Lower small intestine and colon

RESULTS

Time-dependent colon-specific DS coated tablets

The DS core tablets were coated by the coating formulation, consisting of 30 g/L EC, diethyl phthalate (20% of EC, w/w) as a plasticizer and PEG 400 (15% of EC, w/w) as a channeling agent in ethanol solution. The *in vitro* release behavior of the DS coated tablets with different coating levels (3%, 5%, 7%, 9%, and 11%, w/w), was studied. As shown in Figure 1, the coating level exercised a significant effect on the lag time of DS release from the coated tablets. Manifestly, the greater the coating level, the longer the lag time of DS release from the coated tablets. However, once the coating layer was broken up, DS then was rapidly released from the coated tablets (Figure 1). The effects of dissolution medium pH on the release profiles of the DS coated tablets at 7.5% coating level are shown in Figure 2. To be evident, the pH values of media did not exert a significant effect on the DS release pattern from the coated tablets. The *in vitro* release profile of test DS coated tablets at 7.5% coating level was compared with the marketed DS enteric tablets, as shown in Figure 3.

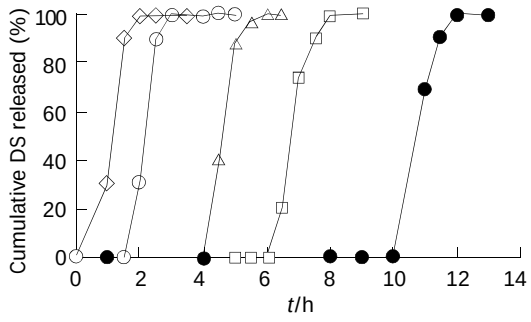

Figure 1 Effect of different coating levels on the DS release from the coated tablets in distilled water. The tablets were coated at five levels of 3% (◇), 5% (○), 7% (△), 9% (□●11%(×) (w / w, total solid applied) (n=6).

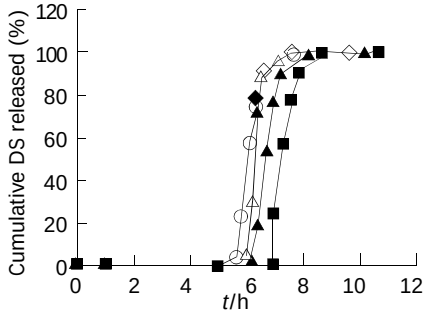

Figure 2 Effect of pH of the dissolution medium on DS release from the coated tablets. The tablets were coated at 7.5% (w / w, total solid applied) level (n=6). pH1.0 (◇), pH2.0 (■), pH5.0 (▲), pH6.8 (○), pH7.6 (△) of the dissolution media.

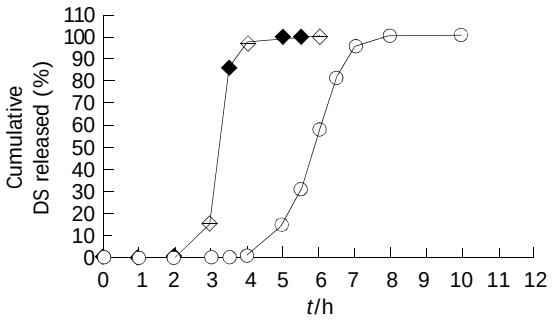

Figure 3 DS dissolution profiles of test coated tablets (○) and the reference enteric coated tablets (◆) (n=6).

The reference enteric tablets started DS release at 2 h, while the test DS coated tablets began to release DS at 4 h, after being put in the dissolution medium. The lag time of DS release from the test tablets was significantly longer than that of reference enteric tablets. Moreover, the cumulative DS release percentage of test tablet was nearly 100% within 7 h.

pH-dependent colon-specific 5-ASA coated pellets

The 5-ASA pellets were coated with combination of Eudragit® L100 -Eudragit® S100 methacrylic acid pH-sensitive copolymers, and their release characteristics were examined by three sequential dissolution media with different pH values in order to mimic pH changes along GI tract. We investigated the effect of combination ratios of Eudragit® L100-Eudragit® S100 in the coating formulation on the release profiles of 5-ASA coated pellets, as shown in Figure 4.

The combination ratios of Eurdragit® L100-Eudragit® S100 in the coating formulation played a significant role in regulating the release behavior of 5-ASA coated pellets. When employing 1:4 (w/w) combination ratio of Eudragit® L100-Eudragit® S100 as the coating formulation, 5-ASA was released less than 1.0% in pH 1.2 dissolution medium (simulated gastric fluid) until 2 h, and less than 3.0% in pH 6.0 (simulated duodenum fluid) at 1 h after changed to fresh medium, and more than 80% in pH 7.2 (simulated lower small intestinal and colonic fluid) at 1.5 h after changed to fresh medium. When the pellets were coated with Eudragit® L100-Eudragit® S100 combination (w/w) ratios of 1:0, 4:1, and 1:1, the cumulative release percentage of 5-ASA was 1.0-3.6% in pH 1.2 until 2 h, 11-37% in pH 6.0 at 1 h, and more than 80% in pH 7.2 at 1.5 h, the results indicating that the earlier measurable release occurred. Pellets coated with Eudragit® S100 alone displayed the slowest release rate, the cumulative release percentage of 5-ASA was less than 0.5% in pH 1.2 up to 2 h, was less than 1.0% in pH 6.0 at 1 h, and was not more than 10% in pH 7.2 at 1.5 h.

The effects of the coating level on the release properties of 5-ASA coated pellets were also examined, with the coating level ranging from 0% to 25% and the combination ratio of Eudragit® L100-Eudragit® S100 set at 1:4 (w/w), as shown in Figure 5. As the coating level and thickness of coating layer increased, the acid-resistant property of coating layer was enhanced. The coating level being 25% (w/w), almost none of the 5-ASA was released from coated pellets in pH 1.2 and pH 6.0 dissolution media. By contrast, the cumulative release percentage of 5-ASA was more than 80% in pH 7.2 at 1.5 h, regardless of the coating levels. Accordingly, this formulation, with the combination ratio Eudragit® L100-Eudragit® S100 being 1:4 (w/w) and the coating level being 25%, would be a promising candidate for designed DS pH-dependent CDDS.

Moreover, we examined the influences of medium pH values on the release characteristics of the 5-ASA coated pellets, utilizing 1:4 (w/w) combination ratio Eudragit® L100-Eudragit® S100 as the coating formulation and setting the coating level at 25%. Five pH values (1.2, 6.0, 6.8, 7.2 and 7.5) of dissolution media were utilized. As shown in Figure 6, pH values of medium notably affected 5-ASA release profiles from the pH-dependent coated pellets. When pH increased from 1.2 to 7.5, the release rate of 5-ASA from the coated pellets was outstandingly enhanced.

In vivo absorption kinetics of time-dependent colon-specific DS coated tablets

Either DS reference formulation (four 25 mg enteric coated tablets) or DS test formulation (four 25 mg EC coated tablets) was orally administered in the two crossover experimental design in dogs at a dose of 100 mg/body, respectively. The concentration-time curve of DS in plasma is illustrated in Figure 7. The pharmacokinetic parameters are calculated and listed in Table 2. The mean lag time of DS absorption from the test

formulation was as long as 5.80 h, while that for the reference formulation was 2.80 h after oral administration. This result was well consistent with the mean *in vitro* lag time of DS release from two formulations, the test tablets being 4 h versus reference enteric tablets being 2 h. In addition, C_{max} of the test and the reference formulations was 8.17 mg/L and 10.05 mg/L, respectively. The relative bioavailability of test formulation versus reference formulation was 86.38%.

Absorption percentage *in vivo* of DS for test formulation was assessed by the Wagner-Nelson method. Both absorption percentage *in vivo* of DS (F(t)) and the cumulative release percentage *in vitro* of DS (f(t)) versus time profiles, demonstrate a similar contour curve in Figure 8. Furthermore, there existed a significant correlation between F(t) and f (t) (r=0.95) for test formulation, indicative of the good relationship between *in vitro* release and *in vivo* absorption processes.

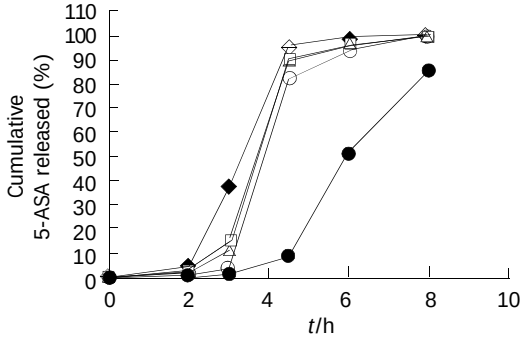

Figure 4 5-ASA release profile of pellets coated at 25% level with various Eudragit® L100-Eudragit® S100 combination ratios of 1:0 (◆), 4:1 (□), 1:1 (△), 1:4 (○) and 0:1 (●) (w/w), using the sequential pH change method (n=6).

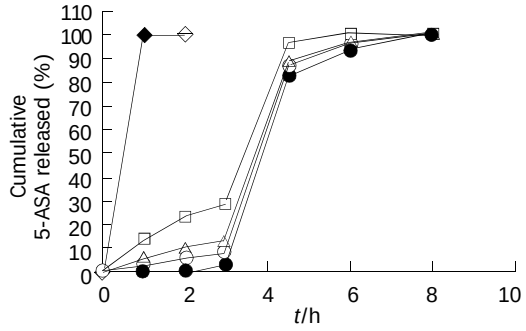

Figure 5 5-ASA release profile of pellets coated at 5 levels of uncoated (◆), 5% (□), 10% (△), 15% (○), 25% (●) (w/w, total solid applied) with Eudragit® L100-Eudragit® S100 combinations of 1:4 (w/w), using the sequential pH change method (n=6).

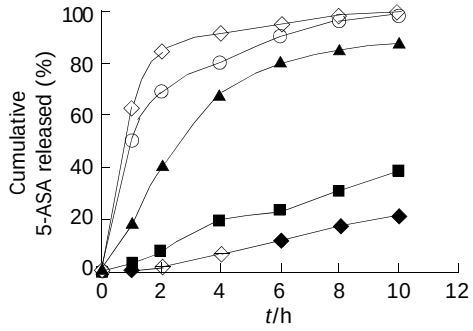

Figure 6 Effect of pH of the dissolution medium on 5-ASA release of coated pellets coated at 25% level with Eudragit® L100-Eudragit® S100 combination ratios of 1:4 (w/w) (n=6). PH 1.2 (◆), pH 6.0 (■), pH 6.8 (▲), pH 7.2 (○), pH 7.5 (◇) of the dissolution media.

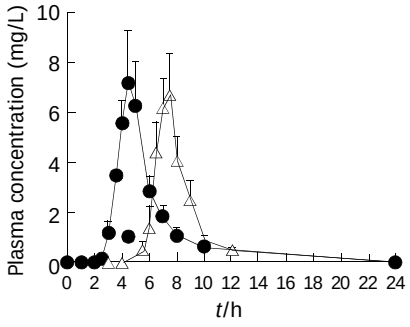

Figure 7 DS plasma concentration-time profiles after oral administration of coated formulation (△) and reference enteric formulation (●) in dogs at a dose of 100 mg/body. Each value represents mean±SE (n=6).

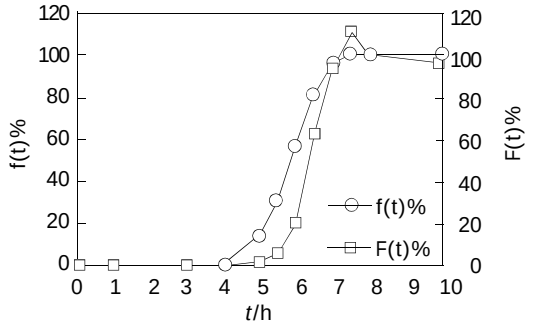

Figure 8 Comparison between the cumulative DS release percentage *in vitro* f(t) and the absorption percentage *in vivo* F(t) of coated formulation (n=6).

Table 2 Pharmacokinetic parameters after oral administration of DS coated formulation and reference enteric formulation in dogs at a dose of 100 mg/body (n=6, mean±SE)

Parameter	Test formulation	Reference formulation
C_{max} (mg/L)	8.17±1.35	10.05±1.66
t_{max} (h)	7.40±0.35	4.50±0.20
K_e (L/h)	0.56±0.06	0.44±0.11
t_{lag} (h)	5.80±0.42	2.80±0.21
$AUC_{0\text{-}tn}$ (mg·h/L)	17.21±2.09	19.91±2.83
F (%)	86.38±10.51	–

DISCUSSION

It has been well found that gastric emptying of a preparation was variable and depended primarily upon whether subjects were fed or not, and upon the properties of the preparation. On the contrary, the transit time in small intestine for the preparation was surprisingly constant at 3±1 h and appeared to be independent of the types of the preparations and whether subjects were fed or not[14]. On the basis of the above understandings, we designed the time-dependent colon-specific drug delivery to achieve no measurable drug release in the upper part of GI tract and a considerable drug release after arrival at colon.

The time-dependent DS coated tablets were prepared by means of the coating technology, with the coating formulation consisting of the water-insoluble EC, the water-soluble channeling agent PEG 400 and the membrane plasticizer diethyl phthalate. Generally, the coating layer of EC was mainly hydrophobic and was moderately impermeable to water molecules. And the water-soluble channeling agent was rapidly dissolved in water, resulting in the formation of numerous micro-channels across the coating layer. Then, water molecules

could penetrate into the tablet core via these channels to cross the hydrophobic EC membrane. Water uptake caused the expansion of the disintegrating agent within the tablet core, resulting in a gradual build-up of pressure within the coated tablets. Once the inside pressure exceeded the critical disrupted value that the coating layer resisted most, the coating layer would be ruptured and release drug in a manner of burst, thus forming the delay effect of drug release from the coated tablets. Taken together, the formation of micro-channels was the first crucial step, and the critical disrupted pressure governed by the coating layer and the expansibility of the disintegrating agent were the key factors for time-dependent controlled release[15].

The release profiles of the DS coated tablets at 7.5% coating level were not affected by the pH values of media (Figure 2). This was reasonably expected, since the channeling agent PEG 400 was pH-insensitive and formation of the micro-channels was not affected by pH. The effects of the coating level on the lag time of DS release from the coated tablets were tested, indicating that the coating level played a significant role in controlling the lag time of release. To increase the coating level would extend the lag time of DS release from the coated tablets (Figure 1). There were two possible mechanisms contributing to this phenomenon. For one thing, since the hydrophobic EC membrane was relatively impermeable to water molecules, substantial effect on the rate of the water molecules diffusion and water uptake, was exerted by the number, size, length and tortuosity of the aqueous micro-channels in the coating layer. The coating level and thickness of the coating layer certainly determined the rate of water uptake, by controlling the formation rate and physical characteristics of the aqueous channels. To be evident, the increase of the coating level would elicit the longer and more tortuous aqueous micro-channels, severely impairing the rate of water uptake. Alternatively, the thicker coating layer developed the higher critical resistant pressure to be surpassed for disrupting the coating membrane, required the greater water uptake to gradually build up inside pressure by the disintegrating agent' s expansion and prolonged the lag time of drug release from the coated tablets[16].

The mean *in vivo* lag time of the DS absorption from coated tablets was significantly longer than that from enteric tablets, being 5.80 h *vs* 2.80 h (Figure 7 and Table 2). The results were in accordance with the *in vitro* lag time of DS release from two formulations, and the lag time of DS release from test tablets was nearly 2 h longer than that from the enteric tablets (Figure 3). Furthermore, the *in vivo* absorption kinetics of the time-dependent DS coated tablets was assessed by the typical Wagner-Nelson method. The absorption percentage *in vivo* versus time profile was analogous to the cumulative release percentage *in vitro* versus time profile, which validated the *in vitro* dissolution conditions and verified the utility of the time-dependent CDDS (Figure 8). The good correlation coefficient (r=0.95) between *in vivo* absorption and *in vitro* release percentages, further confirmed this conclusion.

To our knowledge, there exists a pH gradient along the GI tract, a fact that pH in the stomach is approximately 1.5 in the fasted state, ranges roughly from 5.0 to 7.0 in the small intestine, and from 6.0 to 7.2 in the colon[1]. The pH values at the end of ileum and in the colon are notably higher than the upper GI tract, therefore providing the rationale for developing pH-dependent CDDS. In addition, a novel dosage form, pellets, is the multiple units' drug delivery system, and it is superior to the conventional preparation, such as tablets, for the following reasons. The pellets appear to be less influenced by the physiologic factors, such as the gastric emptying, intestinal transit, than tablets. Moreover, the pellets could be widely and evenly distributed in the GI tract surfaces, which increase the drug-tract contact surface and thus improve bioavailability. Finally, the release failure of the individual unit hardly affects the total release behavior due to the multiple units, whereas tablets do not[17].

Eudragit® L100 and S100 were methacrylic acid pH-sensitive copolymers and began to be dissolved from pH 6.0 and pH 7.0, respectively. The combination utilization of L100 and S100 would be capable of designing the suitable copolymers intended to begin being dissolved from the desired pH environment in the lower GI tract (pH variation range of 6.0-7.0). Clearly, the combination ratio of L100 and S100 exerted a great effect on the 5-ASA release characteristic from the coated pellets. The combination ratios (1:0, 4:1, 1:1, and 1:4, 0:1) of L100 and S100 hardly released drug in pH 1.2 until 2 h, indicating the acid-resistant properties of the coated polymers (Figure 4). After changing to pH 6.0 fresh medium, L100 could to be dissolved and the channels were then quickly created in the coating membrane; conversely, S100 did not. Therefore, the higher the proportion of L100 in the coating formulation, the more channels formed, thus allowing for the higher 5-ASA release[12]. After converting into the pH 7.2 fresh medium, both L100 and S100 could be dissolved; by contrast, the dissolution rate of L100 was faster than S100. Thus the higher amount of L100 in the coating formulation, the faster dissolution and disappearance of the coating layer, leading to rapid release of 5-ASA (Figure 4). The dissolution profile for the 0:1 coating formulation at pH 7.2 demonstrated that the dissolving process of the coating layer of S100 alone was rather slow, resulting in very slow drug release.

Fixing the combination ratio of Eudragit® L100 and S100 at 1:4, the coating level remarkably influenced the 5-ASA release from coated pellets (Figure 5). When the coating level was less than 25%, a measurable 5-ASA release was observed in pH 1.2 and 6.0 media. The coated pellets at 25% coating level scarcely released 5-ASA in pH 1.2 and 6.0 media, and rapidly released in pH 7.2 medium. This coating level of pellets (25%) was significantly higher than that of tablets (10%) in this study, because of the ratio of surface area of pellets considerably greater than tablets. The lower coating level for pellets would form an incomplete closed membrane around pellets, and elicited a measurable drug release in pH 1.2 and 6.0 media (Figure 5). The coating level of pellets 25%, however, could form uninterrupted and homogenous coating layer, swiftly released 5-ASA in pH 7.2, but not in pH 1.2 and 6.0 media. On the other hand, the higher coating level would require the longer processing time, escalation of cost and further 5-ASA was incapable of being rapidly released from pellets in pH 7.2 medium (the coating level $\geqslant$35%, unpublished data). Since the coating copolymers were pH-sensitive, 5-ASA release from the coated pellets was expected to be influenced by the dissolution medium pH, as confirmed in Figure 6.

In summary, two controlled release mechanisms, i.e. time- and pH-dependent, could achieve colonic-specific drug delivery following oral administration. In addition, both CDDS were relatively inexpensive and easy to be manufactured using conventional pharmaceutical coating technique, and provided the promising candidates for specifically delivering drug to the targeted colon region, in particular for DS and 5-ASA in this study, respectively.

REFERENCES

1 **Kinget R**, Kalala W, Vervoort L, van den Mooter G. Colonic drug targeting. *J Drug Target* 1998; **6**: 129-149

2 **Watts PJ**, lllum L. Colonic drug delivery. *Drug Dev Ind Pharm* 1997; **23**: 893-913

3 **Yang L**, Chu JS, Fix JA. Colon-specific drug delivery: new approaches and *in vitro/in vivo* evaluation. *Int J Pharm* 2002; **235**: 1-15

4 **Halsas M**, Penttinen T, Veski P, Jurjenson H, Marvola M. Time-controlled release pseudoephedrine tablets: bioavailability and *in vitro/in vivo* correlations. *Pharmazie* 2001; **56**: 718-723

5 **Halsas M**, Hietala J, Veski P, Jurjenson H, Marvola M. Morning versus evening dosing of ibuprofen using conventional and time-controlled release formulations. *Int J Pharm* 1999; **189**: 179-185

6 **Zou MJ**, Cheng G. The oral colon-specific drug delivery system. *Shenyang Yaoke Daxue Xuebao* 2001; **18**: 376-380

7 **Ardizzone S**, Porro GB. A practical guide to the management of distal ulcerative colitis. *Drugs* 1998; **55**: 519-542

8 **Miller RB**. High-performance liquid chromatographic determination of diclofenac in human plasma using automated column switching. *J Chromatogr* 1993; **616**: 283-290

9 **Pinto JF**, Buckton G, Newton JM. The influence of four selected processing and formulation factors on the production of spheres by extrusion and spheronisation. *Int J Pharm* 1992; **83**: 187-196

10 **Krogars K**, Heinamaki J, Vesalahti J, Marvola M, Antikainen O, Yliruusi J. Extrusion-spheronization of pH-sensitive polymeric matrix pellete for possible colonic drug delivery. *Int J Pharm* 2000; **199**: 187-194

11 **Khan MZ**, Prebeg Z, Kurjakovic N. A pH-dependent colon targeted oral drug delivery system using methacrylic acid copolymers I. Manipulation of drug release using Eudragit L100-55 and Eudragit S100 combinations. *J Control Release* 1999; **58**: 215-222

12 **Khan MZ**, Stedul HP, Kurjakovic N. A pH-dependent colon-targeted oral drug delivery system using methacrylic acid copolymers. II. Manipulation of drug release using Eudragit L100 and Eudragit S100 combinations. *Drug Dev Ind Pharm* 2000; **26**: 549-554

13 **Ashford M**, Fell JT, Attwood D, Woodhead PJ. An *in vitro* investigation into the suitability of pH-dependent polymers for colonic targeting. *Int J Pharm* 1993; **91**: 241-245

14 **Rouge N**, Buri P, Doelker E. Drug absorption sites in the gastrointestinal tract and dosage forms for site-specific delivery. *Int J Pharm* 1996; **136**: 117-139

15 **Xiao YC**, Cheng G, Zou MJ. Studies on coated theophylline tablets for colon-specific delivery using Eudragit NE 30D. *Shenyang Yaoke Daxue Xuebao* 2001; **18**(Suppl): 5-7

16 **Fan TY**, Wei SL, Yan WW, Chen DB, Li J. An investigation of pulsatile release tablets with ethylcellulose and Eudragit L as film coating materials and cross-linked polyvinylpyrrolidone in the core tablets. *J Control Release* 2001; **77**: 245-251

17 **Lu B,** Wang PY, Deng YJ, Zhou Q, Ni D, Xu HN, Xu HL, Liang WQ, Pei YY, Wei SL. New techniques and new dosage forms of drug. 1th ed. *Beijing: People's Medical Publishing House* 1998: 289-305

Edited by Zhang JZ and Chen WW **Proofread by** Xu FM

PO Box 2345, Beijing 100023, China
Fax: +86-10-85381893
E-mail: wjg@wjgnet.com www.wjgnet.com

World J Gastroenterol 2004;10(12):1775-1779
World Journal of Gastroenterology
Copyright ©2004 by The WJG Press ISSN 1007-9327

• BASIC RESEARCH •

Inhibition of Fas/FasL mRNA expression and TNF-α release in concanavalin A-induced liver injury in mice by bicyclol

Min Li, Geng-Tao Liu

Min Li, Geng-Tao Liu, Department of Pharmacology, Institute of Materia Medica and Peking Union Medical College and Chinese Academy of Medical Sciences, Beijing 100050, China
Supported by the Grant from Ministry of Science and Technology of China, No. 94-ZD-02
Correspondence to: Professor Geng-Tao Liu, Department of Pharmacology, Institute of Materia Medica and Peking Union Medical College and Chinese Academy of Medical Sciences, Beijing 100050, China. gtliu2002@yahoo.com
Telephone: +86-10-63165178 **Fax:** +86-10-63017757
Received: 2004-01-02 **Accepted:** 2004-01-16

Abstract

AIM: Bicyclol, 4,4'-dimethoxy-5,6,5',6'-dimethylene-dioxy-2-hydroxymethyl -2'-carbonyl biphenyl, is a new anti-hepatitis drug. The aim of the present study was to investigate the protective effect of bicyclol on concanavalin A (Con A)-induced immunological liver injury in mice and its mechanism.

METHODS: Liver injury was induced by injection of Con A via tail vein of mice and assessed biochemically and histologically. Serum transaminase and tumor necrosis factor alpha (TNF-α) were determined. Liver lesions were observed by light microscope. Expressions of TNF-α, interferon gamma (IFN-γ), Fas and Fas ligand (FasL) mRNA in the livers were measured by RT-PCR.

RESULTS: Serum transaminase level and liver lesions in Con A-induced mice were markedly reduced by oral administration of 100, 200 mg/kg of bicyclol. TNF-α level in serum was also reduced by bicyclol. Con A injection induced up-regulation of TNF-α, IFN-γ, Fas and FasL mRNA expression in liver tissues. Bicyclol significantly down-regulated the expression of IFN-γ, Fas and FasL mRNA, but only slightly affected TNF-α mRNA expression in liver tissues.

CONCLUSION: Bicyclol protects against Con A-induced liver injury mainly through inhibition of Fas/FasL mRNA expression in liver tissues and TNF-α release in mice.

Li M, Liu GT. Inhibition of Fas/FasL mRNA expression and TNF-α release in concanavalin A-induced liver injury in mice by bicyclol. *World J Gastroenterol* 2004; 10(12): 1775-1779
http://www.wjgnet.com/1007-9327/10/1775.asp

INTRODUCTION

Viral hepatitis is a serious health problem worldwide, as more than two billion people alive today have been infected by hepatitis B virus, and 170 million people have been infected by hepatitis C virus[1]. Although a number of drugs such as interferon-2α and lamivudine have been used in the treatment of viral hepatitis, the efficacy of these drugs is still limited and some side effect are severe[2,3]. Therefore, it is necessary to develop new anti-hepatitis drugs. Bicyclol is new synthesized anti-hepatitis drug, chemically named 4, 4'-dimethoxy-5, 6, 5', 6'-dimethylene-dioxy-2-hydroxymethyl- 2'-carbonyl biphenyl. Our previous studies demonstrated that bicyclol has anti-liver injury, anti-liver fibrosis and anti-hepatitis virus activities[4]. Clinical trials indicated that bicyclol markedly normalized the elevated level of serum transaminase in patient with viral hepatitis B, and also inhibited HBV-DNA replication[5]. It is known that the liver injury induced by CCl_4, acetaminophen and D-galactosamine is mainly caused by free radicals and oxidative stress[6,7]. The protection of bicyclol against CCl_4-, acetaminophen-induced liver injury, is closely related to its elimination of free radicals and inhibition of oxidative stress. However, the pathogenesis of human viral hepatitis is different from hepatotoxicants induced liver injury. Human viral hepatitis is a disease resulting from destruction of virus-infected hepatocytes through immune-mediated mechanism[8,9]. Thus, it is necessary to further investigate if there are other mechanisms involved in the protective effect of bicyclol against liver injury in addition to its anti-oxidative activity. Recently, a model of immune-mediated liver injury in mice was established by injection of T cell mitogen Con A, which is an available animal model relevant to human hepatitis and hepatocellular damage[10]. Previous studies demonstrated that activated T cell-mediated cellular immunity is responsible for the liver damages in Con A model. TNF-α released from activated T lymphocytes and Kupffer cells plays a critical role in the process of liver damage and hepatocyte apoptosis[11-13]. In addition, Fas and Fas ligand (FasL) pathway is involved in the pathogenesis of hepatocytes apoptosis and necrosis[14]. Therefore, the present study was to investigate the effect of bicyclol on Con A induced immune-mediated liver injury and its mechanisms. Figure1 shows the chemical structure of bicyclol.

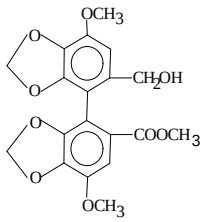

Figure 1 Chemical structure of bicyclol.

MATERIALS AND METHODS

Animals

Male C57BL/6 mice weighing 21-25 g were obtained from the Animal Center of Chinese Academy of Medical Sciences. They were fed standard maintenance diet and water throughout the experiments. All animals received care in compliance with the guidelines of China Ministry of Health.

Reagents

Bicyclol was kindly provided by Professor Zhang CZ in the Department of Pharmaceutical Chemistry of our institute. The purity of bicyclol was over 99% and not dissolved in water. Type IV Con A was purchased from Sigma Chemical Co. (St. Louis, MO, USA). ALT kit was purchased from BHKT Chemical Reagent Co., Ltd (Beijing, China). ELISA kit for

TNF-α determination was provided by Jingmei Biotechnology Co, Ltd (Beijing, China).

Con A-induced hepatitis in mice and drug administration

Control mice were injected pyrogen-free phosphate-buffered saline (PBS). A dose of 23 mg/kg of Con A was injected via tail vein. Bicyclol was suspended in 5 g/L sodium carboxymethylcellulose (Na-CMC) just before use. The 200 mg/kg and 100 mg/kg of bicyclol were administered orally three times, 24, 12, 1 h before Con A injection.

Assay for serum ALT activity and TNF-α levels

Serum from individual mouse was obtained at various intervals after Con A injection. Alanine aminotransferase (ALT) level was determined by a biochemical kit according to the manufacturer's instruction. The assay of serum TNF-α level was performed with specific ELISA kit.

Histopathological examination of liver tissue

Liver samples from individual mouse were fixed in 40 g/L neutral formaldehyde solution, embedded in paraffin, sliced into sections 5-μm of thickness and stained with hematoxylin and eosin for histological examination. The degrees of liver injury were graded based on a score of 0-3[15] and expressed as the mean of 10 different fields of each slide.

Detection of Fas, Fas ligand (FasL), TNF-α, and IFN-γ expression by semiquantitative RT-PCR

Total RNA from mouse liver was extracted by TRIzol reagent (Gibco USA)[16]. RT-PCR was conducted to detect Fas, FasL, TNF-α and IFN-γ gene expression. The primers for Fas were as follows: 5' -TGCACAGAAGGGAAGGAGTA-3' and 5' -ATG GTTTCACGACTGGAGGT-3' ; for FasL: 5' -GACAGCAGTG CCACTTCATC-3' and 5' - TTAAGGCTTTGGTTG GTGAA-3' ; for IFN-γ: 5' -CTCAAGTGGCATAGATGTGG-3' and 5' -ACT CCTTTTCCGCTTCCTGA-3' ; for TNF-α: 5' -GGCGGTGCCT ATGTCTCAG-3' and 5' -GGGCAGCCTTGTC CCTTGA-3' ; and for Cu/Zn SOD: 5' -TCTGCGTGCTGAAG GGCGAC-3' ; and 5' -CTCCTGAGAGTGAGATCACA-3' . mRNA was reversely transcribed with AMV reverse transcriptase and then amplified using *Tfl* DNA polymerase for 35 cycles as follows: at 94 ℃ for 30 s (dissociation), at 60 ℃ for 60 s (annealing), and at 72 ℃ for 90 s (primer extension). PCR amplification products were visualized in 2% agarose gels after staining with ethidium bromide. The density of the PCR products was compared with Cu/Zn SOD, which was used as an internal control. Briefly, the spot density of each band in the gel was measured with the Kodak digital imaging system (Kodak DC120, Digital science 1D system, USA). The percentage of gene expression was calculated by the following equation: (density of cytokine product/density of SOD product) ×100.

Statistical analysis

All data are expressed as mean±SD and analyzed by Student's *t*-test.

RESULTS

Effect of bicyclol on Con A-induced aminotransferase elevation in serum

Injection of Con A to mice caused a time dependent increase in serum ALT levels (Figure 2). ALT levels increased significantly and reached a maximum at 6 h and maintained at plateau for 16 h after Con A injection. Administration of 200 mg/kg and 100 mg/kg of bicyclol to mice for three times significantly reduced the elevated serum ALT levels at 12 h and 16 h after Con A administration (Table 1).

Effect of bicyclol on liver histology

Twelve hours after Con A injection, histological analysis of the liver sections of Con A-treated mice showed widespread areas of necrosis and inflammation within the liver lobules and around the central veins and portal tracts (Figure 3A,B). Extensive lesions were characterized by massive hepatocytes coagulative necrosis, and cytoplasmic swelling of most living hepatocytes and nuclear chromatin condensation were found frequently, which indicated hepatocytes apoptosis. A moderate infiltration of lymphocytes and mononuclear cells in the portal area and around the central vein were also observed. As shown in Figure 3C, bicyclol reduced the areas of lesions and the extent of liver injury induced by Con A. The extent of lymphocyte infiltration in bicyclol treated mice also reduced significantly. The extent of liver necrosis was classified using a four degree score as shown in the footnote of Table 2.

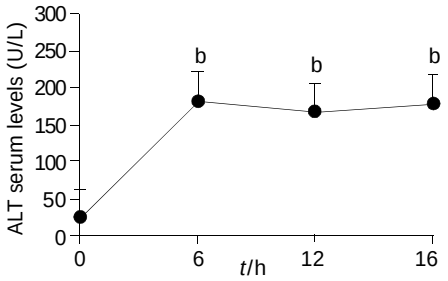

Figure 2 Time-course of Con A-induced liver serum ALT elevation in mice. $^{b}P<0.01$ *vs* other time.

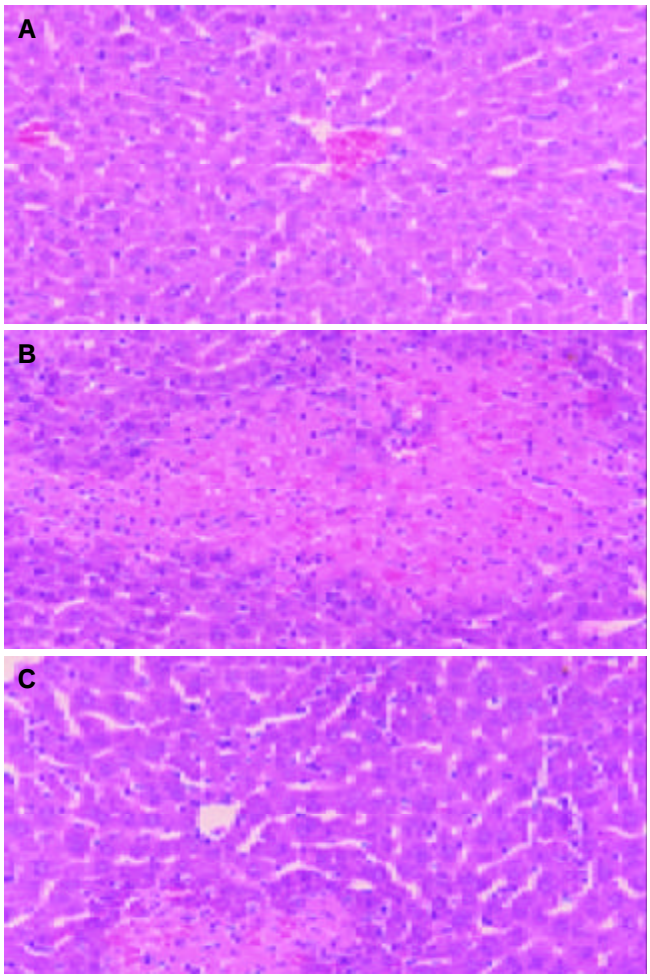

Figure 3 Light micrographs of livers from mice treated with Con A alone or in combination with bicyclol. Original magnification×200. A: normal control mouse. B: Con A injected mouse; C, mouse treated with bicyclol 200 mg / kg.

Table 1 Protection of bicyclol against Con A induced liver injury in mice as determined by ALT(U/L)

Time	Con A alone	Con A+bicyclol 200 mg/kg	Con A+bicyclol 100 mg/kg
12 h	161.5±63.11	27.1±10.8[b]	50.1±15.9[a]
16 h	165.8±8.76	10.6±12.8[b]	30.7±27.4[b]

Data are mean±SD of 8 mice per group. [a]$P<0.05$, [b]$P<0.01$. *vs* Con A alone. Serum ALT levels were measured 12 h and 16 h after Con A injection, respectively.

Table 2 Effect of bicyclol on liver histology by evaluation the degree of liver injury 12 h after Con A injection

Group	Grade of liver injury			
	0	1	2	3
Normal (n=7)	7	0	0	0
Con A alone (n=7)	0	0	0	7
ConA+bicyclol 200 mg/kg (n=8)	3	2	1	2
ConA+bicyclol 100 mg/kg (n=7)	1	2	3	1

Histological degree of liver injury is classified according to the area of coagulative necrosis in hepatic lobules as follows: grade 0, no coagulative necrosis; grade 1, coagulative necrosis area <10%; grade 2, coagulative necrosis area between 10% and 25%; grade 3, coagulative necrosis area >25%.

Lowering effect of bicyclol on serum TNF-α level in Con A-injected mice

Mice were killed at the indicated time points after injection of 23 mg/kg Con A. As shown in Figure 4, serum TNF-α level increased significantly 1-2 h after Con A injection, and then showed a marked decline at 4 h. At 24 h, the level of TNF-α level was still slightly higher than the normal mice but not significantly (Figure 4).

The treatments of mice with bicyclol 200 mg/kg caused a decrease of the elevated TNF-α level by about 50% two hours after Con A injection ($P<0.05$). Bicyclol 100 mg/kg also decreased serum TNF-α concentration about 25% but not significantly statistically (Figure 5).

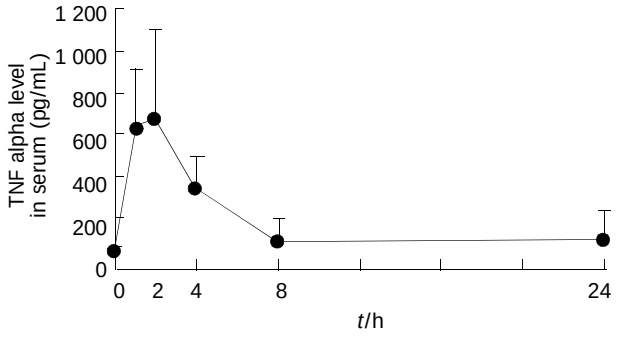

Figure 4 Dynamic changes of serum TNF-α level after Con A injection in mice. Each point represents mean±SD of six mice.

Effect of bicyclol on expressions of liver TNF-α, IFN-γ, Fas and FasL mRNA in Con A-treated mice

One hour after the last administration of bicyclol, mice were injected 23 mg/kg of Con A. The livers were removed 2 h later. Total liver RNA was isolated, reversely transcribed, and amplified by PCR using primers for TNF-α, IFN-γ, Fas and FasL, respectively. Cu/Zn SOD was used as an internal control. As shown in Figure 6, TNF-α and IFN-γ mRNA were undetectable in livers from normal control mice, while the mice injected with Con A showed TNF-α and IFN-γ mRNA expression apparently. Prior administration of bicyclol 200 mg/kg reduced about 40% IFN-γ mRNA expression induced by Con A, but had slight influence on up-regulation of TNF-α mRNA in Con A injected mice.

Although Fas and FasL mRNA levels were detectable in normal control mice, significant increase of both Fas and FasL mRNA levels was demonstrated in Con A challenged mice. Mouse liver Fas mRNA level was more than that of FasL both in normal control and Con A injected groups. Administration of bicyclol down-regulated Fas and FasL mRNA expression to approximately normal level.

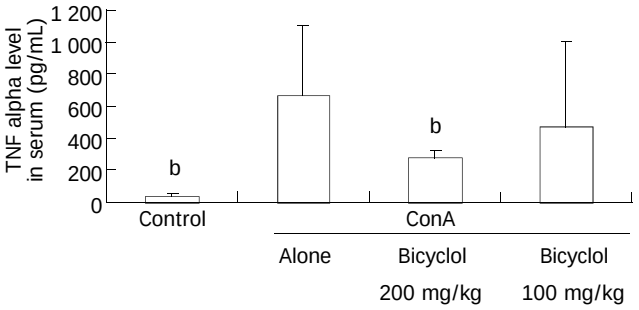

Figure 5 Lowering effect of bicyclol on the elevated serum TNF-α Level induced by Con A injection in mice. Each bar represents mean±SD of 6 mice per group [b]$P<0.01$ *vs* Con A alone.

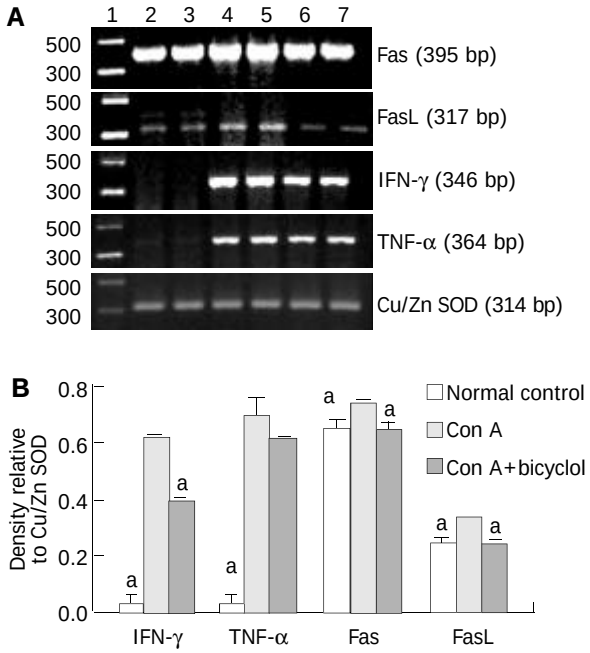

Figure 6 Effect of bicyclol on Con A induced TNF-α, IFN-γ, Fas and FasL mRNA expression determined by RT-PCR. A: Photograph of ethidium bromide-stained amplification products. Lane 1, molecular mass markers; lane 2 and lane 3, control liver; lane 4 and lane 5, liver 2 h after Con A administration alone; lane 6 and lane 7, liver 2 h after injection of Con A in combination with 200 mg/kg bicyclol. B: Relative band intensity of amplification products compared with Cu/Zn SOD mRNA. Data represent the mean of two lanes. Each lane corresponds to the pooled livers from two mice. [a]$P<0.05$ *vs* Con A alone.

DISCUSSION

The immune cell-mediated liver injury is a critical event in the pathogenesis of human viral hepatitis[17-19]. Cell immunity is involved in the immune clearance of virus-infected hepatocytes and at the same time damage virus-infected hepatocytes. This conclusion came from the findings that infiltrating T cells were

observed in the liver tissue of hepatitis patients[20,21]. Con A induced liver injury is a T-cell-dependent hepatitis model, which situation is relevant to human liver injury[22]. In Con A induced hepatitis, T cell activation plays a crucial role in the process of liver injury, because lymphocytes depleted mice or severe combined immunodeficiency disease (SCID) mice can not develop liver injury after Con A injection, and pretreatment of mice with a monoclonal antibody which *in vivo* destroys Thy1.2 antigen-bearing T cells abrogated the susceptibility of these animals toward the hepatotoxicity induced by Con A[10]. In the present study lymphocyte infiltration was observed in the portal area and around the central vein of damaged liver tissue. Biochemical and histological data showed that prior administration of bicyclol, a new anti-hepatitis drug has protective effect against Con A induced liver injury in mice. In order to elucidate how bicyclol exerts its protective effect against Con A induced liver injury, mice were pretreated with bicyclol. The results showed that bicyclol markedly decreased lymphocyte accumulation into liver.

Cytotoxic T lymphocytes play an important role in the pathogenesis of viral hepatitis by inducing hepatocyte apoptosis[23,8]. In the study of Moriyama *et al*.[24] transfer of HBV-specific cytotoxic T lymphocytes can mediate liver cell necrosis in the HBV transgenic murine. As viral hepatitis, hepatocytes apoptosis is a dominant feature of Con A induced hepatitis as measured by DNA fragmentation and morphological observation. The apoptosis cascade can be initiated by a ligand, which binds to its receptors on the cell surface. Ligands such as FasL and TNF-α play an important role in Con A induced hepatitis. Interaction of Fas and FasL is an important pathway that mediates the target cytolysis by cytotoxic T lymphocytes[25]. In *gld/gld* mice, in which FasL is defective, the development of the disease is completely suppressed and in *lpr/lpr* mice, the suppression of Fas mRNA is incomplete, the hepatitis is partially suppressed. Antibody against Fas can block the development of hepatitis[14]. When FasL binds to Fas, the receptor molecules trimerize, leading to clustering of death domains, activation of a series of caspases and the final apoptosis of liver cells[26]. In chronic hepatitis B (CHB), the intensity of FasL mRNA showed a positive correlation with the histological activity and serum alanine aminotransferase level[27]. Immunohistochemical study suggested that Fas antigen expression plays an important role in inflammation in the hepatitis C virus-infected liver[28]. In our previous study, we found that bicyclol inhibited Con A induced DNA fragmentation[29]. To further investigate the mechanism of bicyclol in protection against liver injury, we measured the expression of Fas/FasL in Con A-induced liver injury.

In our study, we found that both FasL and Fas mRNA expressions were up-regulated significantly after Con A injection. Bicyclol down-regulated the expression of FasL and Fas close to normal level. The results explained why bicyclol could inhibit apoptosis of hepatocytes in Con A hepatitis model in our previous experiment[29]. It is known that Fas expression can be activated by IFN-γ to enhance apoptosis. Fas mRNA expression was reduced by 50% in the liver of IFN-$\gamma^{-/-}$ mice compared with that in IFN-$\gamma^{+/-}$ mice[30]. Because IFN-γ can affect the expression of Fas, we further investigated the effect of bicyclol on IFN-γ mRNA expression. Our results indicated that bicyclol reduced the expression of IFN-γ mRNA by about 40% in the livers of Con A treated mice, which was associated with the inhibition of Fas.

TNF-α is another important ligand to induce hepatocyte apoptosis. Activated lymphocytes stimulated the macrophages to release TNF-α and the activated lymphocyte itself is the potential source of TNF-α[31]. This proinflammatory cytokine can produce a direct cytotoxic effect to transcription-inhibited hepatocytes *in vitro* when bound to TNF-R[32]. In addition to the effect on Fas/FasL pathway, bicyclol significantly inhibited the release of TNF-α. Con A significantly increased the release of serum TNF-α and mRNA expression in liver tissue. Bicyclol reduced the serum level of TNF-α by about 50%. It, however, showed a slight effect (10%) on the mRNA expression in liver. It seems that bicyclol inhibited TNF-α release mostly at posttranscriptional level, which needs further investigation.

In conclusion, bicyclol protects mice against Con A-induced liver injury through at least two mechanisms: down-regulation the expression of Fas/FasL mRNA, and prevention of proinflammatory cytokine TNF-α release.

ACKNOWLEDGEMENTS

We thank Ms. Yong-Rong Zhang and Ms. Yan Liu from the Department of Pathology of our institute for their support in the examination of liver morphology by light microscopy. We also thank Ling-Hong Yu for her helpful advice and excellent technical assistance.

REFERENCES

1 **Liu J**, McIntosh H, Lin H. Chinese medicinal herbs for chronic hepatitis B: a systematic review. *Liver* 2001; **21**: 280-286
2 **Haria M**, Benfield P. Interferon-alpha-2a. A review of its pharmacological properties and therapeutic use in the management of viral hepatitis. *Drugs* 1995; **50**: 873-896
3 **Heathcote J**. Treatment of HBe antigen-positive chronic hepatitis B. *Semin Liver Dis* 2003; **23**: 69-80
4 **Liu GT**. The anti-virus and hepatoprotective effect of bicyclol and its mechanism of action. *Chin J New Drug Clin* 2001; **10**: 325-327
5 **Yao GB**, Ji YY, Wang QH, Zhou XQ, Xu DZ, Chen XY. A randomized double-blind controlled trial of bicyclol in treatment of chronic hepatitis B. *Chin J New Drug Clin* 2002; **21**: 457-461
6 **Suematsu T**, Matsumura T, Sato N, Miyamoto T, Ooka T, Kamada T, Abe H. Lipid peroxidation in alcoholic liver disease in humans. *Alcohol Clin Exp Res* 1981; **5**: 427-430
7 **Slater TF**. Necrogenic action of carbon tetrachloride in the rat: a speculative mechanism based on activation. *Nature* 1966; **209**: 36-40
8 **Chisari FV**. Cytotoxic T cells and viral hepatitis. *J Clin Invest* 1997; **99**: 1472-1477
9 **Jacobson Brown PM**, Neuman MG. Immunopathogenesis of hepatitis C viral infection: Th1/Th2 responses and the role of cytokines. *Clin Biochem* 2001; **34**: 167-171
10 **Tiegs G**, Hentschel J, Wendel A. A T cell-dependent experimental liver injury in mice. *J Clin Invest* 1992; **90**: 196-203
11 **Gantner F**, Leist M, Lohse AW, Germann PG, Tiegs G. Concanavalin A induced T-cell mediated hepatic injury in mice: the role of tumor necrosis factor. *Hepatology* 1995; **21**: 190-198
12 **Ksontini R**, Colagiovanni DB, Josephs MD, Edwards CK 3rd, Tannahill CL, Solorzano CC, Norman J, Denham W, Clare-Salzler M, MacKay SL, Moldawer LL. Disparate roles for TNF-alpha and Fas ligand in concanavalin A-induced hepatitis. *J Immunol* 1998; **160**: 4082-4089
13 **Zang GQ**, Zhou XQ, Yu H, Xie Q, Zhao GM, Wang B, Guo Q, Xiang YQ, Liao D. Effect of hepatocyte apoptosis induced by TNF-alpha on acute severe hepatitis in mouse models. *World J Gastroenterol* 2000; **6**: 688-692
14 **Tagawa Y**, Kakuta S, Iwakura Y. Involvement of Fas/Fas ligand system-mediated apoptosis in the development of concanavalin A-induced hepatitis. *Eur J Immunol* 1998; **28**: 4105-4113
15 **Mochida S**, Ohno A, Arai M, Tamatani T, Miyasaka M, Fujiwara K. Role of adhesion molecules in the development of massive hepatic necrosis in rats. *Hepatoloy* 1996; **23**: 320-328
16 **Chomczynski P**, Sacchi N. Single-step method of RNA isolation by acid guanidinium thiocyanate-phenol-chloroform extraction. *Anal Biochem* 1987; **162**: 156-159
17 **Koziel MJ**. The immunopathogenesis of HBV infection. *Antivir Ther* 1998; **3**: 13-24
18 **Chisari FV,** Ferrari C. Hepatitis B virus immunopathogenesis.

Annu Rev Immunol 1995; **13**: 29-60
19 **Koziel MJ**. Cytokines in viral hepatitis. *Semin Liver Dis* 1999; **19**: 157-169
20 **Dienes HP**, Hutteroth T, Hess G, Meuer SC. Immunoelectron microscopic observations on the inflammatory infiltrates and HLA antigens in hepatitis B and non-A, non-B. *Hepatology* 1987; **7**: 1317-1325
21 **Volpes R**, van den Oord JJ, Desmet VJ. Memory T cells represent the predominant lymphocyte subset in acute and chronic liver inflammation. *Hepatology* 1991; **13**: 826-829
22 **Tiegs G**, Gantner F. Immunotoxicology of T cell-dependent experimental liver injury. *Exp Toxicol Pathol* 1996; **48**: 471-476
23 **Koziel MJ**, Dudley D, Wong JT, Dienstag J, Houghton M, Ralston R, Walker BD. Intrahepatic cytotoxic T lymphocytes specific for hepatitis C virus in persons with chronic hepatitis. *J Immunol* 1992; **149**: 3339-3344
24 **Moriyama T**, Guilhot S, Klopchin K, Moss B, Pinkert CA, Palmiter RD, Brinster RL, Kanagawa O, Chisari FV. Immunobiology and pathogenesis of hepatocellular injury in hepatitis B virus transgenic mice. *Science* 1990; **248**: 361-364
25 **Kagi D**, Vignaux F, Ledermann B, Burki K, Depraetere V, Nagata S, Hengartner H, Golstein P. Fas and perforin pathways as major mechanisms of T cell-mediated cytotoxicity. *Science* 1994; **265**: 528-530
26 **Kaplowitz N**. Mechanisms of liver cell injury. *J Hepatol* 2000; **32**: 39-47
27 **Seino K**, Kayagaki N, Takeda K, Fukao K, Okumura K, Yagita H. Contribution of Fas ligand to T cell-mediated hepatic injury in mice. *Gastroenterology* 1997; **113**: 1315-1322
28 **Hiramatsu N**, Hayashi N, Katayama K, Mochizuki K, Kawanishi Y, Kasahara A, Fusamoto H, Kamada T. Immunohistochemical detection of Fas antigen in liver tissue of patients with chronic hepatitis C. *Hepatology* 1994; **19**: 1354-1359
29 **Zhao DM**, Liu GT. Protective effect of bicyclol on concanavalinA-induced liver nuclear DNA injury in mice. *Natl Med J China* 2001; **81**: 844-848
30 **Tagawa Y**, Sekikawa K, Iwakura Y. Suppression of concanavalin A-induced hepatitis in IFN-γ(-/-) mice, but not in TNF-α(-/-) mice: role for IFN-γ in activating apoptosis of hepatocytes. *J Immunol* 1997; **159**: 1418-1428
31 **Gantner F**, Leist M, Kusters S, Vogt K, Volk HD, Tiegs G. T cell stimulus-induced crosstalk between lymphocytes and liver macrophages results in augmented cytokine release. *Exp Cell Res* 1996; **229**: 137-146
32 **Leist M**, Gantner F, Jilg S, Wendel A. Activation of the 55 kDa TNF receptor is necessary and sufficient for TNF-induced liver failure, hepatocyte apoptosis, and nitrite release. *J Immunol* 1995; **154**: 1307-1316

Edited by Zhu LH and Wang XL **Proofread by** Xu FM

PO Box 2345, Beijing 100023, China
Fax: +86-10-85381893
E-mail: wjg@wjgnet.com www.wjgnet.com

World J Gastroenterol 2004;10(12):1780-1784
World Journal of Gastroenterology
Copyright ©2004 by The WJG Press ISSN 1007-9327

• BASIC RESEARCH •

Expression of gonadotropin-releasing hormone receptor and effect of gonadotropin-releasing hormone analogue on proliferation of cultured gastric smooth muscle cells of rats

Lei Chen, Hong-Xuan He, Xu-De Sun, Jing Zhao, Li-Hong Liu, Wei-Quan Huang, Rong-Qing Zhang

Lei Chen, Hong-Xuan He, Rong-Qing Zhang, Department of Biological Science and Biotechnology, Tsinghua University, Beijing, 100084, China
Xu-De Sun, Department of Anaesthesiology, Tangdu Hospital, the Fourth Military Medical University, Xi' an, 710038, Shaanxi Province, China
Lei Chen, Jing Zhao, Li-Hong Liu, Wei-Quan Huang, Faculty of Basic Medicine, the Fourth Military Medical University, Xi' an, 710032, Shaanxi Province, China
Supported by the Natural Science Foundation of China, No. 39770388
Co-correspondents: Wei-Quan Huang
Correspondence to: Professor Rong-Qing Zhang, Institute of Marine Biotechnology, Department of Biological Science and Biotechnology, Tsinghua University, Beijing, 100084, China. rqzhang@mail.tsinghua.edu.cn
Telephone: +86-10-62772899 **Fax:** +86-10-62772899
Received: 2003-12-19 **Accepted:** 2004-02-01

Abstract

AIM: To investigate the expression of gonadotropin-releasing hormone (GnRH) receptor and the effects of GnRH analog (alarelin) on proliferation of cultured gastric smooth muscle cells (GSMC) of rats.

METHODS: Immunohistochemical ABC methods and *in situ* hybridization methods were used to dectect protein and mRNA expression of GnRH receptor in GSMC, respectively. Techniques of cell culture, OD value of MTT test, measure of ^{3}H-TdR incorporation, average fluorescent values of proliferating cell nuclear antigen (PCNA) and flow cytometric DNA analysis were used in the experiment.

RESULTS: The cultured GSMC of rats showed immunoreactivity for GnRH receptor; positive staining was located in cytoplasm. GnRH receptor mRNA hybridized signals were also detected in cytoplasm. When alarelin (10^{-9}, 10^{-7}, 10^{-5} mol/L) was administered into the medium and incubated for 24 h, OD value of MTT, ^{3}H-TdR incorporation and average fluorescent values of PCNA all decreased significantly as compared with the control group ($P<0.05$). The maximum inhibitory effect on cell proliferation was achieved a concentration of 10^{-5} mol/L and it acted in a dose-dependent manner. Flow cytometric DNA analysis revealed that alarelin could significantly enhance ratio of G_1 phase and decrease ratio of S phase of GSMC of rats ($P<0.05$).The maximum inhibitory effect on ratio of S phase was at the concentration of 10^{-5} mol/L and also acted in a dose-dependent manner.

CONCLUSION: Our data suggest that GnRH receptor can be expressed by GSMC of rats. GnRH analogue can directly inhibit proliferation and DNA synthesis of rat GSMC through GnRH receptors.

Chen L, He HX, Sun XD, Zhao J, Liu LH, Huang WQ, Zhang RQ. Expression of gonadotropin-releasing hormone receptor and effect of gonadotropin-releasing hormone analogue on proliferation of cultured gastric smooth muscle cells of rats. *World J Gastroenterol* 2004; 10(12): 1780-1784
http://www.wjgnet.com/1007-9327/10/1780.asp

INTRODUCTION

Gonadotropin releasing hormone (GnRH), a decapeptide synthesized by the neuroendocrine cells in the pro-optic area of brain, plays an important role in regulation of reproductive function. After released from the hypothalamus, GnRH binds to a specific receptor on the plasma membrane of the pituitary gonadotroph, resulting in stimulation of FSH and LH biosynthesis and release. There is evidence that GnRH and its receptors are expressed in numerous extrapituitary tissues, such as syncytiotrophoblast cells[1], human granulosa-Luteal cells[2], human peripheral lymphocytes[3,4] and so on. They are not only expressed in normal tissues, but also widely exist in various carcinoma that derived from reproductive (ovary cancer[5] and prostate cancer[6]) or non-reproductive tissues (breast cancer[7], lung cancer[8], pancreas cancer[9] and hepatocellular carcinoma[10], *et al*). Our previous studies have shown the presence of GnRH and its receptor in rat digestive tract[11], submaxillary gland[12], thyroid glang[13] and pancreas[14] and proposed that GnRH could be classified as a kind of brain-gut hormone. Presently, we first investigated the expression of GnRH receptor in cultured rat gastric smooth muscle cells (GSMC) and investigate the effect of GnRH analogue (alarelin) on the proliferation of cultured GSMC of rats.

MATERIALS AND METHODS

Materials

GnRH anti-idiotypic antibody was prepared by our department[15]. ABC kit was the product of Vector Company (Vector Laboratories Burlingame, CA, U.S.A.). MTT (3-(4, 5-dimethythiazol -zyl-2)-2, 5-diphenyltetrazolium), colleagnase I, PPO (2, 5-diphenyloxazole) and POPOP (1, 4-bis (5-phenyloxazol-2-yl) benzene) were purchased from Sigma Company (Staint Louis, Missouri, U.S.A.). DMEM and Trypsin were the products of Gibco Company (Carlsbad, California, U.S.A.). Alarelin was purchased from Shanghai Lizhu Biochemical and Pharmaceutical Company, Shanghai, China. PCNA (Proliferating cell nuclear antigen) antibody and immunofluorescent kit were purchased from Boster Company (Wuhan, China). ^{3}H-TdR was purchased from Academy of Atomic Energy Sciences of China (Shanghai, China). The 1-3-day-old male Sprague-Dawley rats were purchased from the Center of Laboratory Animal Medicine, the Fourth Military Medical University, (Xi' an, China).

Preparation and culture of GSMC of rats

The culture of GSMC of rats was performed as described previously with modifications[16,17]. 1-3-day-old immature male Sprague-Dawley rats were sterilized by 750 mL/L alchol; removed the stomaches and put them into cool Hanks solution (mmol/L: $CaCl_2$ 1.3, KCl 5.4, KH_2PO_4 0.4, $MgCl_2 \cdot 6H_2O$ 0.4, $MgSO_4 \cdot 7H_2O$ 0.4, NaCl 137, glucose 5.6) immediately. The mucosas were

removed by scrapping with razorblade. The gastric smooth muscle tissues were minced into l.0 mm^3 pieces with tissue chopper, then put them into DMEM containing 1 mg/L collagenase I at 37 ℃ for 30-60 min, and the GSMCs were collected at an interval of 20 min. The cell suspension was centrifuged at 500 r/min for 5 min, washed 2 times in DMEM, then cultured in DMEM containing 100 mL/L calf serum, 100 U/mL pencillin G and 100 U/mL streptomycin under a humidified atmosphere of 50 mL/L CO_2 in air. To obtain pure GSMC and remove the fibroblasts, the cells were preattached in flasks with 10% calf serum under DMEM in a humidified atmosphere of 5% CO_2 or 90 min at 37 ℃. Afterwards, the cells were maintained in fresh DMEM containing 100 mL/L calf serum and removed it per 3 d and subsequently subcultured per 4-5 d by treatment with trypsin (2.5 g/L). The GSMC were identified by "valley and hill appearance"[17] and showed α-actin immunoreactivity, which was located in cytoplasm. The experiments were performed with monolayer of cells from passage 3-5.

Immunocytochemical procedure

The GSMCs (1×10^5/mL) were seeded in a six-well plate containing the coverglasses inside. The cells of passage 3-5 were fixed in 4% paraformaldehyde solution for 30 min at room temperature. The coverglasses were washed 3 times with phosphate-buffered saline (PBS, pH 7.2), and put into methanol-H_2O_2 for 30 min to remove endogenous peroxidase activity. Then they were stained using immunohistochemical ABC method. They were incubated with first antibody, rabbit GnRH anti-idiotypic antibody (1:200 dilution) at 4 ℃ for 18-24 h. Then they were incubabated with second antibody, biotin labeled goat anti-rabbit IgG antibody (1:400 dilution), at room temperature for 2 h, followed by incubation with ABC complex (1:400 dilution), at room temperature for 1 h. Finally, DAB (diaminobenzedin) was used for color developed, and then the slides were washed in distilled water to stop the reaction, dehydrated in alcohol, hyalinized in xylene, and mounted on Canada balsam. The first antibody was replaced by normal and diluted rabbit serum for the negative control.

In situ hybridization

The probe was produced according to the cDNA sequence of the rat' s pituitary GnRH receptor[12,18]. The sequence was: 5' -ATGTATGCCCCCAGCCTTCATGATGGTGATTAGCC TGGATC-3' . The digoxigeni was labeled at 5' -end by the TaKaRa Biotechnology Company, (Dalian, China). The *in situ* hybridization was carried out on the coverglasses after the cells were fixed in 40 g/L paraformaldehyde containing 1 g/L DEPC (Diethyl pyrocarbonate) for 30 min. Then they were processed as follows: The coverglasses were rinsed in 0.01 mol/L PBS (pH 7.2) for 5 min×3, in Proteinase K (1 μg/mL) for 2 min at 37 ℃. They were post-fixed in 40 g/L paraformaldehyde for 5 min, washed in distilled water for 5 min×3. After being dried in the air, each coverglass was applied with the hybridization buffer containing GnRH receptor oligonuclicotide probe (2.0 μg/mL), and hybridization was carried out in sealed humid box at 42 ℃ for 20 h. After that the slides were washed with 2×SSC at 37 ℃ for 5 min×3, 0.1×SSC at 37 ℃ for 10 min×2, they were incubated with mouse-anti-dig antibody at room temperature for 2 h. Thereafter, the slides were washed with 0.5 mol/L TBS for 5 min×3, followed by incubation with biotin-labeled goat-anti-mouse IgG antibody for 1 h at 37 ℃. The slides were washed with 0.5 mol/L TBS for 5 min×3 and incubated with SABC-AP for 30 min at 37 ℃. The sections were rinsed in 0.5 mol/L TBS for 5 min×4, and the alkaline phosphatase reaction was conducted by incubation with complex solution of NBT (Nitrio-blue tetrazolium) and BCIP (5-bromo-4-chloro -3-indo-lyl phosphate) for 20-30 min. Finally, the slides were washed in distilled water to stop the reaction, and then dehydrated in alcohol, hyalinized in xylene, and mounted on Canada balsam. The slides were incubated with normal mouse serum instead of the mouse-anti-dig antibody in absence of the labeled probe for the negative controls.

MTT assay

The cells were trypsinized in a solution of 2.5 g/L trypsin and seeded in a 96-well plate at a density of 10^4 cells/(0.1 mL/well). After the cells were grown for 24 h to approximately 800 g/L subconfluent state, 0.1 mL medium containing 2.5% calf serum and various concentrations (10^{-9}, 10^{-7}, 10^{-5} mol/ L) of alarelin was added to each well, respectively, and incubated for 24 h in a CO_2 incubator. Each concentration was tested in at least 12 wells. The MTT assay was performed as described previously with mondifications[19]. Briefly, 15 μL of MTT solution (5 g/L, PBS, pH 7.2) was added to each well and incubated for 4 h. Then, the medium and MTT were removed and 150 μL of DMSO was added to each well and shaken for 10 min to dissolve the crystal. The OD was determined at 490 nm using an ELISA reader.

^{3}H-TdR incorporation

To observe the role of GnRH analogue in growth regulation of GSMC, a ^{3}H-TdR incorporation assay was performed as previously described[20]. The cells were plated into a 96-well plate at a density of 10^4 cells/(0.1 mL/well). After the cells were grown for 24 h, 0.1 mL medium containing 2.5% calf serum and various concentrations (10^{-9}, 10^{-7}, 10^{-5} mol/L) of alarelin was added to each well, respectively, and incubated for 16 h in a CO_2 incubator. Then the ^{3}H-TdR (2 μCi/mL) was added to each well and continuously incubated for 8 h. Incubation was stopped by adding 1 vol of cold 100 mL/L trichloracetic acid (TCA) which disrupted cells and precipitated the macromolecules. After being washed with a methanol, the precipitate was collected in 9999 fiberglass filter paper, respectively. When the filter paper was dried, 0.5 mL scintillant liquid were mixed and the radioactivity was estimated with a scintillation counter (Backman LS5801). Each concentration was tested in at least 6 wells.

Fluorescent immunocytochemical reaction of PCNA in GSMC

The cells were seeded in six-well plate containing the coverglasses inside. After the cells were grown for 24 h to approximately 800 g/L subconfluent state, 2 mL medium containing 25 mL/L calf serum and various concentrations (10^{-9}, 10^{-7}, 10^{-5} mol/L) of alarelin was added to each well, respectively, and incubated for another 24 h in a CO_2 incubator. Then the monoplayers were fixed in 40 g/L paraformaldehyde solution for 30 min. The cell coverglasses were washed 3 times with PBS (pH 7.2), and then put into methanol-H_2O_2 for 30 min to remove endogenous peroxidase activity. Then PCNA immunofluorescence reaction was carried out according to the manufacturer' instructions. The coverglasses were incubated with the first antibody (mouse antibody, 1:200 dilution) at 4 ℃ overnight, followed by incubation with the second antibody, biotin labeled goat anti-rabbit IgG antibody (1:200 dilution), at room temperature for 2 h. Then the coverglasses were incubated with SABC-fluo Cy3 (1:100 dilution) at room temperature for 1 h. At last, the cells were detected by using the laser confocal microscopy, and scanned the average fluorescent values of PCNA of GSMC. For the negative controls, the first antibody was replaced by normal rabbit serum.

Cell-cycle analysis by flow cytomety

The cells were seeded in 12-well plate at a density of 10^7 cells/(1.5 mL/well). After the cells were grown for 24 h to approximately 800 g/L subconfluent state, 2 mL medium containing 25 mL/L calf serum and various concentrations (10^{-9}-10^{-5} mol/L) of alarelin was added to each well, respectively,

and incubated for another 48 h in a CO_2 incubator. Then the cells were trypsinized in a solution of 2.5 g/L trypsin, fixed in 700 mL/L ethanol and stained by PI (propidium iodide) for DNA analysis. The flow cytometric analyses were performed using EPICS Profile II. DNA content was measured and ratio of each DNA period of cell proliferation was analyzed.

Data analysis

In the proliferation study, the data were expressed as mean±SD. The data were analyzed by SPLM statistical software. $P<0.05$ was considered statistically significant.

RESULTS

Expression and localization of GnRH receptor

Immunocytochemical reaction showed a dark-brown staining in cytoplasm for GnRH receptor immnoreactivity; background was light yellow or no staining; positive cells were identified easily. The two negative controls showed no staining for GnRH receptor. All cultured GSMCs showed immnoreactivity for GnRH receptor in the cytoplasm, but with variations in degrees of intensity of the immunorecativity (Figure 1).

In situ hybridization showed GnRH receptor mRNA hybridized signal was blue, and the background was not stained. The GnRH receptor mRNA hybridization signals could be detected in all cultured GSMCs, but with variation in signal strength between them. The signals were only distributed in the cytoplasm with hybridization negative nuclei (Figure 2). The two negative controls did not show GnRH receptor mRNA hybridized signal.

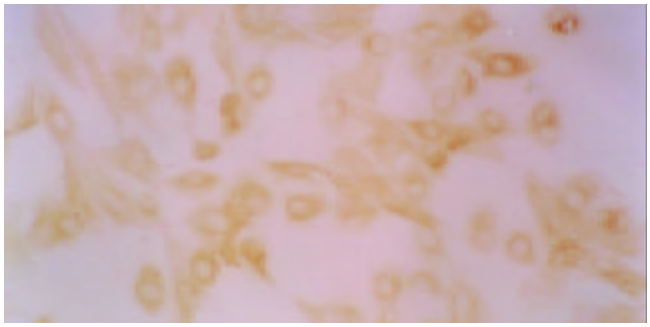

Figure 1 Gastric smooth muscle cells showed GnRH receptor immunoreactivity in cytoplasm. (×200).

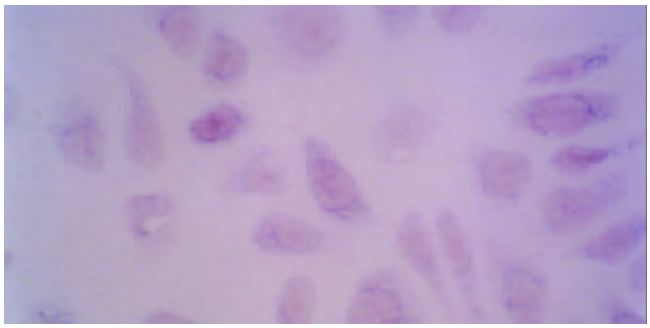

Figure 2 Gastric smooth muscle cells showed GnRH receptor mRNA hybridized signal in cytoplasm. (×400).

Effect of alarelin on GSMC viability

The influence of alarelin on GSMC viability was assessed using the MTT assay. The cell viability in the presence of alarelin was significantly lower than that in the absence of alarelin ($F=59.083$, $P<0.01$). The maximum stimulatory effect on cell viability was achieved at a concentration of 10^{-5} mol/L and it acted in a dose-dependent manner (Table 1).

Table 1 Effects of alarelin on *A* value of MTT of rat GSMC

Group	MTT/A value (n=12)
Control	0.728±0.100
10^{-9} mol/L alarelin	0.533±0.073
10^{-7} mol/L alarelin	0.368±0.029
10^{-5} mol/L alarelin	0.243±0.042

^{3}H-TdR Incorporation assay

To evaluate the functional role of GnRH in GSMC, the cells were treated with different concentrations of alarelin and incubated for 16 h, and then ^{3}H-TdR (2 μCi/mL) was added. After 8 h, ^{3}H-TdR incorporation assays were performed. As shown in Table 2, alarelin inhibited the growth of GSMC in a dose-dependent manner. A significant inhibition of proliferation was detected in the different groups, and the antiproliferative effect was the most evident when the concentration of alarelin at 10^{-5} mol/L ($F=22.33$, $P<0.05$).

Table 2 Effects of alarelin on ^{3}H-TdR Incorporation of rat GSMC

Group	^{3}H-TdR Incorporation (n=6)
Control	1 936.50±440.99
10^{-9} mol/L alarelin	1 448.17±327.72
10^{-7} mol/L alarelin	945.83±374.32
10^{-5} mol/L alarelin	385.83±184.66

The average fluorescent values of PCNA assay

The cells were treated with different concentrations of alarelin (10^{-9}, 10^{-7}, 10^{-5} mol/L) and incubated for another 24 h, and the average fluorescent values of PCNA assays were performed. As shown in Table 3, alarelin significantly inhibited the average fluorescent value in a dose-dependent manner compared with the control group ($F=15.86$, $P<0.01$).

Table 3 Effects of alarelin on average fluorescent values of PCNA in GSMC

Group	Average fluorescent values of PCNA (n=5)
Control	13.48±1.31
10^{-9} mol/L alarelin	11.37±1.99
10^{-7} mol/L alarelin	9.35±1.38
10^{-5} mol/L alarelin	7.37±1.06

Effects of alarelin on GSMC cell cycles

Table 4 showed the ratio of G_1 phase and S phase of DNA period of cell proliferation of each group. The ratio of G_1 phase of DNA in group II- VI were markedly higher than that of the control, but did not increase in a dose-dependent manner ($F=74.94$, $P<0.05$). Moreover, the ratio of S phase of DNA was significantly lower in group II-VI than that in the control and acted in a dose-dependent manner ($F=32.5$, $P<0.05$, except the Group III, V compared with their border groups).

Table 4 Effects of alarelin on GSMC cell cycles (n=4)

Group	Concentration of alarelin	G_1 phase (%)	S phase (%)
Group I	Control	70.80±11.30	17.50±3.40
Group II	10^{-9} mol/L alarelin	80.00±9.42	9.93±1.73
Group III	10^{-8} mol/L alarelin	76.60±8.99	7.10±1.05
Group IV	10^{-7} mol/L alarelin	79.60±7.43	6.60±1.54
Group V	10^{-6} mol/L alarelin	78.50±10.66	5.10±1.01
Group VI	10^{-5} mol/L alarelin	80.20±10.03	3.20±1.20

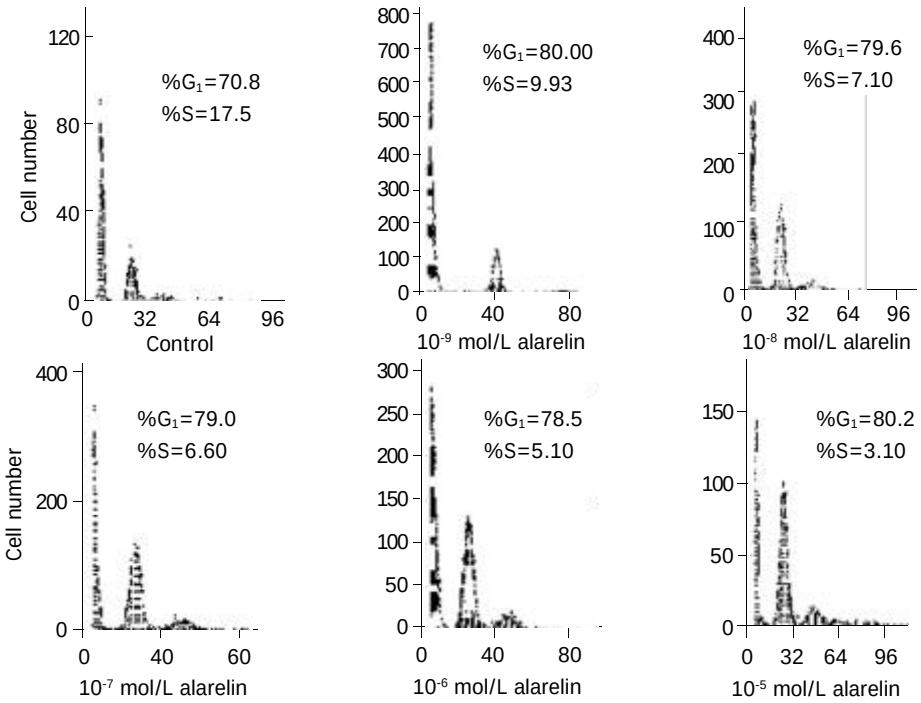

Figure 3 Effects of alarelin on DNA content of GSMCs cell cycles.

DISCUSSION

GnRH anti-idiotypic antibody has been widly applied in immunohistochemical studies of GnRH receptors[11,12,21]. GnRH and its receptor mainly exist in hypothalamus-pituitary axis, and also expressed in extra- hypothalamically, and has extra-pituitary activity. Studies have reported that pancreatic islets have GnRH immunoreactivity[14]. Jan *et al*.[22] reported that GnRH was a possible transmitter in sympathetic ganglion in frog, and our previous studies[4,5] revealed that both GnRH and GnRH receptor were all existed in digestive tract. Our present study revealed, for the first time, that GnRH receptor mRNA was expressed in cultured GSMC of rats. These findings have raised intriguing questions which concern the physiological function of GnRH and its receptor.

GnRH has been suggested to regulate cell growth and proliferation through its receptor in expituitary tissues. GnRH analogues not only have been used and proven to be efficient in treating GnRH receptor-bearing tumors, including carcinomas of the ovary, breast, and endometrium[23-25], but also inhibited the growth and proliferation of normal cell, such as granulose cells and myometrial smooth muscle cells[26,27]. MTT assays and ^{3}H-TdR assays are considered to be the most reliable techniques for measurement of the cell population. Using MTT assays and ^{3}H-TdR assays, we demonstrated that GnRH analogue inhibited growth of normal GSMC of rats in a dose-dependent manner. This inhibitory effect is consistent with the results of Minaretzis *et al*.[26] in granulosa-lutein cells and Chegini *et al*.[27] in myometrial smooth muscle cells. This inhibitory effect of GnRH analogue appears to be receptor-mediated and its exact mechanism of growth inhibitory effect at the receptor level is unclear.

To examine whether GnRH receptor (GnRHR) mediates direct antiproliferative effects, we attempted to assess the effects of alarelin on average fluorescent values of PCNA and cell cycle of GSMC. PCNA, a protein which functions as a cofactor to DNA polymerase delta, has many characteristics which make it an effective marker for evaluating cell proliferation, particularly in S phase[28]. PCNA is a stable cell-cycle regulated nuclear protein, expressed differentially during the cell cycle[29,30], and it is believed to reflect the different stages of the cell cycles, which begins to increase in terminus of G_1, reaches at peak in S phase, and decreases in G_2 and M phases, and this is corresponded with the change of DNA content[28]. In the present study, we found that alarelin inhibited the average fluorescent values of PCNA, and acted in a dose-dependent manner. These might cause by the binding of GnRH analogue with its receptor, which induced the activation of phosphatidylinositol kinase activity, known to stimulate mitogenic response in plasma membranes[31]. By flow cytomety, we demonstrated the GnRH analogue improved the ratios of G_1/G_0 which did not act in a dose-dependent manner, and inhibited the ratios of S phase which acted in a dose-dependent manner. So, the reason of growth inhibition might be that GnRH analogue arrested at G_1/S phase, which inhibits DNA synthesis. These results are consistent with the results of MTT assay, ^{3}H-TdR incorporation and fluorescent value of PCNA.

In summary, we have demonstrated for the first time that GnRH receptor is expressed in GSMC and GnRH analogue has a direct growth inhibitory effect on GSMC of rats that is mediated through GnRH receptor. Our findings strongly suggest that GnRH play an important role in digestive tract.

REFERENCES

1 **Currie WD**, Setoyama T, Lee PS, Baimbridge KG, Church J, Yuen BH, Leung PC. Cytosolic free Ca^{2+} in human syncytiotrophoblast cells increased by gonadotropin-releasing hormone. *Endocrinology* 1993; **133**: 2220-2226

2 **Nathwani PS**, Kang SK, Cheng KW, Choi KC, Leung PC. Regulation of gonadotropin-releasing hormone and its receptor gene expression by 17beta-estradiol in cultured human granulosa-Luteal cells. *Endocrinology* 2000; **141**: 1754-1763

3 **Azad N**, La Paglia N, Jurgens KA, Kirsteins L, Emanuele NV, Kelley MR, Lawrence AM, Mohagheghpour N. Immunoactivation enhances the concentration of luteinizing hormone-releasing hormone peptide and its gene expression in human peripheral T-lymphocytes. *Endocrinology* 1993; **133**: 215-223

4 **Weesner GD**, Becker BA, Matteri RL. Expression of luteinizing hormone-releasing hormone and its receptor in porcine immune tissues. *Life Sci* 1997; **61**: 1643-1649

5 **Furui T**, Imai A, Tamaya T. Intratumoral level of gonadotropin-releasing hormone in ovarian and endometrial cancers. *Oncol Rep*

2002; **9**: 349-352
6 **Leuschner C**, Enright FM, Gawronska-Kozak B, Hansel W. Human prostate cancer cells and xenografts are targeted and destroyed through luteinizing hormone releasing hormone receptors. *Prostate* 2003; **56**: 239-249
7 **Chen A**, Kaganovsky E, Rahimipour S, Ben-Aroya N, Okon E, Koch Y. Two forms of gonadotropin-releasing hormone (GnRH) are expressed in human breast tissue and overexpressed in breast cancer: a putative mechanism for the antiproliferative effect of GnRH by down-regulation of acidic ribosomal phosphoproteins P1 and P2. *Cancer Res* 2002; **62**: 1036-1044
8 **Nechushtan A**, Yarkoni S, Marianovsky I, Lorberboum-Galski H. Adenocarcinoma cells are targeted by the new GnRH-PE66 chimeric toxin through specific gonadotropin-releasing hormone binding sites. *J Biol Chem* 1997; **272**: 11597-11603
9 **Wang L**, Xie LP, Zhang RQ. Gene expression of gonadotropin-releasing hormone and its receptor in rat pancreatic cancer cell lines. *Endocrine* 2001; **14**: 325-328
10 **Yin H**, Cheng KW, Hwa HL, Peng C, Auersperg N, Leung PC. Expression of the messenger RNA for gonadotropin-releasing hormone and its receptor in human cancer cell lines. *Life Sci* 1998; **62**: 2015-2023
11 **Huang W**, Yao B, Sun L, Pu R, Wang L, Zhang R. Immunohistochemical and *in situ* hybridization studies of gonadotropin releasing hormone (GnRH) and its receptor in rat digestive tract. *Life Sci* 2001; **68**: 1727-1734
12 **Yao B**, Huang W, Huang Y, Chui Y, Wang Y, Li H, Pu R, Wan L, Zhang R. A study on the localization and distribution of GnRH and its receptor in rat submaxillary glands by immunohistochemical, *in situ* hybridization and RT-PCR. *Life Sci* 2003; **72**: 2895-2904
13 **Zhou J,** Huang WQ, Ji QH. The expression of gonadotropin-releasing hormone and its receptor in human thyroid gland. *Acta Anatomica Sinica* 2002; **33**: 511-515
14 **Wang L**, Xie LP, Huang WQ, Yao B, Pu RL, Zhang RQ. Presence of gonadotropin-releasing hormone (GnRH) and its mRNA in rat pancreas. *Mol Cell Endocrinol* 2001; **172**: 185-191
15 **Huang WQ**, Sun L, Zhong CL. Preparation and identification of GnRH anti-idiotypic antibody. *Chin J Anatom* 1994; **17**(Suppl): 353-356
16 **Fatigati V**, Murphy RA. Actin and tropomyosin variants in smooth muscles. Dependence on tissue type. *J Biol Chem* 1984; **259**: 14383-14388
17 **Chamley-Campbell J**, Campbell GR, Ross R. The smooth muscle cell in culture. *Physiol Rev* 1979; **59**: 1-61
18 **Kaiser UB**, Zhao D, Cardona GR, Chin WW. Isolation and characterization of cDNAs encoding the rat pituitary gonadotropin-releasing hormone receptor. *Biochem Biophys Res Commun* 1992; **189**: 1645-1652
19 **Chiba K**, Kawakami K, Tohyama K. Simultaneous evaluation of cell viability by neutral red, MTT and crystal violet staining assays of the same cells. *Toxicol In Vitro* 1998; **12**: 251-258
20 **Kang SK**, Choi KC, Cheng KW, Nathwani PS, Auersperg N, Leung PC. Role of gonadotropin-releasing hormone as an autocrine growth factor in human ovarian surface epithelium. *Endocrinology* 2000; **141**: 72-80
21 **Ji QH**, Huang WQ, Sun L, Zhao BQ. Double-labeling immunohistochemical location of glucagon, gonadorelin (GnRH) and GnRH receptor within pancreas of the guinea pig. *J Fourth Milit Med Univ* 1998; **19**: 34-36
22 **Jan YN**, Jan LY, Kuffler SW. A peptide as a possible transmitter in sympathetic ganglia of the frog. *Proc Natl Acad Sci U S A* 1979; **76**: 1501-1505
23 **Grundker C**, Emons G. Role of gonadotropin-releasing hormone (GnRH) in ovarian cancer. *Reprod Biol Endocrinol* 2003; **1**: 65
24 **Sayer HG**, Hoffken K. Hormone therapy, chemotherapy and immunotherapy in breast carcinoma. The best strategy for your patient. *MMW Fortschr Med* 2003; **145**: 40-42
25 **Krauss T**, Huschmand H, Hinney B, Viereck V, Emons G. Hormonal therapy and chemotherapy of endometrial cancer. *Zentralbl Gynakol* 2002; **124**: 45-50
26 **Minaretzis D**, Jakubowski M, Mortola JF, Pavlou SN. Gonadotropin-releasing hormone receptor gene expression in human ovary and granulosa-lutein cells. *J Clin Endocrinol Metab* 1995; **80**: 430-434
27 **Chegini N**, Rong H, Dou Q, Kipersztok S, Williams RS. Gonadotropin-releasing hormone (GnRH) and GnRH receptor gene expression in human myometrium and leiomyomata and the direct action of GnRH analogs on myometrial smooth muscle cells and interaction with ovarian steroids *in vitro*. *J Clin Endocrinol Metab* 1996; **81**: 3215-3221
28 **Galand P**, Del Bino G, Morret M, Capel P, Degraef C, Fokan D, Feremans W. PCNA immunopositivity index as a substitute to 3H-thymidine pulse-labeling index (TLI) in methanol-fixed human lymphocytes. *Leukemia* 1995; **9**: 1075-1084
29 **Kurki P,** Vanderlaan M, Dolbeare F, Gray J, Tan EM. Expression of proliferating cell nuclear antigen (PCNA)/ cyclin during the cell cycle. *Exp Cell Res* 1986; **166**: 209-219
30 **Mathews MB**, Bernstein RM, Franza BR Jr, Garrels JI. Identity of the proliferating cell nuclear antigen and cyclin. *Nature* 1984; **309**: 374-376
31 **Takagi H**, Imai A, Furui T, Horibe S, Fuseya T, Tamaya T. Evidence for tight coupling of gonadotropin-releasing hormone receptors to phosphatidylinositol kinase in plasma membrane from ovarian carcinomas. *Gynecol Oncol* 1995; **58**: 110-115

Edited by Kumar M and Xu FM

PO Box 2345, Beijing 100023, China
Fax: +86-10-85381893
E-mail: wjg@wjgnet.com www.wjgnet.com

World J Gastroenterol 2004;10(12):1785-1788
World Journal of Gastroenterology
Copyright ©2004 by The WJG Press ISSN 1007-9327

• BASIC RESEARCH •

Evaluation of the viability and energy metabolism of canine pancreas graft subjected to significant warm ischemia damage during preservation by UW solution cold storage method

Chun-Hui Yuan, Gui-Chen Li, He Zhang, Ying Cheng, Ning Zhao, Yong-Feng Liu

Chun-Hui Yuan, Gui-Chen Li, He Zhang, Ying Cheng, Ning Zhao, Yong-Feng Liu, Department of Organ Transplantation**,** The First Affiliated Hospital of China Medical University, Shenyang 110001, Liaoning Province, China
Supported by a fund of Liaoning Province key Project, No.0025001
Correspondence to: Dr. Chun-Hui Yuan, Department of Organ Transplantation, The First Affiliated Hospital of China Medical University, Shenyang 110001, Liaoning Provience, China. ychdoctor@hotmail.com
Telephone: +86-24-23256666 **Fax:** +86-24-23265284
Received: 2003-06-05 **Accepted:** 2003-11-06

Abstract

AIM: To evaluate the viability and energy metabolism of long warm ischemically damaged pancreas during preservation by the UW solution cold storage method.

METHODS: The pancreas grafts subjected to 30-120 min warm ischemia were preserved by the UW solution cold storage method for 24 h. The tissue concentrations of adenine nucleotides (AN) and adenosine triphosphate (ATP) and total adenine nucleotides (TAN) were determined by using high performance liquid chromatography (HPLC) and the viability of the pancreas graft was tested in the canine model of segmental pancreas autotransplantation.

RESULTS: The functional success rates of pancreas grafts of groups after 30 min, 60 min, 90 min, 120 min of warm ischemia were 100%, 100%, 67.7%, 0%, respectively. There was an excellent correlation between the posttransplant viability and tissue concentration of ATP and TAN at the end of preservation.

CONCLUSION: The UW solution cold storage method was effective for functional recovery of the pancreas suffering 60-min warm ischemia. The tissue concentration of ATP and TAN at the end of 24 h preservation by the UW solution cold storage method would predict the posttransplant outcome of pancreas graft subjected to significant warm ischemia.

Yuan CH, Li GC, Zhang H, Cheng Y, Zhao N, Liu YF. Evaluation of the viability and energy metabolism of canine pancreas graft subjected to significant warm ischemia damage during preservation by UW solution cold storage method. *World J Gastroenterol* 2004; 10(12): 1785-1788
http://www.wjgnet.com/1007-9327/10/1785.asp

INTRODUCTION

Preservation is necessary if organs for transplantation are removed from donors prior to preparation of the recipient[1-3]. The methods used for preservation of pancreas grafts for experimental transplantation have produced variable results[4,5]. As warm ischemic injury of pancreas graft before and during procurement strongly influences the results of pancreas transplantation, it is important to predict the viability of the ischemically damaged pancreas graft before transplantation[6,7]. Recently we preserved the segmental pancreas in the UW solution after 30-120 min, and our experimental model was heterotopic segmental (left limb) pancreas autotransplantation in totally pancreatectomized dogs, and demonstrated that the UW solution cold storage method was effective for functional recovery of the pancreas suffering 60-min warm ischemia[8]. There are some qualitative differences between warm and cold ischemic injuries[9-12]. In this study we examined the viability and energy metabolism of the pancreas graft after significant warm ischemia and cold storage, and found tissue concentrations of ATP and TAN after preservation by the UW solution cold storage method were excellent markers to predict the posttransplant outcome[13,14].

MATERIALS AND METHODS

Animals

Mongrel dogs of both sexes, weighing 10-15 kg were used for the experiments. UW solution was from China Pharmaceutical Corporation Guangzhou Branch. Chemicals were from Sigma Co.Ltd.

Operative procedures are as follows. Anesthesia was induced and maintained with sodium pentobarbiturate (25 mg/kg). The pancreas was exposed through a midline abdominal incision, and the left limb (tail) was removed with the splenic vessels in preparation for grafting, followed by splenectomy. The segmental pancreas graft was unflushed and left *in situ* for 30-120 min. After warm ischemia the pancreas was flushed with 30-50 mL heparinized cold UW solution (10 000 units/L heparin) and preserved in 50 mL heparinized cold UW solution for 24 h. A splenectomy was performed. The remainder of the pancreas was excised at the time of transplantation. The pancreatic tail was autotransplanted heterotopically, immediately or after preservation, with anastomosis of the splenic vessels to iliac vessels. A proper delicate tube was inserted into the pancreatic duct to drain the pancreatic juice. After operation , the dogs received saline with 100 g/L glucose (30 mL /kg) and 3.2 Mu penicillin for 3-5 days, then standard kennel diets were given.

Experimental protocol

There were two groups of control dogs: group 1, sham-operated group, abdomen was only opened and closed; group 2, no warm ischemia, pancreatic tail was flushed and preserved immediately after being harvested. The experimental group (group 3) was divided into 4 subgroups according to the warm ischemia time: group 3a, 30 min warm ischemia; group 3b, 60 min warm ischemia; group 3c, 90 min warm ischemia; group 3d, 120 min warm ischemia.

Functional studies

Blood glucose concentration was determined daily during the first postoperative week after autotransplantation. An

intravenous glucose tolerance test (IVGTT) was performed one week after transplantation. Glucose, 0.5 g/kg, was administered as a bolus and blood samples were collected serially over a 2-h period for plasma glucose. IVGTT K values were calculated from the plasma glucose levels at the end of 5 to 60 min[15]. Maintenance of normoglycemia for at least five days after transplantation or a key value of IVGTT more than 1.0 one week after transplantation was considered a functional success of pancreas graft. The plasma insulin levels in splenic and peripheral vein one hour after transplantation were examined. The pancreatic juice was collected every day and amylopsin in the pancreatic juice of the first and the seventh days were determined.

Tissue extraction method for adenine nucleotides: After preservation, a part of pancreas was rapidly frozen in liquid nitrogen, lyophilized overnight, and kept at -80 ℃ until analysis. The dry tissue powder was weighed (200 mg) and homogenized in 3 mL of ice cold 0.5 mol/L perchloric acid. The precipitated protein was removed by centrifugation, and 500 μL of supernatant was neutralized by the additions of 50 μL 1 mol/L KOH and 50 μL Tris. Following centrifugation, 10 μL of supernatant was injected into HPLC for analysis.

Measurement of adenine nucleotides

High-performance liquid chromatography (HPLC, Waters, 510 Pump, 486 Detector) was performed on a reverse-phase column of Shim-pack, CLC-ODS (15 cm×3.96 mm, 4 μm) which was equilibrated with 100 mmol/L sodium phosphate buffer (pH 6.0) according to the method of Wynants *et al*.

TAN was calculated as the sum of ATP, adenosine diphosphate (ADP) and adenosine monophosphate (AMP).

Histological studies

Biopsies of the pancreas grafts were taken after cold preservation and one hour after transplantation. For light microscopy, the tissues were fixed in 100 ml/L formalin and stained with hematoxylin and eosin. For electron microscopic studies the tissues were prefixed in 25 g/L glutaraldehyde, postfixed in 25 g/L osmium tetroxide, sectioned at 1 μm, and stained with uranyl acetate and lead citrate.

Statistical analysis

All data were expressed as mean±SD. *F* test was used to compare values of different groups, χ^2 test for comparison of viability. A value of $P<0.05$ was considered statistically significant.

RESULTS

Graft function

Pancreatic graft endocrine function Plasma glucose and IVGTT K values in groups 1, 2, 3a and 3b recovered to normal 2-3 days after transplantation, while groups 3c and 3d did not one week after transplantation(Table1). The plasma insulin levels in splenic and peripheral veins in groups 1, 2, 3a, and 3b were much higher than those in groups 3c, and 3d ($P<0.05$, Table 2).

Pancreatic graft exocrine function The pancreatic juice flow over the pancreatic duct 30 min after transplantation increased gradually and came to a climax on the fourth day after transplantation, and then declined gradually. The daily amounts of pancreatic juice of groups 1, 2, 3 a and 3b were much more than those of groups 3c and 3d ($P<0.05$). The amylase activities in the pancreatic juice of the first and seventh days in groups 1, 2, 3a and 3b were much more than those in groups 3c and 3d ($P<0.05$, Tables 2, 3)

Tissue ATP, ADP, AMP and TAN after preservation The tissue concentrations of ATP, ADP, AMP and TAN after 24-hour preservation in groups 1, 2, 3 a and 3b were much higher than those in groups 3c and 3d ($P<0.05$, Table 4).

Viability of canine pancreas autografts after preservation After significant warm and cold preservation, the functional success rates of groups 2, 3a, 3b, 3c and 3d were 5/5(100%), 6/6(100%), 6/6(100%), 4/6(66.7%) and 0/4(0%), respectively (Table3). The UW cold preservation method was effective for functional recovery of the pancreas after 30 to 60-min warm ischemia (Table 3).

Relationship between posttransplantation viability and tissue ATP and TAN There was no overlap between the lowest ATP in the viable grafts and highest ATP in the nonviable grafts. If ATP level of 4.0 μmol/g dry weight was determined as a critical

Table 1 Plasma glucose and IVGTT K value at the first week after transplantation and plasma insulin level in splenic and peripheral vein one hour after transplantation (mean±SD)

Group	*n*	Plasma glucose (mol/L)	IVGTT K value	In splenic vein (mmol/L)	In peripheral vein (mmol/L)
1	3	5.6±0.9[15]	1.78±0.17[25]	53.4±7.1[35]	8.6±1.3[45]
2	5	6.6±0.9	1.58±0.15	51.3±8.2	8.1±1.2
3a	6	6.7±1.1	1.45±0.12	50.6±7.6	7.5±1.1
3b	6	6.8±0.8	1.42±0.18	47.8±7.6	7.5±0.8
3c	6	11.9±1.3	0.87±0.16	35.0±5.2	3.2±0.7
3d	4	12.9±1.8	0.60±0.13	31.4±8.1	2.7±0.5

[1]F=36.9, $P<0.05$; [2]F=32.9, $P<0.05$; [3]F=7.38, $P<0.05$; [4]F=38.2, $P<0.05$; [5]SNK test: between group 1, 2, 3a, 3b, $P>0.05$; between group 3c, 3d, $P>0.05$.

Table 2 Pancreatic juice flow during the first week after transplantation (mean±SD, mL)

Group	*n*	Pancreatic juice flow / d						
		1	2	3	4	5	6	7
2	5	27±7[18]	70±11[28]	221±17[39]	294±37[49]	136±26[59]	81±21[69]	48±14[79]
3a	6	24±7	74±17	216±36	285± 36	138±24	91±19	53±15
3b	6	24±8	63±15	204±33	287±43	142±4	87±22	41±8
3c	6	12±4	20±6	68±19	69±19	83±18	54±12	30±7
3d	4	7±3	15±8	12±6	16±6	8±3	12±5	10±4

[1]F=9.87, $P<0.05$; [2]F=25.9, $P<0.05$; [3]F=67.4, $P<0.05$; [4]F=88.2, $P<0.05$; [5]F=45.2, $P<0.05$; [6]F=15.9, $P<0.01$; [7]F=13.2, $P<0.01$; [8]SNK test: between group 2, 3a, 3b, $P>0.05$; between group 3c, 3d, $P>0.05$; [9]SNK test: between group 2, 3a, 3b, $P>0.05$.

value for the viability following transplantation, the specificity, sensitivity, predictive value and efficacy were all 100%. And there was also no overlap between the lowest TAN in the viable grafts and highest TAN in the nonviable grafts. If TAN level of 7.0 μmol/g dry weight was determined as a critical value for the viability following transplantation, specificity, sensitivity, predictive value and efficacy were all 100%. Both ATP and TAN were reliable markers for determining the transplantation.

Table 3 Amylase in pancreatic juice of the first and the seventh day and viability after significant warm and cold preservation (mean±SD)

Group	*n*	Amylase (μkat/L)		Functioning grafts/rate(%)
		The first day	The seventh day	
2	5	182±45[13]	359±27[24]	5/(100)
3a	6	183±48	355±37	6/(100)
3b	6	180±42	327±37	6/100)
3c	6	83±24	29±11	4/(66.7)[5]
3d	4	77±30	28±10	0/(0)[5]

[1]F=10.3, P<0.05; [2]F=205.5, P<0.05; [3]SNK test: between group 2, 3a, 3b, P>0.05; [4]SNK test: between group 2, 3a, 3b, P>0.05; between group 3c, 3d, P>0.05. [5]compare with Group 2, P<0.05.

Table 4 Tissue concentration of ATP, ADP, AMP and TAN (mean±SD, μmol/L)

	ATP	ADP	AMP	TAN
Group 1 (n=3)	7.26±0.55[13]	3.33±0.20	1.49±0.34	11.43±1.37[23]
Group 2 (n=5)	5.86±0.52	1.01±0.21	1.51±0.26	7.93±1.30
Group 3a (n=6)	5.28±0.37	1.31±0.35	1.55±0.35	8.02±0.78
Group 3b (n=6)	4.74±0.41	2.01±0.31	1.04±0.24	7.36±0.78
Group 3c (n=6)	2.18±0.21	0.83±0.19	0.81±0.23	4.04±0.51
Group 3d (n=4)	2.11±0.17	0.86±0.21	1.04±0.25	3.33±0.27

[1]F=17.0, P<0.05; [2]F=23.9, P<0.05; [3]SNK test: between group 2, 3a, 3b, P>0.05.

Histologic studies

Under light microscope, the pancreas in groups 1 and 2 stored for 24 h showed normal architecture. After 24 h, preservation vacuolization of the acinar cells and interstitial edema were seen in grafts of groups 3a and 3b, and only mild edema of the islets was evident. Grafts of groups 3c and 3d showed severe edema, and after revascularization there was hemorrhage in the interstitial space.

Under electron microscope, the pancreas in groups 1 and 2 stored for 24 h showed well preserved cells. In grafts of groups 3a and 3b, acinar cells showed no nuclear changes, but rough endoplasmic reticulum (RER) cisternae were dilated. In grafts of groups 3c and 3d, irreversible cell damage was seen in most, but not all, specimens.

DISCUSSION

Pancreas graft injury due to warm ischemia strongly affects the posttransplant outcome[16,17]. Therefore, resuscitation of an ischemically damaged pancreas is essential to enlarge the donor pool using the pancreas graft from the cardiac arrest donor[18]. We have demonstrated that canine pancreases subjected to 60 min of warm ischemia can be resuscitated during preservation by the UW solution preservation method at 4 ℃ for 24 h.

Restoration of cellular function of the pancreas graft subjected to significant warm ischemia by the UW solution cold preservation method will make it possible to use pancreas grafts from cadaver with cardiac arrest[19,20], wait safely for the excision of the pancreas and enlarge the donor pool. Cerra[21,22] reported that the canine pancreatic allografts tolerated warm ischemia up to one hour. Florack *et al*.[23,24]demonstrated that the canine pancreatic autografts tolerated warm ischemia up to 60 min.

On the other hand, the assessment of a pancreas graft viability before transplantation is very important to prevent transplantation of a nonfunctioning allograft especially after significant warm ischemia because there is progressive depletion of ANs during warm ischemia[25], ultimately leading to ischemic damage. But the relationship between the tissue concentration of ANs before transplantation and organ viability after transplantation is controversial[26,27]. In human liver preservation, Lanir *et al*.[28,29] demonstrated a direct correlation between a high ATP concentration and good posttransplant outcome. On the contrary, correlation between the ATP level at the end of cold preservation and viability following transplantation was not proved in the rat liver[30,31].

We have also demonstrated that correlation between high ATP tissue concentration, which is necessary to maintain cellular integrity, and good posttransplant outcome of a canine pancreas graft after preservation by the UW solution cold preservation method[32,33]. It is suggested that tissue concentration of ATP and TAN at the end of 24-h preservation by the UW solution cold preservation method will predict the posttransplant outcome of pancreas graft subjected to significant warm ischemia[34,35]. But the mechanism responsible for the effectiveness of the UW solution cold preservation method in restoration of function of the pancreas graft subjected to significant warm ischemia remains unclear and is under investigation[35-38].

We conclude that the tissue concentration of ATP and TAN at the end of 24-h preservation by the UW solution cold storage method will predict the posttransplant outcome of pancreas graft subjected to significant warm ischemia.

REFERENCES

1 **Pi F**, Badosa F, Sola A, Rosello Catafau J, Xaus C, Prats N, Gelpi E, Hotter G. Effects of adenosine on ischaemia-reperfusion injury associated with rat pancreas transplantation. *Br J Surg* 2001; **88**: 1366-1375

2 **Uhlmann D**, Armann B, Ludwig S, Escher E, Pietsch UC, Tannapfel A, Teupser D, Hauss J, Witzigmann H. Comparison of Celsior and UW solution in experimental pancreas preservation. *J Surg Res* 2002; **105**: 173-180

3 **Wakai A**. Effect of adenosine on ischaemia-reperfusion injury associated with rat pancreas transplantation. *Br J Surg* 2002; **89**: 494

4 **Thayer SP**, Fernandez-del Castillo C, Balcom JH, Warshaw AL. Complete dorsal pancreatectomy with preservation of the ventral pancreas: a new surgical technique. *Surgery* 2002; **131**: 577-580

5 **Fujita H**, Kuroda Y, Saitoh Y. The mechanism of action of the two-layer cold storage method in canine pancreas preservation–protection of pancreatic microvascular endothelium. *Kobe J Med Sci* 1995; **41**: 47-61

6 **Matsumoto S**, Kandaswamy R, Sutherland DE, Hassoun AA, Hiraoka K, Sageshima J, Shibata S, Tanioka Y, Kuroda Y. Clinical application of the two-layer (University of Wisconsin solution/perfluorochemical plus O2) method of pancreas preservation before transplantation. *Transplantation* 2000; **70**: 771-774

7 **Sun B**, Jiang HC, Piao DX, Qiao HQ, Zhang L. Effects of cold preservation and warm reperfusion on rat fatty liver. *World J Gastroenterol* 2000; **6**: 271-274

8 **Kuroda Y**, Tanioka Y, Matsumoto S, Hiraoka K, Morita A, Fujino Y, Suzuki Y, Ku Y, Saitoh Y. Difference in energy metabolism between fresh and warm ischemic canine pancreases during preservation by the two-layer method. *Transpl Int* 1994; **7**(Suppl 1): S441-445

9 **Randhawa P**. Allograft biopsies in management of pancreas transplant recipients. *J Postgrad Med* 2002; **48**: 56-63

10 **Kim Y**, Kuroda Y, Tanioka Y, Matsumoto S, Fujita H, Sakai T, Hamano M, Suzuki Y, Ku Y, Saitoh Y. Recovery of pancreatic tissue perfusion and ATP tissue level after reperfusion in canine pancreas grafts preserved by the two-layer method. *Pancreas* 1997; **14**: 285-289

11 **Matsumoto S**, Kuroda Y, Fujita H, Tanioka Y, Sakai T, Hamano M, Kim Y, Suzuki Y, Ku Y, Saitoh Y. Extending the margin of safety of preservation period for resuscitation of ischemically damaged pancreas during preservation using the two-layer (University of Wisconsin solution / perfluorochemical) method at 20 degrees C with thromboxane A2 synthesis inhibitor OKY046. *Transplantation* 1996; **62**: 879-883

12 **Obermaier R**, Benz S, Kortmann B, Benthues A, Ansorge N, Hopt UT. Ischemia / reperfusion-induced pancreatitis in rats: a new model of complete normothermic *in situ* ischemia of a pancreatic tail-segment. *Clin Exp Med* 2001; **1**: 51-59

13 **Matsumoto S**, Kuroda Y, Fujita H, Tanioka Y, Kim Y, Sakai T, Hamano M, Suzuki Y, Ku Y, Saitoh Y. Resuscitation of ischemically damaged pancreas by the two-layer (University of Wisconsin solution / perfluorochemical) mild hypothermic storage method. *World J Surg* 1996; **20**: 1030-1034

14 **Tanioka Y**, Kuroda Y, Kim Y, Matsumoto S, Suzuki Y, Ku Y, Fujita H, Saitoh Y.The effect of ouabain (inhibitor of an ATP-dependent Na+ / K+ pump) on the pancreas graft during preservation by the two-layer method. *Transplantation* 1996; **62**: 1730-1734

15 **Moorhouse JA**, Granhame GR, Rosen NJ. Relationship between intravenous glucose tolerance and the fasting blood glucose level in healthy and diabetic subjects. *J Clin Endocrinnol Metab* 1964; **24**: 145-159

16 **Troisi R**, Meester D, Regaert B, van den Broecke C, Cuvelier C, Hesse UJ. Tolerance of the porcine pancreas to warm and cold ischemia: comparison between University of Wisconsin and histidine-tryptophan-ketoglutarate solution. *Transplant Proc* 2002; **34**: 820-822

17 **Fujino Y**, Suzuki Y, Tsujimura T, Takahashi T, Tanioka Y, Tominaga M, Ku Y, Kuroda Y. Possible role of heat shock protein 60 in reducing ischemic-reperfusion injury in canine pancreas grafts after preservation by the two-layer method. *Pancreas* 2001; **23**: 393-398

18 **Ludwig S**, Armann B, Escher E, Gabel G, Teupser D, Tannapfel A, Pietsch UC, Hauss J, Witzigmann H, Uhlmann D. Pathomorphologic and microcirculatory changes and endothelin-1 expression in UW-and Celsior-preserved pancreata in experimental pancreas transplantation. *Transplant Proc* 2002; **34**: 2364-2365

19 **Lakey JR**, Kneteman NM, Rajotte RV, Wu DC, Bigam D, Shapiro AM. Effect of core pancreas temperature during cadaveric procurement on human islet isolation and functional viability. *Transplantation* 2002; **73**: 1106-1110

20 **Nagami H**, Tamura K, Kin S, Teramoto M, Ishida T. Beneficial effect of thromboxane A2 synthetase inhibitor (OKY-046) on 24-hr simple hypothermic preservation of the canine pancreas graft. *Int Surg* 1995; **80**: 274-277

21 **Cerra FB,** Adams JR, Eggert DE, Eilert JB, Bergan JJ. Pancreatic function after normothermic ischemia. II. Cadaveric transplanatation. *Am J Surg* 1970; **120**: 693-696

22 **Tsiotos GG**, Sarr MG. Pancreas-preserving total duodenectomy. *Dig Surg* 1998; **15**: 398-403

23 **Florack G**, Sutherland DE, Ascherl R, Heil J, Erhardt W, Najarian JS. Definition of normothermic ischemia limits for kidney and pancreas grafts. *J Surg Res* 1986; **40**: 550-563

24 **Tanioka Y**, Sutherland DE, Kuroda Y, Suzuki Y, Matsumoto I, Deai T. Preservation of dog pancreas before islet isolation with the two-layer method. *Transplant Proc* 1998; **30**: 3419-3420

25 **Iwanaga Y**, Suzuki Y, Okada Y, Mori H, Matsumoto I, Mitsutsuji M, Tanioka Y, Fujino Y, Tominaga M, Ku Y, Kuroda Y. Ultrastructural analyses of pancreatic grafts preserved by the two-layer cold-storage method and by simple cold storage in University of Wisconsin solution. *Transpl Int* 2002; **15**: 425-430

26 **Belzer FO**, Southard JH. Principles of solid-organ preservation by cold storage. *Transplantation* 1988; **45**: 673-676

27 **Kim Y**, Kuroda Y, Tanioka Y, Matsumoto S, Fujita H, Sakai T, Hamano M, Suzuki Y, Ku Y, Saitoh Y. Recovery of adenosine triphosphate tissue levels of grafts preserved by the two-layer method after reperfusion. *Artif Organs* 1996; **20**: 1120-1124

28 **Lanir A**, Jenkins RL, Caldwell C, Lee RG, Khettry U, Clouse ME. Hepatic transplantation survival: correlation with adenine nucleotide level in donor liver. *Hepatology* 1988; **8**: 471-475

29 **Tsujimura T**, Suzuki Y, Takahashi T, Yoshida I, Fujino Y, Tanioka Y, Li S, Ku Y, Kuroda Y. Successful 24-h preservation of canine small bowel using the cavitary two-layer (University of Wisconsin solution / perfluorochemical) cold storage method. *Am J Transplant* 2002; **2**: 420-424

30 **Orii T**, Ohkohchi N, Satomi S, Taguchi Y, Mori S, Miura I. Assessment of liver graft function after cold preservation using 31P and 23Na magnetic resonance spectroscopy. *Transplantation* 1992; **53**: 730-734

31 **Uhlmann D**, Armann B, Ludwig S, Escher E, Pietsch UC, Tannapfel A, Teupser D, Hauss J, Witzigmann H. Comparison of Celsior and UW solution in experimental pancreas preservation. *J Surg Res* 2002; **105**: 173-180

32 **Lakey JR**, Rajotte RV, Warnock GL, Kneteman NM. Cold ischemic tolerance of human pancreas: assessment of islet recovery and *in vitro* function. *Transplant Proc* 1994; **26**: 3416

33 **Shi LJ**, Liu JF, Zhang ZQ, Lu YQ, Shu YG, Chen GL, Xin ZH, Xu JY. Alterations of ATPase activity and erythrocyte oxygen consumption in patients with liver-blood deficiency syndrome. *China Nati J New Gastroenterol* 1997; **3**: 180-181

34 **Humar A**, Kandaswamy R, Drangstveit MB, Parr E, Gruessner AG, Sutherland DE. Prolonged preservation increases surgical complications after pancreas transplants. *Surgery* 2000; **127**: 545-551

35 **Bottino R**, Balamurugan AN, Bertera S, Pietropaolo M, Trucco M, Piganelli JD. Preservation of human islet cell functional mass by anti-oxidative action of a novel SOD mimic compound. *Diabetes* 2002; **51**: 2561-2567

36 **Kim Y**, Kuroda Y, Tanioka Y, Matsumoto S, Fujita H, Sakai T, Hamano M, Suzuki Y, Ku Y, Saitoh Y. Recovery of pancreatic tissue perfusion and ATP tissue level after reperfusion in canine pancreas grafts preserved by the two-layer method. *Pancreas* 1997; **14**: 285-289

37 **Pi F**, Hotter G, Closa D, Prats N, Fernandez-Cruz L, Badosa F, Gelpi E, Rosello-Catafau J. Differential effect of nitric oxide inhibition as a function of preservation period in pancreas transplantation. *Dig Dis Sci* 1997; **42**: 962-971

38 **Matsumoto I**, Suzuki Y, Fujino Y, Tanioka Y, Deai T, Iwanaga Y, Mitsutsuji M, Iwasaki T, Tominaga M, Ku Y, Kuroda Y. Superiority of mild hypothermic (20 degrees C) preservation for pancreatic microvasculature using the two-layer storage method. *Pancreas* 2000; **21**: 305-309

Edited by Hu DK and Zhu LH **Proofread by** Xu FM

PO Box 2345, Beijing 100023, China
Fax: +86-10-85381893
E-mail: wjg@wjgnet.com www.wjgnet.com

World J Gastroenterol 2004;10(12):1789-1794
World Journal of Gastroenterology
Copyright ©2004 by The WJG Press ISSN 1007-9327

• BASIC RESEARCH •

Heme oxygenase-1 in cholecystokinin-octapeptipe attenuated injury of pulmonary artery smooth muscle cells induced by lipopolysaccharide and its signal transduction mechanism

Xin-Li Huang, Yi-Ling Ling, Yi-Qun Ling, Jun-Lin Zhou, Yan Liu, Qiu-Hong Wang

Xin-Li Huang, Yi-Ling Ling, Qiu-Hong Wang, Department of Pathophysiology, Hebei Medical University, Shijiazhuang 050017, Hebei province, China
Yi-Qun Ling, Department of Universal Surgery of Second Hospital, Hebei Medical University, Shijiazhuang 050017, Hebei Province, China
Jun-Lin Zhou, Department of hand Surgery of third Hospital, Hebei Medical University, Shijiazhuang 050017, Hebei province, China
Yan Liu, Department of histogy and embryology, Hebei Medical University, Shijiazhuang 050017, Hebei province, China
Correspondence to: Professor Yi-Ling Ling, Department of Pathophysiology, Hebei Medical University, Shijiazhuang 050017, Hebei province, China. lingyl20@sina.com.cn
Telephone: +86-311-6052263
Received: 2003-07-17 **Accepted:** 2003-07-30

Abstract

AIM: To study the effect of cholecystokinin-octapeptide (CCK-8) on lipopolysaccharide (LPS) -induced pulmonary artery smooth muscle cell (PASMCs) injury and the role of heme oxygenase-1 (HO-1), and to explore the regulation mechanism of c-Jun N-terminal kinase (JNK) and activator protein-1 (AP-1) signal transduction pathway in inducing HO-1 expression further.

METHODS: Cultured PASMCs were randomly divided into 4 or 6 groups: normal culture group, LPS (10 mg/L), CCK-8 (10^{-6} mol/L) plus LPS (10 mg/L) group, CCK-8 (10^{-6} mol/L) group, zinc protoporphyrin 9 (ZnPPIX) (10^{-6} mol/L) plus LPS (10 mg/L) group, CCK-8 (10^{-6} mol/L) plus ZnPPIX and LPS (10 mg/L) group. Seven hours after LPS administration, ulterstructrual changes and content of malondialdehyde (MDA) of PASMCs in each group were investigated by electron microscopy and biochemical assay respectively. HO-1 mRNA and protein of PASMCs in the former4 groups were examined by reverse transcriptase polymerase chain reaction (RT-PCR) and immunocytochemistry staining. Changes of c-fos expression and activation of JNK of PASMCs in the former 4 groups were detected with immunocytochemistry staining and Western blot 30 min after LPS administration.

RESULTS: The injuries of PASMCs and the increases of MDA content induced by LPS were alleviated and significantly reduced by CCK-8 ($P<0.05$). The specific HO-1 inhibitor-ZnPPIX could worsen LPS-induced injuries and weaken the protective effect of CCK-8. The expressions of c-fos, *p*-JNK protein and HO-1 mRNA and protein were all slightly increased in LPS group, and significantly enhanced by CCK-8 further ($P<0.05$).

CONCLUSION: HO-1 may be a key factor in CCK-8 attenuated injuries of PASMCs induced by LPS, and HO-1 expression may be related to the activation of JNK and activator protein (AP-1).

Huang XL, Ling YL, Ling YQ, Zhou JL, Liu Y, Wang QH. Heme oxygenase-1 in cholecystokinin-octapeptipe attenuated injury of pulmonary artery smooth muscle cells induced by lipopolysaccharide and its signal transduction mechanism. *World J Gastroenterol* 2004; 10(12): 1789-1794
http://www.wjgnet.com/1007-9327/10/1789.asp

INTRODUCTION

Lipopolysaccharide (LPS), a main component of Gram-negative bacterial endotoxin, is the main factor to induce endotoxic shock (ES). ES is a common and serious syndrome in clinic and its mortality is very high. The lung is one of the target organs easily insulted in ES. It was demonstrated that lung injury in ES was associated with oxygen free radicals (OFR)[1,2] and the content of cholecystokinin (CCK) in serum was increased when ES occurred. Our previous *in vivo* and *in vitro* studies demonstrated that CCK-8 could protect animals from LPS-induced ES and lung injury, which may be related to its effect on reducing the production of OFR[3-7].

There is a rapid increase in those substances that provide protection against oxidative stress. Among them one is heme oxygenase (HO)-1, which has generated much interest as a novel stress protein that is highly induced by many factors which induce oxidative injury and protect against oxidative stress[8-12]. However, the regulation mechanism of HO-1 expression was still unclear and there were no reports about the relationship between HO-1 and the protection of CCK-8 in LPS-induced ES and lung injury. One of the earliest responses to LPS and CCK-8 is the activation of mitogen-activated protein kinases (MAPKs), including p38, p42/p44 extracellular signal-regulated kinase (ERK) and c-Jun NH_2-terminal kinase (JNK)[13,14]. A slightly later cellular response is the activation of activator protein (AP)-1. AP-1 is a dimeric protein complex containing 2 members of the real family of transcription factors, c-fos and c-Jun. Recent studies showed that, one or more members of AP-1 were likely involved in HO-1 gene transcription[15-18]. The relationship between the activation of these signaling molecules and downstream HO-1 expression represents an active line of investigation. This can provide experimental evidences to elucidate whether the protective mechanism of CCK-8 is associated with HO-1.

Pulmonary artery hypertension (PAH) is the typical pathological change in the early phase of ES. It was reported that the degree and duration of PAH were the important factors of ES accompanied by acute lung injury, and pulmonary artery smooth muscle cells (PASMCs) played an important role in maintaining the tone of pulmonary artery. In the present study, the effect of CCK-8 pretreatment on the injuries of PASMCs induced by LPS was observed, and further investigated the role of HO-1 and the regulation mechanism of c-Jun N-terminal kinase (JNK) and AP-1 signal transduction pathway in inducing HO-1 expression were further investigated.

MATERIALS AND METHODS

Materials

CCK-8 (sulfated), LPS (*E.coli* LPS,serotype 0111:B4), ZnPPIX and Triton X-100 were all purchased from Sigma. Mouse anti-rat phosphorylate JNK(p-JNK) monoclonal antibody, rabbit anti- rat c-fos and HO-1 polyclonal antibody were all purchased from Santa Cruz. DMEM and fetal calf serum (FCS) were purchased from GibcoBRL. Total RNA isolation system and access RT-PCR system were purchased from Promega (USA). SABC kit was purchased from Boshide(China). All other reagents used were of analytic grade.

Methods

Cell isolation and culture Rat PASMCs were prepared as previously described[19]. Briefly, male healthy Sprague-Dawley rats (100-150 g BM, Experimental Animal Center of Hebei Province) were anesthetized with intraperitoneal administration of pentobarbital sodium (35 mg/kg), and pulmonary arteries were obtained. The isolated pulmonary arteries were cleaned of connective tissues, and aseptically opened longitudinally. The adventitia was carefully removed and the luminal surface was scraped with forceps to remove endothelial cells and then minced into 1 mm^2 pieces and plated on culture flasks at 37 ℃ in humidified air containing 50 mL/L CO_2 for 2-3 h , and then cultured in Dulbecco modified Eagle medium (DMEM) supplemented with heat-inactivated 10 mL/L FCS and antibiotics (100 U penicillin, 100 μg/mL streptomycin) and grew until confluence. The medium was changed every 3-4 d, and confluent cells were passaged with 1.25 g/L trypsin solution every 5-7 d, and experiments were performed in an 80% confluent state on the sixth- to eighth-passages from primary culture. Cells were made quiescent by incubation in each medium without FCS for 24 h before LPS or CCK-8 addition. PASMCs in culture were elongated and spindle shaped, grown with the typical hill-and-valley appearance, and characterized by immunocytochemical assay with anti-α-actin monoclonal antibody, demonstrating positive staining in >95% of cells. The cultured PASMCs were randomly divided into 4 or 6 groups: normal culture (control) group, LPS (10 mg/L) group, CCK-8 (10^{-6} mol/L) group, CCK-8 (10^{-6}mol/L) plus LPS (10 mg/L) group, ZnPPIX(10^{-6}mol/L) plus LPS (10 mg/L) group, and CCK-8 (10^{-6}mol/L) plus ZnPPIX (10^{-6}mol/L) and LPS (10 mg/L) group.

Observation of ultrastructrual changes with transmission electron microscopy After treated with LPS, CCK-8 or ZnPPIX, the cells were washed rapidly with PBS and harvested, then fixed with 40 g/L paraformaldehyde/5 g/L glutaraldehyde and postfixed with 40 g/L OsO_4/potassium hexacyanoferrate. After embedded in Epon, thin sections were cut, contrasted with uranyl acetate (20 g/L)/lead citrate (27 g/L) and examined with an EM10 electron microscope as described previously[20].

Assessments of PASMCs malondialdehyde (MDA) content The cells were harvested after treated with LPS or CCK-8 or ZnPPIX and washed rapidly with PBS, then immediately homogenized on ice in 9 volumes of saline. The homogenates were centrifuged at 4 000 r/min at 4 ℃ for 10 min. The MDA content in the supernatants was measured using a MDA assay kit (Nanjing Jiancheng Corp. China).

Analysis of c-fos and HO-1 protein expression by immunocytochemistry Confluent cells were passaged with 2.5 g/L trypsin solution onto 20 mm×20 mm glass sheets in a 6-well plate. After treatment with LPS, CCK-8 or both LPS and CCK-8 for 30 min or 7 h, the cells were treated with 3 mL/L H_2O_2 in methanol to block endogenous peroxide activity. Immunocytochemical staining was performed using rabbit polyclonal antibody against c-fos and HO-1 by an indirect streptavidin/peroxidase technique. Experiments were performed following the manufacturer's recommendations. The cells were incubated with polyclonal anti-rat c-fos and HO-1 antibody for 12 h at 4 ℃ after antigen repair. Biotinylated IgG was added as the second antibody. Horseradish peroxidase labeled streptomycin-avidin complex was used to detect the second antibody. Slides were stained with DAB and examined under a light microscope. The brown or dark brown stained cytoplasm or cell nucleus was considered as positive. Phosphate-buffered saline (PBS) solution was used as negative control. The result of immunocytochemistry was analysed by using the CMIAS-8 image analysis system.

Analysis of HO-1 mRNA by RT-PCR After treatment with LPS, CCK-8 or both LPS and CCK-8 for 7 h, total RNA was extracted from PASMCs. The concentration of RNA was determined from absorbent at 260 nm. The primers for HO-1 and β-actin were as follows: HO-1 (309 bp), 5' -CTT TCA GAA GGG TCA GGT GTC CA-3' ,5' -CTG AGA GGT CAC CCA GGT AGC GG-3' ; β-actin (224 bp), 5' -CGT GGG CCG CCC TAG GCA CCA-3' , 5' -CGG TTG CCT TAG GGT TCA GAG GGG-3' . Polymerase chain reactions(PCR) were performed in a 50 μL reaction volume. Reverse transcriptase polymerase chain reaction (RT-PCR) was run in the following procedures: at 42 ℃ for 45 min, 1 circle; at 95 ℃ for 3 min, at 60 ℃ for 30 s, at 72 ℃ for 30 s, 1 circle; at 94 ℃ for 30 s , at 60 ℃ for 30 s, at 72 ℃ for 30 s, 30 circles; at 94 ℃ for 30 s, at 60 ℃ for 30 s, at 72 ℃ for 6 min, 1 circle. A 10 μL PCR product was placed on to 15 g /L agarose gel and observed by EB staining using a Gel-Pro analyzer.

Western blot analysis of p-JNK protein in PASMCs After treatment with LPS or CCK-8 or both LPS and CCK-8 for 30 min, the cells were harvested and then lysed with ice-cold lysis buffer [50 mmol/LTris (pH 7.5), 150 mmol/LNaCl, 10 g/L Triton X-100, 5 g/L deoxycholic acid, 1 g/L sodium dodecyl sulfate, 1 mmol/L phenylmethysulfonyl (PMSF), 10 mmol/L NaF, 1 mmol/L sodium vanadate, 5 mmol/L EDTA (pH 8.0) and a 40 μg/mL protease inhibitor cocktail] as described previously for 1 h and then centrifuged at 12 000 *g* at 4 ℃ for 10 min. After precipitated unsolubilized fraction was discarded, protein concentration in the supernatant was determined by Coomassie blue dye-binding assay (Nanjing Jiancheng Corp. China). The supernatant containing 30 μg protein was treated with 2×Laemmli buffer, then subjected to SDS-PAGE using 100 g/L running gel for 3 h at 100 V. Protein was transferred to nitrocellulose membrane, and immunoblot analysis was performed as described previously. Briefly, the membrane was incubated successively with 3 mL/L milk in TPBS at room temperature for 1 h, with 1:1 000 diluted mouse anti-rat specific antibody of p-JNK at 37 ℃ for 2 h, and then with horseradish peroxidase-labeled secondary antibody at 37 ℃ for 30 min. After each incubation, the membrane was washed extensively with TPBS and the immunoreactive band was stained with diaminobenzidine (DAB). The brown or dark brown stained strap was considered as positive.

Statistical analysis

Data were reported as mean±SD. Statistical differences between values from different groups were determined by one way ANOVA and Newman-Keuls *q* test. Significance was set at $P<0.05$.

RESULTS

CCK-8 alleviated PASMC injury induced by LPS

PASMCs were harvested at 7 h. There were significantly ultrastructural injuries in LPS group such as seriously swollen mitochondria and mitochondria without or partly without cristallins. CCK-8 could significantly alleviate the above-mentioned changes. While the ultrastructrual injuries induced

by LPS were aggravated and the protective effect of CCK-8 on cells was weakened by ZnPPIX. There was no significant difference between CCK-8 group and control group (Figure 1).

CCK-8 inhibited MDA production

The MDA content of PASMCs was significantly increased in LPS group when compared with control group ($P<0.05$). Compared with the LPS group, the MDA content was further increased in LPS+ZnPPIX group but markedly decreased in CCK-8+L PS group, however the protective effect of CCK-8 was weakened by ZnPPIX. There was no significant difference between CCK-8 group and control group ($P<0.05$) (Table 1).

Table 1 Change of MDA content in PASMCs (mean±SD, n=8)

Group	MDA content (nmol/mL)
Control	4.02±2.18
LPS	23.44±1.25[a]
LPS+CCK-8	14.66±1.66[e]
CCK-8	3.00±2.18
LPS+ZnPP	34.97±1.54[ae]
LPS+CCK-8+ZnPP	29.68±2.18[ec]

[a]$P<0.05$ *vs* Control group, [c]$P<0.05$ *vs* LPS+CCK-8 group, [e]$P<0.05$ *vs* LPS group.

Change of c-fos and HO-1 protein expression

The expressions of c-fos and HO-1 protein in PASMCs were demonstrated by immunocytochemical staining. The results showed that in control group, no brown deposits were present in PASMCs. In contrast, LPS slightly increased the expressions of c-fos and HO-1 protein, some strong positive signals were observed in PASMCs from LPS group. CCK-8 could further enhance the increased expressions of c-fos and HO-1. The dimension and intensity of positive signals were increased also in CCK-8 group (Figure 2).

Table 2 Changes of HO-1 and c-fos protein expression by immumocytochemistry in PASMCs (mean±SD, n=6)

Group	Area (%)		(*A*)	
	HO-1	c-fos	HO-1	c-fos
Control	2.10±0.01	1.18±0.02	0.02±0.009	0.03±0.021
LPS	20.18±0.08[a]	18.95±0.07[a]	0.19±0.07[a]	0.20±0.01[a]
LPS+CCK-8	28.91±0.36[c]	29.87±0.33[c]	0.47±0.04[c]	0.45±0.02[c]
CCK-8	21.27±1.05	20.16±0.98	0.31±0.02	0.33±0.01

[a]$P<0.05$ *vs* Control group, [c]$P<0.05$ *vs* LPS group.

RT-PCR detection of HO-1 mRNA

HO-1 mRNA in PASMCs was detected by PT-PCR analysis. The results showed that the PASMCs of rats 7 h after LPS administration expressed the gene coding for HO-1, because RT-PCR generated a DNA fragment corresponding to the predicted length, 309 bp, of the HO-1 amplification product. The expression of HO-1 increased significantly in LPS and CCK-8 groups compared with control group. The rate of β-actin was (11±2) % in control group, while it increased to (30±6) % and (47±7) % respectively in LPS and CCK-8 groups. The expression of HO-1 increased further in LPS+CCK-8 group compared with LPS group, it increased to (80±8) % in LPS+CCK-8 group. In each cell sample, all β-actin amplification products were 224 bp in length and there was no significant difference in β-actin expression (Figure 3).

Western blot analysis of p-JNK protein

There were a few of activated JNK proteins in control group. JNK could be activated by LPS, significant phosphorylation of JNK was observed in PASMCs 30 min after LPS administration. CCK-8 could significantly enhance LPS-induced phosphorylation of JNK. Phosphorylation of JNK was also observed in cells receiving CCK-8 (Figure 4).

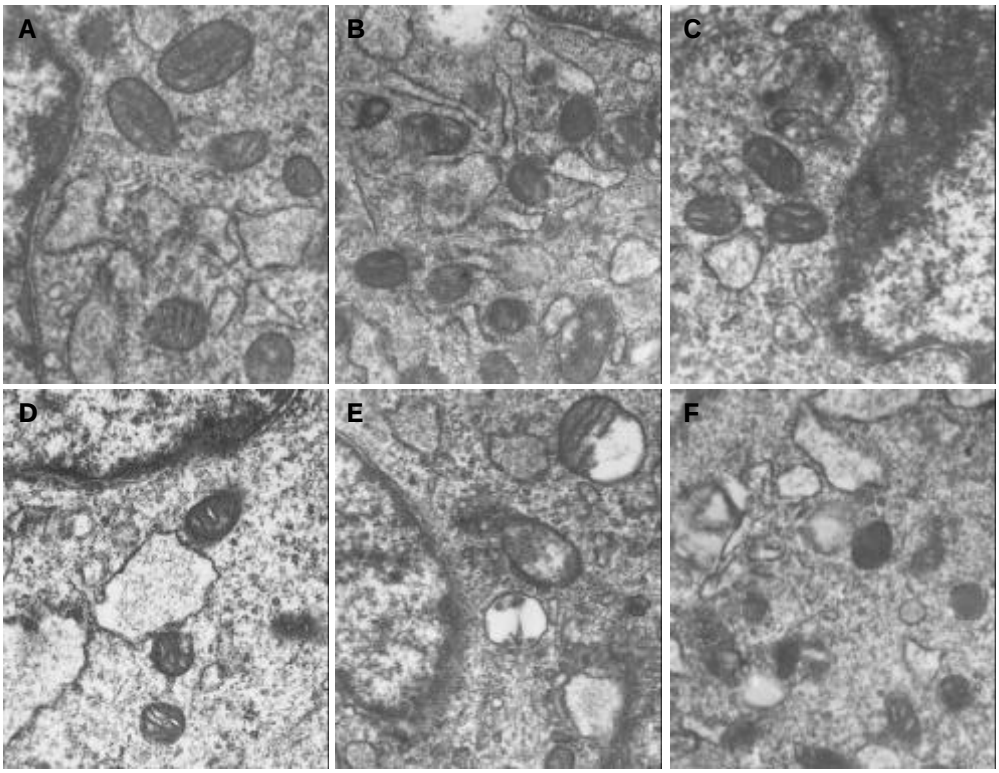

Figure 1 Mitochondria ultrastructural changes shown in EM photograph of PASMCs (×25 000). A: Control group, B: LPS group, C: CCK-8+LPS group, D: CCK-8 group, E: LPS+ZnPP group, F: CCK-8+LPS+ZnPP group.

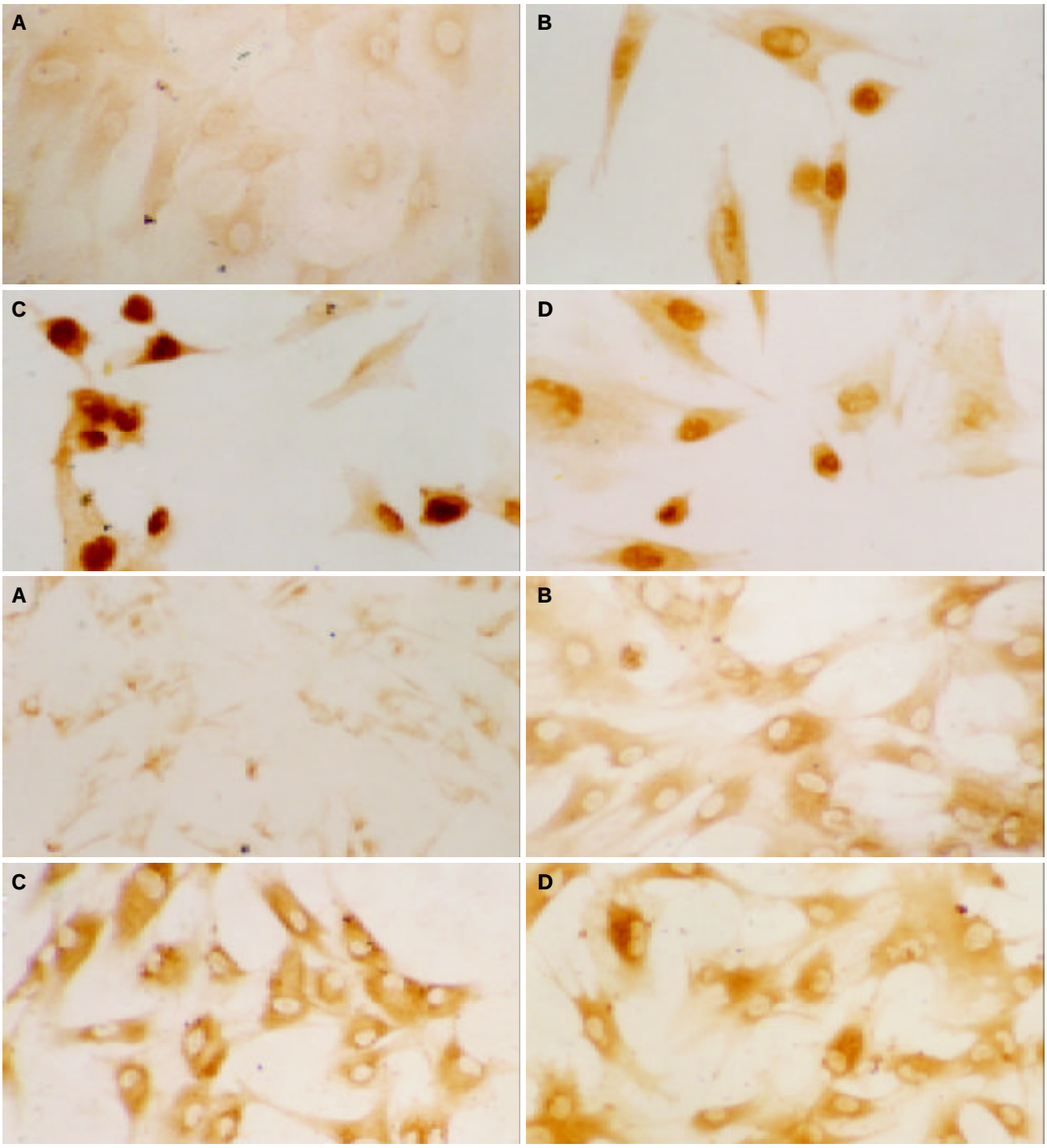

Figure 2 Effect of CCK-8 on LPS-induced c-fos (upper, ×400) and HO-1 (lower, ×200) protein expression in PASMCs. A: Control group, B: LPS group, C: CCK-8+LPS group, D: CCK-8 group.

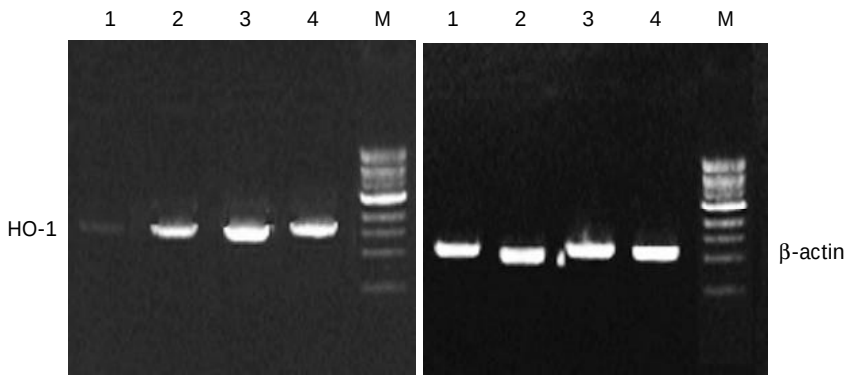

Figure 3 RT-PCR product gel electrophoresis. M: DNA marker, 1: Control, 2: LPS, 3: CCK-8 + LPS, 4: CCK-8.

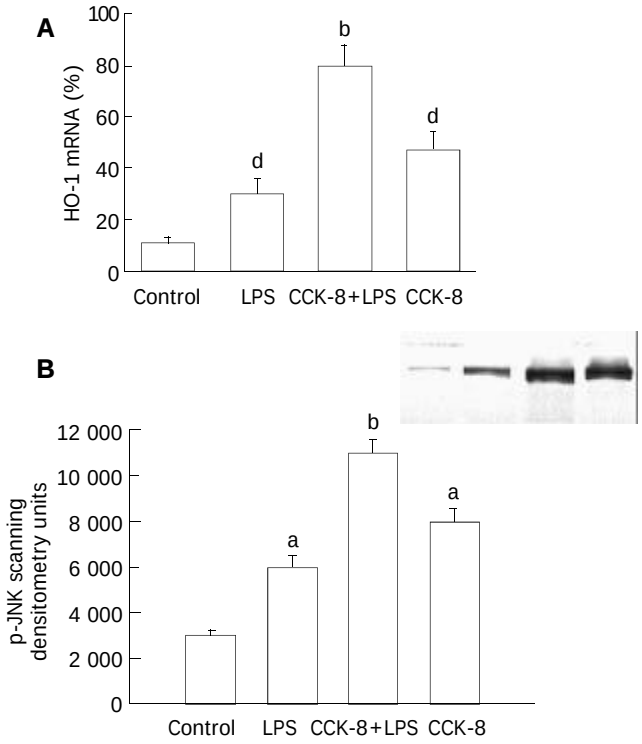

Figure 4 Effect of CCK-8 on LPS-induced HO-1 mRNA expression and JNK activation in PASMCs. A: Effect of CCK-8 on LPS-induced HO-1 mRNA expression in PASMCs. n=3. ^{d}P<0.01 *vs* Control; ^{b}P<0.01 *vs* LPS. B: CCK-8 increases JNK activation induced by LPS in PASMCs. n=3. ^{a}P<0.05 *vs* Control; ^{b}P<0.01 *vs* LPS.

DISCUSSION

CCK is a member of the gastrin-CCK family, first isolated from hog intestine, and shows a widespread distribution in different organs and tissues. The sulfated carboxy-terminal octapeptide (CCK-8), isolated from the central nervous system and digestive tract, is the predominant active form. Our previous *in vivo* and *in vitro* studies demonstrated that CCK-8 could protect animals from LPS-induced ES. Treatment of ES rats and rabbits with CCK-8 could lead to an increase in decreasing mean arterial pressure and a reduction in increasing pulmonary artery pressure. Pathological changes of lung could be ameliorated when CCK-8 was via vessel in advance. CCK-8 could protect pulmonary artery endothelia against detrimental effects and then reverse the inhibition of endothelia-dependent relaxation of pulmonary artery induced by LPS, which might be associated with the above-mentioned protective effect of CCK-8[5-10]. Despite convincing data indicating the protective function of CCK-8 to the organisms in endotoxic shock or to the cells exposed to LPS, the precise mechanism remains unclear.

During stress state induced by administration of LPS, inflammation or therapeutic doses of inhaled oxygen, the bodies would evolve a complex, and redundant network of antioxidants. It has been found that an important arm of the antioxidant response consists of antioxidant enzymes and stress-response proteins[21-23]. One such stress-response protein is HO-1, the rate-limiting enzyme in the oxidative degradation of heme into bilirubin, carbon monoxide (CO) and free iron. HO exists in three isoforms, whereas HO-2 and HO-3 are primarily constitutive. HO-1 also known as heat shock protein 32, has been found to be the only inducible HO isoform[24-27]. There is a strong evidence to support the emerging paradigm that HO-1 is essential in maintaining cellular and tissue homeostasis in various *in vitro* and *in vivo* models of oxidant-induced injury. Recent analyses of HO-1 null mice as well as the first reported HO-1-deficient human have strengthened the emerging paradigm that HO-1 is indeed an important molecule in the host's defense against oxidant stresses such as hypoxia, hyperthermia, and inflammation. It has been considered as one of the most sensitive indicators of cellular injury[28-31]. Recent studies showed that HO-1 was an important regulator of the vascular response to injury. In this experiment we used the specific HO-1 inhibitor-ZnPPIX to study the relationship between induced HO-1 and injuries of PASMCs. The results showed that HO-1 mRNA and protein expression increased after LPS administration and ZnPPIX could worsen LPS-induced injuries, indicating that overexpression of HO-1 in PASMCs can attenuate their injuries induced by LPS. It is undoubtedly one of the adaptive and self-protective responses to the injury.

Given the overall consistency of data that show HO-1 expression is generally a protective response, it is necessary to study the relationship between HO-1 expression and the protection of CCK-8. We found that CCK-8 could ameliorate the ultrastructural injuries of PASMCs induced by LPS. However, the protective effect of CCK-8 was impaired by ZnPPIX. To further demonstrate the role of HO-1 in CCK-8 attenuated injury of PASMCs induced by LPS, the HO-1 expression and signal pathway of HO-1 induction in PASMCs were studied. The candidate upstream signaling pathways for HO-1 regulation were MAPKs, a group of protein kinases that could mediate the nuclear responses of cells to a wide variety of extracellular stresses such as inflammatory cytokines, growth factors, ultraviolet light, and osmotic stress[32-34]. The "classical" MAPKs are the p44 and p42 isoforms. Recently, two novel MAPK-related enzymes have been identified, one is JNK and the other is p38[35]. Although three distinct subfamilies have been described, there is a significant cross talk between the pathway and common downstream target[36]. In our experiment, we found that CCK-8 significantly enhanced LPS-induced overexpression of HO-1 mRNA and protein. We also observed that LPS could also activate c-fos (one of the two members of the real family of AP-1) and JNK in PASMCs, while CCK-8 could further enhance the activation of c-fos and JNK induced by LPS. From all above, the role of MAPKs was potential in HO-1 signal pathway after LPS and CCK-8 administration to PASMCs, HO-1 might be the key for CCK-8 to exert its protective effect.

In summary, administration of CCK-8 can prevent injuries of PASMCs induced by LPS through overexpression of HO-1 mRNA and protein, which may involve c-fos and JNK.

REFERENCES

1 **Liaudet L,** Szabo C, Evgenov OV, Murthy KG, Pacher P, Virag L, Mabley JG, Marton A, Soriano FG, Kirov MY, Bjertnaes LJ, Salzman AL. Flagellin from gram-negative bacteria is a potent mediator of acute pulmonary inflammation in sepsis. *Shock* 2003; **19**: 131-137

2 **Molina PE**, Abunrad NN. Differential effects of hemorrhage and LPS on tissue TNF-α, IL-1 and associate neuro-hormonal and opioid alterations. *Life Sci* 2000; **66**: 399-409

3 Bertolini A, Guarinin S, Ferrari W, Rompianesi E. Caerulein and cholecystokinin reverse experimental heamorrhagic shock. *Neuropeptides* 1986; **8**: 25-31

4 **Guarini S,** Bazzani C, Leo L, Bertolini A. Haematological changes induced by the intravenous injection of CCK-8 in rats subjected to haemorrhagic shock. *Neuropeptides* 1988; **11**: 69-72

5 **Ling YL,** Huang SS, Wang LF, Zhang JL, Wan M, Hao RL. Cholecystokinin-octapeptide (CCK-8) reverses experimental endotoxin shock. *Shengli Xuebao* 1996; **48**: 390-394

6 **Meng AH,** Ling YL, Wang DH, Gu ZY, Li SJ, Zhu TN. Cholecystokinin-octapeptide alleviates tumor necrosis factor-α induced changes in rabbit pulmonary arterial reactivity and injuries of endothelium *in vitro*. *Shengli Xuebao* 2000; **52**: 502-506

7 **Ling YL,** Meng AH, Zhao XY, Shan BE, Zhang JL, Zhang XP. Effect of cholecystokinin on cytokines during endotoxic shock

in rats. *World J Gastroenterol* 2001; **7**: 667-671
8 **Otani K,** Shimizu S, Chijiiwa K, Morisaki T, Yamaguchi T, Yamaguchi K, Kuroki S, Tanaka M. Administration of bacterial lipopolysaccharide to rats induces heme oxygenase-1 and formation of antioxidant bilirubin in the intestinal mucosa. *Dig Dis Sci* 2000; **45**: 2313-2319
9 **Zampetaki A,** Minamino T, Mitsialis SA, Kourembanas S. Effect of heme oxygenase-1 overexpression in two models of lung inflammation. *Exp Biol Med* 2003; **228**: 442-446
10 **Henningsson R,** Alm P, Lundquist I. Evaluation of islet heme oxygenase-CO and nitric oxide synthase-NO pathways during acute endotoxemia. *Am J Physiol Cell Physiol* 2001; **280**: C1242-1254
11 **Otterbein LE,** Choi AM. Heme oxygenase: colors and defense against cellular stress. *Am J Physiol Lung Cell Mol Physiol* 2000; **279**: L1029-1037
12 **Gonzalez A,** Schmid A, Salido GM, Camello PJ, Pariente JA. XOD-catalyzed ROS generation mobilizes calcium from intracellular stores in mouse pancreatic acinar cells. *Cell Signal* 2002; **14**: 153-159
13 **Jarvis BW,** Harris TH, Qureshi N, Splitter GA. Rough lipopolysaccharide from Brucella abortus and Escherichia coli differentially activates the same mitogen-activated protein kinase signaling pathways for tumor necrosis factor alpha in RAW 264.7 macrophage-like cells. *Infect Immun* 2002; **70**: 7165-7168
14 **Zieger M,** Oehrl W, Wetzker R, Henklein P, Nowak G, Kaufmann R. Different signaling pathways are involved in CCK (B) receptor-mediated MAP kinase activation in COS-7 cells. *Biol Chem* 2000; **381**: 763-768
15 **Yuksel M,** Okajima K, Uchiba M, Okabe H. Gabexate mesilate, a synthetic protease inhibitor, inhibits lipopolysaccharide-induced tumor necrosis factor-alpha production by inhibiting activation of both nuclear factor-kappaB and activator protein-1 in human monocytes. *J Pharmacol Exp Ther* 2003; **305**: 298-305
16 **Camhi SL,** Alam J, Wiegand GW, Chin BY, Choi AM. Transcriptional activation of the HO-1 gene by lipopolysaccharide is mediates by 5' distal enhancers: role of reactive oxygen intermediates and AP-1. *Am J Respir Cell Mol Biol* 1998; **18**: 226-234
17 **Lee PJ,** Camhi SL, Chin BY, Alam J, Choi AM. AP-1 and STAT mediate hyperoxia-induced gene transcription of heme oxygenase-1. *Am J Physiol Lung Cell Mol Physiol* 2000; **279**: L175-182
18 **Ryter SW,** Xi S, Hartsfield CL, Choi AM. Mitogen activated protein kinase (MAPK) pathway regulates heme oxygenase-1 gene expression by hypoxia in vascular cells. *Antioxid Redox Signal* 2002; **4**: 587-592
19 **Nelson MT,** Quayle JM. Physiological roles and properties of potassium channels in arterial smooth muscle. *Am J Physiol* 1995; **268**(4 Pt 1): C799-822
20 **Wang YX,** Zheng YM, Abdullaev I, Kotlikoff MI. Metabolic inhibition with cyanide induces calcium release in pulmonary artery myocytes and Xenopus oocytes. *Am J Physiol Cell Physiol* 2003; **284**: C378-388
21 **Haddad JJ.** Glutathione depletion is associated with augmenting a proinflammatory signal: evidence for an antioxidant/pro-oxidant mechanism regulating cytokines in the alveolar epithelium. *Cytokines Cell Mol Ther* 2000; **6**: 177-187
22 **Haddad JJ,** Land SC. Redox signaling-mediated regulation of lipopolysaccharide-induced proinflammatory cytokine biosynthesis in alveolar epithelial cells. *Antioxid Redox Signal* 2002; **4**: 179-193
23 **Wiesel P,** Foster LC, Pellacani A, Layne MD, Hsieh CM, Huggins GS, Strauss P, Yet SF, Perrella MA. Thioredoxin facilitates the induction of heme oxygenase-1 in response to inflammatory mediators. *J Biol Chem* 2000; **275**: 24840-24846
24 **Tenhunen R,** Marver HS, Schmid R. The enzymatic conversion of heme to bilirubin by microsomal heme oxygenase. *Proc Natl Acad Sci U S A* 1968; **61**: 748-755
25 **McCoubrey WK Jr**, Huang TJ, Maines MD. Isolation and characterization of a cDNA from the rat brain that encodes hemoprotein heme oxygenase-3. *Eur J Biochem* 1997; **247**: 725-732
26 **Maines MD.** Heme oxygenae: function, multiplicity, regulatory mechanism, and clinical applications. *FASEB J* 1988; **2**: 2557-2568
27 **Fujiwara T,** Takahashi T, Suzuki T, Yamasaki A, Hirakawa M, Akagi R. Differential induction of brain heme oxygenase-1 and heat shock protein 70 mRNA in sepsis. *Res Commun Mol Pathol Pharmacol* 1999; **105**: 55-66
28 **Agarwal A,** Nick HS. Renal response to tissue injury: lessons from heme oxygenase-1 gene GeneA blation and expression. *J Am Soc Nephrol* 2000; **11**: 965-973
29 **Yachie A,** Niida Y, Wada T, Igarashi N, Kaneda H, Toma T, Ohta K, Kasahara Y, Koizumi S. Oxidative stress causes enhanced endothelial cell injury in human heme oxygenase-1 deficiency. *J Clin Invest* 1999; **103**: 129-135
30 **Lee TS,** Chau LY. Heme oxygenase-1 mediates the anti-inflammatory effect of interleukin-10 in mice. *Nat Med* 2002; **8**: 240-246
31 **Inoue S,** Suzuki M, Nagashima Y, Suzuki S, Hashiba T, Tsuburai T, Ikehara K, Matsuse T, Ishigatsubo Y. Transfer of heme oxygenase 1 cDNA by a replication-deficient adenovirus enhances interleukin 10 production from alveolar macrophages that attenuates lipopolysaccharide-induced acute lung injury in mice. *Hum Gene Ther* 2001; **12**: 967-979
32 **Chan ED,** Riches DW, White CW. Redox paradox: effect of N-acetylcysteine and serum on oxidation reduction-sensitive mitogen-activated protein kinase signaling pathways. *Am J Respir Cell Mol Biol* 2001; **24**: 627-632
33 **Haddad JJ,** Land SC. Redox/ROS regulation of lipopolysaccharide-induced mitogen-activated protein kinase (MAPK) activation and MAPK-mediated TNF-alpha biosynthesis. *Br J Pharmacol* 2002; **135**: 520-536
34 **Tournier C,** Hess P, Yang DD, Xu J, Turner TK, Nimnual A, Bar-Sagi D, Jones SN, Flavell RA, Davis RJ. Requirement of JNK for stress-induced activation of the cytochenrome c-mediated death pathway. *Science* 2000; **288**: 870-874
35 **Widmann C,** Gibson S, Jarpe MB, Johnson GL. Mitogen activated protein kinase: conversation of a three-kinase module from yeast to human. *Physiol Rev* 1999; **79**: 143-180
36 **Whitmarsh AJ,** Shore P, Sharrocks AD, Davis RJ. Integration of MAP kinase signal transduction pathway at the serum response element. *Science* 1995; **269**: 403-407

Edited by Wang XL and Xu FM

PO Box 2345, Beijing 100023, China
Fax: +86-10-85381893
E-mail: wjg@wjgnet.com www.wjgnet.com

World J Gastroenterol 2004;10(12):1795-1797
World Journal of Gastroenterology
Copyright ©2004 by The WJG Press ISSN 1007-9327

• CLINICAL RESEARCH •

Investigation of regurgitation and other symptoms of gastroesophageal reflux in Indonesian infants

Badriul Hegar, Aswitha Boediarso, Agus Firmansyah, Yvan Vandenplas

Badriul Hegar, Aswitha Boediarso, Agus Firmansyah, Department of Pediatrics, Cipto Mangunkusumo Hospital, University of Indonesia, Jakarta, Indonesia
Yvan Vandenplas, Department of Pediatrics, Academisch Ziekenhuis Vrije UniversiteitBrussel, Brussels, Belgium
Correspondence to: Yvan Vandenplas, Department of Pediatrics, Academic Children's Hospital, VUB, Laarbeeklaan 101, 1090 Brussels, Belgium. yvan.vandenplas@az.vub.ac.be
Telephone: +32-24775780 **Fax:** +32-24775783
Received: 2003-09-09 **Accepted:** 2003-12-01

Abstract

AIM: To evaluate the incidence of regurgitation and other symptoms of gastroesophageal reflux in Indonesian infants.

METHODS: In a cross-sectional study at the University Outpatient Clinic for vaccination in Jakarta, 138 mothers of healthy infants less than 12-mo old were prospectively asked to report the frequency of regurgitation.

RESULTS: Whatever the age was, some infants did not regurgitate (from 10% during the first month of life to 67% in 1-year-old infants). Regurgitation of at least once a day was reported in 77% of infants younger than 3 mo. Daily regurgitation decreased to 12% in the 9-12 mo old group. Reported peak prevalence was 81%(26/32) during the first month of life. Regurgitation decreased sharply between the 4-6 and 7-9 mo old groups (from 44% to 9%). The longer the regurgitation persisted, the more frequently the mother perceived regurgitation as a problem. Volume and frequency of regurgitation, back arching, irritability, crying and refusal of feeding were the symptoms causing maternal anxiety. The longer the regurgitation persisted, the more frequently the mothers viewed it as a health problem.

CONCLUSION: Regurgitation occurs frequently in Indonesian infants, and is a frequent cause of concern to mothers.

Hegar B, Boediarso A, Firmansyah A, Vandenplas Y. Investigation of regurgitation and other symptoms of gastroesophageal reflux in Indonesian infants. *World J Gastroenterol* 2004; 10(12): 1795-1797
http://www.wjgnet.com/1007-9327/10/1795.asp

INTRODUCTION

Regurgitation is the effortless return of gastric contents into the mouth, and the most common symptom of infantile gastroesophageal reflux (GER). Few attempts have been made to determine the prevalence of regurgitation and its natural course in infants. In the Western world, evaluation of the natural progression of symptoms of GER at any age has become virtually impossible because of widespread self-treatment and a lack of medical referral. It is not clear how important genetic, racial and ethnic factors may be in the clinical presentation, the prevalence and the natural history of GER disease. In the Eastern part of the world, it is commonly thought that regurgitation is less frequent than in the United States and Europe. For these reasons, determining the prevalence of GER in Indonesian infants is of interest.

MATERIALS AND METHODS

Data were collected from mothers bringing their healthy infants to the Outpatient Clinic of the Cipto Mangunkusumo Hospital, Jakarta, for routine immunization. All infants were born at term and in good general health with adequate nutritional status (P50-97 NCHS). Most of the mothers were from the middle-low socioeconomic class and worked as housewives. The data were obtained by prospectively interviewing mothers using a standard questionnaire about the prevalence of regurgitation during the previous two wk and other descriptive information.

The same author (BH) interviewed 138 consecutive mothers, presenting to the outpatient clinic of one of the local authors. Each interview lasted for 15 to 20 min. All mothers agreed to participate in the study. Age distribution of the infants is listed in Table 1. There were 75 male and 63 female infants. Mothers were asked the number of episodes of regurgitation per day, and whether they considered regurgitation as a health problem, whether the frequency or volume of emesis was a health problem and whether the infant had such symptoms as crying, back arching, irritability, or refusal to feed, as well as whether the symptoms had an adverse impact on the baby's quality of life.

The two-tailed unpaired *t*-test was used, statistical significance was set at $P<0.05$.

Table 1 Age distribution of studied infants

Age (mo)	Infants (*n*)
0-3	74
4-6	34
7-9	21
10-12	9
Total	138

RESULTS

Table 2 summarizes the prevalence and frequency of regurgitation in the infants by month of age. Up to the age of 3 mo, about half of the infants regurgitated more than two times a day, the number was slightly higher in the first mo of life and smaller at 3 mo. In the group regurgitating 1 to 4 times a day, there was a sharp decrease in the number of episodes of regurgitation to almost zero by the age of 7 to 8 mo. Twenty-five percent of the infants regurgitated more than 4 times a day during the first month of life, but from the age of 6 mo all infants regurgitated less than 4 times a day. Table 3 shows the number of mothers who were concerned about regurgitation. The evolution of concern was inversely related to the persistence of regurgitation. During the first month of life, many infants regurgitated, and few mothers expressed their concerns. However, the mothers of older infants with persistent vomiting became concerned about the symptom. Among infants regurgitating more than once a day, about 40% of the mothers asked for medical advice about

the symptom. The reasons for maternal concern are listed in Table 4, and included the excessive volume and frequency of regurgitation, and symptoms suggesting a decreased quality of life of the infants such as food refusal, crying, back arching and irritability. The volume of regurgitation was less frequently considered as a problem than the frequency of regurgitation (9% *vs* 66%). Crying and irritability were the second most frequent reasons for concern among the mothers (57%). Food refusal and back arching were reported as reasons for concern in 26% and 20%, respectively. Mothers of regurgitating infants estimated their infants had an impaired quality of life (75 *vs* 15 %, $P<0.05$). Infants of unconcerned mothers had much less frequent symptoms than infants of concerned mother ($P<0.05$).

Table 2 Daily frequency of regurgitation in 138 healthy infants

Age (mo)	Infants	Daily frequency of regurgitation (%)			
		0	<1	1-4	>4
1	32	3 (10)	3 (10)	18 (55)	8 (25)
2	25	3 (12)	2 (8)	13 (15)	7 (28)
3	17	5 (29)	1 (6)	8 (47)	3 (18)
4	10	6 (60)	1 (10)	3 (30)	0 (0)
5	14	3 (21)	2 (15)	6 (43)	3 (21)
6	10	6 (60)	1 (10)	3 (30)	0 (0)
7	10	6 (60)	2 (20)	2 (20)	0 (0)
8	3	1 (33)	2 (67)	0 (0)	0 (0)
9	8	8 (10)	0 (0)	0 (0)	0 (0)
10	5	4 (80)	0 (0)	1 (20)	0 (0)
11	1	1 (100)	0 (0)	0 (0)	0 (0)
12	3	2 (67)	1 (33)	0 (0)	0 (0)
	138	48(35)	15 (11)	54 (39%)	21 (15%)

Table 3 Number of mothers considering regurgitation as a health problem

	Daily regurgitation frequency (%)			
	<1	1-4	>4	
With concern	3	24	8	35 (25)
Without concern	60	30	13	103 (75)

Table 4 Symptoms of gastroesophageal reflux and number of mothers showing concern

Symptom	*n* (%)
Crying and irritability	20 (57)
Food refusal	9 (26)
Back arching	7 (20)
Excessive frequency of regurgitation	23 (66)
Excessive volume of regurgitation	3 (9)

DISCUSSION

Recent studies have suggested that GER may in part be genetically determined. Thus, its prevalence and severity might be expected to vary according to racial or ethnic background. Radiology is not recommended in the diagnosis of GER. The radiological method of GER evaluation showed a specificity of 50% and a sensitivity of 29%, as compared to 24-h pH monitoring[1]. A genetic influence on the prevalence of GER was supported by the finding that GER symptoms are more frequently encountered in the relatives of GER disease patients[2]. Moreover, the concordance for GER is higher in monozygotic than dizygotic twins[3]. A locus on chromosome 13q, between microsatellite D13S171 and D13S263, has been linked with severe GER in 5 families with multigenerational histories[4], but the same abnormal locus was not found in 5 other families, possibly due to the genetic heterogeneity of GER and different clinical presentations among patients studied[5]. The incidence of hiatal hernia was reported to be much lower in Korea (1.4%) than in Western world (2.3-50%)[6]. Several studies have confirmed the familial segregation of hiatal hernia, Barrett's esophagus, esophageal carcinoma and GER.

There are only a few studies that have attempted to describe the natural history of GER in children. In some of these studies, infantile GER was excluded[7]. Orenstein developed a questionnaire to identify infants with GER[8]. At least regurgitation occurred once a day in half of 0- to 3-mo-old white non-Hispanic infants, and increased up to two thirds at 4 mo and decreased to 5% at 10-12 mo of age[9]. Daily regurgitation was present in 50% of infants younger than 3 mo, in more than 66% at 4 mo, but only in 5% at 1 year of age[8-10]. Nelson and coworkers documented the prevalence of regurgitation in a white non-Hispanic infant population in USA[9]. However, as the authors stated, their findings could not be generalized and investigations of different racial/ethnic and socioeconomic groups are needed to determine differences in prevalence of symptoms in other populations. Also in Japanese infants, regurgitation was common and decreased with age[11].

Our questionnaire intended to report the incidence of regurgitation, not of symptoms suggesting gastro-esophageal reflux (disease). Regurgitation occurred frequently in our small sample size of Indonesian infants. The sample size was relatively small for an epidemiological survey. In fact, the prevalence of regurgitation in our population was the highest ever reported. In the study by Nelson and coworkers, the prevalence of regurgitation peaked at 4 mo of age[9], whereas in our population the prevalence was highest during the first month of life. In a study from northern India, the prevalence of regurgitation in 1-6-mo-old infants was 55%[12]. In our study, 75% of 0-6-mo-old infants regurgitated at least once a day.

Complete resolution of regurgitation was the most common outcome in infant reflux, with a resolution by 10 mo of age in 55%, by 18 mo of age in 60-80% and by 2 years of age in 98%[13,14] In the study by Nelson and coworkers, and in our study, regurgitation was almost completely disappeared by 7 mo[9]. In 6-12-mo old infants, the prevalence of regurgitation was 15% in North India[12], which was similar to the findings in our population if all infants regurgitating at least once per day were considered. If the infants regurgitating less than once a day were included, then the prevalence of regurgitation among 6-12-mo old Indonesian infants was as high as 30%. In all studies evaluating the natural evolution of infant regurgitation, there was a sharp decline around 6-7 mo towards a disappearance at the age of 12 mo[9,12,15].

According to epidemiological data from France, Australia and the United States, excessive regurgitation was a cause of concern and medical consult in about 25% of parents[8-10]. Spilling in infancy was very common, but the majority of children settled by 13 to 14 mo of age. However, those with frequent spilling (>90 d) were more likely to have GER symptoms at 9 years of age[16]. Esophagitis occurred in one quarter of infants with persistent distress[17]. There was a subgroup of otherwise healthy infants, presenting with wheeze and/or stridor, who had isolated swallowing dysfunction and silent aspiration as the cause of their respiratory symptoms[18]. Our findings were similar, 30% of the mothers showed concern over regurgitation. Symptoms causing parental perception that regurgitation might be a problem were comparable in both studies, and included the volume and frequency of regurgitation and symptoms suggesting decreased quality of life such as crying, back-arching and irritability[9]. Parental reports about reflux-related behaviors were similar in Nelson's study and in ours[9]. Despite the concern of parents, pediatricians generally stated

that intervention was not needed[19]. Although a prospective follow-up of 63 regurgitating infants reported a complete disappearance of regurgitation by 12 mo of age, it is interesting that these same infants were reported on a long-term follow-up to have a significant increase in feeding refusal, prolonged eating time, parental distress about feeding and impaired quality of life when compared to non-regurgitating controls[15].

In conclusion, the severity and incidence of GOR were significantly higher in symptomatic than asymptomatic infants[20]. Food allergy might be common in regurgitating infants[21,22]. Recommendations for a diagnostic workup have been published[23,24]. Hydrolysates might treat regurgitation by improving gastric emptying[25]. GER frequently caused apnea in infants[26,27]. GER and regurgitation decreased the quality of life[28] in infants, and increasesd hospital stay and cost[29,30]. Worldwide, racial differences in the prevalence and persistence of infantile regurgitation seem minimal. Regurgitation in Indonesian infants tends to be very frequent, with more than 75% of 0-3-mo-old infants regurgitating at least once a day. Symptoms viewed as being related to GER and causing maternal concern are also similar. For one in three mothers worldwide, the symptom of regurgitation is a cause for concern. Mothers in Indonesia are no exception.

REFERENCES

1 **Aksglaede K**, Pedersen JB, Lange A, Funch-Jensen P, Thommesen P. Gastro-esophageal reflux demonstrated by radiography in infants less than 1 year of age. Comparison with pH monitoring. *Acta Radiol* 2003; **44**: 136-138
2 **Trudgill NJ**, Kapur KC, Riley SA. Familial clustering of reflux symptoms. *Am J Gastroenterol* 1999; **94**: 1172-1178
3 **Cameron AJ**, Lagergren J, Henriksson C. Gastroesophageal reflux disease in monozygotic and dizygotic twins. *Gastroenterology* 2002; **122**: 55-59
4 **Hu FZ**, Preston RA, Post JC, White GJ, Kikuchi LW, Wang X, Leal SM, Levenstien MA, Ott J, Self TW, Allen G, Stiffler RS, McGraw C, Pulsifer-Anderson EA, Ehrlich GD. Mapping of a gene for severe pediatric gastroesophageal reflux to chromosome 13q14. *JAMA* 2000; **284**: 325-334
5 **Orenstein SR**, Shalaby TM, Barmada MM, Whitcomb DC. Genetics of gastroesophageal reflux disease: a review. *J Pediatr Gastroenterol Nutr* 2002; **34**: 506-510
6 **Kim E**. Hiatus hernia and diverticulum of the colon: their low incidence in Korea. *N Engl J Med* 1964; **271**: 764-768
7 **Ashorn M**, Ruuska T, Karikoski R, Laippala P. The natural course of Gastroesophageal reflux disease in children. *Scand J Gastroenterol* 2002; **37**: 638-641
8 **Orenstein SR**, Shalaby TM, Cohn J. Reflux symptoms in 100 normal infants: diagnostic validity of the infant Gastroesophageal reflux questionnaire. *Clin Pediatr* 1996; **35**: 607-614
9 **Nelson SP**, Chen EH, Syniar GM, Christoffel KK. Prevalance of symptoms of gastroesophageal reflux during infancy. A pediatric-based survey. Pediatric Practice Research Group. *Arch Pediatr Adolesc Med* 1997; **151**: 569-572
10 **Chouhou D**, Rossignol C, Bernard Fl. Le reflux gastrooesophagien dans le centres de bilan de sante de l'enfant de moins de 4 ans. *Arch Fr Pediatr* 1992; **49**: 843-845
11 **Miyazawa R**, Tomomasa T, Kaneko H, Tachibana A, Ogawa T, Morikawa A. Prevalence of gastro-esophageal reflux-related symptoms in Japanese infants. *Pediatr Int* 2002; **44**: 513-516
12 **De S**, Rajeshwari K, Kalra KK, Gondal R, Malhotra V, Mittal SK. Gastrooesophageal reflux in infants and children in north India. *Trop Gastroenterol* 2001; **22**: 99-102
13 **Carrè I.** The natural history of the partial thoracic stomach ("hiatal hernia") in children. *Arch Dis Child* 1959; **34**: 344-353
14 **Shepherd RW**, Wren J, Evans S, Lander M, Ong TH. Gastroesophageal reflux in children. Clinical profile, course and outcome with active therapy in 126 cases. *Clin Pediatr* 1987; **26**: 55-60
15 **Nelson SP,** Chen EH, Syniar GM, Christoffel KK. One-year follow-up of symptoms of gastroesophageal reflux during infancy. Pediatric Research Group. *Pediatrics* 1998; **102**: E67
16 **Martin AJ**, Pratt N, Kennedy JD, Ryan P, Ruffin RE, Miles H, Marley J. Natural history and familial relationships of infant spilling to 9 years of age. *Pediatrics* 2002; **109**: 1061-1067
17 **Heine RG**, Cameron DJ, Chow CW, Hill DJ, Catto-Smith AG. Esophagitis in distressed infants: poor diagnostic agreement between esophageal pH monitoring and histopathologic findings. *J Pediatr* 2002; **140**: 14-19
18 **Sheikh S**, Allen E, Shell R, Hruschak J, Iram D, Castile R, McCoy K. Chronic aspiration without gastroesophageal reflux as a cause of chronic respiratory symptoms in neurologically normal infants. *Chest* 2001; **120**: 1190-1195
19 **Aggett PJ**, Agostoni C, Goulet O, Hernell O, Koletzko B, Lafeber HL, Michaelsen KF, Milla P, Rigo J, Weaver LT. Antireflux or antiregurgitation milk products for infants and young children: a commentary by the ESPGHAN Committee on Nutrition. *J Pediatr Gastroenterol Nutr* 2002; **34**: 496-498
20 **Thomas EJ**, Kumar R, Dasan JB, Chandrashekar N, Agarwala S, Tripathi M, Bal CS. Radionuclide scintigraphy in the evaluation of gastro-oesophageal reflux in post-operative oesophageal atresia and tracheo-oesophageal fistula patients. *Nucl Med Commun* 2003; **24**: 317-320
21 **Hill DJ**, Hosking CS, Heine RG. Clinical spectrum of food allergy in children in Australia and South-East Asia: identification and targets for treatment. *Ann Med* 1999; **31**: 272-281
22 **Salvatore S**, Vandenplas Y. Gastroesophageal reflux and cow milk allergy: is there a link? *Pediatrics* 2002; **110**: 972-984
23 **Vandenplas Y**. Diagnosis and treatment of gastroesophageal reflux disease in infants and children. *World J Gastroenterol* 1999; **5**: 375-382
24 **Gold BD**. Epidemiology and management of gastro-oesophageal reflux in children. *Aliment Pharmacol Ther* 2004; **19**(Suppl 1): 22-27
25 **Garzi A**, Messina M, Frati F, Carfagna L, Zagordo L, Belcastro M, Parmiani S, Sensi L, Marcucci F. An extensively hydrolysed cow's milk formula improves clinical symptoms of gastroesophageal reflux and reduces the gastric emptying time in infants. *Allergol Immunopathol* 2002; **30**: 36-41
26 **Sheikh S,** Stephen TC, Sisson B. Prevalence of gastroesophageal reflux in infants with recurrent brief apneic episodes. *Can Respir J* 1999; **6**: 401-404
27 **Wenzl TG**, Silny J, Schenke S, Peschgens T, Heimann G, Skopnik H. Gastroesophageal reflux and respiratory phenomena in infants: status of the intraluminal impedance technique. *J Pediatr Gastroenterol Nutr* 1999; **28**: 423-428
28 **Khalaf MN**, Porat R, Brodsky NL, Bhandari V. Clinical correlations in infants In the neonatal intensive care unit with varying severity of gastroesophageal reflux. *J Pediatr Gastroenterol Nutr* 2001; **32**: 45-49
29 **Ferlauto JJ**, Walker MW, Martin MS. Clinically significant gastroesophageal reflux in the at-risk premature neonate: relation to cognitive scores, days in the NICU, and total hospital charges. *J Perinatol* 1998; **18**: 455-459
30 **Frakaloss G**, Burke G, Sanders MR. Impact of gastroesophageal reflux on growth and hospital stay in premature infants. *J Pediatr Gastroenterol Nutr* 1998; **26**: 146-150

Edited by Wang XL and Xu JY **Proofread by** Xu FM

PO Box 2345, Beijing 100023, China
Fax: +86-10-85381893
E-mail: wjg@wjgnet.com www.wjgnet.com

World J Gastroenterol 2004;10(12):1798-1801
World Journal of Gastroenterology
Copyright ©2004 by The WJG Press ISSN 1007-9327

• CLINICAL RESEARCH •

Severity of gastroesophageal reflux disease influences daytime somnolence: A clinical study of 134 patients underwent upper panendoscopy

Pál Demeter, Katalin Várdi Visy, Nóra Gyulai, Róbert Sike, Tamás G Tóth, János Novák, Pál Magyar

Pál Demeter, Róbert Sike, Tamás G Tóth, Outpatient Clinic of Gastroenterology, St. John' s Hospital, Budapest, Hungary
Katalin Várdi Visy, Nóra Gyulai, Pál Magyar, Department of Pulmonology, Semmelweis Medical University, Budapest, Hungary
János Novák, Dept. of Internal Medicine and Gastroenterology, Pandy Hospital, Gyula, Békés County, Hungary
Correspondence to: Dr. Pál Demeter, St. John' s Hospital, Outpatient Clinic of Gastroenterology, Szõlõskertút 7, Budakeszi 2092, Hungary. pauldemeter@axelero.hu
Telephone: +36-30-9222985 **Fax:** +36-23-457656
Received: 2003-12-10 **Accepted:** 2004-01-16

Abstract

AIM: To asses the relationship between severity of gastroesophageal refluxe disease and Epworth sleepiness scale as an indicator of daytime somnolence.

METHODS: One hundred and thirty-four patients underwent an upper panendoscopy as indicated by the typical reflux symptoms and were also investigated with regard to somnolence. Sleepiness was evaluated by Epworth Sleepiness Scale, which was compared to the severity of endoscopic findings (Savary-Miller/modified by Siewert). Patients with psychiatric disorders or being on sedato-hypnotics as well as shift workers were excluded from the study. The relationship between the severity of the reflux disease and daytime somnolence was analyzed with the help of multivariate regression analysis.

RESULTS: A positive tendency was found between the severity of the reflux disease and the corresponding Epworth Sleepiness Scale. In the case of the more severe type - Savary-Miller III - at least a mild hypersomnia was found. For this group daytime somnolence was significantly higher than in the case of the non-erosive type of Gastroesophageal Reflux Disease representing the mildest stage of reflux disease.

CONCLUSION: The severity of Gastroesophageal Reflux Disease influences daytime somnolence.

Demeter P, Visy KV, Gyulai N, Sike R, Tóth TG, Novák J, Magyar P. Severity of gastroesophageal reflux disease influences daytime somnolence: A clinical study of 134 patients underwent upper panendoscopy. *World J Gastroenterol* 2004; 10(12): 1798-1801
http://www.wjgnet.com/1007-9327/10/1798.asp

INTRODUCTION

Sleep is potentially conducive to the gastro-esophageal reflux events. The physiological antireflux mechanisms – swallowing rate, salivation, the pressure of the upper and the lower esophageal sphincter, gastric emptying - are reduced as well as the the "heartburn-signal" is depressed during the state of sleep[1-6]. Moreover, the typical lying position facilitates the flow of the gastric content towards the esophagus due to the forces of gravitation[2]. Studies of parallel 24 h pH-metry and polysomnography amongst obstructive sleep apneic patients showed that some reflux events coincide with arousals[3]. At the same time, it was also found that some apneic periods contribute to considerable reflux events, while others not. On the other hand, earlier investigations focusing on the relationship between sleep related breathing disorders and Gastroesophageal Reflux Disease (GERD) have indicated the adverse effect of nocturnal reflux events on the sleep structure[4,5]. In this respect some epidemiological studies have suggested a relationship between GERD and daytime sleepiness[6-9]. In 2003 the ProGERD study has established that the effective treatment of GERD reduces sleep disturbances[10]. The results of a Gallup Telephone Survey – conducted on behalf of the American Gastroenterological Association – have shown that the nocturnal heartburn and the regurgitation of gastric content caused frequent awakenings and sleep disturbances, which could affect daytime performance and the quality of life[11]. Therefore it appears that the nighttime reflux could have a considerable impact on the quality of sleep and it can also play a significant role in the developing of restless sleep experienced widely by the patients.

The influence of GERD on daytime cognitive functions has not been analyzed yet. In this study we focused on one of the important cognitive functions, on daytime sleepiness and its relation to the severity of GERD. The aim of the study was to describe the association between the severity of GERD and daytime somnolence.

MATERIALS AND METHODS

The database

The study was conducted by a gastroenterologist in two centers. The patients were referred for upper panendoscopy with the typical symptoms of GERD untreated. Psychiatric patients or those who took sedato-hypnotics and shift workers were excluded. The classification of GERD was based on endoscopic findings and the severity of the esophagitis[12]. We used the conventional Savary-Miller classification of the disease modified by Siewert. The Epworth Sleepiness Scale (ESS) was used as an indicator of daytime somnolence, which is a simple questionnaire measure to asses daytime somnolence amongst patients suffering of sleep-awake disorders[13-15]. The patient data were collated on an Excel 9.0 worksheet, including the severity grades of GERD (0-IV), the Epworth scale (0-24), age, gender and Body Mass Index (BMI).

Statistical methods

The extent and statistical strength of the potential relationship between GERD severity and daytime somnolence was captured by estimating the impact of diagnosed GERD categories on the indicators of sleepiness relative to the two endpoints of the reflux disease severity scale. We relied on the conventional $P<0.05$ critical values regarding the statistical tests of the results. At the same time, we also took into account a somewhat weaker, 10% significance level when evaluating the observed

associations, given the relatively small size of the available sample. We used the *SPSS 9*-software package for the statistical procedures.

RESULTS

Basic descriptions of the study population

The total available population covered 134 patients the descriptive statistics are given in Table 1. This population was characterized by an average age of 52.9 years (std. dev. 16.7), a male/female ratio of 65: 69, and an average BMI of 26.4 (std. dev. 5.1). Using the Savary-Miller definitions as modified by Sievert, our patients displayed the following distribution alongside the endoscopic categorization of reflux disease: 24 (18.9%) GERD 0 subjects, 29(21.6%) GERD I subjects, 56 (41.8%) GERD II subjects, 13(9.7%) GERD III subjects, and 12 (8.9%) GERD IV subjects. Note that we included only the sample of GERD cases with 122 patients into the detailed statistical analysis. The exclusion of GERD IV group was justified on the basis of the consideration that this set of patients is inherently heterogeneous regarding the anatomic abnormalities as well as the severity of the reflux disease itself. Obviously, this could be a confounding factor in relation to the effect on our analyzed dependent variable, the daytime sleepiness.

Table 1 Descriptive statistics of the total study population

Variable	Minimum	Maximum	Mean	SD
Age (yr)	17.00	83.00	52.940	16.752
Male	0	1	0.485	-
BMI	17.54	43.94	26.420	5.133
GERD 0	0	1	0.179	-
GERD I	0	1	0.216	-
GERD II	0	1	0.418	-
GERD III	0	1	0.097	-
GERD IV	0	1	0.089	-
EPWORTH	1.00	24.00	7.440	4.226
		n=134		

Note: The mean values of the dichotomous variables (with cases taking values 0 or 1) refer to frequencies and thus the standard deviation is not an applicable measure for them.

The population means of the Epworth sleepiness scale used as a direct measure of somnolence here was 7.4 (SD. 4.2) (while slightly higher -7.6 (SD4.3) – for the sample covering the GERD 0 and GERD I-IV patients). We created a further dependent variable, "abnormal Epworth", for the observations with an index value greater than 8 taking into account that at least a mild form of hypersomnia could be diagnosed above this level. Since our sample was not primarily directed at patients suffering from sleep disorders, it did not seem to be reasonable to select a higher limit. Nevertheless, the detectable tendencies did not differ qualitatively for the critical Epworth value of 10 from the one, which is presented here. The "abnormal Epworth" took the frequency of 44.8% (and 44.3% after dropping the GERD IV group).

Table 2 shows the patterns for the two above described dependent variables by GERD diagnosis. It is evident that the means for the Epworth indices exhibited increasing values alongside the severity of GERD taking the sub-groups of GERD 0 and GERD I-III together. Whereas GERD I exceeded by 0.5 (6.2% of the population average) and GERD II by 0.7(9.2% of the population average) the 6.7 mean value of our GERD 0 cluster, this difference was already 4.1(54.5% of the population average) in the case of the GERD III group. This increasing tendency reflecting the severity of GERD appeared to be even more characteristic with respect to the frequencies of "abnormal Epworth". Compared with the 29.1% ratio calculated for GERD 0, the observed percentage increments in the presence of hypersomnia were: 8.8% (19.7% of the population average) for GERD I, 17.3%(38.7% of the population average) for GERD II, and 47.8%(106.9% of the population average) for the GERD III group. For information, the table gives our observations for the GERD IV patients as well: we found the lowest group mean value with respect the Epworth index, but the occurrence of hypersomnia went above the population average. This seems to provide a further aspect regarding the heterogeneity of patients diagnosed with GERD IV.

Table 2 Measures of daytime somnolence by GERD groups

GERD	*n*	EPWORTH index Mean (Std. dev.)	"Abnormal" EPWORTH >8 Frequency
GERD 0	24	6.708 (4.639)	0.291
GERD I	29	7.172 (4.036)	0.379
GERD II	56	7.393 (3.706)	0.464
GERD III	13	10.769 (5.890)	0.769
GERD IV	12	6.166 (2.588)	0.500
Total sample	134	7.440 (4.226)	0.447

Notes: 1. The equality of the mean values for the Epworth indices could be rejected at 5% significance level on the basis of the Student *t*-tests for the following pairs of GERD groups: GERD III *vs* GERD II, GERD III *vs* GERD I, GERD III *vs* GERD 0, and GERD III *vs* GERD IV. 2. The Pearson chi-square tests for the frequencies of "abnormal" Epworth indices indicated significant differences at 5% critical value in the case of the following 2x2 tables : GERD III *vs* GERD II, GERD III *vs* GERD I, GERD III *vs* GERD 0.

Statistical analysis and results

To evaluate our observations indicating a positive association between severity of GERD and somnolence more precisely, we performed linear regressions for the variation of the Epworth index and logistic regressions for the probability of "abnormal Epworth" over the sample comprising the GERD 0 and GERD I-III cases. Apart from the categorical variables constructed for the reflux disease classifications, we also included the BMI values, and the observations for gender and age as explanatory variables. Since our estimated models typically gave a better overall fit when measuring age above 50 rather than the number of years directly, we present our result with the former control variable below.

Table 3 summarizes our linear regression analysis. The first two blocks of the table present the results with the inclusion of the additional control variables. Although the sign of the regression coefficient (B) obtained for BMI was positive as expected, the contribution of the variable did not emerge to be statistically significant. At the same time, the higher age was found to reduce the expected value of the Epworth index at $P<0.05$ critical values. As far as the estimates for the GERD categories were concerned, the multivariate regression seemed to support the direct observation that reflux disease severity incurs a positive effect on the extent of the Epworth index. When choosing GERD 0 as the reference category (that is the indicator for this group was excluded), the coefficients for the sub-groups of GERD I-III took positive and increasing values as it is shown by the figures of the first model. These coefficients reached a critical magnitude at the GERD III group, which already proved to be significant at 5% level. In numeric terms, this implied that after filtering out the joint effect of the control variables the Epworth index was estimated to be lifted up by 47.5% of the population mean relative to GERD 0 in the case of the third sub-group of GERD I-III. The negatively

Table 3 Linear regression and dependent variable: Epworth index

	Reference: GERD 0 & control variables			Reference: GERD III & control variables			Reference: GERD 0			Reference: GERD III		
	B	*t*-stat	Signif	B	*t*-stat	Signif	B	*t*-stat	Signif	B	*t*-stat	Signif
Constant	5.210	2.370	0.019	8.743	3.653	0.000	6.708	7.748	0.000	10.769	9.155	0.000
GERD 0				-3.534	-2.410	0.018				-4.061	-2.780	0.006
GERD I	0.503	0.433	0.666	-3.031	-2.125	0.036	0.464	0.397	0.692	-3.597	-2.541	0.012
GERD II	0.635	0.610	0.543	-2.899	-2.178	0.031	0.685	0.662	0.510	-3.376	-2.586	0.011
GERD III	3.534	2.410	0.018				4.061	2.780	0.006			
BMI	0.092	1.254	0.212	0.092	1.254	0.212						
NEM	-0.002	-0.003	0.998	-0.002	-0.003	0.998						
AGE50	-1.557	-1.999	0.048	-1.557	-1.999	0.048						
						n =122						

Table 4 Logistic regression , dependent variable: "abnormal" EPWORTH

	Reference: GERD 0 & control variables				Reference: GERD III & control variables				Reference: GERD 0				Reference: GERD III			
	B	Wald-stat	Signif	Odds ratio	B	Wald-stat	Signif	Odds ratio	B	Wald-stat	Signif	Odds ratio	B	Wald-stat	Signif	Odds ratio
Constant	-0.399	0.153	0.695		-0.399	0.153	0.695		-0.079	0.119	0.729		-0.079	0.119	0.729	
GERD		6.547	0.087			6.547	0.087			7.452	0.058			7.452	0.058	
GERD 0					-1.996	6.126	0.013	0.136					-2.091	6.887	0.008	0.124
GERD I	0.404	0.461	0.497	1.498	-1.592	4.234	0.039	0.204	0.394	0.447	0.503	1.484	-1.696	4.963	0.025	0.183
GERD II	0.704	1.748	0.186	2.023	-1.292	3.118	0.077	0.275	0.744	2.025	0.154	2.104	-1.347	3.592	0.058	0.260
GERD III	1.996	6.126	0.013	7.361					2.091	6.887	0.008	8.095				
BMI	0.023	0.406	0.523	1.023	0.023	0.406	0.523	1.023								
NEM	-0.166	0.174	0.675	0.847	-0.166	0.174	0.675	0.847								
AGE50	-0.408	1.112	0.291	0.664	-0.408	1.112	0.291	0.664								
							n=122									

signed coefficients with decreasing absolute values that were estimated relative to GERD III directly mirrored the results of the first model, but this regression exercise gave an opportunity for further statistical tests (see the second block). Thus, the coefficients obtained for GERD 0 as well as for GERD I, II were significantly (P<0.05) different from zero, and consequently indicated statistically relevant deviations from the expected Epworth value at GERD III serving as the baseline. These two estimations above were repeated without the additional control variables as well (see the third and fourth blocks of Table 3). The coefficients in this case were of course equivalent with the differences of the Epworth means grouped in Table 2. At the same time, the corresponding *t*-values confirmed our previous results indicating that GERD III was associated with a significantly greater sleepiness scale relative to GERD 0, while GERD 0, GERD I and GERD II were associated with a significantly smaller one relative to the GERD III group.

We could reach essentially similar conclusions on the basis of the logistic regressions investigating the occurrences of the "abnormal Epworth" as it is presented in Table 4. The sign of the coefficients (B) obtained for the additional control variables was the same as in the case of the linear regression, but we could not identify a separate significant effect in this case on the basis of the Wald-tests. At the same time, the Wald-statistic referring to the joint effect of the GERD categories (i.e. the "GERD" row of the table) already displayed a weakly significant (P<0.1) value. The estimates relative to GERD 0 gave again increasing coefficients with odds ratios greater than one (see the parameters of the first model). The odds ratio computed for GERD III was different from one at P<0.05. Correspondingly, we found in absolute terms that the estimated ratio of hypersomnia to the normal cases *ceteris paribus* increased by 7.4 times in the GERD III group compared with the least severe reflux disease cluster. At the same time, the increasing odds ratios with values lower than one derived from the logistic regression using GERD III as the reference category showed statistically significant differences in the case all less severe reflux disease groups (the second block of the table). (In this respect, GERD II could be regarded as a "transitory" category between GERD III and the milder disease classes as far as this difference appeared to be only weakly significant.) The regressions re-run without the control variables produced the odds ratios that could be directly calculated from the frequencies of Table 2 (see the third and fourth models of Table 4). The Wald-tests performed on these coefficients indicated again that the probability of hypersomnia to occur was significantly higher for GERD III relative to GERD 0, and significantly lower for GERD 0, GERD I and GERD II relative to GERD III.

DISCUSSION

We raised the question whether the well-known nocturnal symptoms of patients suffering from GERD results in the deterioration of daytime cognitive functions. Daytime sleepiness was chosen to relate the severity of GERD assessed by panendoscopy to the measure of ESS. Our results indicate that the more severe GERD groups categorized by the Savary-Miller classification exhibit a gradually increasing, more "somnolent" result by the ESS. Moreover, while in the group GERD 0 only 29% of patients reaches the mild somnolence value of 8 on ESS, in GERD I this rate grows up to 39% and in GERD II it reaches 46%. In the group of GERD III more than 77% of the subjects suffered of significant somnolence. This relationship was confirmed by the multivariate regression analysis when estimating the ESS result directly as well as

when examining the probability of at least mild hypersomnia, especially with regard to significantly higher somnolence observed in the most severe GERD population.

Our findings seem to imply that there is a significant fragmentation in the sleep structure in the case of severe GERD. Previous investigations already indicated that arousals, which play a major role in the fragmentation of the sleep structure, could be generated by some reflux events[4,16]. The higher positioned and longer than 5 min reflux events are more likely to cause arousals. If the reflux content leaves the esophagus and migrates into the upper respiratory tract, it could irritate the acid sensitive receptors, which are located in the mucus layer[17]. This irritation would lead to the change in muscle tone as a manifestation of arousal producing a motoric restless sleep. In addition, the regurgitation of the acidic gastric fluid may cause discomfort, choking, aspiration, and disturbed sleep with multiple awakenings. The motoric restless sleep is more likely to happen even independently of the pH value of the gastric content, if the refluxate reaches the sensitive pharyngeal level. We, however only assessed patients with the classical self-reported GERD. In fact, patients with extra esophageal symptoms may develop daytime somnolence even earlier and without visible esophagitis.

Finally, it should be noted that GERD is not the dysfunction of acid production but the insufficiency of the LES. So it is important to explore daytime somnolence in the cases of severe and therapy refractory GERD[18]. These cases can be caused by sleep-related breathing disorders, which can augment the symptoms of GERD and cause daytime sleepiness as well.

REFERENCES

1 **Pasricha PJ.** Effect of sleep on gastroesophageal physiology and airway protective mechanisms. *Am J Med* 2003; **115**(Suppl 3A): 114S-118S

2 **Khoury RM**, Camacho-Lobato L, Katz PO, Mohiuddin MA, Castell DO. Influence of spontaneous sleep positions on nighttime recumbent reflux in patients with gastroesophageal reflux disease. *Am J Gastroenterol* 1999; **94**: 2069-2073

3 **Penzel T**, Becker HF, Brandenburg U, Labunski T, Pankow W, Peter JH. Arousal in patinets with gastro-oesophageal reflux and sleep apnoea. *Eur Respir J* 1999; **14**: 1266-1270

4 **Ing AJ**, Ngu MC, Breslin AB. Obstructive sleep apnea and gastroesophageal reflux. *Am J Med* 200; **108**(Suppl 4A): 120S-125S

5 **Orr WC**. Sleep-related breathing disorders. Is it all about apnea? *Chest* 2002; **121**: 8-11

6 **Janson C**, Gislason T, De Backer W, Plaschke P, Bjornsson E, Hetta J, Kristbjarnason H, Vermeire P, Boman G. Daytime sleepiness, snoring and gastro-oesophageal reflux amongst young adults in three European countries. *J Intern Med* 1995; **237**: 277-285

7 **Gislason T**, Janson C, Vermeire P, Plaschke P, Bjornsson E, Gislason D, Boman G. Respiratory symptoms and nocturnal gastroesophageal reflux: a population-based study of young adults in three European countries. *Chest* 2002; **121**: 158-163

8 **Janson C**, Gislason T, De Backer W, Plaschke P, Bjornsson E, Hetta Kristbjarnason H, Vermeire P, Boman G. Prevalence of sleep disturbances among young adults in three European countries. *Sleep* 1995; **18**: 589-597

9 **Suganuma N**, Shigedo Y, Adachi H, Watanabe T, Kumano-Go T, Terashima K, Mikami A, Sugita Y, Takeda M. Association of gastroesophageal reflux disease with weight gain and apnea, and their disturbance on sleep. *Psychiatry Clin Neurosci* 2001; **55**: 255-256

10 **Leodolter A**, Kulig M, Nocon M, Vieth M, Lindner D, Labenz J. Esomeprazole therapy improves sleep disorders in patients with gastroesophageal reflux disease (GERD): A report from the ProGERD study. *Gastroenterology* 2003; **124**(Suppl 1): A-226

11 **Shaker R**, Castell DO, Schoenfeld PS, Spechler SJ. Nighttime heartburn is an under-appreciated clinical problem that impacts sleep and daytime function: the results of a Gallup survey conducted on behalf of the American Gastroenterological Association. *Am J Gastroenterol* 2003; **98**: 1487-1493

12 **Savary M**, Miller G. The esophagus: handbook and atlas of endoscopy. *Solothurn, Switzerland: Verlag Gassman* 1978: 135-142

13 **Johns MW**. A new method for measuring daytime sleepiness: the epworth sleepiness scale. *Sleep* 1991; **14**: 540-545

14 **Johns MW.** Sleep propensity varies with behaviour and the situation in which it is measured: the concept of somnificity. *J Sleep Res* 2002; **11**: 61-67

15 **Roth T**, Roehrs TA. Etiologies and sequele of excessive daytime sleepiness. *Clin Ther* 1996; **18**: 562-576

16 **Orr WC**, Robinson MG, Johnson LF. The effect of esophageal acid volume on arousals from sleep and acid clearance. *Chest* 1991; **99**: 351-354

17 **Thach BT**. Maturation and transformation on reflexes that protect the laryngeal airway from liquid aspiration from fetal to adult life. *Am J Med* 2001; **111**(Suppl 8A): 69S-77S

18 **Wolf S**, Furman Y. Sleep apnea and gastroesophageal reflux disease. *Ann Intern Med* 2002; **136**: 490-491

Edited by Wang XL **Proofread by** Xu FM

PO Box 2345, Beijing 100023, China
Fax: +86-10-85381893
E-mail: wjg@wjgnet.com www.wjgnet.com

World J Gastroenterol 2004;10(12):1802-1805
World Journal of Gastroenterology
Copyright ©2004 by The WJG Press ISSN 1007-9327

• CLINICAL RESEARCH •

Intestinal microecology and quality of life in irritable bowel syndrome patients

Jian-Min Si, Ying-Cong Yu, Yu-Jing Fan, Shu-Jie Chen

Jian-Min Si, Yu-Jing Fan, Shu-Jie Chen, Department of Gastroenterology, Sir Run Run Shaw Affiliated Hospital of Zhejiang University, Hangzhou 310016, Zhejiang Province, China
Ying-Cong Yu, Third People's Hospital of Wenzhou, Wenzhou 325000, Zhejiang Province, China
Supported by Shanghai Sine Pharmaceutical.Co., Ltd. and Wenzhou Science and Technology Bureau, Zhejiang Province, China
Correspondence to: Professor Jian-Min Si, Department of Gastroenterology, Sir Run Run Shaw Affiliated Hospital of Zhejiang University, Hangzhou 310016, Zhejiang Province, China. sijm@163.net
Telephone: +86-571-86090073-2005
Received: 2003-08-02 **Accepted:** 2003-11-19

Abstract

AIM: It has been noticed that gastroenteritis or dysentery plays a role in pathogenesis of irritable bowel syndrome (IBS), and antibiotics can increase functional abdominal symptoms, both of which may be partly due to intestinal flora disorders. This study was to determine the change of gut flora of IBS, a cluster of abdominal symptoms. Because of the chronic course and frequent occurrence of the disease, IBS patients suffered much from it. So the quality of life (Qol) of IBS patients was also evaluated in this study.

METHODS: Twenty-five Rome II criteria-positive IBS patients were recruited, and 25 age and gender-matched healthy volunteers were accepted as control. The fecal flora, including *Lactobacillus, Bifidobacterium, Bacteroides , C. perfringens Enterobacteriacea* and *Enterococus*, were analyzed quantitatively and qualitatively. We also calculated the ratio of *Bifidobacterium* to *Enterobacteriaceae* (B/E ratio) in both IBS patients and controls. In both groups, the data were further analyzed based on age difference, and comparisons were made between the younger and elder subgroups. We also evaluated the quality of life (QoL) of IBS patients and the control group using the Chinese version of SF-36 health questionnaire.

RESULTS: In IBS patients, the number of fecal *Bifidobacterium* was significantly decreased and that of *Enterobacteriaceae* was significantly increased compared with that in healthy controls (both $P<0.05$).The mean microbial colonization resistance (CR) of the bowel in IBS patients was smaller than 1, making a significant difference compared with that in control which was more than 1 ($P<0.01$). There was no significant difference in gut flora between two subgroups. While in control, the elder subgroup presented more *Enterobacteriacea* than the younger one ($P<0.05$). Compared with the control group, IBS patients had significantly lower scores on all SF-36 scales, with the exception of physical functioning. However, there was no significant correlation between quality of life and enteric symptoms in IBS patients.

CONCLUSION: There are intestinal flora disorders in IBS patients, which may be involved in triggering the IBS-like symptoms. IBS patients experience significant impairment in QoL, however, the impairment is not caused directly by enteric symptoms.

Si JM, Yu YC, Fan YJ, Chen SJ. Intestinal microecology and quality of life in irritable bowel syndrome patients. *World J Gastroenterol* 2004; 10(12): 1802-1805
http://www.wjgnet.com/1007-9327/10/1802.asp

INTRODUCTION

Many patients with typical irritable bowel syndrome (IBS) blamed all their bowel symptoms for acute gastroenteritis or dysentery, and it has been shown that intestinal infection does play an important role in the pathogenesis of IBS[1,2]. Although the mechanisms underlying postinfectious IBS are not clear, microbiological environmental alterations may be partly responsible for the pathogenesis. There is even evidence showing that antibiotics can increase functional abdominal symptoms[3]. In some cases, this is due to the colonization of pathogenic bacteria such as *Clostridium difficile*. In others it may be due to changes in bowel flora, which have been shown to persist for many months after a single antibiotic course.

In this study, the changes of intestinal microecology were investigated. Since age or sex may influence the composition of gut flora[4,5], age and sex-matched controls were recruited and the gut flora was also studied. Furthermore, the impact of IBS on quality of life (QoL) was evaluated using SF-36 health questionnaire (Chinese Version). Finally, the correlation between enteric symptoms scores and QoL in IBS patients was analyzed.

MATERIALS AND METHODS

Subjects

From September 2002 to March 2003, 25 Rome II criteria-positive[6] IBS patients diagnosed at the Department of Gastroenterology, Sir Run Run Shaw Affiliated Hospital of Zhejiang University were recruited (8 males, 17 females, mean age 45.40±10.56 years,ranging from 26 to 64 years). Subjects were excluded if they had any organic disease and those who had taken antibiotics or microecological modulators within 2 weeks before study were also ruled out. Twenty-five healthy volunteers (age and gender-matched) were accepted as control. All procedures were approved by the Ethical Committee of Medical College of Zhejiang University.

Bacteriogical analysis of intestinal flora

Selective culture medium for *Lactobacillus* (LBS), *Bifidobacterium* (Bs), *Bacteroides* (NBGT), *Enterococus* (EC) and *Enterobacteriacea* (EMB) was prepared by the Institute of Infectious Diseases, the First Affiliated Hospital of Zhejiang University. The culture medium for *C. perfringen* (TSN) was bought from Biomerieux (French). Glove box (Forma Scientific, Lnc., USA) was also needed.

Bacteriological analysis of intestinal flora was performed using the method that was essentially the same as that established by Okusa *et al*[7]. In brief, 10 g fresh stool was collected and sent to laboratory within 30 min in an anaerobic

jar. After 1 g fresh stool was aseptically quantified and homogenized, then diluted with an anaerobic solution in an anaerobic chamber (decimal dilutions up to 10^{-7} were prepared). Fifty μL of serial dilution volume (10^{-1}, 10^{-3}, 10^{-5}, 10^{-7}) of the specimens was spread over the above agar media with a L-shape stick. Aerobic bacteria were cultivated at 37 ℃ in an incubator for 48 h and anaerobic bacteria were cultivated in glove box (800 mL/L nitrogen, 100 mL/L hydrogen, and 100 mL/L carbon dioxide) at 37 ℃ for 48-72 h. After incubation, morphologically distinct colonies were described, calculated, isolated, and identified by morphology, Gram reaction and API fermentation tests, *etc*. The results were expressed as $\log_{10}$ of the number of bacteria per gram wet weight of feces (colony forming units/g , CFU/g). In our study, 2×10^2 (CFU) were set as the lowest detection limit. The incidence of each bacterial group recorded as the percentage of each bacterial group relative to the total bacteria was calculated. Furthermore, the ratio of *Bifidobacterium* to *Enterobacteriaceae* (B/E ratio) was calculated as the microbial colonization resistance (CR) of the bowel according to literature[8].

Evaluation of enteric symptoms

IBS patients were evaluated by enteric symptom questionnaire[9] which included 6 scales concerning abdominal pain, mucous stool and distention, *etc* (Table 1). Each scale was scored as "0" to "3" according to the severity and frequency of symptoms, whereas a higher score meant a more severe and frequent occurrence. The sum of each score was regarded as the general assessment of enteric symptoms.

Assessment of quality of life

The quality of life (QoL) of IBS patients and controls was evaluated with the Chinese version of short form 36 (SF-36) established by Wang *et al*.[10], which included 8 multiple dimensions as physical functioning (PF), role physical (RP), bodily pain (BP), general health (GH), vitality (VT), social functioning (SF), role emotional (RE) and mental health (MH). Scores were calculated according to corresponding formula and rules. Each dimension was scored from 0 to 100, with higher scores indicating better QoL.

Statistical analysis

Quantitative data were compared using different *t* test according to different situations, with the results expressed as mean±SD. The detection frequency was analyzed by Chi-squares test. The correlation between enteric symptom scores and QoL in IBS patients was detected by Pearson's correlation analysis. A *P* value less than 0.05 was considered statistically significant. All analysis was conducted using SPSS10.0 statistical passage.

RESULTS

Gut flora and microbial colonization resistance and detection frequency

Compared with the control group, IBS patients showed a significant decrease in *Bifidobacterium* but an increase in *Enterobacteriacea* (both $P<0.05$). The mean microbial colonization resistance (CR) of the bowel in IBS patients was smaller than 1, which was significantly different from that in control ($P<0.01$). There were no significant differences in *Lactobacillus*, *Bacteroides*, *Enterococus* between two groups. The detection frequency of *C. perfrigens* in IBS group was much lower than that in the control group ($P<0.01$, Table 2).

Table 2 Number of bacteria and B/E value in two groups (mean±SD, LgN/g stool)

Bacteria (%)	IBS patients (n=25)	Controls(n=25)
Lactobacillus	6.79±1.73 (92)	6.79±1.94 (84)
Bifidobacteria[a]	8.14±2.14 (96)	9.32±1.22 (100)
Bacteroides	10.49±0.56 (100)	10.62±0.79 (100)
C.perfringens[d]	7.32±2.12 (40)	6.66±1.68 (80)
Enterococus	7.96±1.53 (100)	7.49±1.29 (100)
Enterobacteriaceae[a]	9.02±1.04 (100)	8.44±0.95 (100)
B/E value[b]	0.91±0.27 (96)	1.12±0.23 (100)

The data in the bracket mean positive rate (This is applicable for the following tables including flora.). [a]$P<0.05$ flora *vs* control, [b]$P<0.01$ B/E value *vs* control, [d]$P<0.01$ detection frequency *vs* control.

The data were further analyzed based on age difference. Both groups were sorted on ascending order, the first 12 persons were chosen as younger subgroup (mean age 36.25±5.17) and the rest 13 (mean age 53.85±6.14) as elder one. We found that in IBS group, there was no significant difference in gut flora between two subgroups, but CR was smaller than 1 in both subgroups. While in control, the elder subgroup presented more *Enterobacteriacea* than the younger subgroup ($P<0.05$), but smaller CR (Tables 3, 4).

Table 3 Number of bacteria and B/E value in younger subgroup and elder subgroup in IBS group (mean±SD, LgN/g stool)

Bacteria (%)	Younger subgroup (n=12)	Elder subgroup (n=13)
Lactobacillus	6.63±1.83 (100)	6.98±1.70 (84)
Bifidobacteria	7.60±2.65 (100)	8.68±1.38 (92)
Bacteroides	10.52±0.42 (100)	10.47±0.72 (100)
C.perfringens	8.84±1.07 (25)	6.89±2.20 (54)
Enterococus	8.26±1.58 (100)	7.69±1.50 (100)
Enterobacteriaceae	9.16±1.22 (100)	8.90±0.88 (100)
B/E value	0.85±0.33 (100)	0.98±0.19 (92)

QoL of IBS patients

IBS patients experienced significant impairment in QoL (Table 5). Compared with control group, IBS patients had significantly lower scores on all SF-36 scales, with the exception of physical functioning. Decrements in QoL were most pronounced in general heath (GH, mean score 41.40), role physical (RP, mean score 52.00) and vitality (VT, mean score 53.40).Others like mental health (MH), role emotional (RE), bodily pain (BP) and social functioning (SF) were also impaired.

Table 1 Enteric symptom scales

Symptoms	0	1	2	3
Duration of abdominal pain (h/d)	None	<1	2-8	>8
Frequency of abdominal pain (d/wk)	None	1-2	3-5	6-7
Ratio of abnormal shape of stool	None	<1/4	1/4-3/4	>3/4
Ratio of abnormal passage of defecation	None	<1/4	1/4-3/4	>3/4
Ratio of mucous stool	None	<1/4	1/4-3/4	>3/4
Distention or gastrectasia when defecation	None	<1/4	1/4-3/4	>3/4

Table 4 Number of bacteria and B/E value in younger subgroup and elder subgroup of control group. (mean±SD, LgN/g stool)

Bacteria (%)	Younger subgroup (*n*=12)	Elder subgroup (*n*=13)
Lactobacillus	6.18±2.07 (75)	7.20±1.83 (92)
Bifidobacteria	9.32±1.08 (100)	9.32±1.38 (100)
Bacteroides	10.49±0.71 (100)	10.75±0.89 (100)
C.perfringens	6.45±1.82 (83)	6.89±1.59 (77)
Enterococus	7.09±1.49 (100)	7.86±1.00 (100)
Enterobacteriaceae[a]	8.05±1.14 (100)	8.81±0.57 (100)
B/E value	1.19±0.28 (100)	1.06±0.14(100)

[a]*P*<0.05 flora *vs* control.

Table 5 QoL of IBS patients and normal control (mean±SD)

QoL scale	IBS patients (*n* =25)	Controls (*n* =25)
PF	74.40±26.78	85.40±15.53
RP[a]	52.00±44.44	77.00±37.44
BP[b]	73.33±17.57	84.89±16.00
GH[b]	41.40±15.04	73.40±13.52
VT[b]	53.40±16.94	69.60±17.38
SF[b]	75.00±12.50	84.50±12.12
RE[b]	61.33±41.59	96.00±11.06
MH[b]	58.24±16.21	80.00±13.52

[a]*P*<0.05 ,[b]*P*<0.01 *vs* healthy control .

Correlation between QoL and enteric symptoms in IBS patients

Although IBS patients presented a negative correlation between bodily pain (BP) and enteric symptoms (correlation coefficient: 0.347), the difference was not significant (*P*>0.05). While vitality (VT), role emotional (RE), general health (GH) and physical functioning (PF), showed no significant difference with QoL in IBS patients (Table 6).

Table 6 Correlation between enteric symptoms and QoL in IBS (mean±SD)

	Score of QoL	Score of enteric symptoms	Correlation coefficient (*r*)
PF	74.40 (26.78)	7.56 (2.31)	-0.062
RP	52.00 (44.44)	7.56 (2.31)	0.060
BP	73.33 (17.57)	7.56 (2.31)	-0.347
GH	41.40 (15.04)	7.56 (2.31)	-0.137
VT	53.40 (16.94)	7.56 (2.31)	-0.280
SF	75.00 (12.50)	7.56 (2.31)	0.018
RE	61.33 (41.59)	7.56 (2.31)	-0.257
MH	58.24 (16.21)	7.56 (2.31)	0.001

DISCUSSION

The etiology of IBS is still unclear and the pathogenetic mechanisms are only partly understood. Intestinal motility alteration, visceral hypersensitivity, disturbed intestinal reflexes, psychological disorders, food intolerance and gastrointestinal infection and imbalance of gut flora were involved in the pathogenesis of IBS[11]. IBS patients presented various intestinal motility alterations, which were recognized as the basic pathophysiological factor. Evidences have shown that there were gastroparesis and small bowel dysmotility in IBS[12]. The motility index (MI),mean number and peak amplitude of high amplitude propagating contractions (HAPCs) in IBS patients were significantly greater than those in controls. These abnormalities might be related to shortened colonic transit time[13]. The migrating motor complex (MMC) was found to be an important mechanism controlling bacterial growth in the upper small bowel. Its disruption could promote duodenal bacterial overgrowth and bacterial translocation[14].

Food-related microbial alteration of the bowel might be partly responsible for the occurrence of IBS, since many IBS symptoms might be triggered or aggravated by food intake[15]. King and his colleagues found that colonic-gas production, particularly hydrogen, was greater in IBS patients, and both symptoms and gas production were reduced by an exclusion diet. This reduction might be associated with alterations in the activity of hydrogen-consuming bacteria[16].It has been shown that IBS patients have abnormal lactulose breath test (LBT), suggesting the presence of small intestinal bacterial overgrowth (SIBO) or an increased number of enteric organisms. Normalization of LBT could lead to a significant reduction in IBS symptoms[17]. On the other hand, some studies reported that the incidence of IBS was increased after acute gastroenteritis or dysentery. Under the circumstance of infection, an alterant microbiological environment might influence the number of lymphocytes, mast cells and enteroendocrine cells in the mucosa, rapid transit and a tendency to a secretory state was often found[1].

In this study, we found that IBS patients had a decrease of beneficial *Bifidobacteria* and overgrowth of potentially pathogenic *Enterobacteriaceae*. The ratio of B/E was smaller than 1, suggesting impairment of microbial colonization resistance (CR) of the bowel in IBS. Once CR was destroyed by antibiotics or other reasons, bacterial infection or dysbacteriosis might emerge[18].

Intestinal dysbacteriosis may be related to the occurrence of symptoms of IBS, since *Bifidobacteria* are considered to be beneficial to health. It involves in the production of essential mucous nutrients, such as short-chain fatty acids(SCFAs) and lactic acid, by lactose fermentation. They have been shown to eliminate toxins and unnecessary substances, such as hydroxybenzene, ammonia and steroids. They may also participate in the regulation of intestinal functions, such as nutrient synthesis and absorption. *Bifidobacteria* could prevent the overgrowth of potentially pathogenic organisms by bacterial barrier or by producing antibiotics[5,19]. *Enterobacteriaceae*, the main cause of endotoxin, may produce toxins such as ammonia , sulfureted hydrogen[5]. Endotoxin could temporarily impair canine gut absorptive function both in colon and in jejunum, with decreased absorption of water, glucose and eletrolytes, including sodium, chloride, and potassium[20]. When endotoxin of Gram-negative bacteria was administered intravenously in rats, the migrating myoelectric complex was replaced by spike bursts accompanied by rapid transit[21].These effects may contribute to the occurrence of diarrhea. Microecological modulators could prominently relieve IBS-like enteric symptoms, suggesting the close relationship between gut flora and IBS[22,23].

Ageing may affect the flora residing in the gut and outside of it[5]. In our study, we found that the intestinal microecology showed an overgrowth of *Enterobacteriaceae* with age in normal control, implying that age may interact with the gut flora. The overgrowth of *Enterobacteriaceae* may also account for the susceptibility to intestinal infection and endotoxemia in elderly people. *Bifidobacteria* have been shown to have a close relationship with human longevity[5]. While in IBS group, age had no influence on gut flora, since there was intestinal dysbacteriosis in both younger and elder subgroups.

There was a high detection frequency of *C. perfringens* in normal control, without any apparent pathogenic effect. It was supposed that changes of gut flora in IBS might result in a relatively high detection frequency of *C. perfringens* .Therefore, further studies are needed to elucidate this phenomenon.

Anyway, microbial metabolic processes have been going on like in a black box[24]. Although almost all organic compounds and nutrients, fiber, digestive secretions and desquamated

epithelial cells of the host can enter into microorganismic metabolic chains and processes, little is known about this metabolic chain and process. Further studies are still needed. However, there was dysbacteriosis in IBS patients. Whether it is the effect or just cause of IBS remains unclear.

The purpose of focusing on health-related quality of life (HRQL) is to go beyond the presence and severity of symptoms of disease and to examine how patients perceive and experience these manifestations in their daily lives[25].Briefly, HRQL concerns more about the physical, psychological and social functioning.

IBS is not a life-threaten disease. Its impacts include costs associated with diagnosis and treatment, production losses due to morbidity and pain and diarrhea, *etc*.[26]. With a questionnaire, Silk[27] found that IBS impacted significantly on personal relationships and working practices. Some even complained that IBS prevented them from applying for promotion or a new job. IBS patients had impaired quality of life in general health, vitality, social functioning, *etc*[9,28]. According to the research of Gralnek *et al*.[29], IBS patients experienced significantly worse HRQL in some aspects than those with gastroesophageal reflux disease (GERD) or diabetes mellitus (DM). IBS patients had even worse bodily pain, fatigue, and social functioning when compared with dialysis-dependent end-stage renal disease patients,

In our study, we also found that IBS patients had significantly lower scores on all SF-36 scales with the exception of physical functioning, when compared with the age and sex-matched control group. Decrements in QoL were most pronounced in general health, role physical and vitality. However, there was no significant correlation between QoL and enteric symptoms, which might be due to the frequent presence of anxiety, depression, fatigue and anorexia in IBS patients[11,30].Compared with the control, neuroticism, hypochondriasis and depression were significantly more prevalent in IBS patients attending a clinic, which would have a prominently negative influence on QoL. Hypnotherapy was effective in treating IBS, suggesting that psychological factors may play an important role in IBS. Thus the general impacts of IBS may go far beyond those of enteric symptoms, implicating that IBS is a psychosomatic disease.

ACKNOWLEDGMENTS

The authors thank Professor Lan-Juan Li, Directors Yun-Song Yu, Yun-Bo Chen, Zhong-Wen Wu, Dang-Sheng Xiao at Department of Infectious Diseases, First Affiliated Hospital of Zhejiang University for their technical supports.

REFERENCES

1 **Robin CS**. Estimating the importance of infection in IBS. *Am J Gastroenterol* 2003; **98**: 238-241
2 **Wang LH**, Fang XC, Pan GZ. Intestinal infection and irritable bowel syndrome. *Zhonghua Neike Zazhi* 2002; **41**: 90-93
3 **Maxwell PR**, Rink E, Kumar D, Mendall MA. Antibiotics increase functional abdominal symptoms. *Am J Gastroenterol* 2002; **97**: 104-108
4 **Ran L**, Chen ZF, Fu P, Yang BL, Li ZG, Yao JH, Zhao X. A survey on gut flora of 184 cases of healthy populations in Beijing area. *Zhongguo Weishengtaixue Zazhi* 1999; **11**: 10-12
5 **Zhang DR**. Xiao Hua Xi Jibing Yu Weishengtai. The 1st edition. Shanghai: *Shanghai Science Technol Press* 2001: 58-61
6 **Thompson WG**, Longstreth GF, Drossman DA, Heaton KW, Irvine EJ, Muller-Lissner SA. Functional bowel disorder and functional abdominal pain. *Gut* 1999; **45**: 43-47
7 **Okusa T**, Ozaki Y, Sato C, Mikuni K, Ikeda H. Long-term ingestion of lactosucrose increases Bifidobacterium sp. In human fecal flora. *Digestion* 1995; **56**: 415-420
8 **Wu ZW**, Li LJ, Ma WH, Yu YS, Chen YG. A new index for microbial colonization resistance of the bowel-the ratio of B/E. *Zhejiang Yufang Yixue* 2000; **7**: 4-5
9 **Si JM**, Chen SJ, Sun LM. An epidemiological and quality of life study of irritable bowel syndrome in Zhejiang province. *Zhonghua Neike Zazhi* 2003; **42**: 34-37
10 **Wang HM**, Li L, Shen Y. A study on quality of life of inhabitants in Hangzhou area using Chinese version of SF-36. *Zhonghua Yufang Yixue Zazh*i 2001; **35**: 428-430
11 **Xu GM**. Strenghen the study on etiology of irritable bowel syndrome. *Zhonghua Neike Zazhi* 2003; **42**: 73-74
12 **Evans PR**, Bak YT, Shuter B, Hoschl R, Kellow JE. Gastroparesis and small bowel dysmotility in irritable bowel syndrome. *Dig Dis Sci* 1997; **42**: 2087-2093
13 **Chey WY**, Jin HO, Lee MH, Sun SW, Lee KY. Colonic motility abnormality in patients with irritable bowel syndrome exhibiting abdominal pain and diarrhea. *Am J Gastroenterol* 2001; **96**: 1499-1506
14 **Nieuwenhuijs VB**, Verheem A, van-Duijvenbode-Beumer H, Visser MR, Verhoef J, Gooszen HG, Akkermans LM. The role of interdigestive small bowel motility in the regulation of gut microflora, bacterial overgrowth, and bacterial translocation in rats. *Ann Surg* 1998; **228**: 188-193
15 **Simren M**, Mansson A, Langkilde AM, Svedlund J, Abrahamsson H, Bengtsson U, Bjornsson ES. Food-related gastrointestinal symptoms in the irritable bowel syndrome. *Digestion* 2001; **63**: 108-115
16 **King TS**, Elia M, Hunter JO. Abnormal colonic fermentation in irritable bowel syndrome. *Lancet* 1998; **352**: 1187-1189
17 **Mark P**, Evelyn JC, Henry CL. Normalization of lactulose breath testing correlates with symptom improvement in irritable bowel syndrome: a double-blind, randomized, placebo-controlled study. *Am J Gastroenterol* 2003; **98**: 412-419
18 **Van der Waaji D**. History of recognition and measurement of colonization resistance of the digestive tract as an introduction to selective gastrointestinal decontamination. *Epidemiol Infect* 1992; **109**: 315-326
19 **Jiang T**, Savaiano DA. Modification of colonic fermentation by Bifidobacteria and pH *in vitro*. Impact on lactose metabolism, short-chain fatty acid, and lactate production. *Dig Dis Sci* 1997; **42**: 2370-2377
20 **Cullen JJ**, Spates ST, Ephgrave KS, Hinkhouse MM. Endotoxin temporarily impairs canine colonic absorption of water and sodium. *J Surg Res* 1998; **74**: 34-38
21 **Hellstrom PM**, al-Saffar A, Ljung T, Theodorsson E. Endotoxin actions on myoelectric activity, transit, and neuropeptides in the gut. Role of nitric oxide. *Dig Dis Sci* 1997; **42**: 1640-1651
22 **Zhang DR**, Dong XX, Bao YF. Intestinal floral changes in patients with irritable bowel syndrome after ingestion of clostridium butyrium preparation. *Zhongguo Weishengtaixue Zazhi* 1999; **11**: 164-166
23 **Zhang J**, Jin F, Le QL, Zhang ZJ. The effect of Jinshuangqi on irritable bowel syndrome. *Zhongguo Weishengtaixue Zazhi* 2002; **14**: 289-291
24 **Porter J**, Pickup RW. Nucleic acid-based fluorescent probes in microbial ecology: application of flow cytometry.*J Microbiol Methods* 2000; **42**: 75-79
25 **Glise H,** Wiklund I**.** Health-related quality of life and gastrointestinal disease. *J Gastroenterol Hepatol* 2002; **17**(Suppl): S73-85
26 **Boivin M**. Socioeconomic impact of irritable bowel syndrome in Canada. *Can J Gastroenterol* 2001; **15**(SupplB): 8B-11B
27 **Silk DB**. Impact of irritable bowel syndrome on personal relationships and working practices. *Eur J Gastroenterol Hepatol* 2001; **13**: 1327-1332
28 **Hahn BA**, Yan S, Strassels S. Impact of irritable bowel syndrome on quality of life and resource use in the united states and united kingdom. *Digestion* 1999; **60**: 77-81
29 **Gralnek IM**, Hays RD, Kilbournem A, Naliboff B, Mayer EA. The impact of irritable bowel syndrome on health-related quality of life. *Gastroenterology* 2000; **119**: 654-660
30 **Lydiard RB**, Falsetti SA. Experience with anxiety and depression treatment studies: implications for designing irritable bowel syndrome clinical trials. *Am J Med* 1999; **107**: 65S-73S

Edited by Wang XL and Xu FM

PO Box 2345, Beijing 100023, China
Fax: +86-10-85381893
E-mail: wjg@wjgnet.com www.wjgnet.com

World J Gastroenterol 2004;10(12):1806-1809
World Journal of Gastroenterology
Copyright ©2004 by The WJG Press ISSN 1007-9327

• CLINICAL RESEARCH •

Management of nonfunctioning islet cell tumors

Han Liang, Pu Wang, Xiao-Na Wang, Jia-Cang Wang, Xi-Shan Hao

Han Liang, Pu Wang, Xiao-Na Wang, Jia-Cang Wang, Xi-Shan Hao, Department of Gastrointestinal Oncological Surgery, Tianjin Cancer Hospital, Tianjin Medical University. Hexi District, Tianjin 300060, China
Correspondence to: Professor Han Liang, Department of Gastrointestinal Oncological Surgery, Tianjin Cancer Hospital, Tianjin Medical University, Hexi District, Tianjin 300060, China. hanliang86@yahoo.com
Telephone: +86-22-23340123
Received: 2002-08-26 **Accepted:** 2002-10-12

Abstract

AIM: To more clearly define the clinical and pathological characteristics and appropriate diagnosis and treatment of nonfunctioning (NFICTs) islet cell tumors, and to review our institutional experience over the last 30 years.

METHODS: The records of 43 patients confirmed to have nonfunctioning islet cell tumors of pancreas were retrospectively reviewed. Survival was estimated by the Kaplan-Meier methods and potential risk factors for survival were compared with the log-rank tests.

RESULTS: The mean age was 31.63 years (range, 8 to 67 years). There were 7 men and 36 women. Twenty-eight patients had a confirmed diagnosis of nonfunctioning islet cell carcinoma (NFICC) and benign islet cell tumors were found in 15 patients. The most common symptoms in patients with NFICTs were abdominal pain (55.8%), nausea and/or vomiting (32.6%), fatigue (25.6%) and abdominal mass (23.3%). Preoperative ultrasonic and computed tomography localized the tumors in all patients. Forty-three NFICTs were distributed throughout the pancreas, with 21 located to the right of the superior mesenteric vessels, 10 in the body of the pancreas, 6 in the tail of the pancreas, and multiple tumors were found in one patient. Thirty-nine of 43 patients (91%) underwent surgical resection. Surgical treatment was curative in 30 patients (70%) and palliative in 9(21%). The resectability and curative resection rate in patients with NFICC of pancreas were 89% and 61%, respectively. The overall cumulative 5- and 10-year survival rates for patients with NFICC were 58.05% and 29.03%, respectively. Radical operation and diameter of cancer small than 10 cm were positive prognostic factors in females younger than 30 years old. Multivariate Cox regression analysis indicated that radical operation was the only independent prognostic factor, $P=0.007$.

CONCLUSION: Nonfunctioning islet cell tumors of pancreas are found mainly in young women. The long-term results for patients undergone surgery, especially curative resection are good.

Liang H, Wang P, Wang XN, Wang JC, Hao XS. Management of nonfunctioning islet cell tumors. *World J Gastroenterol* 2004; 10(12): 1806-1809
http://www.wjgnet.com/1007-9327/10/1806.asp

INTRODUCTION

Tumors arising from the pancreatic islet cell are rare and represent a heterogeneous group of benign or malignant lesions. Most tumors present with well characterized syndromes, whereas others appear to be nonfunctioning. Functioning tumors, such as gastrinomas, insulinomas, and vasoactive intestinal peptide-secreting tumour (VIPomas), are characterized by extensive production of single polypeptide hormones which lead to specific clinical syndromes. Nonfunctioning tumors, which account for 15% and 52% of tumors, are not associated with clinical syndromes, as they do not produce an excess of any active polypeptide hormones[1,2]. These Lesions tend to occur later and have a different clinical course from their functioning counterparts.

The purpose of this study was to analyze the clinical presentations, diagnosis, management, and prognosis of a large group of patients with nonfunctioning islet cell tumors (NFICTs) of pancreas managed at a single cancer center to determine the natural history and optimum management of such lesions.

MATERIALS AND METHODS

Patients

A total of 43 patients with NFICTs were treated between 1972-2002. The diagnosis of islet cell tumors of pancreas was established by histopathologic examination. Tumors were considered nonfunctional if no clinical symptoms of excess hormone were present.

The disease was considered regional if no evidence of metastases in the liver or elsewhere was found either during surgery or by imaging techniques. Metastases in the liver or elsewhere were considered distant.

Methods

Clinical records were reviewed with regard to patient demographics, clinical features, diagnostic procedures, pathologic findings, operative details, medical treatment, and long-term survival. All patients were followed up by return visits, letters from the follow-up department, correspondence with primary surgeons, or telephone contact within the last months from the conclusion of this study. Survival rate was estimated by the Kaplan-Meier methods, and potential risk factors for survival were compared with the log-rank tests and Cox methods. Ninety-five percent confidence intervals were calculated for specific estimates of survival.

RESULTS

Clinical characteristics

There were 36 females and 7 males with a mean age of 31.63 years and a range of 8 to 67 years and the details are shown in Figure 1. At the time of diagnosis, the median age of male and female patients was 33.57 and 31.25 years, respectively ($P>0.05$). The clinical presentations are illustrated in Table 1. The predominant presentations were abdominal pain, nausea and/or vomiting, fatigue and abdominal pain. None of the patients displayed the clinical features of an endocrine disorder. The duration from the onset of symptoms to diagnosis for all patients ranged from 3 d to 10 years (median 6 mo). Only three patients were asymptomatic, with the tumor found incidentally.

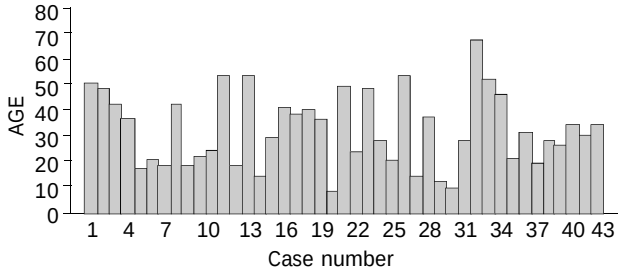

Figure 1 Age distribution in 43 NFICTs patients.

Abdominal ultrasonography (US) and spiral CT were the most commonly employed to detect the primary tumor in all but the patient with emergency operation. Correct prediction of an islet cell tumors based on CT and US results was achieved only in 6(20%) patients. The common diagnosis of CT was carcinoma of pancreas (in 20 patients). Endoscopic retrograde cholangiopancreaticography(ERCP) was performed in 6 patients to determine the cause of obstructive jaundice. Magnetic resonance imaging (MRI) and endoscopic ultrasonography (EUS) localized the tumor and the local extension correctly in 5 and 4 patients, respectively.

Table 1 Clinical presentations

Symptoms	Patients(n=43)	(%)
Abdominal pain	24	55.8
Nausea and/or vomiting	14	32.6
Fatigue	11	25.6
Abdominal mass	10	23.3
Back pain	9	21.0
Jaundice	8	18.6
Weight loss	5	11.6
No symptoms	3	7.0
Acut abdomen	1	2.3

Pathological findings

Confirmation of malignancy was mainly based on the demonstration of local invasion, microscopic vascular or perineural invasion, lymph node metastases, hepatic metastasis or distant metastases. Twenty-eight patients were histopathologically diagnosed as nonfunctioning islet cell carcinoma (NFICC) of pancreas.

The size of islet malignant and benign tumors ranged from 2.5 cm to 15 cm (mean 10 cm) and from 4 cm to 30 cm (mean 9.9 cm), respectively (P>0.05). Metastases were presented in 6 patients at the time of operation. There were 21 tumors located in the head of the pancreas, 10 in tail, 6 in the body, 5 in body and tail (Table 2). Multiple tumors were presented only in one patient.

Table 2 Location of the tumors

Location	Malignant (n=28)	Benign (n=15)
Head	13	8
Tail	8	2
Body	2	4
Body+Tail	4	1
Multiple	1	0

Operative detail and outcome

We performed 30(70%) potentially curative resections, 9(21%) palliative resections, and 4(9.3%) bypass procedures, resulting in a resection rate of 91%. Of the 28 patients with islet cell carcinoma of pancreas, potentially curative resection, palliative resection, palliative bypass and biopsy were performed in 17(61%), 8(28.6%), 3(10.7%) and 1(3.6%), respectively (Table 3). The potentially curative resection was performed in 87% of patients with benign islet cell tumors compared to only 61% of those with NICC (P<0.05). Table 4 shows the type of operative procedures for patients with benign and malignant islet cell tumors. There was no 30-day mortality.

Table 3 Nature operative procedures

Nature	Malignant (n=28)	(%)	Benign (n=15)	(%)
Curative resection	17	61.0	13	87.0
Palliative resection	8	28.6	1	6.7
Palliative bypass	2	5.1	1	6.7
Biopsy only	1	3.6	0	0

Other treatment modalities

A total of 13 cases of NFICC received adjuvant therapy after curative operation, of them 9 patients with NFICC underwent chemotherapy (5 of them with the regimen of FAM and 4 others with 5-FU only) after a curative operation. One of them developed liver metastasis one year later, the another patient died 23 mo postoperatively. The remaining 7 patients were alive with no evidence of disease for a median 45.5 mo (range 15-96 mo). Another 4 patients with malignant tumors underwent radiation plus chemotherapy (three with FAM, and one with 5-FU). All these 4 patients were alive with no evidence of disease for 55.6 mo in average (range 14-124 mo).

Among the patients with NFICC who underwent palliative resection, 4(50%) were given chemotherapy with 5-FU and CF, one developed multiple liver metastasis 13 mo later.

Survival

The cumulative 5- and 10-year survival rates for all patients with NFICC were 58.05% and 29.03%, respectively (Figure 2). Table 5 demonstrates the survival in detail. The median survival of female patients was 120 mo, which was better than the survival for male patients (45 mo, P=0.312, Figure 3). Patients who were

Table 4 Primary operative procedures

Procedure	Malignant (n=28)	(%)	Benign (n=15)	(%)
Pancreatoduodenectomy	8	28.5	2	13.3
Pylorus-preserving pancreatoduodenectomy	0	0	1	6.7
Distal pancreatectomy + splenectomy	7	25.0	5	33.3
Subtotal pancreatectomy + splenectomy	4	14.3	2	13.3
Distal pancreatectomy	2	7.1	0	0
Enucleation	1	3.6	4	26.7
Double bypass	1	3.6	0	0
Biliary bypass	3	10.7	1	6.7
Gastric bypass	1	3.6	0	0
Biopsy only	1	3.6	0	0

younger than 30 years had a better long-term survival than those elder than 30 years, but the difference was not statistical significant (Figure 4, P=0.758). Figure 5 compares survival curves for the curative operations and noncurative groups. Survivals at 5- and 10-years were significant better for patients who underwent PD and STRP than those who underwent palliative operation, P=0.007. As demonstrated in Figure 6, survivals were better for patients with smaller tumors than those with larger ones, but the difference was not statistically significant, P=0.1169.

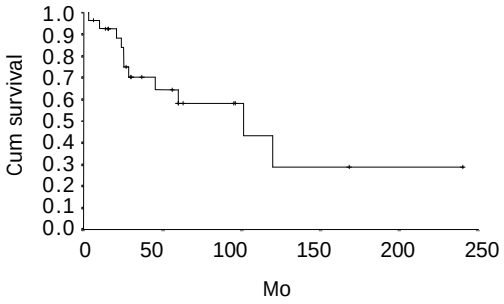

Figure 2 Actual survival for all patients with NFICC (n=28).

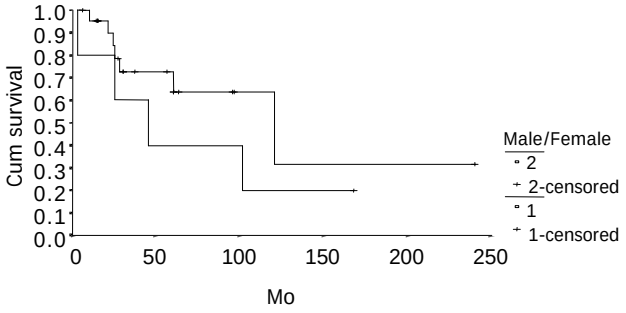

Figure 3 Survival comparison between male (n=5) and female (n=23) patients with NFICC (P=0.312).

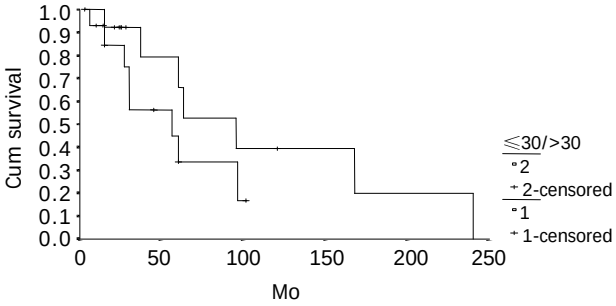

Figure 4 Survival comparison between younger (≤30 years, n=14) and elder (>30 years, n=14) patients with NFICC P=0.7582).

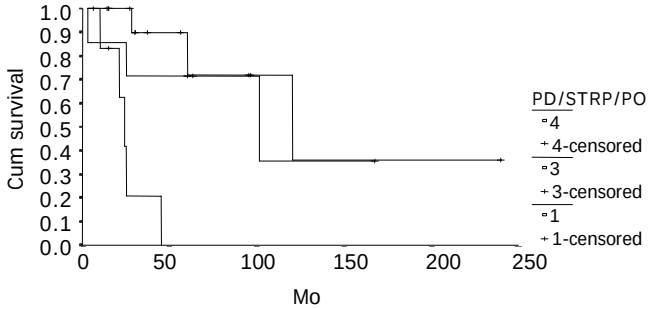

Figure 5 Survival comparison between patients who underwent different operations (PD, n=7; Subtotal resection of pancreas, n=14, palliative operation, n=7, P=0.0005).

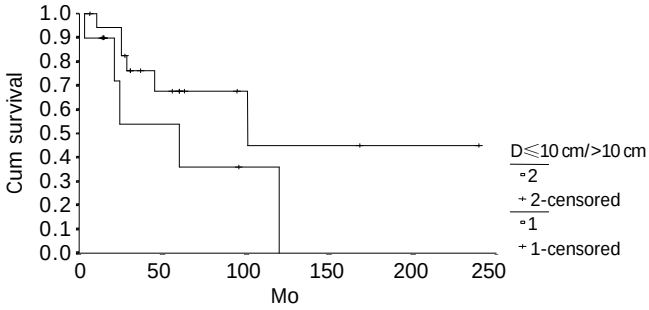

Figure 6 Survival comparison between patients with cancer of different diameters (D≤10 cm, n=18; D>10 cm, n=10, P=0.1169).

Table 5 Survival of patients with NFICC

Patients	n	5-yr survival (%)	10-yr survival (%)	Median survival (mo)
ALL cases	28	58.05	29.03	60±4.35
Male	5	40.00	20.00	45±21.92
Female	23	63.49	31.75	120±44.05
≤30 yr	14	54.17	36.11	120±64.02
>30 yr	14	57.69	0	101
D[1]≤10 cm	18	67.57	49.05	101
D[1]>10 cm	10	36.00	0	60±21.75
PD[2]	7	71.43	35.71	101±56.73
STRP[3]	14	72.00	36.00	120±44.94
PO[4]	7	0	0	24±3.19

[1]Diameter of the cancer, [2]Pancreatoduodenectomy, [3]Subtotal resection of pancreas, [4]palliative operation.

Table 6 Multivariate Cox regression analysis

Factors	Standard Error	Degree of freedom	P value
Sex	2.190	1	0.679
Age	1.292	1	0.821
Location	35.889	1	0.917
Operation	1.528	1	0.007
Tumor Size	117.237	1	0.903
Radial/palliative	117.261	1	0.884

DISCUSSION

NFICTs are developmentally and histologically identical to functioning tumors but differ in their clinical course and outcome. In this group, the mean age at diagnosis (31.63 years) was 20 years younger than those reported by other researchers[3-5], but it was similar to some domestic reports[6-8]. The mean age of the females was 31.25 years, a little bit younger than that of males (33.57 years). It was considered that more male than female patients suffered from islet cell tumors. The ratio of males: females was 1.29:1[9-12]. In contrast to other reports, we found there were more females than males with this disease (F:M=36:7). It was similar to domestic reports [6-8]. The reason is unknown. The difference races may be responsible for this phenomenon.

The clinical presentations of NFICTs were mainly due to mass effects. When tumors were smaller than 5 cm in diameter, most patients were asymptomatic[16]. The symptoms or signs at the time of diagnosis were abdominal pain, weight loss, nausea/vomiting, jaundice and abdominal mass[5-7,10].

Abdominal US and contrast-enhanced spiral CT were used. In this series, abdominal US and CT were used to detect the primary tumor in all but the patients with emergency operation. Correct prediction of a NFICT based on CT and US results was

achieved only in 6(20%) patients. It is believed that the following features appear to be characteristic for NFICTs: a well defined pancreatic mass with a unusually large size, moderate to strong mass hyperdense in the arterial contrastographic phase of either the primary or the hepatic metastases, and no infiltration of vessels of the celiac axis or the proximal superior mesenteric artery[4,13]. A recent report showed that in patients with NFICT, a hypoechoic mass with an irregular central echogenic area on EUS or complete obstruction of the main pancreatic duct on ERCP suggested a malignancy[14].

EUS and laparoscopy could provide accurate preoperative and intraoperative locatization to enhance laparoscopic or open operation[15]. Magnetic resonance imaging, angiography, transabdominal sonography and portal venous sampling could yield an additional accuracy for the diagnosis.

NFICTs of pancreas were believed to be malignant in the presence of distant metastases, or histologic evidence of vascular, lymphatic, or perineural invasion[3,10]. However, because all NFICTs had a similar histologic appearance, the absence of lymphovascular or perineural invasion could not exclude the potential for malignant behavior. Patients who had locally advanced nonmetastatic diseases at diagnosis subsequently died of complications of the primary tumor[11]. It was believed that neither vascular or perineural invasion nor electron microscopy snd any other histologic criteria could accurately predict whether tumor behavior was benign or malignant[5]. Most previous reports have suggested that NFICTs are biologically very aggressive, with a malignancy rate ranging from 82% to 100%[1,11]. However, our findings do not support these previous observations, as we found that the evidence of malignancy based upon evidence of local invasion or presence of metastases could accurately predict the clinical outcome. We believe that the diagnosis of malignancy in NFICTs should be mainly based upon gross findings of local tumor invasion or the presence of metastases. Some reports showed that patients with benign islet tumors were alive at the follow-up time point[16]. The 5 year survival rate of patients with benign tumors in our group was 100%.

Despite of advances in the multidisciplinary management of NFICC of pancreas in recent decades, surgery plays still an important role in providing potentially curative resections, relieving symptoms, and improving long-term survival. The resectable rate of this disease was 24% to 100%[3,4,17] and curative resection was performed only in 61% patients[5]. In current series, the resectable rate was 91%, the curative resection rate for the patients was 61%, which was comparable to that in literature reports. Radical operation could yield a best survival for patients with NFICC, palliative debulking could reduce the mass of tumor, enhance other treatment modalities, it might also prevent other complications such as recurrent pancreatitis, intestinal obstruction, and gastrointestinal bleeding due to direct tumor invasion or varices secondary to splenic vein obstruction[7]. For this reason, noncurative debulking of tumors might improve survival. Repeated resections for respectable recurrences or metastases might be indicated to improve survival also[8].

Tumor size is not included in the diagnostic criteria, but when NFICC is definitely diagnosed, it is helpful to predict the survival. When the diameter was larger than 10 cm, the long-term survival would be poor. On the other hand, female and younger ($\leqslant$30 years) patients would have a better survival.

One third of our patients received adjuvant chemotherapy after radical resection of the primary tumors. Obviously, this was too small a number to make any meaningful observations regarding the efficacy of any specific chemotherapy regimen. Moertel and colleagues[18] reported a large prospective, randomized multi-institutional trial of two regimens using 162 patients with advanced islet cell carcinomas. They concluded that the combination of streptozotocin and 5-fluorouracil could produce a response rate of 63%, which was significantly higher than 34% seen with streptozotocin alone.

REFERENCES

1 **Kent RB 3rd,** van Heerden JA, Weiland LH. Nonfunctioning islet cell tumors. *Ann Surg* 1981; **193**: 185-190
2 **Broughan TA,** Leslie JD, Soto JM, Hermann RE. Pancreatic islet cell tumors. *Surgery* 1986; **99**: 671-678
3 **Eriksson B,** Skogseid B, Lundqvist G, Wide I, Wilander E, Oberg K. Medical treatment and long-term survival in a prospective study of 84 patients with endoctine pancreatic tumors. *Cancer* 1990; **65**: 1883-1890
4 **Bartsch DK,** Schilling T, Ramaswamy A, Gerdes B, Celik I, Wagner HJ, Simon B, Rothmund M. Management of nonfunctioning islet cell carcinomas. *World J Surg* 2000; **24**: 1418-1424
5 **White TJ,** Edney JA, Thompson JS, Karrer FW, Moor BJ. Is there a prognostic difference between functional and nonfunctional islet cell tumors? *Am J Surg* 1994; **168**: 627-629
6 **Zheng X,** Guo K, Tian Y, Li J, Guo R, Zhan Y, Song M, Shen K. Cellular composition and anatomic distribution in nonfunctioning pancreatic endocrine tumors: immunohistochemical study of 30 cases. *Chin Med J* 1998; **111**: 373-376
7 **Lo CY,** van Heerden JA, Thompson GB, Grant CS, Soreide JA, Harmsen WS. Islet cell carcinoma of the pancreas. *World J Surg* 1996; **20**: 878-883
8 **Jiang XS,** Shou NH, LI ZY. Diagnosis and treatment of nonfunctional islet cell tumors. *Zhongguo Putong Waike Zazhi* 1998; **7**: 87-89
9 **Cheslyn-Curtis S,** Sitaram V, Williamson RC. Management of non-functioning neuroendocrine tumours of the pancreas. *Br J Surg* 1993; **80**: 625-627
10 **Legaspi A,** Brennan MF. Management of islet cell carcinoma. *Surgery* 1988; **104**: 1018-1023
11 **Evans DB,** Skibber JM, Lee JE, Cleary KR, Ajani JA, Gagel RF, Sellin RV, Fenoglio CJ, Merrell RG, Hickey RC. Nonfunctioning islet cell carcinoma of the pancreas. *Surgery* 1993; **114**: 1175-1182
12 **Furukawa H,** Mukai K, Kosuge T, Kanai Y, Shimada K, Yamamoto J, Mizuguchi Y, Ushio K. Nonfunctioning islet cell tumors of the pancreas: clinical, imaging and pathological aspects in 16 patients. *Jpn J Clin Oncol* 1998; **28**: 255-261
13 **Procacci C,** Carbognin G, Accordini S, Biasiutti C, Bicego E, Romano L, Guarise A, Minniti S, Pagnotta N, Falconi M. Nonfunctioning endocrine tumors of the pancreas: possibilities of spiral CT characterization. *Eur Radiol* 2001; **11**: 1175-1183
14 **Sugiyama M,** Abe N, Izumisato Y, Yamaguchi Y, Yamato T, Tokuhara M, Masaki T, Mori T, Atomi Y. Differential diagnosis of benign versus malignant nonfunctioning islet cell tumors of the pancreas: the roles of EUS and ERCP. *Gastrointest Endosc* 2002; **55**: 115-119
15 **Spitz JD,** Lilly MC, Tetik C, Arregui ME. Ultrasound-guided laparoscopic resection of pancreatic islet cell tumors. *Surg Laparosc Endosc Percutan Tech* 2000; **10**: 168-173
16 **Yeo CJ,** Wang BH, Anthone GJ, Cameron JL. Surgical experience with pancreatic islet-cell tumors. *Arch Surg* 1993; **128**: 1143-1148
17 **Thompson GB,** van Heerden JA, Grant CS, Carney JA, Ilstrup DM. Islet cell carcinomas of the pancreas: a twenty-year experience. *Surgery* 1988; **104**: 1011-1017
18 **Moertel CG,** Hanley JA, Johnson LA. Strepotozotocin alone compared with streptozoocin plus fluorouracil in the treatment of advanced islet-cell carcinoma. *N Eng J Med* 1980; **303**: 1189-1194

Edited by Wang XL and Xu JY **Proofread by** Xu FM

PO Box 2345, Beijing 100023, China
Fax: +86-10-85381893
E-mail: wjg@wjgnet.com www.wjgnet.com

World J Gastroenterol 2004;10(12):1810-1814
World Journal of Gastroenterology
Copyright ©2004 by The WJG Press ISSN 1007-9327

• BRIEF REPORTS •

Association of -238G/A polymorphism of tumor necrosis factor-alpha gene promoter region with outcomes of hepatitis B virus infection in Chinese Han population

Liang-Ping Lu, Xing-Wang Li, Ying Liu, Guo-Chang Sun, Xue-Ping Wang, Xi-Lin Zhu, Quan-You Hu, Hui Li

Liang-Ping Lu, Hui Li, Department of Epidemiology, Institute of Basic Medical Sciences, Chinese Academy of Medical Sciences; School of Basic Medicine, Peking Union Medical College, Beijing 100005, China
Xing-Wang Li, Department of Internal Medicine, Ditan Hospital, Beijing 100011, China
Xue-Ping Wang, Department of Clinical Laboratory, Ditan Hospital, Beijing 100011, China
Ying Liu, Xi-Lin Zhu, National Laboratory of Medical Molecular Biology, Institute of Basic Medical Sciences, Chinese Academy of Medical Sciences; School of Basic Medicine, Peking Union Medical College, Beijing 100005, China
Guo-Chang Sun, Quan-You Hu, Department of Clinical Laboratory, Shunyi District Hospital, Beijing 101300, China
Supported by the Research Fund for the Doctoral Training Program from the Ministry of Education, No.2000002340 and Beijing Municipal Government Commission for Science & Technology, No. H020920020590
Correspondence to: Hui Li, Department of Epidemiology, Institute of Basic Medical Sciences, Chinese Academy of Medical Sciences; School of Basic Medicine, Peking Union Medical College, 5 Dongdan 3 Tiao, Beijing 100005, China. lihui99360@sohu.com
Telephone: +86-10-65296971 **Fax:** +86-10-65225752
Received: 2003-11-22 **Accepted:** 2003-12-16

Abstract

AIM: To clarify whether -238G/A polymorphism of tumor necrosis factor-α (TNF-α) gene promoter region was associated with outcomes of hepatitis B virus (HBV) infection in Han population of northern China, and to analyze the gene-environment interaction between -238G/A polymorphism and cigarette smoking or alcohol consumption.

METHODS: A case-control study was conducted to analyze the association of TNF-α gene promoter polymorphism with HBV infection outcomes. A total of 207 patients with chronic hepatitis B (HB) and 148 cases of self-limited HBV infection from Ditan Hospital and Shunyi District Hospital in Beijing, respectively were recruited. History of smoking and alcohol drinking was inquired by a questionnaire. The -238G/A polymorphism of TNF-α gene promoter was genotyped by polymerase chain reaction-restricted fragment length polymorphism (PCR-RFLP).

RESULTS: The frequencies of GG and GA genotypes were 98.07% and 1.93% in chronic HB patients and 93.24% and 6.76% in self-limited HBV infection individuals, respectively (χ^2=5.30, *P*=0.02). The frequency of G allele was significantly higher in patients with chronic HB that in individuals with self-limited HBV infection (99.03% *vs* 96.62%, χ^2=5.20, *P*=0.02). Only modestly increased risk of onset of chronic HB was found in smokers (*OR*=1.40, *95% CI*: 0.87-2.28, *P*=0.14) and drinkers (*OR*=1.26, *95%CI*: 0.78-2.05, *P*=0.32). There was a positive interaction between genotype GG and cigarette smoking with an interaction index (II) of 2.95, or alcohol consumption with an II of 1.64.

CONCLUSION: The -238G/A polymorphism of TNF-α gene promoter region is independently associated with different outcomes of HBV infection.

Lu LP, Li XW, Liu Y, Sun GC, Wang XP, Zhu XL, Hu QY, Li H. Association of -238G/A polymorphism of tumor necrosis factor-alpha gene promoter region with outcomes of hepatitis B virus infection in Chinese Han population. *World J Gastroenterol* 2004; 10(12): 1810-1814
http://www.wjgnet.com/1007-9327/10/1810.asp

INTRODUCTION

Human beings are susceptible to HBV. HBV infection in adults is usually clinically inapparent, and the virus is cleared after infection. Only about 5-10% of them become persistently infected and develop chronic liver disease with varied severity[1], which could not be explained completely by the virus itself and environmental factors. Progress of HBV infection might be affected by host genetic susceptibility[2].

Since HBV is not cytolytic for hepatocytes, and hepatocellular injuries caused by HBV infection are predominantly immune-mediated[3-6]. Immune attacks by host against HBV are mainly mediated by a cellular reaction. Cytokines produced by immune cells, such as TNF-α, might play a role in immune pathogenesis of HBV infection.

TNF-α is secreted by macrophages, monocytes, neutrophils, T-cells and NK-cells following the stimulus by bacterial lipopolysaccharides and shows a broad spectrum of biological activities, causing cytolysis and cytostasis in many tumor cell lines *in vitro*. Several lines of evidence suggest the importance of TNF-α in HBV. Patients with acute and chronic hepatitis B have an elevated plasma concentration of TNF-α[7,8]. Some individual differences in cytokine production may be related to genetic components, and certain polymorphism alleles may be associated with higher or lower levels of TNF-α production, which has been ascribed to polymorphisms within the regulatory regions of cytokine genes[9-14].

There were some studies about the association of TNF-α gene promoter polymorphism with progress of the disease[13,15], but ethnic difference could lead to different results. The aim of the present study was to investigate whether the TNF-α promoter polymorphism at position -238 was associated with outcomes of HBV infection in Han people of northern China.

MATERIALS AND METHODS

Study design

Case-control study was used to analyze the association between the polymorphism at position -238 of TNF-α gene promoter and outcomes of HBV infection, as well as the interaction between the gene and smoking or alcohol drinking.

Subjects

The clinical diagnosis for all subjects in this study was based

on references[16,17]. Two hundred and seven patients with chronic HB from Ditan Hospital in Beijing, China during November 2001 to August 2002 were recruited, with inclusion criteria as follows: hepatitis B surface antigen (HBsAg) seropositive, anti-HBs antibodies (anti-HBs) seronegative, abnormally elevated serum alanine aminotransferase level, and duration of chronic HB ⩾2 years. One hundred and forty-eight subjects with self-limited HBV infection were from Shunyi District Hospital in Beijing, China during the same period, with inclusion criteria as positive for both anti-HBs and anti-HBc antibodies only, definitely negative for HBsAg, normal liver function tests, and no history of HBV vaccination. All subjects were Chinese Han people and they were recruited with their informed consent for genetic analysis. Venous blood was drawn from all subjects after an overnight fasting. Serum was separated immediately to detect ALT and blood corpuscles were stored at -70 ℃ to extract DNA and analyze genotypes.

Serological tests

Enzyme-linked immunoadsorbent assay (ELISA) was used for detection of serum HBsAg, anti-HBs, and anti-HBc (IMX; Abbott Diagnostics, North Chicago, IL).

Analysis of TNF-α gene promoter polymorphism

Genomic DNAs were obtained from peripheral blood leukocytes by standard phenol-chloroform extraction[18]. The -238G/A polymorphism in the promoter region of TNF-α gene was detected by PCR-RFLP as described by Miyazoe *et al*[19]. A 152-bp fragment was amplified using primers (5' : 5' AGAAG ACCCCCCTCGGAACC3' and 3' : 5' ATCTGGAGGAAGCG GTAGTG3'). Amplification was performed in a Perkin Elmer thermocycler (2700; Applied Biosystems, Foster City, CA) with 50 ng of genomic DNA, 20 pmol/L of each primer, 200 μmol/L each dNTP, 1.5 mmol/L $MgCl_2$, standard polymerase chain reaction (PCR) buffer and 1U Taq polymerase (Shanghai Biocolor) to 25 μL reaction system. PCR procedure was as follows: predenaturation at 94 ℃ for 2 min, followed by 30 cycles of denaturation at 94 ℃ for 1 min, annealing at 59 ℃ for 1 min and extension at 72 ℃ for 1 min, with a final extension at 72 ℃ for 5 min to terminate the reaction. After amplification, 10 μL PCR product was digested with restriction endonuclease (Msp-I 3U, Takara Bio Cor Dalian) at 37 ℃ for 5 h after addition of appropriate incubation buffer and ddH_2O to 20 μL. The digestion products were separated on 3% agarose gel and visualized directly under UV light with ethidium bromide staining. One base-exchange substitution from A to G position at position -238 created the Msp-I restriction site, resulting in 20- and 132-bp fragments with Msp-I digestion, where -238A allele could not create the Msp-I restriction site, which resulted in an 152-bp fragment.

Cigarette smoking and alcohol consumption

Cigarette smoking and alcohol consumption of the subjects were assessed by their self-report in a questionnaire.

Evaluation of the interaction

The gene-environment interaction was defined according to Rothman *et al*[20], with a formula to estimate interaction index $(II)=OR_{11}/OR_{01}\times OR_{10}$. II>1 was defined as positive, and II<1 as negative.

Statistical analysis

The frequencies of TNF-α promoter region alleles and genotypes were estimated. The Hardy-Weinberg equilibrium and frequencies of the alleles and genotypes between two groups were compared by χ^2 tests with two-tailed *P* values[21]. Odds ratios and their 95% confidence intervals were also calculated as measures of association of the polymorphism with outcomes of HBV infection. All the statistical procedures were performed with SAS version 6.12.

RESULTS

Characteristics of subjects

The main characteristics of study subjects are summarized in Table 1. The average age of the patients with chronic HB and subjects with self-limited HBV infection was 40.06(40.06±14.55) and 37.75(37.75±13.35) years, respectively, without significant difference (t=1.53, P=0.40). The number of men was more in the group of patients with chronic HB that in the group of subjects with self-limited HBV infection (χ^2=36.54, P<0.01). The proportion of married subjects was also different between the two groups (χ^2=6.29, P=0.01), whereas their education level was not statistically different (χ^2=5.66, P=0.06).

Table 1 Main characteristics of study groups

Variable	Chronic HB n=207(%)	Self-limited HBV infection n=148 (%)	P
Age (mean±SD)	40.06±14.55	37.75±13.35	0.40
Male / Female	162 / 45	70 / 78	<0.01
Marital status			0.01
Married	162 (78.26)	131 (88.51)	
Unmarried	45 (21.74)	17 (11.49)	
Education level			0.06
Lower than high school	13 (6.28)	18 (12.16)	
High school	126 (60.87)	94 (63.51)	
Above high school	68 (32.85)	36 (24.32)	

Association of -238G/A polymorphism of TNF-α promoter and behavior factors with outcomes of HBV infection

The distribution of genotype frequencies in patients with chronic HB and subjects with self-limited HBV infection was coincident with Hardy-Weinberg equilibrium (χ^2=0.02, P=0.89; χ^2=0.02, P=0.89).

The genotype distribution and allele frequencies of the -238 polymorphism in both groups are shown in Table 2. The homozygous AA genotype was not found in the study. Two hundred and three (98.07%) patients with chronic HB had GG genotype, significantly increased as compared with subjects with self-limited HBV infection (χ^2=5.30, P=0.02). The frequency of G allele in patients with chronic HB was significantly higher than that in subjects with self-limited HBV infection (99.03% *vs* 96.62%, χ^2=5.20, P=0.02).

The frequency of exposure to cigarette smoking or alcohol consumption in patients with chronic HB was significantly higher than that in subjects with self-limited HBV infection (OR>1), but there was no significant difference between the two groups (χ^2=2.13, P=0.14 and χ^2=0.99, P=0.32).

Multivariate unconditional logistic regression model was used to analyze the association of outcomes of HBV infection with age, sex, cigarette smoking, alcohol consumption and genotypes. It indicated that genotype GG was independently associated with chronic HB after the other factors were controlled (Table 4).

Gene-environmental interaction

As GG genotype was defined as positive exposure in this study, the results of gene-environmental interaction analysis between GG genotype and smoking or alcohol drinking are shown in Tables 5, 6. The odds ratios for smoking exposure alone and GG genotype alone were 0.50 (P=1.00) and 2.60 (P=0.19), respectively, whereas the odds ratio for combination of smoking and GG genotype was 3.84 (P=0.07) in a synergic pattern

Table 2 Genotype and allele frequencies in subjects with chronic HB and self-limited HBV infection

Group	*n*	Genotype (%)[1]			Allele (%)[2]	
		A / A	A / G	G / G	A	G
Chronic HB	207	0 (0.0)	4 (1.93)	203 (98.07)	4 (0.97)	410 (99.03)
Self-limited HBV infection	148	0 (0.0)	10 (6.76)	138 (93.24)	10 (3.38)	286 (96.62)

[1]χ^2=5.30, *P*=0.02, [2]χ^2=5.20, *P*=0.02.

Table 3 Association of behavior factors with risk of chronic HB

Characteristics	Chronic HB (%)	Self-limited HBV infection (%)	OR (95%CI)	*P*
Cigarette smoking			1.40 (0.87, 2.28)	0.14
Yes	74 (35.75)	42 (28.38)		
No	133 (64.25)	106 (71.62)		
Alcohol consumption			1.26 (0.78, 2.05)	0.32
Yes	69 (33.33)	42 (28.38)		
No	138 (66.67)	106 (71.62)		

Table 4 Multivariate logistic regression analysis for determinants of chronic HB

Variable	β	χ^2	*P*	*OR*	*95%CI*
Intercept	-0.5076	7.2203	0.0072	–	–
Sex (Male=1, Female=0)	1.4088	35.1138	<0.0001	4.091	2.567–6.519
-238G / A (GG=1, GA=0)	1.4183	5.1467	0.0233	4.132	1.212–14.085

(II=3.84/ 0.50×2.60=2.95). The odds ratio was 0.78 (*P*=1.00) for alcohol consumption alone and 3.18 (*P*=0.11) for GG genotype alone, respectively, and their combined odds ratio was 4.07 (*P*=0.05), indicating an effect of interaction between them (II=4.07/0.78×3.18=1.64).

Table 5 Case-control analysis for interaction between cigarette smoking and GG genotype

Cigarette smoking	GG genotype	Case[1]	Control[2]	OR (*95%CI*)	*P*
-	-	3	6	1	–
-	+	130	100	2.60 (0.56-13.49)	0.19
+	-	1	4	0.50 (0.01-10.45)	1.00
+	+	73	38	3.84 (0.79-20.73)	0.07

[1]Chronic HB patients, [2]self-limited HBV infection individuals.

Table 6 Case-control analysis for interaction between alcohol consumption and GG genotype

Alcohol consumption	GG genotype	Case[1]	Control[2]	OR (*95%CI*)	*P*
-	-	3	7	1	–
-	+	135	99	3.18 (0.72-15.96)	0.11
+	-	1	3	0.78 (0.02-18.21)	1.00
+	+	68	39	4.07 (0.08-21.25)	0.05

[1]Chronic HB patients, [2]self-limited HBV infection individuals.

DISCUSSION

It is estimated that HBV is present in about 130 million chronic carriers, accounting for 10% of Chinese population[22]. HBV infection can result in acute hepatitis, HBV carriage, chronic hepatitis, liver cirrhosis, even primary hepatocellular carcinoma. One reason of broad spectrum of HBV infection could be attributed to the interaction of genetic and environmental factors. The majority of human genetic studies on HBV infection focused on human leucocyte antigen (HLA) in recent years[23-27]. Several pro-inflammatory cytokines such as interleukin-2 and interferon-γ and TNF-α, have been identified to participate in the process of viral clearance and host immune response to HBV[28,29]. In addition, TNF-α/TNF-α receptor system has an important role in the pathogenesis of liver damage and viral clearance[30].

TNF-α is a principal mediator of inflammation and cellular immune response regulated both transcriptionally and posttranscriptionally[31]. In the past years -238G/A polymorphism in a putative regulation box of the TNF-α gene promoter region has been identified. Genetic polymorphisms in the regulatory regions of various cytokine genes could influence the amount of cytokines produced in response to inflammatory stimuli.

In our study, chronic HB patients and self-limited HBV infection individuals (the same as the patients recovered from HB in other studies) were recruited to examine the TNF-α promoter polymorphism at position –238. The results demonstrated that 98.07% of the patients carried genotype GG, significantly higher than the frequency in those with self-limited infection, suggesting that genotype GG could increase the risk of chronic HB and was different from the report of Hohler[32]. Fifty-three (75%) of 71 subjects with chronic HB were homozygous in TNF-α G/G, lower than the frequency of those with self-limited HBV infection (94%). Ethnic difference could play a certain role in these conflicting results, because the results from several studies suggested that the distribution of TNF promoter polymorphisms in the study subjects was different from those with other racial origins[7,32,33].

The difference in genotype and allele frequency between patients with chronic HB and subjects with self-limited HB infection in our study suggested that GG genotype might have no advantage to antigen presenting, but further study would be needed to demonstrate its significance as a susceptible gene. This difference may be due to the fact that the TNF-α promoter polymorphism at position -238, likely serving as a marker, was in linkage disequilibrium with neighboring genes encoding HLA or other undefined genes, thus possibly influencing the

outcomes of diseases.

Some studies suggested that the TNFA-A allele falling within a putative Y regulation box of the TNF-α promoter, was associated with increased TNF-α expression[34-36], which was inconsistent with other studies[37-40]. It is necessary to carry out the experimental study to confirm the causality between the -238G/A polymorphism of TNF-α promoter gene and the outcome of HBV infection, based on the population study.

The gene of TNF-α is located in the HLA class III region in the short arm of chromosome 6. Some single nucleotide polymorphism (SNP) loci have been found in the promoter region of TNF-α gene. It is speculated that these loci would be in linkage disequilibrium with other unknown mutations or HLA genes. It is important to further demonstrate the association of their constructed haplotypes with outcomes of HBV infection.

Epidemiological findings indicated that alcohol consumption and viral hepatitis could act synergistically to promote the development and progression of liver disease. Patients with viral hepatitis and alcohol consumption accelerated their liver injury with a higher risk of liver cirrhosis and primary hepatocellular carcinoma than those with viral hepatitis alone or alcohol consumption alone[41,42]. Wang[43] reported cigarette smoking and alcohol consumption were independently associated with elevated ALT levels among anti-HCV-seropositive individuals. Our study showed cigarette smoking and alcohol consumption might be risk factors of chronic HB (OR>1), but further study is needed due to lack of evidence that could reveal statistically significant differences between groups of chronic HB and self-limited HBV infection.

The analysis of gene-environmental interaction in this study showed there was a synergic effect between GG genotype and cigarette smoking or alcohol consumption. The very wide confidence interval was due to only one subject who smoked or drank without GG genotype in patient group, which needs a larger sample size to be confirmed.

In summary, different outcomes of HBV infection are independently associated with TNF-α promoter polymorphism at position –238, and there might be a synergic effect between TNF-α promoter gene and cigarette smoking or alcohol consumption in the development of chronic HB.

ACKNOWLEDGMENT

The authors thank Drs.Yi-Fan Chen, Xiu-Yun Ma, Min-Ying Mu, Hao-Dong Cai, Yun-Zhong Wu, Qing-Hua Dong, Zhi-Hai Cheng, Jie Xu from Ditan Hospital and Drs. Guo-Hua Yan, Xiu-Ling Wang, Yi-Liu from Shunyi District Hospital for data and sample collection.

REFERENCES

1 **Chisari FV,** Ferrari C. Hepatitis B virus immunopathogenesis. *Annu Rev Immunol* 1995; **13**: 29-60
2 **Wang FS.** Current status and prospects of studies on human genetic alleles associated with hepatitis B virus infection. *World J Gastroenterol* 2003; **9**: 641-644
3 **Chisari FV.** Rous-Whipple Award lecture. Viruses, immunity, and cancer: lessons from hepatitis B. *Am J Pathol* 2000; **156**: 1117-1132
4 **Jung MC,** Pape GR. Immunology of hepatitis B infection. *Lancet Infect Dis* 2002; **2**: 43-50
5 **Chisari FV.** Cytotoxic T cells and viral hepatitis. *J Clin Invest* 1997; **99**: 1472-1477
6 **Rehermann B.** Immune responses in hepatitis B virus infection. *Seminars Liver Disease* 2003; **23**: 21-37
7 **Bozkaya H,** Bozdayi M, Turkyilmaz R, Sarioglu M, Cetinkaya H, Cinar K, Kose K, Yurdaydin C, Uzunalimoglu O. Circulating IL-2, IL-10 and TNF-alpha in chronic hepatitis B: their relations to HBeAg status and the activity of liver disease. *Hepato Gastroenterol* 2000; **47**: 1675-1679
8 **Tokushige K,** Yamaguchi N, Ikeda I, Hashimoto E, Yamauchi K, Hayashi N. Significance of soluble TNF receptor-I in acute-type fulminant hepatitis. *Am J Gastroenterol* 2000; **95**: 2040-2046
9 **Westendorp RGJ**, Langermans JAM, Huizinga TWJ, Elouali AH, Verweij CL, Boomsma DI, Vandenbrouke JP. Genetic influence on cytokine production and fatal meningococcal disease. *Lancet* 1997; **349**: 170-173
10 **Wilson AG,** Symons JA, McDowell TL, McDevitt HO, Duff GW. Effects of a polymorphism in the human tumor necrosis factor alpha promoter on transcriptional activation. *Proc Natl Acad Sci U S A* 1997; **94**: 3195-3199
11 **Winchester EC,** Millwood IY, Rand L, Penny MA, Kessling AM. Association of the TNF-alpha-308 (G-A) polymorphism with self-reported history of childhood asthma. *Hum Genet* 2000; **107**: 591-596
12 **Sleijffers A,** Yucesoy B, Kashon M, Garssen J, De Gruijl FR, Boland GJ, Van Hattum J, Luster MI, Van Loveren H. Cytokine polymorphisms play a role in susceptibility to ultraviolet B-induced modulation of immune responses after hepatitis B vaccination. *J Immunol* 2003; **170**: 3423-3428
13 **Jazrawi SF,** Zaman A, Muhammad Z, Rabkin JM, Corless CL, Olyaei A, Biggs A, Ham J, Chou S, Rosen HR. Tumor necrosis factor-alpha promoter polymorphisms and the risk of rejection after liver transplantation: a case control analysis of 210 donor-recipient pairs. *Liver Transpl* 2003; **9**: 377-382
14 **McCusker SM,** Curran MD, Dynan KB, McCullagh CD, Urquhart DD, Middleton D, Patterson CC, McIlroy SP, Passmore AP. Association between polymorphism in regulatory region of gene encoding tumour necrosis factor α and risk of Alzheimer's disease and vascular dementia: a case-control study. *Lancet* 2001; **357**: 436-439
15 **Shibue T,** Tsuchiya N, Komata T, Matsushita M, Shiota M, Ohashi J, Wakui M, Matsuta K, Tokunaga K. Tumor necrosis factor α 5'-flanking region, tumor necrosis factor receptor II, and HLA-DRB1 polymorphisms in Japanese patients with rheumatoid arthritis. *Arthritis Rheumatoid* 2000; **43**: 753-757
16 **Lok AS,** Heathcote EJ, Hoofnagle JH. Management of hepatitis B: 2000-summary of a workshop. *Gastroenterology* 2001; **120**: 1828-1853
17 The branch of infectious diseases**,** parasitology and hepatology of Chinese Medical Association. The strategy of prevention and cure in viral hepatitis. *Zhonghua Chuanranbing Zazhi* 2001; **19**: 56-62
18 **Sambrook J,** Russell DW. ed. Molecular Cloning: A Laboratory Manual. 2nd ed. Beijing: *Science Publishing House* 1992: 465-467
19 **Miyazoe S,** Hamasaki K, Nakata K, Kajiya Y, Kitajima K, Nakao K, Daikoku M, Yatsuhashi H, Koga M, Yano M, Eguchi K. Influence of interleukin-10 gene promoter polymorphisms on disease progression in patients chronically infected with hepatitis B virus. *Am J Gastroenterol* 2002; **97**: 2086-2092
20 **Rothman KJ,** Greenland S. ed. Interactions between Causes. Modern Epidemiology, 2nd ed, Boston: *Lippincott Williams Wilkins* 1998: 311-326
21 **Jiang SD,** Lv BZ. ed. Mathematical and Statistical Methods in Medical Genetics. 1st ed. Beijing: *Science Publishing House* 1998: 10-11
22 **Luo KX**. ed. Hepatitis B: Basic Biology and Clinical Science. 2nd ed. Beijing: *People's Medical Publishing House* 2001: 1-6
23 **Almarri A,** Batchelor JR. HLA and hepatitis B infection. *Lancet* 1994; **344**: 1194-1195
24 **Thursz MR,** Kwiatkowski D, Allsopp CE, Greenwood BM, Thomas HC, Hill AV. Association between an MHC class II allele and clearance of hepatitis B virus in the Gambia. *N Engl J Med* 1995; **332**: 1065-1069
25 **Thursz MR**. Host genetic factors influencing the outcome of hepatitis. *J Viral Hepat* 1997; **4**: 215-220
26 **Thio CL,** Carrington M, Marti D, O'Brien SJ, Vlahov D, Nelson KE, Astemborski J, Thomas DL. Class II HLA alleles and hepatitis B virus persistence in African Americans. *J Infect Dis* 1999; **179**: 1004-1006
27 **Diepolder HM,** Jung MC, Keller E, Schraut W, Gerlach JT, Gruner N, Zachoval R, Hoffmann RM, Schirren CA, Scholz S, Pape GR. A vigorous virus-specific CD4+ T cell response may contribute to the association of HLA-DR13 with viral clearance in hepatitis B. *Clin Exp Immunol* 1998; **113**: 244-251

28 **Romero R,** Lavine JE. Cytokine inhibition of the hepatitis B virus core promoter. *Hepatology* 1996; **23**: 17-23

29 **Gonzalez-Amaro R,** Garcia-Monzon C, Garcia-Buey L, Moreno-Otero R, Alonso JL, Yague E, Pivel JP, Lopez-Cabrera M, Fernandez-Ruiz E, Sanchez-Madrid F. Induction of tumor necrosis factor alpha production by human hepatocytes in chronic viral hepatitis. *J Exp Med* 1994; **179**: 841-848

30 **Marinos G,** Naoumov NV, Rossol S, Torre F, Wong PY, Gallati H, Portmann B, Williams R. Tumor necrosis factor receptors in patients with chronic hepatitis B virus infection. *Gastroenterology* 1995; **108**: 1453-1463

31 **Ba DN.** ed. Contemporary Immunological Technology and Application. Beijing: *Peking Medical University and Peking Union Medical College Publishing House* 1998: 52-54

32 **Hohler T,** Kruger A, Gerken G, Schneider PM, Meyer zum Buschenfelde KH, Rittner C. A tumor necrosis factor-alpha (TNF-alpha) promoter polymorphism is associated with chronic hepatitis B infection. *Clin Exp Immunol* 1998; **111**: 579-582

33 **Higuchi T,** Seki N, Kamizono S, Yamada A, Kimura A, Kato H, Itoh K. Polymorphism of the 5'-flanking region of the human tumor necrosis factor (TNF)-alpha gene in Japanese. *Tissue Antigens* 1998; **51**: 605-612

34 **Grove J,** Daly AK, Bassendine MF, Day CP. Association of a tumor necrosis factor promoter polymorphism with susceptibility to alcoholic steatohepatitis. *Hepatology* 1997; **26**: 143-146

35 **Drouet C,** Shakov AN, Jongeneel CV. Enhancers and transcription factors controlling the inducibility of the tumor necrosis factor-alpha promoter in primary macrophages. *J Immunol* 1991; **147**: 1694-1700

36 **Soga Y,** Nishimura F, Ohyama H, Maeda H, Takashiba S, Murayama Y. Tumornecrosis factor-alpha gene (TNF-alpha) -1031/-863, -857 single-nucleotide polymorphisms (SNPs) are associated with severe adult periodontitis in Japanese. *J Clin Periodontol* 2003; **30**: 524-531

37 **Pociot F,** D'Alfonso S, Compasso S, Scorza R, Richiardi PM. Functional analysis of a new polymorphism in the human TNF alpha gene promoter. *Scand J Immunol* 1995; **42**: 501-504

38 **Kaijzel EL,** van Krugten MV, Brinkman BM, Huizinga TW, van der Straaten T, Hazes JM, Ziegler-Heitbrock HW, Nedospasov SA, Breedveld FC, Verweij CL. Functional analysis of a human tumor necrosis factor alpha (TNF-alpha) promoter polymorphism related to joint damage in rheumatoid arthritis. *Mol Med* 1998; **4**: 724-733

39 **Huizinga TW,** Westendorp RG, Bollen EL, Keijsers V, Brinkman BM, Langermans JA, Breedveld FC, Verweij CL, van de Gaer L, Dams L, Crusius JB, Garcia-Gonzalez A, van Oosten BW, Polman CH, Peña AS. TNF-alpha promoter polymorphisms, production and susceptibility to multiple sclerosis in different groups of patients. *J Neuroimmunol* 1997; **72**: 149-153

40 **Uglialoro AM,** Turbay D, Pesavento PA, Delgado JC, McKenzie FE, Gribben JG, Hartl D, Yunis EJ, Goldfeld AE. Identification of three new single nucleotide polymorphisms in the human tumor necrosis factor-alpha gene promoter. *Tissue Antigens* 1998; **52**: 359-367

41 **Khan KN,** Yatsuhashi H. Effect of alcohol consumption on the progression of hepatitis C virus infection and risk of hepatocellular carcinoma in Japanese patients. *Alcohol Alcohol* 2000; **35**: 286-295

42 **Gao B.** Interaction of alcohol and hepatitis viral proteins: implication in synergistic effect of alcohol drinking and viral hepatitis on liver injury. *Alcohol* 2002; **26**: 69-72

43 **Wang CS,** Wang ST, Chang TT, Yao WJ, Chou P. Smoking and alanine aminotransferase levels in hepatitis C virus infection: implications for prevention of hepatitis C virus progression. *Arch Intern Med* 2002; **162**: 811-815

Edited by Zhang JZ and Wang XL **Proofread by** Xu FM

PO Box 2345, Beijing 100023, China
Fax: +86-10-85381893
E-mail: wjg@wjgnet.com www.wjgnet.com

World J Gastroenterol 2004;10(12):1815-1818
World Journal of Gastroenterology
Copyright ©2004 by The WJG Press ISSN 1007-9327

• BRIEF REPORTS •

Hypermethylation of Syk gene in promoter region associated with oncogenesis and metastasis of gastric carcinoma

Shui Wang, Yong-Bin Ding, Guo-Yu Chen, Jian-Guo Xia, Zhen-Yan Wu

Shui Wang, Yong-Bin Ding, Guo-Yu Chen, Jian-Guo Xia, Zhen-Yan Wu, Department of General Surgery, First Affiliated Hospital of Nanjing Medical University, Nanjing 210029, Jiangsu Province, China
Supported by the Science Fund of Department of Science and Technology of Jiangsu Province. 03KJD320138
Correspondence to: Yong-Bin Ding, Department of General Surgery, First Affiliated Hospital of Nanjing Medical University, Nanjing 210029, Jiangsu Province, China. njdyb@sina.com
Telephone: +86-25-86563750 **Fax:** +86-25-86563750
Received: 2003-10-24 **Accepted:** 2003-12-08

Abstract

AIM: To investigate the rrelationship between methylation of Syk (spleen tyrosine kinase) gene in promoter region and oncogenesis, metastasis of gastric carcinoma. The relation between silencing of the Syk gene and methylation of Syk promoter region was also studied.

METHODS: By using methylation-specific PCR (MSP) technique, the methylation of Syk promoter region in specimens from 61 gastric cancer patients (tumor tissues and adjacent normal tissues) was detected. Meanwhile, RT-PCR was used to analyse syk expression exclusively.

RESULTS: The expression of the Syk gene was detected in all normal gastric tissues. Syk expression in gastric carcinoma was lower in 14 out of 61 gastric cancer samples than in adjacent normal tissues (χ^2=72.3, P<0.05). No methylation of Syk promoter was found in adjacent normal tissues. hypermethylation of Syk gene in promoter was detected 21 cases in 61 gastric carcinoma patients. The rate of methylation of Syk promoter in gastric carcinoma was higher than that in adjacent normal tissues (χ^2=25.1, P<0.05). In 31 patients with lymph node metastasis, 17 were found with Syk promoter methylation. A significant difference was noted between two groups (χ^2=11.4,P<0.05).

CONCLUSION: Hypermethylation leads to silencing of the Syk gene in human gastric carcinoma. Methylation of Syk promoter is correlated to oncogenesis and metastasis of gastric carcinoma. Syk is considered to be a potential tumor suppressor and anti-metastasis gene in human gastric cancer.

Wang S, Ding YB, Chen GY, Xia JG, Wu ZY. Hypermethylation of Syk gene in promoter region associated with oncogenesis and metastasis of gastric carcinoma. *World J Gastroenterol* 2004; 10(12): 1815-1818
http://www.wjgnet.com/1007-9327/10/1815.asp

INTRODUCTION

Gastric cancer development and progression are thought to occur through a complex, multistep process, including oncogene activation and mutation or loss of tumor suppressor genes. Determining the function of genetic alterations in gastric carcinoma tumorigenesis and metastasis has been the focus of intensive research efforts for several decades. One group of proteins that play a critical role in gastric cancer cell signaling pathways is tyrosine kinases. The decrease or loss of spleen tyrosine kinase (Syk) expression seems to be associated with increased motility and invasion of malignant phenotype[1-5].

Syk, a non-receptor type of protein-tyrosine kinase that is widely expressed in hematopoietic cells, is one of the two members of the Syk family (Syk and ZAP-70). Syk is activated upon the binding to its tandem Src homology 2 (SH2) domains to immunoreceptor tyrosine-based activation motif (ITAM) and plays an essential role in lymphocyte development and activation of immune cells. Emerging evidence indicates that Syk may be a potent modulator of epithelial cell growth and a potential tumor suppressor in human breast carcinoma[6,7]. But the role of Syk in gastric carcinoma remains unclear, so we examined Syk mRNA expression in human gastric cancer and the adjacent non-cancerous tissues, and explored whether methylation of Syk promoter region was associated with the loss of Syk expression in gastric cancer and the relationship between Syk mRNA expression in gastric cancer tissue and clinicopathological factors in the present study.

MATERIALS AND METHODS

Tissues

Gastric cancer and matched adjacent non-cancerous tissues were obtained during surgical excision from 61 patients with gastric cancer in our department between March 2001 and October 2002. The age of 38 male and 23 female patients was rang from 26 to 78 (mean, 58.1) years. All samples were placed in liquid nitrogen immediately after resection and stored at -70 ℃ until RNA extraction. No patient had received chemotherapy or radiation therapy prior to surgery. All patients were confirmed to have gastric carcinoma by pathologic test.

RNA extraction and semi-quantitative reverse transcription (RT)–polymerase chain reaction (PCR)

Total RNA was isolated from each specimen by Trizol reagent according to the manufacturer's recommendations. Samples were ground into a fine powder using a mortar and pestle, incubated in Trizol solution (100 g/L) for 15 min, and then 1/5 volume of choloform was added. After vigorous agitation for 5 min, the inorganic phase was separated by centrifugation at 12 000 g for 20 min at 4 ℃, RNA was then precipitated in the presence of 1 volume of isopropanol and centrifuged at 10 000 g for 15 min at 4 ℃. RNA pellets were washed with 700 ml/L ice-cold ethanol and then dissolved in diethyl pyrocarbonate (DEPC) - treated H_2O. Total RNA concentration and quantity were assessed by absorbency at 260 nm by using a nucleic acid and protein. Semi-quantitative RT-PCR of 40 pairs of gastric cancer tissues and 15 pair of benign fibroadenoma tissues was performed for intergrin beta1 displaying expression alterations. Five micrograms of total RNA in each hybridization sample was used to synthesize the first strand cDNA with SuperScript preamplification system for first strand cDNA synthesis kit. Then 1 mL product was used as the template to amplify specific fragments in 25 mL reaction mixture under the following conditions:

denaturation at 94 ℃ (3 min); 40 cycles at 94 ℃ (45 s), at 60 ℃ (45 s) and at 72 ℃ (60 s), then extensions at 72 ℃ (3 min). The PCR primers of Syk were as follow: Syk forward, 5' -CATGTCAAGGATAAGAACATCATAGA-3' ; reverse: 5' -AGTTCACCACGTCATAGTAGTAATT-3' . A 514 bp nucleotide fragment of the human Syk cDNA was amplified. In each PCR reaction, primers for the human glyceraldehyde-3-phosphate dehydrogenase (*GAPDH*) gene were used as an internal control. GAPDH primer sequences were as forward: primer 5' -AGAAGGCTGGGGCTCATTTGCAGGG-3' reverse primer 5' -GTCACTGGCGTCTTCACCACCATG-3' . Ten mL RT-PCR reaction product was analyzed by electrophoresis on a 15 g/L agarose gel. The electrophoresis images were scanned by Fluor-S MultiImager and the original intensity of each specific band was quantitated with the software Multi-Analyst. The data were compared after normalized by the intensity of GAPDH. After normalization, the adjusted intensities were calculated for the amplified gene products, and the ratios were calculated. The sequences of PCR primer pairs of intergrin beta1 and GAPDH were designed using Primer3 Internet software program. Their specificity was confirmed by a BLAST Internet software assisted search for a nonredundant necleotide sequence database.

DNA extraction, purification, bisulfite modification and Sequencing

Genomic DNA from cell lines or frozen gastric tissues was extracted by using a Dneasy kit. Genomic DNA was treated with sodium bisulfite. DNA (20 mg/L) was denatured by NaOH (concentration 0.2 mol/L) for 10 min at 37 ℃. Thirty μL of 10 nmol/L hydroquinone and 520 μL of 3 mol/L sodium bisulfate were added, followed by incubation at 50 ℃ for 16 h. The modified DNA was purified using Wizard DNA purification columns. The purified DNA was treated again with NaOH and precipitated. DNA was resuspended in 30 μL of TE buffer (3 mmol/L Tris (P8.0/0.2 mmol/L EDTA) and subjected to PCR amplification using a primer set (forward 5' -GATTAAGATATATTTTAGGGAATATG-3; reverse 5' -CACCTATATTTTATTCACATAATTTC-3) that spanned the Syk CpG island. Fifteen μL reaction containing 30 ng of bisulfite-treated DNA and 1xRDA buffer (67 mmol/L Tris (pH8.8)/16 mmol/L $(NH_4)_2SO_4$, 100 mmol/L 2-mercaptoethanol, 1 g/L BSA) was processed in 30 thermal cycles at 94 ℃ for 45 s, at 58 ℃ for 45 s, and at 72 ℃ for 45 s. One aliquot (2 μL) of diluted PCR Product (40-fold) was subjected to PCR amplification in a 15-μL volume.

Methylation-specificPCR (MSP)

Methylation-specific primers were designed to cover 9 CPG dinucleotides numbered 17-21 (forward) 47-50 (reverse). Similarly, unmethylation-specific primers were designed cover 8 CpG dinucleotides numbered 18-22 b, (forward) and 35-37 (reverse). Primers specific for methylation DNA (forward) 5' -CGATTTCGCGGGTTTCGTTC-3; (reverse) 5' -AAAACGAACGCAACGCGAAAC-3; and unmethylation DNA (forward 5' -ATTTTGTGGGTTTTGTTTGGTG-3, reverse 5' -ACTTCCTTAACACACCCAAAC-3 were added to the same reaction and PCR products were subjected to electrophoresis on a 10 g/L agarose gel. The m-specific primer set yielded a band at 243 bp and the u primer set yielded a band at 140 bp. PCR conditions were 24 cycles at 94 ℃ for 30 s, at 67 ℃ for 30 s, and at 72 ℃ for 30 s.

Statistical analysis

t- test was used to compare the Syk mRNA expression levels with primary gastric cancer, the adjacent non-cancerous tissues. χ^2 test was also used to estimate the relationship between the silencing of Syk mRNA and methylation of Syk promoter region. Values of $P<0.05$ were considered statistically significant.

RESULTS

Expression of Syk in gastric cancer and adjacent non-cancerous tissues

The expression of Syk was found in 14 out of 61 gastric cancer tissues, Syk mRNA expression was detected in all adjacent normal gastric tissue (Figure 1). The rate of expression of Syk in gastric caner tissue was significantly lower than that in adjacent non-cancerous normal gastric tissues ($\chi^2=72.3$, $P<0.05$).

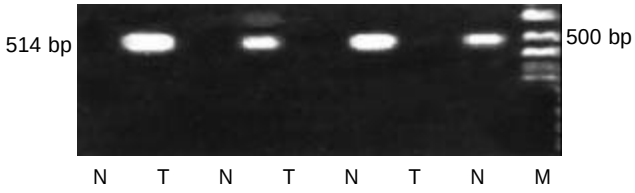

Figure 1 Syk mRNA expression in human gastric cancer and adjacent non-cancerous tissue (RT-PCR detection of Syk mRNA). T: tumor tissue; N: adjacent non-cancerous normal gastric tissue; M: marker.

Syk mRNA expressions were found in 11 out of the 30 gastric cancer patients without lymph node metastasis, but in 3 out of the 31 gastric cancer patients with lymph node metastasis. Expression of Syk mRNA in patients having lymph node metastasis was significantly lower than that in those having no lymph node metastasis ($\chi^2=4.85$, $P<0.05$). Meanwhile no significant difference was found between Syk mRNA expression in the gastric cancer patients and age, tumor size, clinicopathological stage, histological type (data not shown).

Semi-quantitative RT-PCR

A total of 10 μL RT-PCR products were electrophoresed on 15 g/L agarose gel contacting ethidium bromide. The level of GAPDH was used as internal control (Figure 2). The relative expression levels of Syk normalized to the expression level of GAPDH, in the primary gastric cancer tissues and adjacent mammary tissues were, 1.71±1.28 and 3.19±0.59 (mean±SD). A significant difference was found between the level of Syk mRNA expression in the primary gastric cancer tissues and adjacent mammary tissues ($t=2.1$, $P<0.05$). Furthermore, the level of Syk mRNA in patients having lymph node metastasis was significantly lower than that in patients having no lymph node metastasis (1.18±1.13 *vs* 2.14±1.27, $t=3.4$, $P<0.05$).

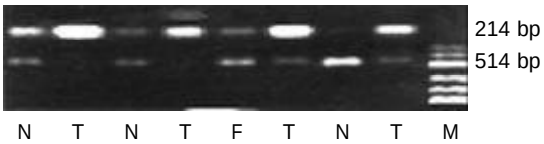

Figure 2 Partial semi-quantitative RT-PCR results in 40 gastric cancer tissues and adjacent non-cancerous tissues. T: tumor tissue; N: adjacent non-cancerous normal gastric tissue; M: marker.

Correlation between methylation of Syk gene in promoter region and oncogenesis, metastasis of gastric carcinoma

MSP was used to analyze the Syk methylation status of gastric carcinoma and its matched normal gastric tissues. Forty nonselective gastric cancers were screened. Among the 61 carcinomas examined, 21 exhibited strong Syk methylation. Representative examples are shown in Figure 3. In contrast to their corresponding carcinomas, the Syk gene of the 61 matched neighboring normal gastric tissues remained unmethylated. The

rate of methylation of Syk promoter in gastric carcinoma was higher than that of adjacent normal tissues (χ^2=25.1, P<0.05).

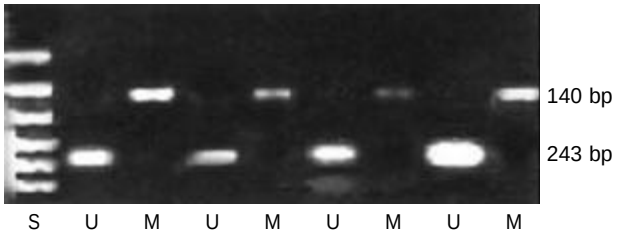

Figure 3 Representative examples of Syk methylation (neighboring normal gastric tissues unmethylated).

As shown in Table 1, of the 31 cases of lymph node metastasis, 17 were found with Syk promoter methylation. Syk promoter methylations in 4 out of 30 without lymph node metastasis were detected. A significant difference was noted between two groups (χ^2=11.4, P<0.05). Correlation between methylation of Syk promoter region and clinicopathologic factors was shown in Table 1.

Table 1 Correlation between methylation of Syk promoter region and clinicopathologic factors (*n*)

Factor	Frequency of Syk promoter region methylation	*P*
Gender		
Male	14 / 38	
Female	7 / 23	0.26
Tumor size		
<3cm	8 / 26	
3	13 / 35	0.61
Depth of invasion		
Mucosa and submucosa	2 / 9	
Muscle and subserosa	7 / 29	
Serosa	12 / 23	0.075
Lymph node metastasis		
Present	17 / 31	
Absent	4 / 30	0.0016
Stage		
I-II	6 / 25	
III-IV	15 / 36	0.24
Tumor location		
Lower third	6 / 15	
Middle third	11 / 35	
Upper third	4 / 11	0.83

Relationship between Syk promoter region hypermethylation and loss of its expression in gastric carcinoma

Syk promoter methylation was found in 21 of 61 gastric tumors. They did not show any detectable Syk. In 40 cases without Syk promoter methylation, Syk mRNA expression was found in 13 cases. Syk promoter methylation was significantly related with loss of Syk expression in gastric carcinoma (χ^2=4.2, P<0.05).

DISCUSSION

Syk is ubiquitously expressed in hematopoietic cells and has been extensively studied as effectors of B cell receptor (BCR) signaling[8-10].It has been found to be involved in coupling activated immunoreceptors to downstream signaling events that mediate diverse cellular responses including proliferation, differentiation and phagocytosis[11-16]. Some reports are of opinions that Syk is a candidated suppressor gene.

In this paper, we explored expression of Syk mRNA in gastric cancer and its adjacent non-cancerous tissues. Our results showed that the level and rate of Syk mRNA expression in gastric cancer tissues were significantly lower than those in adjacent non-cancerous tissues, especially invasive gastric cancer tissues did not show any detectable Syk mRNA expression, indicating that loss of Syk mRNA expression may be correlated to gastric carcinogenesis. Our findings were in agreement with the results of Goodman *et al*.[17,18].

Furthermore, we observed that only four gastric cancer tissues from 31 patients with lymph node metastasis had Syk mRNA expression which was negatively correlated to lymph node metastasis. In B cells, Syk activity was a key regulator of Akt kinase activity after BCR engagement, because Syk induced PI3-K-dependent Akt activation and inhibition of apoptosis[18]. Numerous studies have demonstrated deregulated Akt activity in gastric cancer cells. It is tempting to speculate that Syk may also regulate Akt activity in gastric cells. Syk mRNA expression was reduced during human gastric cancer progression, and then it was unlikely that Syk-dependent signaling contributed to the increased Akt activity observed in gastric cancer cells[19-21]. Findings by Okamura *et al*.[23] suggest that Syk mRNA expression was positively correlated to p53 expression. They found that Syk gene expression was repressed in a *p53*-dependent manner in human colon carcinoma cells, indicating that loss of *p*53 function during tumorigenesis could lead to deregulated Syk activity[7,22]. Study by Mahabeleshwar *et al*.[19] suggested Syk suppressed cell motility and inhibited PI-3 kinase activity and uPA secretion by blocking NF-*k*B activity through tyrosine phosphorylation of I*k*Bα. So loss of Syk expression might contribute to gastric oncogensis and metastasis[18,23].

However, the mechanism of Syk expression loss remains unclear. A number of cancer-associated genes have been shown to be inactivated by hypermethylation of CpG islands during gastric tumorigenesis. About 50% of human genes have clusters of CPG dinucleotides (CPG islands) in their 5' -regulatory sequences. Gene silencing through methylation of these sites has been observed in early developmental stages and aging. Aberrant methylation may lead to deregulation of gene expression. Most notably, tumor suppressor genes, mismatched repair genes, and others such as estrogen receptor, E-cadheria, death-associated protein kinase, and thrombospodin-I, were repressed by CPG island hypermethylation in cancer tissues, inhibition of the transcription of these genes could provide an epigenetic mechanism of clonal selection during tumorigenesis[24,25].

In this study, the 5' CpG island methylation status of the Syk gene in gastric cancer tissues was examined. We found Syk 5' CpG hypermethylation in 35%(21/60) of unselected gastric tumors, whereas all of the matched neighboring normal gastric tissues exhibited unmethylated DNA. We found that the rate of methylation of Syk promoter in gastric carcinoma was significantly higher than that in adjacent normal tissues, suggesting that hypermethylation of Syk promoter region may be associated with oncogenesis of gastric cancer. In addition, the rate of Syk promoter region methylation in the patients with lymph node metastasis is significantly higher than that in the patients without lymph node metastasis, indicating that methylation of Syk promoter methylation is related to lymph node metastasis of gastric cancer. The absence of Syk protein was reflected by the loss of its mRNA expression in gastric cancers, suggesting that the loss of Syk mRNA expression occurs at the transcriptional level. 5' CpG hypermethylation of Syk was reported to be associated with loss or reduction of Syk gene expression, which may provide a new way to treat gastric cancer[26,27].

However, we did not observe any significant correlation between Syk methylation and tumor grade. This may be attributable to a relatively small sample size and the complexity of unselected patient population. Additional detailed studies

using patient cohort should be done needed to examine the value of Syk methylation as a diagnostic or prognostic marker[28,29].

The recent identification of Syk as a potent modulator of gastric epithelial cell growth has generated a need for further exploration of the role of nonreceptor tyrosine kinases in gastric cancer progression and metastasis[28-30]. These initial results offer the promise that novel molecular targets may be identified both for the prevention of gastric cancer development and for inhibition of metastatic gastric cancer spread. The continual elucidation of novel targets such as Syk is a critical part of the endeavor to eradicate gastric cancer. These findings may provide promise molecular targets for the prevention of gastric cancer development[31-33].

ACKNOWLEDGEMENTS

We are grateful for the technical assistance from Mrs. Yu Yue, Laboratory of General Surgery Department, the First Affiliated Hospital of Nanjing Medical University.

REFERENCES

1 **Kim JP.** Surgical results in gastric cancer. *Semin surg oncol* 1999; **17**:132-138
2 **Ding YB**, Chen GY, Xia JG, Zang XW, Yang HY,Yang L. Overexpression of VCAM-1 is associated with oncogenesis, tumor angiogenesis and metastasis of gastric carcinoma. *World J Gastroenterol* 2003; **9**: 1409-1414
3 **Sada K,** Takano T, Yanagi S, Yamamura H. Structure and function of Syk protein-tyrosine kinase. *J Biochem* 2001;**130**: 177-186
4 **Toyama T,** Iwase H, Yamashita H, Hara Y, Omoto Y, Sugiura H, Zhang Z, Fujii Y. Reduced expression of the Syk gene is correlated with poor prognosis in human breast cancer. *Cancer Lett* 2003; **189**: 97-102
5 **Li L**, Shaw PE. Autocrine-mediated activation of STAT3 correlates with cell proliferation in breast carcinoma lines. *J Biol Chem* 2002; **277**: 17397-17405
6 **Coopman PJ,** Do MT, Barth M, Bowden ET, Hayes AJ, Basyuk E, Blancato JK, Vezza PR, McLeskey SW, Mangeat PH, Mueller SC. The Syk tyrosine kinase suppresses malignant growth of human breast cancer cells. *Nature* 2000; **406**: 742–747
7 **Stewart Z,** Pietenpol J. Syk: a new player in the field of breast cancer. *Breast Cancer Res* 2001; **3:** 5-7
8 **Stupack DG,** Li E, Silletti SA, Kehler JA, Geahlen RL, Hahn K, Nemerow GR, Cheresh DA. Matrix valency regulates integrin-mediated lymphoid adhesion via Syk kinase. *J Cell Biol* 1999; **144: 777**-788
9 **Danam RP**, Qian XC, Howell R, Brent TP. Methylation of selected CpGs in the human O^6-methyiguanine-DNA methyltransferase promoter region as a marker of gene silencing. *Mol Carcinogenesis* 1999; **24**: 85-89
10 **Zhang J**, Siraganian RP. CD45 is essential for Fc epsilon RI signaling by ZAP70, but not Syk, in Syk-negative mast cells. *J Immunol* 1999; **163**: 2508-2516
11 **Zhu DM,** Tibbles HE, Vassilev AO, Uckun FM. SYK and LYN mediate B-cell receptor-independent calcium-induced apoptosis in DT-40 lymphoma B-cells. *Leuk Lymphoma* 2002; **43:** 2165-217**0**
12 **Chen L**, Widhopf G, Huynh L, Rassenti L, Rai KR, Weiss A, Kipps TJ. Expression of ZAP-70 is associated with increased B-cell receptor signaling in chronic lymphocytic leukemia. *Blood* 2002; **100:** 4609-4614
13 **Palmieri G**, Tullio V, Zingoni A, Piccoli M, Frati L, Lopez-Botet M, Santoni A. CD94/NKG2-A inhibitory complex blocks CD16-triggered Syk and extracellular regulated kinase activation, leading to cytotoxic function of human NK cells. *J Immunol* 1999; **162**: 7181-7188
14 **Chu DH,** Morita CT, Weiss A. The Syk family of protein tyrosine kinases in T-cell activation and development. *Immunol Rev* 1998; **165**: 167–180
15 **Murphy M**, Schnall R, Venter DJ, Barnett L, Bertoncello I, Thien CB, Langdon WY, Dowtell DD. Tissue hyperplasia and enhanced T-cell signalling *via* ZAP-70 in c-Cbl-deficient mice. *Mol Cell Biol* 1998; **18:** 4872-4882
16 **Zompi S,** Hamerman JA, Ogasawara K, Schweighoffer E, Tybulewicz VL, Di Santo JP, Lanier LL, Colucci F. NKG2D triggers cytotoxicity in mouse NK cells lacking DAP12 or Syk family kinases. *Nat Immunol* 2003; **4**: 565-472
17 **Goodman PA,** Jurana B, Wood CM, Uckun F. Genomic studies of the spleen protein tyrosine kinase locus reveal a complex promoter structure and several genetic variants. *Leuk Lymphoma* 2002; **43**: 1627-1635
18 **Goodman PA,** Wood CM, Vassilev A, Mao C, Uckun FM. Spleen tyrosine kinase (Syk) deficiency in childhood pro-B cell acute lymphoblastic leukemia. *Oncogene* 2001; **20**: 3969-3978
19 **Mahabeleshwar GH**, Kundu GC. Syk, a protein tyrosine kinase suppresses the cell motility and nuclear factor kB mediated secretion of urokinase type plasminogen activator by inhibiting the phosphatidylinositol 3'-kinase activity in breast cancer cells. *J Biol Chem* 2003; **278:** 6209-6221
20 **Paolini R,** Molfetta R, Beitz LO, Zhang J, Scharenberg AM, Piccoli M, Frati L, Siraganian R, Santoni A. Activation of Syk tyrosine kinase is required for c-Cbl-mediated ubiquitination of Fcepsilon RI and Syk in RBL cells. *J Biol Chem* 2002; **277**: 36940-36947
21 **Carter W,** Hoying JB, Boswell C, Williams SK. HER2/neu over-expression induces endothelial cell retraction. *Int J Cancer* 2001; **91:** 295-299
22 **Qiu Y,** Kung HJ. Signaling network of the Btk family kinase. *Oncogene* 2000; **19:** 5651-5661
23 **Okamura S,** Ng C, Koyama K, Takei Y, Arakawa H, Monden M, Nakamura Y. Identification of seven genes regulated by wild-type p53 in a colon cancer cell line carrying a well-controlled wild-type p53 expression system. *Oncol Res* 1999; **11**: 281-285
24 **Dong G,** Loukinova E, Chen Z, Gangi L, Chanturita TI, Liu ET, Van Waes C. Molecular profiling of transformed and metastatic murine squamous carcinoma cells by differential display and cDNA microarray reveals altered expression of multiple genes related to growth, apoptosis, angiogenesis, and the NF-kappaB signal pathway. *Cancer Res* 2001; **61**: 4797-4808
25 **Yuan Y**, Mendez R, Sahin A, Dai JL. Hypermethylation leads to silencing of the SYK gene in human breast cancer. *Cancer Res* 2001; **61**: 5558–5561
26 **Ding YB**, Chen GY, Xia JG, Zang XW, Yang HY,Yang L. Correlation of tumor-positive ratio and number of perigastric lymph nodes with prognosis of gastric carcinoma in surgically treated patients. *World J Gastroenterol* 2004; **10**: 182-185
27 **Buchholz TA,** Wazer DE. Molecular biology and genetics of breast cancer development: a clinical perspective. *Semin Radiat Oncol* 2002; **12:** 285-295
28 **Arber N,** Shapira I, Katan J, Stern B, Fabian I, Halpern Z. Activation of c-k ras mutations in human gastrointest inal tumors. *Gastroentrerology* 2000; **118:** 1045-1050
29 **Balaian L,** Zhong RK, Ball ED. The inhibitory effect of anti-CD33 monoclonal antibodies on AML cell growth correlates with Syk and/or ZAP-70 expression. *Exp Hematol* 2003; **31:** 363-371
30 **Djeu JY**, Jiang K, Wei S. A view to a kill: signals triggering cytotoxicity. *Clin Cancer Res* 2002; **8**: 636-640
31 **Uckun FM**, Sudbeck EA, Mao C, Ghosh S, Liu XP, Vassilev AO, Navara CS, Narla RK. Structure-based design of novel anticancer agents. *Curr Cancer Drug Targets* 2001**; 1:** 59-71
32 **Xu R,** Seger R, Pecht I. Cutting edge: extracellular signal-regulated kinase activates syk: a new potential feedback regulation of Fc epsilon receptor signaling. *J Immunol* 1999; **163**: 1110-1114
33 **Wang L**, Duke L, Zhang PS, Arlinghaus RB, Symmans WF, Sahin A, Mendez R, Dai JL. Alternative splicing disrupts a nuclear localization signal in spleen tyrosine that is require for invasion suppression in breast cancer. *Cancer Res* 2003; **63:** 4724-4730

Edited by Wang XL and Xu CT **Proofread by** Pan BR and Xu FM

PO Box 2345, Beijing 100023, China
Fax: +86-10-85381893
E-mail: wjg@wjgnet.com www.wjgnet.com

World J Gastroenterol 2004;10(12):1819-1821
World Journal of Gastroenterology
Copyright ©2004 by The WJG Press ISSN 1007-9327

• BRIEF REPORTS •

Comparison of nuclear matrix proteins between gastric cancer and normal gastric tissue

Qin-Xian Zhang, Yi Ding, Zhuo Li, Xiao-Ping Le, Wei Zhang, Ling Sun, Hui-Rong Shi

Qin-Xian Zhang, Yi Ding, Xiao-Ping Le, Wei Zhang, Molecular Cell Biology Research Center, Medical College of Zhengzhou University, Zhengzhou 450052, Henan Province, China
Zhuo Li, Ling Sun, Hui-Rong Shi, Henan Key Laboratory of Molecular Medicine, Zhengzhou 450052, Henan Province, China
Supported by the National Natural Science Foundation of China, No. 39170440
Correspondence to: Professor. Qin-Xian Zhang, Molecular Cell Biology Research Center, Medical College of Zhengzhou University, 40 Daxue Lu, Zhengzhou 450052, Henan Province, China. qxz53@zzu.edu.cn
Telephone: +86-371-6977002
Received: 2003-08-05 **Accepted:** 2003-10-22

Abstract

AIM: To study the alteration of nuclear matrix proteins (NMPs) in gastric cancer.

METHODS: The NMPs extracted from 22 cases of gastric cancer and normal gastric tissues were investigated by SDS-PAGE technique and the data were analyzed using Genetools analysis software.

RESULTS: Compared with normal gastric tissue, the expression of 30 ku and 28 ku NMPs in gastric cancer decreased significantly (P=0.002, P=0.001, P<0.05). No significant difference was found in the expression of the two NMPs between the various differentiated grades (P=0.947, P=0.356) and clinical stages of gastric cancer (P=0.920, P=0.243, P>0.05).

CONCLUSION: The results suggested that the alteration of NMPs in gastric cancer occurred at the early stage of gastric cancer development.

Zhang QX, Ding Y, Li Z, Le XP, Zhang W, Sun L, Shi HR. Comparison of nuclear matrix proteins between gastric cancer and normal gastric tissue. *World J Gastroenterol* 2004; 10 (12): 1819-1821
http://www.wjgnet.com/1007-9327/10/1819.asp

INTRODUCTION

Nuclear matrix (NM) is the structural framework of the nucleus comprising the peripheral lamins and pore complexes, an internal ribonucleic protein outside nucleoli[1]. Nuclear matrix proteins (NMPs) are important for a variety of cell functions, including nuclear assembly, replication, transcription, and nuclear integrity[2]. Specific changes of NMPs are associated with many cancers[3-6]. However, the alteration of NMPs in gastric cancer has not been reported. In this paper, the NMPs in gastric cancer and normal gastric tissue were studied by SDS-PAGE and Genetools quantitative analysis software.

MATERIALS AND METHODS

Materials

Twenty-two cases of gastric cancer specimens (with no history of radio- or chemotherapy preoperatively) and normal gastric mucosa were collected from the First Affiliated Hospital of Medical College of Zhengzhou University and the People's Hospital of Henan Province. All the specimens were diagnosed pathologically (well and moderately differentiated cancers in 10 cases, poorly differentiated cancers in 12 cases). According to the PTNM of International Alliance of Anticancer in 1987, the specimens were divided into 4 clinical stages, Nine were at stage I and II, and 13 at stage III and IV.

Preparation of nuclei

The gastric cancers and normal gastric tissues were minced and mixed with STM (0.25 mol/L sucrose, 10 mmol/L Tris-HCl pH 7.4, 5 mmol/L $MgCl_2$) and homogenized with a homogenizer. Nuclei were initially separated by low speed centrifugation at 750 r/min for 10 min. The pellet was suspended with STM containing 5 g/L Triton X-100 for 10 min and centrifuged at 750 r/min for 10 min. The crude nuclei were resuspended with 2 mol/L sucrose and centrifuged at 12 000 *g* for 10 min. The pellet containing purified nuclei was washed with STM.

Extraction of NMPs

The purified nuclei were digested with DNase I (200 U/mL) at room temperature for 45 min prior to low salt (LS) buffer (10 mmol/L Tris-HCl pH 7.4, 0.2 mmol/L $MgCl_2$) extraction and centrifuged at 1 000 r/min for 15 min. The pellet was extracted twice with high salt (HS) buffer (10 mmol/L Tris-HCl pH 7.4, 2 mol/L NaCl, 0.2 mmol/L $MgCl_2$) and centrifuged at 6 000 r/min for 15 min. Washed with LS buffer, the pellet was resuspended with 2×loading buffer and detected for the concentration of proteins in the sample.

SDS-PAGE

A 100 μg proteins were loaded in each well of 100 g/L SDS-polyacrylamide gel. The proteins were electrophoresed at constant voltage of 200 V. The gel was stained with Coomassic brilliant blue R-250 over 4 h. The protein bands were photoed with gel photography system and quantitatively analyzed with Genetools software.

Statistic analysis

Data were analyzed using nonparametric statistics with SPSS 10.0 statistic software and P<0.05 was considered statistically significant.

RESULTS

On the gel stained with Coomassic brilliant blue R-250, many bands were exhibited in both gastric cancer and normal gastric tissue, which suggested that NMPs were abundant in these tissues. The bands of 30 ku and 28 ku NMPs in the gastric cancer were stained more lightly than those in the normal gastric tissue (Figure 1). Analyzed with Genetools quantitative software, the expression of 30 ku and 28 ku NMPs in normal gastric tissues was significantly higher than those in gastric cancer (P<0.05). The difference of the expression of 30 ku and 28 ku NMPs between well and moderately differentiated and

poorly differentiated gastric cancers was not significant (P>0.05). There was no significant difference in the expression of the two NMPs between stageI, II and stage III, IV (P>0.05) (Table 1).

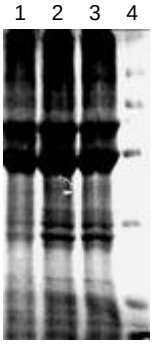

Figure 1 SDS-PAGE of nuclear matrix 1 gastric carcinoma tissue; 2 adjacent cancer tissue; 3 normal tissue; 4 marker.

Table 1 Comparison of the 30 ku, 28 ku bands between gastric cancer tissues and normal tissues

Group	30 ku			28 ku	
	n	*T*	*Z*	*T*	*Z*
Normal tissue group[a]	22	7.25	-3.165	4.33	-3.263
Gastric cancer group	22	12.44		14.19	
Well and moderately differentiated	10	11.60	-0.066	12.90	-0.923
Poorly differentiated	12	11.42		10.33	
Stage I, II	9	11.33	-0.100	13.44	-1.169
Stag III, IV	13	11.62		10.15	

T: mean of rank sum, *Z*: *z* value [a]P<0.05 *vs* gastric cancer.

DISCUSSION

NM is the structural framework of the nucleus[7], and is involved in a variety of cell functions, including DNA replication[8], RNA transcription[9], architecture of chromatin[10], carcinogenesis[11] and apoptosis[12]. The study on the relationship between NMPs and carcinogenesis has been carried out for a few years. In the experiment of Spencer *et al*.[13], specific changes in NMPs of breast cell line were identified by two-dimensional gel electrophoresis. NMP66 was evaluated as a potential biomarker for early breast cancer in large-scale clinical trials[11]. The extent of chromosomal rearrangements correlates positively with the level of expression of the nuclear matrix high mobility group (HMG) proteins HMG I (Y) when tested in three human prostate cancer cell lines (PC-3>DU145>LNCaP)[14]. Using both one-dimensional and high-resolution two-dimensional immunoblot analyses, Leman *et al*.[15] found that, in the transgenic adenocarcinoma of mouse prostate (TRAMP) model, HMG I (Y) was an NMP expressed as two protein bands with a molecular mass of 22-24 ku and HMG I (Y) expression was correlated with neoplastic and malignant properties in late stage of prostate tumor TRAMP model. In 26 pairs of human prostate cancer and normal tissue, Ishiguro *et al*.[16] identified a specific upregulated gene encoding a 55 ku nuclear matrix protein (nmt55) by RT-PCR and real time quantitative PCR. nmt55 gene expression in human prostate cancer tissue was higher (20/26) than that in normal prostate tissue.

NMP22 has been identified as a tumor marker for transitional cell carcinoma of urinary tract[17] and bladder cancer[18-21]. Eissa *et al*.[22] evaluated the diagnostic efficacy of NMP22, fibronectin and urinary bladder cancer antigen (UBC) in comparison with voided urine cytology on the detection of bladder cancer. They found that NMP22 and fibronectin had superior sensitivities compared to UBC and voided urine cytology, while NMP22 and voided urine cytology had the highest specificities. Xu[23] reported that the examination of NMP22 in urine was a rapid and effective way to detect the recurrence of bladder cancer. The urinary NMP22 levels were significantly higher in the renal cell carcinoma group than in the control group. The urinary NMP22 might be used in the evaluation of patients at risk of renal cell carcinoma[24]. Konety *et al*.[25] reported that the BLCA-4 was a very sensitive and specific marker for bladder cancer.

NMPs alterations were also associated with the cancer of digestive tract. Chen *et al*.[26] found that the interaction between HPV-16 E6 and nuclear matrix might contribute to virus induced carcinogenesis in esophageal carcinoma. Brunagel *et al*.[27] analyzed the NMPs expression by high-resolution two-dimensional gel electrophoresis, and found that the NMP composition was able to differentiate liver metastases from normal liver tissue and normal hepatocytes. In 2003, they identified an NMP, calreticulin, which was expressed much more strongly in colon cancer compared to adjacent and normal colon tissue[28]. In our study, we found that the expression of 30 ku, 28 ku NMPs was significantly reduced in gastric cancer when compared with that in the normal gastric tissue (P<0.05). There were no significant differences in the expression of these two proteins between the various differentiation grades and clinical stages of the gastric cancer. The results suggested that the changes of NMPs in gastric cancer might occur at early stage of the tumor development.

Matrix attachment regions (MARs) are postulated to anchor chromatin onto the NM, thereby organizing genomic DNA into topologically distinct loop domains that are important in replication and transcription[29]. The p300-SAF-A interactions at MAR elements of nontranscribed genes might poise these genes for transcription[30]. NM was a key locus for CK2 signaling in the nucleus[31]. Expression of p16 gene was significantly reduced in gastric cancer. The down- regulated expression of 30 ku, 28 ku NMPs in gastric cancer might be related to the down-regulated expression of p16 gene. In our previous study, we found the hypermethylation, mutation and microsatellite instability of p16 gene in gastric cancer. The binding of NMPs to the upstream of p16 gene and its relation to the down regulated expression of p16 gene in gastric cancer will be studied further.

REFERENCES

1 **Leman ES,** Getzenberg RH. Nuclear matrix proteins as biomarkers in prostate cancer. *J Cell Biochem* 2002; **86**: 213-223
2 **Holaska JM,** Wilson KL, Mansharamani M. The nuclear envelope, lamins and nuclear assembly. *Curr Opin Cell Biol* 2002; **14**: 357-364
3 **Pavao M,** Huang YH, Hafer LJ, Moreland RB, Traish AM. Immunodetection of nmt55/p54nrb isoforms in human breast cancer. *BMC Cancer* 2001; **1**: 15
4 **Ishii T,** Okadome A, Takeuchi F, Hiratsuka Y. Urinary levels of nuclear matrix protein 22 in patients with urinary diversion. *Urology* 2001; **58**: 940-942
5 **Brungel G,** Vietmeier BN, Bauer AJ, Schoen RE, Gerzenberg RH. Identification of nuclear matrix protein alterations associated with human colon cancer. *Cancer Res* 2002; **62**: 2437-2442
6 **Leman ES,** Arlotti JA, Dhir R, Greenberg N, Getzengerg RH. Characterization of the nuclear matrix proteins in a transgenic mouse model for prostate cancer. *J Cell Biochem* 2002; **86**: 203-212
7 **Philimonenko VV,** Flechon JE, Hozak P. The nucleoskeleton: a permanent structure of cell nuclei regardless of their transcriptional activity. *Exp Cell Res* 2001; **264**: 201-210
8 **Djeliova V,** Russev G, Anachkova B. Dynamics of association of origins of DNA replication with the nuclear matrix during the cell cycle. *Nucleic Acids Res* 2001; **29**: 3181-3187
9 **Blencowe BJ,** Bauren G, Eldridge AG, Issner R, Nickerson JA,

Rosenina E, Sharp PA. The SRm160/300 splicing coactivator subunits. *RNA* 2000; **6**: 111-120

10 **Cremer T,** Kreth G, Koester H, Fink RH, Heintzmann R, Cremer M, Solovei I, Zink D, Cremer C. Chromosome territories, interchromatin domain compartment, and nuclear matrix: an integrated view of the functional nuclear architecture. *Crit Rev Eukaryot Gene Expr* 2000; **10**: 179-212

11 **Luftner D,** Possinger K. Nuclear matrix proteins as biomarkers for breast cancer. *Expert Rev Mol Diagn* 2002; **2**: 23-31

12 **Wang ZH,** Yu D, Li HK, Chow VW, Ng CC, Chan HB, Cheng SB, Chew EC. Alteration of nuclear matrix protein composition of neuroblastoma cells after arsenic trioxide treatment. *Anticancer Res* 2001; **21**: 493-498

13 **Spencer VA,** Samuel SK, Davie JR. Altered profiles in nuclear matrix proteins associated with DNA *in situ* during progression of breast cancer cells. *Cancer Res* 2001; **61**: 1362-1366

14 **Takaha N,** Hawkins AL, Griffin CA, Issaacs WB, Coffey DS. High mobility group protein I (Y): a candidate architectural protein for chromosomal rearrangements in prostate cancer cells. *Cancer Res* 2002; **62**: 647-651

15 **Leman ES,** Madigan MC, Brunagel G, Takaha N, Coffey DS, Getzenberg RH. Nuclear matrix localization of high mobility group protein I (Y) in a transgenic mouse model for prostate cancer. *J Cell Biochem* 2003; **88**: 599-608

16 **Ishiguro H,** Uemura H, Fujinami K, Ikeda N, Ohta S, Kubota Y. 55 kDa nuclear matrix protein (nmt55) mRNA is expressed in human prostate cancer tissue and is associated with the androgen receptor. *Int J Cancer* 2003; **105**: 26-32

17 **Shao Y,** Zhuang J, Xu SX, Liu DY. Significance of urinary nuclear matrix protein 22 in diagnosis of transitional cell carcinoma of urinary tract. *Aizheng* 2002; **21**: 1005-1007

18 **Friedrich MC,** Hellstern A, Hautmann SH, Graefen M, Conrad S, Huland E, Huland H. Clinical use of urinary markers for the detection and prognosis of bladder carcinoma: a comparison of immunocytology with monoclonal antibodies against Lewis X and 486p3/12 with the BTA STAT and NMP22 tests. *J Urol* 2002; **168**: 470-474

19 **Parekattil SJ,** Fisher HA, Kogan BA. Neural network using combined urine nuclear matrix protein-22 monocyte chemoattractant protein-1 and urinary intercellular adhension molecule-1 to detect bladder cancer. *J Urol* 2003; **169**: 917-920

20 **Mahnert B,** Tauber S, Kriegmair M, Nagel D, Holdenrieder S, Hofmann K, Reiter W, Schmeller N, Stieber P. Measurements of complement factor H-related protein (BAT-TRAK) assay) and nuclear matrix protein (NMP22 assay)-useful diagnostic tools in the diagnosis of urinary bladder cancer? *Clin Chem Lab Med* 2003; **41**: 104-110

21 **Bhuiyan J,** Akhter J, O'Kane DJ. Performance characteristics of multiple urinary tumor markers and sample collection techniques in the detection of transitional cell carcinoma of the baldder. *Clin Chim Acta* 2003; **331**: 69-77

22 **Eissa S,** Swellam M, Sadek M, Mourad MS, Ahmady OE, Khalifa A. Comparative evaluation of the nuclear matrix protein, fibronectin, urinary bladder cancer antigen and voided urine cytology in the detection of bladder tumors. *J Urol* 2002; **168**: 465-469

23 **Xu K,** Tam PC, Hou S, Wang X, Bai W. The role of nuclear matrix protein 22 combined with bladder tumor antigen stat test in surveillance of recurring bladder cancer. *Chin Med J* 2002; **115**: 1736-1738

24 **Ozer G,** Altinel M, Kocak B, Yazicioglu A, Gonenc F. Value of urinary NMP-22 in patients with renal cell carcinoma. *Urology* 2002; **60**: 593-597

25 **Konety BR,** Nguyen TS, Dhir R, Day RS, Becich MJ, Stadler WM, Getzenberg RH. Detection of bladder cancer using a novel nuclear matrix protein, BLCA-4. *Clin Cancer Res* 2000; **6**: 2618-2625

26 **Chen HB,** Chen L, Zhang JK, Shen ZY, Su ZJ, Cheng SB, Chew EC. Human papillomavirus 16 E6 is associated the nuclear matrix of esophageal carcinoma cells. *World J Gastroenterol* 2001; **7**: 788-791

27 **Brunagel G,** Schoen RE, Bauer AJ, Vietmeier BN, Getzenberg RH. Nuclear matrix protein alterations associated with colon cancer metastasis to the liver. *Clin Cancer Res* 2002; **8**: 3039-3045

28 **Brunagel G,** Shah U, Schoen RE, Getzenberg RH. Identification of calreticulin as a nuclear matrix protein associated with human colon cancer. *J Cell Biochem* 2003; **89**: 238-243

29 **Galande S.** Chromatin (dis) organization and cancer: BUR-binding proteins as biomarkers for cancer. *Curr Cancer Drug Targets* 2002; **2**: 157-190

30 **Martens JH,** Verlann M, Kalkhoven E, Dorsman JC, Zantema A. Scaffold/matrix attachment region elements interact with a p300-scaffold attachment factor A complex and are bound by acetylated nucleosomes. *Mol Cell Biol* 2002; **22**: 2598-2606

31 **Wang H,** Yu S, Davis AT, Ahmed K. Cell cycle dependent regulation of protein kinase CK2 signaling to the nuclear matrix. *J Cell Biochem* 2003; **88**: 812-822

Edited by Zhu LH and Xu FM

PO Box 2345, Beijing 100023, China
Fax: +86-10-85381893
E-mail: wjg@wjgnet.com www.wjgnet.com

World J Gastroenterol 2004;10(12):1822-1825
World Journal of Gastroenterology
Copyright ©2004 by The WJG Press ISSN 1007-9327

• BRIEF REPORTS •

Apoptosis of human primary gastric carcinoma cells induced by genistein

Hai-Bo Zhou, Juan-Juan Chen, Wen-Xia Wang, Jian-Ting Cai, Qin Du

Hai-Bo Zhou, Juan-Juan Chen, Wen-Xia Wang, Jian-Ting Cai, Qin Du, Department of Gastroenterology, Second Affiliated Hospital of Zhejiang University, Hangzhou 310009, Zhejiang Province, China
Correspondence to: Dr. Hai-Bo Zhou, Department of Gastroenterology, Second Affiliated Hospital of Zhejiang University, Hangzhou 310009, Zhejiang Province, China. zhouhaibohz@163.com
Telephone: +86-571-87783564
Received: 2003-10-27 **Accepted:** 2004-01-15

Abstract

AIM: To investigate the apoptosis in primary gastric cancer cells induced by genistein, and the relationship between this apoptosis and expression of bcl-2 and bax.

METHODS: MTT assay was used to determine the cell growth inhibitory rate *in vitro*. Transmission electron microscope and TUNEL staining were used to quantitatively and qualitatively detect the apoptosis of primary gastric cancer cells before and after genistein treatment. Immunohistochemical staining and RT-PCR were used to detect the expression of apoptosis-associated genes *bcl-2* and *bax*.

RESULTS: Genistein inhibited the growth of primary gastric cancer cells in dose-and time-dependent manner. Genistein induced primary gastric cancer cells to undergo apoptosis with typically apoptotic characteristics. TUNEL assay showed that after the treatment of primary gastric cancer cells with genistein for 24 to 96 h, the apoptotic rates of primary gastric cancer cells increased time-dependently. Immunohistochemical staining showed that after the treatment of primary gastric cancer cells with genistein for 24 to 96 h, the positivity rates of Bcl-2 proteins were apparently reduced with time and the positivity rates of Bax proteins were apparently increased with time. After exposed to genistein at 20 μmol/L for 24, 48, 72 and 96 respectively, the density of bcl-2 mRNA decreased progressively and the density of bax mRNA increased progressively with elongation of time.

CONCLUSION: Genistein is able to induce the apoptosis in primary gastric cancer cells. This apoptosis may be mediated by down-regulating the apoptosis- associated bcl-2 gene and up-regulating the expression of apoptosis-associated bax gene.

Zhou HB, Chen JJ, Wang WX, Cai JT, Du Q. Apoptosis of human primary gastric carcinoma cells induced by genistein. *World J Gastroenterol* 2004; 10(12): 1822-1825
http://www.wjgnet.com/1007-9327/10/1822.asp

INTRODUCTION

Genistein is a planar molecule with an aromatic A-ring, has a second oxygen atom 11.5 Å from the one in the A ring, a molecular weight similar to those of the steroidal estrogens. It has estrogenic properties in receptor binding assays[1,2], cell culture[3,4], and uterine weight assays[5-7]. Genistein inhibits topoisomerase II[8], platelet-activating factor- and epidermal growth factor-induced expression of c-fos[9], diacylglycerol synthesis[10], and tyrosine kinases[11]. It also inhibits microsomal lipid peroxidation[12] and angiogenesis[13]. Genistein exhibits antioxidant properties[14-16] and was reported to induce differentiation of numerous cell types[17-19]. Moreover, a recent report shows that genistein is a potent cancer chemopreventive agent[20-22]. The anti-tumor activity of genistein might be related to induce the apoptosis of tumor cells but the precise mechanism of antitumor activity is not well understood.

The Bcl-2 family plays a crucial role in the control of apoptosis. The family includes a number of proteins which have homologous amino acid sequences, including anti-apoptotic members such as Bcl-2 and Bcl-x_L, as well as pro-apoptotic members like Bax and Bad[23-26]. Overexpression of Bax has the effect of promoting cell death[27-31]. Conversely, Overexpression of antiapoptotic proteins such as Bcl-2 will repress the function of Bax[32-36]. Thus, the ratio of Bcl-2/Bax appears to be a critical determinant of cell apoptosis[37].

In this study, MTT assay was used to determine the cell growth inhibitory rate. Transmission electron microscope and TUNEL staining method were used to quantitatively and qualitatively detect the apoptosis status of primary gastric cancer cells before and after the genistein treatment. Immunohistochemical staining and RT-PCR were used to detect the expression of apoptosis-associated genes *bcl-2* and *bax*.

MATERIALS AND METHODS

Materials

Genistein and MTT were obtained from Sigma Chemical Co, Ltd. *In situ* cell detection kit, anti-Bcl-2 monoclonal antibody and anti-Bax monoclonal antibody were purchased from Beijing Zhongshan Biotechnology Co, Ltd. Stock solution of genistein was made in dimethylsulfoxide (DMSO) at a concentration of 40 μmol/L. Working dilutions were directly made in the cell culture medium.

Methods

Cell culture Fresh sample from a patient with gastric cancer was obtained in operating room. A single-cell suspension of tumor cells with the concentration of 5×10^5/mL was prepared for seeding. Primary gastric cancer cells were purified after culture.

MTT assay Cells 1×10^5/well in a 96-well plate after incubation for 24 h were treated with different concentrations of genistein (5, 10, 20, 40 μmol/L) for 24, 48 and 72 h respectively. A 10 μL of 5 g/L of MTT was added to the medium triplicate at each dose and incubated for 4 h at 37 ℃. Culture media were discarded followed by addition of 0.2 mL DMSO and vibration for 10 min. The absorbance (*A*) was measured at 570 nm using a microplate reader. The cell growth inhibitory rate was calculated as follows: {(*A* of control group -*A* of experimental group)/(*A* of control group- *A* of blank group)} ×100%.

Transmission electron microscopy Cells treated with 20 μmol/L genistein were harvested after incubation for 24 h. Subsequently

the cells were fixed in 40 g/L glutaral and immersed with Epon 821, imbedded for 72 h at 60 ℃. After that the cells were prepared into ultrathin section (60 nm) and stained with uranyl acetate and lead citrate. Cell morphology was observed by transmission electron microscopy.

TUNEL assay Apoptosis of primary gastric cancer cells was evaluated by using an *in situ* cell detection kit. The cells were treated in the presence or absence of 20 μmol/L genistein for 24 to 96 h and fixed in ice-cold 800 mL/L ethanol for up to 24 h, treated with proteinase K and then 3 mL/L H_2O_2, and labeled with fluorescein dUTP in a humid box for 1 h at 37 ℃. Cells were then combined with POD-horseradish peroxidase, colored with DAB and counterstained with methyl green. Controls received the same treatment except the labeling of omission of fluorescein dUTP. Cells were visualized under light microscope. The apoptotic index (AI) was calculated as follows: AI=(Number of apoptotic cells/Total number)×100%.

Immunohistochemical staining Immunohistochemical staining was done by an avidinbiotin technique. Primary gastric cancer cells treated in the presence or absence of 20 μmol/L genistein for 24 to 96 h were grown on six-well glass plates and were fixed by acetone. After washed in PBS, the cells were incubated in 3 mL/L H_2O_2 solution at room temperature for 5 min. The cells were then incubated with anti-Bcl-2 or anti-Bax monoclonal antibody at a 1:300 dilution at 4 ℃ overnight. After wash of cells in PBS, the second antibody, biotinylated antirat IgG was added and the cells were incubated at room temperature for 1 h. After wash of cells in PBS, ABC compound was added and the cells were then incubated at room temperature for 10 min. DAB was used as the chromagen. After 10 min, the brown color signifying the presence of antigen bound to antibodies was detected by light microscopy and photographed at ×200. Controls were treated the same as the experimental group except the incubation of the primary antibody instead of second antibody. The positive rate (PR) was calculated as follows: PR=(Number of positive cells/Total number)×100%.

RT-PCR The primary gastric cancer cells were treated in the presence or absence of 20 μmol/L genistein for 24 to 96 h and total RNA was extracted. The concentration of RNA was determined by absorption at 260 nm. The primers for Bcl-2, Bax and β-actin were as follows: β-actin (500 bp): 5' GTGGG GCGCCCCAGGCACCA 3' , 5' CTCCTTAATGTCACG CACGATTTC 3' ; bcl-2 (716 bp): 5' GGAAATATGGCGC ACGCT 3' , 5' TCACTTGTGGCCCAGAT 3' ; bax (508 bp): 5' CCAGCTCTGAGCAGATCAT 3' , 5' TATCAGCCCA TCTTCTTCC 3' . Polymerase chain reactions were performed in a 25 μL reaction volume. PCR for Bcl-2 and β-actin was run in the following procedures: at 94 ℃ for 7 min, 1 circle; at 94 ℃ for 1 min, at 72 ℃ for 1 min, 30 cycles; at 72 ℃ for 7 min, 1 circle. PCR for Bax was run in the following procedure: 94 ℃ for 1 min, 60 ℃ for 45 s, 72 ℃ for 45 s, 35 cycles. Ten μL PCR product was placed onto 15 g/L agarose gel and observed by EB staining using Gel-Pro analyzer.

Statistical analysis

Data were analyzed by the paired two-tailed Student' s *t* test, and significance was considered when $P<0.05$.

RESULTS

MTT assay

Primary gastric cancer cells were exposed to increasing concentrations (5 μmol/L to 40 μmol/L) of genistein for 24 to 72 h, respectively. Primary gastric cancer cells showed death in a dose- and time-dependent manner. The data are summarized in Table 1.

Table 1 *A* value of primary gastric cancer cells treated with different concentrations of genistein

	24 h	48 h	72 h
Control	0.400±0.008	0.406±0.007	0.404±0.008
5 μmol/L genistein	0.361±0.002[a]	0.334±0.012[b]	0.305±0.004[b]
10 μmol/L genistein	0.325±0.004[d]	0.313±0.003[b]	0.248±0.004[d]
20 μmol/L genistein	0.308±0.003[d]	0.249±0.002[d]	0.206±0.003[d]
40 μmol/L genistein	0.265±0.004[d]	0.215±0.004[d]	0.159±0.002[d]

[a]$P<0.05$; [b]$P<0.01$; [d]$P<0.001$ *vs* control group.

Morphological changes

After treatment of primary gastric cancer cells with genistein (20 μmol/L) for 24 h, some cells presented apoptotic characteristics including chromatin condensation, appearance of chromatin crescent, nuclear fragmentation that could be seen by transmission electron microscope (Figure 1).

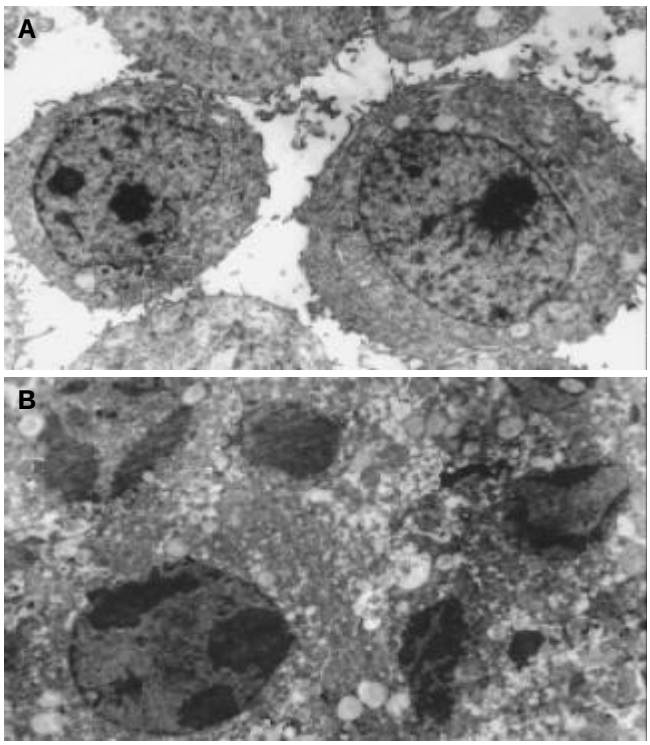

Figure 1 Ultra-microscopic structure of gastric cancer cells induced by genistein. A: Primary gastric cancer cells; B: apoptotic gastric cancer cells (Original magnification: ×4 800).

TUNEL assay

Apoptotic cells were determined by TUNEL assay according to the manufacture' s instructions. Positive staining located in the nucleus. After treatment with genistein (20 μmol/L) for 24 to 96 h, Apoptotic index of the cells was apparently increased with the increase of treatment time ($P<0.05$) (Table 2).

Expression of Bcl-2 proteins

Positive staining located in the cytoplasm. After treatment with genistein (20 μmol/L) for 24 to 96 h, Positivity rate of the cells of Bcl-2 proteins was apparently reduced with the increase of treatment periods ($P<0.05$) (Table 3). This suggested that genistein could down-regulate the expression of Bcl-2.

Expression of Bax proteins

Positive staining located in the cytoplasm. After treatment with genistein (20 μmol/L) for 24 to 96 h, PRs of Bax proteins were apparently increased with increase of treated time ($P<0.05$)

(Table 4). This suggested that genistein could up-regulate the expression of Bax.

Table 2 Apoptotic index (AI) of primary gastric cancer cells treated by genistein

	Control	24 h	48 h	72 h	96 h
AI (%)	1.25±0.30	4.97±0.80	18.44±1.92	35.18±0.35	43.93±1.11
t		-6.13	-13.82	-180.16	-52.80
P		*P*<0.05	*P*<0.05	*P*<0.05	*P*<0.05

P<0.05 *vs* control group; AI: Apoptotic index.

Table 3 Positivity rate (PR) of Bcl-2 in primary gastric cancer cells treated by genistein

	Control	24 h	48 h	72 h	96 h
PR(%)	36.34±0.72	21.62±0.08	10.60±049	7.21±0.45	4.54±0.36
t		31.93	44.67	73.80	59.32
P		*P*<0.01	*P*<0.01	*P*<0.01	*P*<0.01

P<0.01 *vs* control group; PR: Positivity rate.

Table 4 Positivity rate (PR) of Bax in primary gastric cancer cells treated by genistein

	Control	24 h	48 h	72 h	96 h
PR(%)	10.73±0.57	20.63±0.86	34.3±0.81	45.96±0.42	58.61±1.46
t		-57.49	-41.23	-69.53	-51.31
P		*P*<0.001	*P*<0.001	*P*<0.001	*P*<0.001

P<0.01 *vs* control group; PR: Positivity rate.

RT-PCR

After exposed to 20 μmol/L genistein for 24, 48, 72 and 96 h respectively, the density of bcl-2 mRNA decreased progressively and the density of bax mRNA increased progressively with elongation of time by RT-PCR. It suggested that genistein could down-regulate the expression of Bcl-2 and up-regulate the expression of Bax.

DISCUSSION

Populations who consume a diet high in soy are reported to have a lower incidence of breast and prostate cancer. The activity of the soy-derived phytoestrogen, genistein, is thought to account for a portion of the chemopreventative properties of soy; these include an inhibitory effect on tyrosine kinases[11], DNA topoisomerases I and II[8], and ribosomal S6 kinase, antiestrogenicity, antioxidant activity, anti-angiogenesis activity[12], suppression of cell proliferation, induction of differentiation[17-19], and modulation of apoptosis[20-22].

In this study, we found that primary gastric cancer cells showed death in a dose- and time-dependent manner in MTT assay. This suggested genistein was able to restrain the growth of primary gastric cancer cells. It was found that genistein was able to induce the apoptosis of primary gastric cancer cells by transmission electron microscope assay and TUNEL assay. After treatment with 20 μmol/L genistein for 24 to 96 h, PRs of Bcl-2 proteins were apparently reduced and PRs of Bax proteins were apparently increased with increase of treated time by Immunohistochemical staining. After exposed to 20 μmol/L genistein for 24, 48, 72 and 96 h respectively, the density of bcl-2 mRNA decreased progressively and the density of bax mRNA increased progressively with elongation of time by RT-PCR.

Genistein could reduce Bcl-2 expression and enhance bax expression. The ratio of Bcl-2/Bax was decreased when primary gastric cancer cells were treated with genistein, which could trigger the apoptosis of primary gastric cancer cells.

The present study demonstrated that genistein was able to induce the apoptosis in primary gastric cancer. This apoptosis may be mediated by down-regulating the expression of apoptosis-associated gene *bcl-2* and up-regulating the expression of apoptosis-associated gene *bax*. Genistein may be used as a potential chemotherapeutic drug in the anti-gastric carcinoma chemotherapy.

REFERENCES

1 **Shutt DA**, Cox RI. Steroid and phyto-oestrogen binding to sheep uterine receptors *in vitro*. *J Endocrinol* 1972; **52**: 299-310
2 **Mathieson RA**, Kitts WD. Binding of phytooestrogen and estradiol-17beta by cytoplasmic receptors in the pituitary gland and hypothalamus of the ewe. *J Endocrinol* 1980; **85**: 317-325
3 **Martin PM**, Horowitz KB, Ryan DS, McGuire WL. Phytoestrogen interaction with estrogen receptors in human breast cancer cells. *Endocrinology* 1978; **103**: 1860-1867
4 **Makela S**, Davis VL, Tally WC, Korkman J, Salo L, Vihko R, Santti R, Korach KS. Dietary estrogens act through estrogen receptor-mediated processes and show no antiestrogenicity in cultured breast cancer cells. *Environ Health Perspect* 1994; **102**: 572-578
5 **Thigpen JE,** Haseman JK, Saunders H, Locklear J, Caviness G, Grant M, Forsythe D. Dietary factors affecting uterine weights of immatur CD-1 mice used in uterotrophic bioassays. *Cancer Detect Prev* 2002; **26**: 381-393
6 **Folman Y,** Pope GS. The interaction in the immature mouse of potent oestrogens with coumestrol, genistein and other uterovaginotrophic compounds of low potency. *J Endocrinol* 1966; **34**: 215-225
7 **Polkowski K,** Mazurek AP. Biological properties of genistein. A review of *in vitro* and *in vivo* data. *Acta Pol Pharm* 2000; **57**: 135-155
8 **Okura A**, Arakawa H, Oka H, Yoshinari T, Monden Y. Effect of genistein on topoisomerase activity and on the growth of [Val12] Ha-ras-transformed NIH 3T3 cells. *Biochem Biophys Res Commun* 1988; **157**: 183-189
9 **Tripathi YB**, Lim RW, Fernandez-Gallardo S, Kandala JC, Guntaka RV, Shukla SD. Involvement of tyrosine kinase and protein kinase C in platelet-activating-factor-induced c-fos gene expression in A-421 cells. *Biochem J* 1992; **286**(Pt 2): 527-533
10 **Akiyama T**, Ishida J, Nakagawa S, Ogawara H, Watanabe S, Itho N, Shibuya M , Fukami Y. Genistein, a specific inhibitor of tyrosine-specific protein kinases. *J Biol Chem* 1987; **262**: 5592-5595
11 **Dean NM**, Kanemitsu M, Boynton AL. Effects of the tyrosine-kinase inhibitor genistein on DNA synthesis and phospholipid-derived second messenger generation in mouse 10T1/2 fibroblasts and rat liver T51B cells. *Biochem Biophys Res Commun* 1989; **165**: 705-801
12 **Jha HC**, von Recklinghausen G, Zilliken F. Inhibition of *in vitro* microsomal lipid peroxidation by isoflavonoids. *Biochem Pharmacol* 1985; **34**: 1367-1369
13 **Fotsis T**, Pepper M, Adlercreutz H, Fleischman G, Hase T, Montesano R, Schweigerer L. Genistein, a dietary-derived inhibitor of *in vitro* angiogenesis. *Proc Natl Acad Sci U S A* 1993; **90**: 2690-2694
14 **Mitchell JH,** Gardner PT, McPhail DB, Morrice PC, Collins AR, Duthie GG. Antioxidant efficacy of phytoestrogens in chemical and biological model systems. *Arch Biochem Biophys* 1998; **360**: 142-148
15 **Tikkanen MJ,** Adlercreutz H. Dietary soy-derived isoflavone phytoestrogens. Could they have a role in coronary heart disease prevention? *Biochem Pharmacol* 2000; **60**: 1-5
16 **Wei H**, Bowen R, Cai Q, Barnes S, Wang Y. Antioxidant and antipromotional effects of the soybean isoflavone genistein. *Proc Soc Exp Biol Med* 1995; **208**: 124-130
17 **Watanabe T**, Kondo K, Oishi M. Induction of *in vitro* differentiation of mouse erythroleukemia cells by genistein, an inhibitor of tyrosine protein kinases. *Cancer Res* 1991; **51**: 764-768
18 **Miller DR**, Lee GM, Maness PF. Increased neurite outgrowth induced by inhibition of protein tyrosine kinase activity in PC12

pheochromocytoma cells. *J Neurochem* 1993; **60**: 2134-2144

19 **Simon HU,** Yousefi S, Blaser K. Tyrosine phosphorylation regulates activation and inhibition of apoptosis in human eosinophils and neutrophils. *Int Arch Allergy Immunol* 1995; **107**: 338-339

20 **Huang P,** Robertson LE, Wright S, Plunkett W. High molecular weight DNA fragmentation: a critical event in nucleoside analogue-induced apoptosis in leukemia cells. *Clin Cancer Res* 1995; **1**: 1005-1013

21 **Xu LH**, Owens LV, Sturge GC, Yang X, Liu ET, Craven RJ, Cance WG. Attenuation of the expression of the focal adhesion kinase induces apoptosis in tumor cells. *Cell Growth Differ* 1996; **7:** 413-418

22 **Davis JN**, Singh B, Bhuiyan M, Sarkar FH. Genistein-induced upregulation of $p21^{WAFI}$, downregulation of cyclin B, and induction of apoptosis in prostate cancer cells. *Nutr Cancer* 1998; **32**: 123-131

23 **Konopleva M,** Konoplev S, Hu W, Zaritskey AY, Afanasiev BV, Andreeff M. Stromal cells prevent apoptosis of AML cells by up-regulation of anti-apoptotic proteins. *Leukemia* 2002; **16**: 1713-1724

24 **van der Woude CJ**, Jansen PL, Tiebosch AT, Beuving A, Homan M, Kleibeuker JH, Moshage H. Expression of apoptosis-related proteins in Barrett's metaplasia-dysplasia-carcinoma sequence: a switch to a more resistant phenotype. *Hum Pathol* 2002; **33**: 686-692

25 **Panaretakis T,** Pokrovskaja K, Shoshan MC, Grander D. Activation of Bak, Bax and BH3-only proteins in the apoptotic response to doxorubicin. *J Biol Chem* 2002; **277**: 44317-44326

26 **Bellosillo B,** Villamor N, Lopez-Guillermo A, Marce S, Bosch F, Campo E, Montserrat E, Colomer D. Spontaneous and drug-induced apoptosis is mediated by conformational changes of Bax and Bak in B-cell chronic lymphocytic leukemia. *Blood* 2002; **100**: 1810-1816

27 **Matter-Reissmann UB,** Forte P, Schneider MK, Filgueira L, Groscurth P, Seebach JD. Xenogeneic human NK cytotoxicity against porcine endothelial cells is perforin / granzyme B dependent and not inhibited by Bcl-2 overexpression. *Xenotransplantation* 2002; **9**: 325-337

28 **Lanzi C,** Cassinelli G, Cuccuru G, Supino R, Zuco V, Ferlini C, Scambia G, Zunino F. Cell cycle checkpoint efficiency and cellular response to paclitaxel in prostate cancer cells. *Prostate* 2001; **48:** 254-264

29 **Mertens HJ,** Heineman MJ, Evers JL. The expression of apoptosis-related proteins Bcl-2 and Ki67 in endometrium of ovulatory menstrual cycles. *Gynecol Obstet Invest* 2002; **53**: 224-230

30 **Mehta U,** Kang BP, Bansal G, Bansal MP. Studies of apoptosis and bcl-2 in experimental atherosclerosis in rabbit and influence of selenium supplementation. *Gen Physiol Biophys* 2002; **21**: 15-29

31 **Chang WK,** Yang KD, Chuang H, Jan JT, Shaio MF. Glutamine protects activated human T cells from apoptosis by up-regulating glutathione and bcl-2 levels. *Clin Immunol* 2002; **104**: 151-160

32 **Chen GG,** Lai PB, Hu X, Lam IK, Chak EC, Chun YS, Lau WY. Negative correlation between the ratio of Bax to Bcl-2 and the size of tumor treated by culture supernatants from Kupffer cells. *Clin Exp Metastasis* 2002; **19**: 457-464

33 **Usuda J,** Chiu SM, Azizuddin K, Xue LY, Lam M, Nieminen AL, Oleinick NL. Promotion of photodynamic therapy-induced apoptosis by the mitochondrial protein Smac / DIABLO: dependence on Bax. *Photochem Photobiol* 2002; **76:** 217-223

34 **Sun F,** Akazawa S, Sugahara K, Kamihira S, Kawasaki E, Eguchi K, Koji T. Apoptosis in normal rat embryo tissues during early organogenesis: the possible involvement of Bax and Bcl-2. *Arch Histol Cytol* 2002; **65**: 145-157

35 **Jang MH,** Shin MC, Shin HS, Kim KH, Park HJ, Kim EH, Kim CJ. Alcohol induces apoptosis in TM3 mouse Leydig cells via bax-dependent caspase-3 activation. *Eur J Pharmacol* 2002; **449:** 39-45

36 **Tilli CM,** Stavast-Koey AJ, Ramaekers FC, Neumann HA. Bax expression and growth behavior of basal cell carcinomas. *J Cutan Pathol* 2002; **29:** 79-87

37 **Pettersson F,** Dalgleish AG, Bissonnette RP, Colston KW. Retinoids cause apoptosis in pancreatic cancer cells via activation of RAR-gamma and altered expression of Bcl-2 / Bax. *Br J Cancer* 2002; **87**: 555-561

Edited by Zhu LH and Chen WW **Proofread by** Xu FM

PO Box 2345, Beijing 100023, China
Fax: +86-10-85381893
E-mail: wjg@wjgnet.com www.wjgnet.com

World J Gastroenterol 2004;10(12):1826-1829
World Journal of Gastroenterology
Copyright ©2004 by The WJG Press ISSN 1007-9327

• BRIEF REPORTS •

Polymorphisms of interleukin-1B and interleukin-1 receptor antagonist genes in patients with chronic hepatitis B

Ping-An Zhang, Yan Li, Pu Xu, Jian-Min Wu

Ping-An Zhang, Yan Li, Pu Xu, Department of Laboratory Science, Renmin Hospital of Wuhan University, Wuhan 430060, Hubei Province, China
Jian-Min Wu, Department of Laboratory Science, Affiliated Union Hospital of Tongji Medical College, Huazhong University of Science and Technology, Wuhan 430030, Hubei Province, China
Correspondence to: Ping-An Zhang, Department of Laboratory Science, Renmin Hospital of Wuhan University, Wuhan 430060, Hubei Province, China. cydyyjyk@public.wh.hb.com
Telephone: +86-27-88041911-8258
Received: 2003-10-10 **Accepted:** 2003-12-16

Abstract

AIM: To investigate the relationships between polymorphisms of interleukin-1B (IL-1B) promoter region -511C/T and interleukin-1 receptor antagonist gene (IL-1RN) and susceptibility to chronic hepatitis B in Chinese population.

METHODS: Genomic DNA was extracted from the peripheral blood of 190 patients with chronic hepatitis B and 249 normal controls and then subjected to polymerase chain reaction (PCR) amplification. The PCR products were digested by restriction endonuclease *AvaI*. The products of digestion were subjected to 20 g/L gel electrophoresis and ethidium bromide staining.

RESULTS: The frequencies of IL-1B (-511) genotypes CC, CT and TT in patients with chronic hepatitis B were 23.7%, 49.5% and 26.8%, while 26.1%, 47.4% and 26.5% respectively in controls. The results showed that there was no significant difference in the frequencies of alleles or genotypes in IL-1B between patients with chronic hepatitis B and controls. The distributions of IL-1B (-511) genotype CC were significantly different between the two subgroups (HBV-DNA $\leqslant 1\times10^3$ copies/mL as subgroup I, HBV-DNA $>1\times10^3$ copies/mL as subgroup II) of chronic hepatitis B (P=0.029). Only four of the five kinds of polymorphism (1/1, 1/2, 2/2 and 1/4) were found in this study. The frequencies of IL-1RN genotypes 1/1, 1/2, 2/2 and 1/4 were 88.9%, 9.0%, 0.5% and 1.6% in patients with chronic hepatitis B respectively, while were 81.1%, 16.9%, 0.4% and 1.6% respectively in controls. The frequencies of genotype1/2 and IL-1RN allele 2 in patients with chronic hepatitis B were lower than those in controls (P=0.016 and P=0.029, respectively).

CONCLUSION: There is an association between polymorphisms of the promoter region -511C/T of IL-1B and IL-1RN intron 2 and chronic hepatitis B virus infection. Subjects with IL-1RN allele 2 may be resistant to HBV infection, and IL-1B(-511) genotype CC is closely related with HBV-DNA replication, which gives some new clues to the study of pathogenesis of chronic hepatitis B.

Zhang PA, Li Y, Xu P, Wu JM. Polymorphisms of interleukin-1B and interleukin-1 receptor antagonist genes in patients with chronic hepatitis B. *World J Gastroenterol* 2004; 10(12): 1826-1829
http://www.wjgnet.com/1007-9327/10/1826.asp

INTRODUCTION

Hepatitis B virus (HBV) infection is one of the most important chronic viral diseases in the world. An estimated 400 million people worldwide are carriers of HBV, and approximately 250 000 deaths occur each year as a consequence of fulminant hepatic failure, cirrhosis, and hepatocellular carcinoma[1]. When HBV is acquired in adulthood, the majority of infections are cleared, with chronic infection occurring in 5% to 10% of cases. However, the dynamic interaction of the host inflammatory response with HBV, and the subsequent impact of this interaction on the clinical outcome of HBV infection, are not yet fully understood, nor are the underlying mechanisms for persistence of the virus.

Cytokines play an important role in defense against viral infection, indirectly through determination of the predominant pattern of the host response, and directly through inhibition of viral replication[2]. Interleukin(IL)-1 is one of the most proinflammatory agents, and has a central role in inflammation and destruction[3]. The most important members of the IL-1 family are the IL-1α, IL-1β and IL-1 receptor antagonists (ra). IL-1ra is an IL-1 natural competitive inhibitor, acting by occupancy of cell surface receptor without triggering signal transduction[4]. IL-1ra plays a role as an important regulator of inflammation and is currently evaluated in clinical trials. Genes encoding IL-1 are located on the 430 kb region of chromosome 2q13-21, consisting of three homologous genes: IL-1A, IL-1B and IL-1ra (IL-1RN)[5]. Biallelic polymorphisms at positions IL-1A -889, IL-1B -511, and +3 953 have been described, all representing a C/T single nucleotide polymorphism (SNP). IL-1RN contains an 86 bp variable number tandem repeat (VNTR) polymorphism in intron 2[6]. These polymorphisms are located within the regulatory regions of the genes and have potential functional importance by modulating IL-1 protein production, and are related with the development of some diseases[7].

This research was to discuss the relationship between polymorphisms of IL-1 gene and susceptibility to HBV in the Chinese population, and tried to reveal the correlation between the genotype and phenotype distributions, in order to provide a certain scientific basis for prevention and treatment of chronic hepatitis B.

MATERIALS AND METHODS

Subjects

A total of 190 patients with chronic hepatitis B (130 males, 60 females) aged 11-68 years were recruited in Remin Hospital of Wuhan University. The diagnosis of all the patients was confirmed according to the criteria for chronic hepatitis B, and the patients did not have other viral hepatitis. Two hundred and forty-nine control subjects (150 males, 99 females) aged 18-82 years were selected in Wuhan area (HBsAg negative, anti-HBe negative, and anti-HBc negative), and liver, renal, endocrine and cardiovascular disorders were excluded.

PCR preparation

Two microliter peripheral venous blood was collected in an EDTA tube. Genomic DNA was extracted from peripheral

blood leukocytes and frozen at -20 ℃. Each PCR was carried out in 25 μL reaction mixture containing 100-200 ng genomic DNA, 100 μmol/L dNTP, 25 mmol/L $MgCl_2$, 20 pmol/L primers and 1U TaqDNA polymerase (Promega).

IL-1B and IL-1RN polymorphisms

SNP at position -511 in the promoter region (-702-398)of IL-1B was analyzed by the PCR-restriction fragment length polymorphism(RFLP)method[8]. A 304 bp PCR fragment of the IL-1B promoter region was amplified using the following primers: 5'-TGGCATTGATCTGGTTCATC-3' and 5'-GTTTAGGATCTTCCCACTT-3'. PCR conditions were as follows: denaturation at 95 ℃ for 5 min, then 35 cycles at 94 ℃ for 30 s, at 55 ℃ for 30 s, at 72 ℃ for 1 min, and finial extention at 72 ℃ for 5 min. twenty μL of PCR products was digested with 5 U of *AvaI* (TaKaRa, shiga, Japan) at 37 ℃ for 3 h and run on a 20 g/L agarose gel stained with ethidium bromide.

IL-1RN intron 2 contained a VNTR of an 86 bp length of DNA. Oligonucleotides 5'-CTCAGCAACACTCCTAT-3' and 5'-TCCTGGTCTGCAGGTAA-3' flanking this region were used as primers[8]. Amplification conditions were same as the above. The PCR products were analyzed by electrophoresis on a 20 g/L agarose gel stained with ethidium bromide.

HBV-DNA measurement

Serum HBV-DNA level in patients with chronic hepatitis B was detected with the real-time fluorescent quantitative PCR method (reagents supplied by Shanghai Fosun Co. Ltd.) using a Lightcycler PCR system. Results were considered abnormal when HBV-DNA $>1\times10^3$copies/mL.

Statistical analysis

IL-1B(-511) and IL-1RN(intron 2) allelic and genotype frequencies were calculated in patients with chronic hepatitis B and control subjects. Comparison of allelic and genotypes between groups, and association of IL-1B and IL-1RN polymorphisms with HBV-DNA replication were examined for statistical significance with chi-square test. Analysis was completed with SPSS 9.0, and $P<0.05$ was considered statistically significant.

RESULTS

Genotypes of IL-1B and IL-1RN

C/T transition polymorphism of IL-1B(-511) was analyzed by PCR-RFLP. *AvaI* digestion of the PCR products of IL-1B resulted in three genotypes, consisting of TT (intact, 304 bp), CT (three fragments of 304, 190 and 114 bp) and CC (two fragments of 190 and 114 bp), (Figure 1). The intron 2 of IL-1RN polymorphism contained VNTR of 86 bp. There were five alleles in humans, including allele 1 (four repeats, 410 bp), allele 2 (two repeats, 240 bp), allele 3 (five repeats, 500 bp), allele 4 (three repeats, 325 bp) and allele 5 (six repeats, 595 bp). Only four of the five kinds of polymorphism of IL-1RN(1/1, 1/2, 2/2, and 1/4) were found in this study (Figure 2).

Frequencies of IL-1B and IL-1RN genotypes in both groups

The genotype and allele frequencies of IL-1B and IL-1RN in patients with chronic hepatitis B and control subjects were determined, and explored with 2×2 χ^2 test under the Hardy-Weinberg law and shown to represent all population (Tables 1, 2). The frequencies of IL-1B genotypes CC, CT and TT in patients with chronic hepatitis B were 23.7%(45/190), 49.5% (94/190) and 26.8%(51/190), while those in controls were 26.1%(65/249), 47.4%(118/249), and 26.5%(66/249) respectively. The results showed that there was no significant difference in the frequencies of alleles ($\chi^2=0.16$, $P=0.69$) or genotypes ($\chi^2=0.35$, $P=0.84$) in IL-1B between patients with chronic hepatitis B and control subjects.

Only four of the five kinds of polymorphism of IL-1RN (1/1, 1/2, 2/2 and 1/4) were found in this study. The frequencies of 1/1, 1/2, 2/2 and 1/4 were 88.9%, 9.0%, 0.5% and 1.6% in chronic hepatitis B patients, while those in controls were 81.1%, 16.9%, 0.4% and 1.6% respectively. IL-1 RN allele 1 was

Table 1 Comparison of IL-1B(-511) polymorphism between patients with chronic hepatitis B and controls

Group	*n*	Frequency of genotypes (%)			Frequency of alleles (%)	
		CC	CT	TT	C	T
Patients	190	45 (23.7)	94 (49.5)	51 (26.8)	184 (48.4)	196 (51.6)
Controls	249	65 (26.1)	118 (47.4)	66 (26.5)	248 (49.8)	250 (50.2)

Patients *vs* controls, $\chi^2=0.35$, $P=0.84$; $\chi^2=0.16$, $P=0.69$.

Table 2 Comparison of IL-1RN intron 2 polymorphism between patients with chronic hepatitis B and controls

Group	*n*	Frequency of genotypes(%)				Frequency of alleles(%)		
		1/1[a]	1/2[b]	2/2	1/4	1	2[c]	4
Patients	190	169 (88.9)	17 (9.0)	1 (0.5)	3 (1.6)	358 (94.2)	19 (5.0)	3 (0.8)
Controls	249	202 (81.1)	42 (16.9)	1 (0.4)	4 (1.6)	450 (90.4)	44 (8.8)	4 (0.8)

Patients *vs* controls, [a]$\chi^2=5.03$, $P=0.025$; [b]$\chi^2=5.81$, $P=0.016$; [c]$\chi^2=4.76$, $P=0.029$.

Table 3 Association between IL-1B, IL-RN genotypes and HBV copies in chronic hepatitis B patients

Subgroup	*n*	IL-1B genotype (%)				IL-1RN genotype (%)		
		CC[a]	CT	TT	1/1	1/2	2/2	1/4
I	104	31 (29.8)	49 (47.1)	24 (23.1)	93 (89.4)	9 (8.7)	0	2(1.9)
II	86	14 (16.3)	45 (52.3)	27 (31.4)	76 (88.3)	8 (9.3)	1 (1.2)	1(1.2)

HBV-DNA $\leqslant1\times10^3$copies/mL as I, HBV-DNA $>1\times10^3$copies/mL as II, [a]subgroup I *vs* subgroup II, $\chi^2=4.77$, $P=0.029$.

detected in 94.2% of chronic hepatitis B patients and 90.4% of controls, while IL-1RN allele 2 was detected in 5.0% of the patients and 8.8% of controls, The frequencies of genotype 1/2 and IL-1RN allele 2 in patients with chronic hepatitis B were lower than those in controls (χ^2=5.81, P=0.016 and χ^2=4.76, P=0.029 respectively).

Association of IL-1B and IL-1RN polymorphism with HBV-DNA replication

For further analysis of the relationship between IL-1B, IL-1RN polymorphisms and HBV-DNA replication in patients with chronic hepatitis B, the patients were divided into two subgroups (HBV-DNA $\leqslant 1\times10^3$ copies/mL as subgroup I, HBV-DNA $>1\times10^3$ copies/mL as subgroup II). As shown in Table 3, the distributions of IL-1B(-511) genotype CC were of significant difference between the two subgroups (χ^2=4.77, P=0.029).

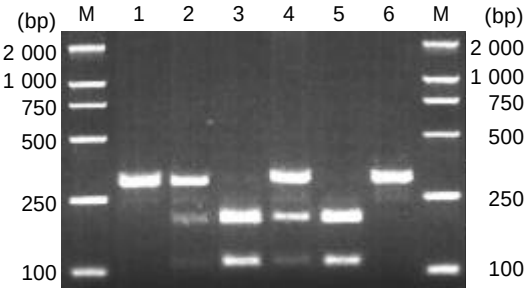

Figure 1 Results of IL-1B(-511) gene typing. Lane M: DNA molecular mass marker; Lanes 1, 6: TT; Lanes 2, 4: CT; Lanes 3, 5: CC.

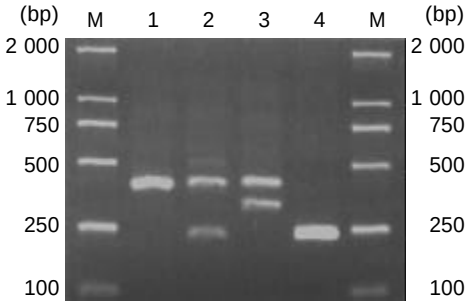

Figure 2 Results of IL-1RN intron 2 VNTR. Lane M: DNA molecular mass marker; Lane 1: 1/1; Lane 2: 1/2; Lane 3: 1/4; Lane 4: 2/2.

DISCUSSION

HBV infection is a major global health problem with an estimated 300 million people chronically infected worldwide[9,10]. Individuals with an inadequate primary immune response to HBV are at increased risk of developing chronic hepatitis B. Age is the strongest host feature associated with chronic infection with 90% infants and 5-10% of adults developing chronic hepatitis B after exposure. In addition, people with the same age, sex and ethnical group were exposed to the same HBV strain, which could cause a broad spectrum ranging from no infection to different clinical outcomes[11]. These data suggest that host genetic factors are responsible for the clinical outcomes of HBV infection. Clearance of HBV requires a coordinated innate and adaptive humoral and cell-mediated immune response. Cytokines are soluble polypeptide molecules that mediate cell-to-cell communication and regulate the intensity and duration of the immune response. Previous studies have shown that the maximal capacity of cytokine production varies among individuals and correlates with SNP in the promoter region of various cytokine genes[12,13]. Furthermore, cytokine gene polymorphisms were associated with liver disease severity in patients with viral hepatitis[14]. In the present study we compared the distributions of IL-1B(-511) and IL-1RN intron 2 VNTR polymorphisms between patients with chronic B and control subjects.

IL-1B is one of the IL-1 gene family members, and located in the proximal region of chromosome 2q13-21. Different polymorphisms have been described in IL-1B, and at least two of them could influence the protein production. One is located in the promoter region at position -511, and the other in exon 5. Pociot *et al*.[15] reported that IL-1B polymorphisms were correlated with IL-1β expression. IL-1B allele T carrier had higher productions of IL-1β than IL-1B allele C carrier. In the study, genotype distributions and allelic frequencies for IL-1B(-511) promoter polymorphisms in patients with chronic hepatitis B and control subjects were not statistically different. Further analysis of the relationship between IL-1B polymorphism and HBV-DNA replication in patients with chronic hepatitis B showed that IL-1B(-511) genotype CC was associated with HBV-DNA replication.

IL-1ra is a naturally occurring anti-inflammatory protein, competitively blocks the binding of IL-1α and IL-1β type I and type II IL-1 receptors, but exerts no agonist activity, despite sharing 30% amino acid sequence homology with IL-1β, and 19% with IL-1α. Il-1ra has been shown to inhibit the effects of IL-1 both *in vitro* and *in vivo*[16]. Increasing evidence showed that IL-1RN polymorphisms were related with susceptibility to individual diseases, including psoriasis, systemic lupus erthematosus, and inflammatory bowel disease[4]. By the study of IL-1RN intron 2 polymorphisms, our results suggested that the distributions of IL-1RN 1/2 genotype and IL-1RN allele 2 in patients with chronic hepatitis B were significantly lower than those in control subjects. A possible explanation of this result could be provided by the fact that carriage of Il-1RN allele 2 of each of these polymorphisms was related with high production of IL-1β[17], which may augment the production of other cytokines, such as IL-2, IL-6 and TNF-α, and trigger the complex immuological processes to eliminate the virus and its complex.

In summary, the findings of this study and others may provide further evidence that genetic factors are important in the pathogenesis of HBV infection. Our results suggest that the carriage of IL-1RN allele 2 may play a protective role in the development of HBV infection and IL-1B CC genotype may be associated with HBV-DNA replication. However, the real roles of IL-1 polymorphisms in the pathogenesis of developing chronic hepatitis B should be further investigated by large population-based studies.

REFERENCES

1 **Perrillo RP**. How will we use the new antiviral agents for hepatitis B? *Curr Gastroenterol Rep* 2002; **4**: 63-71
2 **Koziel MJ**. Cytokines in viral hepatitis. *Semin Liver Dis* 1999; **19**: 157-169
3 **Hutyrova B**, Pantelidis P, Drabek J, Zurkova M, Kolek V, Lenhart K, Welsh KL, Du Bois RM, Petrek M. Interleukin-1 gene cluster polymorphisms in sarcoidosis and idiopathic pulmonary fibrosis. *Am J Respir Crit Care Med* 2002; **165**: 148-151
4 **Ma P**, Chen D, Pan J, Du B. Genomic polymorphism within interleukin-1 family cytokines influences the outcome of septic patients. *Crit Care Med* 2002; **30**: 1046-1050
5 **Nemetz A**, Nosti-Escanilla MP, Molnar T, Kope A, Kovacs A, Feher J, Tulassay Z, Nagy F, Garcia-Gonzalez MA, Pena AS. IL-1B gene polymorphisms influence the course and severity of inflammatory bowel disease. *Immunogenetics* 1999; **49**: 527-531
6 **Garcia-Gonzalez MA**, Lanas A, Santolaria S, Crusius JB, Serrano

MT, Pena AS. The polymorphic IL-1B and IL-1RN genes in the aetiopathogenesis of peptic ulcer. *Clin Exp Immunol* 2001; **125**: 368-375

7 **Moos V**, Rudwaleit M, Herzog V, Hohlig K, Sieper J, Muller B. Association of genotypes affecting the expression of interlukin-1beta or interleukin-1 receptor antagonist with osteoarthritis. *Arthritis Rheum* 2000; **43**: 2417-2422

8 **Kanemoto K**, Kawasaki J, Mjyamoto T, Obayashi H, Nishimura M. Interleukin (IL)-1β, IL-1α, and IL-1 receptor antagonist gene polymorphisms in patients with temporal lobe epilepsy. *Ann Neurol* 2000; **47**: 571-574

9 **Wang FS**. Current status and prospects of studies on human genetic alleles associated with hepatitis B virus infection. *World J Gastroenterol* 2003; **9**: 641-644

10 **Cacciola I,** Cerenzia G, Pollicino T, Squadrito G, Castellaneta S, Zanetti AR, Mieli-Vergani G, Raimondo G. Genomic heterogeneity of hepatitis B virus (HBV) and outcome of perinatal HBV infection. *J Hepatol* 2002; **36**: 426-432

11 **Rapicetta M**, Ferrari C, Levrero M. Viral determinants and host immune responses in the pathogenesis of HBV infection. *J Med Virol* 2002; **67**: 454-457

12 **Giedraitis V,** He B, Huang WX, Hillert J. Cloning and mutation analysis of the human IL-18 promoter: a possible role of polymorphisms in expression regulation. *J Neuroimmunol* 2001; **112**: 146-152

13 **Ben-Ari Z**, Mor E, Papo O, Kfir B, Sulkes J, Tambur AR, Tur-Kaspa R, Klein T. Cytokine gene polymorphisms in patients infected with hepatitis B virus. *Am J Gastroenterol* 2003; **98**: 144-150

14 **Miyazoe S**, Hamasaki K, Nakata K, Kajiya Y, Kitajima K, Nakao K, Daikoku M, Yatsuhashi H, Koga M, Yano M, Eguchi K. Influence of interleukin-10 gene promoter polymorphisms on disease progression in patients chronically infected with hepatitis B virus. *Am J Gastroenterol* 2002; **97**: 2086-2092

15 **Pociot F**, Molvig J, Wogensen L, Worsaae H, Nerup J. A Taq I polymorphism in the human interleukin-1 beta (IL-1 beta) gene correlates with IL-1 beta secretion *in vitro*. *Eur J Clin Invest* 1992; **22**: 396-402

16 **Gabay C**, Smith MF, Eidlen D, Arend WP. Interleukin 1 receptor antagonist(IL-1Ra) is an acute- phase protein. *J Clin Invest* 1997; **99**: 2930-2940

17 **Santtila S**, Savinainen K, Hurme M. Presence of the IL-1RA allele 2 (ILRN*2) is associated with enhanced IL-1 beta production *in vitro*. *Scand J Immunol* 1998; **47**: 195-198

Edited by Zhang JZ and Wang XL **Proofread by** Xu FM

PO Box 2345, Beijing 100023, China
Fax: +86-10-85381893
E-mail: wjg@wjgnet.com www.wjgnet.com

World J Gastroenterol 2004;10(12):1830-1833
World Journal of Gastroenterology
Copyright ©2004 by The WJG Press ISSN 1007-9327

• BRIEF REPORTS •

Effects of tegaserod on Fos, substance P and calcitonin gene-related peptide expression induced by colon inflammation in lumbarsacral spinal cord

Yi-Ning Sun, Jin-Yan Luo

Yi-Ning Sun, Jin-Yan Luo, Department of Gastroenterology, Second Hospital of Xi' an Jiaotong University, Xi' an 710004, Shaanxi Province, China
Correspondence to: Professor Jin-Yan Luo, Department of Gastroenterology, Second Hospital of Xi' an Jiaotong University, Xi' an 710004, Shaanxi Province, China
Telephone: +86-29-87678758
Received: 2003-09-06 **Accepted:** 2003-10-22

Abstract

AIM: To investigate the mechanisms of tegaserod, a partial 5-HT4 agonist, in reducing visceral sensitivity by observing Fos, substance P (SP) and calcitonin gene-related peptide (CGRP) expression in the lumbarsacral spinal cord induced by colonic inflammation in rats.

METHODS: Twenty-four male rats with colonic inflammation induced by intraluminal instillation of trinitrobenzenesulfonic acid (TNBS) were divided into 3 groups. Treatment group 1: intra-gastric administration of tegaserod, 2 mg/kg·d; Treatment group 2: intra-gastric administration of tegaserod, 1 mg/kg·d; Control group: intra-gastric administration of saline, 2.0 mL/d. After 7 d of intra-gastric administration, lumbarsacral spinal cord was removed and processed for Fos, SP and CGRP immunohistochemistry.

RESULTS: In rats of the control group, the majority of Fos labeled neurons was localized in deeper laminae of the lumbarsacral spinal cord (L_5-S_1). SP and CGRP were primarily expressed in the superficial laminae of the spinal cord after TNBS injection. Intra-gastric administration of tegaserod (2 mg/kg·d) resulted in a significant decrease of Fos labeled neurons (22.0±7.7) and SP density (12.5±1.4) in the dorsal horn in the lumbarsacral spinal cord compared to those of the control group (62.2±18.9, 35.9±8.9, $P<0.05$). However, CGRP content in dorsal horn did not significantly reduce in rats of treatment group 1 (1.2±1.1) compared to that of the control group (2.8±2.4, $P>0.05$). Neither Fos expression nor SP or CGRP density in the dorsal horn significantly declined in rats of treatment group 2 compared to those of the control group ($P>0.05$).

CONCLUSION: Tegaserod can significantly reduce Fos labeled neurons in the lumbarsacral spinal cord induced by colonic inflammation. Tegaserod may reduce visceral sensitivity by inhibiting SP expression in the dorsal horn of spinal cord.

Sun YN, Luo JY. Effects of tegaserod on Fos, substance P and calcitonin gene-related peptide expression induced by colon inflammation in lumbarsacral spinal cord. *World J Gastroenterol* 2004; 10(12): 1830-1833

http://www.wjgnet.com/1007-9327/10/1830.asp

INTRODUCTION

Irritable bowel syndrome (IBS) is a common functional gastrointestinal disorder. Its typical feature is recurrent abdominal discomfort or pain associated with disordered defecation. Studies have shown that visceral sensitivity plays an important role in the pathophysiology of IBS[1]. Tegaserod, a partial 5-HT4 agonist, acts selectively on 5-HT4 receptors in the gut. Tegaserod can relieve symptoms in IBS patients with abdominal discomfort or pain and significantly decrease visceral sensitivity[2]. The objectives of the present study were to identify regions of the Fos protein, substance P (SP) and calcitonin gene-related peptide (CGRP) expression in the lumbarsacral spinal cord in response to colonic inflammation induced by intraluminal instillation of TNBS, and to compare the effects of tegaserod on the spinal Fos, SP and CGRP expression induced in the same animal model.

MATERIALS AND METHODS

Animals

Twenty-four adult male Sprague-Dawley rats (The Fourth Military Medical University) weighing 220-250 g were used in this study. The animals were housed in a quiet room with a constant ambient temperature of 20 ℃ with free access to rat chow and water.

Experimental protocol

After 24 h fast, TNBS (100 mg/kg in 300 mL/L ethanol) was administered intrarectally through a silicone rubber catheter introduced 7 cm into the anus under light diethyl-ether anesthesia. To keep TNBS in the colon for a longer time and to avoid leakage, the catheter was slowly withdrawn and the tail of the rat was kept elevating for 8-10 min.

Tegaserod (20 mg, Beijing Novartis Pharmacy Company) was dissolved in 100 mL distilled water. After one day of TNBS instillation, the rats were randomly divided into 3 groups. Each group had eight rats. Treatment group 1: intra-gastric administration of tegaserod 2 mg/kg; Treatmemt group 2: intra-gastric administration of tegaserod 1 mg/kg; Control group: intra-gastric administration of saline 2.0 mL. Tegaserod or saline was administered once daily (10:00AM) for consecutive 7 d after TNBS instillation.

Fos, SP and CGRP immuohistochemistry

One day after the last time of tegaserod or saline administration, the rats were deeply anaesthetized with pentobarbital Na (80 mg/kg, i.p.) and perfused with 100 mL saline followed by 500 mL fixative of 40 g/L paraformaldehyde in 0.1 mol/L phosphate buffer (PH 7.4). L_3-S_2 segments of the spinal cord were removed, post-fixed in the same fixative at 4 ℃ for 2-4 h and then cryoprotected in 200 g/L sucrose overnight. Serial frozen sections of 40-μm thickness cut on a Leitz cryocut. Sections were collected in 0.01 mol/L PBS for immunohistochemistry.

The spinal cord sections were stained for Fos, SP and CGRP using avidin-biotin-peroxidase complex (ABC) method. Free

floating tissue sections were treated in 800 mL/L methanol containing 30 mL/L H_2O_2 to block endogenous peroxidase acitvity for 30 min at room temperature. They were treated with 0.01 mol/L PBS containing 1 g/L Triton ×100 for 20 min at room temperature. The sections were then incubated with a polyclonal rabbit anti-Fos serum (1:3 000, Santa Cruz), polyclonal rabbit anti-SP serum (1:500, Boster) and polyclonal rabbit anti-CGRP serum (1:500, Boster) respectively for 48 h at 4 ℃. After the step, the sections were incubated with biotinylated goat anti-rabbit IgG (1:500, Sigma), and subsequently with the ABC complex (1:500, Sigma) at room temperature for 2 h each. The antigen-antibody reaction sites were visualized by incubation with glucose oxidase-DAB-nickel method for 15-30 min at room temperature. The sections were rinsed in 0.01 mol/L PBS for 3×10 min between transition of these steps. Finally, the sections were mounted onto gelatin-coated slides, dried, dehydrated, cleared and coverslipped.

Fos immunoreative neuronal counts and measurement of the density of dorsal horn SP and CGRP staining

The number of neuronal nuclear profiles expressing Fos was analyzed with computer assisted QUIC menu system. Precise regional localization was done by outlining specific regions and then particles (stained nuclei) were counted in the outlined regions. The number of profiles counted in five sections was averaged for each animal, and comparisons were made between the groups[3].

The density of SP and CGRP staining in the dorsal horn of spinal cord was also measured in specific outlined regions using computer assisted QUIC menu system. The ratio of the area of stained SP or CGRP to the area of the outlined regions was presented as the density of SP or CGRP. The averages were obtained for density measurements from five randomly selected spinal cord sections for each animal, and comparisons were made between treatment and control groups[3].

Statistical analysis

Pictures were taken under BX-60 microscopy with the support of IM50 software. All results are expressed as mean±SD. An unpaired *t*-test was used to compare Fos-IR (immunoreactive) cell count data, SP and CGRP density between the groups. A difference was accepted as significant if the probability was less than 5% ($P<0.05$).

RESULTS

Effect of tegaserod on Fos expression in spinal cord

In animals of the control group, Fos protein was expressed bilaterally in the nuclei of cells of the dorsal horn in L_5, L_6 and S_1 of lumbarsacral spinal cord. The nuclei of Fos-IR neurons were black and there was no cytoplasmic staining. Among 62.2±18.9 neurons exhibited Fos-IR, most of them were distributed in the deeper laminae (III-IV, V-VI) of the dorsal horn. Only few Fos-IR neurons were sparsely distributed in the superficial laminae (I-II) of the dorsal horn (Figure 1A).

After intra-gastric administration of tegaserod 1 mg/kg· d for 7 d, Fos-IR cells in the dorsal horn decreased to 42.6±7.5, but was not significantly different with that of the control group (62.2±18.9, $P>0.05$). After intra-gastric administration of tegaserod 2 mg/kg· d for seven days, Fos-IR neurons in the dorsal horn decreased to 22.0±7.7, a significant difference ($P<0.05$) (Table 1, Figure 2A).

Effect of tegaserod on SP and CGRP expression in spinal cord

In rats of the control group, SP was expressed bilaterally in the superficial laminae (I-II) in the dorsal horn. The density of SP

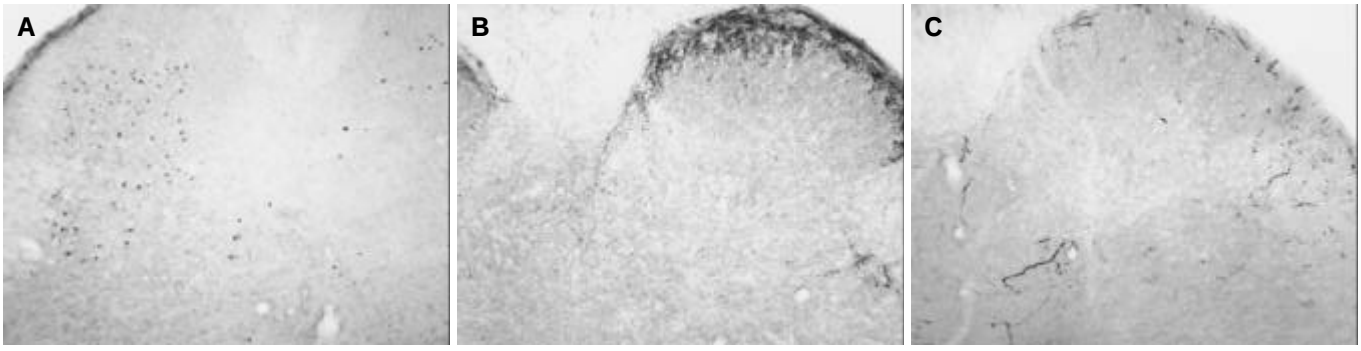

Figure 1 Sections from the control rats. ×10. A: Fos-IR neurons induced by TNBS administration were observed as black spots in the dorsal horn. Note that most Fos-IR neurons were distributed in the deeper laminae of the dorsal horn. B: SP was mainly distributed in the superficial laminae of the dorsal horn. C: CGRP was primarily localized in the superficial laminae of the dorsal horn.

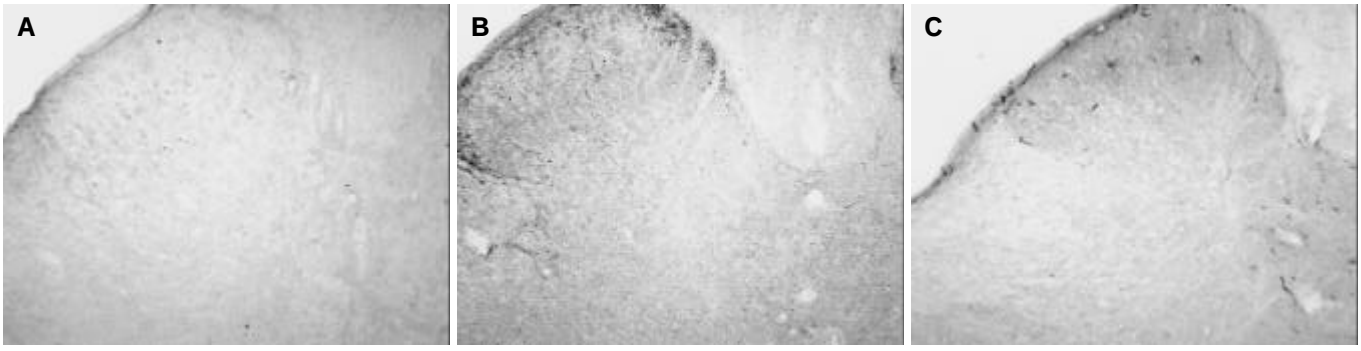

Figure 2 Sections from rats treated with tegaserod 2 mg/kg· d. ×10. A: After treatment with tegaserod, the number of Fos-IR cells was decreased significantly compared with that of the control group. B: Note that the density of SP in rats treated with tegaserod was decreased significantly compared with that of the control rats. C: The density of CGRP was not different between the treatment group and the control group.

was 35.9±8.9. After 7 d of intra-gastric injection of tegaserod 1mg/kg· d, the density of SP in the superficial laminae did not significantly reduce (33.3±3.4, $P>0.05$). However, after intra-gastric administration of tegaserod 2 mg/kg· d for 7 d, the density of SP decreased to 12.5±1.4, a significant difference compared to that of the control group ($P<0.05$) (Table 1, Figures 1B, 2B).

In animals of the control group, most CGRP were expressed in the superficial laminae of the dorsal horn. A few CGRP were distributed in the deeper laminae. The density of CGRP in rats of the control group was 2.8±2.4. The density of CGRP did not significantly decrease in rats treated with tegaserod 1 mg/kg· d for 7 d (2.2±2.3, $P>0.05$). After treatment with tegaserod 2 mg/kg· d for 7 d, the density of CGRP decreased 56.7% compared to that of the control group (1.2±1.1), but there was no significant difference ($P>0.05$) (Table 1, Figures 1C, 2C).

Table 1 Number of Fos-IR neurons and density of SP, CGRP (%) in dorsal horn of rats in various groups

	Fos	SP	CGRP
Treatment group 1 (2 mg/kg·d)	22.0±7.7[a]	12.5±1.4[a]	1.2±1.1
Treatment group 1 (1 mg/kg·d)	42.6±7.5	33.3±3.4	2.2±2.3
Control group	62.2±18.9	35.9±8.9	2.8±2.4

[a]$P<0.05$, *vs* the control.

DISCUSSION

Irritable bowel syndrome is a common functional gastrointestinal disorder. Its typical feature is recurrent abdominal discomfort or pain associated with disordered defecation or a change in bowel habit. Routine investigation revealed no evidence of structural or biochemical abnormality. There is evidence that patients with IBS showed a lower threshold for discomfort and/or pain, increased sensitivity to stimuli, or altered viscerosomatic referral[4]. Therefore, visceral hypersensitivity could play an important role in the pathophysiology of IBS[1].

Tegaserod is a partial 5-HT4 agonist. The absence of blood-brain barrier permeation makes it selectively bind to 5-HT4 receptors in the gastrointestinal tract. Tegaserod has been shown to modulate both gastrointestinal motility and visceral sensitivity[2]. Studies demonstrated that tegaserod produced rapid and sustained improvements of the abdominal pain/discomfort and constipation in IBS patients, especially in female IBS patients[5,6]. These improvements were seen within the first week, and maintained throughout the treatment period. A randomized, double-blind, placebo-controlled study showed that tegaserod reduced the sensitivity to rectal distension in healthy subjects[7].

Fos, one of the inducible transcription factors, serves as a quantifiable marker to identify neuronal populations activated by noxious somatic and visceral stimulations. Noxious stimulation of hollow viscera induced a specific pattern of Fos expression in rat spinal cord that reflected the intensity of the stimulation[8]. Recently, the anti-nociceptive effects of some drugs have been studied in animal models of persistent visceral pain using Fos expression as an independent measure. Lu reported that baclofen, a selective $GABA_B$ receptor agonist, specifically reduced Fos expression in the superficial dorsal horn of spinal cord induced by mustard oil irritation of the colon[3]. A recent study has demonstrated that opiate receptor agonists, especially morphine, attenuate pain related behavior and Fos expression in rat spinal cord neurons following noxious visceral stimulation[9]. Thus, localization of Fos expression can be a useful tool to examine the effectiveness of different analgesic drugs after nociceptive stimulation.

In rats of the control group, Fos protein expression became bilaterally evident as nuclear staining in cells in L_5, L_6 and S_1 of lumbarsacral spinal cord. In the rats, the descending colon was innervated by sensory afferent fibers in the pelvic nerve projecting bilaterally to the lumbarsacral (L_6-S_2) spinal cord[10]. The result was consistent with the viscerotopic organization of the afferent fibers that innervate the descending colon. Most of the Fos-IR neurons were distributed in the deeper laminae (III-IV, V-VI) of the dorsal horn. Few Fos expressed in the superficial laminae (I-II) of the dorsal horn. Imbe demonstrated that Fos-IR cells had the tendency to spread from the superficial laminae to the deeper laminae when deep tissue inflammation became persistent[11]. From the segment and laminae distribution of Fos-IR neurons, we conclude that neurons in the dorsal horn of lumbarsacral spinal cord are activated via sensory afferent fibers in the pelvic nerve by noxious stimulation induced by persistent colonic inflammation. Therefore, tegaserod can dose-dependently prevent sensory neurons in the dorsal horn from being activated by colonic inflammation.

Substance P was released from primary sensory nociceptive neurons in response to noxious stimuli. Up to 80% of dorsal root ganglion (DRG) neurons supplying viscera contained SP, suggesting the importance of SP in transmission of signals from the viscera to the spinal cord[12]. Study of Kishimoto demonstrated that high concentrations of SP were significantly related to abdominal pain[13]. SP could play a pivotal role at the spinal cord level in postsynaptic sensitization, particularly during and after gut inflammation[14]. In the spinal cord, SP releasing from the primary afferents could activate the dorsal horn neurons by inducing an influx of Ca^{2+} throughout voltage-gated Ca^{2+} channels[15].The results of this study showed that the density of SP in the dorsal horn decreased significantly compared to the control group after treatment with tegaserod 2 mg/kg· d for 7 d . Therefore, tegaserod can inhibit SP expression in the dorsal horn of the spinal cord.

CGRP is one of the major neuropeptides expressed in the spinal cord sensory processing region and is widely distributed in the nervous system, particularly in sensory neurons. CGRP, which is generally colocalized with SP in the primary afferent nociceptors, is likely to be involved in pain transmission. CGRP may produce a direct nociceptive effect. CGRP might also enhance SP-induced nociceptive sensation by facilitating the release of SP in the spinal dorsal horn[16]. Compared with that of the control group, the density of CGRP decreased 21.4% in treatment group 1 and 57.1% in treatment group 2, showing an insignificant difference ($P>0.05$). The results suggest that tegaserod may not act on CGRP expression to reduce visceral nociceptive transmission. However, whether a much larger dose of tegaserod can significant decrease CGRP expression in the spinal cord still needs more studies.

The results of the present study showed that tegaserod could significantly decrease Fos and SP expression in the dorsal horn of the spinal cord. Tegaserod can exert antinociceptive effect. This effect is related to SP expression inhibition in the spinal cord. The study of Schikowski showed that in decerebrated cats the static discharge rate of the afferents evoked by rectal distension decreased significantly after intravenous administration of tegaserod. They proposed that 5-HT4 receptor activation had an inhibitory effect on intramural mechanoreceptors in cat rectum[17]. Today there is considerable evidence that serotonin influences nociceptive reflexes at different anatomic levels. For example, intrathecal and iontophoretic applications of serotonin to the dorsal horn produced pain relief, and serotonin antagonists produced hyperalgesia[18]. Ghelardini found that BIMU1 and BIMU8, two 5-HT4 agonists, exerted an antinociceptive effect by centrally potentiating endogenous cholinergic activity[19]. Since there are serotonin-SP and serotonin-Ach neurotransmitter links, we conclude that tegaserod, acting on 5-HT4 receptors in the gut, produces an antinociceptive effect by inhibiting the expression of SP in spinal dorsal horn.

REFERENCES

1 **Bueno L,** Fioramonti J, Delvaux M, Frexinos J. Mediators and pharmacology of visceral sensitivity: from basic to clinical investigations. *Gastroenterology* 1997; **112**: 1714-1743

2 **Lacy BE**, Yu S. Tegaserod: a new 5-HT4 agonist. *J Clin Gastroenterol* 2002; **34**: 27-33

3 **Lu Y,** Westlund KN. Effects of baclofen on colon inflammation-induced Fos, CGRP and SP expresson in spinal cord and brainstem. *Brain Res* 2001; **889**: 118-130

4 **Mertz H,** Naliboff B, Munakata J, Niazi N, Mayer EA. Altered rectal perception is a biological marker of patients with irritable bowel syndrome. *Gastroenterology* 1995; **109**: 40-52

5 **Muller-Lissner SA,** Fumagalli I, Bardhan KD, Pace F, Pecher E, Nault B, Ruegg P. Tegaserod, a 5-HT(4) receptor partial agonist, relieves symptoms in irritable bowel syndrome patients with abdominal pain, bloating and constipation. *Aliment Pharmacol Ther* 2001; **15**: 1655-1666

6 **Novick J,** Miner P, Krause R, Glebas K, Bliesath H, Ligozio G, Ruegg P, Lefkowitz M. A randomized double-blind, placebo-controlled trial of tegaserod in female patients suffering from irritable bowel syndrome with constipation. *Aliment Pharmacol Ther* 2002; **16**: 1877-1888

7 **Coffin B,** Farmachidi JP, Rueegg P, Bastie A, Bouhasira D. Tegaserod, a 5-HT4 receptor partial agonist, decreases sensitivity to rectal distension in healthy subjects. *Aliment Pharmacol Ther* 2003; **17**: 577-585

8 **Traub RJ,** Pechman P, Iadarola MJ, Gebhart GF. Fos-like proteins in the lumbosacral spinal cord following noxious and non-noxious colorectal distention in the rat. *Pain* 1992; **49**: 393-403

9 **Traub RJ,** Stitt S, Gebhart GF. Attenuation of c-Fos expression in the rat lumbosacral spinal cord by morphine or tramadol following noxious colorectal distention. *Brain Res* 1995; **701**: 175-182

10 **Traub RJ,** Murphy A. Colonic inflammation induces fos expression in the thoracolumbar spinal cord increasing activity in the spinoparabrachial pathway. *Pain* 2002; **95**: 93-102

11 **Imbe H,** Iwata K, Zhou QQ, Zuo S, Dubner R, Ren K. Orofacial deep and cutaneous tissue inflammation and trigeminal neuronal activation. Implications for persistent temporomandibular pain. *Cells Tissues Organs* 2001; **169**: 238-247

12 **Palecek J,** Paleckova V, Willis WD. Postsynaptic dorsal column neurons express NK1 receptors following colon inflammation. *Neuroscience* 2003; **116**: 565-572

13 **Kishimoto S,** Kobayash H, Machino H. High concentrations of substance P as a possible transmission of abdominal pain in rats with chemical induced ulcerative colitis. *Biomed Res* 1994; **15**: 133-140

14 **Bueno L,** Fioramonti J. Effects of inflammatory mediators on gut sensitivity. *Can J Gastroenterol* 1999; **13**(Suppl A): 42A-46A

15 **Coderre TJ,** Katz J, Vaccarino AL, Melzack R. Contribution of central neuroplasticity to pathological pain: review of clinical and experimental evidence. *Pain* 1993; **52**: 259-285

16 **Friese N,** Diop L, Chevalier E, Angel F, Riviere PJ, Dahl SG. Involvement of prostaglandins and CGRP-dependent sensory afferents in peritoneal irritation-induced visceral pain. *Regul Pept* 1997; **70**: 1-7

17 **Schikowski A,** Thewissen M, Mathis C, Ross HG, Enck P. Serotonin type-4 receptors modulate the sensitivity of intramural mechanoreceptive afferents of the cat rectum. *Neurogastroenterol Motil* 2002; **14**: 221-227

18 **Gyermek L.** Pharmacology of serotonin as related to anesthesia. *J Clin Anesth* 1996; **8**: 402-425

19 **Ghelardini C,** Galeotti N, Casamenti F, Malmberg-Aiello P, Pepeu G, Gualtieri F, Bartolini A. Central cholinergic antinociception induced by 5-HT4 agonists: BIMU1 and BIMU8. *Life Sci* 1996; **58**: 2297-2309

Edited by Zhao M and Wang XL **Proofread by** Xu FM

PO Box 2345, Beijing 100023, China
Fax: +86-10-85381893
E-mail: wjg@wjgnet.com www.wjgnet.com

World J Gastroenterol 2004;10(12):1834-1835
World Journal of Gastroenterology
Copyright ©2004 by The WJG Press ISSN 1007-9327

• BRIEF REPORTS •

Epidemiological investigation of esophageal carcinoma

Hong Zhang, Shao-Hua Chen, You-Ming Li

Hong Zhang, Shao-Hua Chen, You-Ming Li, Digestive department, the First Affiliated Hospital, Medical College of Zhejiang University, Hangzhou 310003, Zhejiang Province, China
Correspondence to: Professor You-Ming Li, Digestive Department, the First Affiliated Hospital, Medical College, Zhejiang University. No.79 Qingchun Road, Hangzhou, 310003, Zhejiang, China. liyouming@dna.net.cn
Telephone: +86-571-87236603 **Fax:** +86-571-87236611
Received: 2003-11-21 **Accepted:** 2004-01-08

Abstract

AIM: To review the characteristics of esophageal carcinoma in recent 30 years in the epidemiological investigation.

METHODS: A total of 1 520 cases of esophageal carcinoma in the First Affiliated Hospital of Zhejiang University Medical College admitted from 1970 until now were reviewed. Their age, gender, position of carcinoma and histological type were analyzed.

RESULTS: The morbidity of esophageal carcinoma was increasing during the observation period. Compared with the 1970s (9.5%), the ratio of adenocarcinoma significantly increased after the 1980s (19.1%). The difference was significant ($P \leqslant 0.05$).

CONCLUSION: The morbidity of esophageal adenocarcinoma was increasing and advanced clinical study should be strengthened.

Zhang H, Chen SH, Li YM. Epidemiological investigation of esophageal carcinoma. *World J Gastroenterol* 2004; 10(12): 1834-1835

http://www.wjgnet.com/1007-9327/10/1834.asp

INTRODUCTION

Carcinoma of esophagus is one of the most common cancers with a high mortality. Squanmous cell carcinoma and adenocarcinoma account for more than 95% of esophageal tumors[1]. The incidence rate of squamous cell carcinoma of the esophagus in the pathological feature is more frequent compared with adenocarcinoma. Increasing prevalence of adenocarcinoma of the esophagus has been reported from western countries in recent years and its incidence since the 1970s in China is unknown. Our study aimed to make an epidemiological investigation of carcinoma of esophagus and compare the incidence rate of adenocarcinoma and squamous cell carcinoma of the esophagus.

MATERIALS AND METHODS

Medical records of all patients (n=1 520) with adenocarcinoma or squamous cell carcinoma of the esophagus seen at the the First Affiliated Hospital of Zhejiang University Medical College between 1970 and 2001 were reviewed. The following data were retrieved: age, gender, tumor location, history of surgery and pathological features. The patients were divided into 3 groups: group A (211patients) were patients seen from 1970 to 1979, group B (451 patients) were patients from 1980 to 1989 and group C (858 patients) were from 1990 to 2001.

RESULTS

The data of the 1520 patients with adenocarcinoma or squamous cell carcinoma were analyzed. Among them, 236(15.5%) were female and 1 284(84.5%) were male. In group A there were 184 (87.2%) male patients and 27(12.8%) female patients,in group B there were 380(84.3%) male and 71(15.7%) female, in group C there were 720(83.9%) male and 138(16.1%) female. No differences were found between the groups in gender. Among 240 cases of adenocarcinoma of esophagus, 195(81.3%) were male and 45(18.7%) were female. And among 1280 cases of squamous cell carcinoma of the esophagus, 1 089(85.1%) were male and 191(14.9%) were female. No significant difference of sex ratios were found in patients with adenocarcinoma of esophagus and squamous cell carcinoma of the esophagus.

The age distribution of the patients is shown in Table 1. Patients in their 50s are at highest risk for carcinoma of the esophagus in the 1970s. And patients in their 60s are at highest risk for carcinoma of the esophagus since 1980s.

From clinical pathological data, 20, 80, 134 cases with adenocarcinoma and 191, 365, 724 cases with squamous cell carcinoma were found in groups A, B, C, respectively. The proportion of esophageal adenocarcinoma of all groups were 9.5%(20/211), 19.1%(86/451) and 15.6%(134/858), respectively. The difference was significant between groups A and B (P=0.002) and also between groups A and C (P=0.023). And there was no significant difference between groups B and C (P=0.113).

We investigated the location of adenocarcinoma of esophagus (193 cases), whose pathological findings showed the definite location. Two (1.0%) cases were located at the upper esophagus, 15 (7.8%) at the middle and 176 (91.2%) located at the lower esophagus.

Table 1 Age distribution of all patients with carcinoma of esophagus: *n* (%)

Age (yr)	A	B	C
≤30	3 (1.4)	2 (0.4)	5 (0.6)
30-	15 (7.1)	20 (4.3)	26 (3.0)
40-	47 (22.3)	72 (16.0)	162 (18.9)
50-	103 (48.8)	160 (35.5)	250 (29.1)
>60	43 (20.4)	197 (43.7)	415 (48.4)

DISCUSSION

Esophageal cancer is one of the most deadly forms of gastrointestinal cancer in China and death rate from carcinoma of esophagus ranked the third annually. Epidemiological data defined a certain geographical distribution[2]. In high mortality areas of China, Iran and Africa, the incidence of esophageal tumors is approximately equal in men and women[3]. By comparison, in low-incidence regions such as the United States and parts of Europe, there is a significant predilection for males[4]. It was reported that the incidence rate in male is higher than that of female, and the sex ratios (male/female) was 5-10:1. In our study, the male to female

ratio was 5.5:1 and the difference was not significant among groups.

Although squamous cell carcinoma was traditionally considered synonymous with esophageal cancer, the incidence of adenocarcinoma of the esophagus is increasing in most Western industrialized nations in recent years[5,6]. The incidence of esophageal adenocarcinoma increased from 1.5 to 7.0 per 100 000 men and from 0.4 to 1.5 per 100 000 women between 1971 and 1998 in England and Wales[7]. The proportion of adenocarcinomas has increased, probably in connection with the increasing incidence of Barrett's esophagus. But the risk of Barrett's esophageal mucosa advancing to esophageal adenocarcinoma is not well established[8]. Even though the incidence of esophageal adenocarcinoma has been rising in Western populations over the past two decades and squamous cell carcinoma has been declining[9,10], esophageal squamous cell carcinoma remains the predominant type of esophageal malignancy in the remainder of the world.

The mechanism of increased incidence of adenocarcinoma remained to be unclear. Gastroesophageal reflux disease (GERD), Barrett's esophagus, smoking, alcohol drinking and disfunction of esophageal motivation may be associated with the increase of incidence of adenocarcinoma. Adenocarcinoma is an uncommon cause of mortality in patients with Barrett's esophagus. Forty-four patients were confirmed to have Barrett's esophagus and were followed up for 209 patient-years. Only 2 patients developed esophageal adenocarcinoma, resulting in an incidence of one case in 209 patient-years, a 55-fold risk compared with age- and sex-matched population in Scotland[11]. Gastric juice that refluxes into the esophagus can injure esophageal squamous epithelium. When the injury heals through a metaplastic process in which an abnormal columnar epithelium replaces the injured squamous one, the resulting condition is called Barrett's esophagus[12]. Barrett's esophagus is the major risk factor for the development of esophageal adenocarcinoma, which is increasing in incidence faster than any other cancer in the Western world. Barrett's adenocarcinomas are increasing in epidemic proportions for as yet unknown reasons, approximately 0.5-1% of patients with Barrett's will develop adenocarcinoma[13,14]. Although GERD symptoms precede the development of adenocarcinoma of esophagus in many patients, fewer than 50% of patients have pathologic evidence of esophagitis or Barrett's epithelium at presentation.

There are clear racial, gender and site predilections for esophageal adenocarcinoma[15,16]. Our study demonstrated that 176 cases (91.2%) of adnocarcinoma of esophagus were located at the lower esophagus, being different from squamous cell carcinoma of the esophagus which were located mainly at the middle of the esophagus. Adenocarcinoma of esophagus shared with the same location with Barrett's esophagus.

Further study is required to determine the risk factors such as food[17] for the development of esophageal cancer and epidemiological investigation will prove important developing methods of detection and therapeutic intervention of this disease.

REFERENCES

1 **Klimstra DS**. Pathologic prognostic factors in esophageal carcinoma. *Semin Oncol* 1994; **21**: 425-430
2 **Stathopoulos GP**, Tsiaras N. Epidemiology and pathologenesis of esophageal cancer management and its controversial results (review). *Oncol Rep* 2003; **10**: 449-454
3 **Lu JB**, Sun XB, Dai DX, Zhu SK, Chang QL, Liu SZ, Duan WJ. Epidemiology of gastroenterologic cancer in Henan Province, China. *World J Gastroenterol* 2003; **9**: 2400-2403
4 **Blot WJ**. Esophageal cancer trends and risk factors. *Semin Oncol* 1994; **21**: 403-410
5 **Wei JT**, Shaheen N. The changing epidemiology of esophageal adenocarcinoma. *Semin Gastrointest Dis* 2003; **14**: 112-127
6 **Lukanich JM**. Section I: epidemiological review. *Semin Thorac Cardiovasc Surg* 2003; **15**: 158-166
7 **Newnham A**, Quinn MJ, Babb P, Kang JY, Majeed A. Trends in the subsite and morphology of oesophageal gastric cancer in English and Wales 1971-1998. *Aliment Pharmacol Ther* 2003; **17**: 665-676
8 **Zaninotto G**, Costantini M, Molena D, Rizzetto C, Ekser B, Ancona E. Barrett's esophagus. Prevalence, risk of adenocarcinoma, role of endoscopic surveillance. *Minerva Chir* 2002; **57**: 819-836
9 **Powell J**, McConkey CC, Gillison EW, Spychal RT. Continuing rising trend in oesophageal adenocarcinoma. *Int J Cancer* 2002; **102**: 422-427
10 **Younes M**, Henson DE, Ertan A, Miller CC. Incidence and survival trends of esophageal carcinoma in the United States: racial and gender differences by histological type. *Scand J Gastroenterol* 2002; **37**: 1359-1365
11 **Rana PS**, Johnston DA. Incidence of adenocarcinoma and mortality in patients with Barrett's oesophagus diagnosed between 1976 and 1986: implications for endoscopic surveillance. *Dis Esophagus* 2000; **13**: 28-31
12 **Spechler SJ**. Barrett's esophagus and esophageal adenocarcinoma: pathogenesis, diagnosis, and therapy. *Med Clin North Am* 2002; **86**: 1423-1445
13 **Reynolds JC**, Rahimi P, Hirschl D. Barrett's esophagus: clinical characteristics. *Gastroenterol Clin North Am* 2002; **31**: 441-460
14 **Cossentino MJ**, Wong RK. Barrett's esophagus and risk of esophageal adenocarcinoma. *Semin Gastrointest Dis* 2003; **14**: 128-135
15 **Younes M**, Henson DE, Ertan A, Miller CC. Incidence and survival trends of esophageal carcinoma in the United States: racial and gender differences between histological type. *Scand J Gastroenterol* 2002; **37**: 1359-1365
16 **Vega KJ**, Jamal MM. Changing pattern of esophageal cancer incidence in New Mexico. *Am J Gastroenterol* 2000; **95**: 2352-2356
17 **Li K**, Yu P. Food groups and risk of esophageal cancer in Chaoshan region of China: a high-risk area of esophageal cancer. *Cancer Invest* 2003; **21**: 237-240

Edited by Ma JY **Proofread by** Xu FM

PO Box 2345, Beijing 100023, China
Fax: +86-10-85381893
E-mail: wjg@wjgnet.com www.wjgnet.com

World J Gastroenterol 2004;10(12):1836-1837
World Journal of Gastroenterology
Copyright ©2004 by The WJG Press ISSN 1007-9327

• CASE REPORT •

Fathal pulmonary hypertension after distal splenorenal shunt in schistosomal portal hypertension

Roberto de Cleva, Paulo Herman, Vincenzo Pugliese, Bruno Zilberstein, William Abrão Saad, Joaquim José Gama- Rodrigues

Roberto de Cleva, Gastroenterology Department, Hospital Das Clinicas-University of Sao Paulo Medical School
Paulo Herman, Vincenzo Pugliese, Digestive Tract Surgery Division, Hospital Das Clinicas-University of Sao Paulo Medical School
Bruno Zilberstein, Digestive Tract Surgery Division, Hospital Das Clinicas-University of Sao Paulo Medical School
William Abrão Saad, Digestive Tract Surgery Division, Hospital Das Clinicas-University of Sao Paulo Medical School
Joaquim José Gama-Rodrigues, Digestive Tract Surgery Division, Hospital Das Clincas-University of Sao Paulo Medical School
Correspondence to: Roberto de Cleva, Hospital Das Clinicas-Department of Gastroenterology , University of Sao Paulo Medical School, Rua Cel. Artur Godoy, 125 Apto 152. São Paulo–SP–Brazil. CEP 04018-050. roberto.cleva @hcnet.usp.br
Telephone: +55-11-30828000 **Fax:** +55-11-30828000
Received: 2003-09-15 **Accepted:** 2004-01-12

de Cleva R, Herman P, Pugliese V, Zilberstein B, Saad WA, Gama-Rodrigues JJ. Fathal pulmonary hypertension after distal splenorenal shunt in schistosomal portal hypertension. *World J Gastroenterol* 2004; 10(12): 1836-1837
http://www.wjgnet.com/1007-9327/10/1836.asp

INTRODUCTION

Mansonic schistosomiasis is the main cause of portal hypertension in Brazil. Hepatosplenic (HS) form is manifested by hepatomegaly mainly on the left hepatic lobe associated with large splenomegaly and bleeding due to esophageal varices with high mortality rates[1,2].

Pulmonary hypertension in the HS form of mansonic schistosomiasis is described in association with both the acute and chronic forms of the disease, with a prevalence of 5% and may be a serious complication in the evolution of the disease. It can also be the triggering factor for serious complications associated with any form of surgical approach[3,4].

Surgical treatment is indicated for patients with a history of bleeding due to esophageal varix rupture based on world previous experience with endoscopic treatment results[5]. At present, techniques vary in azigo-portal disconnection and splenectomy (APDS) and distal splenorenal shunt (DSRS) for surgical treatment of such patients. All patients submitted to DSRA were carefully evaluated pre-operatively with eletrocardiography, chest X-ray and transthoracic echocardiography to rule out pulmonary hypertension. We report two fatal cases of pulmonary hypertension arising after DSRS.

Case Reports

Case 1 A 33-year-old man was admitted to the Liver and Portal Hypertension Surgical Unit, Hospital das Clí nicas, University of São Paulo Medical School for surgical treatment of portal hypertension due to hepatosplenic mansonic schistosomiasis after previous episode of bleeding esophageal varices. Ultrasound scan of the abdomen revealed discrete hepatomegaly, mainly on the left hepatic lobe associated with splenomegaly. Esophagogastroduodenoscopy revealed four large variceal vessels. The results found in routine laboratory tests were alanine amino transferase (ALT) of 29 U/L (normal: 10-30), aspartate amino transferase (AST) of 20 U/L (normal: 10-36), bilirrubin of 0.8 mg/dL (normal: 0.2- 1.0), gamma-glutamyl transferase of 86 U/L (normal: 7-32), and alkaline phosphatase of 241 U/L (normal: 32-104). The electrocardiogram, chest X-ray and echocardiography were within normal limits. The patient was submitted to DSRS. On the 4th postoperative day he developed progressive dyspnea and dyed 3 h later. The necropsy showed severe pulmonary hypertension, right ventricular dilatation and secondary myocardial infarction. The shunt was pervious.

Case 2 A 25-year-old woman was admitted to the Liver and Portal Hypertension Surgical Unit, Hospital das Clí nicas, University of São Paulo Medical School for surgical treatment of portal hypertension due to hepatosplenic mansonic schistosomiasis after an episode of bleeding esophageal varices. Ultrasound scan of the abdomen revealed discrete hepatomegaly, mainly on the left hepatic lobe associated with splenomegaly. Esophagogastroduodenoscopy revealed two large variceal vessels. The results found in routine laboratory tests were alanine amino transferase (ALT) of 25 U/L (normal 7-45), aspartate amino transferase (AST) of 38 U/L (normal 7-45), bilirrubin of 1.omg/dL(normal 0.2-1-0), gamma-glutamyl transferase of 31 U/L (normal 7-32), and alkaline phosphatase of 96 U/L (normal 32-104). The electrocardiogram, chest X-ray and echocardiography were within normal limits. The patient was submitted to DSRA. One the 7th postoperative day he developed progressive dyspnea and cardiogenic shock. A pulmonary artery catheter was inserted and showed high pulmonary mean artery pressure (64 mmHg) and a reduced cardiac index (CI = 1,2 L/min/m^2). The patient died before the shunt could be occluded. The necropsy showed severe pulmonary hypertension, right ventricular dilatation and secondary myocardial infarction. The shunt was pervious.

DISCUSSION

The treatment of portal hypertension in hepatosplenic schistosomiasis is very different in cirrhotic patients mostly because hepatic function is well preserved in Manson's disease. The surgical treatment has been considered the best alternative for schistosomotic patients with a history of bleeding from esophageal varix rupture because these patients had normal liver function and the only severe complication of the disease was digestive bleeding[2-6].

The two modalities of elective surgical treatment are selective shunt surgery (Warren procedure) or an esophagogastric devascularization procedure with splenectomy (EGDS). Shunt surgeries have been found to be effective for bleeding control, but were associated with postoperative encephalopathy and higher operative mortality rates when compared to devascularization procedures[2,5,6].

Although recognizable as a complication of shunt procedures, acute and fatal pulmonary hypertension have never been previously reported since Warren procedure for treatment of portal hypertension in mansonic schistosomiasis. Some groups in Brazil performed thousands of shunt surgeries for schistosomal portal hypertension, but have never described this important

complication[7-11]. Our group routinely performed a transthoracic echocardiography in order to evaluate pulmonary hypertension. The two patients had a normal pre-operative evaluation and were submitted to DSRS. The necropsy revealed typical findings of acute pulmonary hypertension, suggesting that sub-clinical elevated pulmonary artery pressure be present before surgery. The hyperflow determined by shunt surgery aggravated a previously unsuspected pulmonary hypertension, leading to death. This observation suggests that shunt surgeries should be employed very cautiously in young patients with portal hypertension due to hepatosplenic mansonic schistosomiasis and should be performed only after measurement of pulmonary artery pressure, if indicated.

REFERENCES

1 **Kelner S,** Silveira M. História natural das varizes do esôfago na esquistossomose mansônica hepatoesplênica . In: Kelner S, Silveira M(eds). Varizes de esôfago na esquistossomose mansônica hepatoesplênica. Recife: *Universitária da UFPE* 1997: 55-61

2 **Ferraz AAB,** Bacelar TS, Sılveira MJC, Coelho ARB, Câmara Neto RD, Araújo JR JGC, Ferraz EM. Surgical treatment of schistosomal portal hypertension. *Int Surg* 2001; **86:** 1-8

3 **Ezzat FA,** Abu-Elmagd K, Aly MA, Fathy OM, Ghawlby NA, EL Fiky AM. Selective shunt versus non-shunt surgery for management of both schistossomal and non-schistosomal**.** *Ann Surg* 1990; **212:** 97-108

4 **Ezzat FA,** Aly MA, Bahgat OO. Distal splenorenal shunt for management of variceal bleeding in patients with schistosomal hepatic fibrosis. *Ann Surg* 1986; **204:** 566-574

5 **Sakai P,** Boaventura S, Capacci ML, Macedo TM, Ishioka SZ. Endoscopic sclerotherapy of bleeding esophageal varices. A comparative study of results in patients with schistosomiasis and cirrhosis. *Endoscopy* 1988; **20:** 134-136

6 **Raia S,** Silva LC, Gayotto LCC, Forster SC, Fukushima J, Strauss E. Portal hypertension in schistosomiasis: a long-term follow-up of a randomized trial comparing three types of surgery. *Hepatology* 1994**; 20:** 398-403

7 **Cleva R,** Pugliese V, Zilberstein B, Saad WA, Pinotti HW, Laudanna AA. Hyperdinamic circulation in Manson's hepatosplenic schistosomiasis. *Rev Hosp Clin Fac Med São Paulo* 1998; **53:** 6-10

8 **Cleva R,** Pugliese V, Zilberstein B, Saad WA, Pinotti HW, Laudanna AA. Systemic hemodynamic changes in mansonic schistosomiasis with portal hypertension treated by azygoportal disconnection and splenectomy. *Am J Gastroenterol* 1999; **94:** 1632-1637

9 **Abrantes WL,** Drumond DAF. Anastomose espleno-renal distal em esquistossomóticos - Revisão de 200 pacientes operados há 11 a 22 anos. *Clin Bras Cir* 1995; **2:** 243-254

10 **Pitanga LC.** Selective splenorenal anastomosis: technical details and results of 340 patients subjected in 15 years. *Dig Dis Sci* 1986; **31:** 398 S

11 **Pitanga LC,** Pereira WLM. Anastomose espleno-renal distal na urgência em esquistossomóticos. In: Clínica Brasileira de Cirurgia, Colégio Brasileiro de Cirurgiões-Hipertensão portal. *Estado atual Ed Robe vol 2* 1995

Edited by Wang XL **Proofread by** Xu FM

PO Box 2345, Beijing 100023, China
Fax: +86-10-85381893
E-mail: wjg@wjgnet.com www.wjgnet.com

World J Gastroenterol 2004;10(12):1838-1840
World Journal of Gastroenterology
Copyright ©2004 by The WJG Press ISSN 1007-9327

• CASE REPORTS •

Gastric ulcer penetrating to liver diagnosed by endoscopic biopsy

Ertugrul Kayacetin, Serra Kayacetin

Ertugrul Kayacetin, Department of Gastroenterology, Selcuk University, Meram Medical Faculty, Konya, Turkey
Serra Kayacetin, Department of Pathology, Selcuk University, Meram Medical Faculty, Konya, Turkey
Correspondence to: Dr. Ertugrul Kayacetin, Selcuk Universitesi Meram Tip Fakultesi, Ic Hastaliklari AD, Gastroenteroloji BD, Konya/Turkey. ekayacetin@mynet.com
Fax: +90-332-3236063
Received: 2003-11-12 **Accepted:** 2003-12-24

Abstract

Liver penetration is a rare but serious complication of peptic ulcer disease. Usually the diagnosis is made by operation or autopsy. Clinical and laboratory data were no specific. A 64–year-old man was admitted with upper gastrointestinal bleeding. Hepatic penetration was diagnosed as the cause of bleeding. Endoscopy showed a large gastric ulcer with a pseudotumoral mass protruding from the ulcer bed. Definitive diagnosis was established by endoscopic biopsies of the ulcer base.

Kayacetin E, Kayacetin S. Gastric ulcer penetrating to liver diagnosed by endoscopic biopsy. *World J Gastroenterol* 2004; 10(12): 1838-1840

http://www.wjgnet.com/1007-9327/10/1838.asp

INTRODUCTION

Penetration into the liver is a rare complication of peptic ulcer disease and may lead to unusual complications such as abscess formation or upper gastrointestinal hemorrhage[1,2]. The absolute frequency of this complication in patient with peptic ulcers is not known.

We reported on a patient who presented with upper gastrointestinal bleeding due to a gastric ulcer penetrating into the liver. Diagnosis was based on histologic examination of endoscopic biopsy materials. We also reviewed 13 other reported cases of endoscopically and histologically diagnosed peptic ulcer penetration into the liver[2-13].

CASE REPORT

A 64-year-old man was admitted because of a 2-wk history of weekness, dizziness, and melena. One week before his admission, the patient noted intermittent mild mid-epigastric pain and nause after meals. He had undergone a higly selective vagotomy and primer suture 13 years before for peptic ulcer perforation.

Phiysical examination demonstrated that he was afebrile with a regular heart rate at 88 beats/min and a blood pressure of 110/60 mm Hg. The abdomen was soft, nontender, nondistended, and without organomegaly or masses. Bowel sounds were hyperactive. Rectal examination revealed no masses and the stool was melenic. A nasogastric tube was passed in emergency room, "coffe grounds" material were aspirated from the stomach. Initial laboratory evaluation showed mild leukocytosis (white blood cell counts, 15 800/mm^3; normal, 4-10 10^3/mm^3) and severe anemia (hemoglobin, 4.7 g/dL; normal hemoglobin,14.1 –17.2 g/dL: hematocrit, 13.8%; normal hematocrit, 36.1-50.3%: mean red cell volume, 68.2 fL; normal red cell volume, 82.2-99 fL). The stool was positive for occult blood. Coagulation parameters and liver function tests were within normal limits. The patient had no gastrointestinal symptoms and was not receiving aspirin or nonsteroidal antiinflammatory drugs (NSAIDs). Emergency endoscopy showed a large (4.5 cm) ulcer on the anterior wall of the gastric antrum, with malignant appearance (Figure 1). The ulcer base was covered with fibrin, and the margins were irregular. No active bleeding was present at the time of investigation, but stigmata of recent hemorrhage were detected. Sonographic examination demostrated the "target" sign of the gastric antral area with suggestion of eccentric "tumour" extension into liver (Figure 2). The center of the target was echogenic. Multipl biopsies were taken separately from the ulcer margins and the pseudotumoral mass. Histologic examination of the specimens showed gastric mucosa with granulation tissue and also normal-appearing hepatocytes (Figure 3).

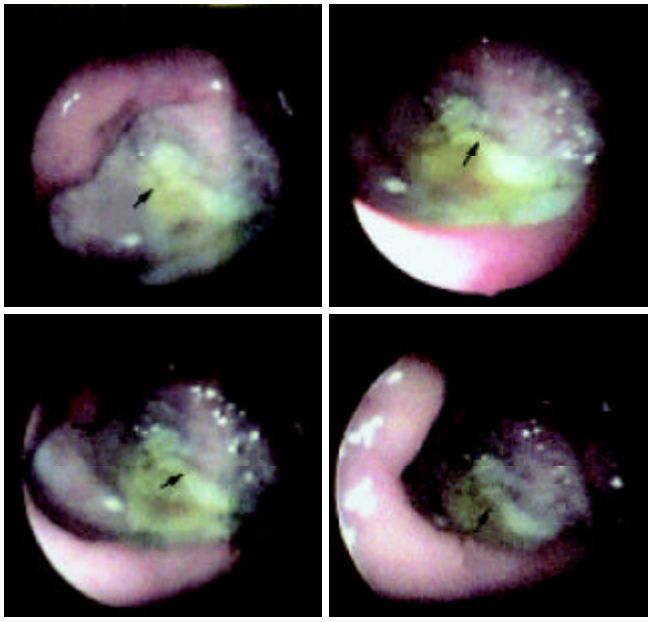

Figure 1 Endoscopic photograph showing a giant deep ulcer (about 4.5 cm in diameter) with malignant appearance (arrow).

Figure 2 Longitudinal ultrasound scan showing the target like appearance (arrows) representing the giant ulcer seen on gastroscopy.

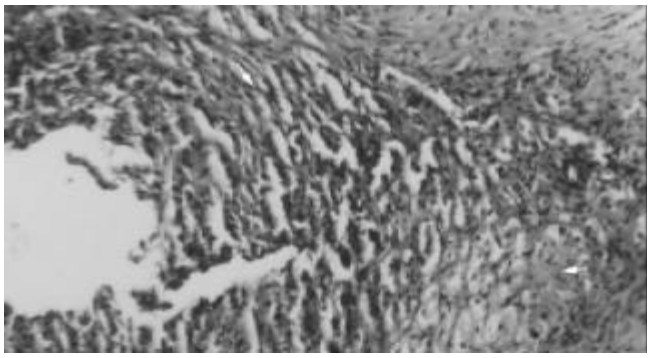

Figure 3 Endoscopic biopsy showing granulation tissue (arrowhead) adjacent to normal-appearance hepatocytes (arrow) (HE ×20).

Urease (CLO test) for *Helicobacter pylori* was negative. Treatment was started with 40 mg of omeprazole twice per day. He received 4 units of packed red blood cells by transfusion. The symptoms improved. The surgery service was than consulted for potential resection, however the patient and family refused surgical intervention. On the 17th d of hospitalization, he died of gastrointestinal bleeding.

DISCUSSION

We reported a very rare case of an endoscopically and histologically proven liver penetration by a gastric ulcer in an older man. In general, penetration into the liver by a peptic ulcer is not a frequent event. We have found only a few reports of liver penetration by gastric ulcer diagnosed by endoscopy . None of them was clinically or radiologically recognised prior to endoscopy. There were thirteen previous case reports of liver penetration in patients with peptic ulcer disease. Four of these cases were for duedonal ulcer and nine were for gastric ulcer. Three of these cases could be diagnosed at the time of surgery, but the other cases were diagnosed on the basis of histologic finding of hepatic tissue on endoscopic biopsies. All of the patients, including ours, showed severe gastrointestinal bleeding. Abdominal pain was described in only 4 patients[7,8,11,13], thus in our case, abdominal pain did not seem to be a common finding. These case reports, including the present one, are summarized in Table1.

Endoscopically, 3 of the patients had a large ulcer crater with a pseudotumoral mass protruding from the ulcer bed, however no histologic signs of malignancy were seen[2,6,7]. Another patient had only a mass without any ulcer[5]. The rest of them had ulcers ranging from 2.5 cm to 9 cm×3 cm in diameter.

The correct diagnosis was established in all the cases by the presence of liver tissue in the histologic examination of endoscopic biopsies. In contrast to the cases, described by Guerrieri and Waxman[9], the liver tissue in this case did not show severe inflammation or inflammatory atypia. The hepatic histological changes found in our case were consistent with those reported by others. All reported cases except two[6,9] had normal liver function tests. This may reflect that local hepatic injury does not cause abnormalities in liver functions. The diagnostic value of liver function tests in cases of ulcer penetration into the liver is very limited.

Table 1 Comparison of published reports of liver penetration by peptic ulcer

Source	Age / Gender	Epigastric Pain / tenderness	Main clinical feature	Location	Endoscopic appearance	NSAIDs	Treatment
Martinez-onsurbe (10)	91 / Female	-	GI bleeding	Anterior wall of antrum	ulcer	?	?
Guerrieri (9)	53 / Male	-	GI bleeding	Lesser curve of antrum	ulcer	?	Antiacids,Op (BII)
Goldman (6)	65 / Male	Tenderness	Nause,anemia	Lesser curve of stomach	ulcer with mass	?	Op (BII)
Park (4)	52 / Male	-	GI bleeding	Lesser curve of antrum	giant ulcer	?	H_2RA
Sperber (3)	69 / Male	Tenderness	GI bleeding	Lesser curve of corpus	ulcer	?	?
Jimenez-Perez(2)	61 / Male	Tenderness	GI bleeding	Lesser curve of corpus	ulcer with mass	?	Op
Castellano (11)	77 / Male	-	GI bleeding	posterior wall of duodenal bulb	ulcer	+	Op (BII)
Castellano (11)	70 / Male	Epigastric pain	GI bleeding	posterior wall of antrum	ulcer	?	Op (BII)
Matsuoka (12)	53 / Male	Tenderness	GI bleeding	Lesser curve of corpus	Giant ulcer	?	H_2RA,Op
Novacek(8)	33 / Female	Epigastric pain	GI bleeding	Posterior wall of duodenal bulb	ulcer	+	PPI,Op
PaddaS (5)	78 / Male	-	GI bleeding	Anterior wall of duodenal bulb	Mass without ulcer	+	H_2RA,Op
Brullet (7)	89 / Female	Epigastric Pain	GI bleeding	Anterior wall of gastric antrum	ulcer with mass	?	Op (BII)
Mostbeck(13)	53 / Male	Epigastric pain	-	Anterior wall of duodenal bulb	ulcer	?	?
Present case	61 / Male	-	GI bleeding	Anterior wall of gastric antrum	giant ulcer	-	PPI

GI Bleeding: gastrointestinal bleeding; Op (BII): subtotal gastrectomy with Billroth II reconstruction; H_2RA: histamine H_2- receptor antagonist; PPI,: proton pump inhibitor.

Larger lesions of the upper gastrointestinal tract have some charecteristic sonographic patterns. These have been described variously as ring sign, pseudo-kidney, target-like and bull's-eye[13,14]. Ultrasonographic examination of the present case showed a 'target' lesion with echogenic centre in the gastric antral area with suggestion of exogastric extension into the liver, leading to the suspicion of hepatic penetration by a gastric tumor as described by Sperber[3]. The center of the ulcer appeared as cavity lesions (hypoechoic area) which were considered secondary to fluid secretions within the cavity of the giant ulcer. Endoscopic ultrasonography is useful for the diagnosis and treatment of a variety of gastrointestinal diseases. We could not perform endoscopic ultrasonography because of its absence in our unit. Endoscopic ultrasonography may be helpful for the diagnosis of gastric ulcer complications such as penetration into an adjacent structure[15]. Only one of the patients was treated succesfully with a histamine H_2-receptor antagonist[4], but an operation was necessary for all other patients. A subtotal gastrectomy with Billroth II reconstruction was performed in 5 cases[6,7,9,11]. In the present case, the patient did not require an emergency operation and was initially treated with a proton pump inhibitor. All patients had uneventful postoperative courses except for 2 patients,of them one died of a sepsis[7], and the other died of pulmonary embolism[11]. The outcome was not given in 3 cases[3,10,13]. These reports indicate that penetration as a serious complication of peptic ulcer disease often required operative treatment. Results of a recent study have not shown a decrease in severe ulcer complications despite the use of histamine- H_2 receptor antagonists[16]. This was likely due to the increase, mean population age in developed countries and the high prevalence of nonsteroidal anti-inflammatory drug use. Lanas *et al*, found that NSAID use was the most important independent risk factor for upper and lower gastrointestinal perforation[17]. Endoscopic studies have shown an increase in the prevalence of peptic ulcers and gastrointestinal perforation in patients who took NSAÝDs regularly[18]. Only three of these cases were regularly using NSAÝDs[5,8,11]. Nonsteoridal antiinflammatory drugs, therefore, seem to be the most important risk factor for ulcer penetration into the liver.

Finally, as in other reported cases, results of the liver function tests in our patient were unremarkable and so did not focalise our attention on the probability of liver process. Endoscopic view of the lesion did not make us suspect penetrating peptic ulcer disease. However, ultrasound was the first procudure to raise suspicion of hepatic penetration by a gastric ulcer. This diagnosis was subsequently confirmed by endoscopic biopsy. A high index of suspicion to make the diagnosis is necessary.

REFERENCES

1 **Isenberg JI**, McQuaid KR, Laine L, Rubin W. Acid peptic disorders In: Yamada T, eds. Text book of gastroenterology. *Philadelphia: J.B Lippincott company* 1991: 1241-1340

2 **Jimenez-Perez FJ,** Munoz-Navas MA. Endoscopic diagnosis of gastric peptic ulcer penetrating into the liver. *Endoscopy* 1991; **23**: 98-99

3 **Sperber AD,** Fenyves D, Barky Y, Yanai-Inbar I, Levy Y. Penetration of gastric ulcers. *Dig Dis Sci* 1991; **36**: 700-702

4 **Park RH,** Russell RI. Liver penetration by peptic ulcer. *Am J Gastroenterol* 1988; **83**: 793

5 **Padda SS,** Moraless TG, Earnest DL. Liver penetration by a duodenal ulcer. *Am J Gastroenterol* 1997; **92**: 352-354

6 **Goldman IS.** Endoscopic diagnosis of hepatic penetration into a gastric ulcer. *Am J Gastroenterol* 1988; **83**: 589-590

7 **Brullet E,** Campo R, Calvet X, Gimenez A. Gastric ulcer penetrating to the liver: endoscopic diagnosis. *Am J Gastroenterol* 1993; **88**: 794-795

8 **Novacek G,** Geppert A, Kramer L, Wrba F, Herbst F, Schima W, Gangl A, Potzi R. Liver penetration by a duodenal ulcer in a young woman. *J Clin Gastroenterol* 2001; **33**: 56-60

9 **Guerrieri C**, Waxman M. Hepatic tissue in gastroscopic biopsy: evidence of hepatic penetration by peptic ulcer. *Am J Gastroenterol* 1987; **82**: 890-893

10 **Martinez-Onsurbe P,** Ruiz-Villaespesa A, Gonzales-Estecha A, Butron-Vila M, de la Iglesia-Ramos M. Cytodiagnosis of gastric ulcer penetration of the liver by examination of endoscopic brushings. *Acta Cytol* 1991; **35**: 464-466

11 **Castellano G,** Galvao A, Vargas J, Canga F, Moreno D, Sanchez F, Solis Herruzo JA. The diagnosis of peptic ulcer penetration in to the liver by endoscopic biopsy. A report of 2 cases and a rewiev of the literature. *Rev Esp Enferm Dig* 1992; **82**: 235-238

12 **Matsuoka T,** Nagai Y, Muguruma K, Yoshikawa K, Higuchi K, Seki S, Satake K. Liver penetration and gastrobronchial fistula: unusual complication of a peptic ulcer. *Am Surg* 1995; **61**: 492-494

13 **Mostbeck G,** Mallek R, Gebauer A, Tscholakoff D. Hepatic penetration by duodenal ulcer: sonographic diagnosis. *J Clin Ultrasound* 1990; **18**: 726-729

14 **Morgan CL,** Trought WS, Oddson TA, Clark WM, Rice RP. Ultrasound patterns of disorders affecting the gastrointestinal tract. *Radiology* 1980; **135**: 129-135

15 **Nakazawa S.** Recent advances in endoscopic ultrasonography. *J Gastroenterol* 2000; **35**: 257-260

16 **Petersen H.** Over the counter sales of histamine-2 receptor antagonists. *Scand J Gastroenterol Suppl* 1988; **155**: 20-22

17 **Lanas A,** Serrano P, Bajador E, Esteva F, Benito R, Sainz R. Evidence of aspirin use in both upper and lower gastrointestinal perforation. *Gastroenterology* 1997; **112**: 683-689

18 **Higham J,** Kang JY, Majeed A. Recent trends in admissions and mortality due to peptic ulcer in England: increasing frequency of haemorrhage among older subjects. *Gut* 2002; **50**: 460-464

Edited by Wang XL and Xu FM

PO Box 2345, Beijing 100023, China
Fax: +86-10-85381893
E-mail: wjg@wjgnet.com www.wjgnet.com

World J Gastroenterol 2004;10(12):1841-1843
World Journal of Gastroenterology
Copyright ©2004 by The WJG Press ISSN 1007-9327

• CASE REPORTS •

Inflammatory pseudotumor of the liver in association with a gastrointestinal stromal tumor: A case report

Oswens S. Lo, Ronnie T. Poon, Chi Ming Lam, Sheung Tat Fan

Oswens S. Lo, Ronnie T. Poon, Chi Ming Lam, Sheung Tat Fan, Centre for the Study of Liver Disease and Department of Surgery, The University of Hong Kong, Pokfulam, Hong Kong, China
Correspondence to: Dr. Ronnie T. Poon, Department of Surgery, University of Hong Kong Medical Centre, Queen Mary Hospital, 102 Pokfulam Road, Hong Kong, China. poontp@hkucc.hku.hk
Telephone: +852-28553641 **Fax:** +852-28175475
Received: 2003-10-20 **Accepted:** 2003-12-30

Abstract

Inflammatory pseudotumor of the liver is a rare benign lesion that can mimic a malignant liver neoplasm. A case of inflammatory pseudotumor of the liver found in association with a malignant gastrointestinal stromal tumor (GIST) of the small bowel was reported. The inflammatory pseudotumor was misdiagnosed as a metastasis from the GIST by frozen section. A correct diagnosis was made only after histopathological examination of the paraffin section of the resected specimen. This case is particularly interesting because of the association of the two rare pathological entities and the diagnostic dilemma that arose from the similarity of their histological appearances. To our knowledge, this association has not been reported in the literature.

Lo OS, Poon RT, Lam CM, Fan ST. Inflammatory pseudotumor of the liver in association with a gastrointestinal stromal tumor: A case report. *World J Gastroenterol* 2004; 10(12): 1841-1843
http://www.wjgnet.com/1007-9327/10/1841.asp

INTRODUCTION

Inflammatory pseudotumors of the liver are rare benign lesions characterized by proliferating fibrovascular tissue mixed with inflammatory cells. They are associated with fever, pain and a mass effect, and are commonly mistaken for malignant tumors or liver abscesses. Usually the radiological or cytological examinations fail to differentiate hepatic pseudotumors from liver neoplasms. We report a patient with an inflammatory tumor of the liver who was found to have a malignant gastrointestinal stromal tumor (GIST) of the small bowel at the same time, with special emphasis on their possible etiological association and the diagnostic dilemma.

CASE REPORT

A 46-year-old housewife was admitted to our hospital in January 1998 with right upper quadrant abdominal pain and low grade fever for one week. Blood tests showed leukocytosis (16.7×10^9/L) and raised erythrocyte sedimentation rate (ESR) (92 mm/h). Serum alkaline phosphatase (138IU/L) was slightly increased but hepatic parenchymal enzymes were normal. The levels of serum alpha-fetoprotein (AFP) and carcinoembryonic antigen (CEA) were within normal ranges. Hepatitis B and C viral serology tests were negative. Repeated blood culture did not reveal any bacterial growth.

In view of the mildly deranged liver function, an abdominal ultrasonography was performed which showed a space-occupying lesion in the right hepatic lobe. No dilated intrahepatic or common bile ducts were noted. Helical computer tomography (CT) scan showed a heterogeneous lesion of 10 cm in size in the right lobe of the liver (Figure 1). The right portal vein was displaced anteriorly. Radiologist commented that it could be a large multi-septated liver abscess, but the possibility of a liver tumor could not be excluded.

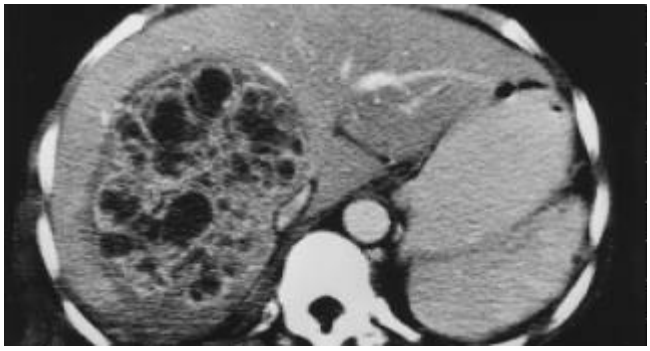

Figure 1 Contrast CT scan showing heterogeneous contrast enhancement in the lesion with a multi-septated appearance.

The patient was treated initially with intravenous cefotaxime and metronidazole, and the fever subsided after 1 wk of antibiotics treatment. However, due to the large size of the lesion and the worry about possible malignancy, surgical exploration was decided. Intraoperatively, in addition to the liver mass, a 10 cm soft tissue tumor was found in the ileum at 15 cm from the ileocecal valve. The tumor and a segment of the small bowel were resected and frozen section examination showed a spindle cell tumor. Trucut biopsy of the liver mass and frozen section suggested a metastastic spindle cell tumor. In view of an isolated hepatic metastasis without lymph node involvement or other evidence of metastasis, an extended right hepatectomy with a 1 cm resection margin from the tumor was performed (Figure 2).

Figure 2 Yellowish firming well-circumscribed mass in the right hepatectomy specimen.

Histopathological examination of the paraffin section of the small bowel tumor confirmed the diagnosis of a malignant GIST. Microscopic examination of the paraffin section of the liver "tumor" showed that it was composed of fascicles of spindle fibroblasts and myofibroblasts admixed with chronic inflammatory cells, which were mainly lymphocytes and plasma cells. The overall pathological features were those of an inflammatory pseudotumor of the liver.

The patient recovered well after the operation and was discharged without complication. The patient had regular follow-up in our outpatient clinic with yearly CT scan. After 4 years of follow-up, the patient was in good health and there was no evidence of tumor recurrence or further liver lesion.

DISCUSSION

Inflammatory pseudotumor of the liver is a rare clinical and pathological entity. Pack and Baker first described it in a patient after right hepatic lobectomy in 1953[1]. To date, there have been fewer than 80 cases reported in the literature[2-7]. These "tumors" were so named because of the difficulty in distinguishing them from malignant lesions preoperatively, as in the case of our patient. Histologically, these tumors are composed of densely hyalinized collagenous tissue infiltrated by a variety of cells, mainly plasma cells and the enigmatic plump spindle cells, although monocytes and lymphocytes have also been found[3]. The pathogenesis and etiology of inflammatory pseudotumors of the liver are uncertain. Some authors suggested that they might be attributed to a septic origin from aberrant inflammatory reaction to migrating microorganisms from large bowel[2]. Though bacterial culture growths, such as Escherichia coli and Klebsiella pneumoniae, have been reported in a few cases[8], no definite microorganism could be isolated from the specimens in most cases. Other authors suggested that Epstein Barr viral infection might play a role in the pathogenesis of inflammatory pseudotumors[9], but this still needs to be verified by further studies.

In the reported cases, patients with an inflammatory pseudotumor of the liver usually complained of non-specific symptoms at first presentation, such as abdominal pain, fever, weight loss and malaise. Elevated ESR, leukocytosis and mildly elevated hepatic transaminases and bilirubin were typical. Inflammatory pseudotumor has been reported in children as young as 3 mo of age and in adults up to 83 years of age[4,5], with male preponderance. Schmid reported that more patients with inflammatory pseudotumors were observed in Southeast Asians (54.7%) when compared with other Western counterparts[4]. As hepatitis B infection is common in Southeast Asia, hepatocellular carcinoma is the most common liver tumor encountered in this area. However, inflammatory pseudotumor should be included in the differential diagnosis of a hepatic mass, especially in those patients with normal hepatitis B screening and AFP level.

The recommended therapeutic approach for inflammatory pseudotumors of the liver is still controversial, though surgical resection is generally considered as an overtreatment[8,10]. Spontaneous regression of the lesion was reported in some cases, and cases that regressed with the use of antibiotics[11] or nonsteroidal anti-inflammatory drugs[12] have also been reported. When the inflammatory pseudotumors caused major complications, such as biliary obstruction[13] and portal hypertension[14], the patients might need surgical resection or even liver transplantation[15]. Although most authors believed that inflammatory pseudotumors had a benign behavior, there have been some reports of invasive course and mortality[2].

To our knowledge, this is the first patient reported to have an inflammatory pseudotumor in association with a small bowel GIST. The exact etiological link between the two is uncertain. However, the presence of an ileal GIST could potentially enhance entry of enteric bacteria into the portal circulation, which could then result in an inflammatory pseudotumor if the hypothesis of an infective etiology is true. In our patient, frozen section examination of the hepatic mass suggested that it was a metastasis from the malignant small bowel GIST, but we proceeded with hepatic resection in view of the absence of other obvious extrahepatic metastasis. In the past, patients with hepatic metastases from malignant GIST or leiomyosarcoma were considered to have poor prognosis even after surgical resection[16,17]. Hence, hepatic resection was usually not offered to patients with liver metastasis from gastrointestinal leiomyosarcoma. However, recently some authors advocated that aggressive surgical resection for liver metastasis might provide survival benefit to the patients[18,19]. In a recent report from a single institution, a median survival of 40 mo and a 5-year survival rate of 33% were observed after hepatic resection for hepatic metastases from leiomyosarcoma[17]. We adopted a similar approach and performed a major hepatectomy. The final pathology of the liver lesion turned out to be an inflammatory pseudotumor, and the patient had survived without any disease recurrence for four years by the time of writing the manuscript. Our case illustrated the difficulty in differentiating an inflammatory pseudotumor from a malignancy not only in the preoperative imaging but also even by frozen section examination. The histological appearance of an inflammatory pseudotumor and a GIST is particularly difficult to differentiate. The surgeons should be aware of their possible association as illustrated in this case. A favorable long-term outcome may be expected with resection of the GIST together with hepatic resection for the inflammatory pseudotumor in the liver.

REFERENCES

1 **Pack G,** Backer H. Total right hepatic lobectomy. Report of a case. *Ann Surg* 1953; **138:** 253-258

2 **Horiuchi R,** Uchida T, Kojima T, Shikata T. Inflammatory pseudotumor of the liver. Clinicopathologic study and review of the literature. *Cancer* 1990; **65:** 1583-1590

3 **Shek TW,** Ng IO, Chan KW. Inflammatory pseudotumor of the liver. Report of four cases and review of the literature. *Am J Surg Pathol* 1993; **17:** 231-238

4 **Schmid A,** Janig D, Bohuszlavizki A, Henne-Bruns D. Inflammatory pseudotumor of the liver presenting as incidentaloma: report of a case and review of the literature. *Hepatogastroenterology* 1996; **43:** 1009-1014

5 **Lee SL,** DuBois JJ. Hepatic inflammatory pseudotumor: case report, review of the literature, and a proposal for morphologic classification. *Pediatr Surg Int* 2001; **17:** 555-559

6 **Ciftci AO,** Tanyel FC. Inflammatory pseudotumor of the liver. *J Pediatr Surg* 2001; **36:** 1737-1738

7 **Sakai M,** Ikeda H, Suzuki N, Takahashi A, Kuroiwa M, Hirato J, Hatakeyama SI, Tsuchida Y. Inflammatory pseudotumor of the liver: case report and review of the literature. *J Pediatr Surg* 2001; **36:** 663-666

8 **Torzilli G,** Inoue K, Midorikawa Y, Hui AM, Takayama T, Makuuchi M. Inflammatory pseudotumors of the liver: prevalence and clinical impact in surgical patients. *Hepatogastroenterology* 2001; **48:** 1118-1123

9 **Arber DA,** Weiss LM, Chang KL. Detection of Epstein-Barr Virus in inflammatory pseudotumor. *Semin Diagn Pathol* 1998; **15:** 155-160

10 **Gluszek S,** Kot M, Czerwaty M. Inflammatory pseudotumor of the liver treated surgically. *Hepatogastroenterology* 1999; **46:** 2959-2960

11 **Jais P,** Berger JF, Vissuzaine C, Paramelle O, Clays-Schouman E, Potet F, Mignon M. Regression of inflammatory pseudotumor of the liver under conservative therapy. *Dig Dis Sci* 1995; **40:**

752-756
12 **Hakozaki Y,** Katou M, Nakagawa K, Shirahama T, Matsumoto T. Improvement of inflammatory pseudotumor of the liver after nonsteroidal anti-inflammatory agent therapy. *Am J Gastroenterol* 1993; **88:** 1121-1122
13 **Pokorny CS,** Painter DM, Waugh RC, McCaughan GW, Gallagher ND, Tattersall MH. Inflammatory pseudotumor of the liver causing biliary obstruction. Treatment by biliary stenting with 5-year follow-up. *J Clin Gastroenterol* 1991; **13:** 338-341
14 **Heneghan MA,** Kaplan CG, Priebe CJ Jr, Partin JS. Inflammatory pseudotumor of the liver: a rare cause of obstructive jaundice and portal hypertension in a child. *Pediatr Radiol* 1984; **14:** 433-435
15 **Kim HB,** Maller E, Redd D, Hebra A, Davidoff A, Buzby M, Hoffman MA. Orthotopic liver transplantation for inflammatory myofibroblastic tumor of the liver hilum. *J Pediatr Surg* 1996; **31:** 840-842
16 **DeMatteo RP,** Lewis JJ, Leung D, Mudan SS, Woodruff JM, Brennan MF. Two hundred gastrointestinal stromal tumors: recurrence patterns and prognostic factors for survival. *Ann Surg* 2000; **231:** 51-58
17 **Lang H,** Nussbaum KT, Kaudel P, Fruhauf N, Flemming P, Raab R. Hepatic metastases from leiomyosarcoma: A single-center experience with 34 liver resections during a 15-year period. *Ann Surg* 2000; **231:** 500-505
18 **Chen H,** Pruitt A, Nicol TL, Gorgulu S, Choti MA. Complete hepatic resection of metastases from leiomyosarcoma prolongs survival. *J Gastrointest Surg* 1998; **2:** 151-155
19 **DeMatteo RP,** Shah A, Fong Y, Jarnagin WR, Blumgart LH, Brennan MF. Results of hepatic resection for sarcoma metastatic to liver. *Ann Surg* 2001; **234:** 540-547

Edited by Wang XL **Proofread by** Xu FM

PO Box 2345, Beijing 100023, China
Fax: +86-10-85381893
E-mail: wjg@wjgnet.com www.wjgnet.com

World J Gastroenterol 2004;10(12):1844-1847
World Journal of Gastroenterology
Copyright ©2004 by The WJG Press ISSN 1007-9327

• CASE REPORTS •

Human cyclosporiosis in Turkey

Süleyman Yazar, Saban Yalcln, Ýzzet Sahin

Süleyman Yazar, Saban Yalcın, Ýzzet Sahin, Department of Parasitology, Medical Faculty, Erciyes University, 38039, Kayseri-Turkey
Correspondence to: Süleyman Yazar, Department of Parasitology, Medical Faculty, Erciyes University, 38039, Kayseri, Turkey. syazar@erciyes.edu.tr
Telephone: +90-352-4374937 **Fax:** +90-352-4375285
Received: 2003-10-08 **Accepted:** 2004-01-09

Abstract

Six patients infected with *Cyclospora cayetanensis* who sought medical care at three different hospitals in Turkey are herein presented. Four patients were male and the others were female and their ages ranged from 7 to 62 years. The first patient was HIV-positive and presented with watery diarrhea with a frequency of up to 18 times a day for more than ten months and diagnosed as cyclosporiosis in Kayseri, 1996. The second patient was also HIV positive and diagnosed as cyclosporiosis in Kayseri, 2000. The third patient was an acute myeloblastic leukemia (AML) patient and diagnosed in Istanbul, 2000. The fourth patient was idiopathic hepatic cirrhosis complaining of diarrhea and weakness and diagnosed in Kayseri, 2001. The fifth and sixth patients were immunocompetent patients complaining of diarrhea and diagnosed in Izmir and Kayseri, 2002. Diarrhea occurring from one to ten times a day continued for 7 to 70 d in the last 5 patients. Treatment with a trimethoprim/sulfamethoxazole compound was done for all patients. Both symptomatic and parasitologic improvements were quickly observed. In summary, *C. cayetanensis* infection is rare in Turkey and most patients infected with this pathogen tend to be immunosuppressive individuals at present.

Yazar S, Yalcln S, Sahin ý. Human cyclosporiosis in Turkey. *World J Gastroenterol* 2004; 10(12): 1844-1847
http://www.wjgnet.com/1007-9327/10/1844.asp

INTRODUCTION

The genus *Cyclospora* is in the subclass Coccidia, phylum Apicomplexa. This genus is taxonomically related to coccidian genera in humans. This organism is a unilocular parasite previously known as cyanobacterium-like or coccidian-like body (CLB) and, in recent years, a new coccidian pathogen, *Cyclospora*, has been putatively identified[1,2]. The organisms are seen as nonrefractile spheres and are acid-fast variable with the modified Kinyoun's acid-fast stains, those are unstained appear as glassy, wrinkled spheres. Modified acid-fast stains stain the oocysts from light pink to deep red, some of which may contain granules or have a bubbly appearance. The oocysts autofluoresce (strong green or intense blue) under UV epifluorescence[3]. The first known human cases of illness caused by *Cyclospora* infection (i.e., cyclosporiosis) were reported in the medical literature in 1979[4]. Our aim in this study was to present cases of human cyclosporiosis in Turkey and to review the literature.

MATERIALS AND METHODS

We evaluated all of the human cases in our country retrospectively which were belongs to Kayseri (three cases), Istanbul (one case) and Izmir (one case) regions between 1996 and 2002[5-9]. Following these, we determined a new case with *C. cayetanensis* in December 2002. In this study, we discuss all of the six cases with cyclosporiosis in Turkey.

RESULTS

Case 1[5]

A 50 year-old woman with acquired immune deficiency syndrome (AIDS) was admitted in December 1996 for chronic diarrhea, vomiting, and fever to the Erciyes University Medical Faculty Hospital. There was preceding history of episodic watery diarrhea, vomiting, and weight loss along with intermittent fever over a period of one year. She was cachectic, with mild abdominal tenderness and alert, thrush and palpable small cervical lymph nodes. She had anemia (Hb 8.4 g/L). Enzyme immunoassays for HIV antibodies were positive and the T4/T8 ratio was 0.6 in serum. *E. coli* and *Proteus* spp. were found at 10^4 cfu/mL from urine specimens. Microscopical analysis of the stool revealed numerous spherical double walled microorganisms 8-9 μm in diameter, some with internal granulation. After Kinyoun's acid fast staining of the stool, the organisms appeared faint pink to red in colors, some cysts not taking up the stain and appearing as "ghosts" . Empty cysts varied in shape but had generally collapsed into crescents. The organisms were identified as *Cyclospora* sp. The patient was treated with TMP/SMZ (160/800 mg) bid for three weeks. Following treatment, re-examination of a stool sample revealed no more organisms and diarrhea stopped. This case was the first report of *Cyclospora* infection in Turkey.

Case 2[6]

A 40-year old man with AIDS was evaluated parasitologically for the etiologic agent of his persistent diarrhea for two months in Erciyes University Medical Faculty Hospital in 2000. Stool samples were examined by conventional coprological methods such as fresh preparation, iodine stain, and flotation. Suspicious organisms (8-10 μm in diameter) were seen in stool, which were stained with Kinyoun's acid-fast stain and identified as *C. cayetanensis*. He was treated with TMP/SMZ (160/800 mg) bid for two weeks. We could not find the organism in the stool samples after the treatment and diarrhea stopped.

Case 3[7]

In 2000, at the Istanbul University Medical Faculty Hospital there was another 7 year-old male patient with acute myeloblastic leukemia (AML). A sudden diarrhea developed while bone narrow transplantation was being planned. The patient's stool samples were examined with respect to pathogen bacteria and fungi and rotavirus. None of them was determined, isolated and/or seen. Two stool specimens, which were taken in one-week interval, also were examined with modified trichrome, acid fast and safranin staining methods. In microscopic examinations, *C. cayetanensis* oocysts were seen with all three staining methods. After four weeks of therapy with trimethoprim-sulphamethoxazole (15 mg/kg.d) diarrhea stopped and in the new stool specimens, *C. cayetanensis* oocysts were not encountered.

Case 4[8]

A 52 year-old male patient with idiopathic hepatic cirrhosis

complaining of diarrhea and weakness was accepted to the gastroenterology clinic of Erciyes University Medical Faculty Hospital in 2001. In the patient's history, there were watery, bad smelling, bloodless episodes of diarrhea, fever, cold, sweating, and a 10 kg lost of weight which all began three weeks prior to hospitalization. The patient had never traveled to a foreign country. Physical examination did not reveal any abnormalities except subicteric conjunctivas and a hyperemic tongue. The patient was apyretic. In laboratory examination, blood values were found as Hb: 14.2 g/dL, white blood cells: 4 900/mm^3 , platelets: 69 000/mm^3 . Biochemical values were as follows: K: 2.9 mmol//L (↑), *P*: 1.7 mg/dL (↑), Ca: 7.6 mg/dL (↑), Mg: 0.9 mg/dL (↑), uric acid: 9.3 mg/dL (↑), total bilirubin: 4.2 mg/dL (↑), AST: 165 U/L (↑), ALT: 76U/L (↑), CK-MB: 120 U/L (↑), albumin: 2.8 gr/dL (↑), acetone, protein and bilirubin were (+) in urine. Anti-HBs Ag and Anti-HAV were positive and other hepatitis markers were negative. Anti-HIV antibodies were found to be negative by ELISA test. In abdominal USG, liver with lobule contour was smaller than normal size, and its echo was increased. Widespread intraperitoneal exudate was seen.

In order to find out the causative etiologic agent of diarrhea, stool samples were examined by different methods and stained using modified Kinyoun's acid-fast stain. Following examination, acid-fast variable wrinkled spheres approximately 9 µm in diameter, were seen and diagnosed as *C. cayetanensis*. Confirmation of the diagnosis was established by fluorescent microscope (380 to 420 nm excitation filter), which showed bright green to intense blue autofluorescent oocysts.

Consequently, this organism was diagnosed as *C. cayetanensis*. The patient was treated with TMP/SMZ (160/800 mg) bid for 7 d. Following treatment, re-examination of a stool sample, however, did not reveal the presence of any organisms.

Case 5[9]

A 30 year-old female patient complaining of diarrhea and weakness was admitted to the gastroenterology clinic of Atatürk State Hospital in I zmir, 2002. In the patient's history, there were watery diarrhea, fever, nausea which all began one week prior to admission to hospital**.** Stool samples were examined by conventional coprological methods such as fresh preparation, iodine stain, flotation, modified Ritchie's method and modified Kinyoun's acid-fast stain. Acid-fast variable wrinkled spheres were seen and diagnosed as oocysts of *C. cayetanensis*. Confirmation of the diagnosis was established by fluorescent microscope. After one-week therapy with trimethoprim-sulphamethoxazole for 7 d, diarrhea stopped and in the new stool specimens, *C. cayetanensis* oocysts were not seen. This patient was different from the other four cases in Turkey because there were no abnormalities in immunologic tests of the patient. That is, she was an immunocompetent patient.

Case 6

A 62-year-old male patient complaining of diarrhea was admitted to the Erciyes University Medical Faculty Hospital in October 2002. This case was not reported anywhere. In the patient's history, there were watery, bad smelling diarrhea, fever, sweating, which all began one week before admission to hospital. Stool samples were examined by conventional coprological methods. Acid-fast variable oocysts were seen and diagnosed as oocysts of *C. cayetanensis* (Figure 1).

After one-week therapy with trimethoprim-sulphamethoxazole (160/800 mg) bid for 7 d diarrhea stopped and in the new stool specimens, *C. cayetanensis* oocysts were not encountered and all the symptoms disappeared. This patient was also immunocompetent similar to case 5. There were no abnormalities in immunologic tests of the patient.

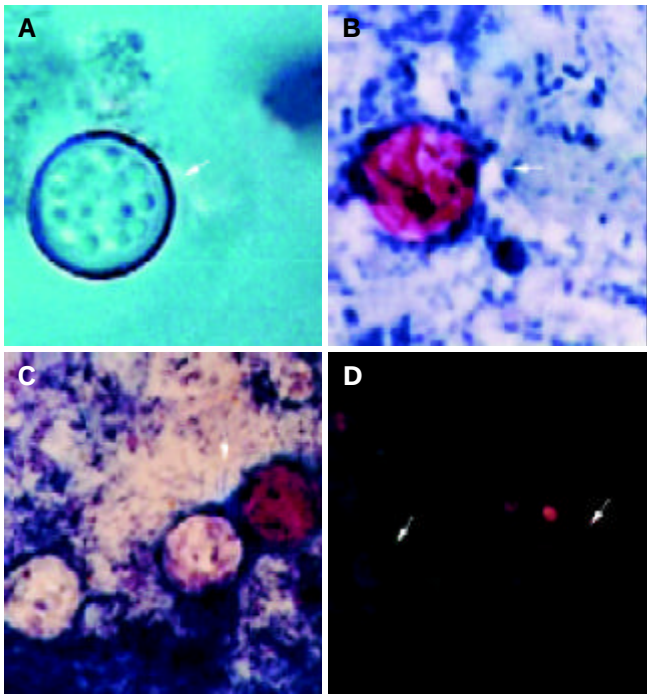

Figure 1 *Cyclospora* oocysts in stool smear preparations. A: *Cyclospora* oocysts in native preparation (original magnification. ×1 000). B: Acid-fast stained *Cyclospora* oocysts (Modified Kinyoun's acid-fast stain: original magnification. ×1 000). C: Acid-fast stained and unstained *Cyclospora* oocysts (Modified Kinyoun's acid-fast stain: original magnification. ×1 000). D: *Cyclospora* oocysts' autofluorescense in wet preparation with fluorescent microscope of 380-420 nm wavelength. (×400).

DISCUSSION

Cyclospora organisms were first reported in the intestines of moles in 1870 by Eimer, and Schneider introduced the genus *Cyclospora* in 1881. The first report of human *Cyclospora* infection came from Papua New Guinea in 1979[4].

Cyclospora oocysts in freshly excreted stool are non-infectious. The oocysts are thought to require days to weeks outside the host under favorable environmental conditions to sporulate and thus to become infectious. Direct person-to-person transmission by fecal exposure is unlikely, because excreted oocysts must sporulate to become infective[10].

C. cayetanensis constitutes a significant cause of chronic and intermittent diarrhea in immunocompromised patients especially those with AIDS. A study in Haiti has documented the occurrence of chronic diarrhea in most patients with AIDS[11]. *Cyclospora* infection has also been reported in patients with severe AIDS in other areas[12,13]. Lontie *et al*.[14] reported 2 cases of intestinal *Cyclospora* infection in immunocompetent Belgians. In Turkey, there were 6 cases between 1996 and 2002, 2 of them were AIDS patients[5,6], 1 of them was an AML patient[7], 1 of them was idiopathic hepatic cirrhosis[8] and the last two patients were immunocompetent individuals[9,10].

Both epidemiological and environmental data suggested that the organism be waterborne[1]. The transmissibility of *Cyclospora* through water depends on the probability that the water source of interest could become contaminated and that the water treatment would kill or remove oocysts. *Cyclospora* oocysts, like *Cryptosporidium* oocysts, probably are highly chlorine resistant, but they could be more easily removed by conventional filtration because they are about twice as big as *Cryptosporidium* oocysts[10].

In 1994, an outbreak of *Cyclospora* occurred among British soldiers and dependents stationed in a small military base detachment in Pokhara, Nepal. That outbreak was epidemiologically

Table 1 Similarities and differences between *Cryptosporidium parvum* and *Cyclospora cayetanensis*[10]

Similarities	*C. cayetanensis*	*C. parvum*
Acid-fast staining of oocysts	Variable acid-fast	Acid-fast
Number of infective units (sporozoites) per sporulated oocyst	4	4
Completion of life cycle within humans	Yes, except for sporulation	Yes
Multiplication outside the host (e.g. in water or food)	No	No
Differences		
Size of oocysts	8-10 μm in diameter (intermediate in size between *Cryptosporidium parvum* and *Isospora belli*)	Average width of 4.5 μm and average length of 5 μm
Number of organisms in stools of symptomatic nonimmune hosts	Typically excreted in low to moderate number	Often excreted in somewhat higher numbers
Autofluorescence of oocyst wall	Yes	No
Internal morphology of sporulated oocysts	Each oocyst has 2 internal sporocysts, each contains 2 sporozoites	The 4 sporozoites are naked within the oocyst
Infectivity of oocysts in freshly excreted stool	Must sporulate outside host to become infectious	Fully sporulated and infectious when excreted (sporozoites can be visualised when oocysts are excreted
Zoonotic potential	Host range unknown	Infects virtually all commonly known wild and domestic mammals
Location in enterocytes of small bowel	Intracytoplasmic within a parasitophorous vacuole in apical supranuclear region	Intracellular, extracytoplasmic, within a parasitophorous vacuole at luminal surface of enterocyte
Susceptibility to antimicrobial agents	Treatment with TMP-SMZ leads to both clinical and parasitologic cure	Some antimicrobial agents (e.g. paromomycin) may cause clinical improvement, but no agents has been consistently demonstrated to provide parasitologic cure

linked to drinking water, because the organism was identified in the water source[15].

In the 1990s, at least 11 definite and probable food born outbreaks of cyclosporiosis, affecting at least about 3 600 people, were documented, all of which occurred in North America[10]. The outbreak that brought cyclosporiosis to prominence in North America and definitively established that *Cyclospora* was transmissible through food, occurred in 1996 in the United States and Canada and was linked to a third country, Guatemala, which was the source of implicated fresh raspberries[16].

The symptoms presenting in one patient (watery diarrhea, nausea, weight loss, and abdominal pain) were similar to those classically *Cyclospora* infection[11,13,17]. Since the oocysts of *Cyclospora* are acid-fast like those of *Cryptosporidium*, we recommend that all laboratories screening for the latter parasite include precise measurements of oocysts. *Cyclospora* oocysts are 8-10 μm in diameter (intermediate size between *Cryptosporidium parvum* and *Isospora belli*). *Cryptosporidium parvum* oocyts have an average width and length of 4.5 μm 5 μm, respectively. It is possible that many cases of diarrhea reported to be due to *Cryptosporidium* might actually be due to *Cyclospora* because size discriminations are not often made. *Cyclospora* organisms have now been isolated in chronic diarrhea and this infection should be carefully distinguished from cryptosporidiosis[1,11,18]. A list of some of the similarities and differences between these two organisms is shown in Table 1.

The treatment for *Cyclospora* infections cotrimoxasole (TMP-SMZ) was given for 7-10 d (longer, if symptoms persist)[19]. The adult dosage was 160 mg TMP plus 800 mg SMZ orally twice daily. In a double blind, placebo controlled trial among Peruvian children, a three-day course of TMP (5 mg/kg.d) plus SMZ (25 mg/kg.d) decreased the duration of oocyst excretion, but few symptomatic children were treated to address the effect on duration of diarrhea[20]. Alternative treatments have not yet been identified. Limited data suggest that the following drugs are ineffective: albendazole, azithromycin, nalidixic asid, norfloxacin, tinidazole, metronidazole, quinacrine, tetracycline, and diloxanide furoate. Approaches to alternative treatment of patients who could not tolerate TMP-SMZ therapy include observation and symptomatic treatment[21-25]. In a small, randomized, controlled-trial comparing oral TMP-SMZ and ciprofloxacin for treatment of and secondary prophylaxis for *Cyclospora* infection in HIV infected Haitians, ciprofloxacin (500 mg twice daily for 7 d as therapy and thrice weekly for 10 wk as secondary prophylaxis) was moderately effective, though it was less active than TMP-SMZ[26]. These results suggest that ciprofloxacin might be an alternative for patients who cannot tolerate TMP-SMZ. However, these results should be confirmed in a large number of patients as well as in non-HIV population.

Sporadic cases of infection may be part of widespread outbreaks and should in any case be reported to public health officials. Pubic health personals and clinicians should also be aware that stool examination for *Cyclospora* should be specifically required in case of clinical suspicion of *Cyclospora* infection (protracted or relapsing diarrheal episode)[10]. In conclusion, this organism should be considered in the differential diagnosis of unexplained diarrhea in both immunosuppressive and immunocompetent patients. However, further studies are needed to confirm the causative association with other diseases and to determine the incidence and epidemiological features of this organism.

REFERENCES

1 **Long EG**, Ebrahimzadeh A, White EH, Swisher B, Callaway

CS. Alga associated with diarrhea in patient with acquired immunodeficiency syndrome and in travelers. *J Clin Microbiol* 1990; **28**: 1101-1104
2 **Ortega YR**, Sterling CR, Gilman RH, Cama VA, Diaz F. Cyclospora species a new protozoon pathogen of humans. *N Engl J Med* 1993; **328**: 1308-1312
3 **Garcia SL**, Bruckner AD. Intestinal protozoa: Coccidia and Microsporidia in Diagnostic medical parasitology. Washington, D.C: *American Society Microbiol* **1997**: 54-89
4 **Ashford RW**. Occurrence of an undescribed coccidian in man in Papua New Guinea. *Am Trop Med Parasit* 1979; **73**: 497-500
5 **Koc AN**, Aygen B, Sahin ý, Kayabas Ü. Cyclospora sp. associated with diarrhea in a patient with AIDS in Turkey. *Tr J Med Scien* 1998; **28**: 557-558
6 **Yazar S**, Aygen B, Koc AN, Altunoluk B, Alp E, Sahin I. A diarrheal case caused by Cyclospora cayetanensis: Case report. *Erciyes Med J* 2000; **22**: 48-51
7 **Büget E**, Büyükbaba BÖ, Kırkoyun UH, Agırbaslı H, Yalman N, Anak S, Can E, Gedikoglu G. Türkiye'de ilk kez belirlenen Cyclospora cayetanensis etkenli diyare olgusu. *J Turks Mic Soc* 2000; **30**: 162-165
8 **Yazar S**, Yaman O, Demirtas F, Yalcın S, Yücesoy M, Sahin ý. Cyclospora cayetanensis associated with diarhea in a patient with idiopathic compensated hepatic cirrhosis. *Acta Gastro-Enterol Belg* 2002; **65**: 241-244
9 **Turk M**, Turker M, Ak M, Karaayak B, Kaya T. Cyclosporiasis associated with diarrhoea in an immunocompetent patient in Turkey. *J Med Microbiol* 2004; **53**: 255-257
10 **Herwaldt BL**. Cyclospora cayetanensis: A review, focusing on the outbreaks of cyclosporiasis in the 1990s. *Clin Inf Dis* 2000; **31**: 1040-1057
11 **Pape JW**, Verdier RI, Boncy M, Boncy J, Johnson WD Jr. Cyclospora infection in adults infected with HIV clinical manifestations, treatment and prophylaxis. *Ann Intern Med* 1994; **121**: 654-657
12 **Madico G**, Gilman RH, Miranda E, Cabrera L, Sterling CR. Treatment of *Cyclospora* infection with co-trimoxasole. *Lancet* 1993; **342**: 122-123
13 **Hart AS**, Ridinger MT, Soundarajan R, Peters CS, Swiatlo AL, Kocka FE. Novel organisms associated with chronic diarrhea in AIDS. *Lancet* 1990; **335**: 169-170
14 **Lontie M**, Degroote K, Michiels J, Bellers J, Mangelschots E, Vandepitte J. Cyclospora sp.: a coccidian that causes diarrhea in travellers. *Acta Clin Belg* 1995; **50**: 288-290
15 **Rabold JG**, Hoge CW, Shlim DR, Kefford C, Rajah R, Echeverria P. Cyclospora outbreak associated with chlorinated drinking water. *Lancet* 1994; **344**: 1360-1361
16 **Herwaldt BL**, Ackers ML. Cyclospora working group. An outbreak in 1996 of cyclosporiasis associated with imported raspberries. *N Engl J Med* 1997; **336**; 1548-1556
17 **Albert MJ**, Kabir I, Azim T, Hossain A, Ansaruzzaman M, Unicomb L. Diarrhea associated with Cyclospora Sp. in Bangladesh. *Diagn Microbiol Infect Dıs* 1994; **19**: 47-49
18 **Soave R**. Cyclospora: An overview. *Clin Infect Dis* 1996; **23**: 429-437
19 **Hoge CW**, Shlim DR, Ghimire M, Rabold JG, Pandey P, Walch A, Rajah R, Gaudio P, Echeverria P. Placebo-controlled trial of cotrimoxazole for Cyclospora infections among travellers and foreign residents in Nepal. *Lancet* 1995; **345**: 691-693
20 **Madico G**, McDonald J, Gilman RH, Cabrera L, Sterling CR. Epidemiology and treatment of Cyclospora cayatanensis infection in Peruvian children. *Clin Infect Dis* 1997; **24**: 977-981
21 **Soave R**, Herwaldt BL, Relman DA. Cyclospora. *Infect Clin Dis North Am* 1998; **12**: 1-12
22 **Shlim DR**, Cohen MT, Eaton M, Rajah R, Long EG, Ungar BL. An alga-like organism associated with an outbreak of prolonged diarrhea among foreigners in Nepal. *Am J Trop Med Hyg* 1991; **45**: 383-389
23 **Shlim DR**, Pandey P, Rabold JG, Walch A, Rajah R. An open trial of trimethoprim along against Cyclospora infection. *J Travel Med* 1997; **4**: 44-45
24 **Connor BA**, Shlim DR, Scholes JV, Rayburn JL, Reidy J, Rajah R. Pathologic changes in the small bowel in nine patients with diarrhea associated with a coccidian-like body. *Ann Intern Med* 1993; **119**: 377-382
25 **Wurtz R**. Cyclospora: a newly identified intestinal pathogen of humans. *Clin Infect Dis* 1994; **18**: 620-623
26 **Verdier RI**, Fitzgerald DW, Johnson WD Jr, Pape JW. Trimethoprim-sulfamethoxazole compared with ciprofloxacin for treatment and prophylaxis of *Isospora belli* and *Cyclospora cayetanensis* infection in HIV infected patients. *Ann Intern Med* 2000; **132**: 885-888

Edited by Wang XL and Xu FM